| | |
|---|---|
| **Titre:** Title: | Accounting for Cold Working and Residual Stress Effects on the Axial Strength of HSS Bracing Members |
| **Auteur:** Author: | Ihor Koval |
| **Date:** | 2018 |
| **Type:** | Mémoire ou thèse / Dissertation or Thesis |
| **Référence:** Citation: | Koval, I. (2018). Accounting for Cold Working and Residual Stress Effects on the Axial Strength of HSS Bracing Members [Mémoire de maîtrise, École Polytechnique de Montréal]. PolyPublie. https://publications.polymtl.ca/3317/ |



| | |
|---|---|
| **URL de PolyPublie:** PolyPublie URL: | https://publications.polymtl.ca/3317/ |
| **Directeurs de recherche:** Advisors: | Robert Tremblay |
| **Programme:** Program: | Génie civil |

UNIVERSITÉ DE MONTRÉAL

# ACCOUNTING FOR COLD WORKING AND RESIDUAL STRESS EFFECTS ON THE AXIAL STRENGTH OF HSS BRACING MEMBERS

IHOR KOVAL

DÉPARTEMENT DES GÉNIES CIVIL, GÉOLOGIQUE ET DES MINES

ÉCOLE POLYTECHNIQUE DE MONTRÉAL

MÉMOIRE PRÉSENTÉ EN VUE DE L'OBTENTION

DU DIPLÔME DE MAÎTRISE ÈS SCIENCES APPLIQUÉES

(GÉNIE CIVIL)

AOÛT 2018

UNIVERSITÉ DE MONTRÉAL

ÉCOLE POLYTECHNIQUE DE MONTRÉAL

Ce mémoire intitulé :

# ACCOUNTING FOR COLD WORKING AND RESIDUAL STRESS EFFECTS ON THE AXIAL STRENGTH OF HSS BRACING MEMBERS

présenté par : KOVAL Ihor

en vue de l'obtention du diplôme de : Maîtrise ès sciences appliquées

a été dûment accepté par le jury d'examen constitué de :

M. MASSICOTE Bruno, Ph. D, président

M. TREMBLAY Robert, Ph. D, membre et directeur de recherche

M. ROGERS Colin A., Ph. D, membre

# ACKNOWLEDGEMENT

I would like to thank my supervisor Professor Robert Tremblay for his valuable professional guidance and encouragement during these past years. With his help, I was able to develop and improve my skills as a researcher and an engineer. The experience and knowledge I gained throughout this project will stay with me for a lifetime.

I would also like to thank my father Viacheslav, my mother Kateryna and my sister Arianne for their continued support, words of encouragement and inspiration.

# RÉSUMÉ

Les profilés HSS couramment utilisés comme membrures diagonales dans les contreventements concentriques sont habituellement formés à froid. Le processus de laminage en continu utilisé pour ces HSS induit un gradient sur la limite élastique de l'acier ($F_y$) sur le contour de la section à cause de l'écrouissage de l'acier. Par exemple, pour des profilés HSS carrés ou rectangulaires, $F_y$ dans les coins est beaucoup plus élevée que dans les parois droites. Le processus de laminage en continu induit aussi des contraintes résiduelles longitudinales et transversales importantes. Dans la conception sismique, les forces de conception dans les connexions, colonnes et les poutres dépendent des forces réelles obtenues dans les contreventements HSS. Pour cette raison, il est important de tenir compte de la variation du $F_y$ sur les parois droites et des contraintes résiduelles lorsqu'on détermine les résistances probables en tension et compression des diagonales de contreventement lors de la conception.

Une revue de littérature approfondie a été effectuée pour étudier la variation de la limite élastique $F_y$ et les profils de contraintes résiduelles dans les sections HSS formées à froid. Une étude statistique a été effectuée sur la limite élastique des profilés HSS carrés, rectangulaires et circulaires de plusieurs nuances (ASTM A500, G40.21, ASTM 1085) à partir de valeurs obtenues d'essais en traction recueillies auprès d'usines nord-américaines. Les données obtenues de la revue de littérature et de l'analyse statistique auprès des fabricants ont été utilisées pour bâtir un modèle détaillé de la variation de $F_y$ et des contraintes résiduelles sur les parois droites et les coins des profilés HSS carrés. La résistance moyenne à la traction a été déterminée basée sur ce modèle et des nuances de l'équation CSA S136 pour tenir compte de l'écrouissage. Par la suite, un modèle numérique sur OpenSees a été construit avec ces propriétés pour obtenir la résistance en compression des diagonales de contreventement HSS. Les résistances en traction et compression ont ensuite été comparées aux dispositions sismiques actuelles de la norme CSA S16 pour déterminer la résistance probable des diagonales de contreventements HSS formés à froid.

On a constaté que ces dispositions sous-estiment la résistance réelle des profilés HSS formés à froid. Il est en effet nécessaire de tenir compte de la variation du $F_y$ et des contraintes résiduelles sur le périmètre de la section pour obtenir des résultats représentatifs du comportement réel. La limite élastique dans les coins peut être posée égale à la contrainte de rupture $F_u$ obtenue de

l'éprouvette prélevée au centre des parois droites des profilés. Si cette valeur n'est pas disponible, une équation a également été proposée sur la base du rapport *D/t* et la valeur nominale de $F_y$.

La valeur moyenne de la limite élastique obtenue des essais de traction, sur des éprouvettes prélevées au centre des parois droites des profilés HSS carrées et rectangulaires, a été 1.30$F_y$ pour les trois nuances d'acier pour une limite d'un *KL/r* de 200. Pour une limite de *KL/r* de 100 à 200, pour les profilés HSS circulaires, cette valeur est de 1.22$F_y$ pour du ASTM A500 et ASTM A1085, et 1.26$F_y$ pour du CSA G40.21. Pour une limite de *KL/r* des HSS circulaires inférieure à 100, cette valeur est de 1.24$F_y$ pour du ASTM A500, 1.27$F_y$ pour du ASTM A1085 et 1.30$F_y$ pour du CSA G40.21.

Pour les sections rectangulaires et carrées, se basant sur le modèle proposé de la variation de $F_y$ et les variations de l'équation CSA S136 pour tenir compte de l'écrouissage, la limite élastique probable $R_yF_y$ pour le calcul de $T_u$ et $C_u$ devrait être égale 1.50$F_y$ (515 MPa). Cette nouvelle valeur est supérieure à la valeur de $R_yF_y$ de 460 MPa qui est présentement spécifiée dans la norme CSA S16. Pour les HSS circulaires, la limite élastique probable $R_yF_y$ devrait être égale à la valeur de l'éprouvette prélevée sur la paroi du mur présentée dans le paragraphe précédent.

La résistance pondérée à la traction $T_r$ du HSS, basée sur l'aire nominale, peut être déterminée à partir d'une moyenne pondérée basée sur le modèle proposé de la variation de $F_y$ et les nuances de l'équation pour tenir compte de l'écrouissage du CSA S136. Cette étude a été réalisée sur les sections rectangulaires et carrées. Pour ces sections, les résultats ont montré que l'on pouvait utiliser une résistance pondérée à la traction basée sur une valeur moyenne égale à 500 MPa pour des sections dont le *KL/r* ne dépasse pas 200.

Pour déterminer la résistance ultime en compression $C_u$, l'effet combiné de la limite élastique et les contraintes résiduelles varie selon l'élancement de la diagonale. Pour un défaut de rectitude de L/480, les résultats montrent que la résistance en compression des diagonales peut être approximée par l'équation de la norme CSA S16 avec $n$ = 1.34. Pour un défaut de rectitude de L/6000, la résistance en compression des diagonales peut être approximée par l'équation de la norme CSA S16 avec $n$ = 2.24 pour des élancements inférieurs à 0.75. Pour des élancements supérieurs à 0.75, la résistance en compression se rapproche graduellement à l'équation de la norme CSA S16 avec $n$ = 1.34. Pour des élancements supérieurs à 0.75, la résistance en compression se rapproche graduellement à l'équation de la norme CSA S16 avec $n$ = 1.34. Pour des élancements supérieurs

à 1.00, la résistance en compression des diagonales peut être approximée par l'équation de la norme CSA S16 avec $n$ = 2.24.

# ABSTRACT

Cold-formed hollow structural shapes (HSSs) are commonly used for bracing members in concentrically braced frames. The continuous rolling process used for the fabrication of HSSs results in yield strength properties that vary along the perimeter of the cross-section due to strain hardening. For instance, higher yield strength is observed in the corners of square and rectangular HSSs compared to the values obtained from tensile tests on coupons taken from the HSS walls. The forming process also induces longitudinal and transverse residual stresses that affect the compressive resistance of HSS members. In seismic design, design forces for brace connections, columns and beams depend on the actual resistance of the bracing members and it is important that the variation in yield strength properties and residual stress effects be properly accounted for when determining brace probable resistances in tension and compression for design.

An extensive literature review was performed to determine the yield strength and residual stress magnitudes across the section of cold-formed HSS profiles. Statistical data on mill tensile coupon tests on square, rectangular and circular HSS sections was then collected from North American manufacturers for several steel grades (ASTM A500, G40.21, ASTM 1085). The data from the literature review and North American manufacturers was used to construct a detailed model representing the yield strength and residual stress distribution across the sections of cold-formed HSS profiles. Average full section tensile strengths were then determined based on this model. A numerical model was built with OpenSees and a parametric study was performed to investigate the compressive resistance of bracing members. The tensile and compressive strengths from these models were compared to current CSA S16 seismic design provisions for the probable resistance of cold-formed HSS bracing members.

It was found these provisions underestimate the actual strength of the cold-formed sections. It is indeed necessary to account for the cross-sectional yield strength gradient and residual stresses to obtain accurate results. The actual yield strength for the corners can be approximately set equal to the steel ultimate tensile stress $F_u$ from tensile tests performed on coupons taken from the middle of the walls. If this value is not available, an equation is also proposed based on the D/t ratio and nominal yield strength.

For rectangular and square profiles of all three steel grades and a *KL/r* limit of 200, the average yield strength obtained from mid-wall tensile coupons was $1.30F_y$. For circular profiles and a *KL/r*

range of 100 to 200, this was value was 1.22$F_y$ for the ASTM A500 and ASTM A1085 steel grades, and 1.26$F_y$ for the CSA G40.21 steel grade. For circular profiles and a *KL/r* limit below 100, this value was 1.24$F_y$ for the ASTM A500 steel grade, 1.27$F_y$ for the ASTM A1085 steel grade and 1.30$F_y$ for the CSA G40.21 steel grade.

For rectangular and square profiles, the probable resistance $R_yF_y$ to determine $T_u$ and $C_u$ should be 1.50$F_y$ (515 MPa). This new value is superior to the current $R_yF_y$ of 460 MPa found in the CSA S16 standard. For circular HSS profiles, the probable resistance $R_yF_y$ should be equal to the mid-wall tensile coupon value determined in the previous paragraph.

The factored tensile resistance $T_r$, based on the nominal area, of the HSS member can be determined from a weighted average based on the proposed $F_y$ variation across the section and variations of the CSA S136 standard equation to account for strain hardening. This study was performed on square and rectangular HSS profiles. For these profiles, it was shown an average $T_r$ value of 500 MPa can be used for *KL/r* ratios below 200.

To determine the ultimate compressive resistance $C_u$, the combined effect of the yield strength and residual stress varies with the slenderness of the diagonal. For an out-of-straightness of L/480, results show that the compressive resistance of the HSS diagonals can be approximated by the CSA S16 standard equation with $n$ = 1.34. For an out-of-straightness of L/6000, the compressive resistance of the diagonals can be approximated by the CSA S16 standard equation with $n$ = 1.34 for slenderness ratios below 0.75. For slenderness ratios above 0.75, the compressive resistance gradually decreases towards the CSA S16 standard equation with $n$ = 1.34. For slenderness ratios above 1.00, the compressive resistance of the HSS diagonals can be approximated by the CSA S16 standard equation with $n$ = 1.34.

# TABLE OF CONTENTS

# LIST OF TABLES

# LIST OF FIGURES

# LIST OF SYMBOLS AND ABBREVIATIONS

| | |
|---|---|
| $A_{eff}$ | Effective area |
| $A$ | Hollow section area |
| $B$ | Hollow section width |
| $C$ | Ratio of corner to total cross-sectional area |
| $D$ | Hollow section height |
| $E$ | Elastic modulus |
| $Q$ | Effective to gross area ratio |
| $P_y$ | Yield force |
| $P_{Stheor}$ | Theoretical stub column strength |
| $R_yF_y$ | Probable yield strength |
| $\phi$ | Steel resistance factor |
| $n$ | Column strength parameter |
| $\lambda$ | Slenderness ratio |
| $\beta$ | Reliability index |
| $\alpha_r$ | Coefficient of separation |
| $\delta$ | Curvature |
| $\sigma_{stub}$ | Stub column yield stress |
| $\sigma_{coupon}$ | Yield strength of coupon taken from center of flat wall |
| $\sigma_{ys}$ | Stub column stress |
| $\sigma_{0.2}$ | 0.2% proof stress |
| $\sigma_{rt,max}$ | Maximum through thickness residual stress |
| $\sigma_y$ | Yield stress |
| $F_y$* | An equivalent nominal yield strength |

| | |
|---|---|
| $F_y$ | Yield strength |
| $F_u$ | Ultimate tensile stress |
| $F_{ynom}$ | Nominal yield strength |
| $F_{yc}$ | Corner yield strength |
| $F_{yv}$ | Strip coil virgin yield strength |
| $F_{ya}$ | Average cross section yield strength |
| $F_{uv}$ | Strip coil virgin ultimate tensile stress |
| $\rho_m$ | Material ratio |
| $\rho_g$ | Geometric bias ratio |
| $\rho_p$ | Professional ratio |
| $\rho_r$ | Steel resistance factor |
| $V_r$ | Coefficient of variation of resistance factor |
| $V_m$ | Coefficient of variation of material ratio |
| $V_g$ | Coefficient of geometric bias |
| $V_p$ | Coefficient of resistance factor |
| *CHS* | Circular hollow section |
| *RHS* | Rectangular hollow section |
| *HSS* | Hollow structural section |
| *SHS* | Square hollow section |
| $RSD_{flat}$ | Residual stress of flat |

# LIST OF APPENDICES

# CHAPTER 1 INTRODUCTION

## 1.1 Historical context

Cold-formed square hollow structural sections (HSS) are commonly used for compression members such as columns, truss members and bracing members of building structures. Today's manufacturing methods for cold-formed steel HSS profiles involve a forming process by continuous rolling as shown Figure 1-1. In the first stage, a steel plate is bent to create a circular hollow section (CHS) and welded together. For rectangular hollow sections (RHS) and square hollow sections (SHS), a second rolling stage is performed to transform the CHS into the desired rectangular or square shape. In the second stage, additional cold working is induced to create the flat walls and sharp 90° corners of the final cross-section shape.

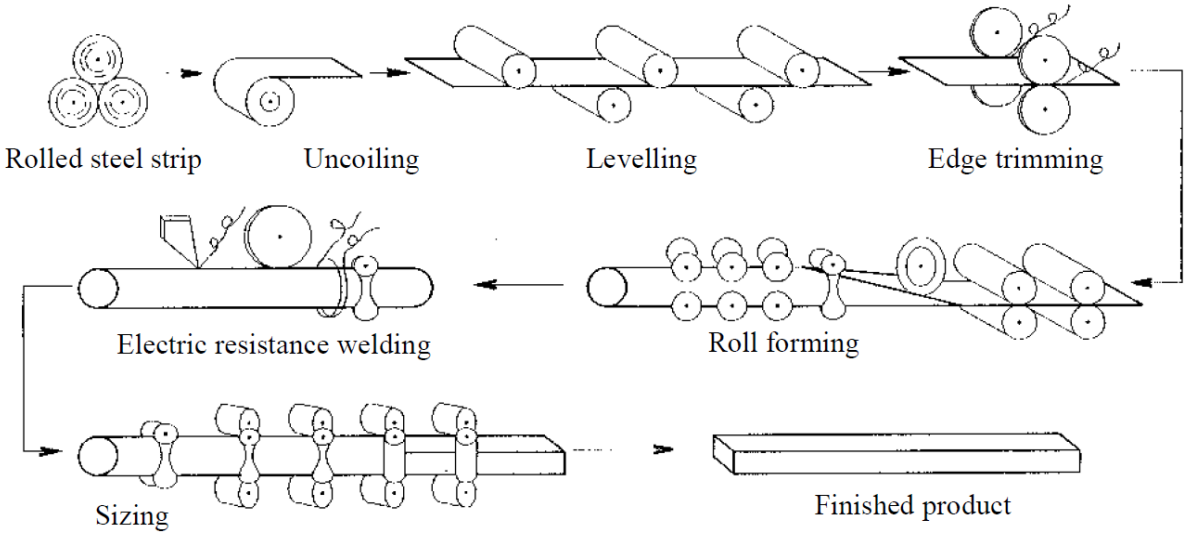


Figure 1-1: Cold-rolled forming process of cold-formed hollow structural members (Wilkinson, 1999)

Various investigations have shown that "cold-formed steel is subject to strain hardening of the material; this increases the yield strength and, in most cases, also the ultimate tensile stress, at the expense of some reduction in ductility" (Britvec et al., 1970). As noted in the same reference, "structural economy can be improved if the design of such members is based on the as-formed properties, rather than on the properties of the flat sheet, strip, or plate before forming". Britvec et

al. (1970) performed a comprehensive study that led to an equation that accounts for the strain-hardening effects on the yield strength of cold-formed steel profiles. This equation is still in use in the CSA S136 standard for the design of cold-formed steel structural members (CSA, 2016).

In Canada, the design of cold-formed HSS members is however performed in accordance with the CSA S16 standard for the design of steel structures (CSA 2014). In this standard, the factored tensile and compressive resistances of HSSs, $T_r$ and $C_r$, respectively, are based on the nominal steel yield strength, $F_y$, and there is no equation to account for increased yield strength from cold forming. In standards regulating the fabrication of HSS members such as the general requirement for rolled or welded steel (CSA 2004; ASTM 2003 and ASTM 2013), minimum yield strength requirements for rectangular and square HSSs are verified by means of tensile tests performed on coupons taken at mid-width of the walls. Hence, the design of these HSS members does not account for the likely higher yield strength present in the sharp 90° corners from cold working done in the second rolling stage. Cold forming of HSSs also induces significant residual stresses in the longitudinal direction as well as in the transverse directions. Despite residual stresses in HSS and W-shapes are very different, the compressive resistance of cold-formed HSS members in CSA S16 is determined with the equation originally developed for W-shapes, as was proposed by Davison and Birkemoe (1983) from numerical and experimental investigations.

Hollow structural sections producers however take advantage of cold forming effects on yield strength as they generally use plate material exhibiting lower yield strengths and rely on strain hardening to satisfy the required minimum yield strength requirement in the finished tube[1]. Hence, the specified minimum yield strength used in design should be representative of the actual yield strength present on the perimeter of CHSs and walls of SHSs and RHSs while underestimating the yield strength in the corners of SHSs and RHSs. In practice, however, because the extent of cold forming and its effects on $F_y$ vary with the plate thickness and the size of the cross-sections, yield strengths measured on the perimeters of CHSs and walls of SHSs and RHSs still vary significantly between producers and as a function of the section size, as revealed by the survey done by Schmidt and Bartlett (2002a) for CSA G40.21-350W HSSs. This is shown in Figure 1-2.

[1] Bradley Fletcher, Atlas Tube, Personal communication, 2017.

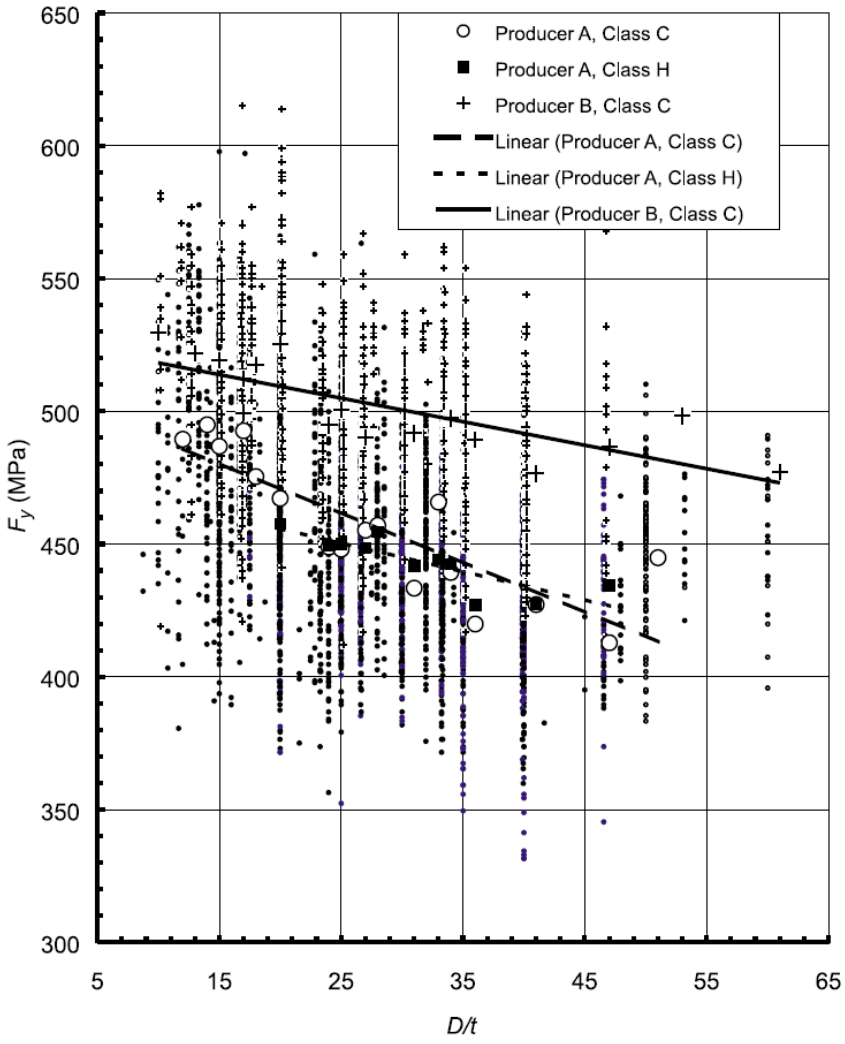


Figure 1-2: Measure yield strength for cold-formed HSS members (Schmidt & Bartlett, 2002a)

In Figure 1-2, the parameter $D$ used in the $D/t$ ratio for SHS and RHS is the equivalent diameter taken equal to 2(b+d)/(π). The plots show that $F_y$ typically greatly exceeds the 350 MPa minimum yield strength value and $F_y$ generally increases for stockier sections (smaller $D/t$) requiring more pronounced cold working.

When designing for HSS members for non-seismic loads the $F_y$ increase due to cold-forming is ignored. This results in a non-optimized design. In seismic force resisting systems, CHS and SHS profiles are commonly used as bracing members for concentrically braced steel frames. CBFs can be designed as Type MD (moderately ductile) or Type LD (limited ductility) category. In CSA S16, CBFs of these two categories must be designed and detailed such that seismic input energy can be dissipated through tensile yielding and inelastic buckling of the bracing members. The

bracing members must therefore be detailed to achieve this inelastic response. Moreover, design forces for brace connections, beams and columns are based on lateral loads required to attain the probable tensile and compressive resistances of the bracing members, $T_u$ and $C_u$, respectively. It is therefore important to properly account for the increase of yield strength due to cold forming and residual stress effects on axial resistances when using cold-formed HSS profiles.

This is not the case in current practice. In CSA S16, the probable yield strength, $R_yF_y$ that must be used to determine probable brace resistances in seismic design is set to 460 MPa, i.e. a value that approximately corresponds to the average $F_y$ in the survey by Schmidt and Bartlett (2002). It does not account for the variation with the $D/t$ ratio. For SHSs and RHSs, the value is based on tensile tests performed on coupons taken from the HSS walls and does not account for the greater $F_y$ expected in the HSS corners.

For SHS and RHS members, it would be possible to obtain more uniform and economical designs in seismic applications if the increase in yield strength was taken into account for the calculation of $T_r$ and $C_r$ through an equation like the one available in the CSA S136 standard. The CSA S136 equation was developed based on tests conducted on very thin channels made from low yield material (260 MPa) fabricated by break forming. It may therefore not reflect $F_y$ values resulting from today's continuous rolling methods, steel grades and HSS profiles currently used for construction with thickness up to 22.5 mm. Similarly, the study by Davison and Birkemoe (1983) was likely performed on HSS members that were not manufactured using current forming processes. More realistic values for $C_r$ could therefore be obtained if actual residual stress conditions were taken into account in the equations used in CSA S16. For seismic design, safer design would be achieved if the actual yield strength and residual stress properties were considered in the calculation of the probable tensile resistance $T_u$ and probable compressive resistance $C_u$ specified in CSA S16 for cold-formed HSS bracing members.

In Canada, the industry often substitutes CSA G40.21 HSS with ASTM A500 tubing. The latter are fabricated using less stringent tolerances and lower strength material. Recently, a new ASTM standard, A1085, was developed in the U.S. for HSS profiles. The requirements in this standard are comparable to those specified for CSA G40.21-350W HSS, except that a maximum yield strength value of 485 MPa is specified. It is expected that the industry will eventually adopt this new standard. Meanwhile, CSA G40.21 and ASTM A500 will still be in use in Canada. Hence, a

study on HSS properties should examine products manufactured in accordance with these three standards.

## 1.2 Problem statement

Due to the significant increase in actual yield strength of the HSS bracing members, it is believed that the factored resistance $T_r$ for seismic design may not be appropriate and should be improved. In addition, the probable resistance of HSS bracing members in concentrically braced seismic resisting systems proposed by current seismic design provisions (CSA S16) is not representative of the actual strength of the member. This probable resistance is taken from mill certificates that are based on the strength of a coupon taken from the mid-section. It is assumed a yield strength gradient is present across the full cross-section due to the strain hardening of the material. The corners also undergo greater cold work than the flat wall. This significantly increases their yield strength compared to the rest of the cross-section. In addition, the final properties of the member due to the cold-forming process are highly dependant on the equipment, usage, calibration and the virgin coil which also exhibits non-uniform properties. This leads to a very large variation in the $F_y$ of the mid-section coupon. The CSA S136 standard presents an equation which can be used to estimate the yield strength of the corners. However, this equation was developed for a much thinner material that was cold-formed using different processes compared with what is done to manufacture HSS today. The CSA S16 standard does not account for the increased yield strength from the corners. Residual stresses are not directly accounted for either as the column strength of cold-formed members is based on an equation originally developed for W-shapes which exhibit a very different residual stress pattern. Since the seismic design provisions in the CSA S16 standard are based on capacity design, this means the actual forces in the beams, columns and other members are associated with tension yielding or compression buckling of the HSS braces. In addition, the North American industry has been moving from ASTM A500 steel grades to ASTM A1085 and CSA G40.20/G40.21 steel grades which show more consistent properties.

## 1.3 Objectives and scope of research

The goal of this investigation is to propose new values for the factored tensile resistance $T_r$ and for the probable resistances $T_u$ (gross yielding) and $C_u$ that should be used for HSS bracing members used for the seismic design of Type MD and Type LD steel CBFs. These new values should account

for the variability in the yield strength of HSS members currently used for construction. For SHS and RHS, it must also account for the yield strength gradients across the walls, the increase in yield strength in the corners and the actual residual stress distribution.

## 1.4 Methodology

The following steps are taken to obtain an accurate model of the actual yield strength gradient and residual stress distribution of a HSS bracing member:

- Review available literature on material properties of cold-formed members.
- Determine representative yield strength and residual stress theoretical models based on previous investigations.
- Compile yield strength values from mill certificates from North American manufacturers.
- Perform a statistical analysis of the test results and propose reasonable magnitudes and distribution for the yield strength and residual stress gradients.
- Propose a final yield strength and residual stress distribution model to determine the strength of cold-formed HSS bracing members.

The following steps are taken to study the effect of the actual tensile and compressive resistances of HSS bracing members:

- Determine the average probable tensile resistance $R_yF_y$ of HSS bracing members from the proposed model and the CSA S136 equation to be used to calculate $T_u$ and $C_u$.
- Perform a reliability analysis to determine the nominal yield strength that should be used for the factored tension resistance $T_r$ of HSS bracing members.
- Design sample braced frames to determine the most common HSS sizes being used in low-rise buildings in Canada and examine the possible savings that can be gained from accounting for the actual yield strength in design.
- Develop an OpenSees model of SHS bracing members that accounts for the increased yield strength in the corners, the yield strength gradient across the flat walls and the actual residual stress distribution.

- Perform a parametric study on several A1085 HSS bracing members to assess the impact of the actual yield strength and residual stresses on their compressive resistances with respect to Canadian column strength curves.
- Propose recommendations with respect to $T_r$, $T_u$ and $C_u$ for tensile and compressive resistances of cold-formed HSS bracing members to be used for seismic design.

## 1.5 Outline of thesis

This investigation is composed of the five following chapters. Chapter 1 presents the introduction, objectives and the problem addressed in this thesis. Chapter 2 presents an comprehensive literature review which summarizes research into cold-formed members over the past 60 years. The review is centered around the material properties of these sections, specifically the yield strength and residual stresses. Chapter 3 provides a statistical analysis of experimental values determined from the reviewed literature in Chapter 2 and mill certificates from North American manufacturers. Different steel grades are compared. A detailed yield strength and residual stress model is proposed for numerical modelling. Average factored tension resistance values are obtained from a reliability analysis. An economic study is performed in Chapter 4 based on assumed $F_y$ and $R_y F_y$ values. Expected weight saving are evaluated for typical concentrically braced frames with SHS braces for low-rise buildings in Canada. The most commonly used sections are identified based on these analyses. A parametric study is then performed to determine the impact of an increased yield strength and residual stress distribution on Canadian column compression design curves. Chapter 5 presents the conclusion and recommendations of this thesis.

# CHAPTER 2 LITERATURE REVIEW

This chapter provides a comprehensive review of the literature of cold-formed members over the past 60 years. It is mostly centered on the material properties such as the yield strength and residual stress of the cold-formed HSS members. It is separated in four sections; each section approximately covers two decades. Each section has an introduction and a summary to facilitate the reading. The reviewed articles are presented in the introduction and a short overview of the findings for each treated article is presented in the summary. A conclusion is also presented at the end of this chapter where the main findings from the full chapter are reported. The S136-16 standard equation developed in the 1960s to account for the increased yield strength from cold work of forming is presented in the first Section 2.1 of this review. The first residual stress and yield strength gradient models that were proposed in the late 1960s to the early 1980s are discussed in the second Section 2.2. A more detailed residual stress model that was proposed in the 1990s is presented in the third Section 2.3 and the differences with respect to the model presented in Section 2.2 are explained. In the final Section 2.4, investigations performed in the past 20 years are presented and their findings are compared to the first three sections.

## 2.1 Accounting for the increased yield strength from cold work of forming according to the S136-16 standard

The first major research effort into the increased yield strength of cold-formed members was undertaken by Britvec, Chajes, Karren and Winter during a sponsored investigation by the American Iron and Steel Institute at Cornell University, New York. The goal of this investigation was to determine the as-formed properties of cold-formed sections. Since these properties are different from the original plate used to form the member, Britvec et al. state that accounting for these changes would improve the structural economy of the project. In 1970, a condensed account of this investigation was published to constitute the basis of the provisions for the 1968 edition of the *Specification for the Design of Cold-Formed Steel Structural Members*. The four papers listed below were summarized in this account (Britvec et al., 1970):

- *Effects of Cold-Straining on Structural Sheet Steels* (Chajes et al., 1963).
- *Corner Properties of Cold-Formed Steel Shapes* (Karren, 1967).
- *Effects of Cold-Forming on Light-Gage Steel Members* (Karren & Winter, 1967).
- *Cold-Forming Effects in Thin-Walled Steel Members* (Uribe & Winter, 1969).

In 2016, the current Specification for the Design of Cold-Formed Steel Structural Members (CSA S136-16) still permits to account for the strength increase in cold-formed members based on the same equation as proposed in 1968. This section gives a summary of the research leading to equation (2-1) which is referred to as equation (C-A7.2-1) in the CSA S136-16 standard.

$$\frac{F_{yc}}{F_{yv}} = \frac{B_c}{\left(\frac{R}{t}\right)^m} \tag{2-1}$$

$$\frac{\mathrm{F}_{yc}}{\mathrm{F}_{yv}} = \frac{B_c}{(\frac{R}{t})^m}$$

$$B_c = 3.69\frac{F_{uv}}{F_{yv}} - 0.819\left(\frac{F_{uv}}{F_{yv}}\right)^2 - 1.79$$

$$m = 0.192\frac{F_{uv}}{F_{yv}} - 0.068$$

The basic theory behind uniform cold stretching is established in the first paper (Chajes et al., 1963). The second paper proposes mathematical formulations to account for the yield strength increase in corners based on virgin properties of the coil. The third paper compares experimental results on a sectioned channel to full section tensile tests and proposes a method to account for the increased yield strength in the full section. The fourth paper was not included as it concentrated on joist cords and was exterior the scope of this investigation.

As it is explained by (Chajes et al., 1963), previous research had already shown that corners in light-gage steel sections exhibit increased yield strength through testing of corner. However, no theory was proposed to explain this. Therefore, it was judged necessary, by Chajes et al., to understand the basic theory behind uniform stretching before tackling the corners. This objective was set in the fist paper titled "*Effects of Cold-Straining on Structural Sheet Steels*" (Chajes et al., 1963).

To achieve this, light-gage steel sheets from mild carbon structural steel were subjected to uniform cold stretching. (Chajes et al., 1963) tested a total of five different types of mind carbon which were extracted from the straightened coil used to further produce structural members. Table 2-1

presents the chemical composition of the tested sheets and Figure 2-1 shows the coupons taken from the coil. It is important to note (Chajes et al., 1963) refer to the specimens in the axial direction of the future member as transverse specimens.

Table 2-1: Material properties (Chajes et al., 1963)

| Material | Gage | Chemical Composition by Random Check Analysis | | | | Tensile Properties | | |
|---|---|---|---|---|---|---|---|---|
| | | C | Mn | S | P | Yield Strength, in psi | Ultimate Strength, in psi | % Elong. 2 inch gage length |
| 1. Cold Reduced Annealed, Temper-Rolled Killed, Sheet Coil | 16 | 0.15 | 0.40 | 0.024 | 0.008 | 38,300 | 51,100 | 40 |
| 2. Cold Reduced Annealed, Temper-Rolled Rimmed, Sheet Coil | 16 | 0.09 | 0.39 | 0.028 | 0.008 | 36,400 | 50,700 | 35 |
| 3. Hot Rolled Semi-Killed Sheet Coil | 16 | 0.04 | 0.32 | 0.025 | 0.008 | 37,500 | 49,000 | 37 |
| 4. Hot Rolled Rimmed Sheet Coil | 16 | 0.08 | 0.32 | 0.045 | 0.008 | 40,500 | 50,700 | 35 |
| 5. Hot Rolled Semi-Killed Sheet Coil | 10 | 0.18 | 0.50 | 0.029 | 0.008 | 37,000 | 57,500 | 36 |

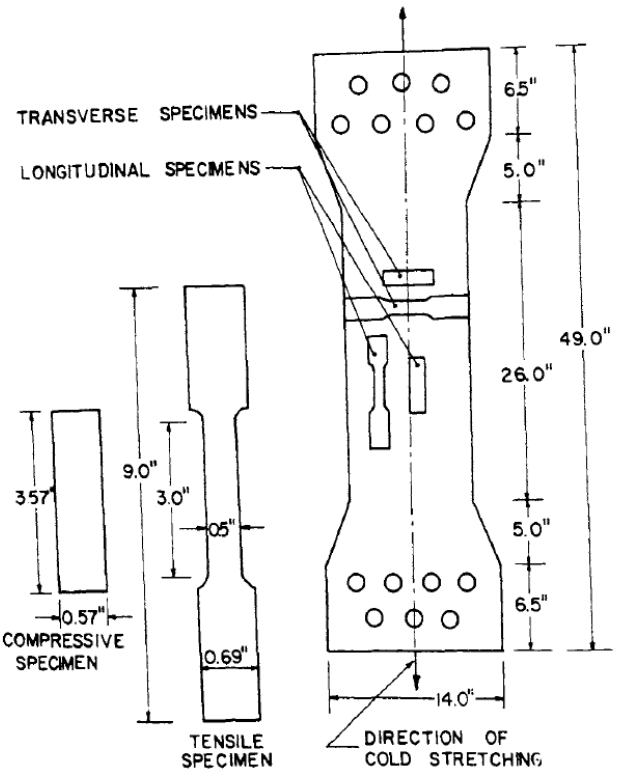


Figure 2-1: Plate used in cold stretching operation and typical tensile and compressive specimens (Chajes et al., 1963)

(Chajes et al., 1963) performed both tensile and compressive tests on the coupons to determine the stress-strain curve after plastically deforming the coil sheet to various degrees. Figure 2-2 presents the typical stress-strain curve obtained from the tested coupons. The results available in the report show there was an increase in yield strength in both tensile and compressive coupons in both directions except for the cold-reduced killed steel. However, Britvec et al. found the increase is strongly dependent on the amount of cold work done and does not display the same increase in all directions.

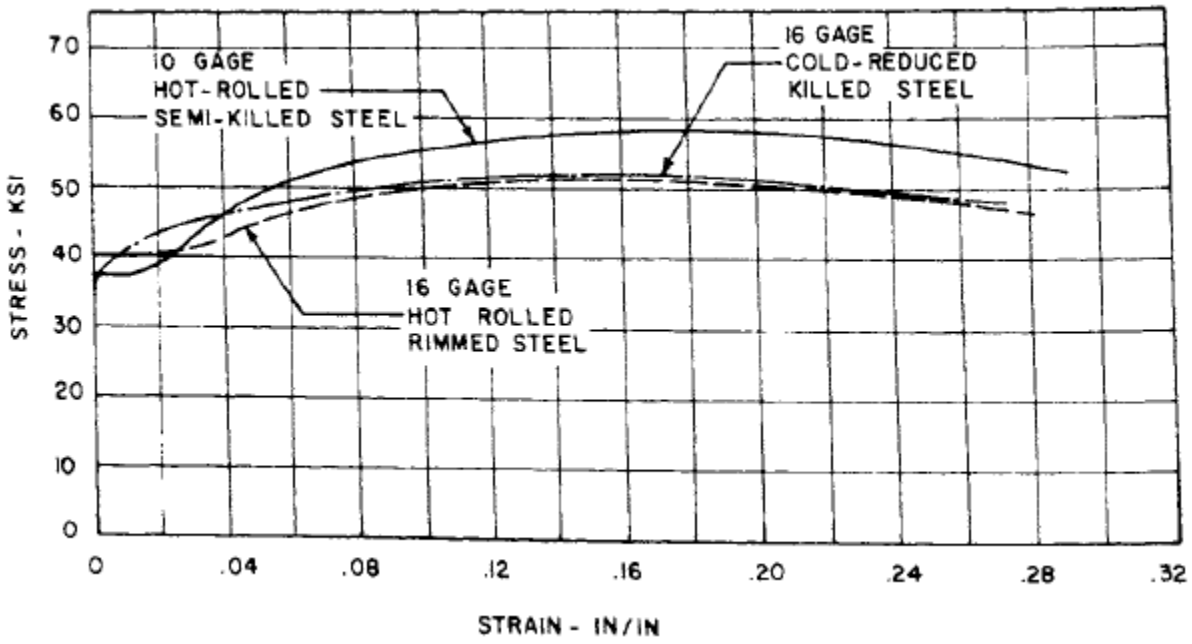


Figure 2-2 :Typical stress-strain curve for tested coils (Chajes et al., 1963)

For example, as reported by Chajes et al. (1963), the 10-gage hot rolled semi-killed steel had an 89% tensile yield strength increase from the virgin coil in the longitudinal direction and about half in the transverse direction (axial direction of future specimen) for 10% of cold stretching. The opposite is seen in compressive specimens with a significantly higher increase in the transverse direction compared to the longitudinal direction. Britvec et al. attributed these variations to the Bauschinger effect in the longitudinal direction and the inverse Bauschinger effect in the transverse direction.

The authors (Chajes et al., 1963) further studied the effects of the ultimate to yield strength ratio and aging of the material. It is reported that a higher ultimate to yield strength ratio will result in a higher yield strength increase. Aging of the material will also result in an increase of yield strength

for all steels except for the cold reduced killed steel. An important secondary effect of aging noted by Chajes et al. (1963) is the recovery of the well-defined yield point of mild steel. Figure 2-3 illustrates this effect. The dashed line represents the specimen right after cold stretching while the solid line represents the specimens after being aged at 100°C for 30 min. Nevertheless, it is reported not all specimens recovered the yield plateau as it was strongly dependent on manufacturing type and chemical composition.

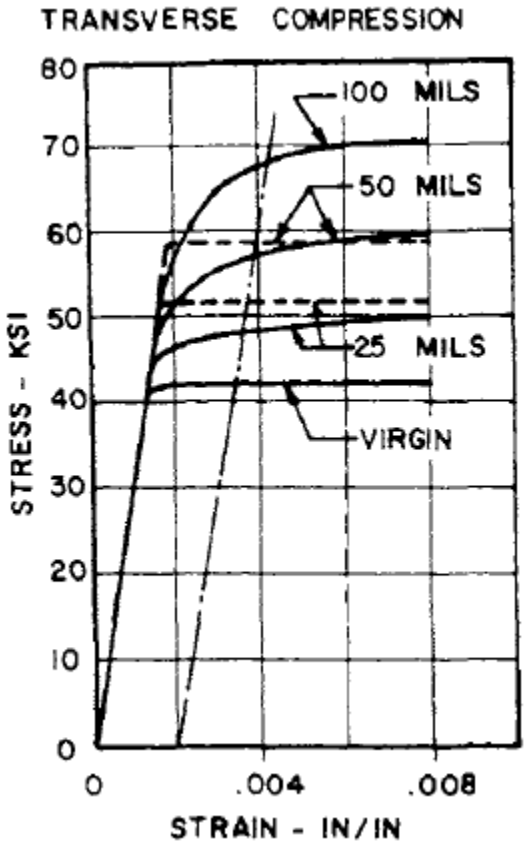


Figure 2-3: Aging effects on hot rolled semi-killed steel (Chajes et al., 1963)

Just as the increase in yield strength, Chajes et al. (1963) found the increase in ultimate tensile stress is strongly dependent on the amount of cold stretching. However, this increase is significantly less than the increase in yield strength. Most sheets displayed an increase in ultimate tensile stress of about 10% while the cold reduced killed steel had no increase at all. In addition, this increase is fully attributed to strain aging and not strain hardening by which the difference between the killed reduced steel and the rest is explained.

To continue, Chajes et al. (1963) examined the percentage of elongation which showed a significant decrease with increasing stretching. Once again, it was found the killed cold reduced steel was the only exception with a significant smaller reduction. For a 10% permanent elongation, the percentage elongation decreased from 35 to 12%. This reduction in ductility was attributed to strain hardening and aging of the material. This is justified in the investigation by the cold reduced killed non-aging steel only showing a decrease of 9% to the same 10% permanent elongation.

The second part of the investigation performed in Cornell University consisted in developing a method to predict the yield strength of cold-formed corners from the yield strength of the virgin material. This was achieved in the paper titled "*Corner Properties of Cold-Formed Steel Shapes*" (Karren, 1967). To this end, the virgin tensile and compressive properties of an un-straightened coil sheet and the as-formed properties of corners were determined. (Karren, 1967) does not specify the actual shapes of the profiles that the coil was used for. However, they do specify the forming process that was used to create the corner (roll formed, press-braked, and coin press-braked) as well as the *a/t* ratio which represents the interior corner radius to thickness ratio. The chemical properties of the materials are also described with an added four additional carbon steels to the ones studied in the first paper. In parallel, Karren developed an analytical model for the yield strength of the corner. To verify their model, they compared the analytical results to the experimental ones and concluded they were in reasonable agreement. A short overview of the development of the model is presented below.

Karren (1967) assumed the strain hardening function can be expressed by the power function in equation (2-2).

$$\sigma = k(\varepsilon)^n \tag{2-2}$$

As long as the logarithmic plot of the stress-strain curve is linear, equation (2-2) can be simplified to equation (2-3) for uniaxial tension expressed in terms of true stress and strain. Figure 2-2 shows the tensile stress-strain curves of the virgin materials confirming the applicability of this equation (Karren, 1967).

$$\sigma' = k(\varepsilon')^n \tag{2-3}$$

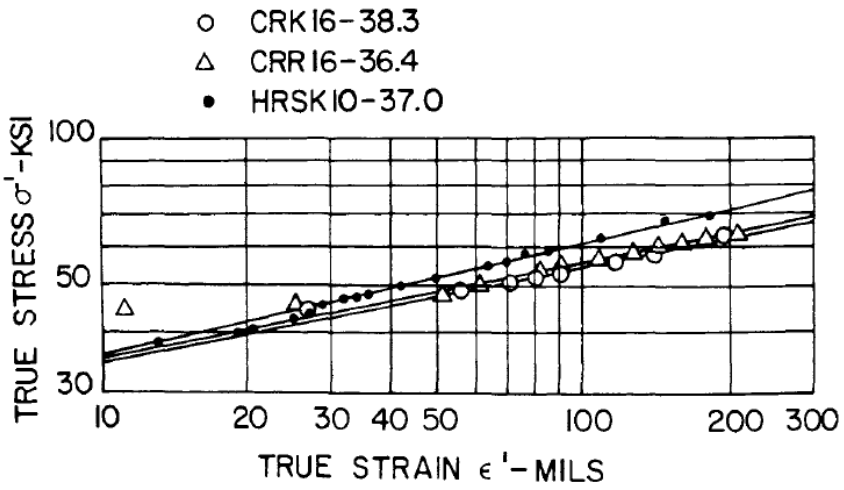


Figure 2-4: Tensile stress-strain curves of virgin materials in terms of true stress and true strain (Karren, 1967)

The factors *k* and *n* were determined experimentally and are related to the virgin ultimate tensile stress and the virgin yield stress by equations (2-4) and (2-5) developed by Karren.

$$k = 2.8\sigma_u - 1.55\sigma_y \tag{2-4}$$

$$n = 0.225\frac{\sigma_u}{\sigma_y} - 0.120 \tag{2-5}$$

Once the factors were established, it was necessary define the circumferential strain at any point of the corner for a simplified model. The model assumes uniform curvature and tangential strain. The following assumptions were posed by Karren (1967) to simplify the model:

- *Isotropic material under plastic conditions.*
- *Elastic strains are negligible in comparison to plastic ones.*
- *Shearing stresses cause plastic deformations, not normal stresses.*
- *Ratios of principal strains remain constant.*
- *Principal axes do not rotate with respect to the element.*
- *Same tensile and compressive stresses in terms of true stress.*
- *No Bauschinger effect is present.*
- *No change in volume as result of plastic deformations.* (Britvec et al., 1970, p.60)

By applying these simplifications, Karren (1967) developed the following relationship for the circumferential strain (also named tangential strain) in equation (2-6).

$$\varepsilon_\theta = \frac{l - \mathrm{l}_o}{\mathrm{l}_o} = \frac{r - \mathrm{r}_o}{\mathrm{r}_o} = \frac{r}{\mathrm{r}_o} - 1 \tag{2-6}$$

Further simplifying the equation and applying the assumptions Karren (1967) presented the generalized strain in equation (2-7).

$$\varepsilon = \frac{2}{\sqrt{3}} \ln(1 + \varepsilon_\theta) = \frac{2}{\sqrt{3}} \ln \frac{r}{\mathrm{r}_o} \tag{2-7}$$

Where $r_o$ represents the radius to the fiber of zero strain, $r$ is the exterior radius of the corner, and $\varepsilon_\theta$ is the engineering strain in the tangential direction.

An important assumption for this model that contradicts findings from the previous paper is the removal of the inverse Bauschinger effect. Karren (1967) explains this by stating that "*the increase in tensile yield strength in the longitudinal direction from a compressive plastic strain in the tangential direction is offset by the reduction from the equal tensile plastic strain in the radial direction*" (Britvec et al., 1970, p.70). Previous experimental research is also referred to confirm this affirmation.

Since the Bauschinger effect is absent, the overall yield strength will be the weighted average of the yield strength of all fibers composing the corner. Since the equation for the generalized strain has been developed and confirmed by experimental values, it is simply necessarily to apply it to the stress-strain equation for uniaxial tension and integrate it over the corner area. Through some mathematical simplifications and the previously defined assumptions Karren (1967) obtained the relationship in equation (2-8). Further details of the calculations can be found in Karren's paper.

$$\sigma_{yc} = \frac{kb}{(\frac{a}{t})^m} \tag{2-8}$$

$$b = 0.945 - 1.315n$$

$$m = 0.803n$$

The generalized strain equation was further experimentally verified in Karren's paper by the Photogrid Method and the results are presented in Figure 2-5. The main conclusions drawn by the authors from this comparison are the lack of significant strains in the longitudinal direction (confirms condition of plane strains), a small reduction in thickness, and the presence of significant radial pressure in some of the forming processes (roll forming). This led Karren (1967) to propose a second model which will included a uniformly distributed radial pressure.

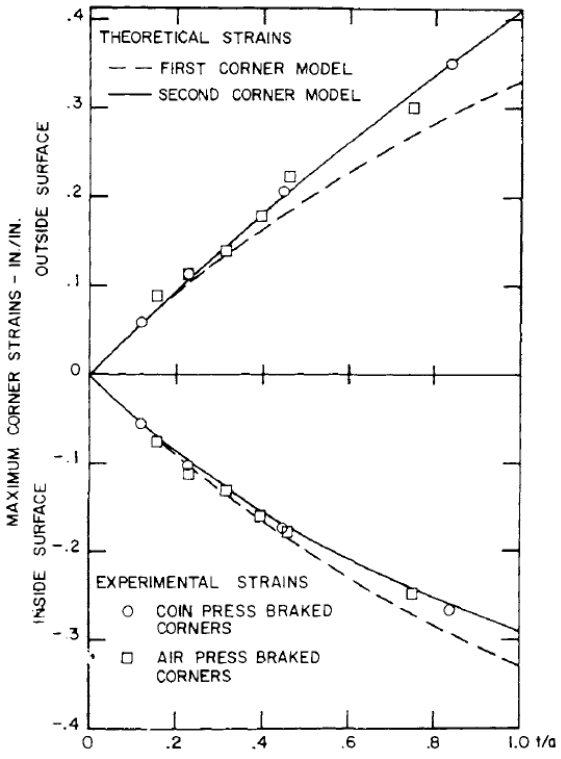


Figure 2-5: Maximum corner strains by Photogrid Method, full line, and corner strains by equation (2-8), dashed line (Karren, 1967)

Karren (1967) determined an equation for the new neutral axis while accounting for the radial pressure, however the amount of radial pressure applied during the process is unknown. Therefore, the authors proceeded to trial and error to obtain the location of the zero-strain axis which ends closer to the interior surface. The new neutral axis is given in equation (2-9).

$$\sigma_o = \sqrt{(ab)} \tag{2-9}$$

By integrating equation (2-9) in the previously defined steps, Karren (1967) obtained the factors relating to the corner yield stress in equation (2-10).

$$\frac{\sigma_{yc}}{\sigma_y} = \frac{\frac{kb}{\sigma_y}}{(\frac{a}{t})^m} \tag{2-10}$$

$$b = 1.0 - 1.3n$$

$$m = 0.855n + 0.035$$

By performing some algebraic manipulations and replacing the *k* and *n* variables in equation (2-10) with equations (2-4) and (2-5), it is possible to obtain equation (2-11) which is equation (C-A7.2-1) in the CSA S136-16 standard (CSA 2016). It can be concluded that the equation to account for increased yield strength in cold-formed sections in the 2016 version of the standard is virtually the same as the one developed in the 1960s by Karren (1967).

$$\frac{\mathrm{F}_{yc}}{\mathrm{F}_{yv}} = \frac{B_c}{(\frac{R}{t})^m} \tag{2-11}$$

$$B_c = 3.69\frac{F_{uv}}{F_{yv}} - 0.819\left(\frac{F_{uv}}{F_{yv}}\right)^2 - 1.79$$

$$m = 0.192\frac{F_{uv}}{F_{yv}} - 0.068$$

$F_{yc} = corner\ yield\ stress$
$F_{yv} = virgin\ yield\ stress$
$F_{uv} = virgin\ ultimate\ tensile\ strength$
$R = inside\ bend\ radius$

Once the equation for the increased yield strength is established, Karren (1967) verified the results by testing corners in tension and compression. The factors determined in the tests were the proportional limit, the yield strength, the tensile ultimate tensile stress and the percentage elongation.

In nonaging materials, Karren (1967) determined the compressive and tensile yield strengths are approximately equal while aging materials had compressive strengths 5 to 15% higher than tensile strengths. It is also determined the forming method has no significant influence on corner properties.

As Karren (1967) explained, as the a/t ratio (interior radius over thickness) decreases the corners showed a significantly higher increase in yield strength as well as gradual yielding while high a/t ratios showed sharper yielding and smaller increase in yield strength. This is explained by various fibers having achieved different levels of effective yield stress in corners with small a/t ratios. Therefore, the fibers will plastify at different strengths producing a gradual stress-strain yielding curve.

Figure 2-7 shows some of the results obtained by Karren (1967) when comparing theoretical values to experimental values in compression and tension. It is important to note the author took the same *k* and *n* for the tensile and compressive models. Therefore, the theoretical curve is equal for both.

As Karren (1967) noted, the curves show that experimental values tend to be conservative when compared to the theoretical models. It was also determined ultimate tensile stress increases significantly less than yield strength. For example, for one high cold worked material, the yield strength increased by 69% and the ultimate tensile stress increased by 45% compared to the virgin.

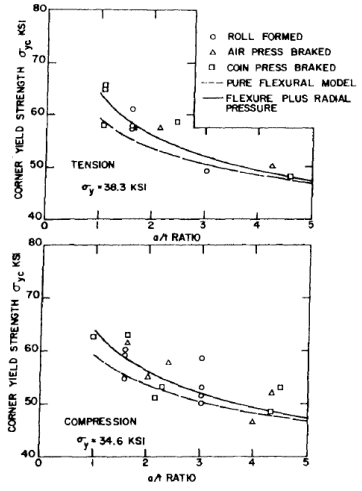


Fig. 12. Yield strength of corners versus *a/t* ratio for CRK16-38.3 steel.

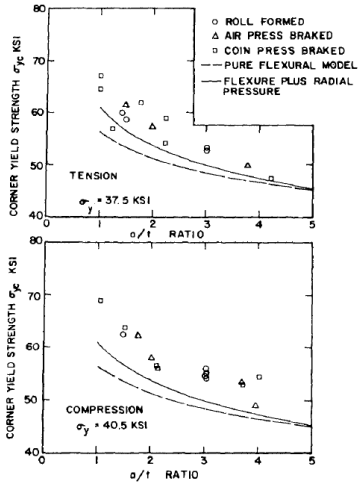


Fig. 13. Yield strength of corners versus *a/t* ratio for HRSK16-37.5 steel.

Figure 2-6 : Comparison between theoretical prediction of corner yield strength and experimental results – Part 1 (Karren, 1967)

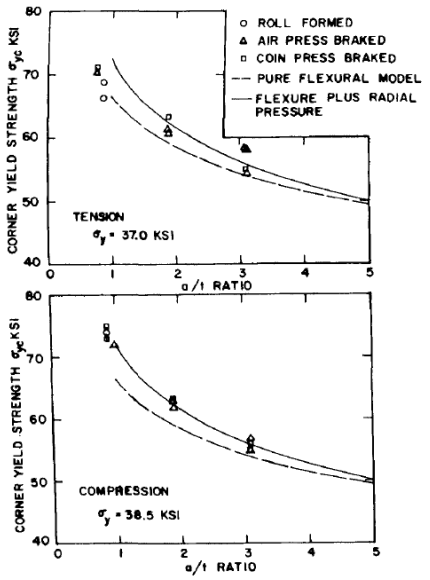


Fig. 14. Yield strength of corners versus $a/t$ ratio for HRSK10-37.0 steel.

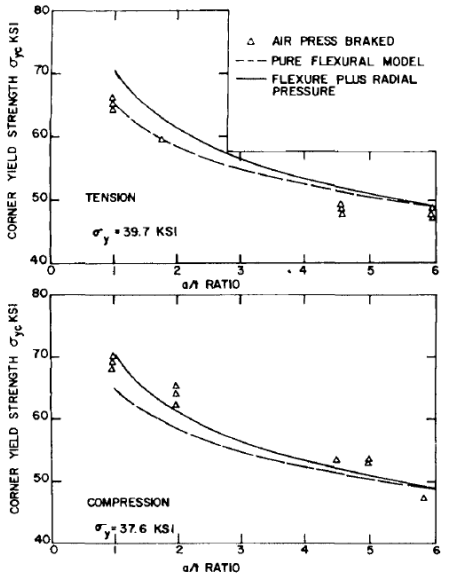


Fig. 15. Yield strength of corners versus $a/t$ ratio for HRSK16-39.7 steel.

Figure 2-7 : Comparison between theoretical prediction of corner yield strength and experimental results – Part 2 (Karren, 1967)

After establishing an equation for corner yield strength, the third part of the investigation presented by Britvec et al. (1970) focused on studying the effects of cold forming on flats and the stability of the cold-formed sections. This was published in the paper titled "*Effects of Cold-Forming on Light-Gage Steel Members"* (Karren & Winter, 1967). To achieve this, Karren and Winter (1967) tested several roll-formed channels and joist chords. The virgin properties of the sheet used to produce the sections were tested, as well as the corners of the as-formed sections. The as-formed member was also sectioned, and the properties of the flats were determined. Figure 2-8 gives an example of the results. Full-section tensile and compressive tests were done as well. The compressive tests were separated into stub column tests and laterally supported tests.

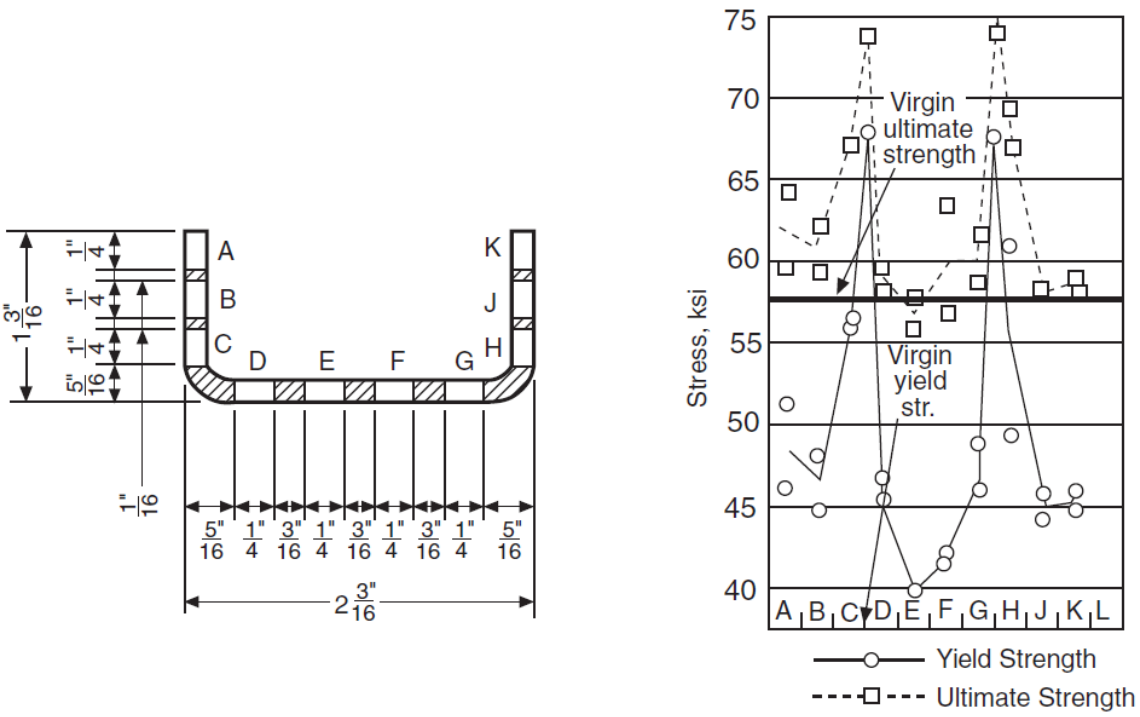


Figure 2-8: Sectioned coupon properties for virgin and as-formed state (Karren & Winter, 1967)

It was found in this investigation Karren and Winter (1967), the corner yield strength was as much as 100% higher than the virgin material, the reduction in percentage of elongation varied from 20% to 90% highly reducing ductility. The maximum ultimate tensile stress increase was of 47% above the virgin value. Flat specimens regained their sharp yielding characteristics after aging and corner specimens did not.

Karren and Winter (1967) determined the change in yield strength of the flats greatly varies with the method of fabrication. Press-braked members exhibit increases of the order of 6%, while roll-formed sections exhibit increases ranging from 17 to 50%. The largest reduction in percentage of elongation is of 26% rendering a small decrease in ductility. It is found strain hardening and aging are the two factors contributing to the increased yield strength. The effect of aging is assumed to have a uniform distribution through the flats. The effect of strain hardening is strongly dependent on the roll design, the human operator, wear and tear of the rolls and other manufacturing aspects. Therefore, Karren and Winter (1967) did not attempt to predict the increase through an equation as it was done for the corners.

Karren and Winter (1967) created composite curves from the flat and corner coupon results by taking a weighted average of the results and comparing them to the full-section results. An example of such curve is provided in Figure 2-9. The elongation for full sections was found to range from 32 to 48% which is significantly larger than the elongation for the individual coupons meaning the ductility wasn't as affected. It was found yield strength in laterally-supported compressive members was larger than the tensile yield strength and stub column compressive strength. The lower stub column resistance is attributed to the flats buckling locally before the corners can achieve their full yield strength.

The authors proposed equation (2-12) based on the weighted average to account for the increased yield strength. This is the same equation as the one available in the CSA S136-16 standard.

$$\sigma_{ys} = C\sigma_{yc} + (1 - C)\sigma_{yf} \tag{2-12}$$

The $\sigma_{yc}$ (corner yield strength) factor is to be determined from equation (2-10), while the $\sigma_{yf}$ (flat yield strength) factor can be determined by taking the weighted average of flat tensile coupons. The *C* factor is the ratio of corner to flat area.

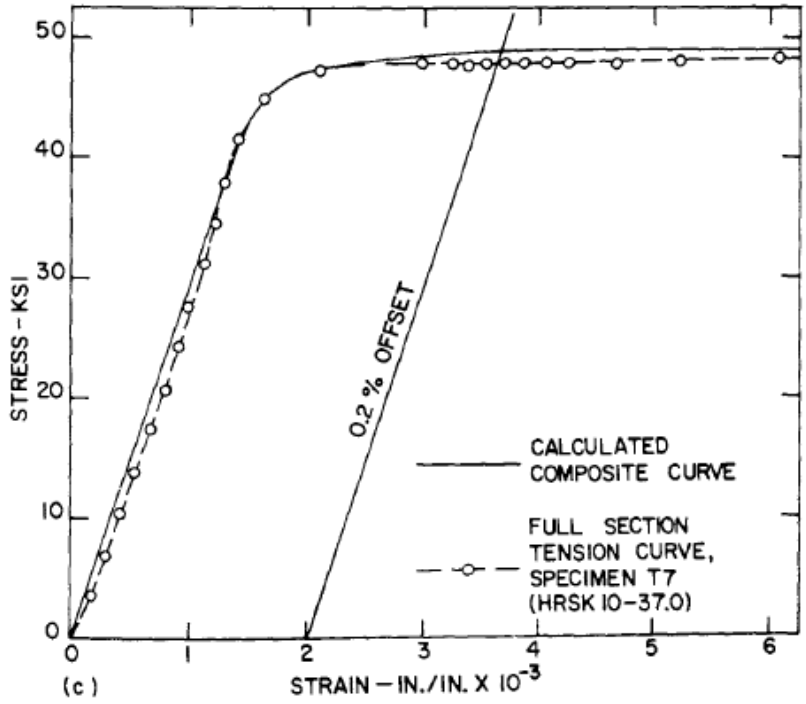


Figure 2-9: Composite curve of flat and corner average vs. experimental results from full tensile section (Karren & Winter, 1967)

The same equation is proposed for sections in tension and compression with the equation being based on tensile results only. Karren and Winter (1967) justify this by stating the tensile sections are more conservative than the compressed sections. Table 2-2 compares the calculated values to the experimental values.

Table 2-2: Calculated results to experimental results (Karren & Winter, 1967)

| Average Flat Tensile Yield Strength, $\sigma_{yf}$, in kips per square inch | Calculated Tensile Full-Section Yield Strength, $\sigma_{ys}$, in kips per square inch | Full-Section Tests | | | Ratio of Tensile Yield Strength to Calculated tensile Full-Section Yield Strength | Ratio of Compressive Yield Strength to Calculated tensile Full-Section Yield Strength |
|---|---|---|---|---|---|---|
| | | Tensile Yield Strength, in kips per square inch | Compressive Yield Strength, in kips per square inch | Ultimate Strength, in kips per square inch | | |
| (8) | (9) | (10) | (11) | (12) | (13) | (14) |
| 37.9 | 40.0 | 39.4 | 37.8 | 48.8 | 0.98 | 0.94 |
| 39.7 | 41.5 | 42.5 | 44.9 | 51.1 | 1.02 | 1.08 |
| 43.8 | 46.0 | 45.6 | 51.0 | | 0.99 | 1.11 |
| 45.6 | 49.9 | 47.8 | 55.4 | 59.5 | 0.96 | 1.11 |
| 46.8 | 50.6 | 50.0 | 53.5 | 61.7 | 0.99 | 1.06 |

Finally, Uribe and Winter (1969) performed tests on pin-ended chord sections, but this report was not included as it was outside the scope of this investigation.

#### 2.1.1.1 Summary

To summarize, it was determined in the first paper (Chajes et al., 1963) that for a uniformly stretched strip there is an increase in yield strength in compression and tension for most materials. However, the increase was not the same in all directions. For example, a tensile coupon had a yield strength increase of 90% in tension and half in compression after 10% of cold stretching. This was attributed to the Bauschinger effect. It was further determined this increase in yield strength is due to strain hardening and aging of the material. There was also a modest increase in ultimate tensile stress, up to 10%, but this was strictly attributed to material aging. It was found highly cold worked materials lose the well-defined yield plateau. However, the sharp plateau of the stress-strain curve can be recovered after the aging of the material for most sections if the cold stretching was below 10% of permanent elongation. Elongation also tended to decrease as the amount of cold stretching increased. For 10% of permanent elongation the decrease was up to 35%. The reduced killed steel was an exception for most properties. It already exhibited gradual yielding before cold stretching and this did not change with aging. Its elongation decreased significantly less than all other steels and its yield strength in compression did not increase. The proportional limit also decreased in longitudinal compression and transverse tension.

In the second paper (Karren, 1967), an equation to account for the increased yield strength in the corners from the virgin strength of the coil and the interior radius over thickness ratio was determined. This was achieved by expressing the strain hardening function as a power function and determining its factors experimentally from the true stress-strain curve of the material in logarithmic form. Two models were proposed. The first model assumed uniform curvature and tangential strain. The proposed equation is compared to strain measurements obtained by the Photogrid method and it was concluded it is necessary to include radial pressure. The final equation was virtually the same equation as seen in the S136-16 standard. This section also included experimental tests on corner coupons. It was determined compressive strengths were 5 to 15% higher in compression than in tension for aging materials. It was established the increase in yield strength is significantly higher as the *a/t* (interior radius over thickness) ratio decreases. It was again confirmed the ultimate tensile stress increases significantly less than the yield strength.

In the third paper (Karren & Winter, 1967), an equation to determine the increase in yield strength for the full section based on tensile results of the flat coupons was established. The equation is a

weighted average of the flat coupon yield strength and the corner yield strength which was obtained with the previously proposed equation. The authors determined the corner yield strength can be up to 100% higher than the virgin material and the elongation can decrease from 20 to 90%. Ultimate tensile stress increased up to 47% compared to the virgin material. Corners did not regain their sharp yield plateau as flat coupons did. Roll-formed sections exhibited significantly higher increases in yield strength compared to press-braked sections. The increase in yield strength ranged from 17 to 50% for these sections. It was found the decrease in elongation of the full section wasn't nearly as pronounced as the coupons. Finally, it was concluded the equation to account for the yield increase in the full section was in good agreement with experimental results.

The last paper (Uribe and Winter, 1969) was omitted from this review as it was outside the scope of this investigation.

## 2.2 Residual stress model, yield strength gradient and multiple column strength concept

This section of this chapter concentrates on residual stress and column strength models for cold-formed sections. Research from four different papers is included. The groundwork for today's column strength curves was established in the first paper by Bjorhovde and Tall (1971), however, no cold-formed sections were included. Kamani (1974) further studied seamless cold-formed sections and proposed a yield strength and longitudinal residual stress gradient. Davison (1977) performed a comprehensive investigation on the residual stress distributions of cold-formed HSS members based on previous research conducted in the late 1960s and early 1970s and proposed a model to account for this parameter in numerical analysis. Bjorhovde (1977) added the properties of several additional regular cold-formed sections in the fourth paper. Davison and Birkemoe (1983) summerized Davison's (1977) findings and added new information in the last investigation. All five investigations propose column strength curves. The titles of the papers are summerized below:

- *Maximum Column Strength and the Multiple Column Curve Concept* (Bjorhovde & Tall, 1971).
- *Stub Column Data and the Prediction of Compression Behaviour of Hollow Structural Sections* (Kamani, 1974).
- *A Theoretical Investigation of the Column Behaviour of Hollow Structural Steel Sections* (Davison, 1977).
- *Strength and Behaviour of Cold-formed HSS Columns* (Bjorhovde, 1977).
- *Column Behavior of Cold-formed Hollow Structural Steel Shapes* (Davison & Birkemoe, 1983).

The first report being looked at is titled "*Maximum Column Strength and the Multiple Column Curve Concept*" (Bjorhovde & Tall, 1971) which was part of a project named "*Residual Stresses in Thick Welded Plates*" (Bjorhovde et al., 1972). The purpose of this investigation was to develop a set of curves to predict the strength of columns. At the time, only one curve was available for all sections. It is pointed out, it is inaccurate to use one curve to portray all sections due to their inherently different properties. This point is supported in Figure 2-10 which shows the curves of 69 different sections with various properties and materials.

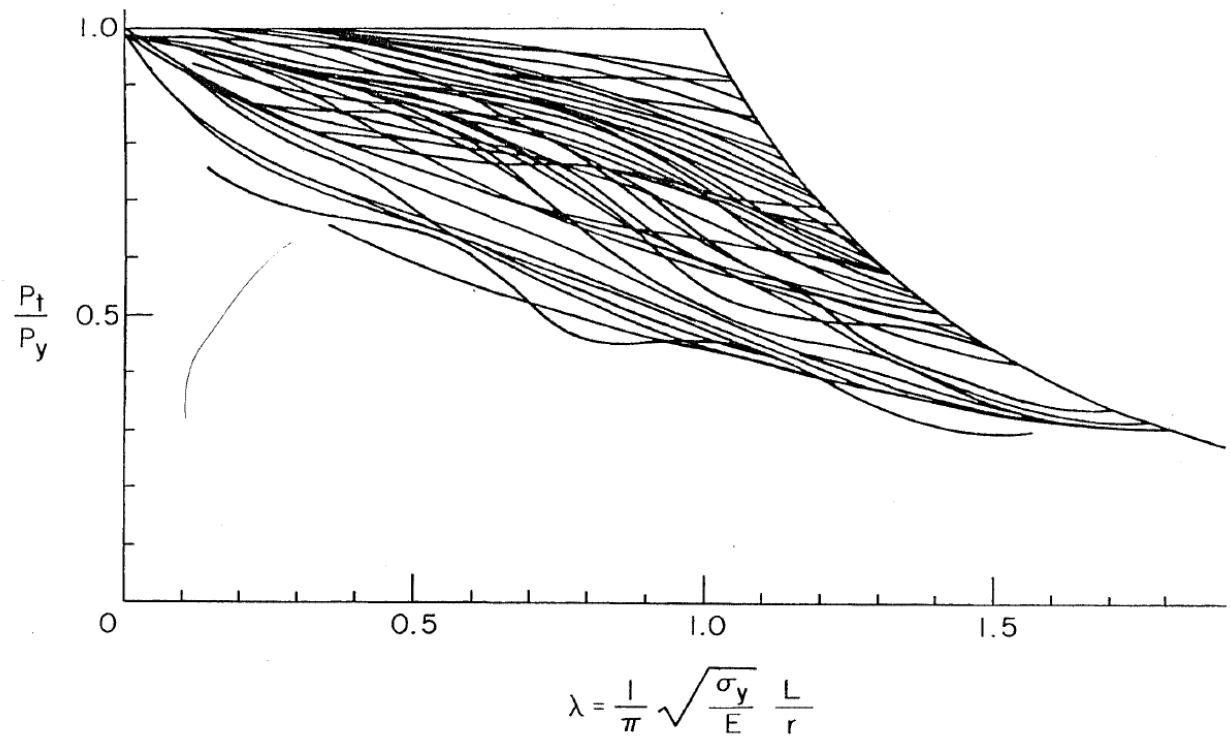


Figure 2-10: The assembly of 69 tangent modulus column curves (Bjorhovde & Tall, 1971)

This figure was obtained from a previous investigation in which different curves were constructed using the tangent modulus theory. As Bjorhovde and Tall (1971) point out, a major shortcoming of this theory is that it cannot account for out-of-straightness. To overcome this weakness, the authors performed a similar investigation using the maximum strength theory. Figure 2-11 shows the difference between both theories.

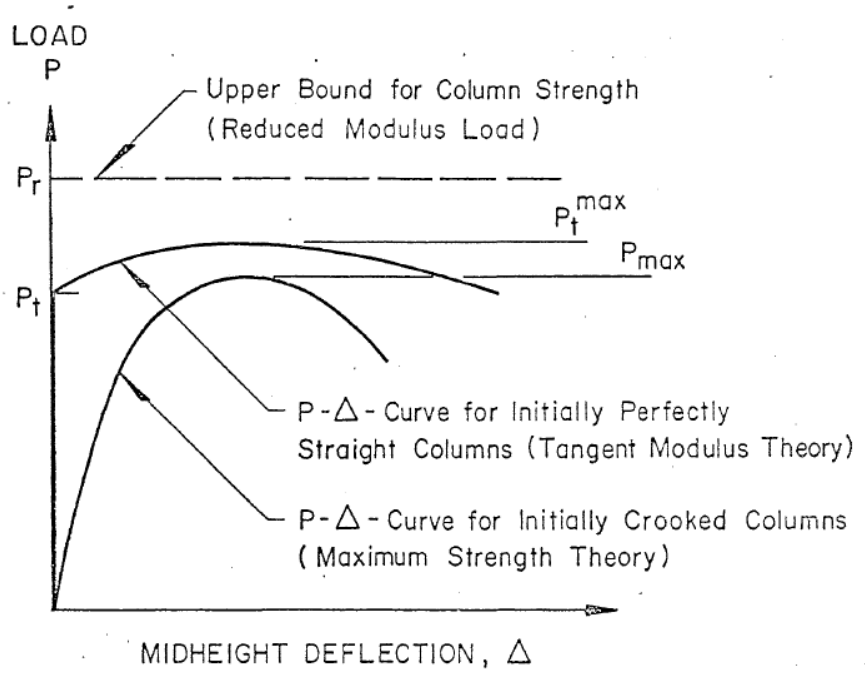


Figure 2-11: Schematic illustration of the various inelastic column strength concepts (Bjorhovde & Tall, 1971)

To construct the new curves using the maximum strength theory, Bjorhovde and Tall (1971) used a fiber based numerical computer program which was available at the time named MAXLD2. This program was specifically developed for this investigation. The yield strength, the manufacturing method, the size of the shape, the cross section of the column, the bending axis and the out-of-straightness parameters were taken into account. Only W type roll-formed columns, H type columns and welded-box columns of various steel grades and sizes were analyzed. Experimental values such as the yield strength and residual stress were included in the numerical model. Bjorhovde and Tall (1971) made several assumptions to simplify the numerical model such as an idealized linearly elastic-plastic stress-strain relationship in all fibers, a sin-wave deflection after loading, plane sections, uniform residual stresses, elastically unloading yielded fibers, a yield strength gradient and stresses at the mid-height of the column. For further details on the numerical model Bjorhovde and Tall's investigation can be consulted. Figure 2-12 provides the results of the numerical model. Since there were too many curves, Bjorhovde and Tall only included the upper and lower bands.

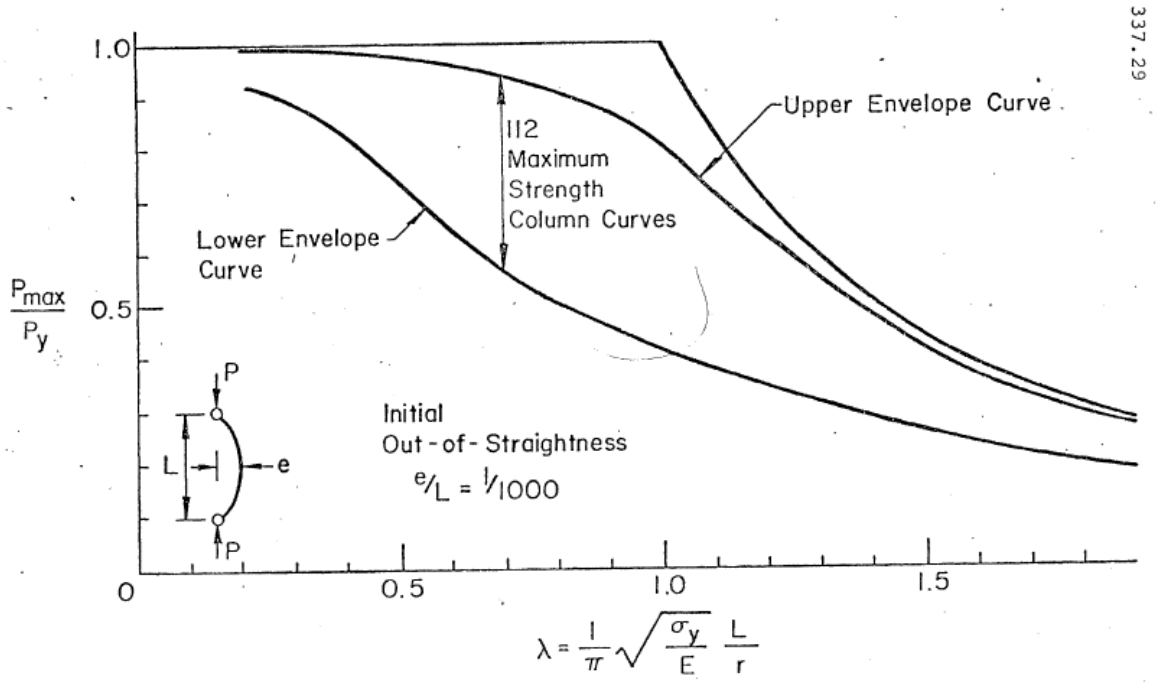


Figure 2-12: The band of all 112 maximum strength column curves (Bjorhovde & Tall, 1971)

Based on these results, Bjorhovde and Tall (1971) studied several new curve possibilities to represent all available sections the best they could. It was finally decided to include three curves. This number was chosen to have enough variety, but not to overwhelm the user. The first group, as described by Bjorhovde and Tall, would mostly englobe high strength steels, hybrid H-shapes with A514 flanges and stress-relieved sections of all steel grades. These sections would be mostly located on the upper side of the band. The second group would represent the central band and would be the most diverse, while the third group would be the least diverse and mostly represent heavy rolled, heavy welded and light welded wide-flange universal mill shapes. Figure 2-13 and Table 2-3 to Table 2-5 present the obtained curves along with the proposed groups.

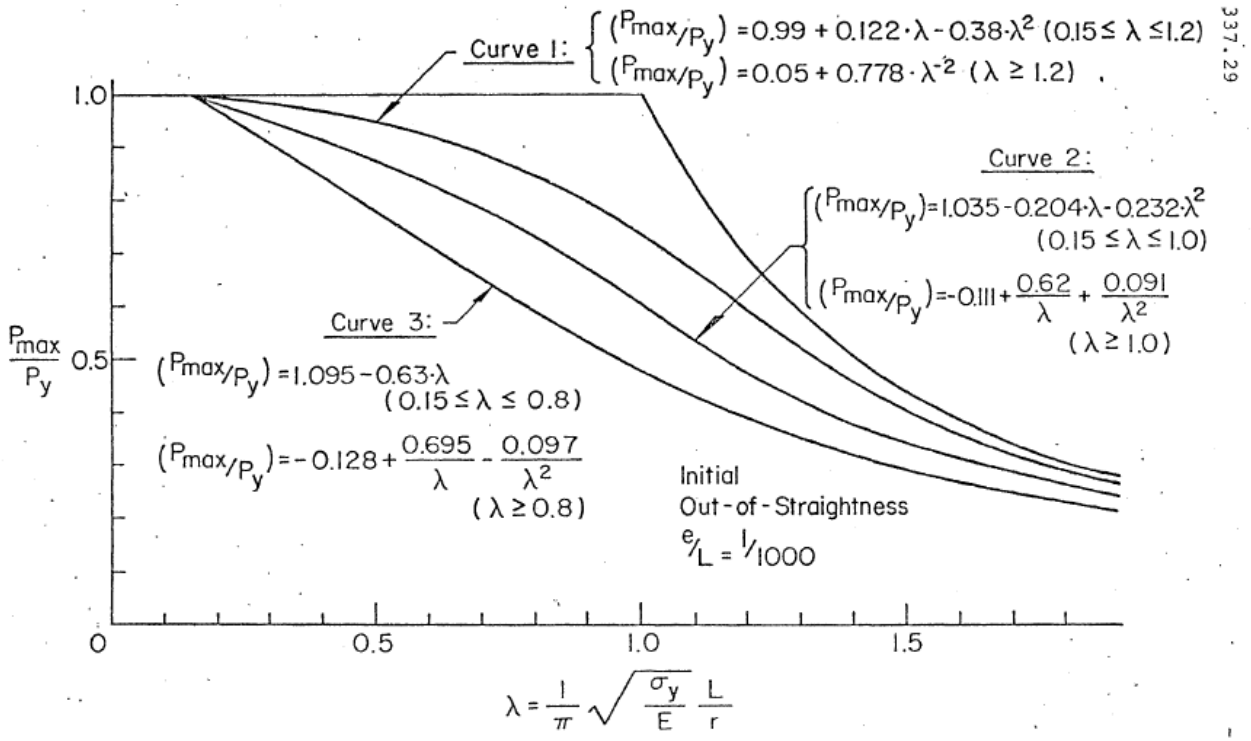


Figure 2-13: Proposed maximum strength columns and group descriptions – Column curves (Bjorhovde & Tall, 1971)

Table 2-3: Proposed maximum strength columns and group descriptions – Sections belonging to group 1 (Bjorhovde & Tall, 1971)

COLUMN TYPES BELONGING TO COLUMN STRENGTH CATEGORY 1
(MAXIMUM STRENGTH STUDY)
(Notation as in Tables 1 through 4)

| Material+ | Manufacturing Method | Shape* | Light or Heavy | Axes |
|---|---|---|---|---|
| A242 | R1 | W | L | S |
| A514 | R1 | W | LH | SW |
| A514 | We/FC | H | L | S |
| A514 | We/UM | H | L | S |
| A514 | We | B | L | SW |
| Hybrid: | | | | |
| F1 A514 &Web A441 | We/FC | H | L | SW |
| F1 A514 &Web A36 | We/FC | H | L | SW |
| All stress-relieved columns (regardless of steel grade, manufacturing method, shape, size, and axes). | | | | |

* B = Box-shape.

\+ Included among the A514-steels are the special extra-high strength steels, such as USS 5Ni-Cr-Mo-V ($\sigma_y$ = 130 ksi).

Table 2-4: Proposed maximum strength columns and group descriptions – Sections belonging to group 2 (Bjorhovde & Tall, 1971)

COLUMN TYPES BELONGING TO COLUMN STRENGTH CATEGORY 2
(MAXIMUM STRENGTH STUDY)
(Notation as in Tables 1 through 4, and 14)

| Material | Manufacturing Method | Shape | Light or Heavy | Axes |
|---|---|---|---|---|
| A7/A36 | Rl | W | L | S |
| A7/A36 | We/FC | H | LH | SW |
| A7/A36 | We | B | LH | SW |
| A242 | Rl | W | L | W |
| A572(50) | We/FC | H | LH | SW |
| A441 | We/FC | H | H | SW |
| A441 | We/UM | H | H | SW |
| A514 | We/FC | H | L | W |
| A514 | We/UM | H | L | W |
| Hybrid: | | | | |
| Fl A441 &Web A36 | We/FC | H | L | SW |
| Fl A441 &Web A36 | We/UM | H | L | SW |

Table 2-5: Proposed maximum strength columns and group descriptions – Sections belonging to group 3 (Bjorhovde & Tall, 1971)

COLUMN TYPES BELONGING TO COLUMN STRENGTH CATEGORY 3
(MAXIMUM STRENGTH STUDY)
(Notation as in Tables 1 through 4, and 14 and 15)

| Material | Manufacturing Method | Shape | Light or Heavy | Axes |
|---|---|---|---|---|
| A7/A36 | Rl | W | H | SW |
| A7/A36 | We/UM | H | LH | SW |

This investigation (Bjorhovde & Tall, 1971) represents the groundwork for today's column curves. As it was seen from the types of columns included in the groups, cold-formed HSS sections were not included in this investigation.

To fill this gap, significant experimental research was performed in the 1970s on cold-formed HSS members. One such example is a paper titled "*Stub Column Data and the Prediction of Compression Behaviour of Hollow Structural Sections*" (Kamani, 1974). The goal of this investigation was to undertake an experimental study in cold-formed hollow sections to determine their stub-column strength, yield strength and residual stress distribution in order to propose a

column curve for these sections. The studied columns in this investigation were seamless, therefore they don't fully represent the roll-formed columns studied in this thesis. However, some interesting results were obtained, therefore they were shortly summarized below.

The experimental part of the investigation performed by Kamani (1974) consisted in testing a 4 x 4 x 3/8" section. Figure 2-14 presents the coupon distribution for the tensile tests and residual stress measurements. Stub column results, residual stress measurements and yield strength coupon results are shown in Figure 2-15, Figure 2-16 and Figure 2-17.

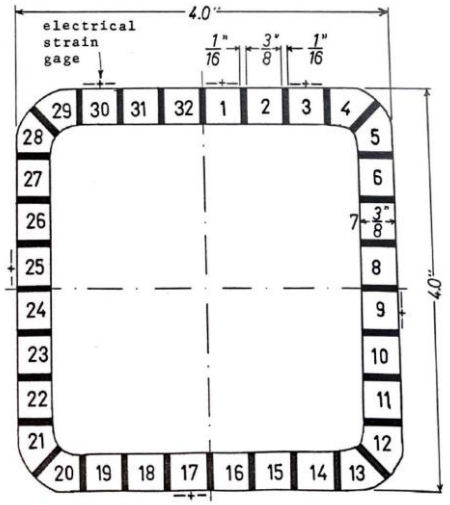


Figure 2-14: Coupon distribution for residual stress measurements and tensile tests (Kamani, 1974)

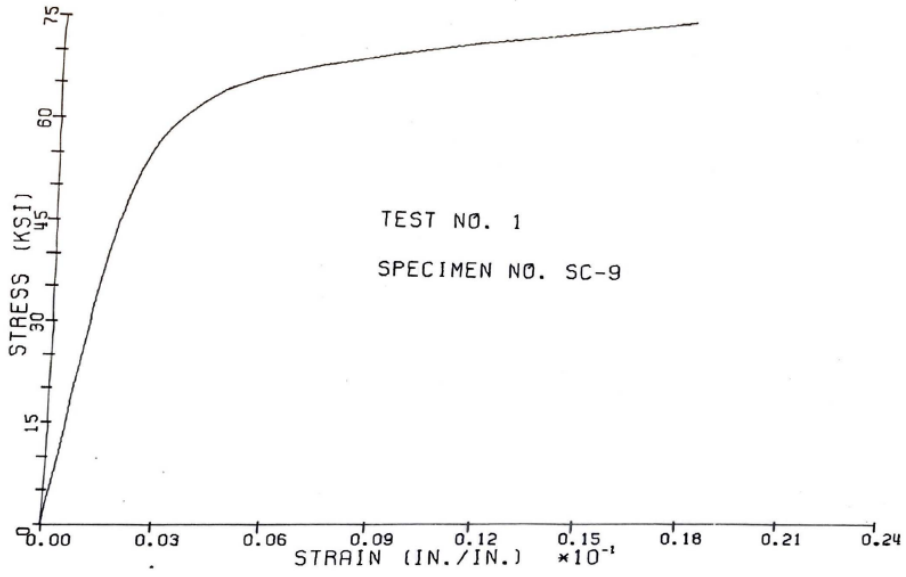


Figure 2-15: Stub-column stress strain curve (Kamani, 1974)

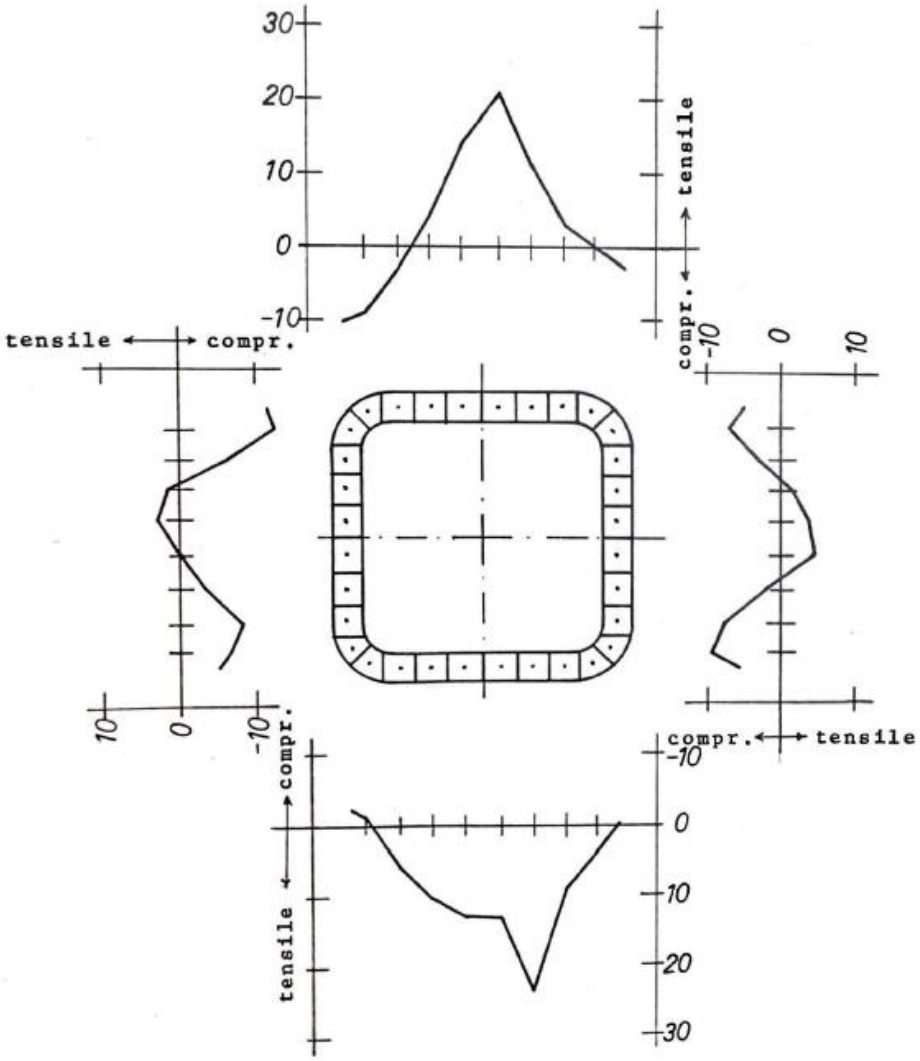


Figure 2-16: Longitudinal residual stress distribution across the section (Kamani, 1974)

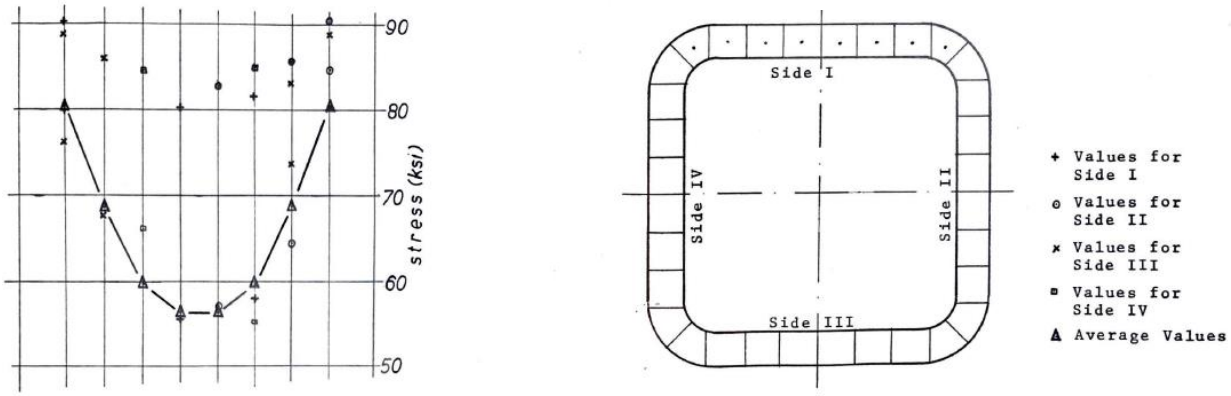


Figure 2-17: Stub column, residual stress, and tensile coupon measurements (Kamani, 1974)

After determining the experimental properties for the section, Kamani (1974) included these results in the analytical model. Material properties were included through two different methods and two different models were studied. The first column curve was plotted using the average stub-column data and the second one was plotted using residual stress and coupon data. The two analytical models that were studied were the tangent modulus model and the maximum strength model.

As explained by Kamani (1974), the first method that was analyzed was the tangent modulus model. This method to determine the column curve consists in evaluating the tangent modulus at various stress levels from the stub-column results. This is later related to the slenderness at that position. To determine the tangent modulus Kamani used three different methods: differentiation formulas by parabolic interpolation, approximating the Ramberg-Osgood equation and the least-squares curve-fitting approximation. The results from the three methods are shown in Figure 2-18.

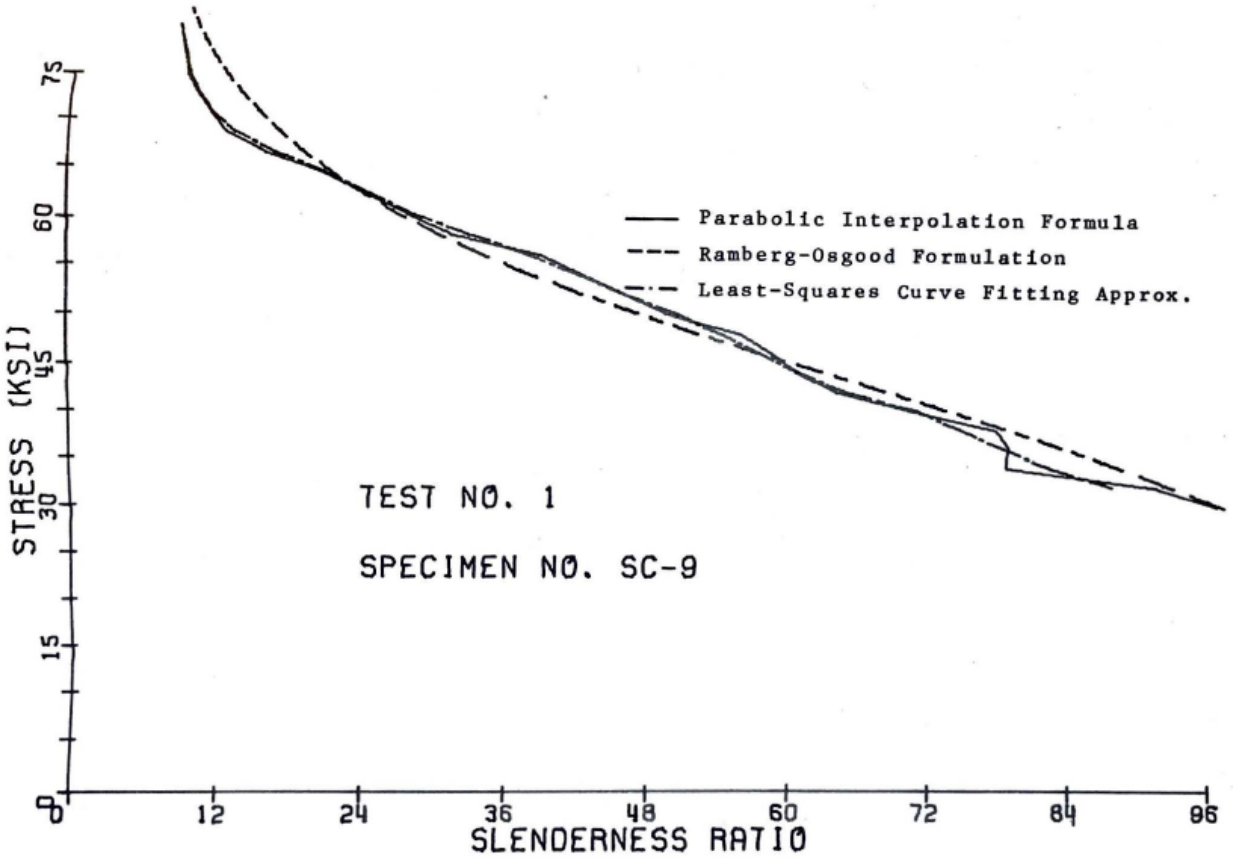


Figure 2-18: Comparison of column curves obtained from various approximate methods (Kamani, 1974)

For the second method Kamani considered three scenarios. The first scenario had a residual stress pattern and a “flat-top” yielding steel. The second scenario had variable yield strength across the section but no residual stress. The third scenario has a residual stress pattern and a yield strength distribution. A computer program based on a fiber discretization model was specifically written by Kamani to apply the residual stress and yield strength patterns. The following steps were applied by Kamani for the computation of the model: (1) the model was discretized into fiber areas, (2) residual stresses were included by applying an initial strain, (3) the moment of inertia was reduced after each increment which was used to recalculate the slenderness. For further details of Kamani’s numerical model his thesis can be consulted (Kamani, 1974).

To include the yield strength, Kamani (1974) used four different Ramberg-Osgood parameters to account for the difference in non-linear behaviour from the flats and the corners. The parameters and the obtained curves are presented in Figure 2-19. A parametric study was also performed to evaluate the impact of the residual stress. A curve was obtained with zero residual stress and one where residual stress was included. The final results for the column strength model are shown in Figure 2-20. In Figure 2-21 the column strength model is compared with the tangent modulus model. The final part of the investigation was to determine which longitudinal residual stress profile would best represent actual results. Figure 2-22 presents these results.

Table 2-6: Ramberg-Osgood approximation parameters (Kamani, 1974)

| COUPON NO. ON SIDE I | $\sigma_{0.2}$ | $\sigma_{0.1}$* | n | B | E |
|---|---|---|---|---|---|
| 1,32 | 56.48 | 53.2 | 11.586 | 96.57 | 30,500 |
| 2,31 | 59.86 | 57.0 | 14.158 | 92.85 | 30,500 |
| 3,30 | 68.75 | 66.3 | 19.102 | 95.18 | 30,500 |
| 4,29 | 80.47 | 78.6 | 29.480 | 99.35 | 30,500 |
| | (KSI) | (KSI) | | | (KSI) |

*Interpolated values

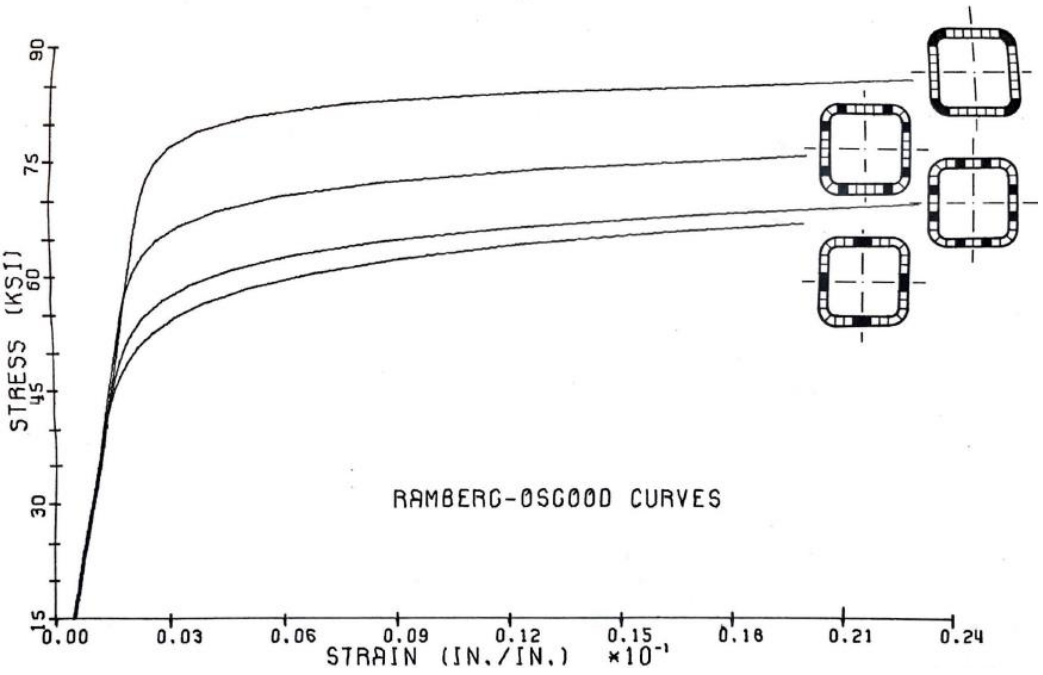


Figure 2-19: Ramberg-Osgood approximation curves for the averaged stress-strain values (Kamani, 1974)

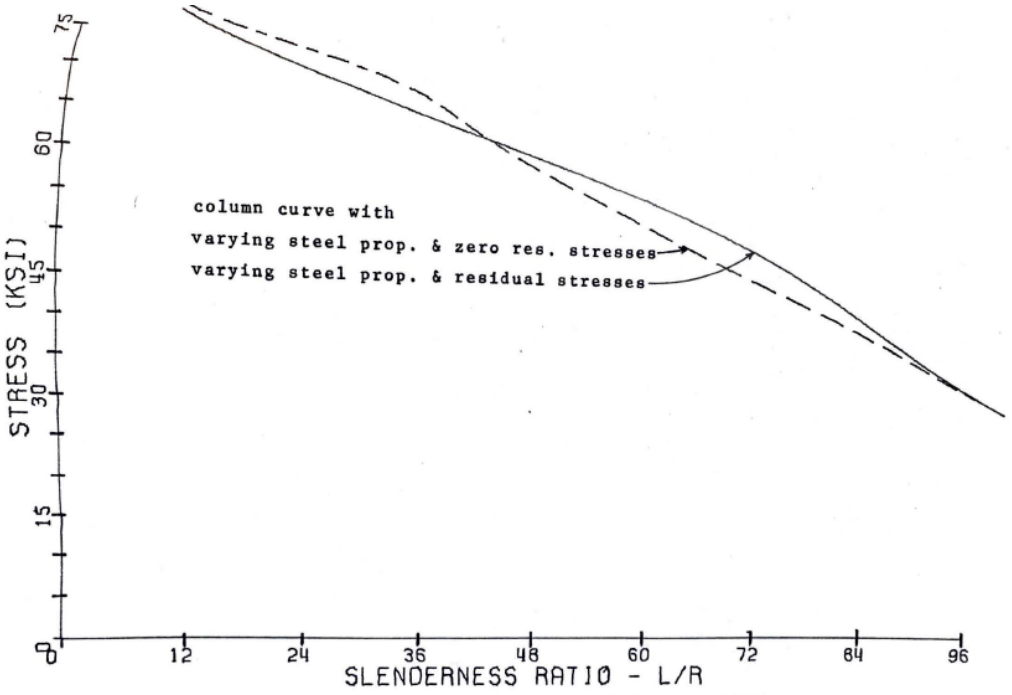


Figure 2-20: Maximum strength model with and without residual stress (Kamani, 1974)

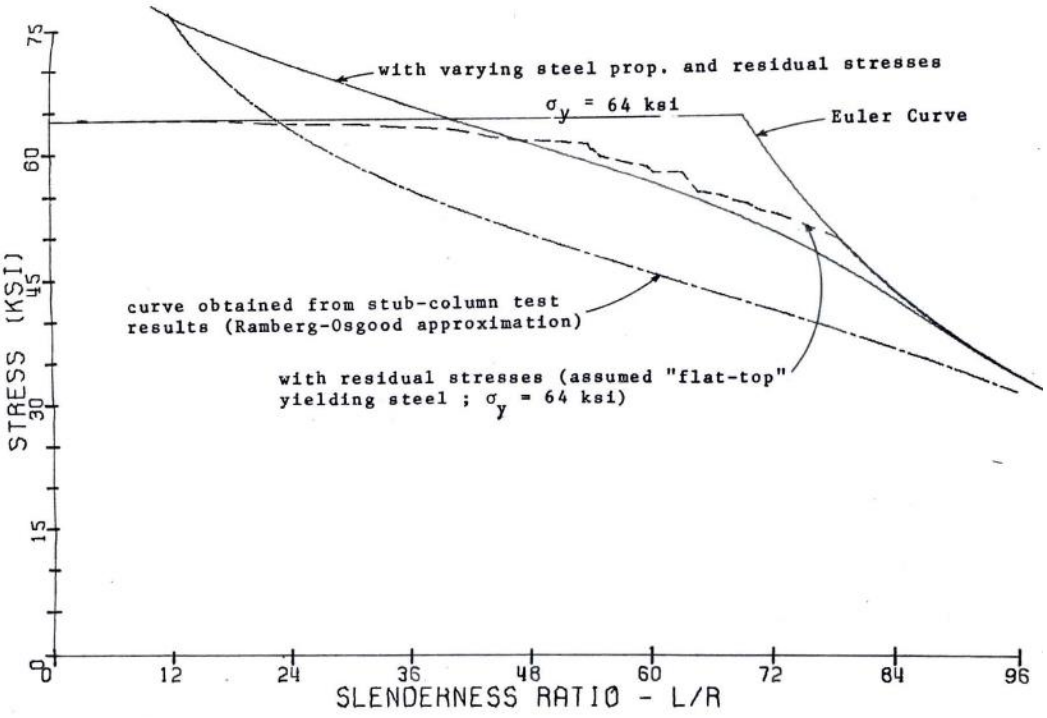


Figure 2-21: Comparison between the case with and without residual stress and comparison between different model types (Kamani, 1974)

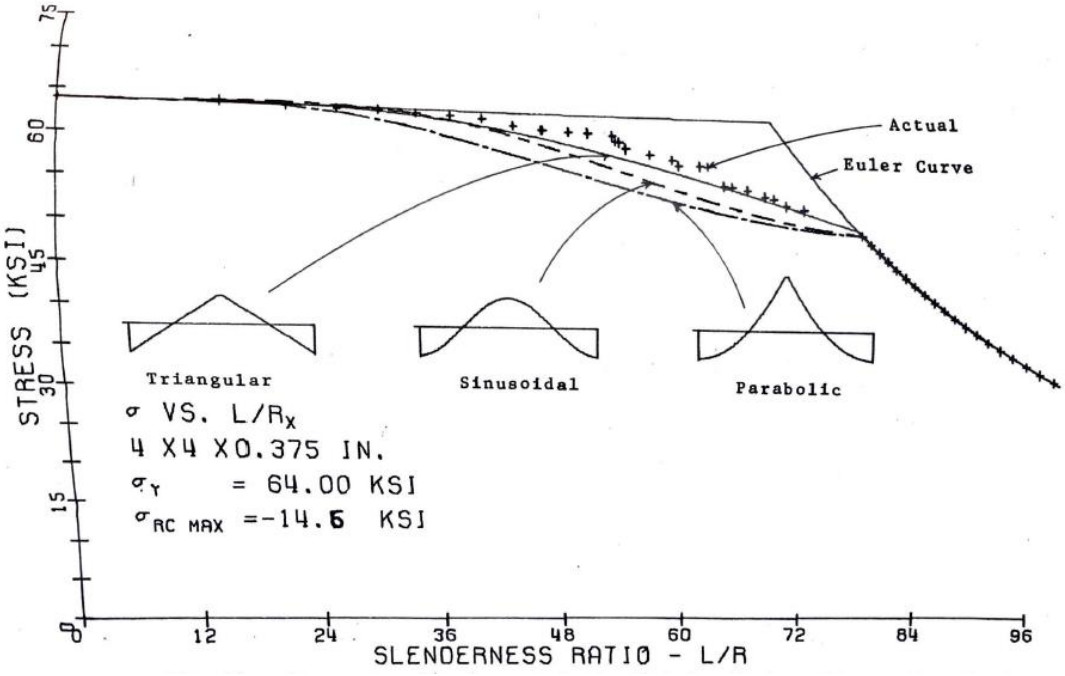


Figure 2-22: Proposed residual stress distribution vs actual residual stress (Kamani, 1974)

Kamani (1974) concluded the Ramberg-Osgood curve drawn from stub column results with the tangent modulus model is very conservative and the material properties of the section significantly affect the behaviour. Therefore, it is important to include actual material properties. The triangular longitudinal residual stress distribution is seen as the most efficient to represent the actual behaviour.

The next paper being reviewed is titled "*A Theoretical Investigation of the Column Behaviour of Hollow Structural Steel Sections*" (Davison, 1977). This investigation summarized and consolidated residual stress models for cold-formed HSS sections proposed by various researchers from the late 1960s to the mid 1970s and a final model was proposed by Davison. The model was later verified by Key (1990) and no significant adjustments were made. The goal of Davison's thesis was to perform an experimental investigation of several types of cold-formed sections and to propose a theoretical model to include the residual stress distribution in numerical models. The experimental investigation concentrated on heat-treated columns, but models were developed for all types of cold-formed sections. It was found in Davison's investigation the general residual stress profile was similar for all studied cold-formed sections. The parameter which would vary in the numerical model would be the magnitude of the residual stress.

The first section of Davison's thesis (1977) consisted in determining experimentally material variations in several cold-formed HSS members. From this information, analytical residual stress and yield strength gradient models were proposed. The models were than compared with experimental values and the best model was used for numerical simulations. These properties were then input into a tangent-modulus column strength model to investigate the effects of each of the studied parameters. This was further repeated in a maximum strength theory which included initial out-of-straightness. Finally, Davison generated column curves from the tangent-modulus and maximum strength analytical models and compared them to experimental results.

The foundation of Davison's investigation (1977) was based on Ringle's research in 1969 where regular cold-formed sections were analyzed. Ringle's paper was titled "*Effects of cold roll-forming on the mechanical properties of square welded steel tubes*" (Ringle, 1969). It was not possible to find it, but Davison included a summary in his literature review. Ringle studied the strain history of cold-formed sections undergoing roll forming. Davison summarized the strain history obtained by Ringle it in Table 2-7.

Table 2-7: Strain history during cold-forming process (Davison, 1977)

| Fibre | Forming Operation | Strain |
|---|---|---|
| Outside | (1) Bending | Tension $+\varepsilon_{B_1}$ |
| | (2) Pressure + Welding | Compression $-\varepsilon_m$ |
| | (3) Reverse bending | Compression $-\varepsilon_{B_2}$ |
| Mid-plane | (1) Bending | None |
| | (2) Pressure + Welding | Compression $-\varepsilon_m$ |
| | (3) Reverse bending | None |
| Inside | (1) Bending | Compression $-\varepsilon_{B_1}$ |
| | (2) Pressure + welding | Compression $-\varepsilon_m$ |
| | (3) Reverse bending | Tension $+\varepsilon_{B_2}$ |

Ringle (1969) was also the first to propose the bending (through thickness) and membrane (perimeter) component for cold-formed members in the transverse direction. While the direction normal to the longitudinal axis (transverse) was identified as having the primary strains, it was also found these strains cause deformation in the longitudinal direction. To understand the nature of bending residual stress, Davison (1977) provided Figure 2-23 where the stress-strain diagram is shown in terms of moment and curvature for a section undergoing uniform bending in the transverse direction (perpendicular to the axial direction of the profile).

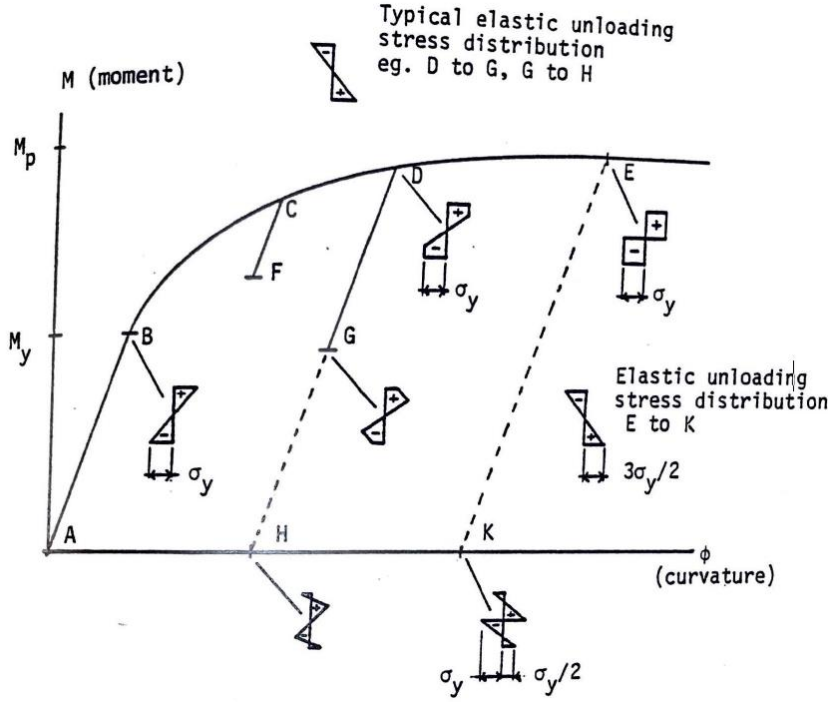


Figure 2-23: Nature of bending residual stresses (Davison, 1977)

It is explained in Davison's investigation (1977) that for a single unstressed plain bar the moment-curvature relationship can be represented by the ABCDE curve where the element is fully restrained. If the element is partially released, its residual stress distribution will be as shown next to point G. For a fully released element, it's residual stress distribution will be as shown next to point H and K. By knowing the elastic unloading distribution, which can be easily measured from the rotation of the released coupon and adding the remaining residual stress of the fully released coupon, the state of residual stress within the member can be determined. Therefore, the distribution next to E can be determined by adding the distribution next to K to the elastic unloading distribution between E and K.

Since the geometric form of the final through thickness residual stress would be difficult to determine as it is dependant on the number and type of plastic deformations it experiences, Davison analyzed simpler geometric distributions which could be implemented into the model. Davison looked at previously defined profiles by Kato and Aoki (1978) and Giaux (1972) which he considers to strongly resemble to the profile seen at G. In Figure 2-24, the profiles proposed by Kato and Aoki (1978), and Giaux (1972) are shown as well as two profiles proposed by Davison (1977). The final chosen profile for the through thickness residual stress is the trapezoid. Davison considers it to be a closer representation of the actual state of residual stress within the member compared to the triangle. It is also pointed out the exterior face is always in tension while the interior face is in compression.

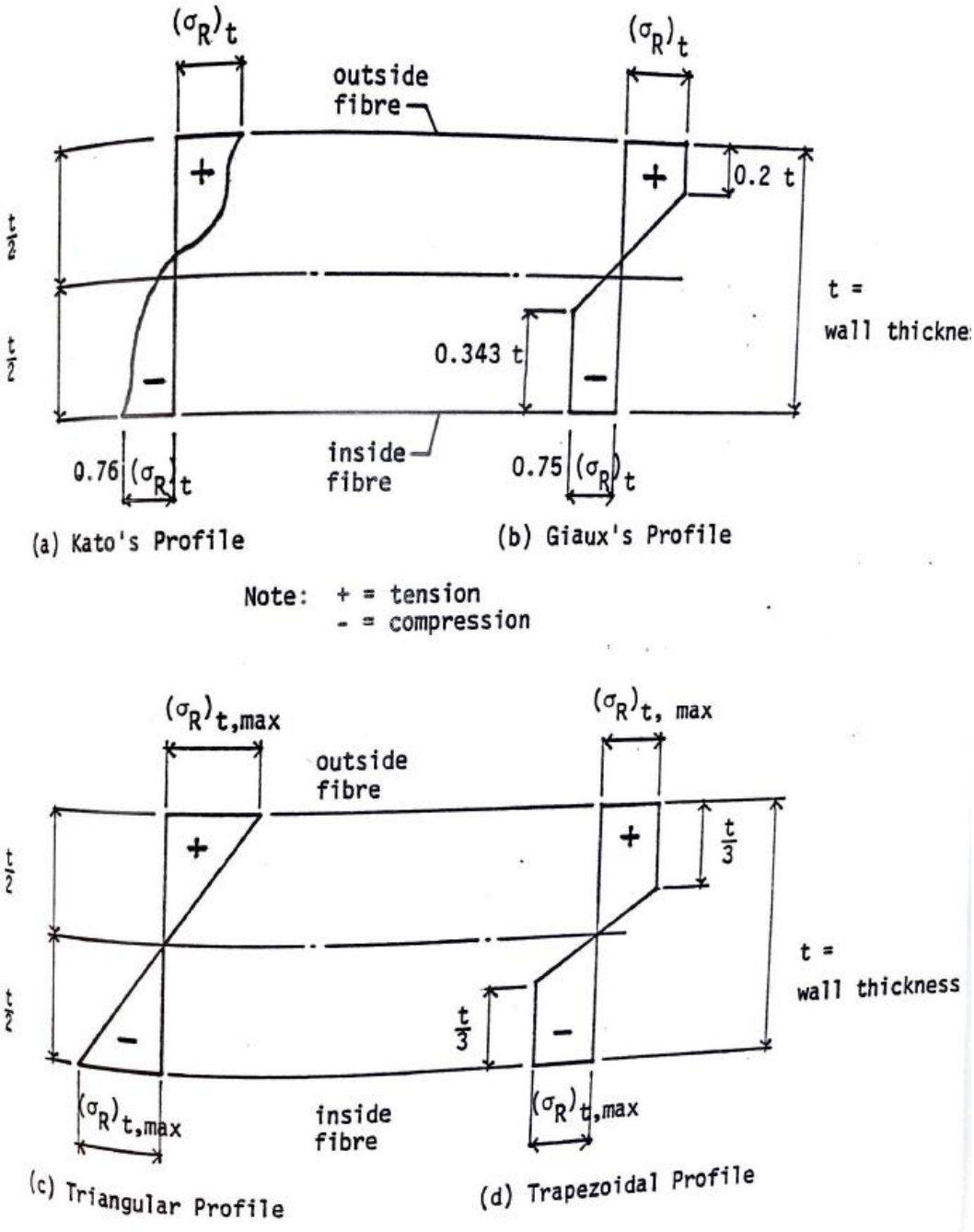


Figure 2-24: (a) Kato and Aoki (1978) and (b) Giaux (1972) through thickness residual stress profiles and (c) & (d) Davison's proposed profiles (Davison, 1977)

After the residual stress pattern was assigned, Davison (1977) proceeded to determine the magnitudes to be applied on this gradient. Table 2-8 presents residual stress measurements obtained from various researchers at the time including Davison himself.

Table 2-8: Maximum longitudinal through thickness residual stress magnitudes (Davison, 1977)

| REF. NO. | TUBE SIZE (inches) | TUBE* TYPE | w/t | COUPON YIELD $\sigma_y$ (ksi) | MAXIMUM RESIDUAL STRESS† $(\sigma_R)_{t,max}/\sigma_y$ | |
|---|---|---|---|---|---|---|
| | | | | | Triangular | Trapezoidal |
| 20 | 4 x 2 x 0.187 | CF | 17.4 | 65.0 | 0.690 | 0.479 |
| 21 | 4 x 4 x 0.375 | CFS | 6.7 | 56.2 | 0.446 | 0.309 |
| 22 | 4 x 4 x 0.375 | HF | 6.7 | 35.7 | 0.056 | 0.039 |
| | 5 x 3 x 0.375 | HF | 9.3 | 36.1 | 0.053 | 0.037 |
| | 5 x 5 x 0.437 | CF | 7.4 | 67.9 | 0.413 | 0.286 |
| | 6 x 4 x 0.437 | CF | 9.7 | 66.7 | 0.535 | 0.370 |
| | 8 x 8 x 0.500 | CF, HCW | 12.0 | 58.2 | 0.460 | 0.318 |
| | 8 x 8 x 0.500 | CF, LCW | 12.0 | 62.5 | 0.433 | 0.299 |
| 1 | 8 x 8 x 0.375 | CF, HT | 17.3 | 64.2 | 0.531 | 0.359 |
| | 8 x 8 x 0.450 | CF, HT | 13.8 | 54.6 | 0.529 | 0.366 |
| | 12 x 12 x 0.375 | CF, HT | 28.0 | 62.5 | 0.544 | 0.376 |

ymbols:
CF - cold formed, seamed
CFS - cold formed, seamless
HF - hot formed
HCW - heavy cold work
LCW - light cold work
HT - heat treated

e:
Values of $(\sigma_R)_t/\sigma_y$ for tubes from Refs. [1,20,21] are based on coupon curvature measurements; values from Ref. [22] are based on surface strains accurate to ± 10%.

To complete the full residual stress profile, it was necessary to determine the perimeter residual stress distribution since the in-situ residual stress is the sum of both the perimeter and through thickness distributions. Only one coupon located at the center of the section was measured in this paper. However, previous measurements from earlier research were included. Davison (1977) based his distribution on these previous measurements. Figure 2-25 presents a few perimeter residual stress patterns proposed by past research (Kamani, 1974; Sherman, 1969 and Schuster, 1975).

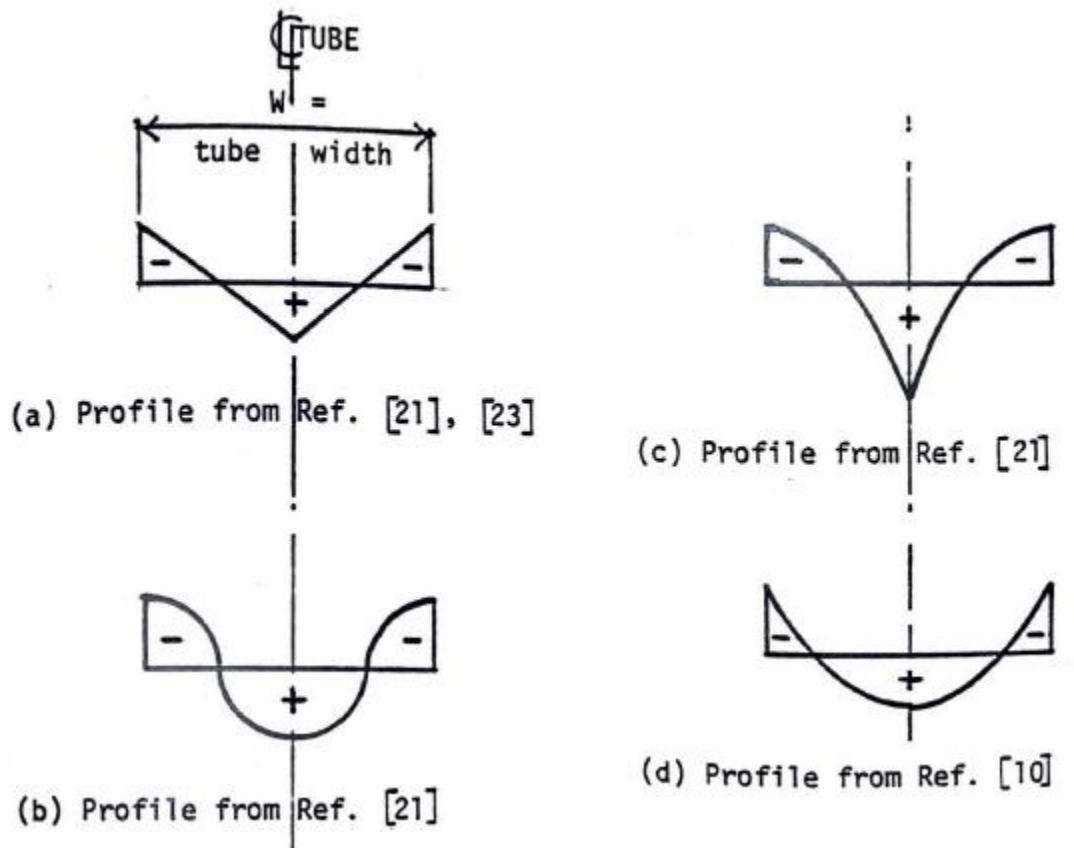


Figure 2-25: Possible perimeter residual stress patterns (Davison, 1977)

Davison (1977) points out research performed by Kamani (1974) which identified that the shape is not as important as the magnitude of the perimeter residual stress. It is finally concluded the triangular shape (a in Figure 2-25) would provide the most accurate model. The magnitude of the longitudinal perimeter residual stresses is provided in Table 2-9 and Table 2-10. The final residual stress model for heat treated cold-formed sections is provided in Figure 2-26. The total in-situ (in place) residual stress for the coupon is the sum of the perimeter residual stress and the through thickness residual stress.

Table 2-9: Measurements for longitudinal perimeter residual stress (Davison, 1977)

| REF. NO. | TUBE SIZE (inches) | TUBE* TYPE | w/t | YIELD† $\sigma_y$ (ksi) | MAXIMUM RESIDUAL STRESS $(\sigma_R)_{p,max}/\sigma_y$** | | | |
|---|---|---|---|---|---|---|---|---|
| | | | | | CORNER | | CENTRE LINE | |
| | | | | | PROFILE(1) | PROFILE(2) | PROFILE(1) | PROFILE(2) |
| 20 | 4 x 2 x 0.187 | CF | 17.4 | 65.0 | | -0.308 | | +0.308 |
| 21 | 4 x 4 x 0.375 | CFS | 6.7 | 63.8 | | -0.229 | | +0.229 |
| 22 | 4 x 4 x 0.375 | HF | 6.7 | 35.7 | +0.056 | +0.097 | -0.364 | -0.097 |
| | 5 x 3 x 0.375 | HF | 9.3 | 36.1 | +0.0 | | -0.278 | |
| | 5 x 5 x 0.437 | CF | 7.4 | 67.9 | -0.245 | | +0.294 | |
| | 6 x 4 x 0.437 | CF | 9.7 | 66.7 | -0.195 | | +0.330 | |
| | 8 x 8 x 0.500 | CF, HCW | 12.0 | 58.2 | -0.206 | | +0.378 | |
| | 8 x 8 x 0.500 | CF, LCW | 12.0 | 62.5 | -0.288 | -0.361 | +0.485 | +0.361 |

*Symbols:
CF - cold formed, seamed
CFS - cold formed, seamless
HF - hot formed
HCW - heavy cold work
LCW - light cold work

†Note:
$\sigma_y$ based on tensile coupon yield for Ref. [22]; based on stub column yield for Refs. [20,21].

**Note:
Values listed under profile(2) Ref. [22] considered to be representative for hot and cold formed tube types.

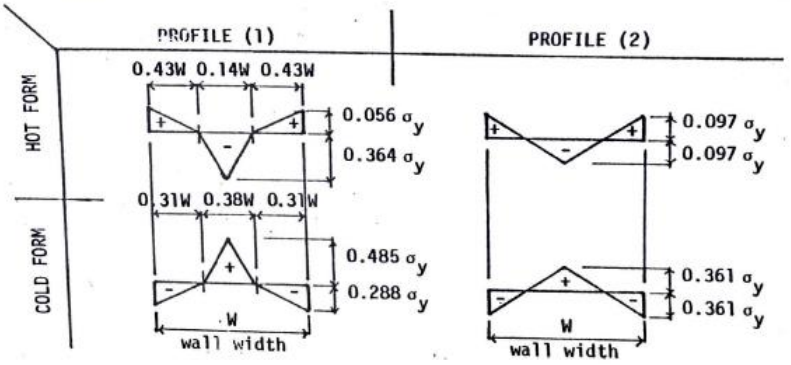


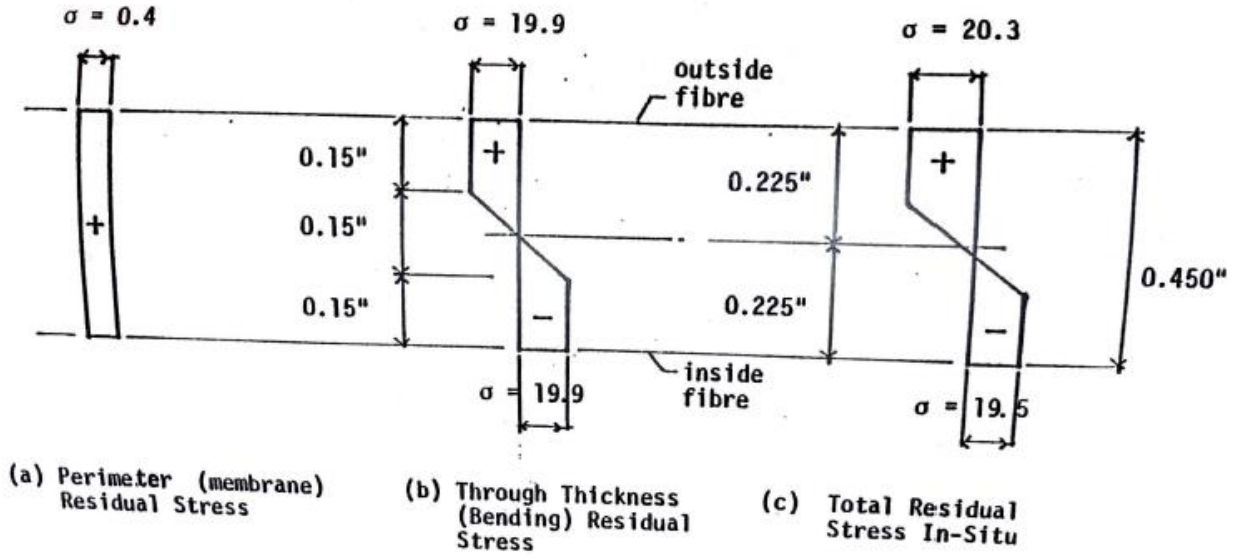


Figure 2-26: In-situ residual stress after sum of perimeter and through thickness (Davison, 1977)

Table 2-10: Final proposed residual stress distribution (Davison, 1977)

| TUBE TYPE | YIELD STRENGTH* CHARACTER | MAXIMUM PERIMETER† (MEMBRANE) RESIDUAL STRESS $(\sigma_R)_{p,max}/\sigma_y$ | | MAXIMUM THROUGH THICKNESS†† (BENDING) RESIDUAL STRESS $(\sigma_R)_{t,max}/\sigma_y$ | |
|---|---|---|---|---|---|
| | | Corner | Centerline | Inside Face | Outside Face |
| Hot formed seamless as formed | Uniform or cross-section | +0.097 | -0.097 | -0.038 | +0.032 |
| Cold formed seamless as formed | Variable or cross-section | -0.229 | +0.229 | -0.309 | +0.309 |
| Cold formed seamed heat treated | - ditto - | -0.006 | +0.006 | -0.359<br>-0.366<br>-0.376 | +0.359<br>+0.366<br>+0.376 |
| Cold formed seamed as formed | - ditto - | -0.364 | +0.364 | -0.350 | +0.350 |

*Refer to Figs. 2.6 and 2.7 for typical cold formed variations.
†Based on Table 11, Fig. (a) below.
††Based on Table 10, Fig. (b) below.
$\sigma_y$ = average cross-sectional yield strength.

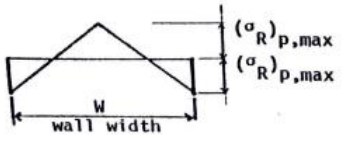


Fig. (a) Perimeter (Membrane) Residual Stress Profile

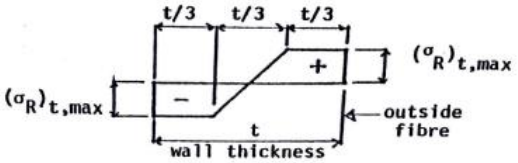


Fig. (b) Through Thickness (Bending) Residual Stress Profile

For coupon yield strength tests, Davison (1977) tested a HSS of 8 x 8 x 0.375, 8 x 8 x 0.450 and 12 x 12 x 0.375. Coupons were taken from various positions ranging from the centerline of the flat wall all the way to the corner to obtain a yield strength gradient. The tested coupons and the results for one section are presented in Figure 2-28.

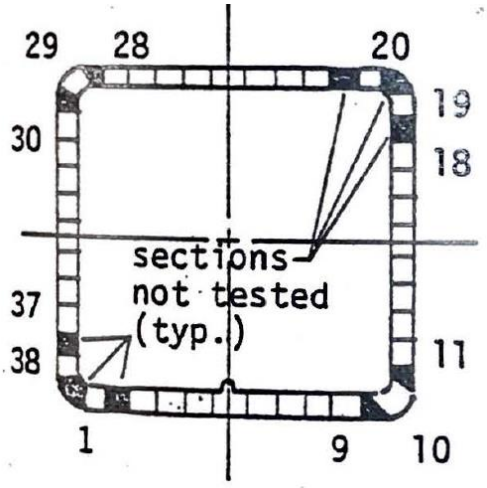


Figure 2-27: Sectioned profile with all tested coupons (Davison, 1977)

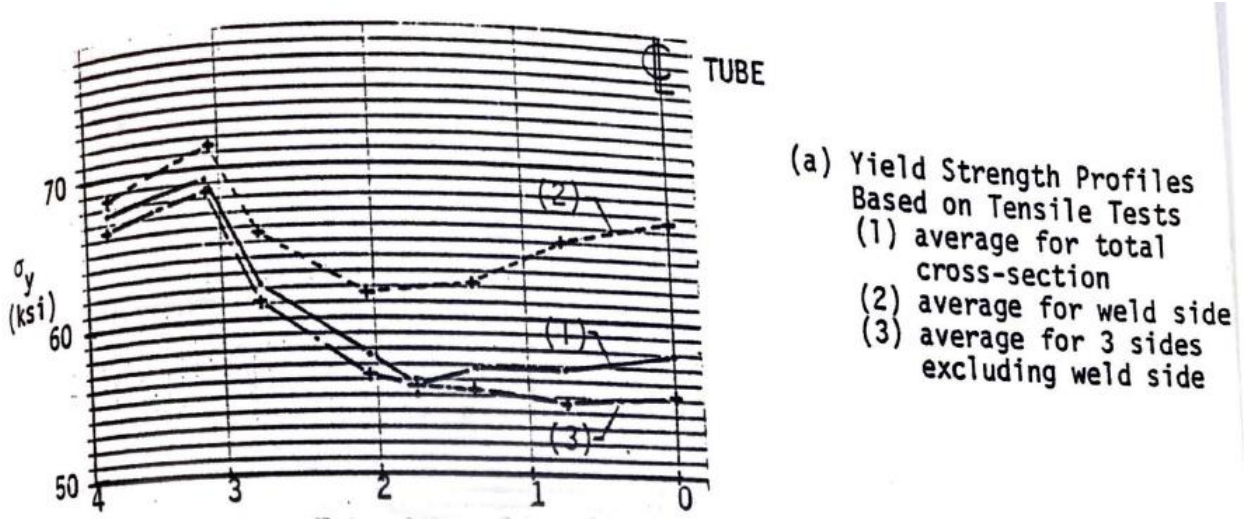


Figure 2-28: Yield strength distribution (Davison, 1977)

Davison further compared the results with predictions made by Karren (1967) and Lind and Shroff (1975). The equation which was used from Karren's formulation is the same as the one found in the S136-16 standard to account for increased yield strength in the corners. This comparison is presented in Figure 2-29.

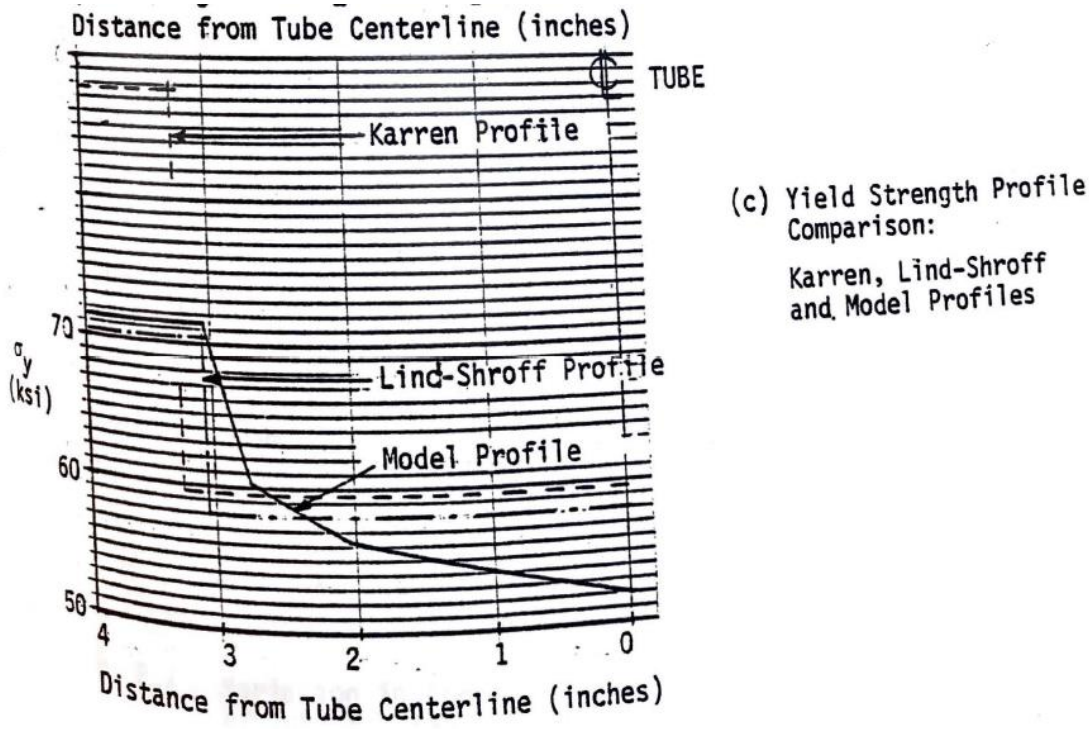


Figure 2-29: Comparison between yield strength prediction models and model profile based on actual results (Davison, 1977)

Davison (1977) notes Karren's profile (1967) overestimates the corner yield strength and Lind-Shroff's curve is more convenient for this section. It is also noted by Davison two yield strength gradients can be drawn from the results. For sections with a high w/t ratio, the yield strength of the flat is fairly constant up until the corner. For sections with a low w/t ratio, the yield strength gradient of the flat section gradually increases towards the yield strength of the corners as shown in Figure 2-28. The yield strength and residual stress gradients applied to the model are finally presented in Figure 2-30. This model was used to analyze the effect of the yield strength, perimeter and through thickness residual stress. Some parameters were varied while others were held constant to determine their effects.

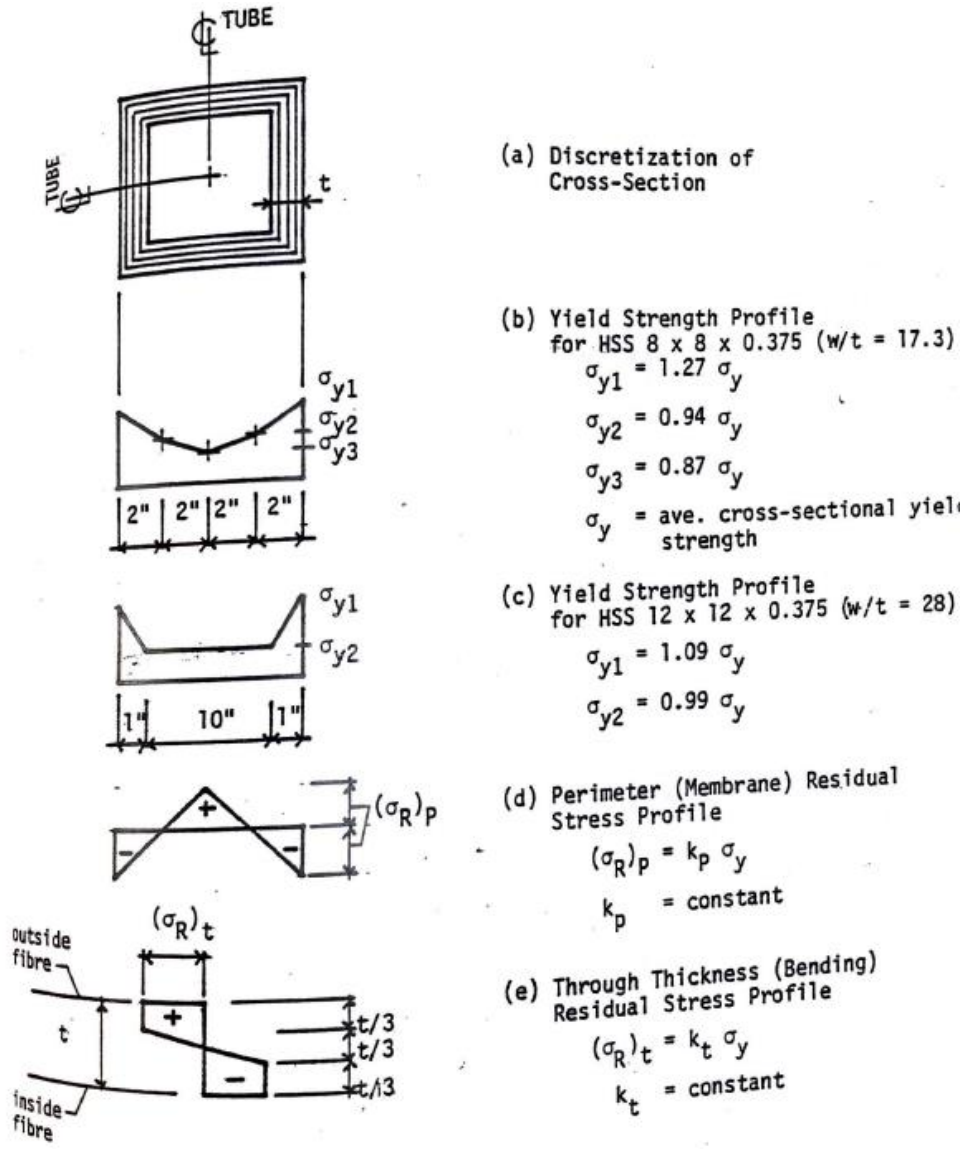


Figure 2-30: Tangent modulus model (Davison, 1977)

Davison (1977) concluded the perimeter residual stress decreases the column strength when the yield strength is kept the same for all the elements. In the case the yield strength has a gradient, the column strength decreases for some profiles and increases for others. This difference can be attributed to profiles with low w/t ratios (column strength increases) and high w/t ratios (column strength decreases). The through thickness residual stress decreased column strength for all cases. It is also noted the effects of all the parameters were greater for profiles with low w/t ratios.

The second part of Davison's thesis (1977) consisted in studying the column strength model. This was done to investigate the effects of an initial out-of-straightness on each of the previously defined parameters and to model the behaviour of full HSS columns. The column properties were previously discussed in a thesis published by Salvarinas (1977). Since this thesis (Salvarinas, 1977) was an experimental investigation on heat-treated members and the properties were summarized by Davison, it is not directly included in this review. The computer program (MAXLD) used by Davison was the same as the one used by Bjorhovde and Tall (1971) with similar assumptions to the ones previously described.

Three cases were studied for the maximum column strength model by Davison (1977). The first combination has a yield strength gradient but zero residual stresses. The through thickness residual stress was added to the second combination and the third combination had both the perimeter and through thickness residual stresses. Davison states it is important to study the effects of the perimeter residual stress as Sherman (1969) found it can decrease the column strength by up to 40%.

An experimental study was also conducted to determine the initial out-of-straightness of the specimens. A total of 20 HSS specimens were measured. It was determined long specimens had a single curvature over their whole length while short specimens exhibited a single curvature over part of their length. The final curvature considered in the model was half a sin wave up to the center of the specimen. The maximum mean out-of-straightness was found to be of 1/5400 for short specimens and 1/6200 for long specimens. Davison (1977) decided to include crookedness values of 1/1000, 1/2000, 1/4000 and 1/8000 in his model to study its effects.

The general parametric study was very similar to the tangent modulus model. Davison (1977) concluded the tangent modulus model represents an upper bound for the maximum strength model. The maximum strength model had virtually the same behaviour as the tangent modulus model for

large perimeter and though thickness residual stress gradients with an out-of-straightness of 1/8000. Initial crookedness decreases the effects of residual stress. Residual stresses decreased the column strength with its greatest impact on columns of intermediate length. If the perimeter and through thickness residual stresses are of the same intensity they cause similar decreases in column strength. The through thickness residual stress has a significantly greater impact on the column behaviour than the perimeter residual stress as the perimeter residual stress is close to zero in heat-treated sections.

The final section in Davison's thesis (1977) consisted in proposing an SSRC curve for heat-treated HSS members. Figure 2-31 provides the results obtained by Davison.

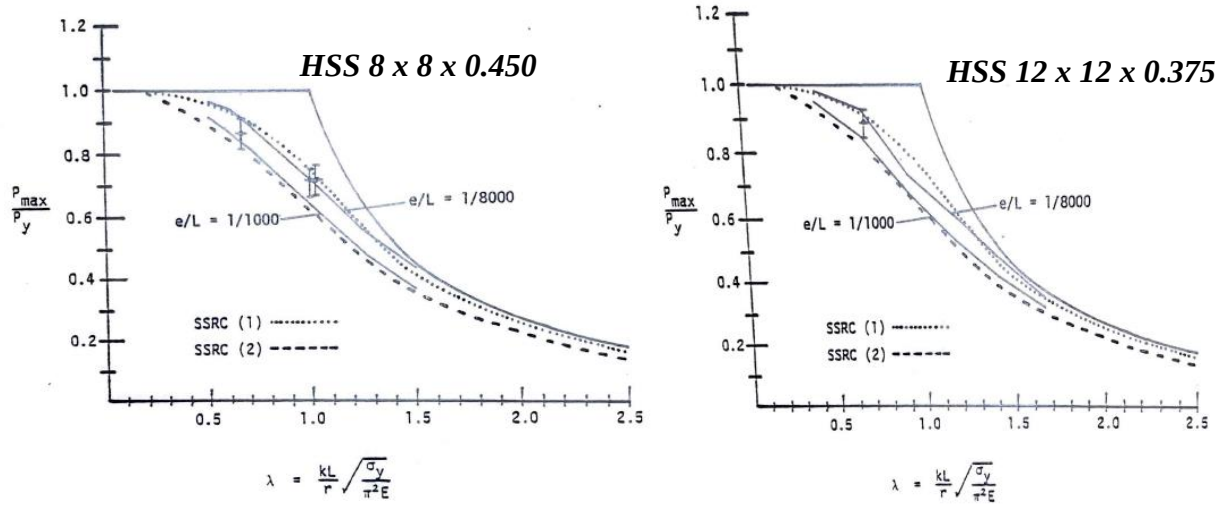


Figure 2-31: Comparison of heat treated HSS sections with SSRC curves (Davison, 1977)

Davison (1977) concluded the models fall between curve 1 and curve 2. If the out-of-straightness is closer to 1/1000 the model is very close to curve 1, but for more conservative out-of-straightness values the model is closer to curve 2. To propose a final curve, Davison compared the results to the curve bands as seen in Bjorhovde and Tall's (1971) investigation. It was determined the results fell on the upper band of curve 2 and closer to the center in curve 1. Curve 1 was finally proposed.

Bjorhovde (1977) completed previous investigations by adding regular cold-formed sections which had not been investigated since Ringle (1969) in a thesis titled "*Strength and Behaviour of Cold-formed HSS Columns*". This investigation was undertaken by Bjorhovde who also participated in the 1971 paper to propose the groundwork for current column curves. The goal of this investigation was to determine material properties of Canadian cold-formed structural tubes. The selected

profiles are shown in Table 2-11 and were chosen to cover the most used Canadian HSS sections of the time with the most varying properties.

Table 2-11: Tested sections (Bjorhovde, 1977)

| | |
|---|---|
| Test series A: | HSS 2x2x1/4 |
| Test series B: | HSS 4x4x1/4 |
| Test series C: | HSS 4x4x1/2 |
| Test series D: | HSS 6x6x1/4 |
| Test series E: | HSS 6x6x1/2 |
| Test series F: | HSS 8x8x1/4 |
| Test series G: | HSS 8x8x1/2 |

None of the sections in Table 2-11 were heat-relieved. One 8 x 8 x 1/4 heat relieved section was added to the list. All sections were CSA G40.21 grade 50W which was seen as the most commonly used grade at the time. Bjorhovde (1977) performed cross-sectional measurements, out-of-straightness measurements, tensile coupon tests on flat wall, weld and corner regions of the profile, stub column tests, and long column tests on pin-ended columns. Some flat coupon specimens were also taken close to the corner, but not at the corner itself. The tensile coupon specimen distribution is shown in Figure 2-32. Table 2-12 and Figure 2-33 provide tensile coupon and stub-column results. Full coupon results normalized with respect to the yield strength are presented in Chapter 3.

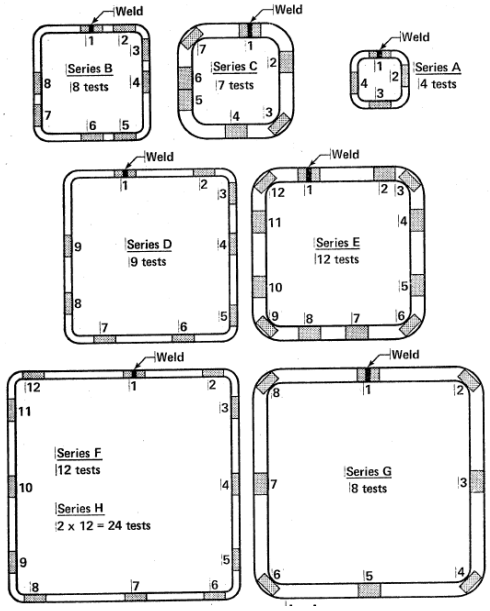


Figure 2-32: Tension coupon specimen locations (Bjorhovde, 1977)

Table 2-12: Tensile coupon measurements (Bjorhovde, 1977)

Comparison of Mechanical Properties for Test Shapes (1)

| Series HSS | | Yield Strength (ksi) | | | Tensile Strength (ksi) | | | Elongation in 2" (%) | | | Fracture (2) Toughness (Charpy) (ft-lb) |
|---|---|---|---|---|---|---|---|---|---|---|---|
| | | CSA Min. | Mill Test Cert. | Av. (3) of Tension Tests | CSA Min. | Mill Test Cert. | Av. (3) of Tension Tests | CSA Min | Mill Test Cert. | Average of Tests | |
| A | 2x2x1/4 | 50 | 67.8 | 67.7 | 65 | 79.0 | 69.9 | 22 | 22.0 | 15.5 | -(4) |
| B | 4x4x1/4 | 50 | 57.5 | 60.3 | 65 | 70.4 | 64.3 | 22 | 34.0 | 30.6 | 82 |
| C | 4x4x1/2 | 50 | 65.8 | 76.0 | 65 | 84.7 | 81.2 | 22 | 26.0 | 19.1 | 134 |
| D | 6x6x1/4 | 50 | 54.5 | 54.4 | 65 | 65.6 | 60.6 | 22 | 27.0 | 25.5 | -(4) |
| E | 6x6x1/2 | 50 | 60.9 | 68.8 | 65 | 74.7 | 73.6 | 22 | 28.0 | 25.3 | 136 |
| F | 8x8x1/4 | 50 | 56.3 | 58.5 | 65 | 71.8 | 69.1 | 22 | 39.0 | 28.1 | 61 |
| G | 8x8x1/2 | 50 | 67.9 | 62.9 | 65 | 78.3 | 71.0 | 22 | 35.0 | 28.6 | 206 |
| H (5) | 8x8x1/4 | 50 | -(4) | 63.7 | 65 | -(4) | 71.1 | 22 | -(4) | 30.0 | -(4) |

(1) For numbers and locations of tension test specimens in test shapes, see Figure 2.
(2) Fracture toughness values are not required for Grade 50W steels, but are shown here for information only. These data are mill test values, generally the average of 3 tests. Test temperater was -20°F (-29°C) in all cases.
(3) All test values for yield and tensile strength are based on zero strain rate, which is not used for standard mill tests.
(4) Data not available.
(5) Stress-relieved (annealed) sections.

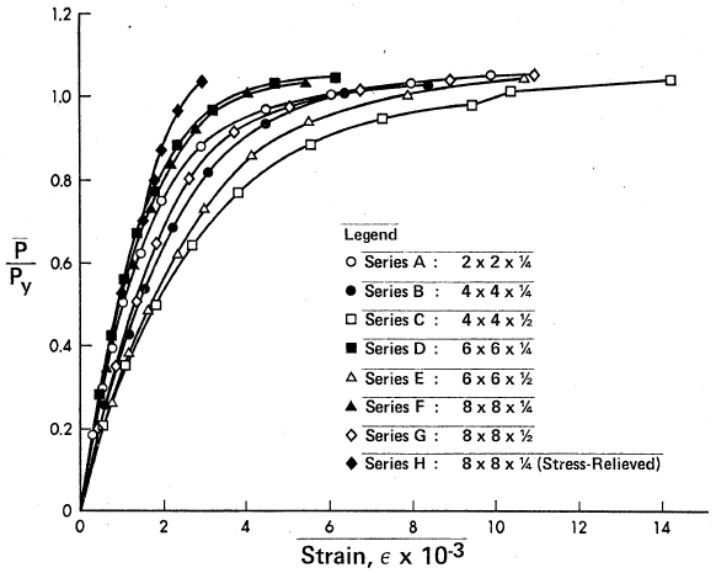


Figure 2-33: Stub column results (Bjorhovde, 1977)

Bjorhovde (1977) notes actual cross section measurements tend to be lower than the nominal values. The highest out-of-straightness was of 1/730, most specimens had an out-of-straightness ranging from 1/2000 to 1/5000 and many had an out-of-straightness of well below 1/10000. The mean was computed at 1/6384 and the maximum out-of-straightness was mostly found within the center quarter of the length of the specimen. The yield strength tended to be significantly higher than the specified nominal yield strength. For example, specimen C exhibited a yield strength more than 50% higher than the nominal value. The ultimate tensile stress was also higher than the nominal ultimate tensile stress except for specimen D. Bjorhovde (1977) also notes the significant differences between the mill tests and the laboratory tests and attributes this discrepancy to the strain rate. It is pointed out strain rate increases the yield strength. Laboratory tests were taken at static conditions with zero strain rate. The ductility requirements are mostly satisfied except for the A and C sections. Tension specimens in the welded areas exhibited significantly higher yield strengths. For some specimens, the weld strength was up to 10% higher than the flat coupon specimen but ductility was reduced up to 15.5%. The flat coupons at the center and those close to the corners show no significant differences for profiles B, D, F and H. However, the corner strength for profiles C and E was about 10% higher than the center flat. The corner elongation was however decreased up to 16%. The residual stress was determined from the proportional yield limit from the stub column tests. It was noted previous studies ranged longitudinal residual stresses in cold-formed members from 50 to 75%. Bjorhovde determined residual stresses for these sections ranged

from 58 to 80%. Figure 2-34 presents the residual stress measurements taken by Bjorhovde based on the first yield condition (proportional limit).

| | |
|---|---|
| A - HSS 2x2x1/4 : | $\sigma_{rc} = 0.42\ \sigma_y = 32.9$ ksi |
| B - HSS 4x4x1/4 : | $\sigma_{rc} = 0.26\ \sigma_y = 17.9$ ksi |
| C - HSS 4x4x1/2 : | $\sigma_{rc} = 0.34\ \sigma_y = 26.8$ ksi |
| D - HSS 6x6x1/4 : | $\sigma_{rc} = 0.20\ \sigma_y = 11.8$ ksi |
| E - HSS 6x6x1/2 : | $\sigma_{rc} = 0.36\ \sigma_y = 26.5$ ksi |
| F - HSS 8x8x1/4 : | $\sigma_{rc} = 0.30\ \sigma_y = 18.6$ ksi |
| G - HSS 8x8x1/2 : | $\sigma_{rc} = 0.38\ \sigma_y = 27.0$ ksi |
| H - HSS 8x8x1/4 : (stress-relieved) | $\sigma_{rc} = 0.11\ \sigma_y = 7.3$ ksi |

Figure 2-34: Residual stress measurements based on proportional limit (Bjorhovde, 1977)

It is indicated by Bjorhovde (1977) the smallest section exhibits the highest residual stress measurements. Several sections with the same thicknesses show very similar results and the stress relieved section shows very little residual stress. Stub column results tend to be higher than tensile yield strength coupons. Bjorhovde explains this by the fact that the coupon tests only represent a sample and the increased corner strength was not included in the average as much as it could have been. Finally, pin-ended column tests are shown in Figure 2-35.

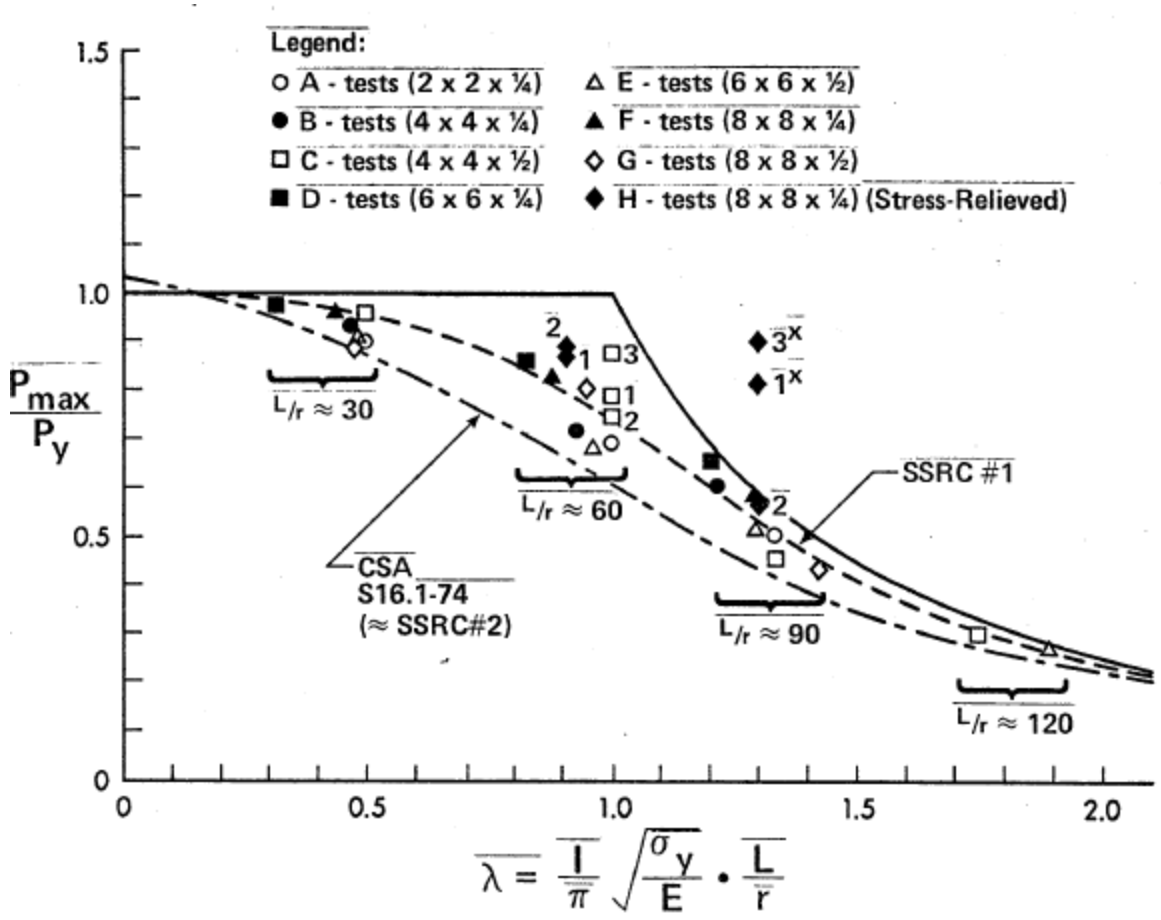


Figure 2-35: Pin-ended column results with respect to SSRC curves (Bjorhovde, 1977)

Bjorhovde (1977) finally states that the column strength data would indicate most of the tested sections would belong to the SSRC curve 1 and all results fall within the 95% confidence interval of this curve.

The fifth paper of these series is titled "*Column Behavior of Cold-formed Hollow Structural Steel Shapes"* (Davison & Birkemoe, 1983). This was an article that summarized all of the research performed in the 1970s and was based on Davison's thesis (1977). While most of the results were the same as the ones reported in the 1977 thesis, some new figures, data, distributions and conclusions were added. Several explanations were also developed and rephrased. In total, five different sections were included in this article along with their respective material properties: Cold-formed heat treated, non-heat treated, seamless non-heat treated, seamed partially heat treated, and seamed fully heat treated. A realistic column curve model was built which included the residual stress distribution and yield strength gradient.

To account for the cross-sectional yield strength distribution, Davison and Birkemoe (1983) proposed two models. An exponential distribution was applied to sections with low w/t ratios and a step-function for sections with high w/t ratios. These two models are justified with experimental data presented in Figure 2-36 and Figure 2-37. The dots in Figure 2-37 represent the coupon yield strength over stub column strength, 0.0 represents the center of the flat and 1.0 represents the center of the corner.

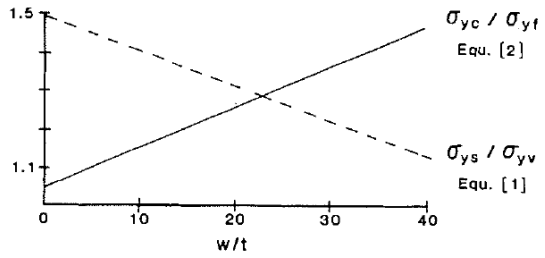


Figure 2-36: Corner and stub column strength over virgin coil strength (Davison & Birkemoe, 1983)

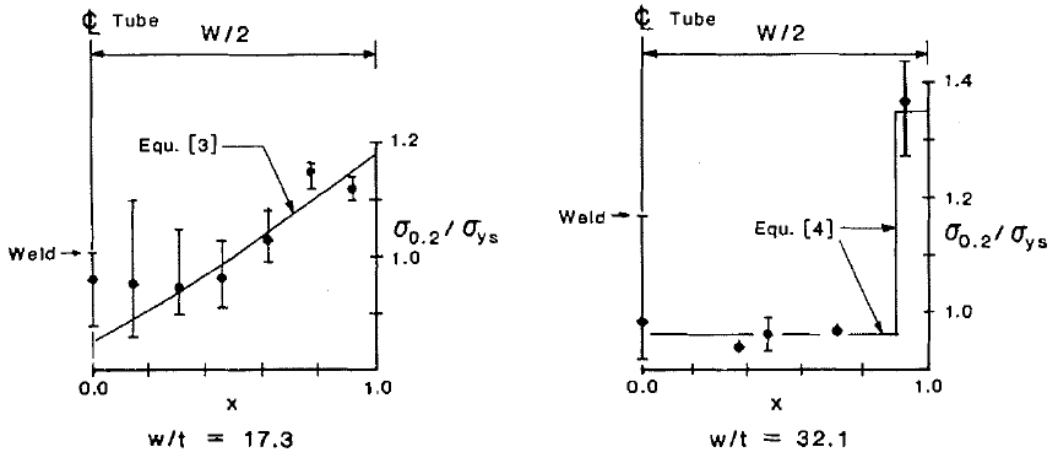


Figure 2-37: Yield strength gradient for two sections with different w/t ratios (Davison & Birkemoe, 1983)

Equation (2-13) is to be applied to sections with *w/t* ratios below 17.3 and (2-14) is to be applied on sections with a w/t above 32.1.

$$\frac{\sigma_{0.2}}{\sigma_{ys}} = 0.85e^{0.33x} \qquad (2\text{-}13)$$

$$\frac{\sigma_{0.2}}{\sigma_{ys}} = 0.96; \qquad x < 0.90 \tag{2-14}$$

$$\frac{\sigma_{0.2}}{\sigma_{ys}} = 1.36; \qquad 0.90 \leq x \leq 1.0$$

Davison and Birkemoe (1983) set up the equations so the average yield strength equals to 1.0 (average yield strength of the whole flat). It was also noted sections in between the *w/t* limits proposed by this equation show a hybrid behavior, however, Davison and Birkemoe made no attempt to model it through an equation.

Davison and Birkemoe (1983) observed a distinct difference between heat treated and non-heat-treated sections, the latter displaying a highly non-linear behavior. To account for this behavior, Ramberg-Osgood parameters were determined from tensile coupon tests. An example of a regular stress-strain curve for cold-formed sections is provided Figure 2-38.

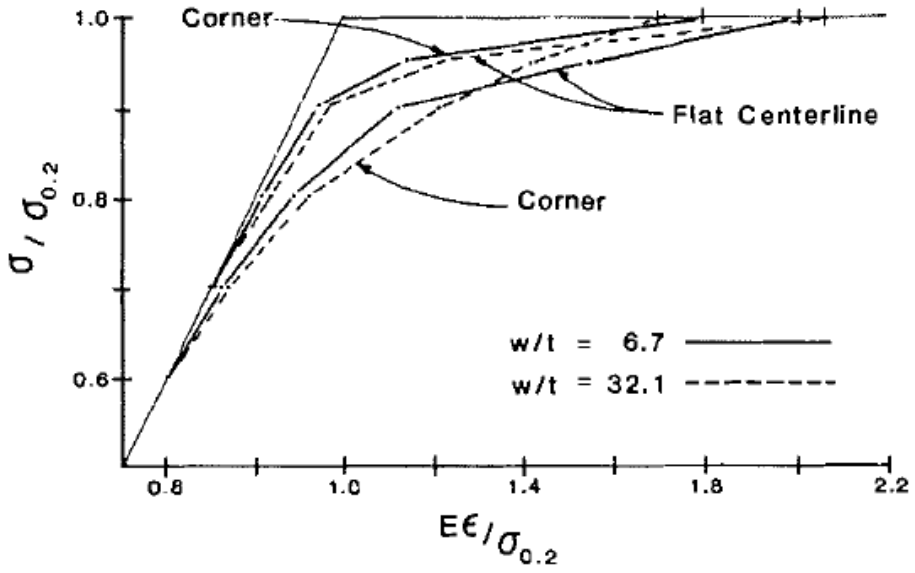


Figure 2-38: Variation in material stress-strain nonlinearity in non-heat treated regular CF (*w/t* = 32.1) and seamless CF (*w/t* = 6.7) tensile coupons (Davison & Birkemoe, 1983)

After establishing a model for the yield strength distribution, Davison and Birkemoe (1983) incorporated the residual stress gradient. Two types of residual stress gradients in the longitudinal direction (axial) were identified by the authors. One is called the perimeter (membrane) residual stress and it accounts for the variation in the residual stress across the section perimeter. The second

is called the through thickness residual stress and accounts for the variation through the section's thickness (bending). The perimeter residual stress will cause the released coupon to change in length while the bending residual stress will cause the coupon to exhibit curvature. Figure 2-39 illustrates both gradients. The actual residual stress in the tube in the longitudinal direction is the arithmetic sum of both the through thickness residual stress and the perimeter residual stress.

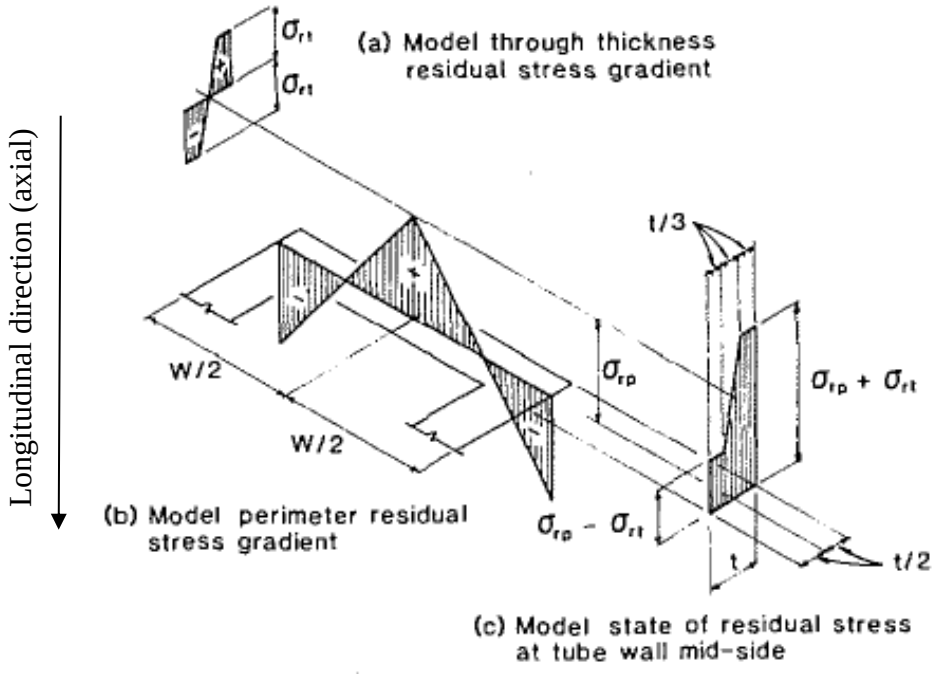


Figure 2-39: Residual stress on cross section (Davison & Birkemoe, 1983)

Davison and Birkemoe based the through thickness residual stress model distribution on a simplified version of a slightly different model proposed by Kamani (1974) and Schuster (1975). This model is justified by the notion that the section goes through several plastic bending deformations followed by an elastic rebound. Therefore, part of the section will have plastified while the rest is still in its elastic state. Davison and Birkemoe (1983) judged the model to be accurate enough to be an average representation of the actual behavior.

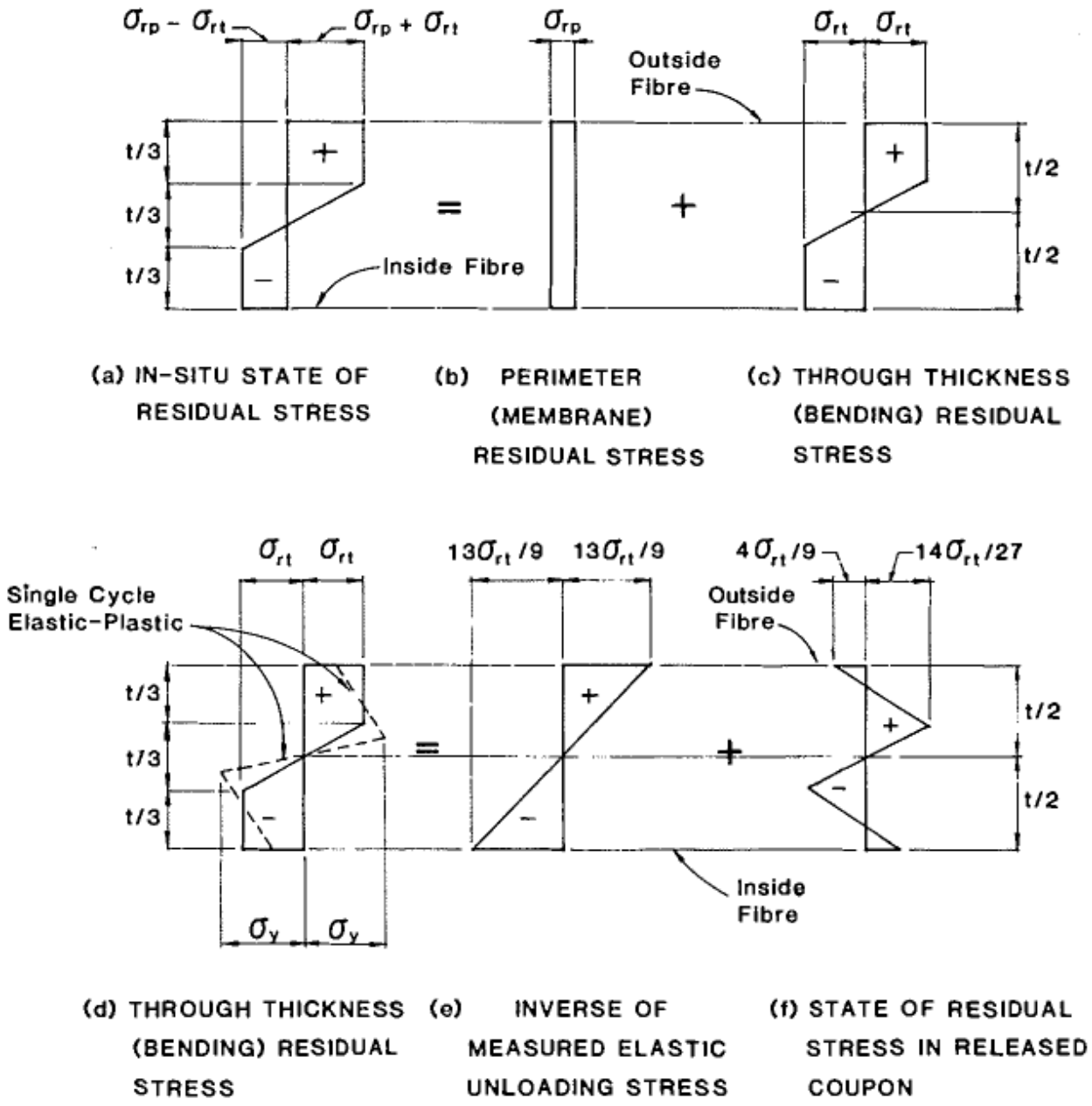


Figure 2-40: Model state of residual stress through the tube wall (Davison & Birkemoe, 1983)

Once a basic distribution model was established, Davison and Birkemoe (1983) proceeded to assign residual stress values. They note, it was not possible to directly measure the through thickness residual stress since not all of it is released from the coupon upon extraction. The remaining residual stress within the coupon is shown by Figure 2-40-f. As the coupon unloads elastically and changes in length, it releases the membrane stress shown in Figure 2-40-b. As it bends from the same elastic unloading stress, it releases the bending stress shown on Figure 2-40-e to reach the equilibrium

state shown by Figure 2-40-f. The maximum elastic unloading stress in Figure 2-40-e is determined through experimental data by strain-stress or curvature measurements. The through thickness residual stress within the member is the sum of Figure 2-40-e (elastic unloading stress) and Figure 2-40-f (residual stress remaining in the coupon after it's been released from all restraints). To determine the actual maximum through thickness residual stress, Davison and Birkemoe assume that the bending moment caused by Figure 2-40-e is equivalent in magnitude to the bending moment caused by Figure 2-40-d (their areas are the same). The relationship in equation (2-15) is obtained from this assumption where $\sigma_{EL}$ is the measured unloading stress and $\sigma_{rt,max}$ is maximum through thickness residual stress within the member.

$$\sigma_{rt,max} = 9\sigma_{EL}/13 \tag{2-15}$$

If the curvature was measured instead of the stress, Davison and Birkemoe propose the relationship in equation (2-16).

$$\sigma_{rt,max} \approx 36Et\delta/(13L^2) \tag{2-16}$$

For the perimeter residual stress distribution, Davison and Birkemoe (1983) adopted a linear profile across the section as shown by Figure 2-39-b. The maximum values are located at the mid-section flat wall and the corners; equal in magnitude but opposite in sign. The edges are in compression while the mid-wall is in tension. Davison and Birkemoe acknowledge this is not the most accurate profile that exists, but they justify its application with its simplicity and previous research done by Kamani (1974). Kamani determined the magnitude of the membrane residual stress is a far more critical factor to the final strength of the column than the geometric shape. The maximum values were determined by measurements on the experimental coupon data.

Davison and Birkemoe (1983) also observed that the coupons adjacent to the corners exhibit a smaller through thickness residual stress than the coupons closer to the centerline. This was not included in the model.

The final residual stress obtained from the proposed model (Davison & Birkemoe, 1983) was compared to experimental values measured on the exterior, interior and center surface. The results are shown in Figure 2-41.

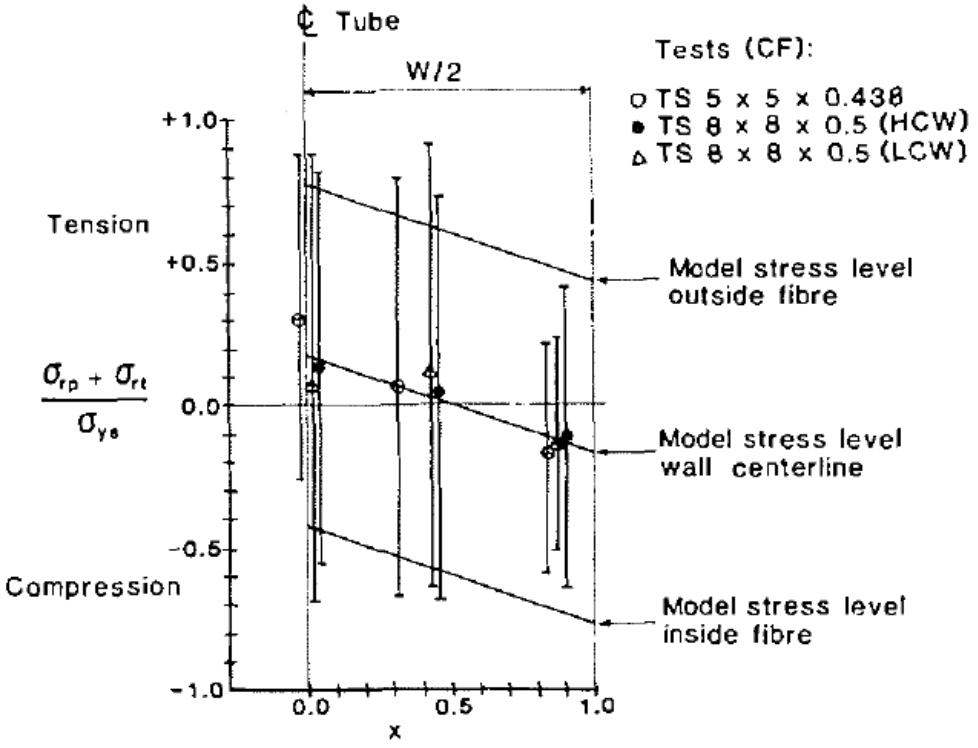


Figure 2-41: Comparison of CF residual stress levels: Model vs. mean test values (Davison & Birkemoe, 1983)

It was pointed out by Davison and Birkemoe (1983) the model is conservative on the tube corners and unconservative at the flat centerline. Nevertheless, it is an accurate representation of the general behavior. A table summarizing the proposed model values to be used for each HSS type is shown in Table 2-13. An important observation to note is that these values are normalized with respect to the stub column strength.

Table 2-13: Model parameter based on mean experimental values (Davison & Birkemoe, 1983)

| HSS type | Material $\sigma-\epsilon$ behaviour | Max. perimeter (membrane) residual stress $\sigma_{rp}/\sigma_{ys}$ | | Max. through thickness (bending) residual stress $\sigma_{rt}/\sigma_{ys}$ | |
|---|---|---|---|---|---|
| | | Corner | Centreline | Inside fibre | Outside fibre |
| CF | Nonlinear | −0.17 | +0.17 | −0.60 | +0.60 |
| CFS | Nonlinear | −0.17 | +0.17 | −0.24 | +0.24 |
| CFHT | Linear | −0.10 | +0.10 | −0.36 | +0.36 |
| HT | Linear | 0.0 | 0.0 | 0.0 | 0.0 |

NOTE: For yield strength gradients see Fig. 2*b*.

The final parameter that Davison and Birkemoe (1983) applied to the model was the initial crookedness. The authors argue that the maximum initial crookedness for the SSRC 1976 design curves of e/L = 1/1000 is not representative of cold-formed HSS profiles. Based on previous experimental research performed by Salvarinas (1977) and Bjorhovde (1977), Davison and Birkemoe propose an initial crookedness of e/L = 1/5800 for their model. They also performed the analysis with the value of e/L = 1/1000 to compare the results to the maximum allowed crookedness.

Having established all the model parameters and distributions, the column behaviour was studied in the final section of the article. Davison and Birkemoe (1983) studied two column models, a tangent modulus model where the column is perfectly straight and a maximum strength theory model which accounts for an initial crookedness. The tangent modulus theory was mainly used to establish an upper bound to the maximum strength theory. As it was noted by the authors, this is due to the maximum strength theory load exceeding the tangent load theory at low crookedness values while the tangent modulus load theory is too conservative at mid-height displacements.

Davison and Birkemoe (1983) further performed a parametric study on the yield strength gradient, the through thickness residual stress and the perimeter residual stress. One or two of the parameters was held constant while the other parameter could vary. The parameters were held at the values proposed in Table 2-13. For slenderness values of 0.2 to 1.6 and crookedness values ranging from e/L = 1/1000 to 1/5800, it was determined the yield strength gradient had almost no effect on the maximum column strength if residual stress was present. Yield strength could vary according to the exponential and step models proposed earlier. When studying the residual stress parameter, the yield strength gradient could only vary through the exponential model. It was determined the perimeter residual stress has little effect on the maximum strength while through thickness residual stress had a significant effect. At a slenderness of 1.6, keeping the membrane and yield strength gradients constant produced results 26% greater than with the through thickness residual stress. Keeping the through thickness residual stress constant produced results varying from 99% to 103% compared to when all three parameters were present. As Davison and Birkemoe noted, this clearly showed the through thickness residual stress was the most critical parameter affecting column strength. To confirm the models experimentally, the authors compared stub column tests from previous research to their tangent modulus model results in Figure 2-42.

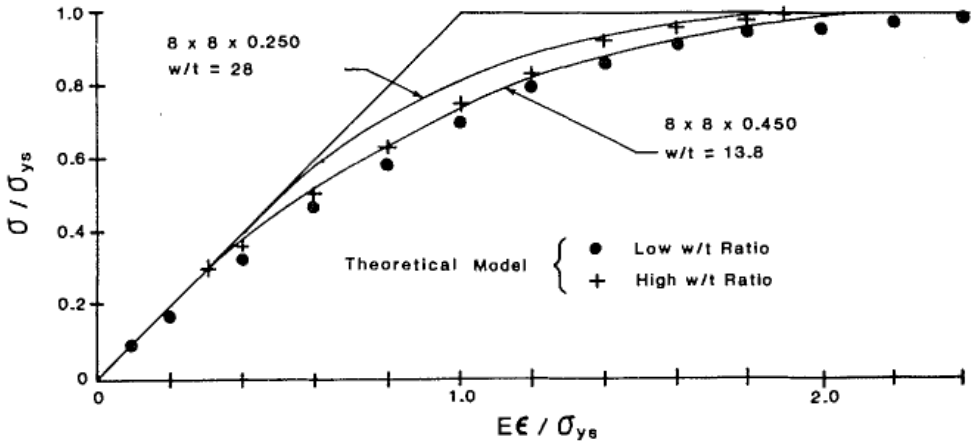


Figure 2-42: Comparison of HSS stub column results to tangent modulus model for CF shapes (Davison & Birkemoe, 1983)

Davison and Birkemoe (1983) determined the tangent modulus model agrees well with experimental results for low *w/t* values but is too conservative for high *w/t* ratios. For the full section measurements, the tangent modulus model was mostly above the experimental results.

As pointed out by Davison and Birkemoe (1983), maximum strength model results were always above the experimental results for an initial crookedness of e/L = 1/1000 and the majority were above the experimental results for an initial crookedness of e/L = 1/5800. This is shown in Figure 2-43.

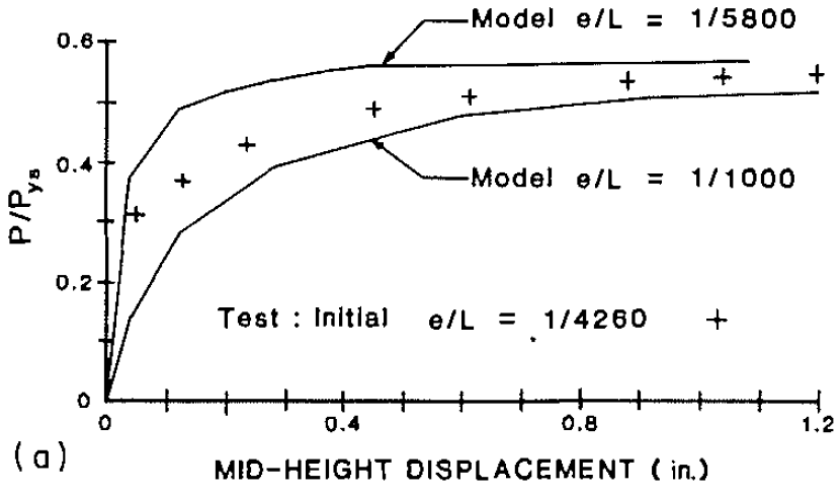


Figure 2-43: Comparison of load-displacement curves for full-sized column tests with maximum strength theory for cold-formed non-heat-treated section 8 x 8 x 0.450 (Davison & Birkemoe, 1983)

It was determined in the article member crookedness reduced the effects of the increased yield strength and residual stress. However, its effect was found to be more significant on the increased yield strength parameter. Davison and Birkemoe (1983) proposed a crookedness of e/L = 1/5800 to represent cold-formed HSS members. Figure 2-44 presents the theoretical curves compared to the maximum, minimum and mean strength.

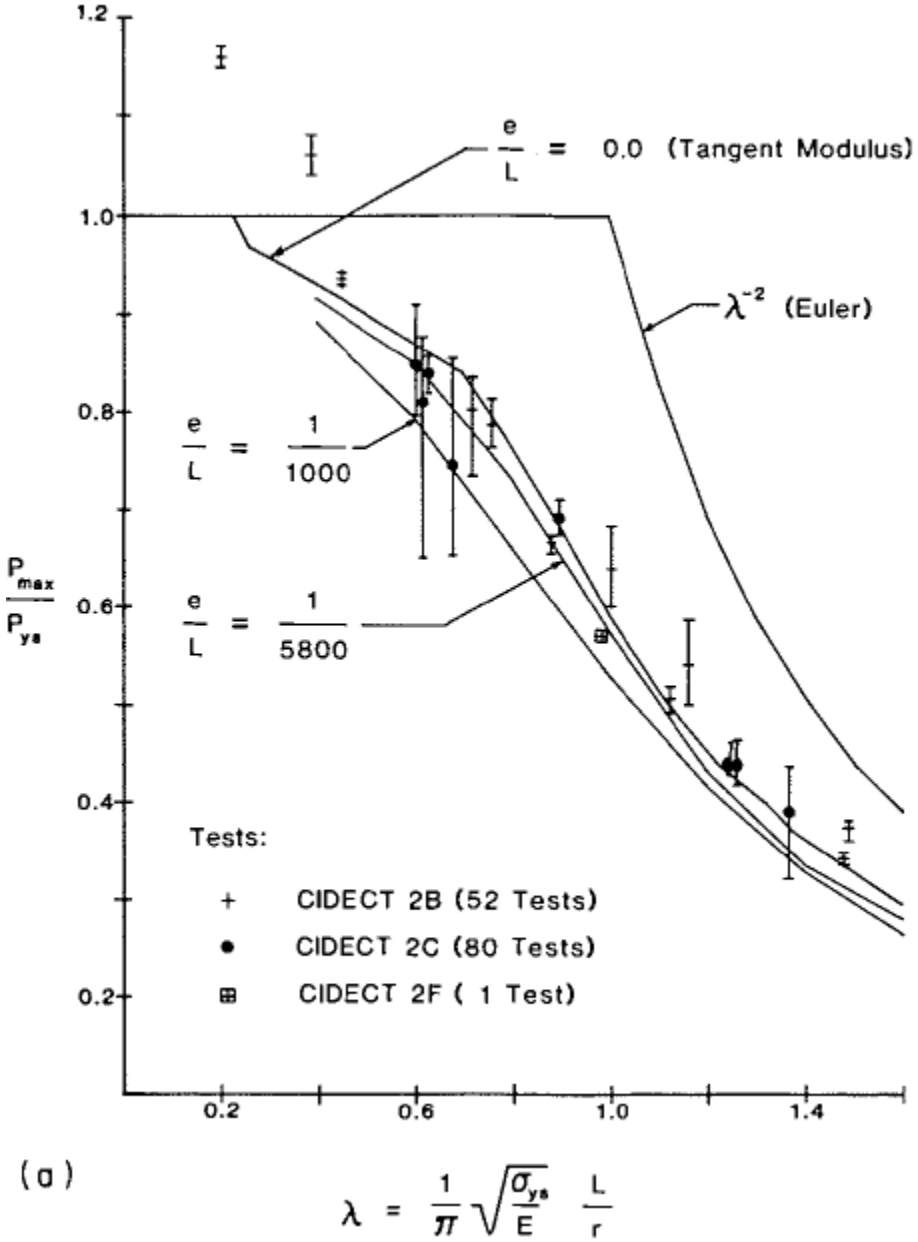


Figure 2-44: Comparison-strength curves from full-sized column tests and theory for cold-formed non-heat-treated HSS (Davison & Birkemoe, 1983)

Finally, Davison and Birkemoe (1983) proposed the appropriate Structural Stability Research Council (SSRC, 1976) curve to represent cold-formed HSS members which were not included in the original formulation. To recommend the appropriate curve, the authors took the band of curves representing curve 1 and 2 from the SSRC and verified whether the obtained theoretical curves fall within those bands. It was concluded CF and CFS curves fall within the band for curve 2, while CFHT and HT curves fall within the band for curve 1. Figure 2-45 shows the results for the CF and CFS section.

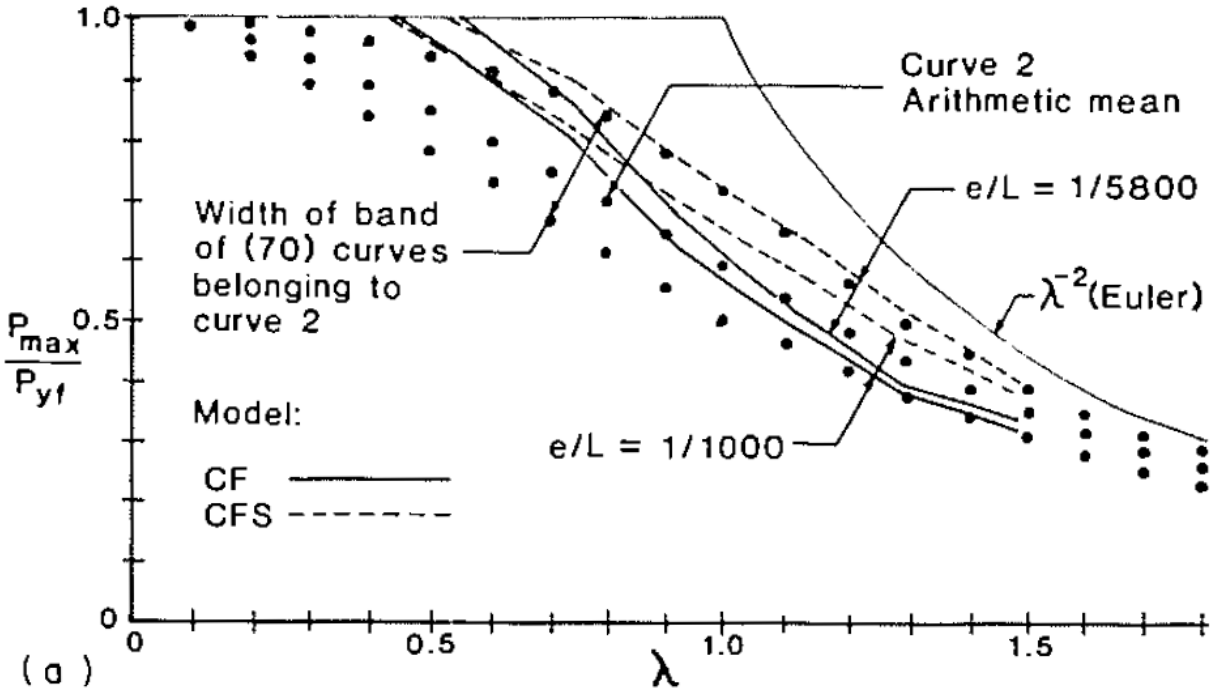


Figure 2-45: Comparison of SSRC curves with theoretical maximum strength curves for CF and CFS sections (Davison & Birkemoe, 1983)

#### 2.2.1.1 Summary

To summarize, this section of Chapter 2 concentrated on researched performed in the 1970s right after the 1960s research effort in Cornell University (Britvec et al., 1970). Bjorhovde and Tall (1971) studied the maximum column curve concept in the first investigation titled "*Maximum Column Strength and the Multiple Column Curve Concept*" (Bjorhovde & Tall, 1971). Only one column strength curve was available at the time. Bjorhovde and Tall concluded this was not acceptable as steel sections manufactured by different methods had inherently different properties. Previous research had already proposed several curves based on the tangent modulus theory, but the out-of-straightness cannot be accounted for in this formulation. To adress this issue, Bjorhovde and Tall developped a maximum strength model. A numerical fiber based model was built specifically for that task and the authors included W type roll-formed columns, H type columns and welded-box columns of various steel grades and sizes. Experimental values from the properties these profiles such as yield strength, residual stress and out-of-straightness were included in the model. Bjorhovde and Tall proposed three different groups to best represent the sections, but not to overwhelm the designer. These groups however, did not include cold-formed profiles.

The second investigation was a thesis titled "*Stub Column Data and the Prediction of Compression Behaviour of Hollow Structural Sections*" (Kamani, 1974). This thesis addressed the lack of cold-formed sections in the previously proposed SSRC curves. However, the profiles studied by Kamani were seamless. This investigation was still included due to interesting results which can be applied to regular roll-formed profiles. Kamani sectioned the profile to obtain a yield strength and residual stress distribution across the section. It was found the yield strength at the corners is significantly larger than the mid-wall flat. Kamani also found a yield strength gradient across the flat wall. The strength was found to increase somewhat linearly from the center to the edges up until the corner yield strength. Three longitudinal residual stress profiles were studied in this investigation. It is important to note, Kamani's profiles only represent the membrane residual stress component. One was triangular, one was sinusoidal, and one was parabolic. Kamani considered the triangular one to best represent the experimental results. The residual stress was found to be in tension at the center and in compression at the edges. The residual stress component linearly increased from the compressive edge up to the tensile mid-wall section. The magnitudes at the mid-wall and edge of the wall are the same. It was also determined the slight variations in the three residual stress profiles aren't as important as the actual magnitudes and these have a minimum impact on the model. These

experimental results were included in two analytical models to obtain the column curve. The first model was a tangent modulus model and was mainly used to study the effect of the residual stress. This model included stub-column results and residual stress measurements. It was concluded by Kamani residual stress does not always decrease the strength and this depends on the slenderness ratio. The second model was the maximum strength model. In order to include the yield strength gradient from the coupon results, Kamani proposed three different Ramberg-Osgood coefficients. These coefficients were to account for the difference in the strain-stress curve between the mid-wall flat and the corners. As the coupons approached the corners the stress-strain curve lost its sharp yield plateau. Finally, Kamani compared the tangent modulus results versus the maximum strength results and concluded the tangent modulus model was far too conservative.

The third investigation was titled "*A Theoretical Investigation of the Column Behaviour of Hollow Structural Steel Sections*" (Davison, 1977). This thesis represents the groundwork for residual stress gradient models in cold-formed sections. An experimental investigation was carried on heat treated cold-formed sections, but results from several types of sections were included to construct the residual stress model. Davison finally proposed a trapezoidal through thickness longitudinal residual stress model and a triangular perimeter longitudinal residual stress model as proposed by Kamani (1974). The through thickness residual stress model is also named *bending residual stress* and the perimeter residual stress model is also named *membrane residual stress*. The final residual stress distribution would be the algebraic sum of the through thickness and perimeter residual stresses. The yield strength gradient was also studied. Two different gradients were proposed. One for sections with low *w/t* ratios and a second one for sections with large *w/t* ratios. The gradient proposed by Kamani (1974) where the yield strength linearly increases from the flat to the corners is applied to sections with low *w/t* ratios. For sections with high *w/t* ratios the yield strength would be constant in the flat portion of the wall and suddenly increase at the corners with a step-function. Magnitudes for residual stress and yield strength were proposed for several types of cold-formed sections. Davison proceeded to a similar exercise as the one performed by Kamani (1974). He used a tangent modulus model to study the effect of each parameter at first and then repeated the procedure with the maximum strength model and finally proposed an SSRC curve. It was concluded perimeter residual stress decreases the column strength if no yield strength gradient is included. If a yield strength gradient is present, this depends on the section's *w/t* ratio. The through thickness residual stress decreased column strength for all cases. Out-of-straightness in the member

was also studied. It was concluded the mean out-of-straightness was of 1/5400 for short members and 1/6200 for long members. This is significantly smaller than the 1/1000 value proposed in the standard at the time. Therefore, Davison proceeded to analyse the effect of out-of-straightness on the model. It was concluded the tangent modulus model represents an upper bound for the column strength model and they show the same behaviour for high out-of-straightness values. It was found initial crookedness decreases the effects of residual stress. Residual stresses have the highest impact on columns of intermediate length. Davison finally states most of the maximum column strength model results fall in the center of SSRC curve 1 and the upper band of curve 2. Curve 1 is proposed for these sections.

Since no regular cold-formed sections had been tested after Ringle (1969), Bjorhovde (1977) filled this gap by adding the properties of eight regular cold-formed sections. This was done in a thesis titled "*Strength and Behaviour of Cold-formed HSS Columns*" (Bjorhovde, 1977). Several measurements on out-of-straightness, flat and corner coupons and stub column strength were taken. Residual stress was determined from the proportional limit on stub column stress-strain curves. The mean out-of-straightness for these sections was determined to be 1/6384 which is once again significantly lower than the code prescribed limit of the time. The yield strength (average of tension coupons) was up to 50% higher than the nominal strength (to add in conclusion). The ultimate tensile stress also increased, but not nearly as much. The weld had a yield strength of up to 10% higher than the mid-wall flat coupon. Elongation in the weld was reduced by up to 15.5%. Some profiles showed no signficant differences between the mid-wall flats and the flats close to the corners but for other profiles the difference was up to 10%. The corner elongation was up to 16% lower than the flat coupons. Longitudinal residual stresses were determined to be between 58 to 80% of the yield strength of the section. Previous research had proposed longitudinal residual stresses of 50 to 75%. A large difference in residual stress is also observed with respect to the column thickness and size. Finally, Bjorhovde notes that 95% of pin-ended column results fall within curve 1 of the SSRC (1974).

The final investigation titled "*Column Behavior of Cold-formed Hollow Structural Steel Shapes"* (Davison & Birkemoe, 1983) summarized Davison's research (1977) and added some new results and insights. For example, a new exponential equation was proposed to model the increased yield strength in sections with a *w/t* ratio lower than 17.3 and a step-function was proposed for sections with a *w/t* ratio above 32.1. It was noticed sections in between those two limits would experience

a hybrid behaviour, but no equation was given. Another equation was given to model the through thickness residual stress (bending) from the elastic unloading stress of the released coupon. This equation was based on the assumption that the magnitude of the elastic unloading stress is the same as the magnitude of the through thickness residual stress within the section. The model was confirmed by experimental values. Davison and Birkemoe concluded it is a good representation of the general residual stress behaviour. Maximum model parameters based on mean measurements were also proposed. Finally, column curves corresponding to the SSRC (1974) curve 2 were proposed for regular cold-formed and seamless cold-formed sections, while the SSRC (1974) curve 1 was proposed for heat treated sections.

## 2.3 Improved residual stress model and plastic collapse mechanism for slender cold-formed sections

After the 1970s research effort, a new series of major investigations into the behavior of cold-formed sections continued at the University of Sydney, Australia. This comprehensive research effort was undertaken by Key, Hancock, Hassan, and later Wilkinson. It started in the mid 1980s and continued up to the late 1990s. Most investigations were on regular cold-formed sections with a nominal yield strength of 350 MPa. The authors paid specific attention to very slender sections and concentrated their efforts on determining plastic-collapse mechanisms and post-ultimate behavior. A large investigation was also performed on the residual stress of cold-formed HSS profiles. An additional residual stress component was identified that was implicitly included in Davison and Birkemoe's model (1983) but not explicitly measured. Based on these results, new residual stress models were proposed. It was also determined Davison and Birkemoe's model was in good agreement with the new model. The following papers are summarized in this section:

- *An Experimental Investigation of the Column Behavior of Cold-formed Square Hollow Sections* (Key and Hancock, 1985).
- *Plastic Collapse Mechanisms for Cold-formed Square Hollow Section Columns* (Key and Hancock, 1986).
- *Column Behavior of Cold-formed Hollow Sections* (Key et al., 1988).
- *The Behavior of Cold-Formed Square Hollow Section Columns, 1990* (Key, 1988).
- *A Theoretical Investigation of the Column Behavior of Cold-Formed Square Hollow Sections* (Key and Hancock, 1993).
- *The Plastic Behavior of Cold-formed Rectangular Hollow Sections* (Wilkinson, 1999).

The first investigation is titled "*An Experimental Investigation of the Column Behavior of Cold-formed Square Hollow Sections*" (Key & Hancock, 1985). The goal of this investigation was to determine properties of Australian cold-formed HSS members. The results were further compared to previous European and North American research and an appropriate curve was proposed. The authors pointed out that SSRC and European curves did not include cold-formed HSS shapes in their research. This was a problem because the use of cold-formed HSS sections had been significantly growing. Key and Hancock chose to test normal strength sections with a nominal yield strength of 350 MPa. The sections produced by cold-formed electric resistance welding which is equivalent to Birkemoe and Davison's (1983) regular CF sections. The sections were strain aged for 15 min at 150℃. Table 2-14 presents the tested profiles. Key and Hancock specifically tested tubes with very high *b/t* ratios. It is explained these were chosen since the available tubes with low *b/t* ratios fell in a range where "inelastic local buckling could significantly alter the column strength and post-ultimate response, especially when the possible deleterious effect of residual stress is considered" (Key & Hancock, 1985).

Table 2-14: Performed tests and studied profiles (Key & Hancock, 1985)

| Section Geometry D x B x t (mm) | b/t | TESTS PERFORMED | | | | |
|---|---|---|---|---|---|---|
| | | Yield stress | Residual stress | Out of straightness | Stub Column | Pin-ended Column |
| 76 x 76 x 2.0 | 36.1 | Yes | No | Yes | 1 | 12 |
| 152 x 152 x 4.9 | 29.1 | Yes | Yes | Yes | 1 | 8 |
| 203 x 203 x 6.3 | 30.3 | Yes | No | Yes | 2 | 6 |
| 254 x 254 x 6.3 | 38.3 | Yes | No | No | 2 | No |

Notes: 1. Number in table is total number of tests performed for that section.

To measure residual stress, Key and Hancock (1985) placed electric strain gages on the outer and inner surfaces. After the initial measurements, the tube was sliced longitudinally to release the remaining residual stress and additional measurements were taken. Tensile residual stress was found to exist on the outer surface and compressive residual stress on the inner surface. Key and Hancock reported the following observations:

- *Average residual surface stress equals to approximately half of actual yield strength.*

- *The net membrane residual stress was found to be around 30 MPa tensile at the center and 40 MPa compressive at the edges near the corner which is very small compared to the overall stress. Released bending residual stress is approximately equal to 200 MPa. Applying Birkimoe's equation* [(2-15)] *it gives a pure through thickness residual stress of 140 MPa.*
- *Welding only produced about 80 MPa tensile membrane residual stress which is still relatively small.*
- *Some symmetry is seen at the weld line.* (Key and Hancock, 1985, p.7)

On average, Key et al. (1988) reported the membrane residual stress was found to be approximately 15% of the yield stress and the bending residual stress (through thickness) was found to be approximately 70% of the actual yield strength.

To measure yield strength, the member was sectioned as shown in Figure 2-46 and the yield strength was determined for each coupon.

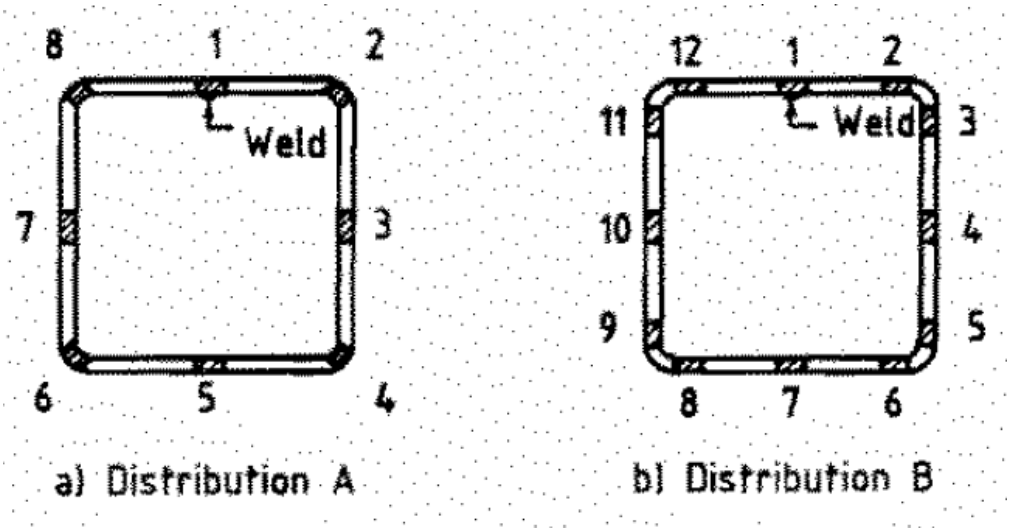


Figure 2-46: Yield strength coupon locations (Key & Hancock, 1985)

Figure 2-47 provides an example of the results obtained by Key and Hancock (1985). The cross shaped represents the yield strength while the circle shaped symbol represents the ultimate tensile stress. Key and Hancock (1985) reported that while the increase in corner yield strength is evident, the distribution about the face is quite flat. The average yield strength is around 400 MPa and the authors state the small variation in the yield strength distribution for the flat part is not likely to affect the results.

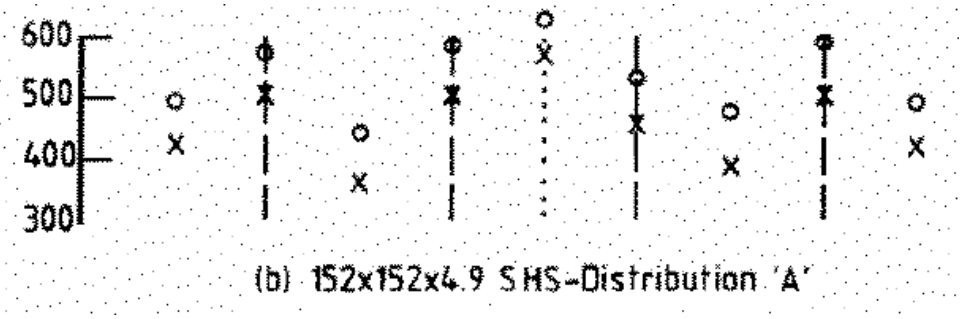


Figure 2-47: Yield strength results for sectioned member (Key & Hancock, 1985)

Key and Hancock (1985) also compared the virgin material yield strength to the corner yield strength. For the studied sections, the virgin material had a yield strength ranging from 300 MPa to about 330 MPa. By analyzing the $\sigma_u/\sigma_y$ relationship as well as the maximum elongation, it is concluded the ductility of the material decreases after cold forming. The virgin material had an elongation at ultimate ranging from 15 to 20%, while the worked flats had an elongation ranging from approximately 5 to 10% and for the corners it ranged from 2 to 4%. Nevertheless, it is reported this was not an issue since full section stub column tests still exhibited significant deformation. Table 2-15 summarizes their results. A significant difference can be seen between the two 76 x 76 x 2.0 sections in the yield strength. Key and Hancock (1985) state the only explanation for this discrepancy was that the profiles came from different production lines. This significant variation is an example of the impact of the production line, equipment and calibration of the rollers during the production of cold-formed sections.

Table 2-15: Summary of yield strength results (Key & Hancock, 1985)

| Specimen | Virgin Material | | | | Formed Material | | | | | $\frac{\sigma_Y \text{ formed}}{\sigma_Y \text{ virgin}}$ |
|---|---|---|---|---|---|---|---|---|---|---|
| | $\sigma_Y$ | $\sigma_U$ | $\Delta L/L$ | $\sigma_U/\sigma_Y$ | Location | $\sigma_Y$ | $\sigma_U$ | $\Delta L/L$ | $\sigma_U/\sigma_Y$ | |
| 76 x 76 x 2.0 (Series 1) | 327 | 457 | 19% | 1.40 | Face<br>Corner | 425<br>531 | 499<br>588 | 5.4%<br>2.3% | 1.17<br>1.11 | 1.30<br>1.62 |
| 76 x 76 x 2.0 (Series 2) | 327 | 457 | 19% | 1.40 | Face<br>Corner | 370<br>476 | 449<br>522 | 9.0%<br>2.8% | 1.21<br>1.10 | 1.13<br>1.46 |
| 152 x 152 x 4.9 | 302 | 454 | 14.8% | 1.50 | Face<br>Corner | 416*<br>498 | 475*<br>573 | 5.4%<br>2.8% | 1.14<br>1.15 | 1.38<br>1.65 |
| 203 x 203 x 6.3 | 312 | 511 | 20.6% | 1.64 | Face<br>Corner | 395<br>520 | 494<br>604 | 8.7%<br>4.2% | 1.25<br>1.16 | 1.27<br>1.67 |
| 254 x 254 x 6.3 | 312 | 511 | 20.6% | 1.64 | Face<br>Corner | 405<br>487 | 479<br>555 | 8.4%<br>3.3% | 1.18<br>1.14 | 1.30<br>1.56 |

Notes: 1. * Centre face yield stress factored to take account of yield stress variation across face.
2. $\Delta L/L$ = % elongation up to ultimate in 25 mm gauge length.
3. All stresses in MPa.

To continue, Key and Hancock (1985) discuss the general difference in stress-strain behavior between corner and flat coupons. The main difference being the distinct yield plateau in flat coupons, while corner coupons exhibit gradual yielding. The 1960s research is invoked (Britvec et al., 1970), and strain aging is attributed as the main factor to justify this difference. It is justified that strain aging returns the highly non-linear curve to its original state, but large plastic strains render its effects negligible. Therefore, the return to the well-defined yield plateau is only seen in flat coupons as they did not sustain significant plastic strains.

Table 2-16: Stub column tests (Key & Hancock, 1985)

| Specimen | b/t | $P_{Sult}$ (kN) | $P_{Scoup}$ (kN) | $\frac{P_{Sult}}{P_{Scoup}}$ | $P_{Yn}$ (kN) | $\frac{P_{Sult}}{P_{Yn}}$ |
|---|---|---|---|---|---|---|
| 76 x 76 x 2.0 (Series 1) | 36.1 | 243 | 252 | 0.96 | 204 | 1.19 |
| 76 x 76 x 2.0 (Series 2) | 36.1 | - | - | - | 204 | |
| 152 x 152 x 4.9 | 29.1 | 1283 | 1194 | 1.07 | 984 | 1.30 |
| 203 x 203 x 6.3 | 30.3 | 2010<br>2015 | 1970 | 1.02<br>1.02 | 1691 | 1.19<br>1.19 |
| 254 x 254 x 6.3 | 38.3 | 2420<br>2500 | 2515 | 0.96<br>0.99 | 2139 | 1.13<br>1.17 |

After defining the residual stress and yield strength distribution, Key and Hancock (1985) performed stub column tests to define the overall section behavior. The sections and results are presented in Table 2-16 where $P_{Scoup}$ is the coupon weighted average and $P_{ny}$ is the nominal yield load. It is pointed out sections with high b/t ratios are more likely to exhibit local buckling, hence lose part of their maximum strength compared to the weighted coupon average. The stub column failure load is 13 to 30% greater than the nominal yield load. It is also noted that if the $P_{ult}/P_{Scoup}$ ratio is less than unity the column suffered from inelastic local buckling and did not achieve its full strength. Key (1988) explains this difference in behavior is clearly seen when comparing the two sections with a b/t approximately equal to 30 versus the other sections with a b/t of 36 and 38. It is

further pointed out that as the b/t ratio reaches approximately 40, the column fails with no prior warning. This is due to each side behaving as a separate plate laterally supported by the adjacent sides. If local buckling and plasticity occur almost simultaneously the column experiences sudden failure which referred as "violent load shedding" (Key, 1988). This behavior is amplified if the initial imperfection is small.

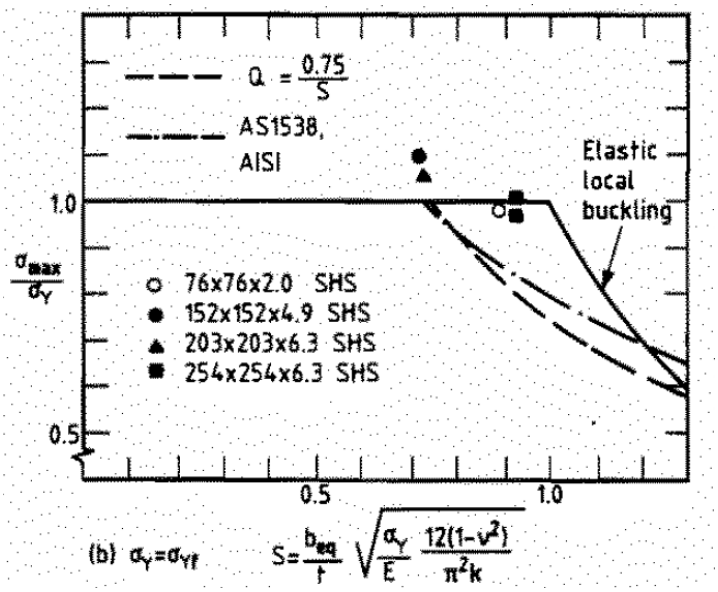


Figure 2-48: Stub column maximum strength (Key & Hancock, 1985)

Key and Hancock (1985) also discuss the effective width of the section and its impact on the theoretical stub column compressive strength. They present several equations to account for it, mostly based on previous research by Von Karman (1932). They further compare theoretical stub column strength calculated with the nominal yield strength to the one calculated with the weighted coupon average yield strength. In both cases the effective width is accounted for through the Q factor. Key and Hancock present this in equation (2-17) where Q is the ratio between the effective area and the gross area. It is concluded theoretical stub column strength calculated with the weighted coupon average yield strength is much closer to the experimental value. It is also determined the flat plate loses its full effectiveness at a slenderness value approximately equal to 0.73 (Key et al., 1988). This is equal to a w/t value of approximately 33.3 for a nominal yield strength of 350 MPa. These results are shown in Figure 2-48.

$$P_{Stheor} = A_{eff}\sigma_y = QA\sigma_y = QP_y \tag{2-17}$$

After having performed the stub column tests, Key and Hancock (1985) continued with pin-ended column tests. Both concentric and eccentric tests were performed along with out-of-straightness measurements. The maximum tested slenderness values L/r were up to 100.

The average out of straightness was determined to be L/7700 and L/9560 depending on the axis which Key and Hancock (1985) mostly attribute to the alignment of the rolls. In a paper published later (Key et al., 1988), Key et al. determined an average out-of-straightness of L/6600 and L/1100. The code limit of the time employed an out-of-straightness of L/1000 (Key et al., 1988). A single curvature is noted for the out-of-straightness of large profiles. The smaller profiles exhibit an irregular shape which the authors attribute to post manufacturing handling. There is no correlation between the weld location and maximum out-of-straightness location (Key et al., 1988). There is also no correlation between the direction of buckling failure and the weld (Key et al., 1988). Figure 2-49 presents the normalized results for all combined sections.

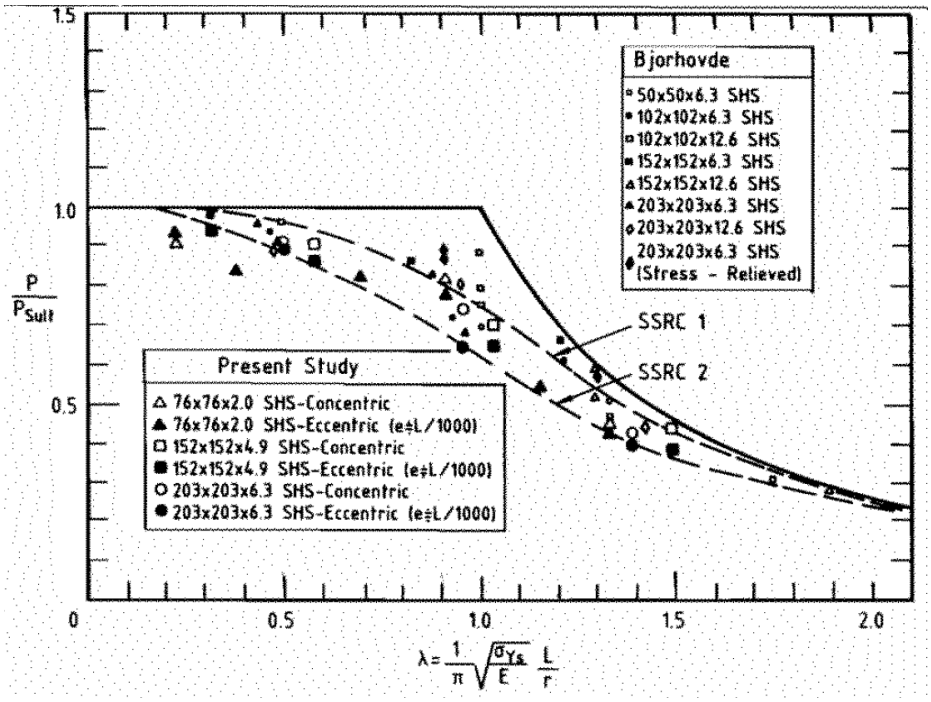


Figure 2-49 : Pin ended column results for Hancock and Bjorhovde (Key & Hancock, 1985)

As explained by Key and Hancock (1985), the two main failure mechanisms are either an overall column bending mode or a plastic hinge mechanism mode. An example of these mechanisms is presented in Figure 2-50 which compares the normalized load-axial deformation graphs for different L/r values.

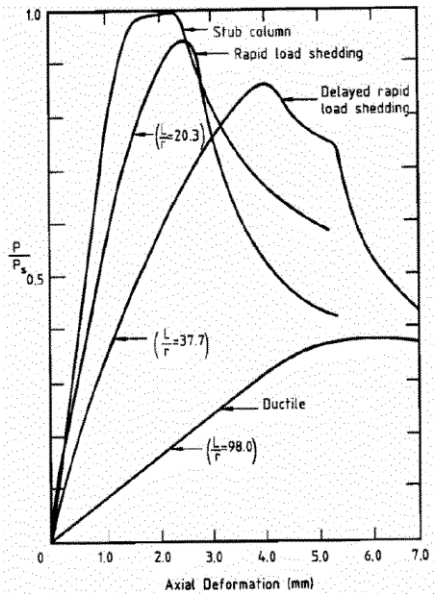


Figure 2-50: Load-axial deformation curves for 152 x 152 x 4.9 section (Key & Hancock, 1985)

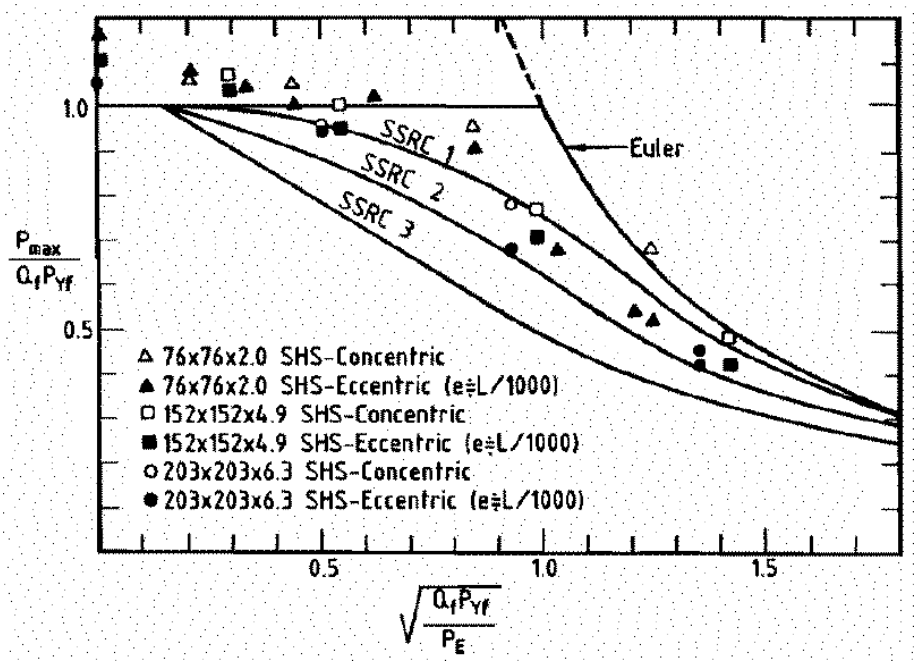


Figure 2-51: Experimental results compared to the SSRC curves and normalized to the average coupon yield strength (Key & Hancock, 1985)

Finally, Key and Hancock (1985) compared the European (ECS) and American (SSRC, 1978 and AISI, 1969) design curves to their experimental results and proposed an appropriate Australian curve. The theoretical column curves were calculated using the average coupon yield strength, not including the weld, and the effective area with the Q factor as explained previously. The out of

straightness in the analytical model was assumed to be sinusoidal with a maximum value of L/1000. Figure 2-51 presents the experimental results compared to the SSRC curves.

Key and Hancock (1985) apply Rotter's formulation (1981) to represent the new curve in a simple way and base their curve on the SSRC curve 2. They present the new curve in equation (2-18).

$$\frac{P_{Stheor}}{QP_y} = \frac{\lambda^2 + 1 + n}{2\lambda^2} - \left(\left(\frac{\lambda^2 + 1 + n}{2\lambda^2}\right)^2 - \frac{1}{\lambda^2}\right)^{\frac{1}{2}} \tag{2-18}$$

$$n = 0.293(\lambda - 0.15) > 0$$

$$\lambda = \lambda_n + c * a$$

$$\lambda_n = \frac{1}{90}\left(\frac{L}{r}\sqrt{\frac{Q\sigma_y}{250}}\right)$$

$$a = \frac{2100(90\lambda_n - 13.5)}{(90\lambda_n)^2 - 15.3(90\lambda_n) + 2050} > 0$$

The term *c* is a factor that shifts the curve from the central SSRC curve 2. The term *c* ranges approximately from -1.0 to 1.0 with the extremes approximately corresponding to the SSRC curves 1 and 3. If the term *c* is zero the curve will fall on the SSRC curve 2. It is found that the c term produces the best mean fit to the experimental results when it is equal to -0.5. This column curve formulation is proposed to represent the cold-formed HSS design curve. Key and Hancock (1985) also compared the proposed curve to the experimental results while using the nominal yield strength value instead of the coupon average. An example of these results is presented in Figure 2-52.

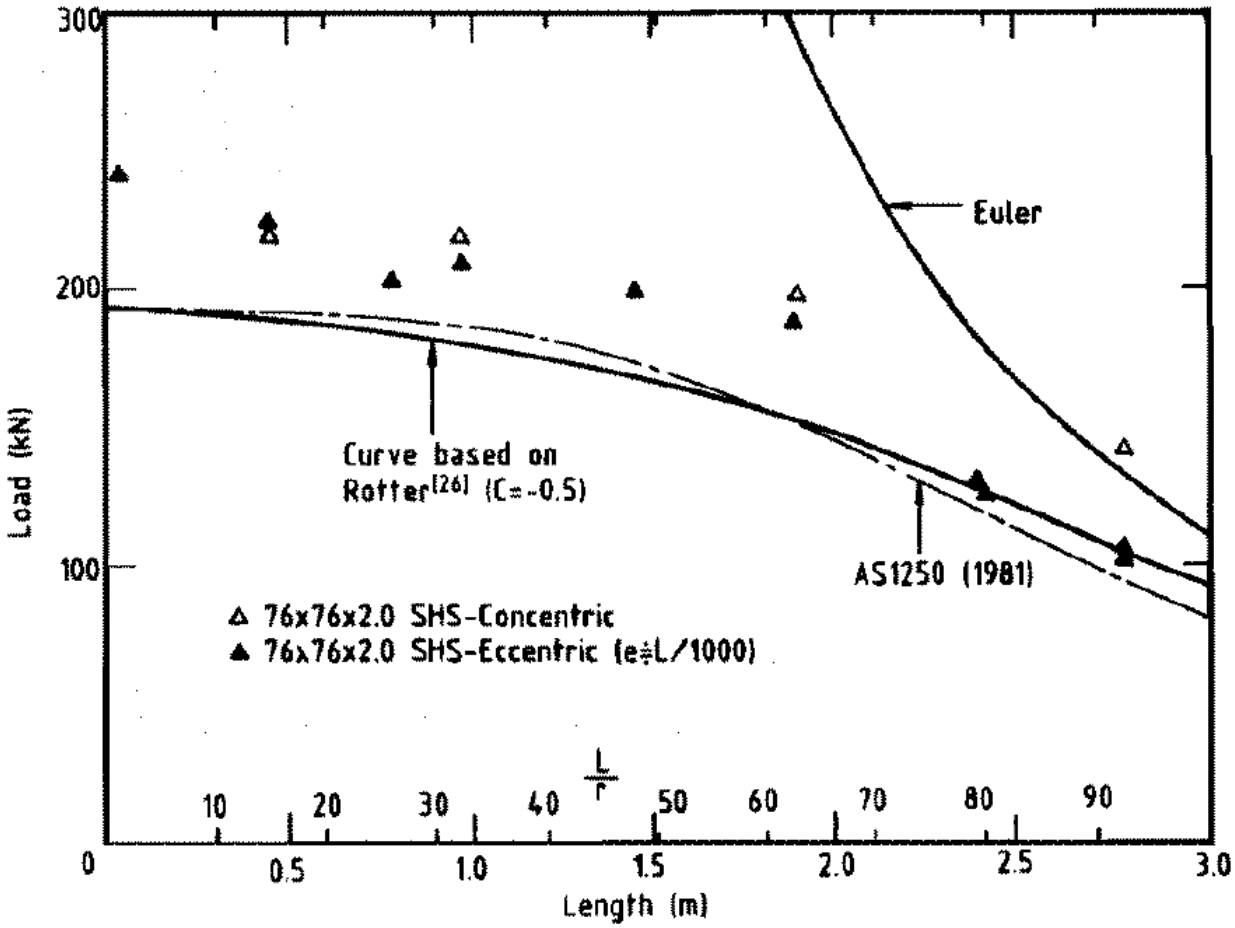


Figure 2-52: Proposed column curve based on the nominal yield strength compared to experimental results (Key & Hancock, 1985)

The main observation (Key & Hancock, 1985) is that the experimental results are significantly above the proposed column curve at low slenderness values but represent a good fit at high slenderness values. This is attributed to the complex yield stress distribution in the profile.

After studying slender sections in the previous paper, Key and Hancock (1986) decided to address one of the problems they noticed in a new paper titled "*Plastic Collapse Mechanisms for Cold-formed Square Hollow Section Columns*". The problem addressed in this paper is the sudden post-ultimate load shedding due to the plastic hinge occurring at the same time and place as local buckling. This behavior is very dangerous when a ductile response is expected as it leads to brittle behavior. Key and Hancock (1986) analyzed the plastic collapse mechanisms for the HSS members proposed by the previous research (Key & Hancock, 1985) and develop their own for stub and pin-ended columns. Key et al. (1988) noted, one major shortcoming of previously defined plastic

collapse mechanisms is that most mechanisms consider a single plate under uniaxial compression and the overall behavior is modeled as the composite of four such plates. These models also don't account for specific corner yielding or the increased yield strength across the section.

The model proposed by Key and Hancock (1986) accounts for the increased yield strength and has four components which are the plate folding mechanism, corner yielding and folding corner restraint. However, it does not account for residual stress as the authors state it should not significantly affect results in this case. Figure 2-53 represents an illustration of the stub column model.

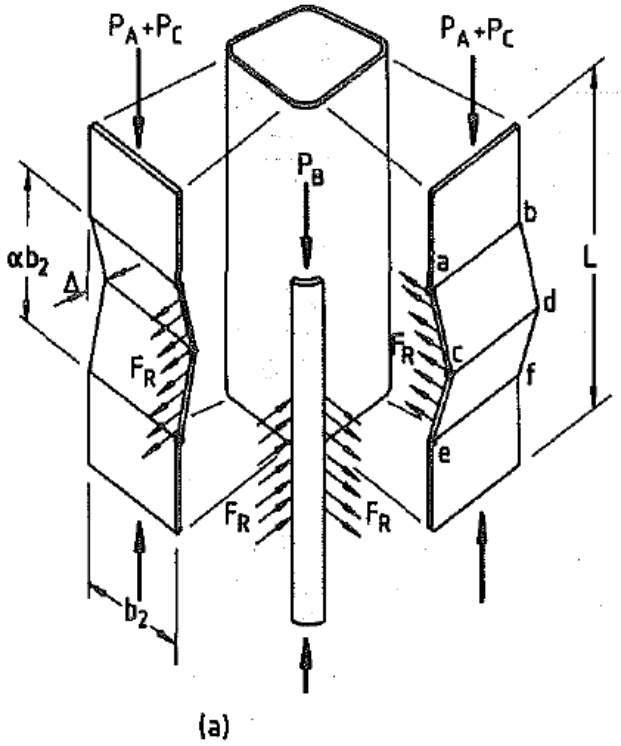


Figure 2-53: Stub column plastic mechanism model (Hancock & Key, 1986)

The plate folding component is composed of three plastic hinges, however, the author states it is safe to simplify it by a straight line. The corners immediately yield to stay in kinematic equilibrium with the plate folding mechanism. In case of large deformations, a plastic hinge takes place between the corners and plates to allow for the plate to deform since the corners cannot open to follow the plate's out of plane deformation. Key and Hancock (1986) confirm this behavior experimentally. Figure 2-54 gives an example of the theoretical model presented by the authors compared to the theoretical results and models proposed by other researchers.

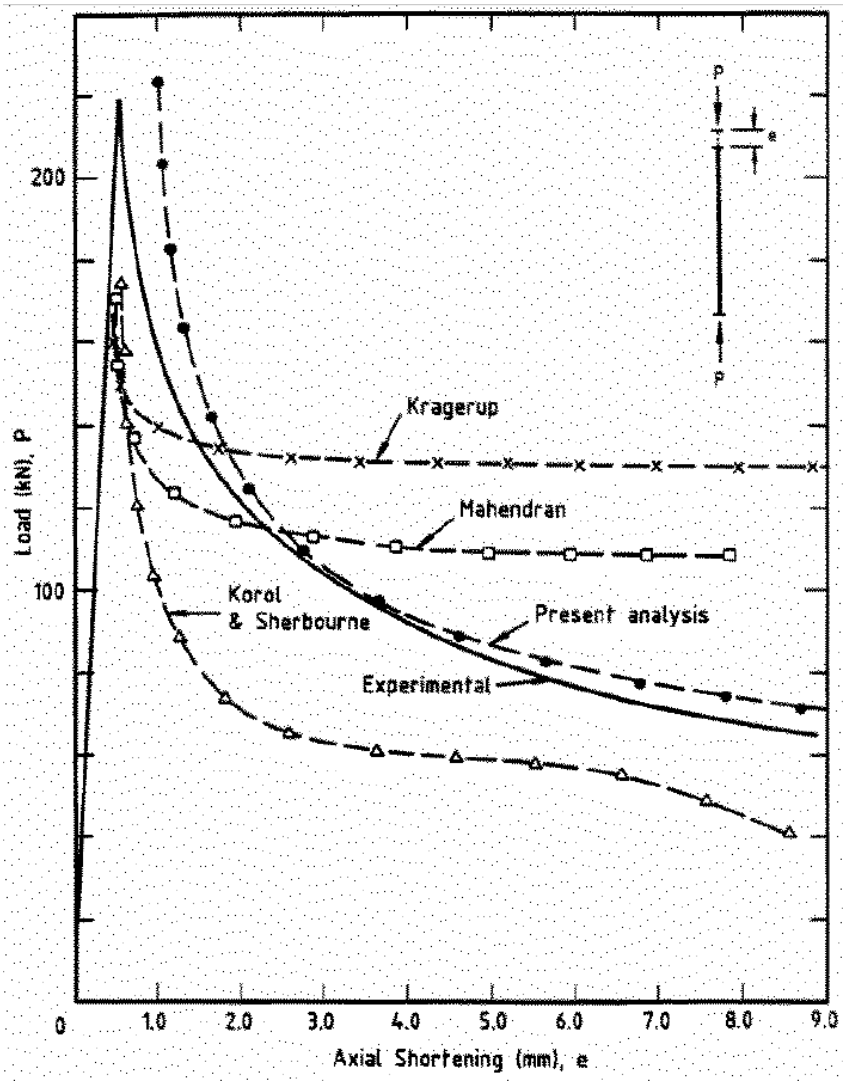


Figure 2-54: Comparison of theoretical plastic mechanisms for section 76x76x2.0 (Hancock & Key, 1986)

It is concluded by Key (1988), the theoretical results are in well agreement with experimental values except for the low slenderness sections. The general shape is considered to properly represent the overall behavior. Nevertheless, the theoretical model underestimates the load by about 20% in all cases except for one. This discrepancy is attributed to overall plastic straining at ultimate load which the model does not account for. This theory is further reinforced since the discrepancy increases as the slenderness decreases and slender sections are subjected to higher strain hardening.

Key and Hancock (1986) compared their results with previous research and explain the advantages of their model. One disadvantage noted by Key et al. (1988) with respect to previous research is that the model tends to reach an artificial load plateau not present in experimental values. This is

explained by the full yield assumption in the corners. The discrepancy with experimental results showed by models from other investigations is explained by the slenderness of the tested sections. The slenderness ranged from 60 to 80 and previous investigations used a single plate to model the behavior. Key et al. (1988) explain it is clear from the results this is not enough.

The pin-ended column model proposed by Key and Hancock (1986) is almost the same as the stub column model except for the additional channel folding mechanism. Figure 2-55 presents an illustration of the model.

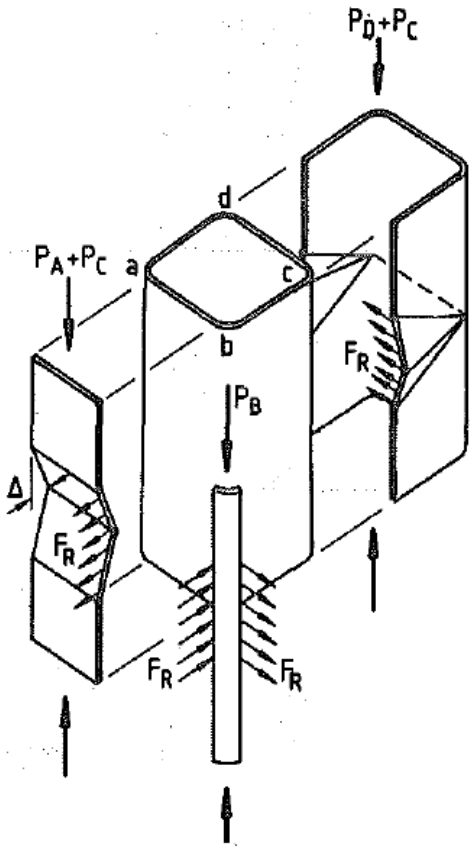


Figure 2-55: Pin-ended column plastic mechanism model (Hancock & Key, 1986)

The same conclusions drawn for the stub column model can be applied to the pin-ended column model. The models give a good general representation of the behavior but lose accuracy when the slenderness decreases. Key et al. (1988) also noted there are two post-ultimate equilibrium paths. For the first one, the whole column buckles with no local deformation. For the second one, a plastic mechanism develops where most of the deformation is concentrated, usually towards the center of the column. In cases of short columns, a specific slenderness steep post-ultimate shedding

mechanism can develop which greatly affects the ductility of the section. It is finally suggested to evaluate the ductility of these sections using the ductility index and the simplified response curve to have a proper estimate of this parameter.

The previous investigations are further summarized in an article titled "*Column Behavior of Cold-formed Hollow Sections*" (Key et al., 1988). This article is briefly summarized below as it mostly comes back to the previously discussed investigations (Key and Hancock, 1985; Key and Hancock, 1986) and the concepts that were brought forward. For example, reduced material ductility due to strain hardening and the sudden load shedding. This instability occurs after the maximum load has been reached in moderately slender sections with a b/t ranging from 30 to 50 (Key et al, 1988). The previously seen spatial plastic mechanism models are also discussed and are proposed as a way to determine the section's ductility after it has reached its ultimate load. The limiting plate slenderness values present at the time of the publication are also verified through ductility analysis. Finally, it is concluded the AISI class A column curve (1980) is more suitable to represent cold-formed hollow sections than the class B curve.

In parallel to the research into the yield strength, residual stress, out of straightness and post ultimate behavior in the previous papers, Key et al. (1988) constructed a rigorous large displacement nonlinear finite strip analysis model to investigate and document the load-deformation behavior of cold-formed square hollow sections. Key et al. (1988) chose sections with a very high ratio of width to wall thickness. This made local instability a significant factor. The main motivation to study these sections is that thin-walled members had gained significant ground in construction projects during that time. It was considered thin-walled members were generally more efficient in terms of cost and overall stability (Key et al, 1988). This part of the research is addressed in Key's thesis (1988) titled "*The Behavior of Cold-Formed Square Hollow Section Columns*". The finite strip model in this thesis accounts for large displacements, plasticity and initial conditions of geometric imperfection and residual stress. It also includes local and torsional buckling. The main factor added in Key's (1988) thesis, in comparison to previous papers (Key & Hancock, 1985; Key & Hancock, 1986) is the through thickness residual stress.

The goal of the elaborate finite strip method presented by Key (1988) is to be able to properly assess the ultimate load and post ultimate behavior of the section. Key (1988) provided a comprehensive review of the finite strip method and the differences between the finite element

method and the finite strip method. In summary, the finite strip method is presented as a simplification of the finite element method where the section can only buckle in the longitudinal direction. This is achieved by applying a differentiable smooth series in the longitudinal direction and a simple polynomial function in the transversal direction. Figure 2-56 provides an illustration of this approach. Key (1988) used a finite strip nonlinear elastic-plastic analysis for his model where he included large displacements, material yielding, elastic-plastic and rounded material stress-strain curves, residual stresses, initial geometric imperfections and membrane displacements at the corners. Material yielding is accounted for by applying a rigorous layer approach for the through-thickness treatment of plasticity. Residual stress can vary across the section perimeter and through the thickness. The solution algorithm in his model applied the modified Newton-Raphson method which was chosen over the standard method to reduce the computation time required. Key (1988) bypassed one of the shortcomings of the modified method which lowers its accuracy at large displacements by updating the stiffness matrix during the iteration at some cases.

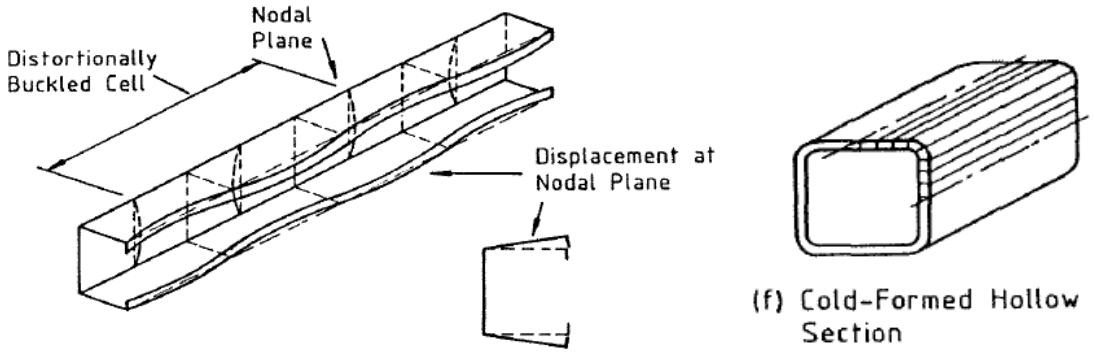


Figure 2-56: Distortionally buckled member (left) and typical section for finite strip discretization (right) (Key, 1988)

The experimental section of Key's thesis (1988) provides data on yield strength distribution, residual stress and out of straightness which was further applied to the finite strip model. The author questions the applicability of the column strength curves as not enough data is available for Australian sections. Since Key's thesis was aimed at understanding the effects of local instability, sections with high b/t ratios were chosen. Table 2-17 provides the sections tested by Key along with the predicted critical elastic buckling stress according to the finite strip model. The sections had a nominal yield strength of 350 MPa and were produced from a semi-killed steel strip with a

nominal yield strength of 250 MPa. They were first rolled into a tubular section with an electric resistance weld and then further roll formed into a square HSS.

Table 2-17: Cold-formed hollow sections tested (Key, 1988)

| Section Geometry $D \times B \times t$ (mm) | $b/t$ | Area of Section ($mm^2$) | $\sigma_{cr}$ † (MPa) |
|---|---|---|---|
| 76 × 76 × 2.0 | 36.1 | 583 | 532.7 |
| 152 × 152 × 4.9 | 29.1 | 2810 | 808.6 |
| 203 × 203 × 6.3 | 30.3 | 4830 | 747.6 |
| 254 × 254 × 6.3 | 38.3 | 6110 | 471.8 |
| $E = 2.0 \times 10^5$ MPa<br>$\sigma_Y = 350$ MPa nominal | | | |

†Elastic critical buckling stress from Program BFINST

This manufacturing process induces residual stress patterns which vary both around the section and through the wall thickness. Key (1988) also identified the roll drag, oversize and undersize feedstock, and forming speed among the factors which can influence the residual stress magnitude at the end of the process. An important reason why the author proceeds to tests specific Australian sections for residual stress is the difference between the manufacturing methods in various factories and different countries. Another significant contribution the author brings in his thesis is the measurement of the through thickness residual stress which Key (1988) states had not been measured in Davison and Birkemoe's (1983) research and was only based on a simplified theoretical model and surface strain measurements from released coupons.

Key (1988) measured the through thickness residual stress using a spark erosion layering technique and the longitudinal released surface strains were measured using electrical resistance strain gauges with the sectioning technique. It is important to note that in Davison and Birkemoe's (1983) paper the "bending" residual stress model includes both the "bending" and "layering" models presented by Key (1988). However, while in Davison and Birkemoe's paper the model is based on theory, Key actually measures the distribution.

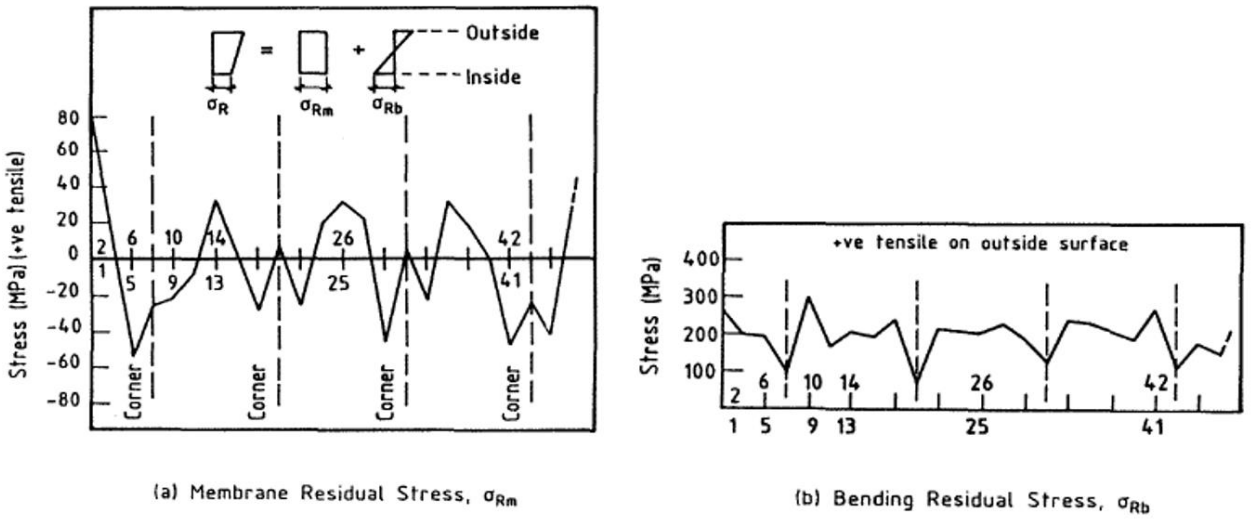


Figure 2-57: Measured residual stress values - Longitudinal (Key, 1988)

The sectioning technique applied by Key (1988) consisted in cutting a 125 mm coupon from a 450 mm section. The coupon was equipped with strain gauges on the exterior and interior faces which were read to determine the released surface strain and curvature. These measures were used to determine the membrane residual stress distribution (across the section's perimeter).

The spark layering technique which Key (1988) used to determine the through thickness variation of the residual stress consisted in three separate steps illustrated in Figure 2-58. The first step was the panel removal after which strains were measured on the exterior and interior surface and corresponds to Figure 2-58-a. This step is equivalent to Figure 2-40-e from Davison and Birkemoe's (1983) paper (elastic unloading stress). This is the step after which Davison and Birkemoe stopped and assumed a theoretical model. A similar distribution and result to Davison and Birkemoe's findings can be seen where the exterior surface is in tension while the interior surface is in compression. This represents the "bending" layer in Key's (1988) thesis. The magnitude of the measured values is also similar. The second step consists in removing small blocks from the panel which is in equilibrium at this stage. This step corresponds to Figure 2-58-b and yields negligent residual stress values. The final step in Figure 2-58-c consists in removing small layers from the block. This provides a new distribution of residual stress and is equivalent to Figure 2-40-f in Davison and Birkemoe's paper (1983) (state of residual stress in released coupon). The measured values for the membrane residual stress and the released bending residual stress are shown in Figure 2-60.

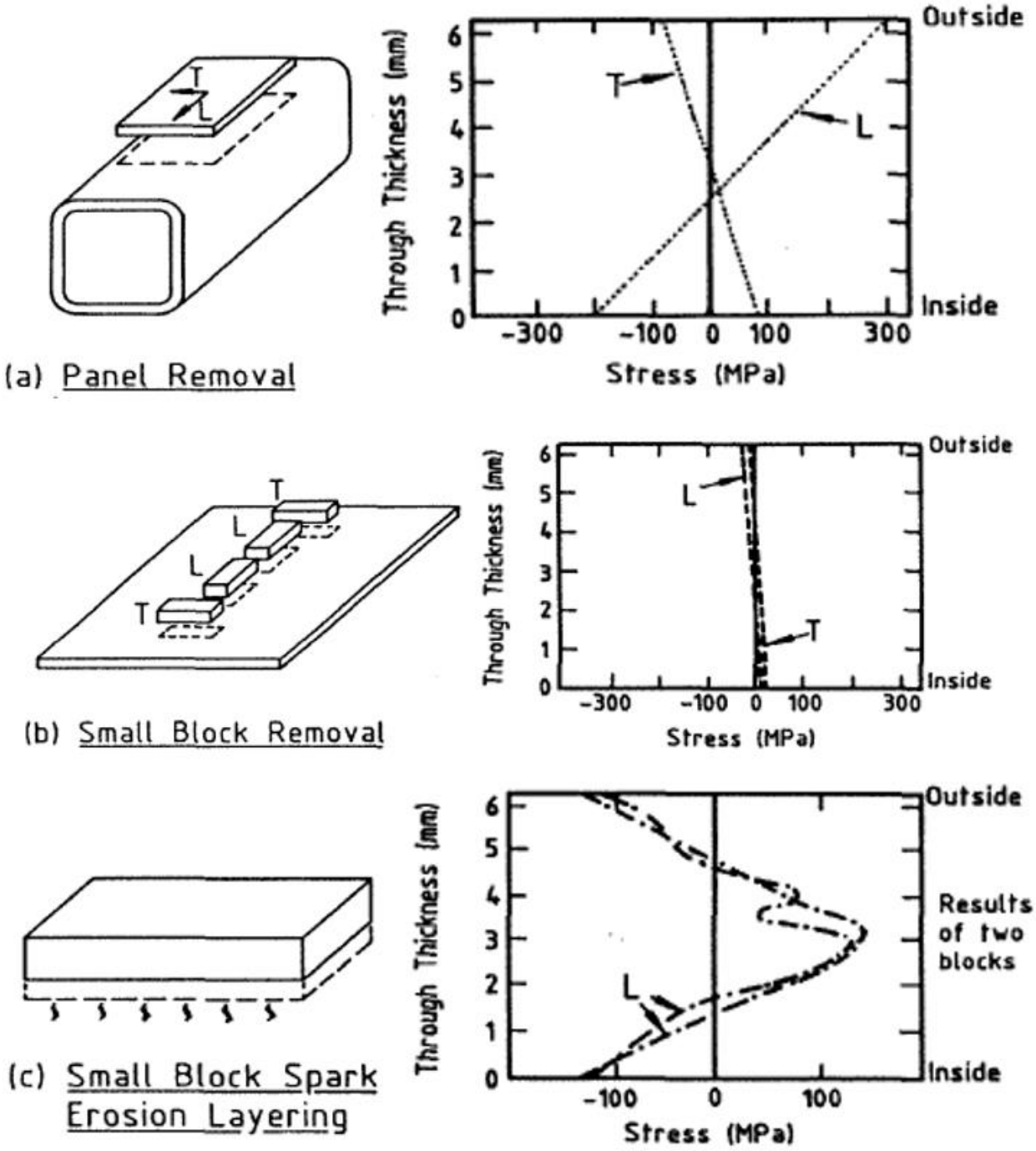


Figure 2-58 : Spark layering technique procedure - Longitudinal (Key, 1988)

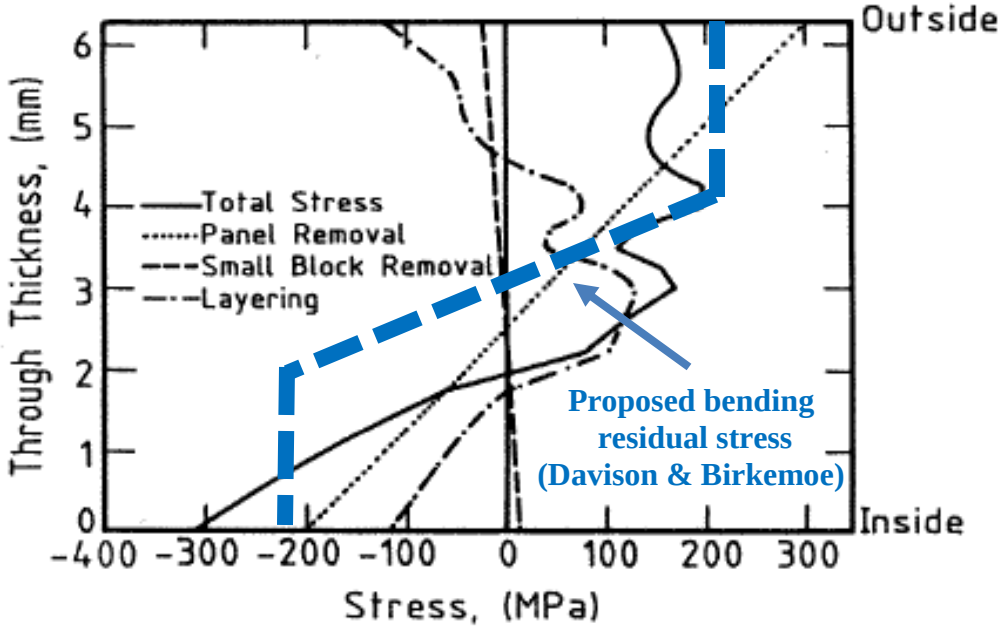


*Note: The fat dashed blue line represents Davison and Birkemoe's (1983) distribution.*

Figure 2-59: Measured final through thickness residual stress in longitudinal direction (Key, 1988)

The final through thickness residual stress distribution in Key's (1988) thesis corresponds of the algebraic sum the "membrane", "bending" and "layering" components corresponding to Figure 2-60. The transverse residual stress was also determined, and its proposed model is shown in Figure 2-61. It can be seen both Key's (1988) and Davison and Birkemoe's (1983) models are quite similar. The main difference arises from the geometric shape Davison and Birkemoe gave to the remaining residual stresses within the coupon which would correspond to the layering residual stresses in Key's model. This shape was slightly different but both models seem to be equivalent judging by Figure 2-59.

The final residual stress profiles with their values, in Key's (1988) model, are shown in Figure 2-62. The values were of 30 MPa for the membrane component, the bending component had a maximum of 200 MPa with the through thickness distribution shown in Figure 2-62-a, the layering component had a maximum of approximately 130 MPa with the through thickness distribution shown in Figure 2-62-b. Key specifies that the factor X shown in Figure 2-62 refers to the fact that residual stress values for the through thickness distribution in Figure 2-60 are not for the same section as the membrane distribution shown in Figure 2-62. Figure 2-60 refers to section 254 x 254

x 6.3 while Figure 2-62 refers to section 152 x 152 x 4.9. The residual stress measured in 152 x 152 x 4.9 is 20% smaller than the residual stress measured in 254 x 254 x 6.3.

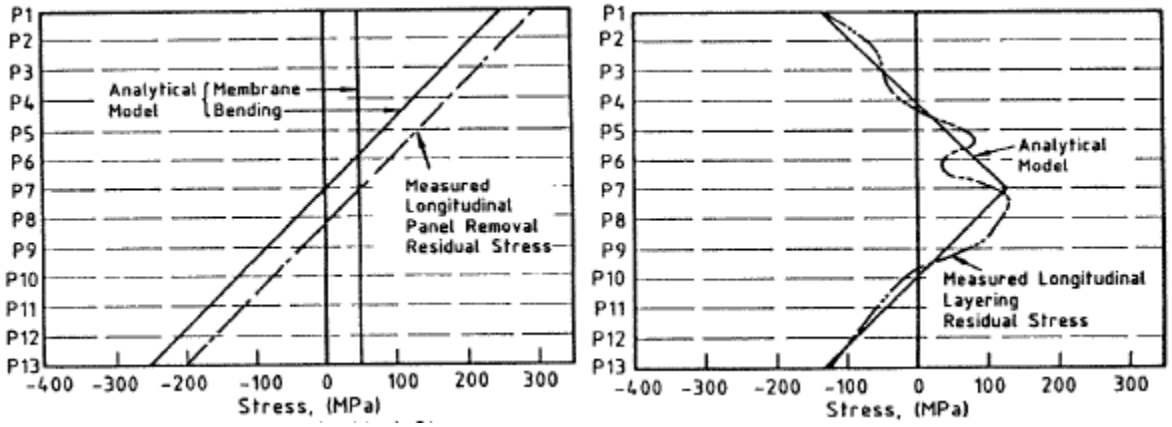


Figure 2-60 : Adopted through thickness residual stress profile - Longitudinal (Key, 1988)

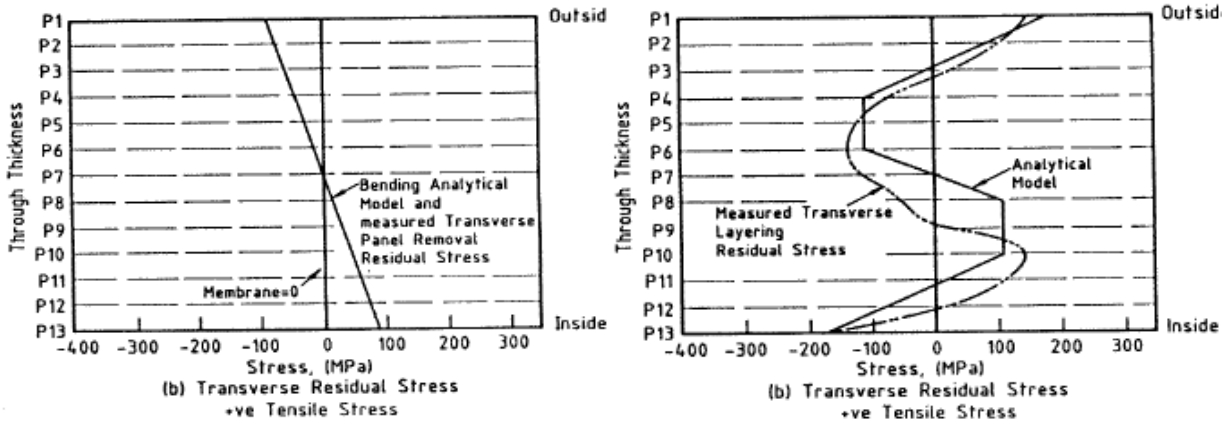


Figure 2-61: Adopted residual stress profile – Transverse (Key, 1988)

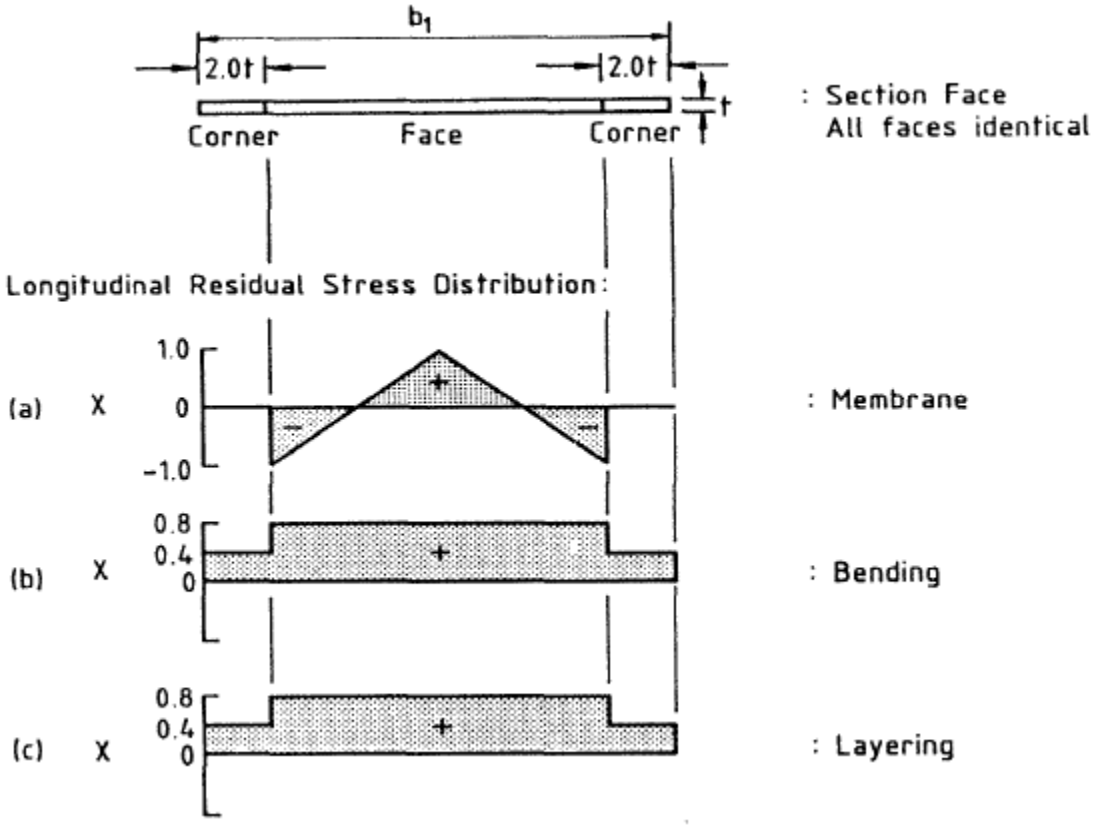


Figure 2-62 : Adopted residual stress profile across the section (Key, 1988)

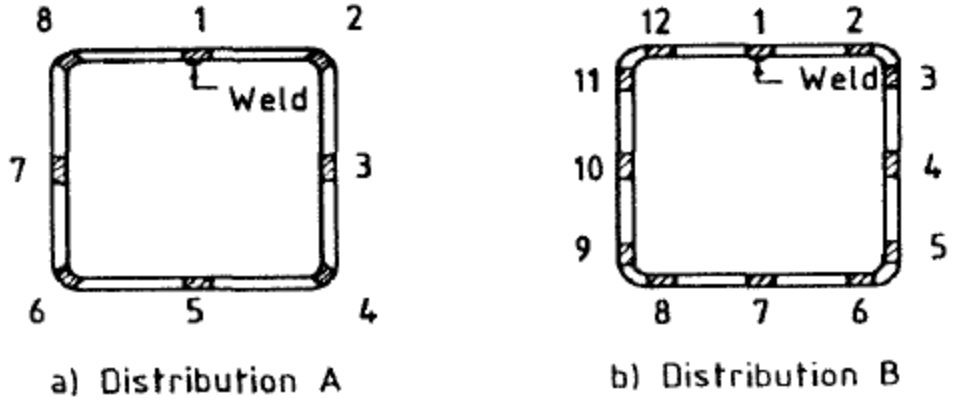


Figure 2-63 : Tensile coupon positions (Key, 1988)

As it is already known at this stage, cold work increases the yield strength of the section while reducing ductility. This increase is not uniform with the corners being subjected to a significantly higher increase than the flat wall of the HSS. To implement this behavior in his thesis, Key (1988) sectioned a tube and took tensile coupons from different positions to obtain the yield strength distribution variation across the tube's face. The three sections tested were 76 x 76 x 2.0, 203 x

203 x 6.3 and 254 x 254 x 6.3 with the coupon positions shown in Figure 2-63. Figure 2-64 shows some of the obtained results and Table 2-18 shows a summary of the results for all the tested sections.

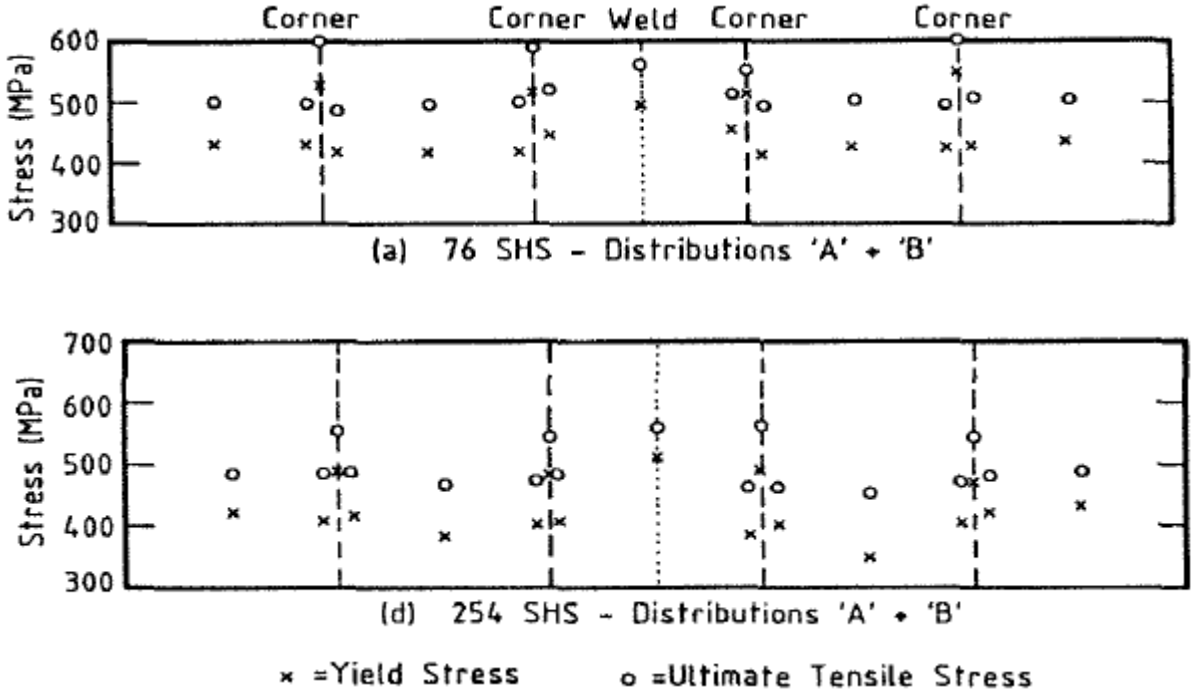


Figure 2-64 : Tensile stress in sectioned coupons (Key, 1988)

Table 2-18: Average yield strength per section (Key, 1988)

| SECTION | VIRGIN MATERIAL | | | | FORMED MATERIAL | | | | | |
|---|---|---|---|---|---|---|---|---|---|---|
| | $\sigma_Y^*$ (Mpa) | $\sigma_U^*$ (Mpa) | $\epsilon_{un}^*$ (%) | $\sigma_U^*/\sigma_Y^*$ | Location | $\sigma_Y$ (Mpa) | $\sigma_U$ (Mpa) | $\epsilon_{un}$ (%) | $\sigma_U/\sigma_Y$ | $\sigma_Y/\sigma_Y^*$ |
| 76 SHS | 327 | 457 | 19 | 1.40 | Face | 425 | 499 | 5.4 | 1.17 | 1.30 |
| (Series 1) | | | | | Corner | 531 | 588 | 2.3 | 1.11 | 1.62 |
| 76 SHS | 327 | 457 | 19 | 1.40 | Face | 370 | 449 | 9.0 | 1.21 | 1.13 |
| (Series 2) | | | | | Corner | 476 | 522 | 2.8 | 1.10 | 1.46 |
| 152 SHS | 302 | 454 | 14.8 | 1.50 | Face† | 416 | 475 | 5.4 | 1.14 | 1.38 |
| | | | | | Corner | 498 | 573 | 2.8 | 1.15 | 1.65 |
| 203 SHS | 312 | 511 | 20.6 | 1.64 | Face | 395 | 494 | 8.7 | 1.25 | 1.27 |
| | | | | | Corner | 520 | 604 | 4.2 | 1.16 | 1.67 |
| 254 SHS | 312 | 511 | 20.6 | 1.64 | Face | 405 | 479 | 8.4 | 1.18 | 1.30 |
| | | | | | Corner | 487 | 555 | 3.3 | 1.14 | 1.56 |

†Centre face yield stress and UTS factored by 1.05 (see main text).

It is important to note Key (1988) did not obtain a detailed distribution for the 152 x 152 x 4.9 section and the values in Table 2-18 assume the same distribution as the 203 x 203 x 6.3 section. It is noted by Key, the increase of yield strength in the flat section is not as pronounced as it could be in his investigation due to the b/t ratio being very large. However, previous research had already established this tendency. The ductility of the material decreased after the cold work compared to the virgin material. This is particularly pronounced in the corners which have an ultimate to yield strength ratio of 1.14. Key defines ductility as the ability of the material to undergo plastic deformation without fracture. As Key points out, it was previously found that to ensure the ductility of the material, uniform elongation should be greater than 3%, ultimate to yield ratio should be greater than 1.05 and local elongation should be greater than 20%. Significant differences in strain-stress curves are also noted between the flats and corners as the flats display a well-defined yield plateau and some rounding while the corners display no yield plateau and significant rounding. Key noted that strain aging the section can help it recover part of its virgin yield plateau. This is only true for sections that have undergone strains below 10% in the direction transverse to subsequent testing. Key specifies this was established in the 1960s research performed by Britvec et al. (1970).

Table 2-19: Stub column strength results (Key, 1988)

| SECTION | b/t | Stub Column Length (mm) | $P_{Sult}$ (kN) | $P_{Ycoup}$ (kN) | $\frac{P_{Sult}}{P_{Ycoup}}$ | $P_{Yn}$ (kN) | $\frac{P_{Sult}}{P_{Yn}}$ |
|---|---|---|---|---|---|---|---|
| 76 SHS (Ser. 1) | 36.1 | 300 | 243 | 252 | 0.96 | 204 | 1.19 |
| 76 SHS (Ser. 2) | 36.1 | 300 | – | – | – | 204 | – |
| 152 SHS | 29.1 | 510 | 1283 | 1194 | 1.07 | 984 | 1.30 |
| 203 SHS | 30.3 | 1010 | 2010 | 1970 | 1.02 | 1691 | 1.19 |
| | | | 2015 | | 1.02 | | 1.19 |
| 254 SHS | 38.3 | 1280 | 2420 | 2515 | 0.96 | 2139 | 1.13 |
| | | | 2500 | | 0.99 | | 1.17 |

After defining a residual stress model and determining the yield strength distribution of the tested tubes, Key (1988) determined their stub column strength. Table 2-19 presents the obtained results where the ultimate stub column strength is compared to the nominal strength, the factored coupon

yield strength, and the nominal yield strength. The factored coupon yield strength consists of the weighted average between the flat and corner yield strength that was determined earlier.

The various properties determined throughout the Australian study (Key, 1988) were included in the finite strip model. The residual stress distribution adopted in the model is shown in Figure 2-62 and Figure 2-60. The yield strength distribution adopted in the model is shown in Figure 2-65. The flats were modeled with an elastic plastic curve while the corners were modeled with a Ramberg-Osgood equation with an *n* factor of 15.

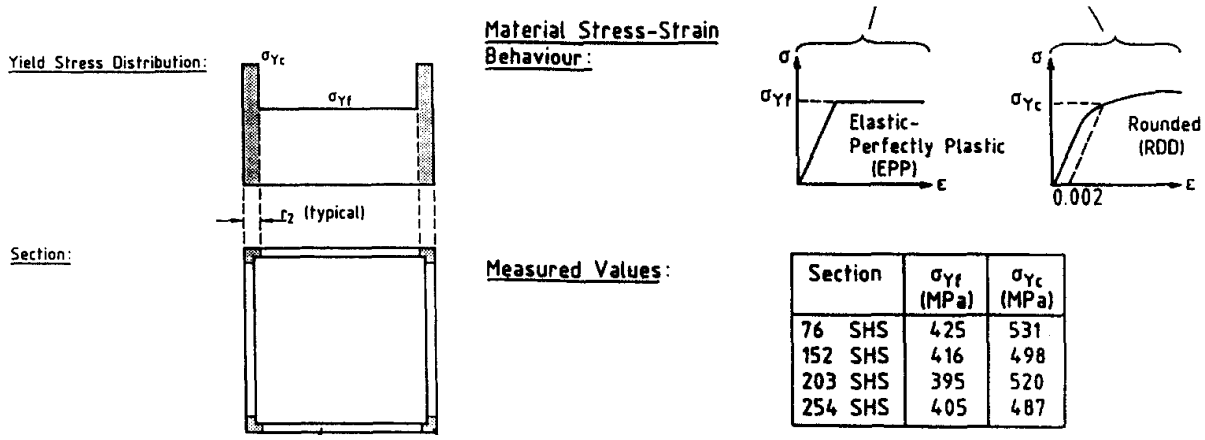


| Section | $\sigma_{Yf}$ (MPa) | $\sigma_{Yc}$ (MPa) |
|---|---|---|
| 76 SHS | 425 | 531 |
| 152 SHS | 416 | 498 |
| 203 SHS | 395 | 520 |
| 254 SHS | 405 | 487 |

Figure 2-65: Yield stress distribution adopted in theoretical model (Key & Hancock, 1993)

The next section in Key's (1988) investigation consisted of comparing the experimental stub and pin ended column tests to the finite strip model which was based on experimental properties. Figure 2-66 shows the finite element discretization adopted by Key for the pin and stub column models.

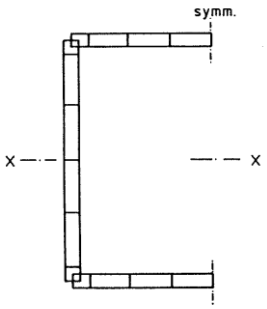


Figure 2-66 : Finite strip discretization (Key, 1988)

The length of the experimental stub column was of at least three times the section width while the finite strip model had a length of about one section width. Key (1988) chose this to represent a local buckle wavelength of the section. Parametric studies were performed to determine the

influence of various parameters on the section's behavior. At first the author proceeded to analyze certain parameters on a nominal section with no increased yield strength or residual stress. Those parameters were the bow-out of the section's face and whether using rounded corners was necessarily in contrast to two strips forming a rectangular corner. Key determined both factors had little effect on the final results and did not include them. Another two parameters which were included in the analysis were the shape of the stress-strain curve (rounded or purely elastic-plastic) and the local geometric imperfections. An adverse and sympathetic imperfection was studied. It was determined the small geometric imperfections measured on the actual section had a significant impact on the ultimate load. A sympathetic imperfection can decrease the ultimate load up to 14.4%. An adverse imperfection resulted in a decrease in ultimate load of up to 5.2%.

Key (1988) also found it wasn't necessary to model the actual rounded corner. Two strips forming a right angle were enough to obtain accurate results. Another factor studied in the model was the face bow-out of the section. Key found this parameter does not significantly influence the model with only a very slight increase in ultimate stress (0.6%) and it was not included in his model.

An extensive parametric study was conducted by Key (1988) to determine the influence of the various residual stress parameters specified earlier. Key used thirteen-layer points through the section to illustrate the residual stress variation. Each layer point represented the average of all the parameters. In Key's words, the following conclusions were reported from the parametric study on the stub column:

- *Membrane residual stress is in tension over the central part of the section and in compression closer to the edges. Its influence over the pre-ultimate behavior and ultimate load is not significant and only results in a slight increase at ultimate load.*
- *Once the bending residual stress is added a significant difference in behavior can be seen. The ultimate load is decreased between 1.9 and 5.4% and the axial stiffness is reduced from 3.5 to 9.1 percent for a* $\sigma_m/\sigma_o$ *of 0.7.*
- *The addition of the layering component does not significantly affect the behavior at ultimate load but does reduce the axial stiffness.*
- *The addition of the transverse residual stress decreases the ultimate load by up to 1.2% and decreases the axial stiffness in the early stages of loading.* (Key, 1988, p.215)

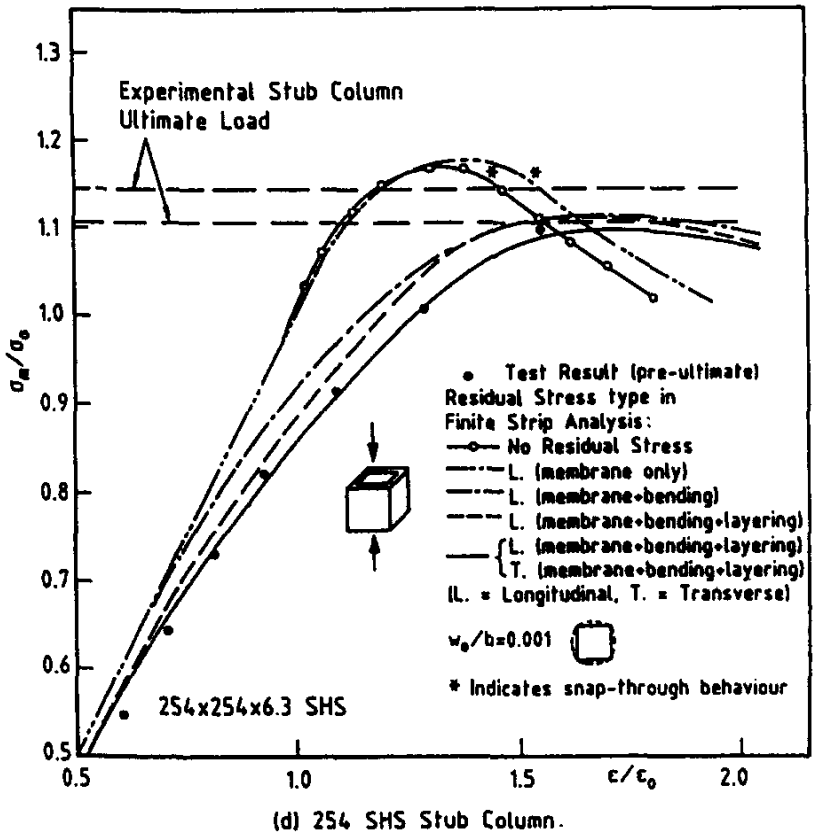


(d) 254 SHS Stub Column.

Figure 2-67: Residual stress parametric study (Key & Hancock, 1993)

Key (1988) concluded that his finite element model is generally in good agreement with the experimental investigation except for one section where it was not possible to explain the discrepancy when evaluating the stub column strength. The ductility was also evaluated, and it was concluded slender sections show a far better agreement with experimental results than stockier sections. However, Key reported adopting an experimentally measured Ramberg-Osgood (n=15) rounded stress-strain curve for corners resulted in a better agreement between experimental and theoretical ductility ratios. Finally, the plastic mechanism model is introduced in the finite strip model and the behavior is compared. It is determined the ultimate load and post-ultimate behavior is in good agreement with the experimental results. Figure 2-67 shows the residual stress influence over the section behavior for one section.

After analyzing stub column behavior Key (1988) proceeded to test pin-ended columns by loading them concentrically and eccentrically at an imperfection of 1/5000, previously defined average by (Key & Hancock, 1985), and 1/1000. A similar parametric study to the stub column was conducted and is summarized in Figure 2-68.

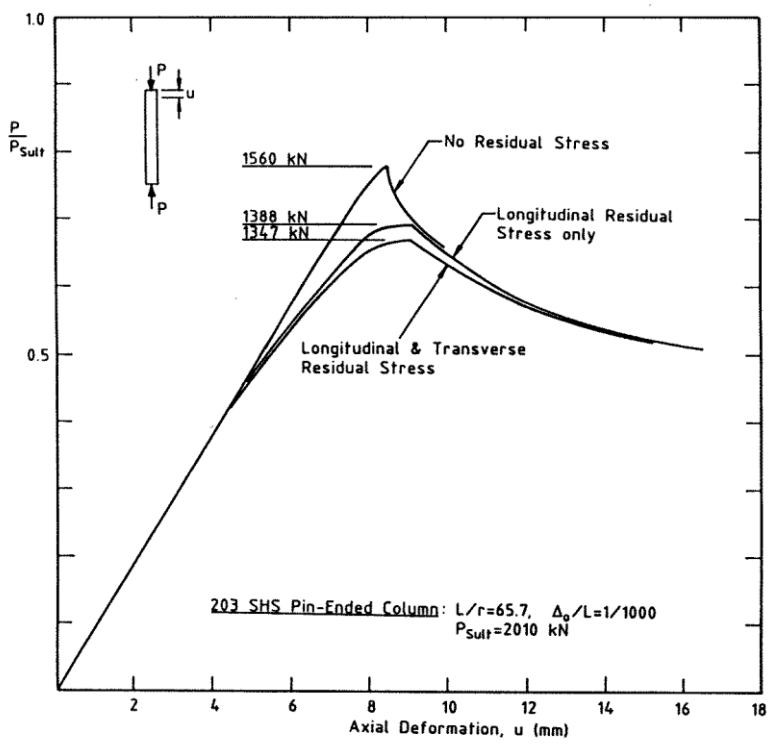


Figure 2-68: Influence of Residual Stress on SHS Pin-Ended Column Behaviour (Key, 1988)

Key (1988) found that including the transverse residual stress in the 203 SHS section with a 1/1000 imperfection decreases the maximum load by 3.1% and considers it an important factor in the final behaviour. The difference between the layering residual stress versus the membrane and bending residual stresses is insignificant (0.25%). The difference between a case with all residual stresses and no residual stress was determined at 15.8%.

The difference between the code proposed 1/1000 imperfection and the average 1/5000 measured imperfection (Key, 1988) was studied. It was found the 1/1000 imperfection overestimates the maximum load by 2.9 to 6.6% for the 203 SHS section (b/t = 30.3) which was loaded eccentrically in this case. This was partly attributed to the sinusoidal imperfection distribution in the model and a uniform distribution in the experimental specimen. The 1/5000 imperfection overestimated the maximum load by 1.4 to 6.9% compared to experimental results.

It is also reported the 76 SHS section (b/t = 36.1) did not show the same level of agreement between the experimental results and the theoretical model. The eccentric maximum load was 11.5% to 13.8% lower for the model compared to the experimental values. The column failed due to a sudden plastic mechanism formation as previously explained by Key (1988).

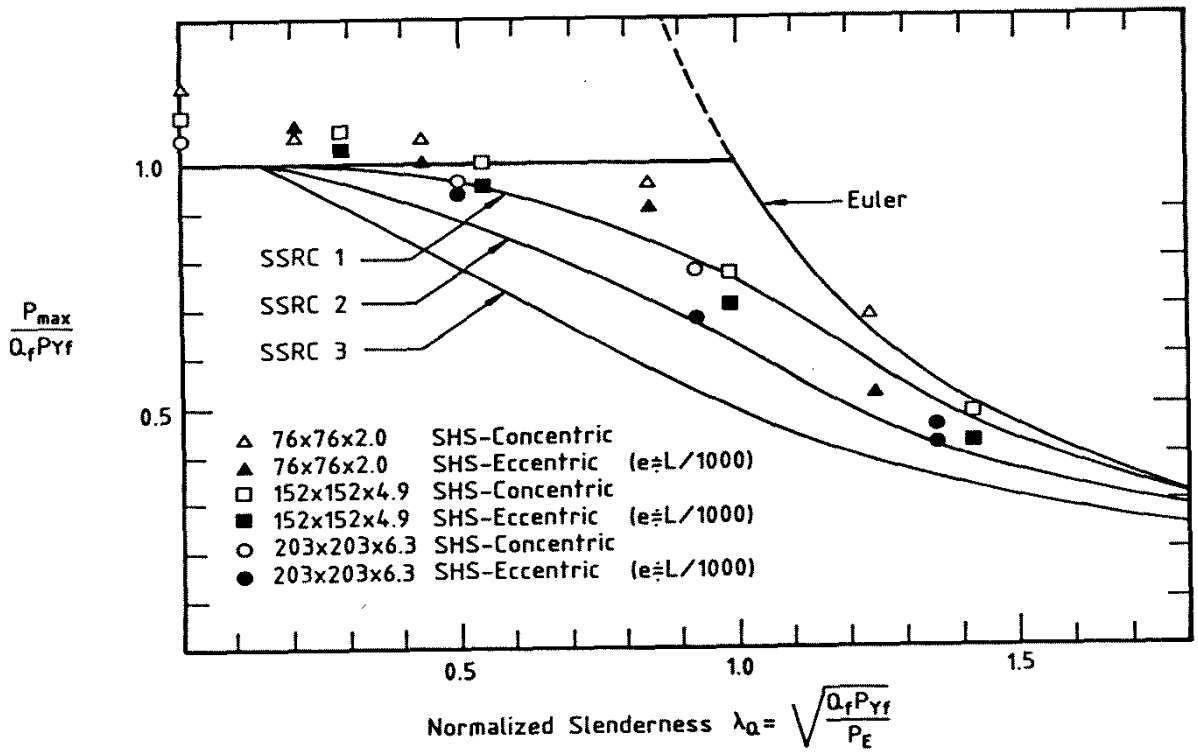


Figure 2-69: Comparison of Test Results and Codes (Key, 1988)

Finally, the last section of Key's thesis (1988) consisted in comparing the design curves to the experimental results in order to determine their accuracy. Figure 2-69 summarizes the results. The L/1000 value represents the eccentricity at which the load was applied. The results are normalized with respect to $P_{yf}$ which is the yield load based on the average obtained from the coupons.

Based on these results, Key (1988) proposes to classify the current sections under the SSRC curve 2. It is pointed out this is in agreement with previous research performed by Bjorhovde (1977) and Davison and Birkemoe (1983), who tested Canadian produced sections, and Kato (1977) who Japanese produced sections. It is however noted that Kato came to the conclusion that Curve 1 was more appropriate for cold-formed SHS sections when the results were normalized with respect to the minimum specified yield stress and Curve 2 was more appropriate when the results were normalized according to the average stub column yield stress.

The eight years of extensive research on cold-formed hollow sections undertaken at the University of Sydney were finally summarized in a paper titled "*A Theoretical Investigation of the Column Behavior of Cold-Formed Square Hollow Sections*" (Key & Hancock, 1993). Any new information available in this paper has already been included throughout the previous review.

Wilkinson (1999) further added another paper titled "*The Plastic Behavior of Cold-formed Rectangular Hollow Sections*". The author's goal was to assess the suitability of cold-formed HSS members in the plastic design of portal frame structures. Wilkinson developed appropriate design rules for cold-formed SHS and RHS members and specifically addresses slenderness limits. He studied C350 and C450 material grade members and carried out an experimental investigation composed of bending tests, connection tests and tests on pinned-base portal frames to achieve this goal. A finite element analysis was also performed to simulate bending tests along with a parametric study on the elements influencing the results. While the current investigation is on concentrically braced frames and not portal frames, Wilkinson did report relevant results regarding material properties.

The C350 grade material are standard 350 MPa nominal yield strength members, while the C450 grade material undergoes in-line galvanization. Both material grades start with the same 300 MPa virgin coil, but the C450's grade yield strength increases to 450 MPa due to the additional in-line galvanization process. The respective tensile strengths were of 430 and 500 MPa. Wilkinson (1999) also points out previously identified behavior patterns in cold-formed steel, such as the fact it does not have a well-defined yield plateau, and strain hardening begins right after yielding. The corners also tend to have a much smaller ductility ratio compared to the flat sections of the specimen due to the extensive cold work they are subjected to. The yield stress of the section increases as the corner radius decreases. This means more cold work has been applied to the corner.

Wilkinson (1999) determined various section properties through tensile coupon tests, full section tensile tests and stub column tests. Coupon tests were taken on three of the flat faces excluding the weld and the corners.  Figure 2-70 shows the position of the coupons.

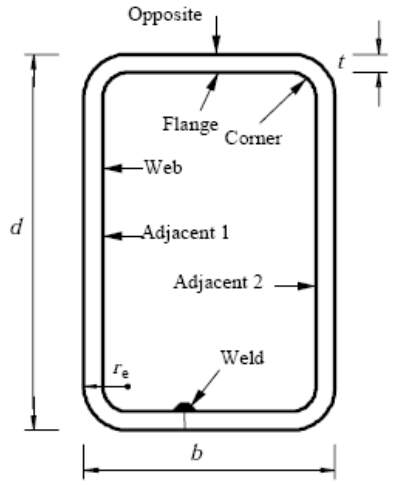


Figure 2-70: Typical RHS section (Wilkinson, 1999)

Figure 2-71 shows an example of the yield strength distribution obtained from the faces and corners in Wilkinson's tests. The rest of Wilkinson's results were included in Chapter 3.

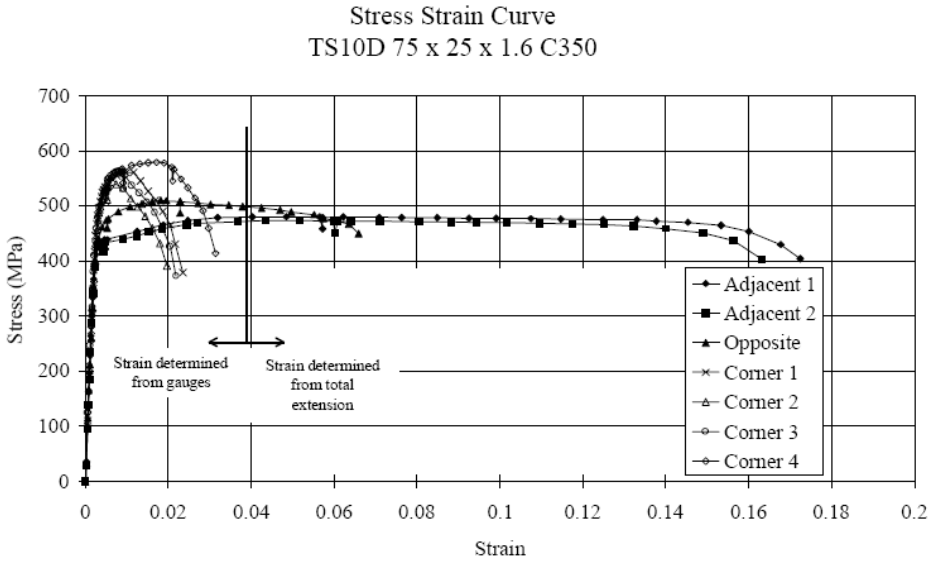


Figure 2-71: Typical stress strain curve for cold-formed sections (Wilkinson, 1999)

Wilkinson (1999) reported the increase in yield strength is not uniform across the faces. The face located opposite to the weld is about 10% higher than the yield strength of the adjacent faces, and the corner's yield strength is approximately 20% higher than the opposite face. It is also noted that as the D/t ratio decreases a clear difference is seen between the flat specimens and the corner specimens.

Figure 2-72 shows the stress strain curve where the full section results are compared to the coupon results. The tested sections had a D/t ratio of 42. It is noted the specimen fractured at the corner and the fracture moved to the web until the whole member was sectioned. Wilkinson (1999) also performed stub column tests and reports the maximum load was 10 – 20% higher than the weighted average of the adjacent face coupons.

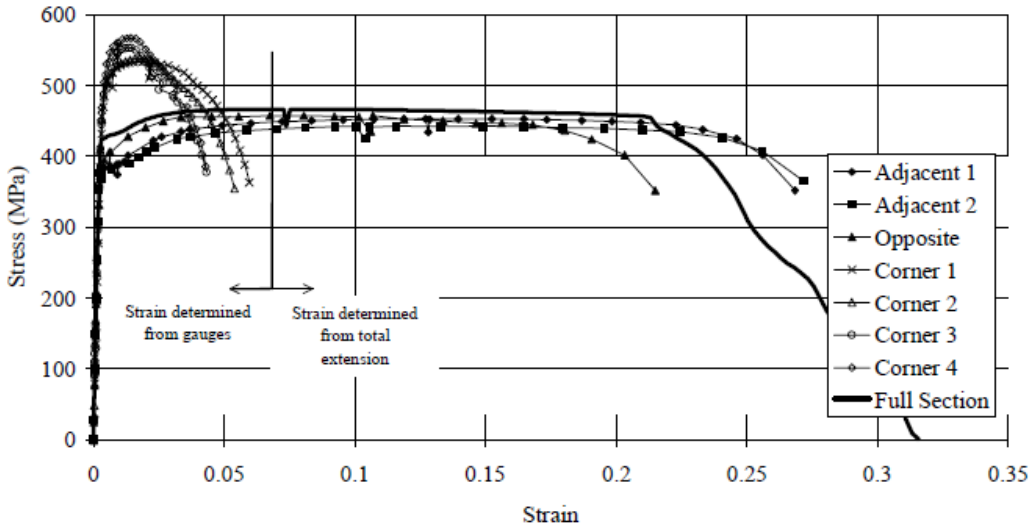


Figure 2-72 : Full section test vs coupon tests (Wilkinson, 1999)

A short mention of residual stress is also presented with an interesting observation. Wilkinson (1999) did not explicitly include residual stress in his numerical model, but it is stated the bending residual stress is already included in the coupon data. This is explained by the fact the coupon was straightened when introduced in the testing machine after being significantly bent when originally removed from the section. Hence the bending component was reintroduced at the testing stage. As for the layering residual stresses, it is stated they are already included in the full section tests. The only residual stress component which was completely ignored was the membrane component which Wilkinson states does not play a big role in the final behavior due to its significantly smaller magnitude. Finally, Wilkinson reported average residual stress magnitudes presented by Key and Hancock (1993) which were of 80 MPa for the membrane residual stress, 300 MPa for the bending residual stress and 100 MPa for the layering residual stress.

#### 2.3.1.1 Summary

To summarize, a major investigation into cold-formed HSS members from the mid 1980s up to the late 1990s was undertaken at the University of Sydney. This investigation was led by Key, Hancock, Hassan and later Wilkinson. The investigation confirmed previous findings in the 1970s research effort, in particular, Davison and Birkemoe's (1983) theoretical residual stress model. The research effort at University of Sydney, however focused on very slender sections. Specifically, the interaction between local buckling and post-ultimate behavior. The tested sections were regular cold-formed 350 MPa HSS sections up until Wilkinson's research. Wilkinson added sections with a nominal yield strength of 430 MPa.

In the first investigation, titled "*An Experimental Investigation of the Column Behavior of Cold-formed Square Hollow Sections*" (Key & Hancock, 1985), the properties of four different sections were determined. An experimental investigation was performed on the yield strength, residual stress, out-of-straightness, stub column strength and pin-ended column strength of the HSS members. It was observed that the average longitudinal residual stress is about half of the nominal yield strength. For the 350 MPa nominal yield strength sections the membrane residual stress was of about 30 to 40 MPa. The released bending residual stress was of about 200 MPa which corresponds to a 140 MPa through thickness residual stress according to Davison and Birkemoe (1983) research. A residual stress of only 80 MPa was determined on the welding line. On average, the membrane residual stress was set at about 15%, while the bending residual stress was set at about 70% of the actual yield strength. The yield strength distribution was determined from a sectioned member. Coupons were taken from the center of the flat, the corner and the flat part next to the corner. The average yield strength was determined at about 400 MPa and the flat section was fairly uniform. The corners and the weld were significantly higher. This observation confirms Davison and Birkemoe's proposition (1983) for a step function to be used for sections with high b/t ratios. A distinct stress-strain curve was seen in the corners compared to the flats. The flat coupons had regained their sharp yield plateau, while corner coupons had a rounded curve with an inelastic behavior. This is explained by strain aging. It is noted the material is able to regain its original sharp yield as long as it doesn't experience significant strains. It was shown cold work significantly decreases the ductility of the material. Elongation decreased by 10% compared to the virgin material. This was seen for individual coupons, however, full stub column sections still showed significant elongation. The stub column strength was 13 to 30% greater than the nominal

yield strength. The average out-of-straightness was determined at 1/6600. Finally, the experimental results were compared to North American and European column strength curves. The SSRC curve 2 was considered to be the best fit to represent the tested sections. Key and Hancock (1983) also propose a new curve by adjusting the SSRC curve.

A problem that was noticed in very slender sections is the sudden post-ultimate load shedding and it is addressed in the second investigation titled "*Plastic Collapse Mechanisms for Cold-formed Square Hollow Section Columns*" (Key & Hancock, 1986). This research is included for completion of the investigation conducted at University of Sydney, but it is not fully relevant to the current review. Key and Hancock (1986) proposed a model of a plastic collapse mechanism that accounts for corner yielding and increased yield strength across the section. One model was proposed for the stub column and another one for the pin-ended column. The stub column model was composed of three mechanisms: Corner yielding, plate folding and folding corner restraint. The pin-ended column mechanism was exactly the same as the stub column one except for a channel folding mechanism that was added. The models were compared to experimental results and the authors concluded they are in good general agreement with each other.

The last two investigations were finally summarized in an article titled "*Column Behavior of Cold-formed Hollow Sections"* (Key & Hancock, 1988). Some new information was added such as the slenderness at which columns are most likely to experience a sudden load-shedding plastic mechanism collapse. This slenderness was established to coincide to a b/t ratio ranging from 30 to 50. The AISI column strength curves were also studied and it was concluded the class A curve is the most appropriate for cold-formed sections.

The third investigation was a thesis titled "*The Behavior of Cold-Formed Square Hollow Section Columns*" (Key, 1988) in which cold-formed sections were analyzed through a large displacement nonlinear finite strip analysis model. Key concentrated his research on slender sections and post-ultimate behavior. This investigation was a major step in the study of residual stresses in cold-formed sections. It was separated in two parts. The first part was composed of an experimental investigation to determine the residual stress pattern and yield strength gradient in cold-formed sections. The residual stress investigation went a step further than Davison's investigation in 1977. Davison only determined the elastic unloading bending stress of a coupon and proposed the bending residual stress from theoretical assumptions. Key actually measured the bending stress in

the released coupon through a spark erosion layering technique and proposed a third component to the residual stress distribution. Key's model (1988) is composed of a membrane, bending and layering component. Davison's model (1977) has a membrane and bending component which already includes Key's layering component. Key does not dispute Davison and Birkemoe's (1983) findings and states both models are in good agreement with each other. The membrane residual stress was measured at approximately 30 MPa in Key's investigation. It was found to be in tension over the central part and in compression at the edges. The released bending residual stress was found to be approximately 200 MPa and was somewhat uniform across the section except for the corners where it dropped to approximately 120 MPa (seen in Key's figures). The layering component had a maximum of approximately 130 MPa. A similar distribution to the longitudinal direction was obtained in the transverse direction for the released bending residual stress but of much smaller magnitude. The layering transverse residual stress had a complicated trapezoidal shape with maximum magnitudes similar to the longitudinal one. Key's theoretical model included both the longitudinal and transverse residual stresses. The yield strength of the flat sections was of approximately 400 MPa and no significant variation between the center and the coupons closer to the edges was seen. The corner yield strength was of approximately 500 MPa. A step function model was adopted for the yield strength gradient as proposed by Davison and Birkemoe (1983). This is once again explained by the very high b/t ratio of the tested sections. It is noted the ductility of the material decreases as cold work increases. The corners show a very good representation of this theory as their yield to ultimate ratio is of only 1.14. Once again, the difference between the rounded corner stress-strain curves and the sharp yielding flat coupon curves is noted. Strain aging can help recover the yield plateau as long as the sections have undergone strains below 10% in the direction transverse to subsequent testing. Key adopted an elastic plastic curve for the flats and a Ramberg-Osgood curve equation with an n factor of 15 for the corners. The stub column strength was 13 to 30% higher than the nominal yield strength. The author studied the effects of several parameters through the finite strip model. It was determined taking two square corner strips was enough to obtain accurate results and rounding them to represent the actual geometric shape was not necessary. Local geometric imperfections significantly affected the behavior decreasing the ultimate load up to 14.4% for a sympathetic imperfection and 5.2% for an adverse imperfection. The membrane and layering components of residual stress did not significantly affect results but slightly reduced the axial stiffness. The transverse residual stress decreased the ultimate stress up

to 1.2% and decreased the axial stiffness at early loading stages. The bending residual stress has a very significant impact and the ultimate load is decreased from 1.9 to 5.4%. The axial stiffness was decreased from 3.5 to 9.7%. Finally, the plastic mechanism was added to the finite strip model. it was concluded experimental results are in good agreement with the theoretical stub column model. The pin-ended column model was evaluated at an imperfection of 1/5000 and 1/1000. It was concluded both imperfection levels in the model overestimate the maximum load. The section with a b/t of 30.3 showed far better agreement with the experimental results than the section with a b/t of 36.1. Key finally compared the experimental values to the SSRC curves. Curve 2 was proposed for cold-formed sections, but at low slenderness values curve 1 is more representative.

The eight years of research were finally summarized in an article titled "*A Theoretical Investigation of the Column Behavior of Cold-Formed Square Hollow Sections*" (Key & Hancock, 1993).

The final investigation in this section is titled "*The Plastic Behavior of Cold-formed Rectangular Hollow Sections*" (Wilkinson, 1999). The goal in thesis was to assess the suitability of cold-formed HSS members in the plastic design of portal frame structures. Appropriate design rules for cold-formed SHS and RHS members were developed and slenderness limits were addressed. Two steel grades were tested: C350 and C450. A finite element analysis to simulate bending tests was performed and experimentally determined material properties were included in the model. A parametric study was also performed to assess the impact of various properties. Wilkinson reviewed and confirmed several affirmations that were made about cold-formed steel in previous investigations. These affirmations are the following: " *(a) there is no yield plateau in corners, (b) the corners have a much smaller ductility ratio than the flats, (c) strain hardening begins right after yielding, (d) the corner ductility ratio is significantly smaller than the flats due to the extensive cold work, (e) as the corner radius decreases, the yield strength increases*" (Wilkinson, 1999, p351-352). It was observed the face opposite to the weld has a yield strength 10% higher than the faces adjacent to the weld. The corner's yield strength tends to be approximately 20% higher than the opposite face. As the D/t ratio increases (check increase or decrease) a clear difference is seen between the flat and corner specimens. Specimens mostly fractured at the corners and the fracture moved towards the web until the whole member was sectioned. The stub column results were 10 to 20% higher than the weighted average of the adjacent face coupons. Finally, while the residual stress was not specifically studied, Wilkinson reported average values from Key's paper (1988). An average of 80 MPa was reported for the membrane residual stress, 300 MPa for the bending

residual stress and 100 MPa for the layering residual stress. It is interesting to point out Wilkinson reported 80 MPa as the average value for membrane residual stress as being reported by Key (1988). This was the value reported by Davison and Birkemoe (1983) and Key actually specified he obtained a significantly smaller value. Key (1988) states Davison and Birkemoe's value (1983) of 80 MPa seems too high compared to the average 30 MPa Key measured.

## 2.4 Recent developments in the research of cold-formed members

During the last part of the 20th century, research into cold-formed sections had been highly localized. The first major effort was undertaken by researchers in North America who developed the CSA S136 standard equation to account for strain hardening and increased yield strength in cold-formed sections. In the 1970s, another research effort was undertaken by North American and universities to develop the multiple column curve concept and the first residual stress model for cold-formed sections was developed. During the mid-1980s to the late 1990s a significant effort was undertaken at University of Sydney, Australia. These series of investigations added a new residual stress component to the previously defined model and confirmed previous results. The 21st century research into cold-formed sections wasn't as centralized as the previous brackets and articles were around the world. A significant number of articles were written in China where thick cold-formed members only appeared and began to take market value in the late 1990s. Thick cold-formed sections had been available in North America for several decades at that point. Several articles were also published where non-carbon cold-formed members were studied. Some articles centered their research on stainless steel sections while others studied high strength steel sections. Several residual stress measurements were taken, and most confirmed previous models proposed in the 1970s and 1990s. The list of studied articles in this section is provided below.

- *Shake Table Resting of Tubular Steel Bracing Members,* (Elghazouli et al., 2005).
- *Seismic Behavior of HSS Bracing Members according to Width–Thickness Ratio under Symmetric Cyclic Loading* (Han et al., 2007).
- *Experimental study on compressive strengths of thick-walled cold-formed sections* (Guo et al., 2007).
- *Residual Stresses in Roll-formed Square Hollow Sections* (Li et al., 2009).
- *Comparative Experimental Study of Hot-rolled and Cold-formed Rectangular Hollow Sections* (Gardner et al., 2010).
- *The Cold Work of Forming Effect in Steel Structural Members* (Gao and Moen, 2010).
- *Material Properties of Thick-wall Cold-rolled Welded Tube with a Rectangular Square Hollow Section* (Hu et al., 2011).

- *Cold-forming Effect Investigation on Cold-formed Thick-walled Steel Hollow Sections* (Li et al., 2010).
- *Experimental Investigation on Longitudinal Residual Stresses for Cold-formed Thick-walled Square Hollow Sections* (Tong et al., 2012).
- *Strength Enhancement in Cold-formed Structural Sections – Part I: Material testing* (Afshan et al., 2013).
- *Strength Enhancement in Cold-formed Structural Sections – Part II: Predictive models* (Rossi et al., 2013).
- *Direct-formed and Continuous-formed Rectangular Hollow Sections – Comparison of Static Properties* (Sun & Packer, 2014).
- *Modelling and Probabilistic Study of the Residual Stress of Cold-formed Hollow Steel Sections* (Liu et al., 2017).
- *Residual stress measurements on cold-formed HSS hollow section columns, 2016* (Somodi & Kovesdi, 2016).
- F*lexural buckling resistance of cold-formed HSS hollow section members* (Somodi & Kovesdi, 2017).

The first article addressed in this section is titled "*Shake Table Resting of Tubular Steel Bracing Members*" (Elghazouli et al., 2005). An experimental investigation was carried out into the seismic response of cold-formed HSS members in concentrically braced steel frames. Three different braces were subjected to shake table tests representing realistic seismic loads. Figure 2-73 presents the shake table setup and Table 2-20 presents the tested section properties.

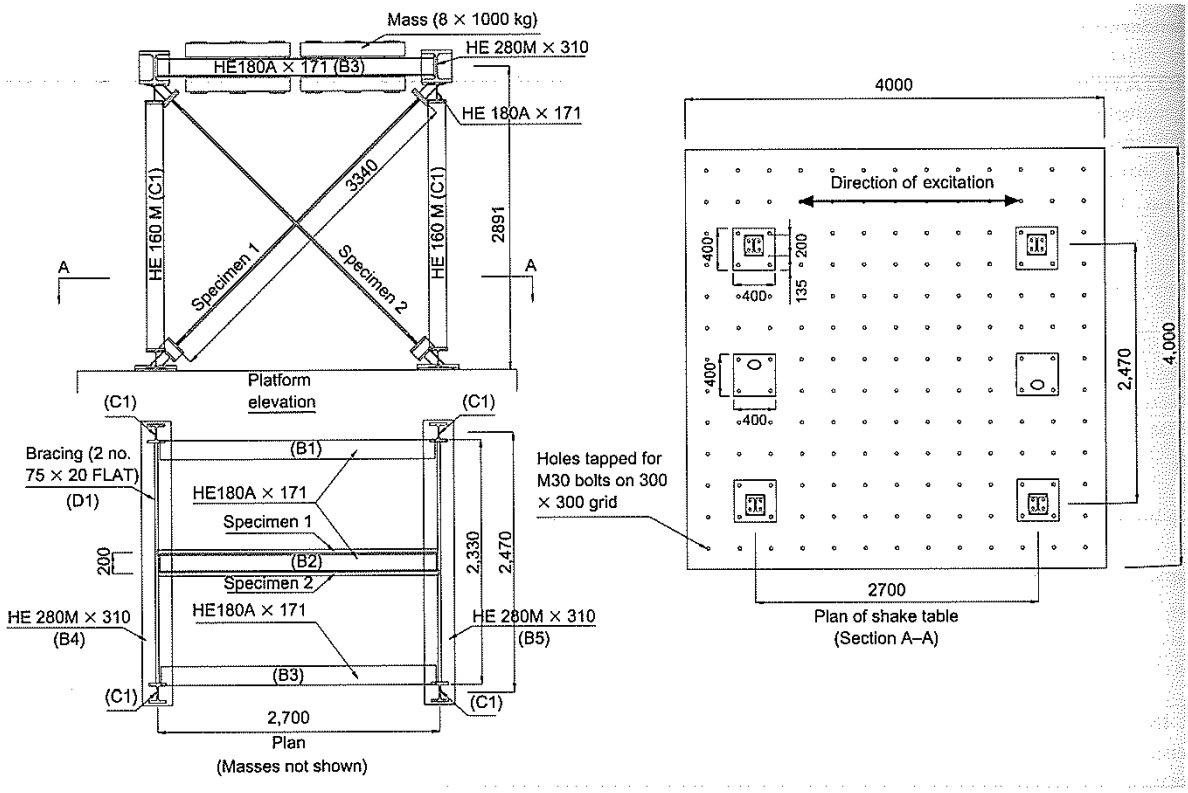


Figure 2-73: Shake table setup for CBF tests (Elghazouli, et al., 2005)

Table 2-20: Shake table setup for CBF tests (Elghazouli, et al., 2005)

| Specimen reference | Section size: mm | $f_y$: N/mm$^2$ | $f_u$:N/mm$^2$ | $\bar{\lambda}$ |
|---|---|---|---|---|
| H20A | 20 × 20 × 2·0 | 283·1 | 345·9 | 2·48 |
| H20B | 20 × 20 × 2·0 | 306·7* | 388·9* | 2·58* |
| H20C | 20 × 20 × 2·0 | 391·5 | 461·3 | 2·91 |
| H50A | 50 × 25 × 2·5 | 332·9 | 354·5 | 1·95 |
| H40A | 40 × 40 × 2·5 | 358·4 | 407·7 | 1·33 |
| H40B | 40 × 40 × 2·5 | 395·9 | 435·4 | 1·39 |

*Estimated values for replacement second brace are $f_y = 407{\cdot}6$ N/mm$^2$, $f_u = 493{\cdot}5$ N/mm$^2$, $\bar{\lambda} = 2{\cdot}97$.

The braces had 3050 mm in clear length and were pin-ended with nominally rigid connections. The measured imperfection was reported at 0.2%. The yield strength is reported in Figure 2-73 and was obtained from a full section tensile test. Elghazouli et al. (2005) also tested flat coupons and determined the average strength according to the Eurocode 3 equation (1993) which accounts for increased yield strength due to cold working effects. This equation is the European equivalent to the S136-16 strain hardening equation discussed earlier. It is reported the full section strength was about 10% higher than the average strength based on the Eurocode 3 equation. The average strength in the Eurocode 3 equation was determined from a coupon sample. Another interesting observation brought by Elghazouli et al. is that the two H20B braces in Figure 2-73 have significantly different yield strengths even though both have the same geometries. This is explained by both sections coming from different packs. It is seen they almost have 100 MPa in difference. This subsequently caused an asymmetric response during the seismic excitation and disproportionate inelastic deformation in one direction.

The final results are presented in Table 2-21 where Elghazouli et al. (2005) compared the actual yield strength determined from the section tensile tests ($N_y$) and the maximum tensile force measured in the braces during the tests ($N_t$).

Table 2-21: Normalized response parameters (Elghazouli, et al., 2005)

| Specimen reference | $N_t/N_y$ | $N_t/N_u$ | $V_s/V_y$ | $V_s/V_u$ | $\Delta_u$% | $\mu_m$ | $\mu_p$ | $\mu_p/\mu_m$ |
|---|---|---|---|---|---|---|---|---|
| H20A | 1·32 | 1·08 | 1·44 | 1·18 | 1·4 | – | – | – |
| H20B | 1·36* | 1·11* | 1·56 | 1·27 | 2·5 | 6·5 | 7·8 | 1·20 |
| H20C | 1·16 | 0·99 | 1·45 | 1·23 | 3·4 | 7·7 | 6·4 | 0·83 |
| H50A | 1·17 | 1·09 | 1·22 | 1·15 | 2·6 | 5·6 | 4·1 | 0·73 |
| H40A | 1·27 | 1·12 | 1·24 | 1·09 | 5·1 | 12·8 | 15·4 | 1·20 |
| H40B | 1·11 | 1·01 | 1·21 | 1·10 | 4·8 | 12·6 | 12·8 | 1·02 |

*Estimated values based on the average material properties of the two braces.

Elghazouli et al. (2005) determined the actual maximum tensile strength measured during the shake table test is about 30% higher than the section yield strength from the full tensile test ($N_t/N_y$). The ultimate tensile stress is about 10% higher. The tensile strength discrepancy is attributed to strain hardening and strain rate effects while the ultimate tensile stress discrepancy is attributed to just strain rate effects. The actual yield strength from the section tests ($N_y$) is compared to the

characteristic yield strength ($N_{nom}$). It is found it was 25% higher on average and up to 40% for some specimens. Elghazouli et al. determined the maximum tensile force in the brace for a realistic seismic scenario is underestimated by over 50%.

The article (Elghazouli et al., 2005) continued with a discussion of the actual measured shear per story for the shake table tests ($V_s$) versus the theoretical shear calculated from the yield strength measured from the section tensile tests ($V_y$ and $V_u$). The values for the ultimate shear $V_u$ were 20 to 40% greater and the values for the yield shear $V_y$ were 20 to 60% greater than the theoretical values based on full section tests.

Elghazouli (2005) wrote that a strength enhancement factor of 60% is recommended with respect to the actual measured yield strength and 100% with respect to the characteristic yield strength.

Finally, the section's ductility was addressed, and it was concluded (Elghazouli et al., 2005) conventional methods for evaluating ductility demand provided reasonable predictions. It was also recommended to re-evaluate the current member slenderness limits as it was concluded members with higher slenderness levels demonstrate satisfactory performance.

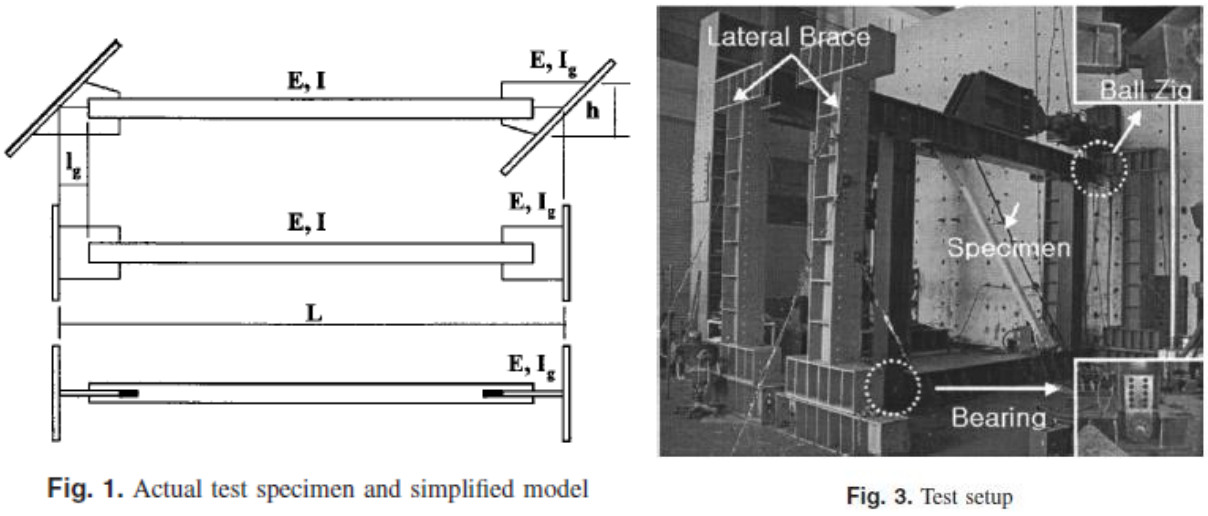


**Fig. 1.** Actual test specimen and simplified model

**Fig. 3.** Test setup

Figure 2-74: Test setup and simplified model (Han et al., 2007)

Another interesting study which was published slightly later is titled "*Seismic Behavior of HSS Bracing Members according to Width–Thickness Ratio under Symmetric Cyclic Loading*" (Han et al., 2007). The goal of this study was to carry out an experimental investigation to determine the effects of the width-thickness ratio on the seismic behaviour of cold-formed hollow structural members. The authors took 11 SHS specimens with different width to thickness ratios and applied

a quasi-static reversed cyclic load with symmetric tension and compression displacements to simulate seismic loading. The specimens had a w/t ratio ranging from 8 to 28. The specimens were of Korean origin but were fabricated to conform to the ASTM 500 Grade B specification ($F_y$ = 317 MPa, $F_u$ = 400 MPa). Tensile coupons were also taken from the specimens. Figure 2-74 presents the experimental setup and the simplified model while Figure 2-75 presents the tensile coupon placement and the tested sections.

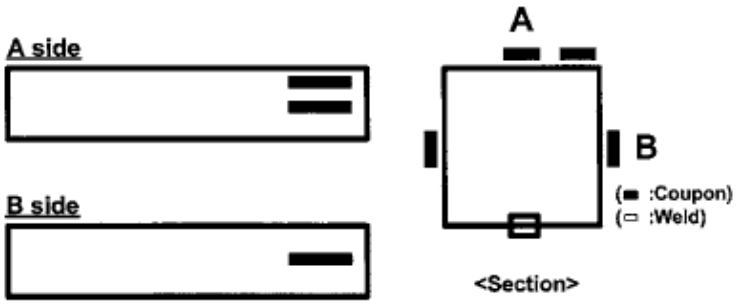


| Specimen | Section (width × thickness) (mm) | $w/t^f$ |
|---|---|---|
| S 77-28 | 100 × 100 × 3.2 | 28.25 |
| S 80-22 | 100 × 100 × 4 | 22.00 |
| S 82-19 | 100 × 100 × 4.5 | 19.22 |
| S 70-18 | 125 × 125 × 6 | 17.83 |
| S 85-14 A | 100 × 100 × 6 | 13.67 |
| S 85-14 B | 100 × 100 × 6 | 13.67 |
| S 85-14 C | 100 × 100 × 6 | 13.67 |
| S 69-11 | 125 × 125 × 9 | 10.89 |
| S 90-8 A | 100 × 100 × 9 | 8.11 |
| S 90-8 B | 100 × 100 × 9 | 8.11 |
| S 90-8 C | 100 × 100 × 9 | 8.11 |

Figure 2-75 : Tensile coupon placement and tested sections (Han et al., 2007)

Han et al. (2007) concentrated their research on the w/t influence over the actual yield strength, the buckling sequence, the energy dissipation capacity and the fracture and strain distributions. Yield strength results are reported in Table 2-22. The results per coupon were not available and Table 2-22 represents the average of all coupons.

Table 2-22: Tensile coupon tests (Han et al., 2007)

| Specimen | Young's modulus $E$ (MPa) | Yield strength $F_y^{(*)}$ (MPa) | Ultimate strength $F_u^{(*)}$ (MPa) | Yield ratio $(F_y^{(*)}/F_u^{(*)})$ | Elongation strain (%) |
|---|---|---|---|---|---|
| S 77-28 | 193,000 | 394 | 448 | 0.88 | 28.9 |
| S 80-22 | 192,000 | 411 | 453 | 0.87 | 30.0 |
| S 82-19 | 194,000 | 421 | 461 | 0.91 | 28.8 |
| S 70-18 | 191,000 | 405 | 456 | 0.89 | 31.7 |
| S 85-14 A | 197,000 | 399 | 441 | 0.91 | 28.3 |
| S 85-14 B | 190,000 | 410 | 452 | 0.90 | 29.7 |
| S 85-14 C | 189,000 | 408 | 456 | 0.89 | 30.8 |
| S 69-11 | 198,000 | 402 | 462 | 0.87 | 29.8 |
| S 90-8 A | 197,000 | 425 | 456 | 0.93 | 31.1 |
| S 90-8 B | 196,000 | 392 | 440 | 0.89 | 28.7 |
| S 90-8 C | 193,000 | 395 | 430 | 0.92 | 28.9 |

It was reported (Han et al., 2007) the actual yield strength was significantly higher than the nominal yield strength and the ratio of actual yield strength to specified ultimate tensile stress ranged from 0.87 to 0.93.

Han et al. (2007) classified three buckling and fracture sequences: the local buckling sequence, overall-local buckling sequence, and overall buckling sequence. It was reported specimen 100 x 100 x 3.2 (w/t = 28) undergoes the first sequence where it only experiences local buckling at the $7^{th}$ cycle of loading followed by full fractures at the $13^{th}$ cycle. Specimens with moderate w/t ratios (w/t = 14 – 22) experienced an overall buckling sequence at the $7^{th}$ cycle followed by a local buckling sequence. These specimens had a significantly better seismic behaviour than the previous specimen. Finally, the specimens with a small w/t ratio ($w/t \leq 10$) mostly experienced an overall buckling sequence and fractured early at their slotted end. The 125 x 125 x 9 specimen had some local buckling occur at the midsection before fracture. When comparing the fracture life, Han et al. wrote that specimens with low w/t ratios do not necessarily have a longer fracture life as stated in previous research. This was due to previous research studying the fracture life of specimens under compression-oriented loading. Therefore, this conclusion does not stand for symmetric compression and tension loading. When it comes to energy dissipation, Han et al. concluded specimens with a w/t ratio of 14 have the greatest energy dissipation capacity. Moving away from the w/t ratio of 14 in either direction reduces the dissipation capacity. The strain was concentrated at the midsection for specimens with higher w/t ratios. Specimens with a mid range w/t ratio had a uniform strain distribution and specimens with very low w/t ratios had a strain concentration at the end of the sections.

Another article published the same year by researchers from China and Australia was titled "*Experimental study on compressive strengths of thick-walled cold-formed sections*" (Guo et al., 2007). The experimental properties of thick cold-formed members were determined in this investigation. The study consisted in testing 18 stub columns with thicknesses ranging from 8 to 12 mm and a D/t ratio ranging from 27.6 to 47.7. In total, 24 flat and 24 corner coupons from the sections along with the virgin properties of the strip used to form the member were tested. The nominal yield strength of the virgin strip was of 235 MPa. Figure 2-76 presents the coupon distribution and Table 2-23 presents the results.

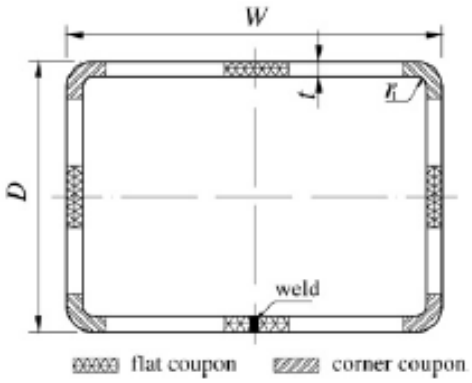


Fig. 1. Definition of symbols.

Figure 2-76: Coupon distribution (Guo et al., 2007)

Table 2-23: Coupon test distribution and results (Guo et al., 2007)

| Specimen | $\sigma_y$ (MPa) | $\sigma_u$ (MPa) | $\varepsilon_u$ (%) | Comparison | | | |
|---|---|---|---|---|---|---|---|
| | | | | $\frac{\sigma_{y(\text{flat coupon})}}{\sigma_{y(\text{virgin material})}}$ | $\frac{\sigma_{y(\text{corner coupon})}}{\sigma_{y(\text{virgin material})}}$ | $\frac{\varepsilon_{u(\text{flat coupon})}}{\varepsilon_{u(\text{virgin material})}}$ | $\frac{\varepsilon_{u(\text{corner coupon})}}{\varepsilon_{u(\text{virgin material})}}$ |
| R1-V | 259.1 | 376.9 | 23.05 | | | | |
| R1-F | 269.0 | 448.4 | 20.86 | 1.04 | 1.43 | 0.90 | 0.44 |
| R1-C | 371.8 | 619.7 | 10.19 | | | | |
| R2-V | 261.4 | 379.4 | 24.19 | | | | |
| R2-F | 273.0 | 454.0 | 21.07 | 1.04 | 1.49 | 0.87 | 0.39 |
| R2-C | 389.4 | 649.0 | 9.47 | | | | |
| R3-V | 258.1 | 430.2 | 25.86 | | | | |
| R3-F | 266.2 | 443.7 | 21.16 | 1.03 | 1.45 | 0.82 | 0.32 |
| R3-C | 374.7 | 624.5 | 8.20 | | | | |
| R4-V | 261.0 | 381.1 | 23.54 | | | | |
| R4-F | 272.1 | 453.6 | 21.26 | 1.04 | 1.31 | 0.90 | 0.41 |
| R4-C | 342.6 | 571.0 | 9.74 | | | | |
| S1-V | 259.8 | 433.1 | 23.53 | | | | |
| S1-F | 267.8 | 446.3 | 21.56 | 1.03 | 1.49 | 0.92 | 0.42 |
| S1-C | 386.0 | 643.3 | 9.97 | | | | |
| S2-V | 256.4 | 427.4 | 25.74 | | | | |
| S2-F | 269.16 | 448.6 | 20.76 | 1.05 | 1.44 | 0.81 | 0.33 |
| S2-C | 369.20 | 615.3 | 8.48 | | | | |
| | | | Mean | 1.04 | 1.44 | 0.87 | 0.39 |

Note: V = Flat coupons taken from virgin material; F = Flat coupons taken from cold-formed sections; C = Corner coupons taken from cold-formed sections.

It was reported (Guo et al., 2007) the flat sections increased in average by about 1.04 compared to the virgin strip and the corners increased on average by about 1.44. The elongation at fracture significantly decreased compared to the virgin strip. The ratio was of 0.87 for the flats and 0.39 for the corners.

Stub column tests were compared (Guo et al., 2007) to the values proposed by the Chinese (2002) and Australia/New Zealand (1996) codes. These results are presented in Table 2-24. It was concluded in this article (Guo et al., 2007), the design strengths predicted by the standards using material properties obtained from coupon tests (flat coupon average, corner strength estimated from

flat coupon) were quite conservative while those obtained from a full section (weighted average of corner and flat coupon yield strength) were far less conservative.

Table 2-24: Experimental results versus design standard (Guo et al., 2007)

Capacity comparison of column specimens

| Specimen | Test | Comparison | | | |
|---|---|---|---|---|---|
| | $N_{exp}$ (kN) | $\frac{N_{exp}}{N_{AS/NZS}}$ | $\frac{N_{exp}}{N^*_{AS/NZS}}$ | $\frac{N_{exp}}{N_{GB}}$ | $\frac{N_{exp}}{N^*_{GB}}$ |
| R1-1 | 2415 | 1.43 | 1.37 | 1.48 | 1.25 |
| R1-2 | 2452 | 1.40 | 1.34 | 1.45 | 1.23 |
| R1-3 | 2418 | 1.35 | 1.29 | 1.40 | 1.19 |
| R2-1 | 3533 | 1.56 | 1.47 | 1.65 | 1.37 |
| R2-2 | 3618 | 1.59 | 1.50 | 1.69 | 1.39 |
| R2-3 | 3572 | 1.60 | 1.51 | 1.69 | 1.39 |
| R3-1 | 4149 | 1.48 | 1.31 | 1.50 | 1.21 |
| R3-2 | 4198 | 1.56 | 1.39 | 1.61 | 1.29 |
| R3-3 | 4219 | 1.55 | 1.38 | 1.60 | 1.28 |
| R4-1 | 1899 | 1.49 | 1.27 | 1.49 | 1.19 |
| R4-2 | 1616 | 1.26 | 1.08 | 1.26 | 1.01 |
| R4-3 | 1685 | 1.31 | 1.12 | 1.31 | 1.04 |
| S1-1 | 3310 | 1.35 | 1.24 | 1.31 | 1.08 |
| S1-2 | 3325 | 1.31 | 1.20 | 1.28 | 1.05 |
| S1-3 | 3310 | 1.32 | 1.21 | 1.28 | 1.06 |
| S1-4 | 3250 | 1.23 | 1.13 | 1.22 | 1.00 |
| S2-1 | 3920 | 1.31 | 1.12 | 1.31 | 1.08 |
| S2-2 | 4080 | 1.32 | 1.13 | 1.31 | 1.08 |
| | Mean | 1.41 | 1.28 | 1.44 | 1.18 |

*Note: $N_{AS/AZS}$ is cold-formed standard equation with coupon average while $N*_{AS/AZS}$ is cold-formed standard equation with full section tensile results*

Important additional residual stress research was published in an article titled "*Residual Stresses in Roll-formed Square Hollow Sections*" (Li et al., 2009). A Chinese experimental investigation on the residual stress of roll-formed square hollow sections was reported on. Li et al. studied the difference between the residual stress magnitude and distribution in circle-to-rectangle forming (CRF) and flat-strip-to-rectangle forming (FRF). Figure 2-77 shows both forming processes.

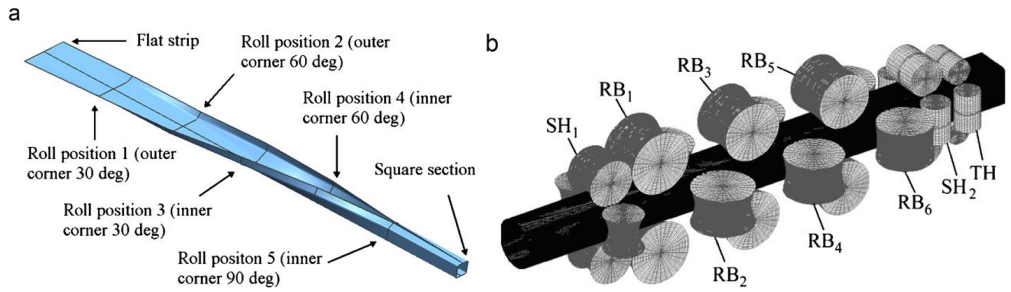


Figure 2-77: Roll-formed square hollow section: (a) FRF and (b) CRF (Li et al., 2009)

Table 2-25: Tested cross section and average material properties (Li et al., 2009)

| Specimen | $b$ (mm) | $t$ (mm) | $r$ (mm) | $\sigma_y$ (N/mm$^2$) | $\sigma_u$ (N/mm$^2$) | Process | Remark |
|---|---|---|---|---|---|---|---|
| A | 135 | 12 | 24 | 272 | 533 | FRF | |
| B | 135 | 12 | 24 | 266 | 542 | CRF | |
| C | 135 | 10 | 15 | 248 | 555 | CRF | TH |
| D* | 100 | 10 | 15 | 392 | 698 | FRF | |
| E | 100 | 12 | 15 | 263 | 561 | FRF | |
| F | 200 | 5 | 5 | 246 | 553 | CRF | |
| G | 200 | 8 | 12 | 389 | 669 | FRF | |
| H* | 300 | 12 | 24 | 384 | 677 | FRF | |
| I | 400 | 16 | 32 | 371 | 688 | FRF | IS |
| J | 400 | 12.5 | 25 | 362 | 691 | FRF | IS |

*Note*: * represents gradual yielding material. IS means the inside surface of specimen is measured; TH means the distribution of residual stresses through thickness is measured.

The X-Ray diffraction method was used in this investigation (Li et al., 2009) to determine residual stress values on the exterior and interior surfaces and the through thickness variation. The tested sections ranged from 100 to 400 mm in width and the thickness ranged from 5 to 16 mm. Coupons were only taken on the flat faces of the specimen. An average coupon yield strength is provided in Table 2-25. Through thickness residual stress measurements on what concerns the CRF method were only taken on one section.

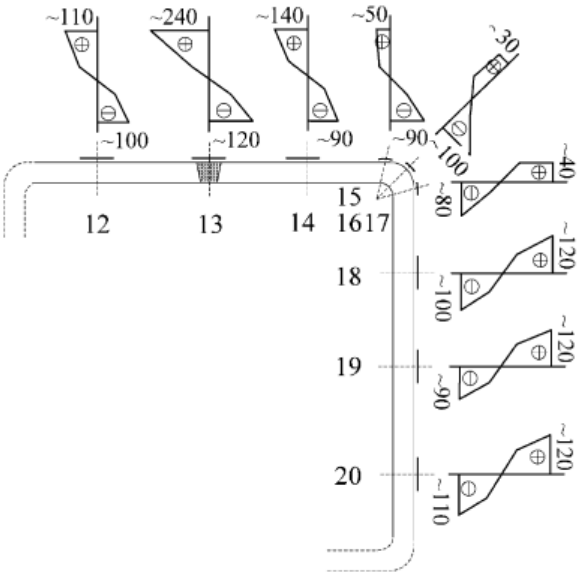


**Fig. 18.** Transversal residual stress along thickness of specimen C (135 × 135 × 10-CRF) (average transversal residual stress on depth 0.0, 2.5, 5.0 and 7.5 mm was 105.6, 63.0, −41.2 and −97.9 N/mm$^2$, respectively).

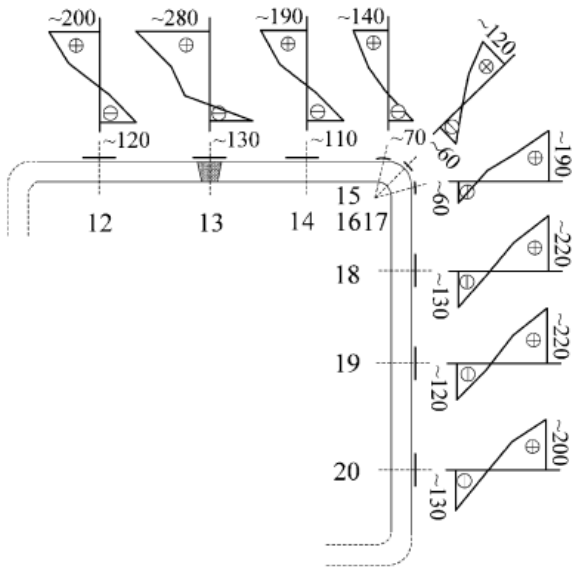


**Fig. 19.** Longitudinal residual stress along thickness of specimen C (135 × 135 × 10-CRF) (average longitudinal residual stresses at depths 0.0, 2.5, 5.0 and 7.5 mm were 194.3, 111.4, 3.8 and −103.8 N/mm$^2$, respectively).

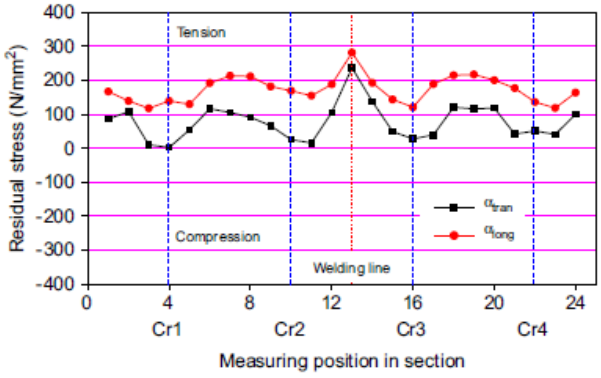


**Fig. 10.** Residual stress distributions on outside surface of specimen C (135 × 135 × 10-CRF) (average transversal residual stress was 77.7 N/mm$^2$, average longitudinal residual stress was 173.4 N/mm$^2$).

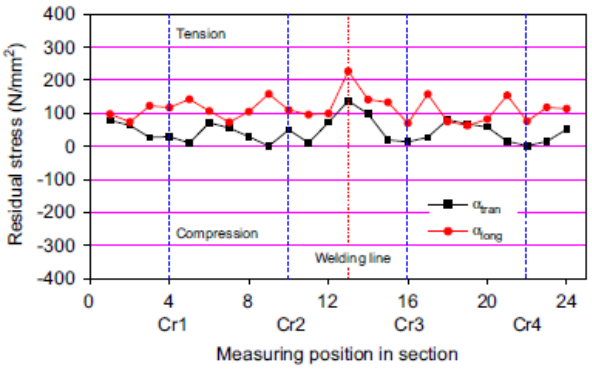


**Fig. 13.** Residual stress distributions on outside surface of specimen F (200 × 200 × 5-CRF) (average transversal residual stress was 45.2 N/mm$^2$, average longitudinal residual stress was 113.3 N/mm$^2$).

Figure 2-78: Residual stress distribution (Li et al., 2009)

On the exterior surface, it was determined (Li et al., 2009) transversal residual stresses are typically below the 70% of the yield strength while longitudinal residual stresses can reach up to 90% of the yield strength. The maximum residual stress is always on the welding line. On the interior surface, the measured residual stresses were typically below 30% of the yield strength for the transverse component and below 40% for the longitudinal component. Figure 2-78 shows the results for the exterior and interior surfaces as well as through thickness measurements.

Li et al. (2009) determined the through thickness residual stress distribution is bi-linear. Li et al. stated that their results are in good agreement with the residual stress model proposed by Key

(1988) and Hancock (1993), but there is no clear explanation on why the previously measured results did not provide bi-linear distributions. Finally, it is concluded longitudinal residual stresses in CRF sections are far greater than those in FRF sections. The author's explanation about the inconsistency reads as follows (Li et al., 2009, p.511):

> *"This through thickness variations of residual stresses are in general agreement with the model reported by Key and Hancock [9]. Although the model they proposed was only based on the experimental data at the center of one face of square hollow sections, the experiment results in this paper verified their model. The reason for these differences could be attributed to that there is no springback at final stand because bent strip is welded together to form the square hollow section before coming out of the rolls."*

To continue, Gardner et al. (2010) analyzed the major differences between cold-formed sections and hot-rolled sections in Europe in an article titled "*Comparative Experimental Study of Hot-rolled and Cold-formed Rectangular Hollow Sections*". An experimental investigation was carried on both section types where material properties were determined. Tensile coupon tests on flats and corners, stub column tests and residual stress tests were performed. Geometric imperfections were also determined and tests on a simple continuous beam were performed. The authors examined 5 cold-formed and 5 hot-rolled sections for which results are presented in Table 2-26. The added *C* next to the name represents the corner coupon. The flat coupon was taken directly opposite to the weld and the corner coupon was adjacent to the flat as shown in Figure 2-79.

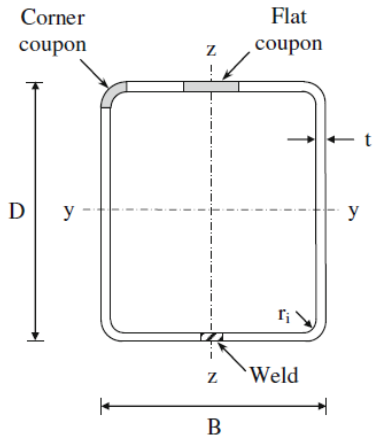


Figure 2-79: Tensile coupon distribution (Gardner et al., 2010)

Table 2-26: Material properties of cold-formed sections versus hot-rolled sections (Gardner et al., 2010)

Mill certificate (virgin) and measured tensile material properties of test specimens.

| Tensile test specimen | Mill certificate (virgin) material properties | | Measured tensile material properties | | | |
|---|---|---|---|---|---|---|
| | $\sigma_{y,mill}$ (N/mm$^2$) | $\sigma_{u,mill}$ (N/mm$^2$) | $\sigma_{y,exp}$ (N/mm$^2$) | $\sigma_{u,exp}$ (N/mm$^2$) | $E_{exp}$ (N/mm$^2$) | $\varepsilon_{f,exp}$ (−) |
| SHS 100 × 100 × 4-HR | 491 | 569 | 488 | 570 | 212600 | 0.33 |
| SHS 100 × 100 × 4-CF | 378 | 423 | 482 | 500 | 208300 | 0.29 |
| SHS 100 × 100 × 4-CF-C | – | – | 522 | 567 | 199900 | 0.15 |
| SHS 60 × 60 × 3-HR | 478 | 574 | 449 | 555 | 215200 | 0.31 |
| SHS 60 × 60 × 3-CF | 395 | 423 | 361 | 402 | 207400 | 0.49 |
| SHS 60 × 60 × 3-CF-C | – | – | 442 | 471 | 208000 | 0.21 |
| RHS 60 × 40 × 4-HR | 482 | 561 | 468 | 554 | 213800 | 0.37 |
| RHS 60 × 40 × 4-CF | 445 | 471 | 400 | 452 | 212000 | 0.21 |
| RHS 60 × 40 × 4-CF-C | – | – | 480 | 570 | 202400 | 0.15 |
| SHS 40 × 40 × 4-HR | 523 | 576 | 496 | 572 | 212300 | 0.34 |
| SHS 40 × 40 × 4-HR-C | 523 | 576 | 499 | 578 | 215500 | 0.37 |
| SHS 40 × 40 × 4-CF | 383 | 413 | 410 | 430 | 201600 | 0.38 |
| SHS 40 × 40 × 4-CF-C | – | – | 479 | 507 | 210900 | 0.17 |
| SHS 40 × 40 × 3-HR | 520 | 565 | 504 | 581 | 219600 | 0.36 |
| SHS 40 × 40 × 3-CF | 430 | 456 | 451 | 502 | 212900 | 0.24 |
| SHS 40 × 40 × 3-CF-C | – | – | 534 | 589 | 196700 | 0.16 |

There appears to be an inconsistency in the paper as it is clearly stated the nominal values for yield strength were of 235 MPa for cold-formed sections and 355 MPa for hot-rolled sections. However, when analyzing the values presented in Table 2-26, the yield strength of the virgin strip for cold-formed sections is higher than the nominal value. As it is determined in various investigations, the industry usually uses a virgin strip of lower yield strength and accounts for the enhancement during the cold-forming processes for final section to reach the required nominal strength. It is also clearly stated in the article (Gardner et al., 2010) the mill certificate value is of the strip used to form the section and not of the formed section tested at the mill. If this was the case, the discrepancy could be explained by different equipment or experimental procedures used at the mill and the lab. It is not clear why the virgin strip used to form the section would have higher yield strength values than the formed section or even the nominal yield strength.

Gardner et al. (2010) further analyzed the effect of corner radii to thickness ratio, and ultimate to yield strength ratio for the virgin strip. The results are presented in Figure 2-80 and are compared to the CSA S136 standard (1996). Previous results from Guo et al. (2007), Key et al. (1988), Wilkinson (1999), and Key and Hancock (1993) were also included. Gardner et al. (2009) confirmed the tendencies expressed by previous investigations. As the corner radii decreases the yield strength increases. As the ultimate to yield ratio of the virgin strip increases, the corner yield strength also increases. Gardner et al. (2009) then determined the mean ratio between the corner

yield strength and virgin strip yield strength. The CSA S136 (1996) standard equation (2-11) was adjusted to that ratio to better conform to the experimental values. Equation (2-19) was obtained.

$$\frac{F_{yc}}{F_{yv}} = \frac{B_c}{(\frac{R}{t})^m} \tag{2-19}$$

$$B_c = 2.90\frac{F_{u,mill}}{F_{y,mill}} - 0.752\left(\frac{F_{uv}}{F_{yv}}\right)^2 - 1.09$$

$$m = 0.23\frac{F_{uv}}{F_{yv}} - 0.041$$

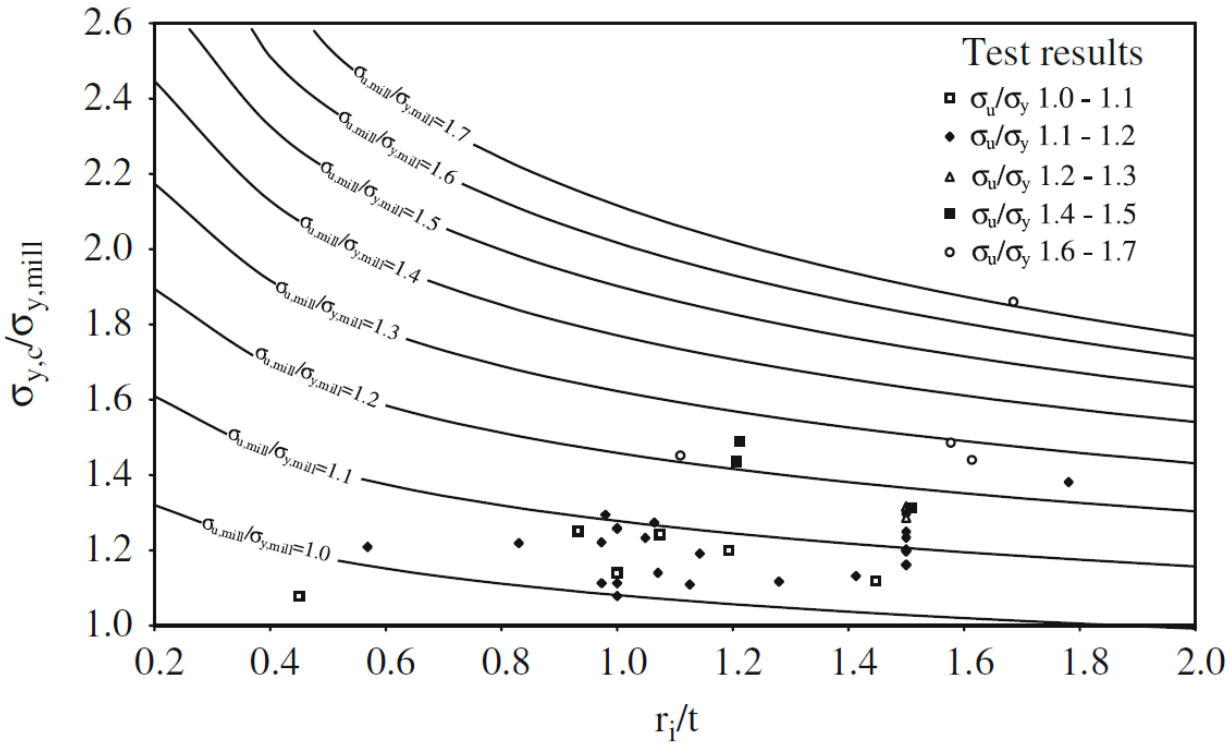


Figure 2-80: Corner material strength data and AISI predictive model (Gardner et al., 2010)

It is important to note there was a mistake in the paper (Gardner et al., 2010) when the CSA S136 equation was reported. It is not clear whether this was just a typo, or the wrong equation was used. Gardner et al. reported equation (2-20) as the CSA S136 standard equation. The factor in front of the $F_{uv}/F_{yv}$ should be 0.192 and not 0.92.

$$\frac{F_{yc}}{F_{yv}} = \frac{B_c}{(\frac{R}{t})^m} \quad (2\text{-}20)$$

$$B_c = 3.69\frac{F_{uv}}{F_{yv}} - 0.819\left(\frac{F_{uv}}{F_{yv}}\right)^2 - 1.79$$

$$m = \mathbf{0.92}\frac{F_{uv}}{F_{yv}} - 0.068$$

Table 2-27: Residual stress measurements (Gardner et al., 2010)

Bending residual stress values for cold-formed sections.

| Specimen | Flat faces | | | |
|---|---|---|---|---|
| | $\sigma_{bl}$ (N/mm$^2$) | $\sigma_{br}$ (N/mm$^2$) | $\sigma_{bl}/\sigma_{0.2}$ | $\sigma_{br}/\sigma_{0.2}$ |
| 100 × 100 × 4-CF | 287 | 191 | 0.60 | 0.40 |
| 60 × 60 × 3-CF | 262 | 175 | 0.73 | 0.48 |
| 60 × 40 × 4-CF | 356 | 237 | 0.89 | 0.59 |
| 40 × 40 × 4-CF | 379 | 253 | 0.92 | 0.62 |
| 40 × 40 × 3-CF | 362 | 241 | 0.80 | 0.53 |
| Mean | | | 0.79 | 0.52 |

| Corner regions | | | |
|---|---|---|---|
| $\sigma_{bl}$ (N/mm$^2$) | $\sigma_{br}$ (N/mm$^2$) | $\sigma_{bl}/\sigma_{0.2}$ | $\sigma_{br}/\sigma_{0.2}$ |
| 253 | 121 | 0.49 | 0.23 |
| 267 | 130 | 0.60 | 0.29 |
| 501 | 389 | 1.04 | 0.81 |
| 370 | 211 | 0.77 | 0.44 |
| 338 | 171 | 0.64 | 0.32 |
| | | 0.71 | 0.42 |

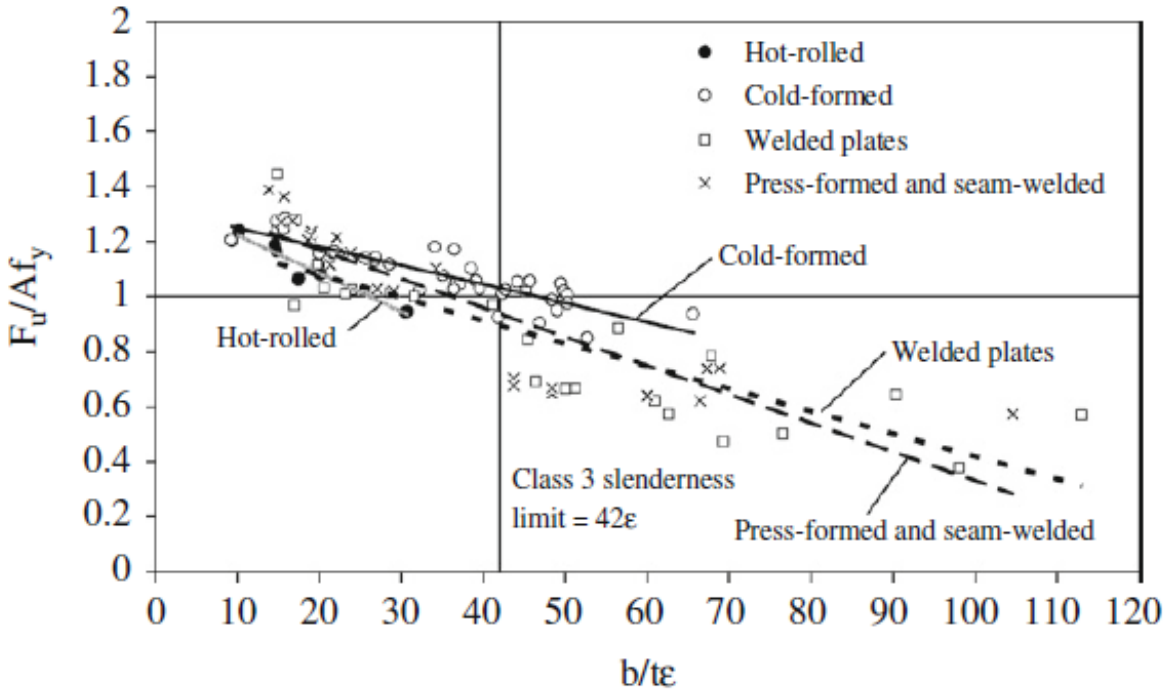


Figure 2-81: Normalized stub column resistance versus plate slenderness (Gardner et al., 2010)

Residual stress predictions in the article (Gardner et al., 2010) were made from surface strain measurements. Gardner et al. determined tensile stresses were present on the exterior surface and compressive stresses were present on the interior surface. Table 2-27 presents the reported residual stress measurements. Gardner et al. assumed two residual stress models. The first denoted $\sigma_{bl}$ represents a linearly varying residual stress. The second denoted $\sigma_{br}$ represents a rectangular block. The authors stated a factor of 1.5 was applied to the longitudinal model compared to the rectangular block. The values were normalized with respect to the previously obtained tensile values.

Stub column tests results (Gardner et al., 2010) are reported in Figure 2-81 where they were compared to results obtained in previous studies. The stub column strength was normalized by the product of the measured tensile strength and the gross area. It is seen the stub column strength varied linearly from approximately 1.3 at very low slenderness values (b/t ≈ 10) to 0.9 at very high slenderness values (b/t ≈ 75). Finally, geometric imperfections were determined to be of the same magnitude in both cold-formed and hot-rolled sections.

In the third article published by Gao and Moen (2010), titled "*The Cold Work of Forming Effect in Steel Structural Members*", the finite element parameters necessary to properly model cold-formed sections were analyzed. The authors stated that research and design of finite element models for

cold-formed sections is often inconsistent. Gao and Moen wrote that some researchers propose to ignore cold bending effects in finite element simulations to obtain results matching the experiment, while others use modeling protocols which include residual stresses and increased yield stress at cold-bent locations. It is also brought up that the CSA S136 (2007) standard equation (2-11) to account for strain hardening is empirically derived and does not explicitly account for residual stresses. To address these problems, Gao and Moen utilized finite element simulations to study the mechanics of cold bending.

The main factor addressed in this article (Gao and Moen, 2010) are metal plasticity laws such as isotropic or kinematic hardening. Isotropic hardening is described as a law mostly used in single loading conditions while kinematic hardening is used in cyclic loading conditions. Figure 2-82 illustrates both laws.

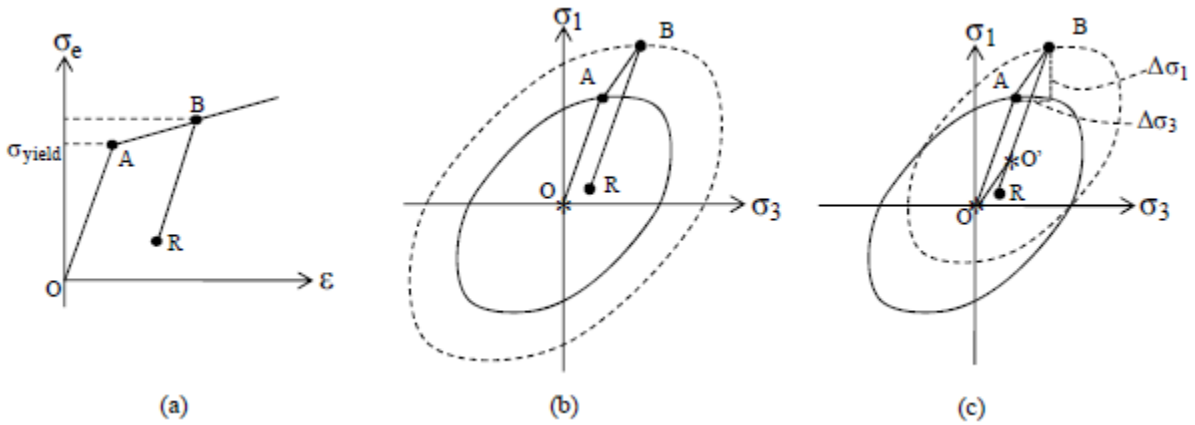


Figure 2-82: Hardening with residual stresses from cold bending: (a) stress-strain curve, (b) isotropic hardening with expanding yield surface, and (c) kinematic hardening with shifting yield surface (Gao and Moen, 2010)

The main difference between isotropic and kinematic hardening is that in isotropic hardening the surface remains the same shape but expands in size while in kinematic hardening the surface remains in the same shape and size but translates in space (Kelly, 2012). Kinematic hardening also accounts for the Bauschinger effect where hardening in tension will lead to softening in compression (Kelly, 2012). Gao and Moen (2010) posed the hypothesis that to reproduce the cyclic nature of the loading applied to cold-formed members, it is necessary to use a combination of isotropic and kinematic hardening.

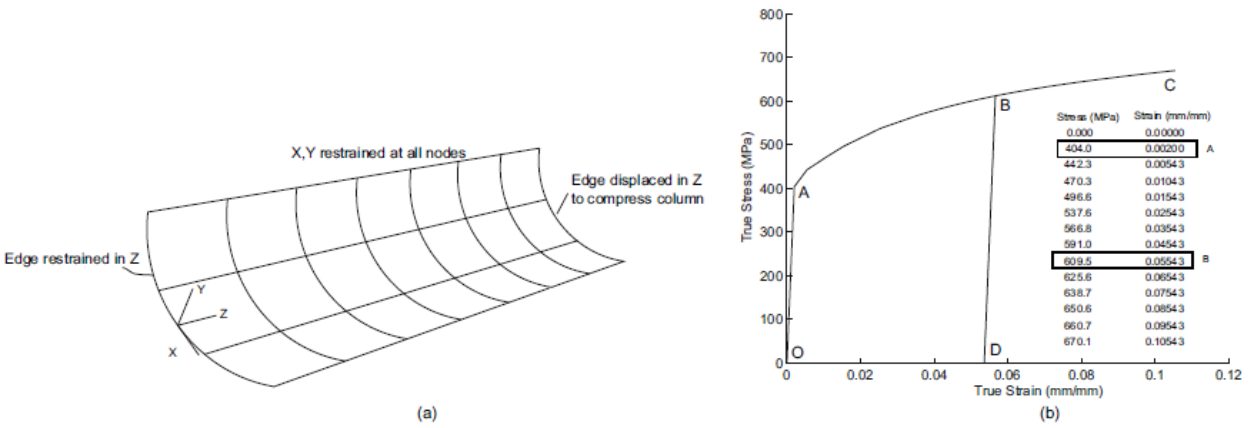


Figure 2-83: (a) Finite element model boundary conditions and loading and (b) assumed stress-strain curve (Gao and Moen, 2010)

Gao and Moen (2010) modeled a 120 mm column strip of 2.6 mm in thickness with a radius of 305 mm. A modified Riks nonlinear solution method was applied and 9 reduced integration shell elements were used. Figure 2-83 presents the model on the left and the assumed stress-strain curve on the right.

Gao and Moen (2010) studied four different cases: isotropic hardening with a virgin stress-strain curve, isotropic hardening with a modified stress-strain curve to simulate increased yield stress, isotropic hardening including residual stresses and effective plastic strains and isotropic-kinematic hardening including residual stresses and equivalent plastic strains. The residual stress distribution was calculated from an equation developed to simulate the cold forming process and predict the residual stress distribution in the member based on an available stress-strain curve (Moen et al., 2008). Figure 2-84 provides the adopted distribution of residual stress in this article.

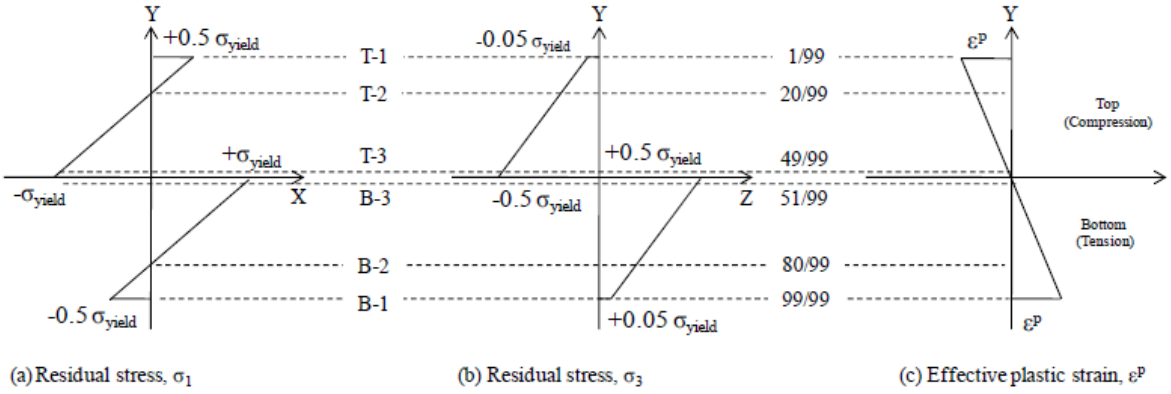


Figure 2-84: Residual stress distribution in finite element model (Gao & D. Moen, 2010)

It was determined by Gao and Moen (2010), the case with increased yield strength provides 40% higher results than the baseline case with a virgin yield strength. The third case where both residual stress and increased yield strength are accounted for shows similar results but with a softer yield knee. The final case which applies combined isotropic and kinematic plasticity laws falls back to the baseline model. The authors mentioned this result was unexpected. It is explained by the yield lag due to the residual stress, which the isotropic model fails to account for, and the Bauschinger effect. The authors finally recommended the isotropic-kinematic hardening plasticity law which includes residual stresses and the equivalent plastic strains case for cold-bent modeling.

An experimental investigation into the manufacturing process of cold rolling was carried out in an article titled "*Material Properties of Thick-wall Cold-rolled Welded Tube with a Rectangular Square Hollow Section*" (Hu et al., 2011). The authors analyzed flat and corner coupons, parent plate coupons (virgin strip) and stub columns from thick-wall cold-rolled welded tube sections. Two section sizes were chosen (250 x 250 x 9.2 and 200 x 300 x 9.2 – D/t = 35) and the yield strength was determined throughout the whole rolling process which consisted of 15 passes. Figure 2-85 presents the location of tensile coupons on the formed section and the virgin strip. Corner coupons were taken during the whole process while flat coupons were only taken after the section was welded. Figure 2-86 provides the yield strength of the coupons after each pass.

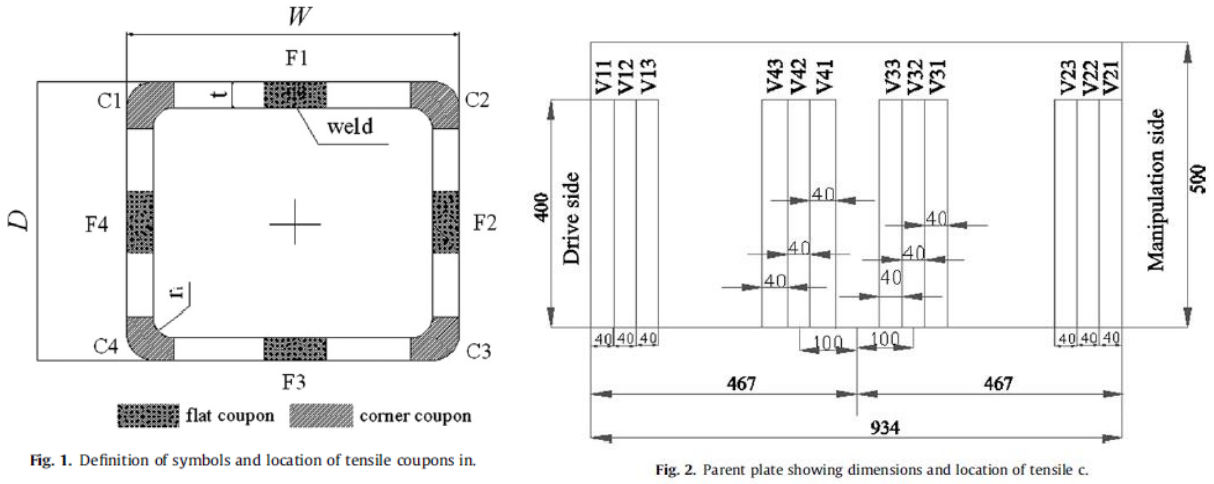


Fig. 1. Definition of symbols and location of tensile coupons in.

Fig. 2. Parent plate showing dimensions and location of tensile c.

Figure 2-85: Tensile coupon distribution and virgin strip coupon distribution (Hu et al., 2011)

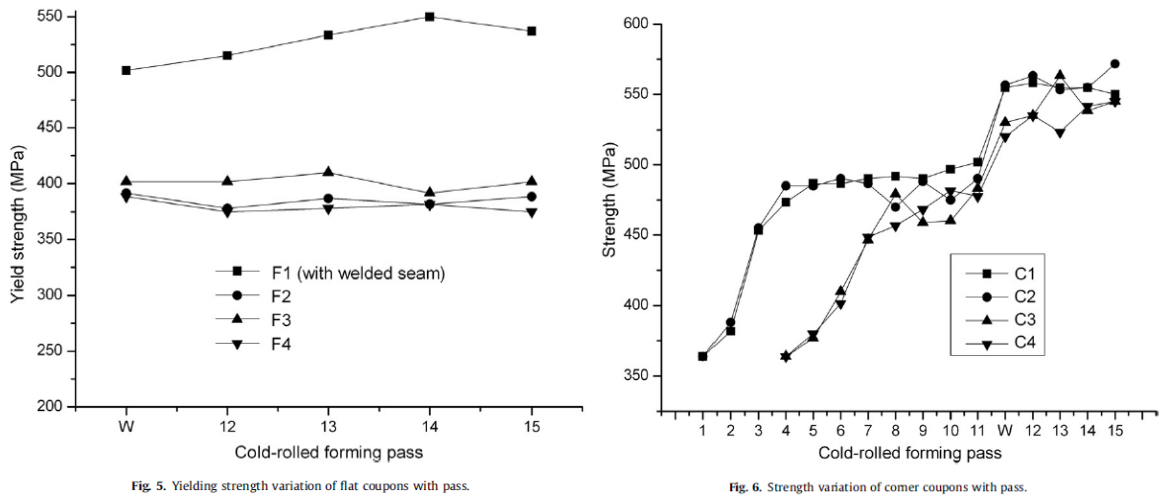


Fig. 5. Yielding strength variation of flat coupons with pass.

Fig. 6. Strength variation of corner coupons with pass.

Figure 2-86: Yield strength in tensile coupons after each pass (Hu et al., 2011)

Hu et al. (2011) noticed significant differences in the virgin steel before it even underwent any treatment. The elongation for the center was respectively 27.4% higher than the edges and the yield strength was also higher at the very edge. The properties were however symmetrical with respect to the center. It was determined the ratio of flat coupon to virgin strip was of 1.1, while the ratio of corner coupon to virgin strip was of 1.47. Elongation ratios decreased to 0.79 for the flat section and 0.40 for the corner section compared to the virgin strip. In the second part of the article, Hu et al. compared stub column strength to design values proposed by the Chinese (2002) and Australia/New Zealand (1996) standard for cold-formed structures (equivalent to the North American CSA S136 standard). The $N_{AZ/NZS}$ equations take the flat coupon average, while the $N^{*}_{Az/NZS}$ equation uses the full section tensile strength. Table 2-28 provides their results.

Table 2-28: Stub column results compared to Chinese and Australia/New Zealand cold-formed standards (Hu et al., 2011)

Capacity comparison of column specimens.

| Specimen | Test | Comparison | | | |
|---|---|---|---|---|---|
| | $N_{exp}$ (KN) | $\frac{N_{\exp}}{N_{AS/NZS}}$ | $\frac{N_{\exp}}{N^{*}_{AS/NZS}}$ | $\frac{N_{\exp}}{N_{GB}}$ | $\frac{N_{\exp}}{N^{*}_{GB}}$ |
| S1 | 3600 | 1.19 | 1.11 | 1.12 | 1.20 |
| S2 | 3725 | 1.24 | 1.16 | 1.17 | 1.25 |
| S3 | 3650 | 1.23 | 1.14 | 1.16 | 1.24 |
| Rl | 3490 | 1.22 | 1.15 | 1.15 | 1.18 |
| R2 | 3350 | 1.17 | 1.10 | 1.10 | 1.13 |
| R3 | 3340 | 1.17 | 1.10 | 1.10 | 1.12 |
| | Mean | 1.20 | 1.13 | 1.13 | 1.19 |

Li et al. (2012) studied the material properties if three cold-formed sections in an article titled "*Cold-forming Effect Investigation on Cold-formed Thick-walled Steel Hollow Sections*". What is particularly interesting in this paper is that the authors attempted to determine the yield strength distribution within the corner. This was done by taking tensile tube coupons from the center and edges of the corner coupon. These tubes were named rounded specimens. The specimen distribution is shown in Figure 2-87.

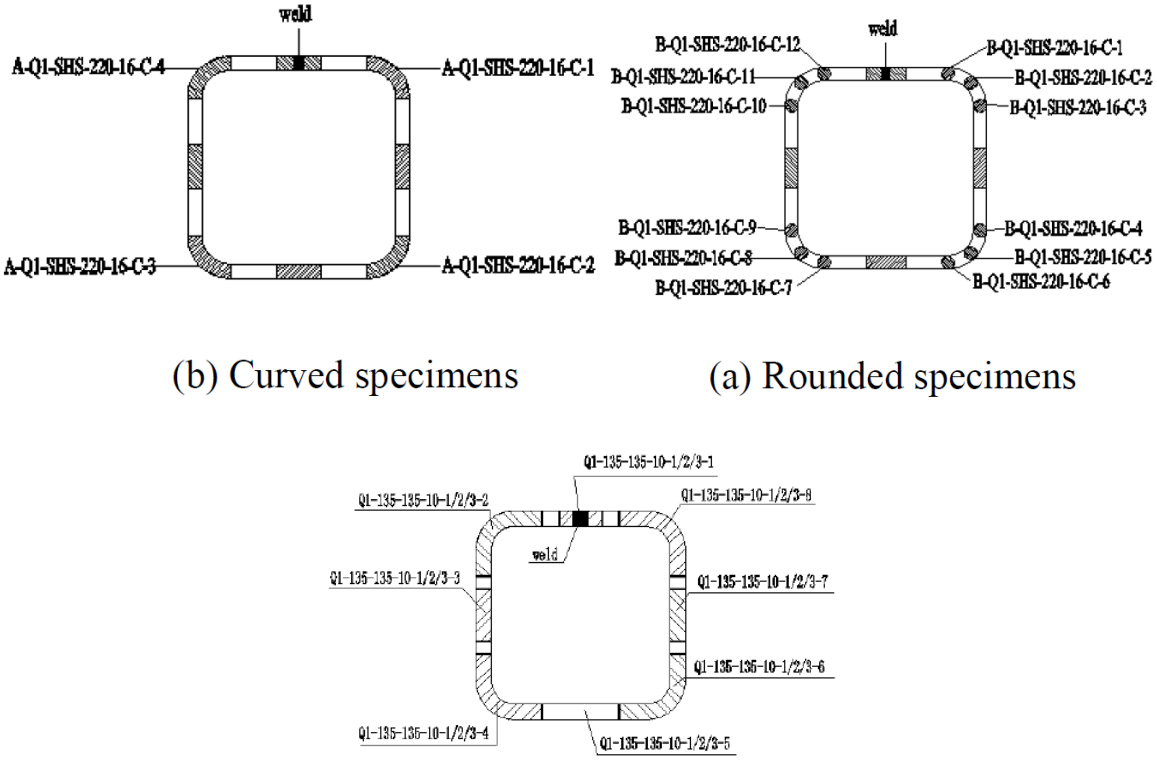


Figure 2-87: Flat and corner coupon distribution (Li et al., 2012)

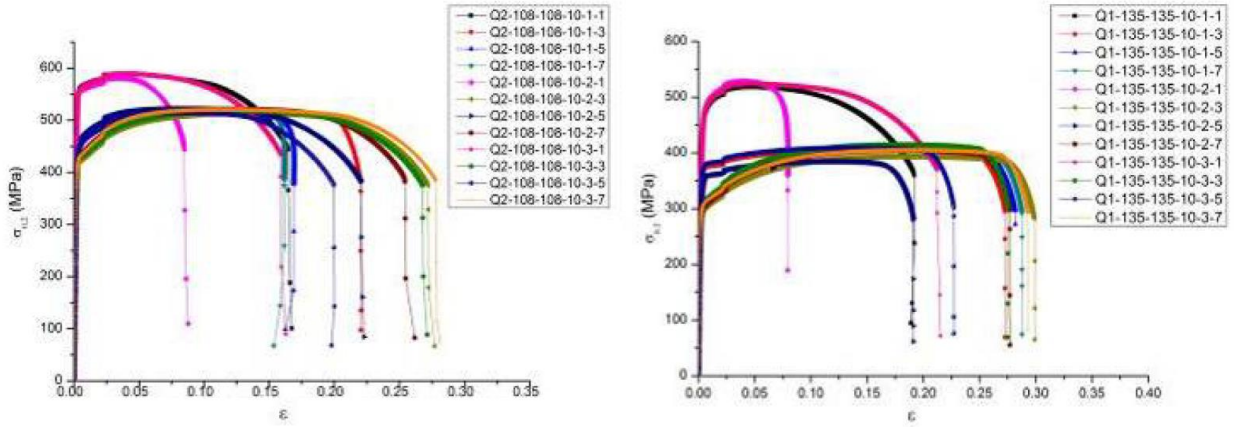


(a) Section type: 108-108-10 (b) Section type: 135-135-10

Figure 2-88: Obtained stress-strain curves for tested coupons (Li et al., 2012)

To continue, Li et al. (2012) performed flat tensile coupon tests and stub column tests which were later compared to design strengths. Three sections were tested for tensile coupons (108 x 108 x 10 – d/t = 13.75, 135 x 135 x 10 – D/t = 17 and 220 x 200x 16 – D/t = 17.5) with nominal yield strengths of 345 MPa for the first section and 235 MPa for the other two. The 345 MPa section was also tested in compression along with another section with the same yield strength (250 x 250 x 8 – D/t = 40). Results for regular tensile coupons are presented in Figure 2-88 and results for tube corner coupons are presented in Figure 2-89 and Figure 2-90.

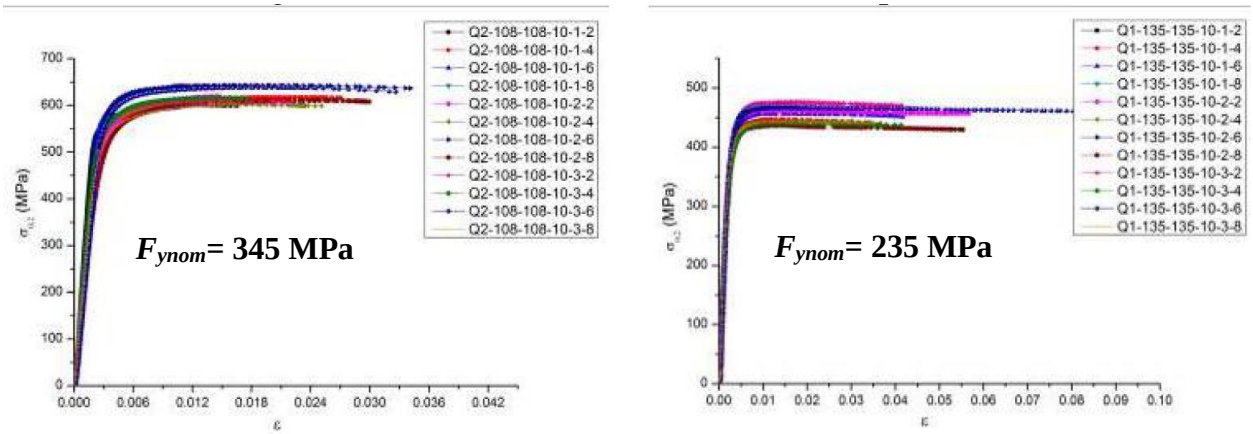


(a) Section type: 108-108-10 (b) Section type: 135-135-10

Figure 2-89: Tube coupon results – Part 1 (Li et al., 2012)

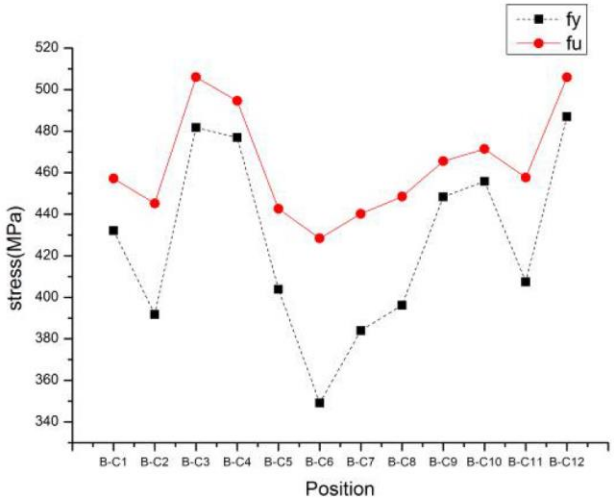


(c) Section type: 220-220-16

Figure 2-90: Tube coupon results – Part 2 (Li et al., 2012)

It was concluded (Li et al., 2012) there is a significant difference in yield strength between the flat coupons, the corner coupons and the weld. The weld and corner coupons showed significantly higher yield strengths than the flat coupons but also presented highly decreased ductility. The rounded specimens did not show any particular distribution pattern.

Li et al. (2012) reported stub columns failed by yielding. Specimens with smaller width to thickness ratios experienced crushing accompanied by the cracking of the weld. Specimens with higher width to thickness ratios experienced some local instability.

The coupon yield strength was further normalized with respect to the "*minimum yield strength of all flats*" (Li et al., 2012) to draw a trend with respect to the width to thickness ratio. Results were expressed as the radius to thickness ratio (R/t) and centerline length of section to inner radius ratio ($L_s$/t). Li et al. (2012) did not specify this, but it is understood from the minimum strength they meant the strength from the lowest flat and not the average of all flats.

Li et al. (2012) concluded the yield strength of the flats adjacent to the weld did not depend on the b/t ratio. Li et al. wrote that the mean yield strength was of 1.10 for opposite flats, 1.01 for adjacent flats and 1.04 for the average of all three compared to the minimum strength. When analyzing the yield strength of corner coupons an increase ranging from 17 to 67% was noted. An increase in strength with the R/t ratio was clearly noted as well. The ultimate tensile stress increase was less pronounced, only ranging from 7 to 24% and averaging at 16%. Li et al. finally compared stub

column results to the cold-formed standards in North America (2001), Australia/New Zealand (2005), Europe (2006) and China (2002) in Figure 2-91. It was concluded the values obtained in the standards are unconservative for low R/t ratios. This was attributed to the presence of residual stresses.

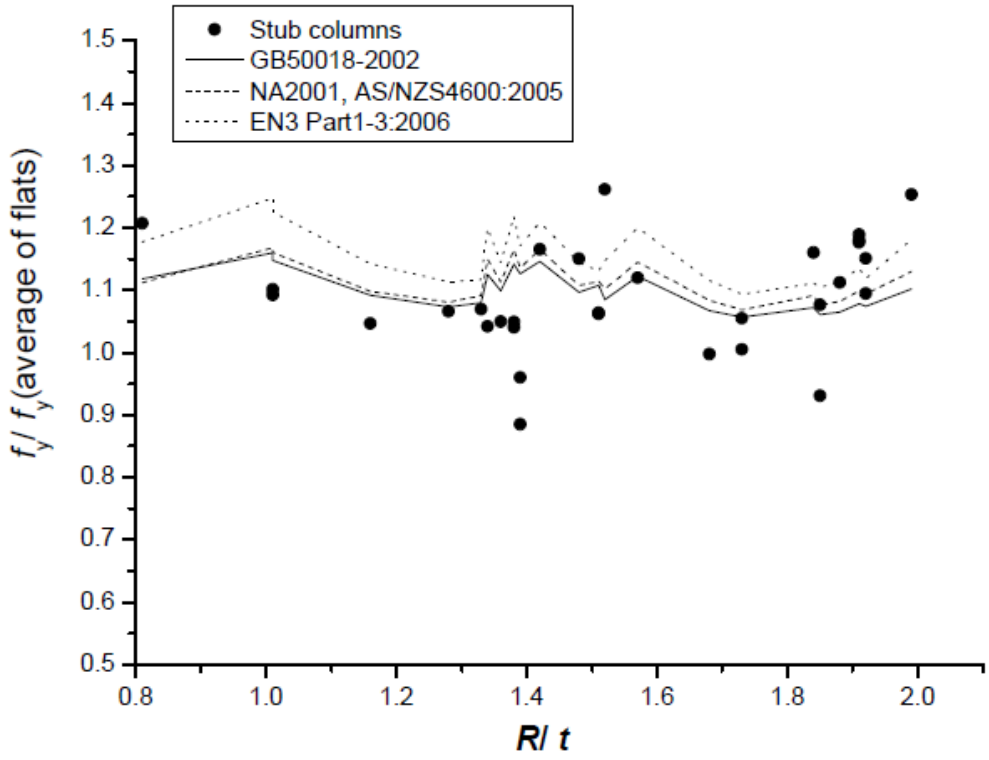


Figure 2-91: Stub column strengths compared to cold-formed standards (Li et al., 2012)

Tong et al. (2012) determined the longitudinal residual stress distribution in thirteen cold-formed sections through the hole-drilling method and the X-ray diffraction technique in an article titled "*Experimental Investigation on Longitudinal Residual Stresses for Cold-formed Thick-walled Square Hollow Sections*". Tong et al. compared directly formed cold-formed sections and indirectly formed ones. The directly formed sections were formed into the proper SHS directly from the coil strip (denoted with *S*), while the indirect sections were first formed into a tube before being converted into an SHS (denoted with *C*).

The hole-drilling method to measure residual stress consists in measuring strain gauge deformation on the surface of a section after drilling a hole in the vicinity of the gauge and releasing trapped stresses (Tong et al., 2012). The X-ray diffraction method consists in projecting an X-ray beam into the crystal lattice of the material and measuring its diffracted characteristics (Fitzpatrick et al.,

2005). To measure the through-thickness residual stress, Tong et al. (2012) stripped the outer surface up to the measured point as shown in Figure 2-92. A tensile coupon at the center of the face opposite to the flat was also taken. The results are presented in Figure 2-93 and Figure 2-94.

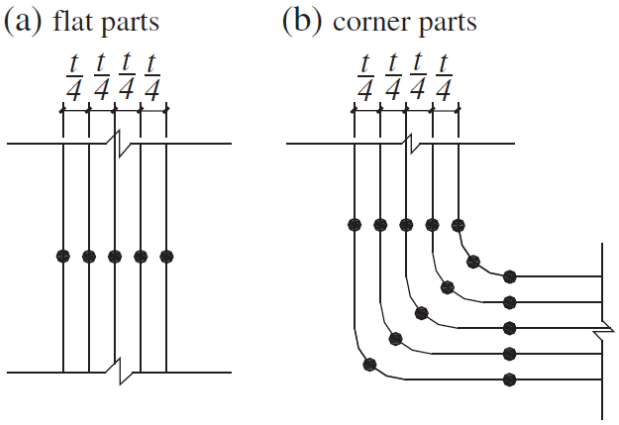


Figure 2-92: Through thickness measurement position (Tong et al., 2012)

| Series | $E_0$ (GPa) | Average of $E_0$ (GPa) | $\sigma_{0.2}$ (MPa) | Average of $\sigma_{0.2}$ (MPa) | $\sigma_u$ (MPa) | Average of $\sigma_u$ (MPa) | $\varepsilon_f$ (%) | Average of $\varepsilon_f$ (%) |
|---|---|---|---|---|---|---|---|---|
| S-135×10 | 208.7 | 204.6 | 403 | 386 | 452 | 437 | 22.60 | 22.5 |
| | 205.2 | | 383 | | 433 | | 23.10 | |
| | 199.9 | | 371 | | 425 | | 21.90 | |
| C-135×10 | 185.4 | 183.7 | 394 | 391 | 445 | 445 | 20.40 | 20.8 |
| | 200.2 | | 374 | | 438 | | 21.80 | |
| | 165.5 | | 404 | | 453 | | 20.30 | |
| S-300×16 | 202.9 | 200.6 | 276 | 273 | 400 | 398 | 27.40 | 27.4 |
| | 200.9 | | 286 | | 395 | | 28.20 | |
| | 198.0 | | 257 | | 400 | | 26.50 | |

Figure 2-93: Material properties of test specimens (Tong et al., 2012)

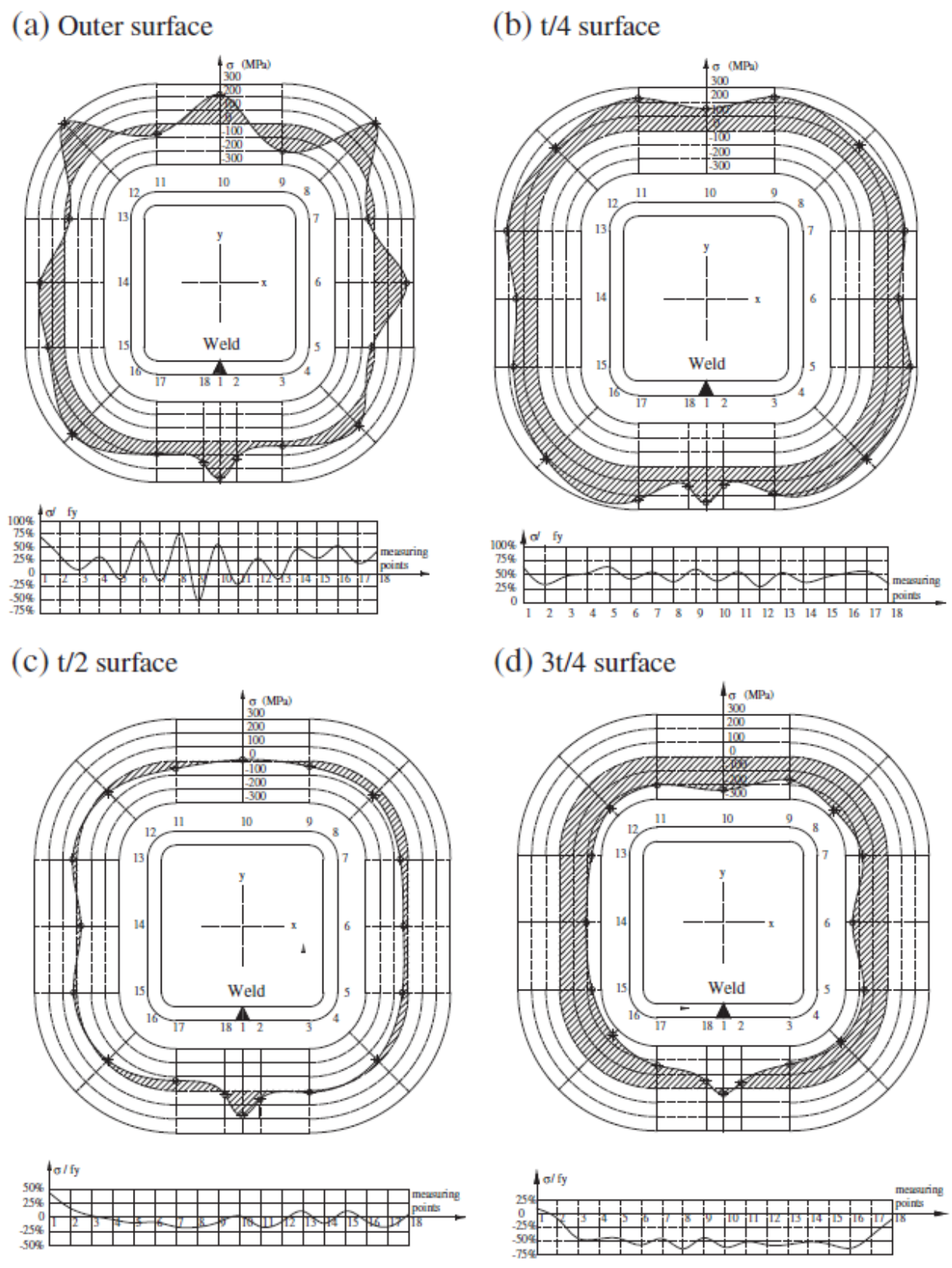


Figure 2-94: Residual stresses for C-135 x 10 using hole-drilling method (Tong et al., 2012)

After taking the measurements, Tong et al. (2012) compared the longitudinal residual stress results obtained by the X-ray method and the hole drilling method. It was reported the results are in good agreement with each other. The hole drilling method yielded results varying from 52 to 61% of the material yield strength while the X-ray method yielded results ranging from 43 to 67%. The mean value was of respectively 29.16% and 29.41% of the yield strength. To understand the mean value statement, it is necessary to consult Figure 2-95 where position 1 corresponds to the weld. Positions 5, 11, 17 and 23 correspond to corners. Tong et al. reported the longitudinal residual stress was in tension on the outer surface and in compression on the inner surface. The stresses were small in the middle along the section thickness and corners exhibited higher residual stress magnitudes than flats for directly formed specimens. For indirectly formed specimens, the residual stress magnitudes are either approximately equal or smaller for the corners. Figure 2-94 provides the results and distribution along the thickness for the indirectly formed section.

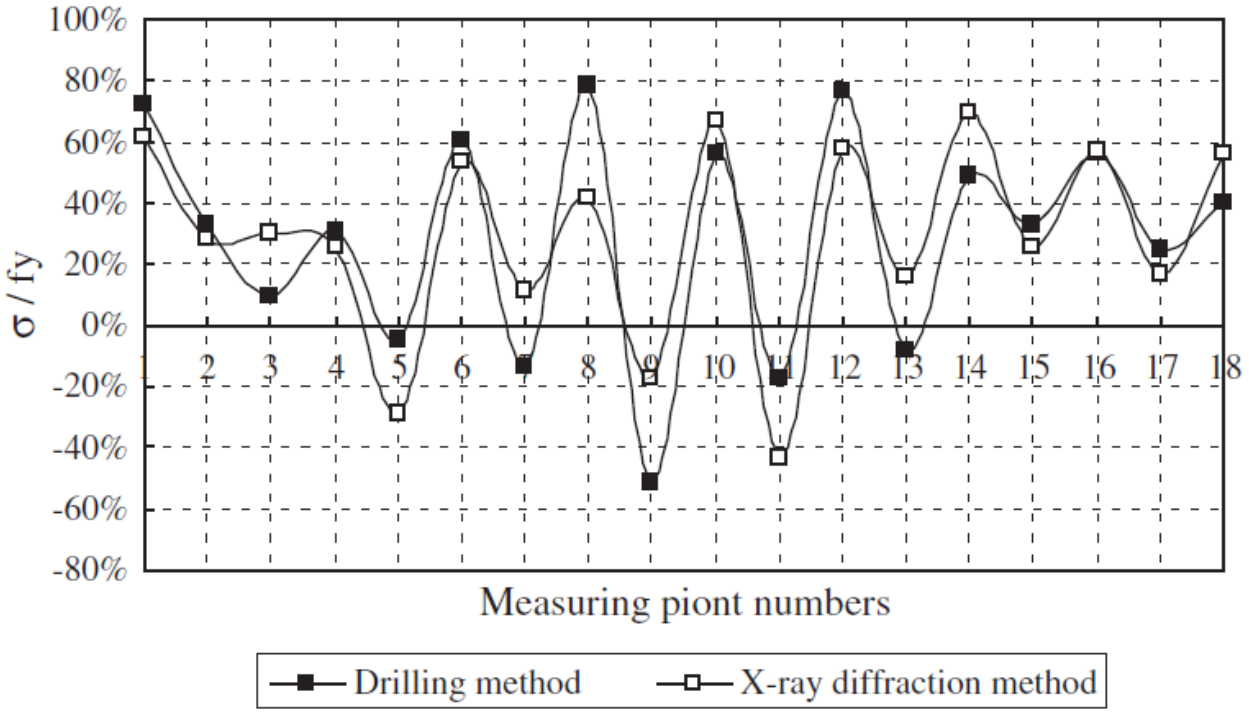


Figure 2-95: Comparison of hole drilling method and diffraction method (Tong et al., 2012)

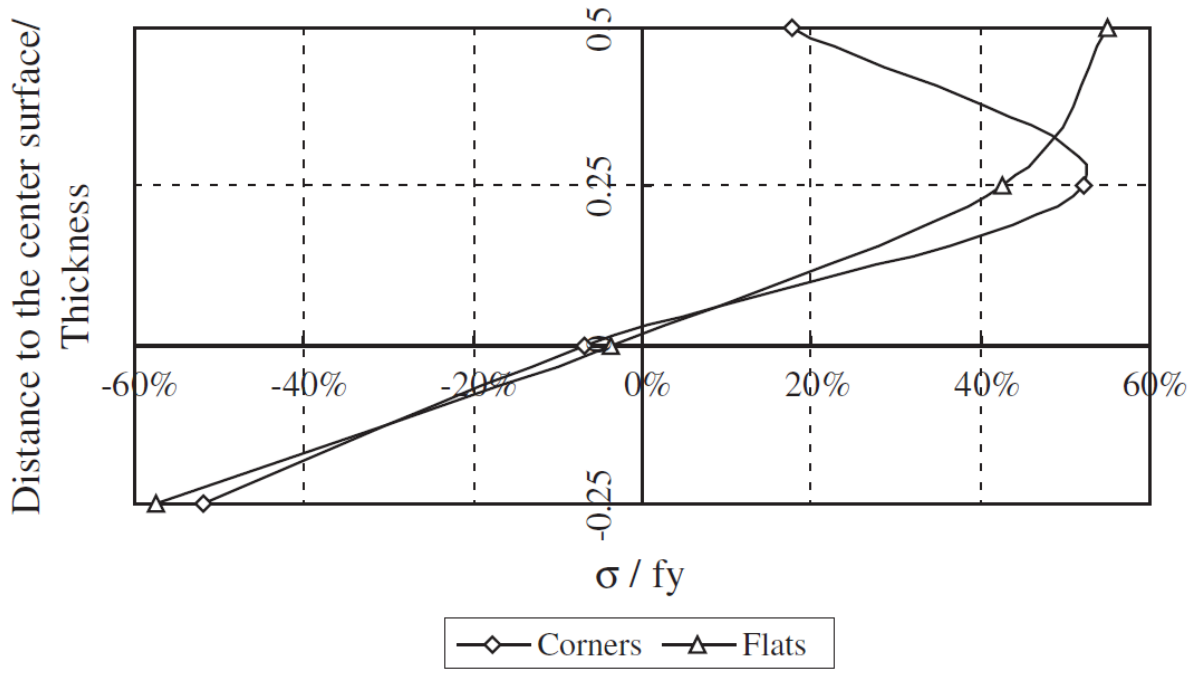


Figure 2-96: Through thickness distribution – C-135 x 10 (Tong et al., 2012)

Finally, Tong et al. (2012) provided equation (2-21) to model the residual stress in both directly and indirectly formed cold-formed sections. The obtained distribution can be seen in Figure 2-97 for the indirectly formed section.

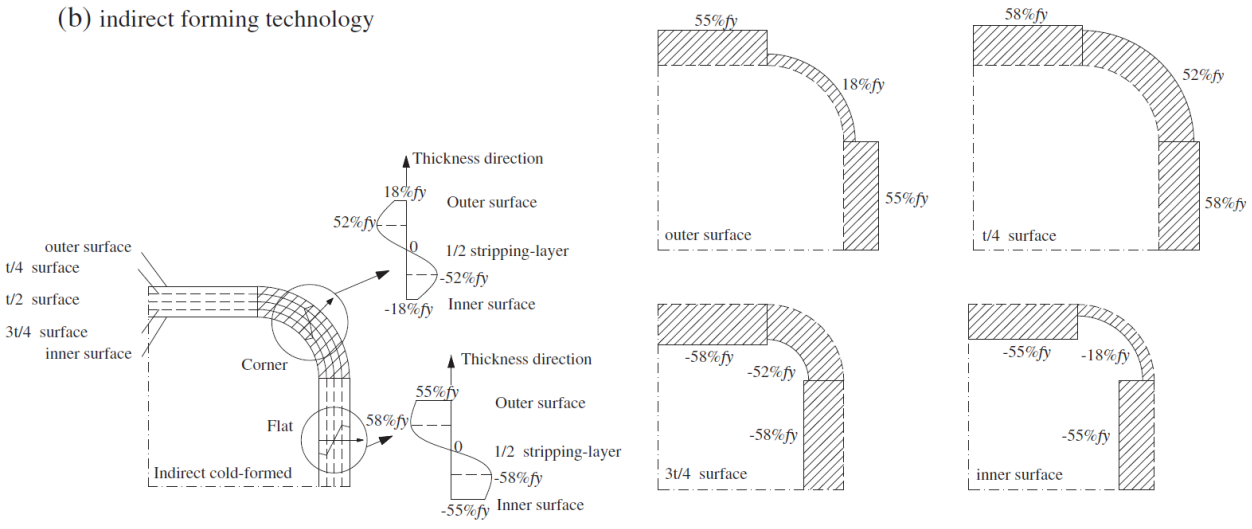


Figure 2-97: Proposed longitudinal residual stress distribution (Tong, et al., 2012)

$$\sigma_{corners} = 0.52 \cdot f_y \cdot \sin\pi\left(1.55\frac{x}{t} + 0.112\right) \qquad (0 \le x \le t/4)$$

$$\sigma_{corners} = 0.52 \cdot f_y \cdot \sin 2\pi\frac{x}{t} \qquad (t/4 \le x \le 3t/4)$$

$$\sigma_{corners} = 0.58 \cdot f_y \cdot \sin\pi\left(1.55\frac{x}{t} - 1.663\right) \qquad (3t/4 \le x \le t)$$

$$\sigma_{flats} = 0.58 \cdot f_y \cdot \sin\pi\left(0.41\frac{x}{t} + 0.397\right) \qquad (0 \le x \le t/4)$$

$$\sigma_{flats} = 0.58 \cdot f_y \cdot \sin 2\pi\frac{x}{t} \qquad (t/4 \le x \le 3t/4)$$

$$\sigma_{flats} = 0.58 \cdot f_y \cdot \sin\pi\left(0.41\frac{x}{t} - 0.808\right) \qquad (3t/4 \le x \le t)$$

(2-21)

The next paper titled "*Strength Enhancement in Cold-formed Structural Sections*" is composed of two parts (Afshan et al., 2013; Rossi et al., 2013). The first part (Afshan et al., 2013) consisted in defining the material properties of cold-formed sections such as the flat and corner yield strength increase. The second part (Rossi et al., 2013) consisted in proposing an equation to predict the final flat and corner yield strength based on the virgin strip.

In total, the material properties of eighteen sections were determined in this paper (Afshan et al., 2013). Twelve were Square Hollow Sections, five Rectangular Hollow Sections and one was a Circular Hollow Section. Several materials were tested such as ferritic, duplex, lean duplex, stainless and carbon steel. Tensile coupon tests and full section tensile tests were performed, and the coupon distribution is shown in Figure 2-98.

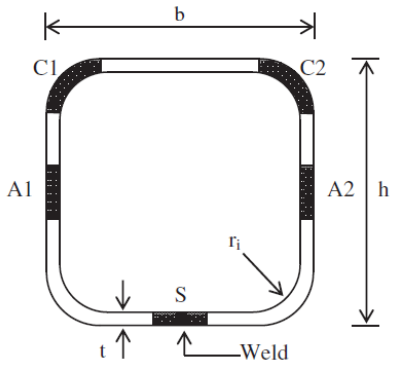


Figure 2-98: Location of tensile coupon tests (Afshan et al., 2013)

The Ramberg-Osgood parameter *n* was also determined in this paper (Afshan et al., 2013) and the results are provided in Table 2-29 along with the tensile coupon results. Afshan et al. concentrated their research on stainless steel and only a few carbon sections were presented. To simplify the figure, only the results for carbon steel sections are included which are relevant to this investigation.

Table 2-29: Yield strength properties of tested sections (Afshan et al., 2013)

Mechanical properties as stated in the mill certificates.

| Cross-section | Material grade | $\sigma_{0.2,mill}$ (N/mm$^2$) | $\sigma_{1.0,mill}$ (N/mm$^2$) | $\sigma_{u,mill}$ (N/mm$^2$) | $A_5$ (%) |
|---|---|---|---|---|---|
| SHS 150×150×6 | S355J2H | 420 | –[a] | 529 | 31 |
| RHS 200×100×5 | S355J2H | 478 | –[a] | 546 | 27 |
| RHS 150×100×6 | S355J2H | 384 | –[a] | 511 | 24 |
| SHS 200×200×6 | S355J2H | 475 | –[a] | 549 | –[a] |

[a] Values were not provided.

Summary of key material properties for the tensile flat coupons.

| Coupon reference | E (N/mm$^2$) | $\sigma_{0.2}$ (N/mm$^2$) | $\sigma_{1.0}$ (N/mm$^2$) | $\sigma_u$ (N/mm$^2$) | $\varepsilon_u$ (%) | $\varepsilon_{pl,f}$ (%) | R–O parameters | | |
|---|---|---|---|---|---|---|---|---|---|
| | | | | | | | n | $n'_{0.2,u}$ | $n'_{0.2,1.0}$ |
| SHS 150×150×8 – A1 | 205,400 | 512 | 567 | 711 | 25.5 | 49.0 | 5.7 | 3.5 | 2.6 |
| SHS 150×150×8 – A2 | 192,000 | 525 | 589 | 745 | 29.8 | 54.8 | 4.9 | 3.8 | 2.9 |
| SHS 150×150×8 – S | 191,000 | 560 | 647 | 704 | 16.6 | 43.7 | 4.7 | 6.5 | 6.0 |
| SHS 150×150×6 – A1 | 195,000 | 393 | 395[d] | 514 | 14.70 | 27.9 | 7.9 | – | – |
| SHS 150×150×6 – A2 | 191,000 | 408 | 425[d] | 529 | 15.80 | 31.9 | 6.9 | – | – |
| SHS 150×150×6 – S | 210,800 | 532 | 572 | 631 | 5.80 | 17.1 | 15.6 | 2.4 | 2.3 |
| RHS 200×100×5 – A1 | 195,000 | 421 | 456 | 494 | 9.6 | 23.0 | 5.8 | 3.8 | 3.2 |
| RHS 200×100×5 – A2 | 191,300 | 436 | 465 | 503 | 11.7 | 30.7 | 8.1 | 2.4 | 2.9 |
| RHS 200×100×5 – S | 210,800 | 624 | 655 | 664 | 3.1 | 13.7 | 9.9 | 2.0 | 1.6 |
| RHS 150×100×6 – A1 | 196,000 | 363 | 390 | 434 | 16.4 | 33.9 | 5.4 | 3.7 | 3.0 |
| RHS 150×100×6 – A2 | 206,900 | 375 | 398 | 449 | 16.5 | 32.4 | 8.4 | 2.8 | 2.5 |
| RHS 150×100×6 – S | 197,000 | 561 | 578 | 580 | 1.6 | 9.9 | 10.1 | 3.3 | 2.9 |
| SHS 200×200×6 – A1 | 208,042 | 419 | 458 | 522 | 14.6 | 35.0 | 7.5 | 3.6 | 2.9 |
| SHS 200×200×6 – A2 | 202,380 | 419 | 459 | 526 | 14.6 | 36.2 | 6.4 | 3.6 | 2.9 |
| SHS 200×200×6 – S | 192,600 | 517 | 546 | 580 | 6.3 | 17.5 | 14.8 | 3.1 | 2.7 |

Summary of key material properties for the tensile corner coupons.

| Coupon name | E (N/mm$^2$) | $\sigma_{0.2}$ (N/mm$^2$) | $\sigma_{1.0}$ (N/mm$^2$) | $\sigma_u$ (N/mm$^2$) | $\varepsilon_u$ (%) | $\varepsilon_{pl,f}$ (%) | R–O parameters | | |
|---|---|---|---|---|---|---|---|---|---|
| | | | | | | | n | $n'_{0.2,u}$ | $n'_{0.2,1.0}$ |
| SHS 150×150×6 – C1 | 197,300 | 602 | 644 | 649 | 2.6 | 15.4 | 9.9 | 4.7 | 9.6 |
| SHS 150×150×6 – C2 | 196,300 | 608 | –[d] | 639 | 1.2 | 10.8 | 10.1 | 3.2 | – |
| RHS 200×100×5 – C1 | 180,500 | 531 | –[b] | –[c] | – | – | 4.2 | – | – |
| RHS 200×100×5 – C2 | 200,300 | 540 | –[b] | –[c] | – | – | 5.3 | – | – |
| RHS 150×100×6 – C1 | 201,500 | 545 | –[d] | 565 | 0.9 | 13.4 | 10.8 | 1.6 | – |
| RHS 150×100×6 – C2 | 210,000 | 528 | –[d] | 542 | 0.7 | 12.7 | 8.8 | 1.1 | – |
| SHS 200×200×6 – C1 | 220,000 | 584 | –[d] | 615 | 0.9 | 12.1 | 8.9 | 1.5 | – |
| SHS 200×200×6 – C2 | 197,300 | 599 | 631 | 633 | 1.4 | 13.1 | 11.3 | 3.4 | 4.1 |

The second part (Rossi et al., 2013), which addressed the predictive models for the yield strength increase in cold-formed sections, was fully based on stainless steel sections. Nevertheless, Rossi et al. compared the results obtained from the proposed equations to carbon steel and concluded their equation can be applied to any metallic non-linear material. The predictive model was based on several previously developed models. The first model was proposed by Cruise and Gardner (2008)

who developed a model for cold-rolled and press-braked stainless-steel sections. It was concluded the two main parameters determining the increase in yield strength are the strain experienced during the cold-rolling process and the potential for strength enhancement. Another simpler power model was also proposed by Ashraf et al. (2013) for cold-rolled sections which was based on a model for press-braked sections proposed by Gardner and Nethercot (2004). Rossi further proposed a new model (2011) where she considered the inverted compound Ramberg-Osgood material model proposed by Abdella (2006) and the strains considered in Cruise and Gardner (2008). The models proposed by Rossi et al. were compared to experimental values and the results are shown in Table 2-30. It is important to note that out of the 158 experimental tests that were used for comparison, only 20 were of carbon steel. Out of those 20, 9 were of sections with a nominal yield strength of 355 MPa and 11 were of sections with a nominal yield strength of 235 MPa.

Table 2-30: Comparison between predictive models and experimental results (Rossi et al., 2013)

Comparison of the predictive models and test data for the 0.2% proof strength of the flat faces of cold-rolled sections ($\sigma_{0.2,f,pred}/\sigma_{0.2,test}$).

| Predictive model | | Cruise and Gardner [4] | Rossi [5] |
|---|---|---|---|
| All | Mean | 1.10 | 0.97 |
| | COV | 0.21 | 0.20 |
| Carbon steel | Mean | (1.25) | 0.99 |
| | COV | (0.20) | 0.18 |
| Stainless steel | Mean | 1.06 | 0.97 |
| | COV | 0.20 | 0.21 |

Comparison of the predictive models and test data for the 0.2% proof strength of the corner regions of cold-formed sections ($\sigma_{0.2,c,pred}/\sigma_{0.2,test}$).

| Predictive model | | Cruise and Gardner [4]Gardner et al. [13] | Rossi [5] |
|---|---|---|---|
| All | Mean | 0.97 | 1.06 |
| | COV | 0.11 | 0.14 |
| Carbon steel | Mean | 0.97 | 0.98 |
| | COV | 0.11 | 0.09 |
| Stainless steel | Mean | 0.97 | 1.08 |
| | COV | 0.12 | 0.14 |

Rossi et al. (2013) explain that while model proposed by Rossi (2008) gave accurate results, it was deemed too difficult to be practically used in design. To solve this issue, Rossi et al. studied a simple power law model and a tri-linear model based on the model proposed by Rossi (2008). It was determined the power law model was more accurate. The comparison between the two is shown in Table 2-31.

Table 2-31: Comparison between power law model and tri-linear model (Rossi, Afshan, & Gardner, 2013)

Comparison of the proposed predictive models and test data for the 0.2% proof strength of flat faces of cold-rolled sections ($\sigma_{0.2,f,pred}/\sigma_{0.2,test}$).

| Predictive model | | Linear model | Power model |
|---|---|---|---|
| All | Mean | 0.89 | 1.01 |
| | COV | 0.21 | 0.20 |
| Carbon steel | Mean | 0.96 | 1.00 |
| | COV | 0.17 | 0.19 |
| Stainless steel | Mean | 0.87 | 1.01 |
| | COV | 0.22 | 0.20 |

Comparison of the proposed predictive models and test data for the 0.2% proof strength of corner regions of cold-formed sections ($\sigma_{0.2,c,pred}/\sigma_{0.2,test}$).

| Predictive model | | Linear model | Power model |
|---|---|---|---|
| All | Mean | 0.92 | 0.96 |
| | COV | 0.14 | 0.14 |
| Carbon steel | Mean | 0.93 | 0.92 |
| | COV | 0.07 | 0.08 |
| Stainless steel | Mean | 0.92 | 0.97 |
| | COV | 0.16 | 0.15 |

Rossi et al. (2013) proposed equation (2-22) based on virgin properties for both flats and corners and equation (2-23) for the overall yield strength of the section for roll-formed sections. Rossi et al. suggested the corner strength should be extended by 2t beyond the radius.

$$\sigma_{0.2,f,pred} = 0.85\left[p\left(\varepsilon_{f,av} + \varepsilon_{t,0.2}\right)^{q}\right] \qquad \text{but} \leq \sigma_{u,mill} \tag{2-22}$$

$$\sigma_{0.2,c,pred} = 0.85\left[p\left(\varepsilon_{c,av} + \varepsilon_{t,0.2}\right)^{q}\right] \qquad \text{but} \leq \sigma_{u,mill}.$$

$$p = \frac{\sigma_{0.2,mill}}{\varepsilon_{t,0.2}^{q}}$$

$$q = \frac{\ln\left(\sigma_{0.2,mill}/\sigma_{u,mill}\right)}{ln\left(\varepsilon_{t,0.2}/\varepsilon_{u}\right)}.$$

For cold-rolled sections: (2-23)

$$\sigma_{0.2,section} = \frac{\left(\sigma_{0.2,c,pred}A_{c,rolled}\right) + \left(\sigma_{0.2,f,pred}\left(A - A_{c,rolled}\right)\right)}{A} \tag{17}$$

where, $A_{c,pb} = A_c = (n_c\pi t/4)(2r_i + t)$, $A_{c,rolled} = A_c + 4n_c t^2$, $A$ = gross cross-sectional area of the section and $n_c$ is the number of 90° corners in the section.

Finally, the predictive model (Rossi et al., 2013) was compared to the European equations in EN 1993-1-4 and EN 1993-1-1 to account for the increased yield strength (similar to the CSA S136 standard). It was determined the proposed equations offer strength enhancements of 19 and 36% on average with respect to the European standards.

Another interesting article titled "*Direct-formed and Continuous-formed Rectangular Hollow Sections – Comparison of Static Properties*" was published by Sun and Packer (2014). This article was based on Sun's thesis (2014) titled "*Mechanical Behaviour of Cold-Formed Hollow Structural Section Material*". Except for some changes in the nomenclature, the article was a summary of several chapters of the thesis. The investigation compared the tensile stress-strain behaviour, ductility, compressive stress-strain behaviour of the entire cross-section and longitudinal residual stresses of sections going through three different manufacturing methods. The sections were produced by direct-forming, continuous forming and continuous forming with stress-relieving heat treatment. Table 2-32 presents the tested sections.

Table 2-32: Tested sections (Sun, 2014)

| RHS ID | Nominal sizes | $B_{nom}/t_{nom}$ | Manufacturing standard / grade |
|---|---|---|---|
| DF19 | 152x152x7.95 mm | 19 | N/A (Domex) |
| DF12 | 152x152x12.7 mm | 12 | CAN/CSA-G40.20-04/G40.21-04 Gr. 350W Class C |
| DF24 | 152x152x6.35 mm | 24 | CAN/CSA-G40.20-04/G40.21-04 Gr. 350W Class C |
| CF12 | 152x152x12.7 mm | 12 | CAN/CSA-G40.20-04/G40.21-04 Gr. 350W Class C |
| CFH12 | 152x152x12.7 mm | 12 | CAN/CSA-G40.20-04/G40.21-04 Gr. 350W Class H |
| CF24 | 152x152x6.35 mm | 24 | CAN/CSA-G40.20-04/G40.21-04 Gr. 350W Class C |
| CFH24 | 152x152x6.35 mm | 24 | CAN/CSA-G40.20-04/G40.21-04 Gr. 350W Class H |

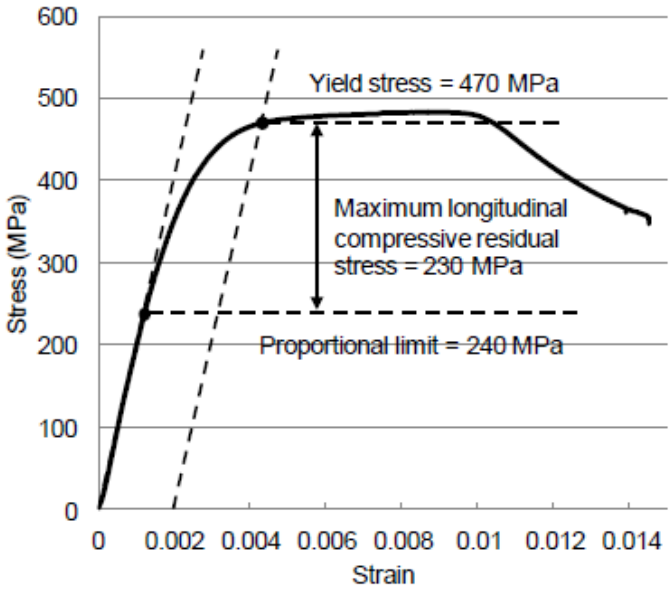


Figure 2-99: Approximation of longitudinal residual stress from stub column results (Sun, 2014)

Sun (2014) conducted an experimental investigation to determine the yield strength of flat and corner coupons along with stub column specimens. Residual stress measurements were also performed using the sectioning technique. The sectioning technique consists in attaching strain gauges to the exterior and interior surfaces, cutting the section into longitudinal strips and then measuring the strain change in the section. The strip will exhibit axial deformation and bending, which can then be converted into unloading stresses. The unloading stress represents an approximation of the residual stresses within the section. This is the same technique as used by Davison and Birkemoe (1983) which they used to determine the average magnitudes to apply to the residual stress model. The full-section tensile properties were not measured and were determined from the weighted average of the flat and corner coupon results. These are further compared with the stub column results. Sun also determined the approximate magnitude of the longitudinal residual stress from stub column results by subtracting the proportional limit yield strength to the actual yield strength as shown in Figure 2-99. Table 2-33 presents the yield strength results. Table 2-34 compares tensile results to stub column results. Figure 2-100 and Figure 2-101 present flat coupon versus corner coupon results for the continuously formed sections. Figure 2-102 presents the elongation differences between flat and corner coupons. Finally, Table 2-35 and Figure 2-103 present residual stress measurements.

Table 2-33: Coupon test results (Sun, 2014)

| | | Flat face | | Corner | | Entire cross-section | | $f_{y,avg}$ difference between flat face and entire cross-section |
|---|---|---|---|---|---|---|---|---|
| RHS ID | $B_{nom}/t_{nom}$ | Area ($mm^2$) | $f_{y,avg}$ (MPa) | Area ($mm^2$) | $f_{y,avg}$ (MPa) | Area ($mm^2$) | $f_{y,avg}$ (MPa) | |
| DF19 | 19 | 3867 | 723 | 708 | 770 | 4575 | 730 | 1% |
| DF12 | 12 | 5228 | 427 | 1636 | 615 | 6864 | 472 | 10% |
| DF24 | 24 | 3240 | 402 | 382 | 539 | 3622 | 416 | 4% |
| CF12 | 12 | 4991 | 457 | 1692 | 590 | 6683 | 491 | 7% |
| CFH12 | 12 | 4991 | 483 | 1692 | 570 | 6683 | 505 | 5% |
| CF24 | 24 | 3036 | 340 | 379 | 483 | 3415 | 356 | 5% |
| CFH24 | 24 | 3036 | 363 | 379 | 463 | 3415 | 374 | 3% |
| | | Flat face | | Corner | | Entire cross-section | | $f_{u,avg}$ difference between flat face and entire cross-section |
| RHS ID | $B_{nom}/t_{nom}$ | Area ($mm^2$) | $f_{u,avg}$ (MPa) | Area ($mm^2$) | $f_{u,avg}$ (MPa) | Area ($mm^2$) | $f_{u,avg}$ (MPa) | |
| DF19 | 19 | 3867 | 779 | 708 | 807 | 4575 | 783 | 1% |
| DF12 | 12 | 5228 | 522 | 1636 | 649 | 6864 | 552 | 6% |
| DF24 | 24 | 3240 | 473 | 382 | 567 | 3622 | 483 | 2% |
| CF12 | 12 | 4991 | 599 | 1692 | 676 | 6683 | 618 | 3% |
| CFH12 | 12 | 4991 | 606 | 1692 | 637 | 6683 | 614 | 1% |
| CF24 | 24 | 3036 | 448 | 379 | 528 | 3415 | 457 | 2% |
| CFH24 | 24 | 3036 | 464 | 379 | 531 | 3415 | 471 | 2% |

Table 2-34: Full-sectional tensile versus compressive properties (Sun, 2014)

| | | $f_{y,avg}$ | | | $f_{u,avg}$ | | |
|---|---|---|---|---|---|---|---|
| RHS ID | $B_{nom}/t_{nom}$ | Tensile (MPa) | Compressive (MPa) | Tensile / compressive | Tensile (MPa) | Compressive (MPa) | Tensile / compressive |
| DF19 | 19 | 730 | 720 | 1.01 | 783 | 801 | 0.98 |
| DF12 | 12 | 472 | 500 | 0.94 | 552 | 580 | 0.95 |
| DF24 | 24 | 416 | 470 | 0.89 | 483 | 482 | 1.00 |
| CF12 | 12 | 491 | 550 | 0.89 | 618 | 658 | 0.94 |
| CFH12 | 12 | 505 | 580 | 0.87 | 614 | 584 | 1.05 |
| CF24 | 24 | 356 | 390 | 0.91 | 457 | 446 | 1.02 |
| CFH24 | 24 | 374 | 410 | 0.91 | 471 | 426 | 1.11 |

Note: There are differences between the full-sectional tensile and compressive properties because the full-sectional tensile properties were calculated based on local tensile properties obtained from tensile coupon tests.

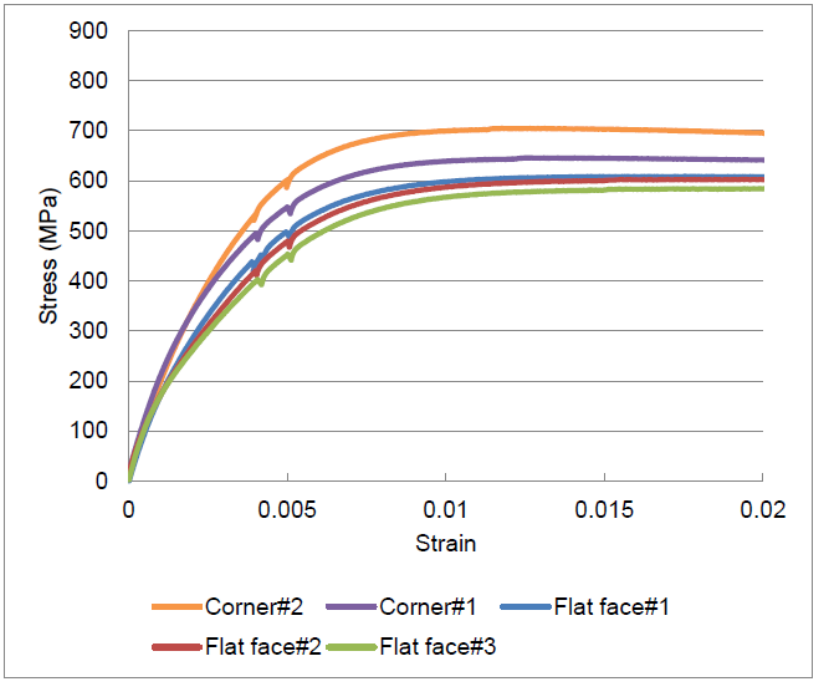


Figure 2-100: Tensile coupon results CF12 – RHS 152 x 152 x 12.7 – Continuously formed (Sun, 2014)

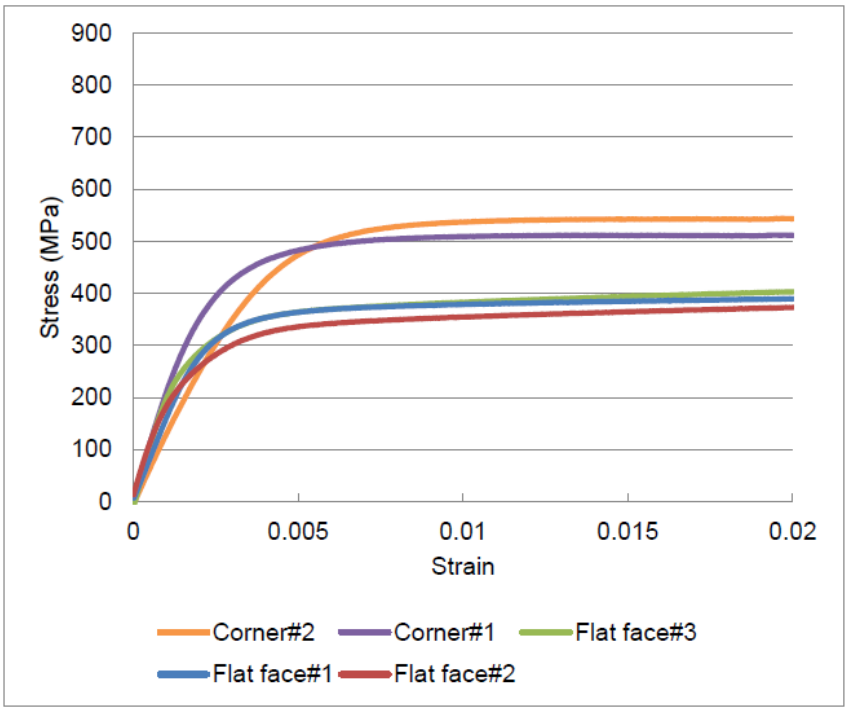


Figure 2-101: Tensile coupon results CF24 – RHS 152 x 152 x 12.7 – Continuously formed (Sun, 2014)

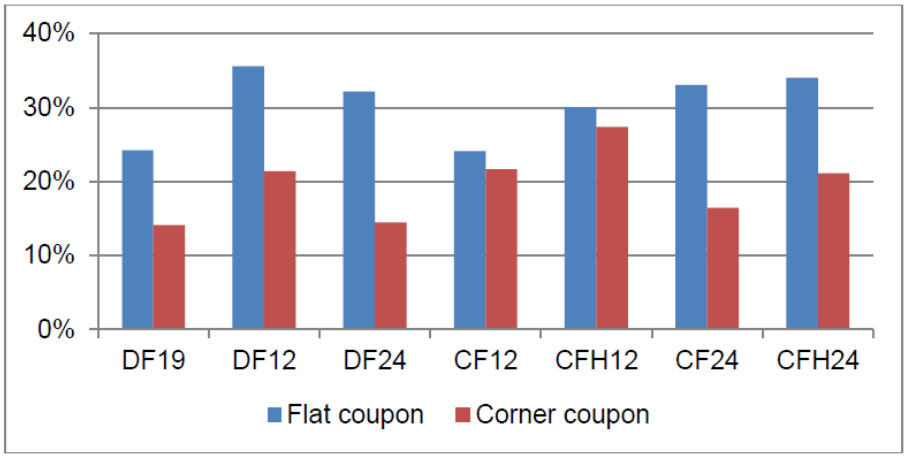


Figure 2-102: Elongation differences (Sun, 2014)

Table 2-35: Residual stress measurements (Sun, 2014)

| RHS ID | $B_{nom}$ / $t_{nom}$ | Average of $\sigma_{rs,out}$ / $f_y$ (tensile) | Average of $\sigma_{rs,in}$ / $f_y$ (compressive) | Max. compressive $\sigma_{rs}$ / $f_y$ (from residual stress measurements) | Max. compressive $\sigma_{rs}$ / $f_y$ (from stub column test results) |
|---|---|---|---|---|---|
| DF12 | 12 | 39.0% | 37.6% | 60.2% | 52.0% |
| DF24 | 24 | 36.1% | 28.1% | 56.7% | 48.9% |
| CF12 | 12 | 60.0% | 60.0% | 91.1% | 74.5% |
| CFH12 | 12 | 24.1% | 24.5% | 37.2% | 31.0% |
| CF24 | 24 | 51.8% | 47.4% | 74.9% | 61.5% |
| CFH24 | 24 | 19.4% | 16.1% | 28.5% | 17.1% |

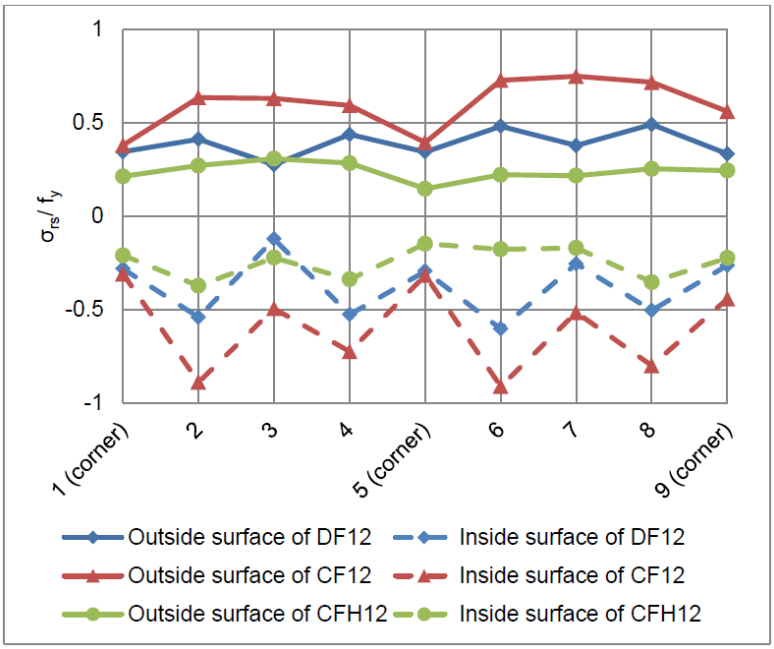


Figure 2-103: Residual stress measurements (Sun, 2014)

Sun (2014) concluded the difference between nominal yield strength and the experimental yield strength can be quite significant. The difference was up to 38% for the flat coupons and 76% for the corners. There was also no clear yield point as the material began to yield progressively. There was only a slight increase in ultimate tensile stress compared to the yield strength increase.

When analyzing the stub column behaviour, Sun and Packer (2014) wrote there was a relatively large difference on the proportional limit to overall compressive yield strength ratio with respect to b/t ratios for continuously formed sections. The proportional limit to overall compressive thickness ratio for the directly formed sections was very similar regardless of the b/t ratio. These observations led Sun and Packer to determine that longitudinal residual stress is affected by the b/t ratio. It is explained sections with larger b/t ratios would have a lower longitudinal residual stress. These results are shown in Table 2-36.

Table 2-36: Proportional limit over stub column yield strength ratio (Sun & Packer, 2014)

Key stub column test results.

| RHS ID | L (mm) | A ($mm^2$) | E (GPa)[a] | $f_y$ (MPa) | $f_u$ (MPa) | $\sigma_p$ (MPa) | $\sigma_p/f_y$ |
|---|---|---|---|---|---|---|---|
| DF1 | 498.0 | 4662 | 179.5 | 720 | 801 | 320 | 44.4% |
| DF2 | 499.8 | 6678 | 176.3 | 500 | 580 | 240 | 48.0% |
| DF3 | 599.5 | 3549 | 214.0 | 470 | 482 | 240 | 51.1% |
| CF1 | 501.5 | 6565 | 170.2 | 550 | 658 | 140 | 25.5% |
| CFH2 | 498.3 | 6565 | 180.4 | 580 | 584 | 400 | 69.0% |
| CF3 | 599.8 | 3366 | 197.4 | 390 | 446 | 150 | 38.5% |
| CFH4 | 599.7 | 3366 | 204.3 | 410 | 426 | 340 | 82.9% |

[a] Some Young's modulus values are lower than the nominal (200 GPa), since shim material was used for alignment control due to non-perfect machining of the ends of some stub columns.

The corner ductility significantly decreased for all types of sections. The flat coupon ductility only significantly decreased for the continuously formed section. The section with a b/t ratio of 12 had a much larger decrease in ductility than the section with a b/t of 24. Sun (2014) explained previous research (Feldmann et al., 2012) had demonstrated that the amount of cold work sustained by a section is directly proportional to its b/t ratio. This means the yield strength gradient and ductility reduction for a section with a b/t of 12 should be about twice as the one for a section with a b/t of 24. Heat treatment brings back the material's original ductility.

The residual stress measurements were compared with the stub column predictions from the proportional limit and were found to be in good agreement with each other. Sun reported "*maximum*

*longitudinal residual stresses were found between the centrelines of the flat faces and the corners, which is in good agreement with measurements reported by other researchers such as Davison and Birkemoe, Key, Hancock and Gardner*" (Sun, 2014, p.30). It was also found continuously-formed HSS sections had the highest level of residual stresses from all the section types. As the b/t ratio increased the average longitudinal residual stress deceased.

After determining the experimental values, Sun (2014) constructed a column model based on the tangent modulus theory for a perfectly straight member and incorporated the results. The author justified a perfectly straight member by stating that HSSs tend to have a very high level of straightness in practice. The adopted residual stress distribution for the theoretical model is shown in Figure 2-104.

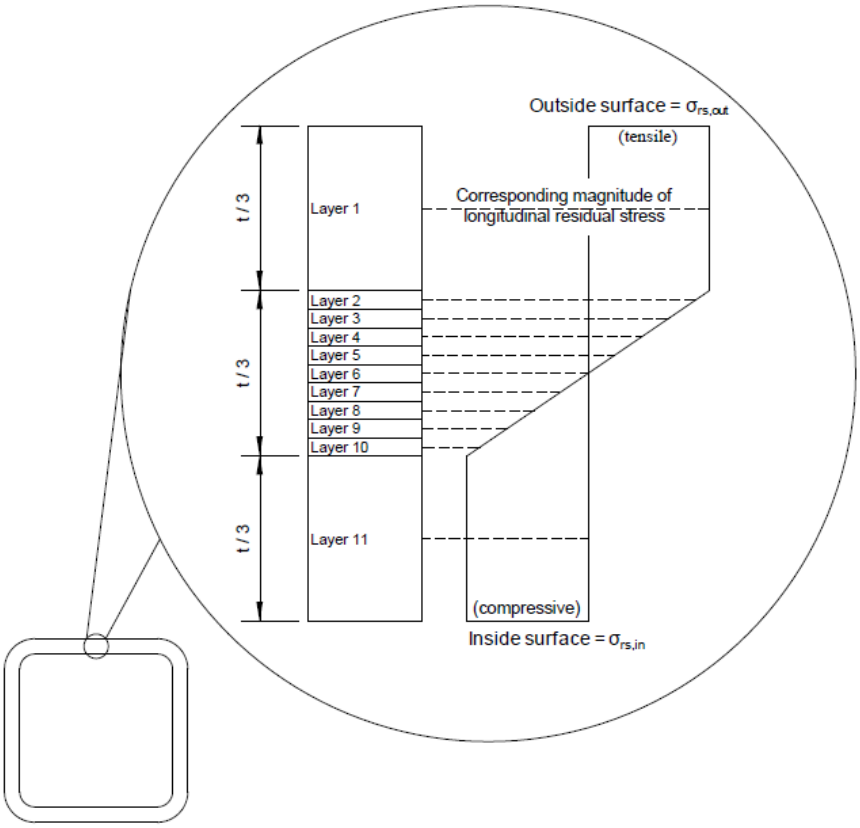


Figure 2-104: Residual stress distribution applied to column model (Sun, 2014)

Finally, Sun (2014) compared the results obtained from the column model to previously determined experimental results and to the current design curves. This comparison is shown in Figure 2-105

and Figure 2-106. The author also performed Charpy V-Notch impact toughness tests and high strain rate behaviour. For information on these results, Sun's thesis can be consulted.

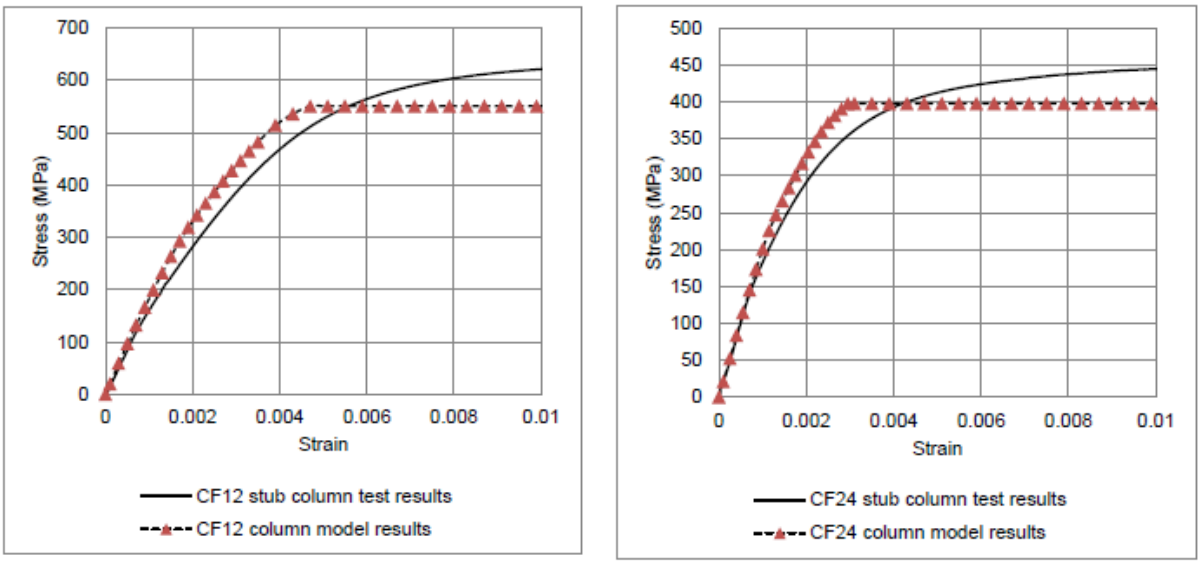


Figure 2-105: Tangent modulus model versus stub column experimental values (Sun, 2014)

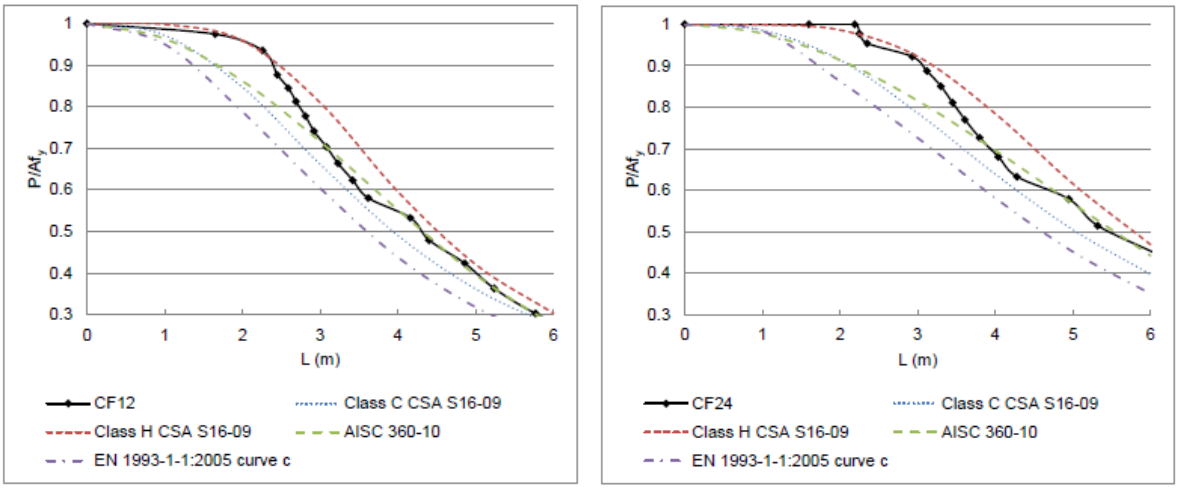


Figure 2-106: Comparison of column model with design curves and experimental values (Sun, 2014)

Liu et al. (2017) proposed a method to approximate the residual stress distribution in cold-formed steel members and to include it in a beam element-based nonlinear frame analysis in an article titled "*Modelling and Probabilistic Study of the Residual Stress of Cold-formed Hollow Steel Sections*". The authors also performed a probabilistic study of several HSS frames.

The residual stress distribution proposed by Liu et al. (2017) is the one proposed by Key and Hancock (1993). However, as Liu et al. wrote, a distribution of such complexity can only be implemented into a Shell Finite-Element or Finite-Strip model. Therefore, Liu et al. approximated the effects of the components by modifying the perfectly-plastic stress-strain curve. For further details on the equations and assumptions to achieve this Liu et al.'s paper can be consulted.

It was considered the bending longitudinal residual stress is enough to obtain accurate results. To confirm this, Liu et al. (2017) compared a simple beam with all six components and just the bending component. A cubic polynomial function was proposed for the stress-strain curve accounting for bending residual stress. The results are seen in Figure 2-107.

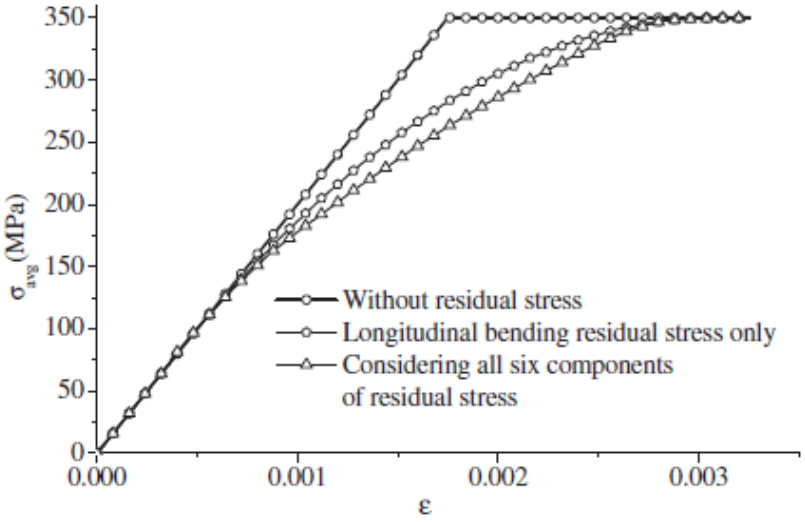


Figure 2-107: Comparison of effects of different residual stress components (Liu et al., 2017)

Liu et al. (2017) used a beam element-based geometric and material nonlinear analysis to study the influence of residual stresses in frames. To trace the spread of plasticity, a 3D plastic zone beam-column element was built in ABAQUS with a 200 mm mesh size. The slenderness of the columns was set close to unity to obtain the maximum effects from the residual stress. Two frame configurations were studied as shown in Figure 2-108 with 500 kN point loads at each beam-column intersection.

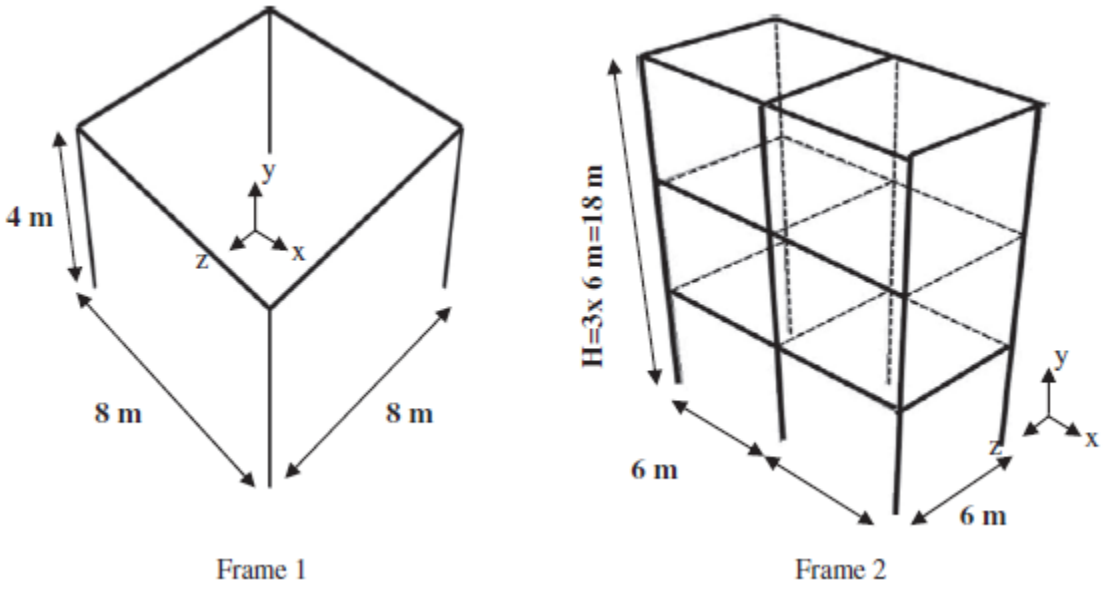


Figure 2-108: Studied frame configurations (Liu et al., 2017)

Liu et al. (2017) studied four cases of residual which they described as follows:

- *Case 1: No residual stress.*
- *Case 2: The stress-strain curve accounting for all six components of residual stress.*
- *Case 3: The stress-strain curve accounting for the longitudinal bending residual stress.*
- *Case 4: The stress-strain curve using the approximate polynomial function.* (Liu et al., 2017, p.991)

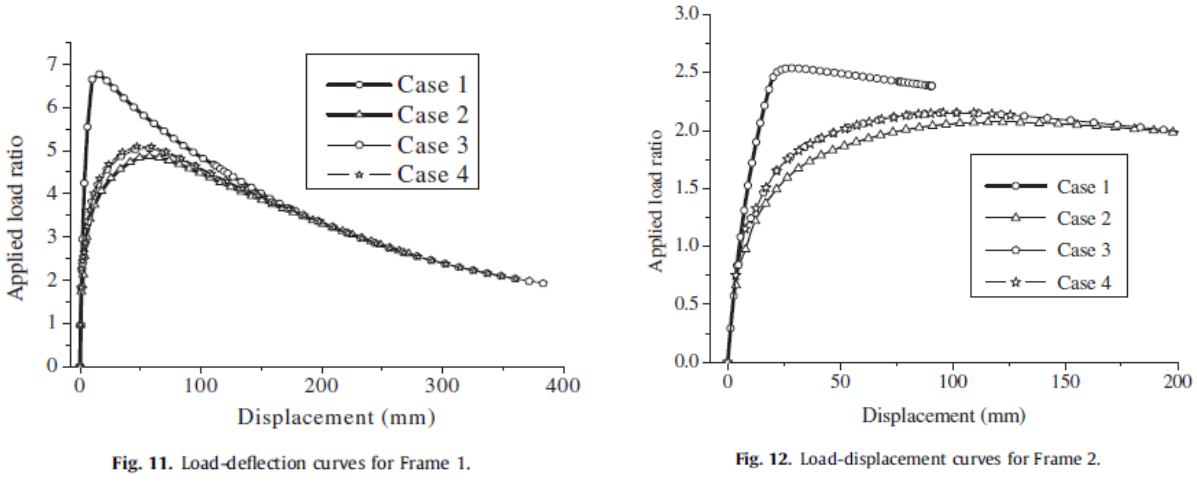


Figure 2-109: Parametric study on residual stress – Graphs (Liu et al., 2017)

Table 2-37: Parametric study on residual stress – Numerical values (Liu et al., 2017)

Comparison of the ultimate load factors of Frames 1 and 2.

| Case | Frame 1 | Error (%) | Frame 2 | Error (%) |
|---|---|---|---|---|
| Case 1 | 6.77 | 39.14 | 2.54 | 22.71 |
| Case 2 | 4.86 | – | 2.07 | – |
| Case 3 | 5.05 | 3.91 | 2.15 | 3.86 |
| Case 4 | 5.10 | 4.94 | 2.15 | 3.86 |

The results are shown in Figure 2-109 and Table 2-37. Liu et al. (2017) concluded the case with only the longitudinal bending residual stress represents a small enough error to justify not including all six components. After determining it is only necessary to apply the longitudinal bending residual stresses to obtain accurate results, Liu et al. took a bending residual stress with a maximum value of $0.7F_y$ with a coefficient of variation of 0.05 for their model where $F_y$ is the uniaxial yield stress of the section. This value was based on previous literature, specifically Davison and Birkemoe's (1983) suggestion. A total of eight moment resistant frame configurations were studied with sections of a nominal yield strength of 450 MPa. This gave a maximum bending residual stress of 315 MPa. Finally, a Monte Carlo simulation was carried out to assess the effect of the uncertainty in the residual stress of the member. Liu et al. determined it is important to include the residual stress in the model, but its uncertainty can be treated as deterministic.

The final articles to be included in this review are a European set published in 2016 and 2017. The articles are the following:

- *Residual stress measurements on cold-formed HSS hollow section columns* (Somodi & Kövesdi, 2016).
- F*lexural buckling resistance of cold-formed HSS hollow section members* (Somodi & Kövesdi, 2017).

Both of these articles were aimed at high strength steel cold-formed HSS members. However, the Somodi and Kövesdi (2016 and 2017) provided good comparisons with normal strength members and drew conclusions for both which makes them of great interest to this investigation.

Somodi and Kövesdi (2016) studied the residual stress distribution in continuously formed cold-rolled sections and tested grades ranging from S420 to S960 in the first article. The main issues

addressed by the authors were the lack of residual stress information on high strength steels and whether the b/t ratio affects material properties.

The residual stresses on the surface were determined (Somodi & Kövesdi, 2016) using two methods which are the sectioning technique and the Laser-Falconeye method. The second method was deemed far more precise and was used to confirm the results obtained with the sectioning technique. Flat and corner coupon yield strength was also measured. Figure 2-110 and Table 2-38 provide some of the results on residual stress measurements and tensile coupon strength.

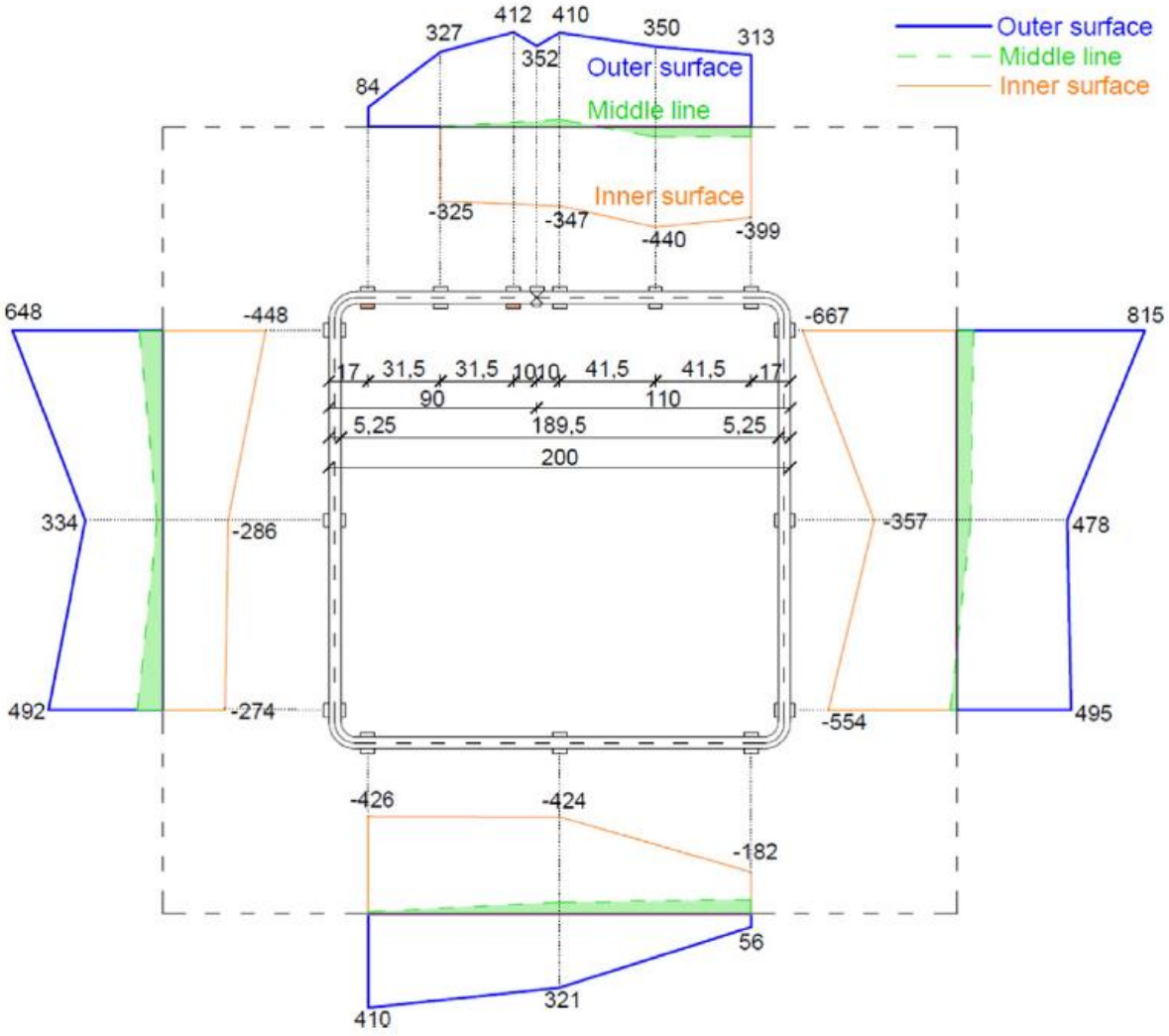


Figure 2-110: Residual stress measurements – CF5 200 x 5 (Somodi & Kövesdi, 2016)

Table 2-38: Tensile coupon strength measurements (Somodi & Kövesdi, 2016)

Residual stress results on the cold-formed test specimens.

| Specimen | Material properties | | Residual stresses [MPa] | | | | Residual stress/yield strength ratios | | | |
|---|---|---|---|---|---|---|---|---|---|---|
| | Plate | | | | | | | | | |
| | *fy* [MPa] | *fu* [MPa] | Outside | | Inside | | Outside | | Inside | |
| | | | Mean | Max | Mean | Min | Mean | Max | Mean | Min |
| CF5-120 × 6_V | 624 | 656 | 518 | 637 | −488 | −630 | 83% | 97% | −78% | −96% |
| CF5-130 × 4_V | 573 | 649 | 557 | 729 | −452 | −649 | 97% | 112% | −79% | −100% |
| CF5-200 × 5_V | 567 | 648 | 408 | 815 | −387 | −667 | 72% | 126% | −68% | −103% |
| CF7-150 × 8_R | 742 | 839 | 579 | 711 | −551 | −786 | 78% | 85% | −74% | −94% |
| CF7-150 × 4_V | 799 | 874 | 534 | 889 | −561 | −815 | 67% | 102% | −70% | −93% |
| CF9-120 × 6_R | 1088 | 1182 | 452 | 549 | −386 | −408 | 42% | 46% | −35% | −35% |
| CF9-120 × 4_R | 1049 | 1207 | 502 | 643 | −619 | −746 | 48% | 53% | −59% | −62% |
| CF9-150 × 7_R | 1114 | 1199 | 391 | 557 | −353 | −511 | 35% | 46% | −32% | −43% |
| CF4.2-100 × 3_R | 458 | 552 | 320 | 469 | −292 | −361 | 70% | 85% | −64% | −65% |
| CF4.2-120 × 6_R | 506 | 551 | 331 | 466 | −326 | −544 | 65% | 85% | −64% | −99% |
| CF4.2_150 × 5_R | 479 | 561 | 351 | 601 | −331 | −606 | 73% | 107% | −69% | −108% |
| CF4.6_150 × 8_R | 508 | 563 | 467 | 561 | −489 | −627 | 92% | 100% | −96% | −111% |
| CF4.6_120 × 4_R | 559 | 598 | 297 | 423 | −349 | −421 | 53% | 71% | −62% | −70% |

The following conclusions, as reported by Somodi and Kövesdi (2016), were drawn from these measurements:

- *Tension stresses are measured on the outer surface of the specimens.*
- *Compression stresses are measured in the inner surface.*
- *Membrane stresses are close to zero.*
- *Bending stresses are the dominant residual stresses.*
- *The residual stresses in the corner zone are significantly smaller than the values measured in the middle of the plates.*
- *The residual stresses in the middle of the plates are slightly smaller than the residual stresses close to the corner zone, the difference depends on the b/t ratio of the tested girder.*
- *Residual stresses are slightly reduced in the welding zone.* (Somodi & Kövesdi, 2016, p.712)

Transverse residual stresses were also measured (Somodi & Kövesdi, 2016) and were determined to be significantly smaller than longitudinal residual stresses. They were always opposite in sign to longitudinal stresses and the absolute value was about half of the longitudinal stress.

Figure 2-111 compares residual stress measurements with respect to the b/t ratio. Results from previous research are also included. Somodi and Kövesdi (2016) concluded it was not possible to establish a clear tendency for indirectly formed sections with a b/t ratio ranging from 10 to 40.

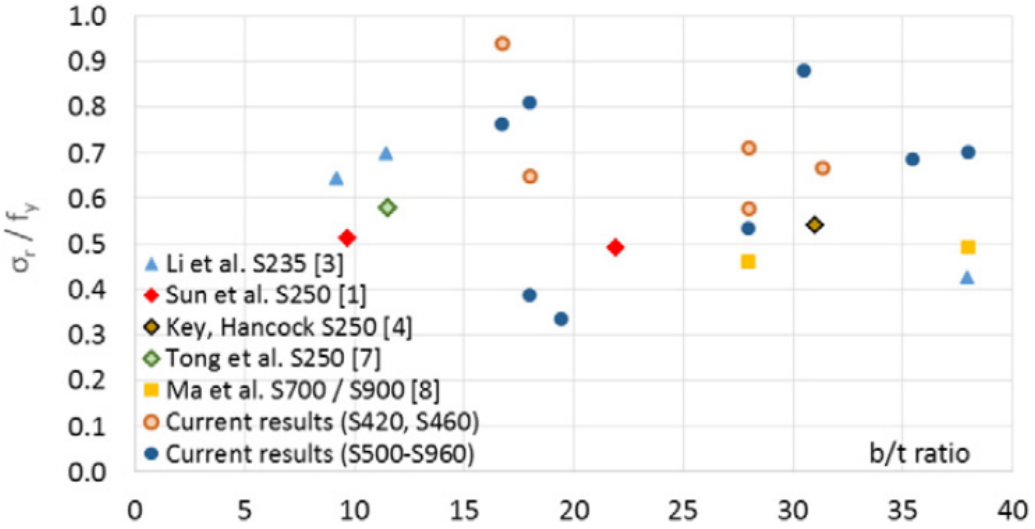


Figure 2-111: Residual stress measurements with respect to b/t ratio (Somodi & Kövesdi, 2016)

An important note has to be made with regards to Sun's results (2014). As it is seen in Figure 2-111 Sun's results are reported as 50% of the actual yield strength. In the previous section, these same results were reported as approximately 50 and 60% in Table 2-35. This discrepancy arises because Somodi and Kövesdi (2016) took the results from Sun and Packer's article (2014), while the results in the current review were reported from Sun's thesis (2014). Both set of results are correct, but the results from the thesis represent the average measured from the sectioning method, while the results in the article were determined from the proportional limit.

Somodi and Kövesdi (2016) noted a clear relationship can be seen between the nominal yield strength and the residual stress for normal strength sections. As the nominal yield strength increases so does the residual stress. The authors report the relationship is quasi-linear. High strength steels show the opposite where the residual stress decreases with an increase of nominal yield strength. This difference in behaviour is explained by high strength steels having a far stronger Bauschinger effect.

Somodi and Kövesdi (2016) proposed two equations to approximate the average longitudinal bending residual stress based on the nominal yield strength. Equation (2-22) is for high strength steel grades ranging from S500 to S960 and equation (2-25) is for normal strength steel with grades ranging from S235 to S460.

$$\sigma_{rb,flat} = \pm\left(1.28 - \frac{f_y}{1270\ \ MPa}\right) \cdot f_y \tag{2-24}$$

$$\sigma_{rb,flat} = \pm\left(0.8 \cdot f_y - 67\ \text{MPa}\right) \tag{2-25}$$

As for residual stress in corners, Somodi and Kövesdi (2016) concluded it is approximately 55% of the residual stress of the flats. It was also reported that while the average bending residual stress is not dependant on the b/t ratio, the difference between the center of the flat and the edges of the flat is actually affected by this parameter. For small b/t ratios, the residual stress at the center is much closer to the residual stress at the edges. For high b/t ratios, the difference in residual stress between the center and the flats is more significant. However, the authors state, there is not enough data to draw a final conclusion, but the tendency is clear. Figure 2-112 shows the sectioning technique results compared to the laser Falconeye results. Figure 2-113 shows additional through thickness measurements. The authors state both methods are in good agreement with each other.

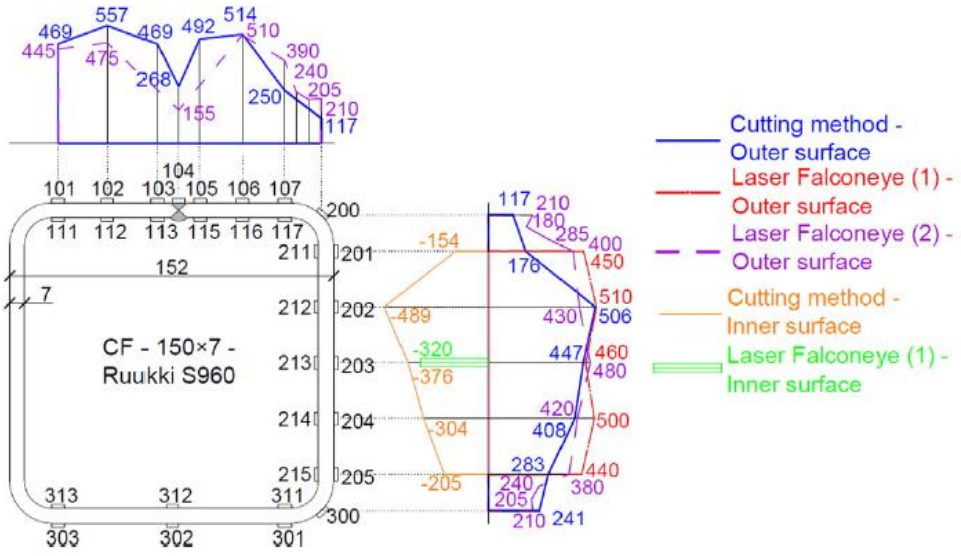


Figure 2-112: Residual stress measurements by the sectioning technique versus the laser Falconeye technique (Somodi & Kövesdi, 2016)

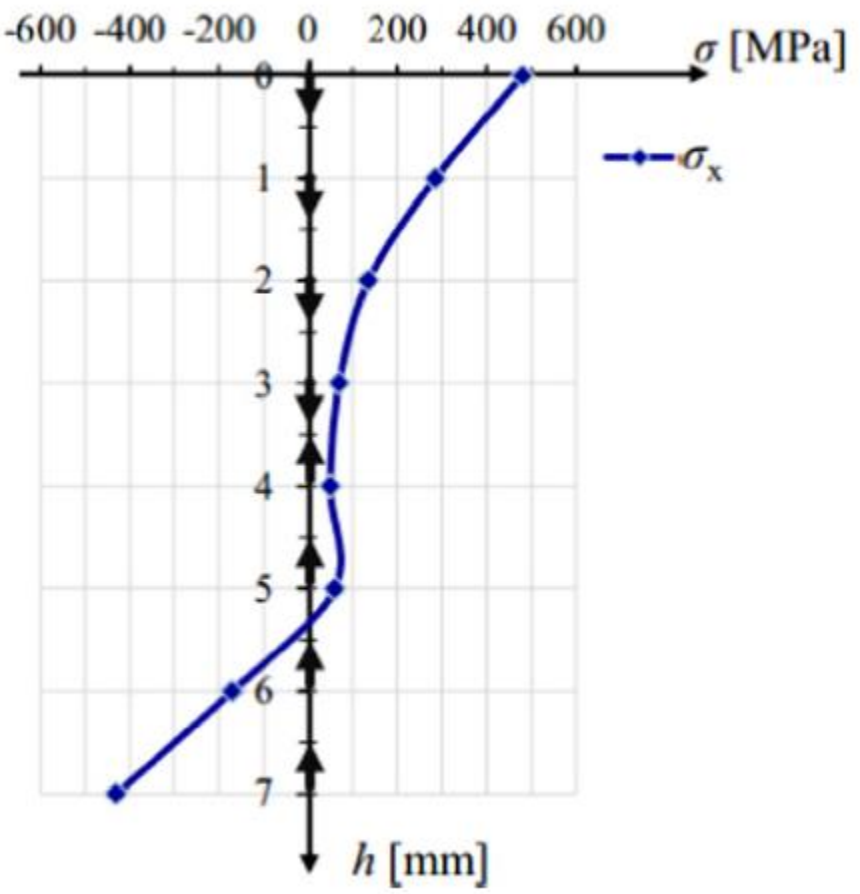


Figure 2-113: Through thickness residual stress measurements (Somodi & Kövesdi, 2016)

Finally, Somodi and Kövesdi (2016) propose several recommendations for numerical modeling. No particular yield strength gradient is proposed. The authors consider the bending residual stresses to be dominant and the membrane residual stresses to be close to zero. It is considered the residual stresses are in tension in the outer surface and compression in the inner surface. There is a variation in residual stress with respect to the b/t ratio. As the b/t ratio decreases, the residual stress at center is increased up to the magnitude at the edge of the flat wall.

For the second article, Somodi and Kövesdi (2017) studied the EN 1993-1-1 column buckling resistance curves and determined whether a new curve needed to be developed for high strength steel. A total of 45 global buckling tests were carried out on grades ranging from A460 to A960. The authors measured several properties such as the residual stress, global imperfections, buckling resistance, etc.

The geometric imperfection for high strength steels was concluded (Somodi & Kövesdi, 2017) to be no different to normal strength steels and no particular tendency was noticed with the material grade but a small tendency could be noticed with respect to the b/t ratio. Figure 2-114 and Figure 2-115 provides various results on global imperfection.

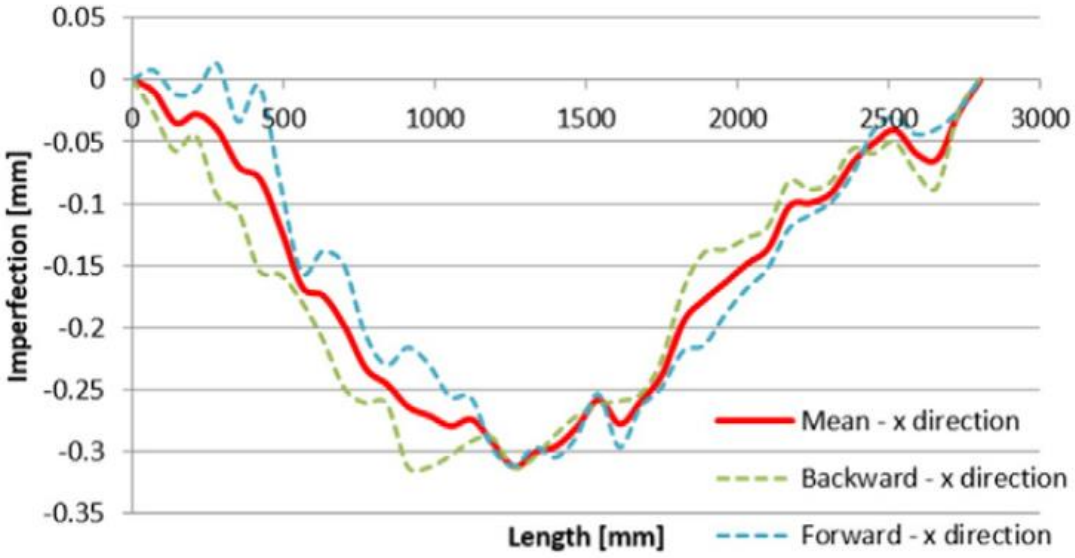


Figure 2-114: Global imperfection results – Brute results (Somodi & Kövesdi, 2017)

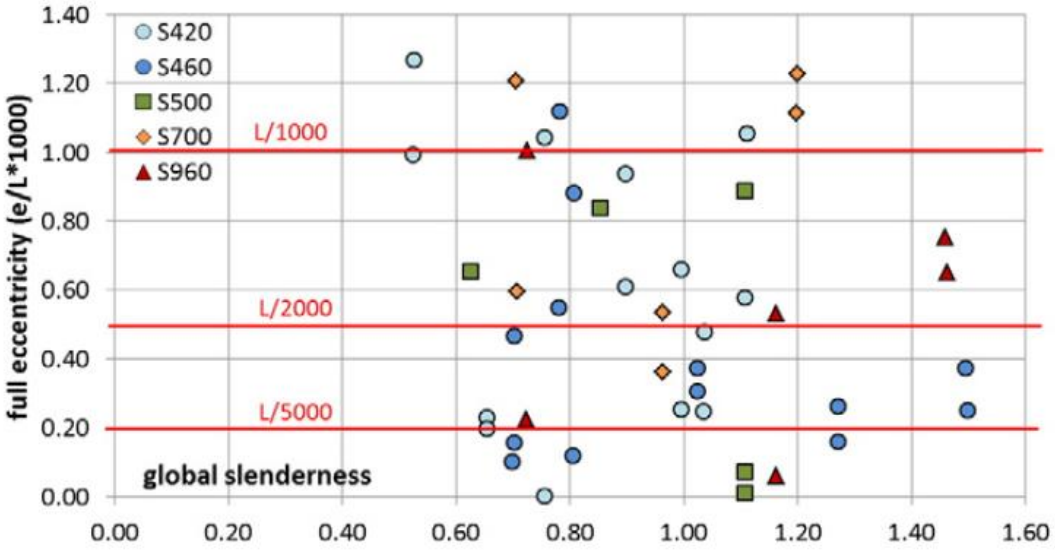


Figure 2-115: Global imperfection results – Normalized (Somodi & Kövesdi, 2017)

Somodi and Kövesdi (2017) found the average imperfection was of L/8000 which is much smaller than the L/750 required in European standards. After performing the experimental tests, the authors

determined the buckling reduction coefficients. The results are shown in Figure 2-116 and Figure 2-117.

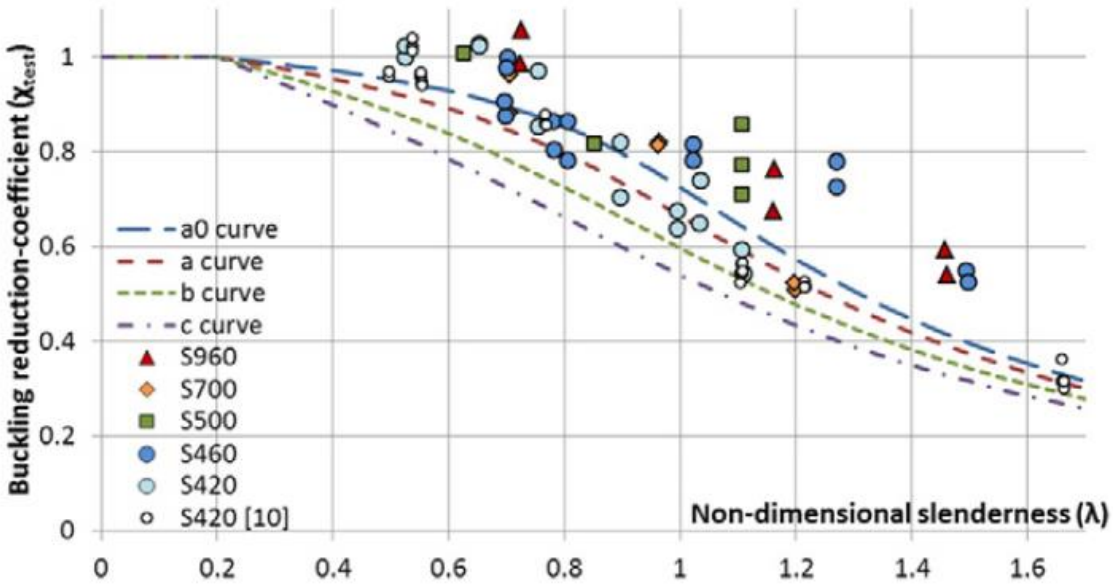


Figure 2-116: Buckling reduction coefficients – Based on actual values (Somodi & Kövesdi, 2017)

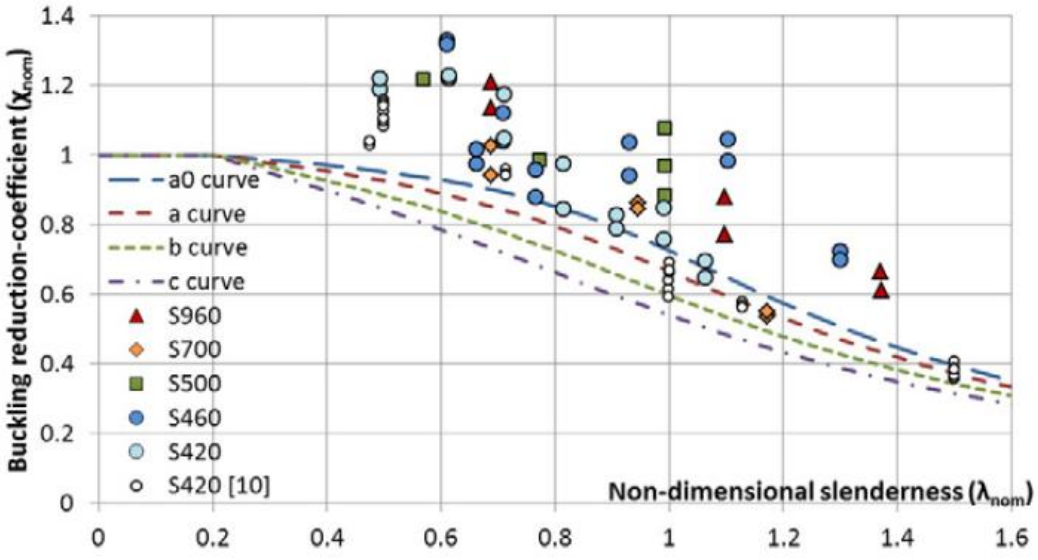


Figure 2-117: Buckling reduction coefficients – Based on nominal values (Somodi & Kövesdi, 2017)

Based on these results, Somodi and Kövesdi (2017) considered the buckling Curve b to be appropriate for high strength steels. This was determined based on safety margins according to the 2.3% quantile method and the predefined partial safety factor. It was deemed Curve a does not satisfy the safety margins.

Somodi and Kövesdi (2017) also built a parallel numerical model to determine the flexural buckling resistance. The model was developed on ANSYS 14.5 based on full solid eight node rectangular 3-D elements and the Newton-Raphson approach for the non-linear analysis. The residual stress distribution was determined in the previous paper (Somodi & Kövesdi, 2016). No particular distribution was applied for the increased yield strength. A uniform yield strength obtained from standard coupon tests was applied. The model was hinged at the ends. The effects of yield strength, residual stress and the material model law were studied separately to determine its effects. The linear elastic hardening plastic and Ramberg-Osgood models were compared.

Somodi and Kövesdi (2017) determined yield strength results increase the buckling reduction factor while the residual stress significantly decreases it for high slenderness ratios and has no effect on it for low slenderness ratios (below 0.6). As Somodi and Kövesdi explained, this is due to the tension and compression component of the residual stress gradient cancelling each other out when the specimens have a dominant plastic failure mechanism. The results for the two material models are shown in Figure 2-118.

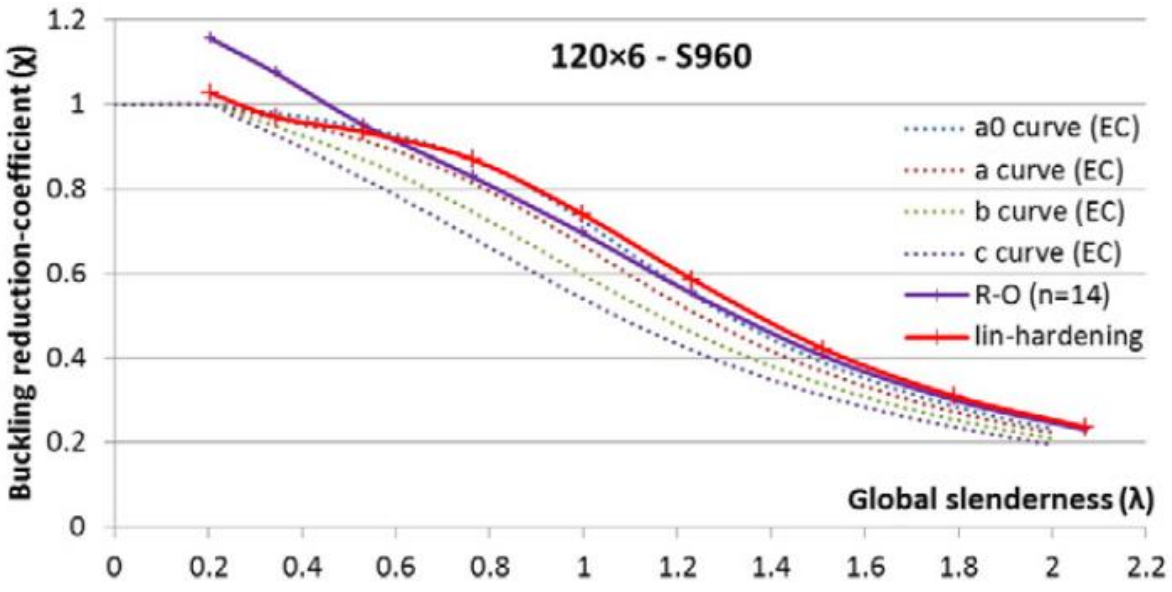


Figure 2-118: Buckling curve with material models (Kovesdi & Somodi, 2017)

Finally, Somodi and Kövesdi (2017) performed a numerical analysis on a hinged column. The results are shown in Figure 2-119. Based on these results, the authors proposed a new buckling curve for high strength steels and consider the buckling *Curve c*, which is already used in the European standard, to be appropriate for normal strength steels.

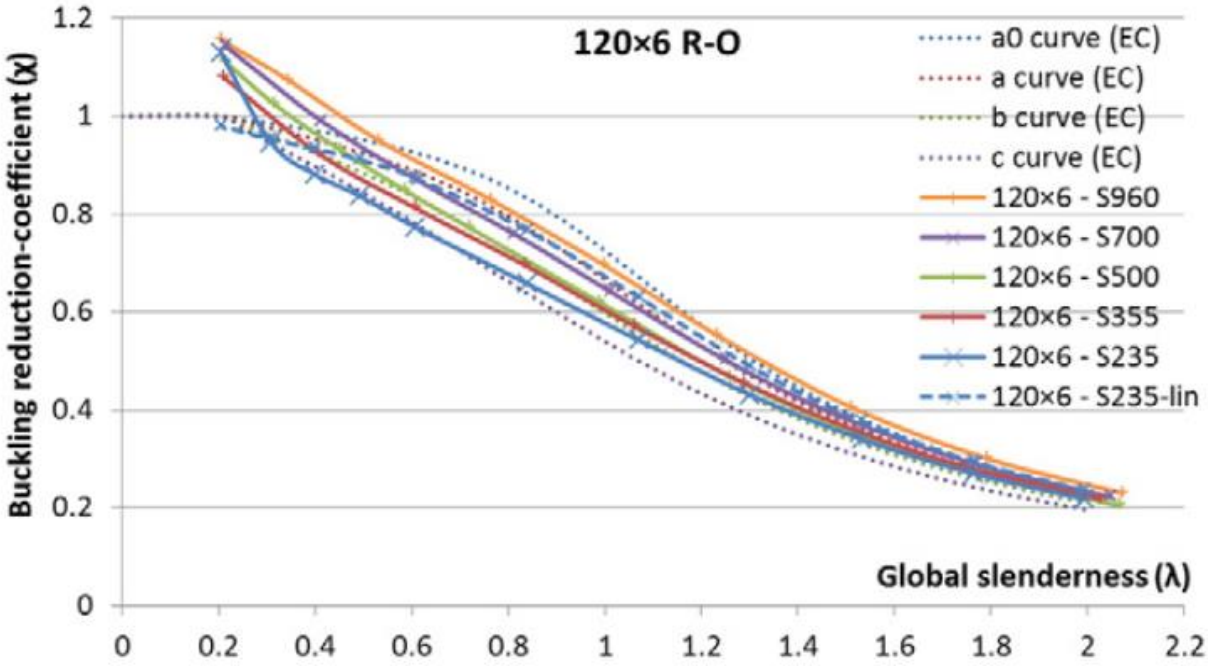


Figure 2-119: Buckling curve for different material grades (Kovesdi & Somodi, 2017)

#### 2.4.1.1 Summary

This final section of the literature review covered cold-formed HSS research from the early 2000s up until 2017. As opposed to the previous sections, this review was not centered on one particular research effort. Instead, a vast number of investigations from different places around the world were covered. It can be specifically noticed several investigations were undertaken in China in recent decades which has greatly developed its cold-formed steel industry. Most of the investigations covered in this section confirmed the residual stress models proposed by Davison and Birkemoe (1983), and Key and Hancock (1993). Several trends and observations were also validated.

The first paper (Elghazouli et al., 2005) was titled "*Shake Table Resting of Tubular Steel Bracing Members"*. An experimental investigation was performed on one concentrically braced frame configuration subjected to realistic seismic loads. Several braces were tested on the same configuration. Material properties of the brace sections were measured and compared to the actual properties obtained from the shake table analysis. Elghazouli et al. determined the average yield strength of the section according to the Eurocode 3 equation to account for increased yield strength in cold-formed sections (equivalent to S136 standard equation). This was then compared to full tensile section tests. It was determined the strength was underestimated by approximatly 10%. After subjecting the brace to seismic loads within the concentrically braced frame, it was found the actual yield strength of the brace was 11 to 36% higher than the previously measured full section tensile strength. The ultimate load was up to 10% higher. Elghazouli et al. concluded the yield strength of the section was underestimated by an average of 25% and up to 40% for some specimens when compared to the characteristic strength of the member. The story shear was calculated based on the measured full section yield strength ($V_y$) and the actual yield strength within the frame ($V_s$). Elghazouli et al. state that the story shear from the measured full section yield strength ($V_y$) is the most likely value to be used in design. It is found the real shear ($V_s$) was 20 to 60% greater than the shear from the yield strength ($V_y$) and 20 to 40% greater than the shear from the ultimate tensile stress ($V_u$). Elghazouli et al. finally recommended a 60% strength enhancement factor with respect to the actual measured yield strength and a 100% enhancement factor with respect to the characteristic yield strength in seismic design.

The second article was published by Han et al. (2007) and was titled "*Seismic Behavior of HSS Bracing Members according to Width–Thickness Ratio under Symmetric Cyclic Loading*". The authors studied the effects of width to thickness ratio on the actual yield strength, buckling sequence, energy dissipation capacity, fracture and strain distributions. Several braces were subjected to symmetric tension and compression loading simulating an earthquake. It is determined the ratio of the actual yield strength from the flat coupon average to the specified ultimate tensile stress ranged from 0.87 to 0.93. Specimens with low w/t ratios mostly followed a local buckling sequence. Specimens with a mid range w/t ratio mostly followed an overall-local buckling sequence. Specimens with high w/t ratios mostly followed an overall buckling sequence. Han et al. concluded specimens with low w/t ratios do not have a longer fracture life in compression and tension loading sequences. It is also stated these results contradict other investigations. A significant difference was seen for the energy dissipation capacity according to the w/t ratios. Han et al. concluded the optimum w/t ratio for energy dissipation is of 14. Moving away from this value in any direction decreases the dissipation capacity. Specimens with mid range w/t ratios had their strain uniformly distributed, while specimens with low w/t ratios had a concentration of strain at the end of the sections.

Guo et al. (2007) studied the compressive strengths of 18 cold-formed sections with a D/t ratio ranging from 27.6 to 47.7 in an article titled "*Experimental study on compressive strengths of thick-walled cold-formed sections*". The sections were formed from a virgin strip of 235 MPa, and the authors compared the final yield strength in several coupons to the virgin yield strength. Coupons were taken from the center of each flat and each corner. It was determined the flat coupon yield strength increased by a ratio of approximately 1.04 compared to the virgin strip and the corner coupons increased by approximately 1.44. The elongation decreased significantly: 0.87 for the flats and 0.39 for the corners. Stub column results were then compared to the Chinese and Australian equations to account for increased yield strength in cold-formed sections. One equation was based on only flat coupons, while the second equation was based on a weighted average of the flat and corner coupons. Both of these equations are similar in nature to the CSA S136 standard equation to account for strain hardening. The main difference is the first equation estimates the corner yield strength from the flat coupons, while the second equation uses the actual corner yield strength. It is concluded the equation which only uses flat coupon results is very conservative. The second equation is also conservative but not as much as the first one.

Li et al. (2009) conducted an extensive experimental investigation into residual stresses of cold-formed members. The results were reported in an article named "*Residual Stresses in Roll-formed Square Hollow Sections*". Residual stresses of directly formed members (from strip to square or rectangle) and indirectly formed members (from strip to circle to square or rectangle) were determined with the X-Ray technique and then compared. Both transverse and longitudinal residual stresses were determined. Yield strength measurements were also taken from coupons at the center of the flat faces and an average was determined. Li et al. observed transverse residual stresses typically below 70% of the yield strength and longitudinal residual stresses up to 90% of the yield strength on the exterior surface. Maximum residual stresses were measured on the welding line on the interior surface. These stresses were typically below 30% in the transverse direction and below 40% in the longitudinal direction. Li et al. found their residual stress measurements are in good agreement with Key and Hancock's model (1993). However, Li et al. suggests a bi-linear model should be used which is slightly different from Key and Hancock's model.

Gardner et al. (2010) published an article titled "*Comparative Experimental Study of Hot-rolled and Cold-formed Rectangular Hollow Sections*". The difference between cold-formed and hot-rolled sections in Europe were studied in this investigation. The authors performed tensile coupon tests on flats and corners, stub column tests, residual stress and geometric measurements. It is not possible to comment on the actual yield strength results for flats as the virgin strip yield strength values were often higher than the flat coupon values. This is a very unusual occurrence and it is not specifically addressed in the article. Gardner et al. mentioned there is insufficient data and in general, there is a small strength enhancement. Previously observed tendencies were confirmed. A higher ultimate to yield ratio of the virgin strip and a tighter corner radius increased the yield strength in the formed section. Gardner et al. determined the mean ratio of the corner yield strength to coil yield strength. This ratio was used to adjust the CSA S136 standard equation to account for increased yield strength. A new equation was finally proposed. Next, Gardner et al. measured residual stress values from surface strain measurements. They did not provide an interior and exterior measurement, instead an average was given according to a rectangular through thickness residual stress model and a linear one. A mean residual stress of 0.79, normalized to the yield strength, was proposed for the linear model and 0.52 for the rectangular block model. Finally, the stub column strength was measured and compared to the b/t ratio. Gardner et al. observed the stub column ultimate resistance varied linearly from 1.3, at very low slenderness values, to 0.9 at very

high slenderness values. The stub column resistance was normalized with respect to the measured yield strength.

Gao and Moen (2010) built a finite element model to simulate cold-formed bending. The results were reported in an article titled "*The Cold Work of Forming Effect in Steel Structural Members*". The authors studied the isotropic and kinematic plasticity laws. It was assumed is it necessary to combine both laws to obtain a proper response. A parametric study was conducted where four different cases were studied: isotropic hardening with a virgin stress-strain curve, isotropic hardening with a modified stress-strain curve to simulate increased yield stress, isotropic hardening including residual stresses and effective plastic strains and isotropic-kinematic hardening including residual stresses and equivalent plastic strains. It was found the final case where all factors are taken into account returned to the baseline model. This was explained by the Bauschinger effect.

Hu et al. (2011) published an article titled "*Material Properties of Thick-wall Cold-rolled Welded Tube with a Rectangular Square Hollow Section*" where the manufacturing process of cold rolling was studied. The authors analyzed flat and corner coupons, parent plate coupons (virgin strip) and stub columns from thick-wall cold-rolled welded tube sections. Coupons were taken from the production line at different stages of the cold forming process. The coil strip was also analyzed before it underwent any treatment. The elongation at the center was up to 27.4% higher than the edges. The yield strength to virgin strength ratio was of 1.1 for the flats and 1.47 for the corners. Elongation ratios decrease by 0.79 for the flat coupons and 0.40 for the corners. Hu et al. also compared the column strength to the Chinese and Australian/New Zealand design values. It was concluded the design equations underestimate actual stub column strengths from 10 to 24%.

Li et al. (2012) performed an experimental investigation on the material properties of thick walled cold-formed sections. The results were reported in an article titled "*Cold-forming Effect Investigation on Cold-formed Thick-walled Steel Hollow Sections*". Tensile strength coupons were taken from the center of the flats and the corners. The corners were also discretized, and round tensile tubes were taken from the edges and center of the corner. The side opposite to the weld had a yield strength on average 10% higher than the lowest flat coupon. On average, all flat coupons had a yield strength 4% higher than the lowest flat. This might not appear much, but when comparing the actual yield strength to the nominal yield strength, the lowest flat was already 22% higher than the nominal yield strength. Li et al. do not provide this value, but it can be read from

the graphs. Li et al. concentrated their analysis on comparing the sides between each other. The corners were approximately 17 to 67% higher than the minimum flat yield strength. A clear pattern was noted in the increase of yield strength for the corners with respect to the R/t ratio. The ultimate stress increase is far less pronounced, ranging only at 7 to 24% and averaging at 16%. Finally, Li et al. compared the stub column strength to the average of all flats and the Chinese, Australia/New Zealand and European equations to account for cold-forming. It was determined the results from the equations are unconservative for low R/t ratios and the stub column strengths are actually lower than the values proposed by the equation.

The next article, titled "*Experimental Investigation on Longitudinal Residual Stresses for Cold-formed Thick-walled Square Hollow Sections*" (Tong et al., 2012), determined the longitudinal residual stress distribution in thirteen cold-formed sections through the hole-drilling method and the X-ray diffraction technique. Directly and indirectly formed sections were studied. Results for the indirectly formed sections (studied in this thesis) ranged from 52 to 61% of material yield strength were obtained by the hole drilling method. Results ranging from 43 to 67% of material yield strength were obtained by the X-Ray method. Residual stresses were in tension on the outer surface and compression on the inner surface. The residual stress in corners was either slightly smaller or equal to the residual stress in flats. From the obtained through thickness distribution, the corner residual stress is almost equal from the inner surface to $3/4^{th}$ of the thickness. At the outer surface the corner residual stress is about half of the flat residual stress. Finally, a series of equations were proposed to model the longitudinal residual stress. The proposed distribution is close to the model proposed by Davison and Birkemoe (1983).

A set of two articles titled "*Strength Enhancement in Cold-formed Structural Sections – Part I: Material testing*" and "*Strength Enhancement in Cold-formed Structural Sections – Part II: Predictive models*" were published by Afshan et al. (2013) and Rossi et al. (2013). The first article (Afshan et al., 2013) consisted in defining the material properties of cold-formed sections such as the flat and corner yield strength. The second article (Rossi et al., 2013) consisted in proposing an equation to predict the final flat and corner yield strength based on the virgin strip. Eighteen sections of five different materials were tested. It was found the main parameters which dictate the yield strength increase are the amount of cold work the section is subjected to and the potential for strength enhancement. Rossi et al. did an extensive review of several models which were determined previously and proposed an equation based on a power law model. A separate equation

was developed for the corner and the flat section. Rossi et al. centered their research on stainless steel, but the predictive models were compared to other material types as well. It was determined the predictive equation can be applied to any metallic structural section. Finally, Rossi et al. compared their predictive model to the European equations to account increased yield strength in cold-formed sections. It was determined the new predictive model offers strength enhancements of 19% (stainless steel) and 36% (carbon steel).

Sun and Packer (2014) published a paper titled "*Direct-formed and Continuous-formed Rectangular Hollow Sections – Comparison of Static Properties*" which was based on Sun's thesis (2014) titled "*Mechanical Behaviour of Cold-Formed Hollow Structural Section Material*". This investigation compared the tensile stress-strain behaviour, ductility, compressive stress-strain behaviour of the entire cross-section and longitudinal residual stresses of sections going through three different fabrication methods. Sun (2014) also picked sections with different b/t ratios to assess its impact. A significant difference in yield strength could be seen between the CF24 (b/t = 24) and CF12 (b/t = 12) continuously rolled sections (CF). The CF24 section had an overall yield strength close to the nominal value. The CF12 section had a yield strength 40% higher than the nominal value. Flat face coupons were 31% above the nominal value and corner coupons were 70% above the nominal value. The CF24 sections had a slightly lower yield strength than the nominal value for flat coupons. The corner coupons were 40% above the nominal value. The ultimate tensile stress was 33% (CF12) and 0% (CF24) above the nominal value for the flats, and 50% (CF12) and 17% (CF24) for the corners. Stub column results were approximately 10% higher than average tensile yield strength results. Elongation decreased significantly more for the corners than the flat coupons. Average surface longitudinal residual stress measurements were found be around 50 to 60% of the actual yield strength. The outer surface was in tension while the inner surface was in compression. Finally, Sun (2014) constructed a column model based on the tangent modulus theory and applied the previously defined material properties. It was concluded the model was in good agreement with the experimental stub column results.

Liu et al. (2017) proposed a method to approximate residual stress distribution in cold-formed steel members by modifying the stress-strain curve in an article titled "*Modelling and Probabilistic Study of the Residual Stress of Cold-formed Hollow Steel Sections*". A polynomial equation was developed to approximate the stress-strain curve. The equation was developed with all six residual stress parameters proposed by Key and Hancock (1993). A parametric study on a simple beam was

later performed to determine the necessity of including all six parameters. The authors concluded just including the longitudinal bending residual stress parameter is accurate enough for engineering purposes based on the beam model. A second parametric study was then carried on two portal frame configurations using beam element-based geometric and material nonlinear analysis. The spread of plasticity was traced using a 3D plastic zone beam-column element modelled in ABAQUS. The elements were purposely designed so the slenderness was close to unity to obtain the maximum residual stress effects. The authors studied a total of four cases. The first case had no residual stress at all. The second case accounted for all six components of residual stress and the third case only accounted for the bending component. The fourth case used the developed approximate polynomial curve. It was concluded the polynomial function gave an accurate representation of the behaviour. Finally, Liu et al. performed a probabilistic study on residual stress to determine the effects of its uncertainty. It was concluded residual stress must be accounted for in numerical models, but its effects can be treated as deterministic.

The final two papers were published in 2016 and 2017. The papers were titled "*Residual stress measurements on cold-formed HSS hollow section columns*" (Somodi & Kövesdi, 2016) and "F*lexural buckling resistance of cold-formed HSS hollow section members*" (Somodi & Kövesdi, 2017). Both of these articles were aimed at high strength cold-formed HSS members. However, the authors provided good comparisons with normal strength members and drew conclusions for both which makes them interesting for this research. In the first article (Somodi & Kövesdi, 2016), residual stress measurements on high strength steel sections were taken using the sectioning technique and the Laser-Falconeye method. Sections with several b/t ratios were studied to determine its effects on residual stress. It was concluded tension stresses are present on the outer surface and compression stresses on the inner surface. Membrane residual stresses were close to zero. Bending residual stresses were dominant. Residual stresses at the corners were significantly smaller than those at the flat wall. Residual stresses were slightly smaller in the welding zone. No clear tendency could be established for the residual stress magnitude with respect to the b/t ratio. However, a quasi-linear relationship was seen between the nominal yield strength and the residual stress magnitude. The authors proposed two equations to account for the longitudinal residual stress. One is for high strength sections and the second one is for normal strength sections. The equation for normal strength sections gave an average longitudinal residual stress of approximately 213 MPa for a nominal yield strength of 350 MPa. This is approximately equivalent to the values

measured by Davison and Birkemoe (1983) and Key and Hancock (1993). Corner residual stresses were determined to be 55% of the residual stress in the flat wall. This conclusion was not universally confirmed by previous investigations. European column strength curves were studied in the second article (Somodi & Kövesdi, 2017) and a new curve for high strength steel was determined. Some new properties were also measured, such as geometric imperfections. No particular difference in imperfection was noticed between high strength and normal strength steels. A small tendency in imperfection is observed with respect to the b/t ratio. The average imperfection was determined to be at L/8000. The authors compared the experimental values to European buckling curves and determined Curve b should be applied to high strength members and Curve a should be applied to normal strength members. Finally, a numerical model was built to determine the flexural buckling resistance. A uniform yield strength obtained from standard coupon tests was applied to the model along with the residual stress distribution determined in the previous article. It was found yield strength results in an increase of the buckling reduction factor while the residual stress resulted in a significant decrease of the factor for high slenderness ratios and had no effect on it for low slenderness ratios (below 0.6).

## 2.5 Literature review summary

An extensive literature review was performed in this chapter, starting from the first development of the CSA S136 standard equation to account for increased yield strength from cold work of forming, up to recent developments in the research of cold-formed sections.

The first major research effort into cold-formed sections was undertaken by Britvec et al. at Cornell University in the 1960s and lasted a decade. A semi-empirical equation was established to account for the increased yield strength in the corners of cold-formed sections. It was determined the increase is dependant on the ultimate to yield ratio of the virgin strip that was used to form the section, and the corner bent radius. A smaller corner radius would imply more cold work was performed to bend the corner. The increase in yield strength is directly proportional to the amount of cold work the section has been submitted to. The ultimate tensile stress of the virgin strip represents an upper bound to the increase of corner yield strength. The ratio of the virgin yield to ultimate tensile stress represents the amount of strain hardening the corner can sustain. A small increase in the ultimate tensile stress of the corner was also seen. It was also determined the ultimate tensile stress of the corner does not increase from strain hardening. The increase is fully due to aging of the material. Finally, the virgin strip stress-strain curve tends to have a very sharp yield point. This property is lost due to cold work, but if the sustained strain is not significant it can be recovered with the aging of the material. Today's CSA S136 (2016) equation to account for the increased yield strength from cold working is still the same equation as proposed by Britvec et al. in the 1960s. It has not been updated since.

The investigation into cold-formed sections continued in the 1970s in North America and Japan. Several researchers undertook experimental investigations to determine the yield strength and residual stress of cold-formed HSS members. Davison and Birkemoe, Kamani and Bjorhovde took full cross-sectional readings to establish a yield strength gradient across the section. It was determined the yield strength is at its minimum at the center of the flat and increases linearly towards the edges. Corners tend to have a yield strength significantly higher than the flat. A residual stress model was also determined. It was found the residual stress can be approximated by a membrane (perimeter gradient) and a bending (through thickness gradient) component. The membrane component has equal magnitudes at the edges and center of the section. However, the edges are in compression while the center is in tension. The bending component has a trapezoidal

shape and is split into three parts. The outer fiber was determined to be in tension and the inner fiber in compression. The multiple column strength curve concept was also studied. It was proposed by most investigations to use the equivalent to the $n$ = 1.34 curve in today's standard (CSA S16, 2014). One investigation proposed to use the $n$ = 2.24 curve (Kato, 1977).

A major investigation into cold-formed sections was undertaken in Australia in the mid 1980s up to the late 1990s by Key, Hancock, Hasan and Wilkinson. The sudden load shedding collapse mechanism of slender sections was studied. Several yield strength and residual stress measurements were taken. An additional residual stress component was identified, and a more detailed residual stress model was proposed. The new component was called the "layering" residual stress and it measured the residual stress in released coupons. This component was implicitly included in Davison and Birkemoe's (1983) research. The overall residual stress model was very close to the one previously proposed.

Several researchers continued to determine the yield strength in corners and residual stress distributions with recently developed techniques, such as the X-Ray diffraction method, in the past decade. Most of these investigations confirmed Davison and Birkemoe's trapezoidal model. However, the magnitudes were slightly different, and equations were proposed to estimate the average residual stress. Some investigations, also found that the residual stress in corners is significantly smaller than the residual stress in the flat wall. Other observations which were previously made were also confirmed. For example, the residual stress being in tension on the outer surface and in compression on the inner surface. Several investigations centered around the yield strength of the weld and the ratios between the different flat faces. It was determined the yield strength in the weld can be as high the yield strength of corners and the face opposite to the weld tends to have a higher yield strength than the adjacent faces. It was also confirmed the average yield strength of the section increases as the b/t ratio decreases. New updated equations to account for the increase in yield strength of corners were also proposed in other investigations. All of these equations were based on the ultimate to yield strength ratio of the coil and the corner radius to thickness ratio as was determined by Britvec et al. at Cornell University in the 1960s. Most proposed equations were updated versions of the CSA S136 (2016) standard equation.

Data from the previously seen investigations was compiled and summarized in the next chapter in order to establish trends on the corner yield strength, the yield strength gradient of the flat wall, and residual stresses of cold-formed HSS members.

# CHAPTER 3 EXPERIMENTAL INVESTIGATION, PROBABLE TENSILE RESISTANCE AND FACTORED TENSILE RESISTANCE

In this chapter, a collection of experimental data from various sources is presented and analyzed. This data is used to establish the probable yield strength $R_yF_y$ (average cross-sectional yield strength) used to calculate the probable tensile resistance $T_u$. An equivalent nominal yield strength ($F_y$*) to be used in the current equation of the factored tensile resistance $T_r$ assuming a $\phi$ of 0.9 and the nominal area is then determined based on the probable tensile resistance $T_u$.

Coupon data on the yield strength ($F_y$) and ultimate tensile stress ($F_u$) is collected from several investigations seen in Chapter 2. Tables and figures are prepared to summarize these findings. This is done to propose a representative yield strength gradient across the section walls and determine the average increase in yield strength in the corners from cold working. By knowing the yield strength gradient across the flat walls and the increase in yield strength in the corners, the average cross-sectional yield strength of the cold-formed section can be established.

Mill certificate data is compiled from North American manufacturers on $F_y$ and $F_u$ properties of rectangular, square and circular HSS members. For square and rectangular members, the yield and ultimate tensile stress values were those obtained at the center of the flat walls. Several steel grades were analyzed and compared. This was necessary due to trends in the industry where the ASTM A1085 grade, which is very close to Canadian CSA G40.21 grade, is expected to eventually replace the ASTM A500 grade. The variation of the yield strength is analyzed with respect to the b/t ratio of the section to establish a tendency. The D/t ratio is also commonly used in this chapter. This ratio is often used in research into cold-formed HSS members and has a direct correlation to the b/t ratio. Both of these ratios are equivalent to each other.

Data for mill certificates is adjusted to reflect the yield strength distribution across the section. This is done by computing an average yield stress over the cross-section to be used as $R_yF_y$ in the calculation of the probable brace resistances in seismic design. This average value is obtained using three different yield strength distribution models. The first one is based on the yield strength distribution proposed from data obtained in Chapter 2. In other two models, the mill certificate value is applied over the full flat width of the walls. The yield strength of the corners ($F_{ycorner}$) is determined according to the CSA S136 (2016) equation to account for increased yield strength. For the *S136A* model, since mill data was not available for the virgin strip, the calculation of $F_{ycorner}$ is

done using ratio of the ultimate to yield strength obtained from the nominal values. For the *S136B* model, the $F_y$ and $F_u$ values are based on the mill certificates.

For the calculation of a factored tensile resistance $T_r$ that accounts for the actual material properties of HSS members, it is proposed to determine an equivalent nominal ($F_y$*) to be used in the current equation $T_r$ assuming $\phi$ 0.9 and the nominal area. The computation of the $F_y$* is performed in accordance to the procedure used by Kennedy et Aly (1980) for the determination of $\phi$ factors except that $F_y$* is the searched value, instead of the resistance factor, to achieve the required level of reliability index in limit state design.

Finally, the residual stress model for cold-formed HSS members based on the review presented in Chapter 2 is determined. The model proposed by Davison and Birkemoe (1983) is compared to recent models to determine if it is still accurate.

## 3.1 Experimental data from previous investigations and corner yield strength increase

In this section, yield and ultimate tensile stress data is compiled from a total of 19 investigations. All sections were formed by cold-rolling. Most sections had a nominal yield strength of 345 MPa and a nominal ultimate tensile stress of 450 MPa. Some sections had a yield strength of 317 and 235 MPa. A few investigations did not mention the nominal steel grade. A nominal yield strength was assumed if the value seemed reasonable based on the results and other investigations by the same researchers. All sections were made from regular carbon steel. One section was heat-treated, but it was still included in the investigation as the full cross-sectional yield strength was determined which was quite rare. Investigations from around the world were included, so not all sections are North American. Other investigations were Chinese, Australian and European. Table 3-1 summarizes the compiled research articles and Table 3-2 provides a list of the available yield strength data each provided along with the article refence.

Table 3-1: List of previous investigations and the type of data each provided

| **Investigations used to compile data on yield strength** |
|---|
| **Direct-formed and continuous-formed rectangular hollow sections-Comparison of static properties** (Sun & Packer, 2014) |
| **-Strength enhancements in cold-formed structural sections — Part I Material testing** (Afshan et al., 2013) |
| **Experimental investigation on longitudinal residual stresses for cold-formed thick-walled square hollow sections** (Tong, et al., 2012) |
| **Cold-forming Effect Investigation on Cold-formed Thick-walled Steel Hollow Sections** (Li et al., 2012) **– 235 and 345 MPa** |
| **Materials properties of thick-wall cold-rolled welded tube with a rectangular or square hollow section** (Hu et al., 2011) |
| **Comparative experimental study of hot-rolled and cold-formed rectangular hollow sections** (Gao & Moen, 2010) |
| **Residual stresses in roll-formed square hollow sections** (Li et al., 2009) |
| **Seismic Behavior of HSS Bracing Members according to Width–Thickness Ratio under Symmetric Cyclic Loading** (Han et al., 2007) **– 317 MPa** |
| **Experimental study on compressive strengths of thick-walled cold-formed sections** (Guo et al., 2007) **– 235 MPa** |
| **THE PLASTIC BEHAVIOUR OF COLD-FORMED RECTANGULAR HOLLOW SECTIONS** (Wilkinson, 1999) |
| **Square and Rectangular Hollow Sections Subject to Combined Actions** (Key & Hancock, 1993) |
| **The Behaviour of Cold-Formed Square Hollow Section Columns** (Key, 1988) |
| **COLUMN BEHAVIOR OF COLD-FORMED HOLLOW SECTIONS** (Key et al., 1988) |
| **Column behaviour of cold-formed hollow structural steel shapes** (Davison & Birkemoe, 1983) |
| **Strength and behaviour of cold-formed HSS columns** (Bjorhovde, 1977) |
| **An experimental investigation of the column behaviour of hollow structural steel sections** (Salvarinas, 1977) **– HEAT TREATED** |
| **A theoretical investigation of the column behaviour of hollow structural steel sections (**Davison, 1977) |
| **Stub column data and the prediction of compression behaviour of hollow structural shapes** (Kamani, 1974) **– SEAMLESS** |

A “full section” in Table 3-2 means most coupons from Figure 3-1 were provided. A “partial face” in Table 3-2 means only the distribution for one face was provided. The “corner” and “flat” distributions in the “detailed” section mean the data for most corners and coupons from the center of each flat face was provided. If the provided “corner” and “flat” face is in average, it means the authors did not provide the individual values for each corner. The gross data was not in the same form in all investigations. Some investigations provided the values in a percentage. If this was the case, the data was transformed to a numerical yield strength value and normalized with respect to the nominal yield strength. In Figure 3-1, the corners are split into three sections. Only one value is actually provided for all three and the same value is used for all three sections. Corners in Figure 3-1 were originally discretized into three parts to obtain the value at the edges and center of the corner. After studying previous investigations, it was determined this exercise was only performed in one investigation (Li et al., 2012). It was determined in this investigation the results were inconsistent. Li et al. concluded the average of the corner should be taken. A total of 81 sections were included in the data. Out of the 81, some type of data for the corner yield strength was obtained for 47 sections. Some investigations provided data for each of the four corners, some provided an average, while others only tested one corner. To simplify the results, when data for all four corners was provided an average was taken. The same was done when data for the center flat coupon for all sides was provided. Finally, thirteen investigations shown in Figure 3-2 provided information on corner yield strength. Detailed measurements can be found in Appendix D.

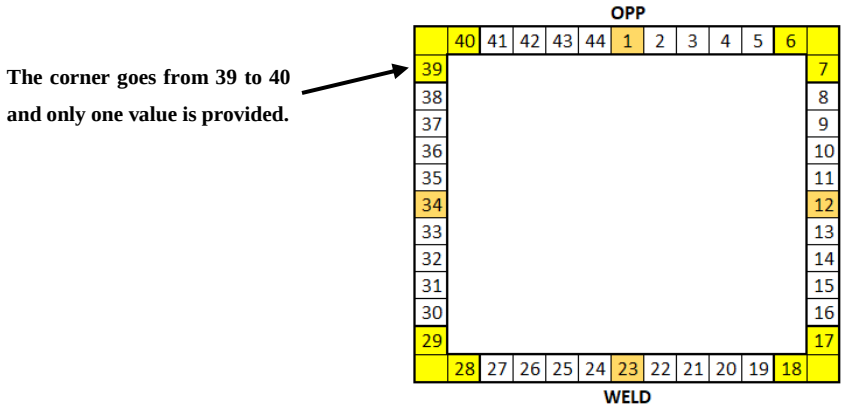


Figure 3-1: Coupon distribution

Table 3-2: Data provided by each investigation

| Heat treatment | Nominal yield strength (Mpa) | Detailed | | | | Average | | |
|---|---|---|---|---|---|---|---|---|
| | | Full section | Partial face | Corner | Flat | Corner | Flat | |
| NONE | 345 | | | | | | | (Sun & Packer, 2014) |
| NONE | S355J2 | | | X | X | | | (Afshan, Rossi, & Gardner, 2013) |
| NONE | Assumed350 | | | | | | X | (Tong, et al., 2012) |
| NONE | 345 and 235 | | | X | X | | | (Li, Wen, Want, & Shen, 2012) |
| NONE | Assumed 350 | | | X | X | | | (Hu, Ye, & Li, 2011) |
| NONE | Not available | | | X | X | | | (Gao & D. Moen, 2010) |
| NONE | Not available | | | | | | X | (Li, Zeng, Ma, Guo, & Lai, 2009) |
| NONE | 317 | | | | | | X | (Han, Kim, & A. Foutch, 2007) |
| NONE | 235 | | | | | X | X | (Guo, Zhu, Pi, & Ton-Loi, 2007) |
| NONE | 345 | | | X | X | | | (Wilkinson, 1999) |
| NONE | 345 | | | | | X | X | (Key & Hancock, 1993) |
| NONE | 345 | | | X | X | X | X | (Key, 1988) |
| NONE | 345 | | | | | X | X | (Key, Hasan, & Hancock, 1988) |
| NONE | 345 | | X | | | | | (Davison & Birkemoe, 1983) |
| NONE | 345 | | X | X | | | X | (Bjorhovde, Strength and Behaviour of Cold-formed HSS Columns, 1977) |
| HEAT TREATED | 345 | X | | | | | | (Salvarinas, 1977) |
| NONE | 345 | X | X | X | X | | | (Davison T. A., 1977) |
| NONE | 345 | | X | X | | | | (Kamani, 1974) |

The results are shown in Figure 3-2 to Figure 3-6. Results were taken with respect to the D/t ratio defined by equation (3-1) and normalized with respect to the nominal yield strength.

$$\frac{\mathrm{D}}{\mathrm{t}} = \frac{(2 * B) + (2 * D)}{\pi * t} \tag{3-1}$$

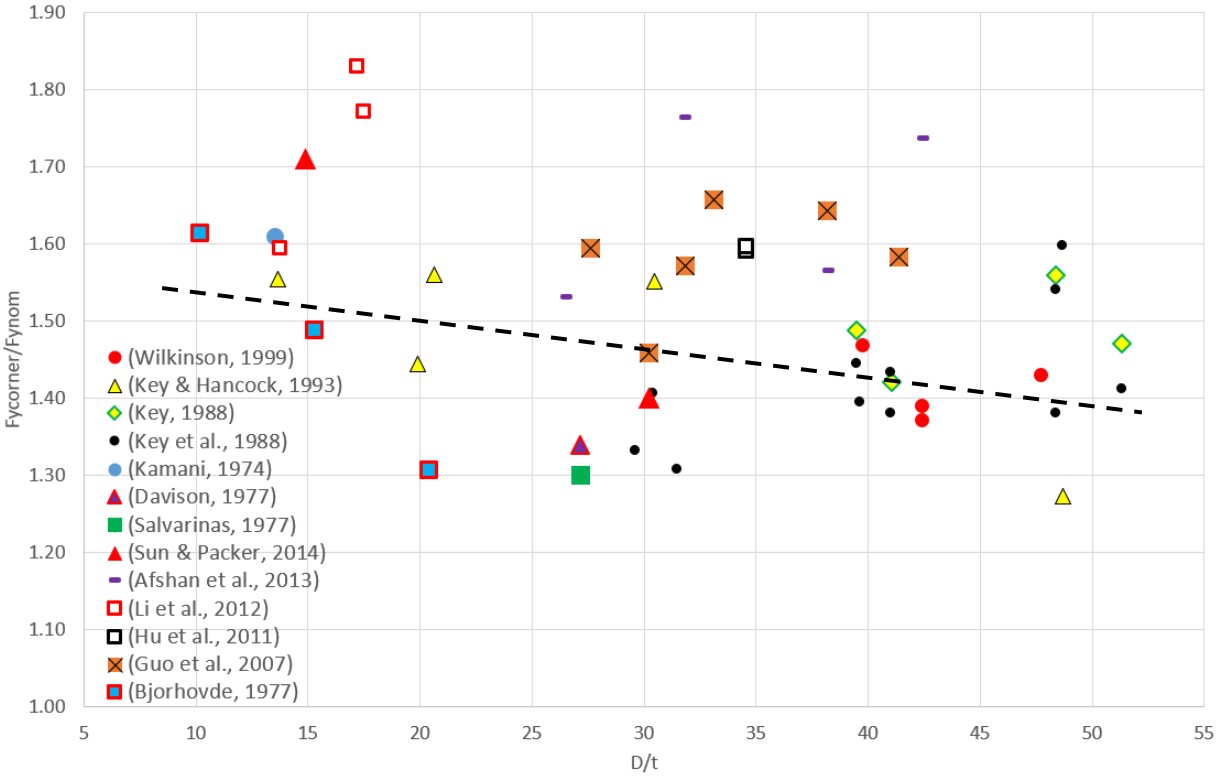


Figure 3-2: Average normalized yield strength of corners by investigation

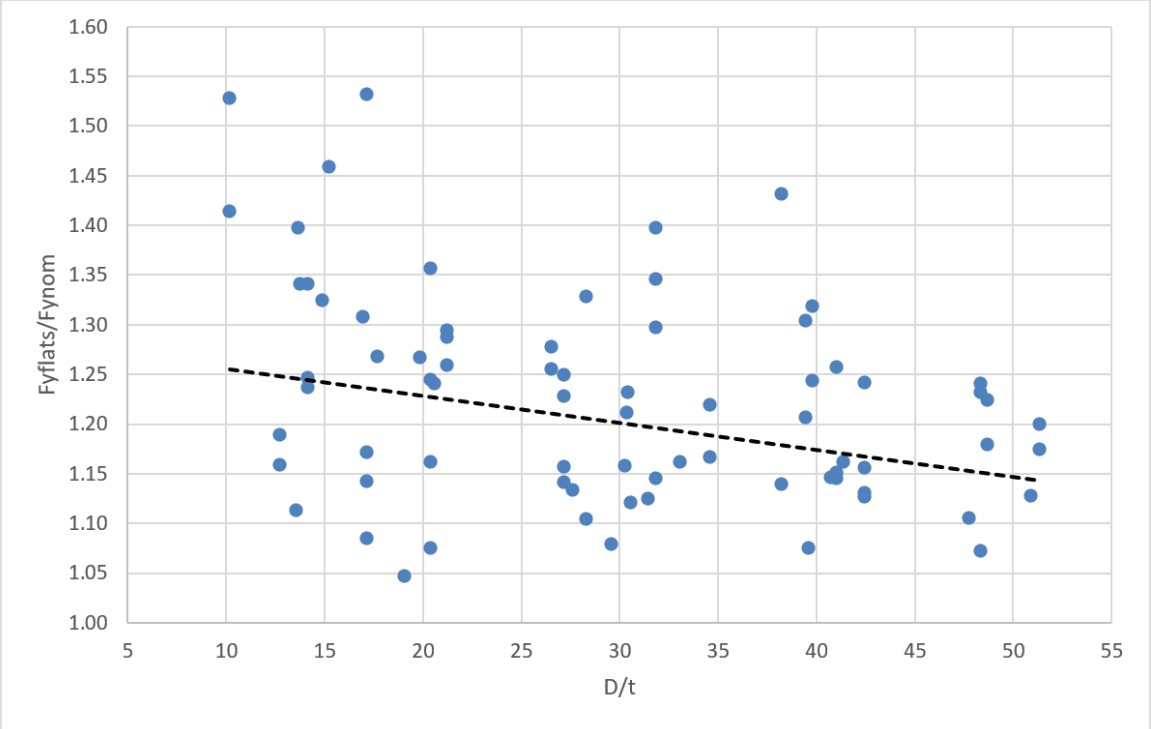


Figure 3-3: Average normalized yield strength from flat sections – Including weld

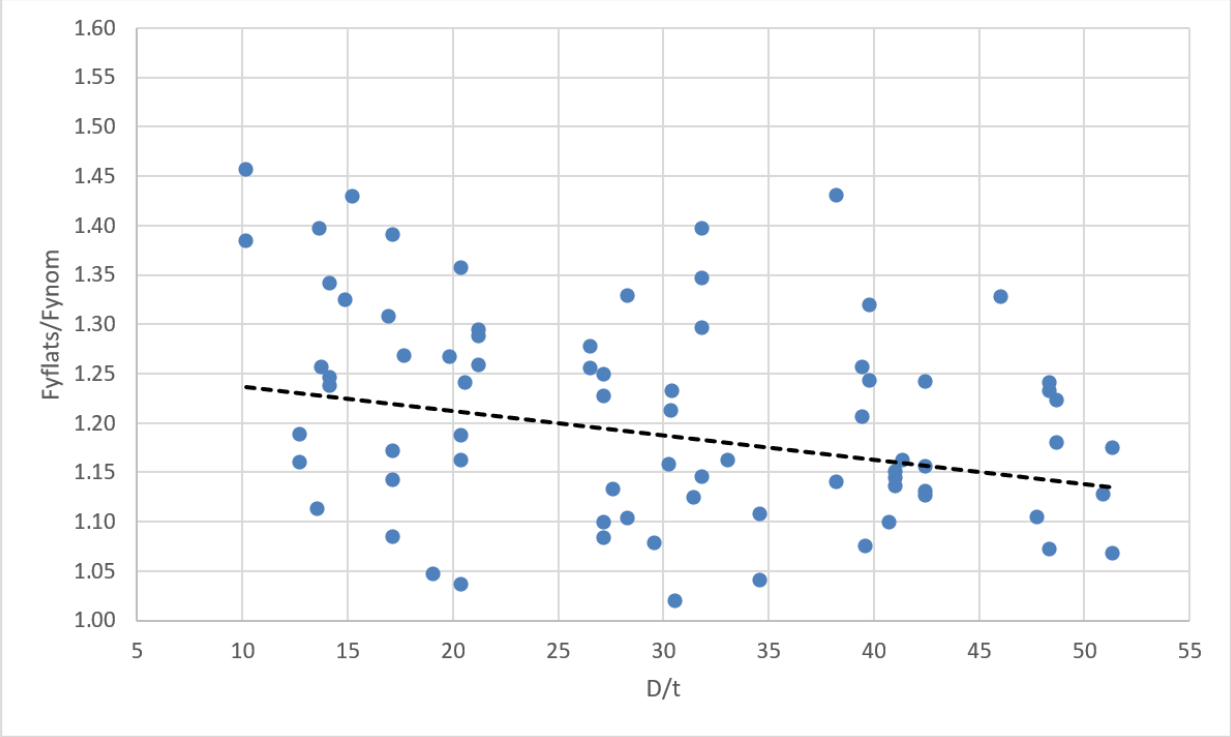


Figure 3-4: Average normalized strength from flat sections – Excluding weld

By analyzing Figure 3-2, Figure 3-3 and Figure 3-4, it is clear the average yield strength of the flat coupons decreases as the D/t ratio increases. The same behaviour can be seen for corner coupons. The weld increases the average yield strength of the flat coupons by about 3% for low D/t ratios. For high D/t ratios, the average yield strength of the flat coupons strength is almost the same whether we include the weld or not. The maximum reported corner yield strength was about 85% above the nominal yield strength. The lowest reported corner yield strength was about 30% above the nominal yield strength. It can be seen in Figure 3-2 that the upper bound limit of the corner yield strength decreases as the D/t ratio increases. The lower bound limit seems to flatten at 30%.

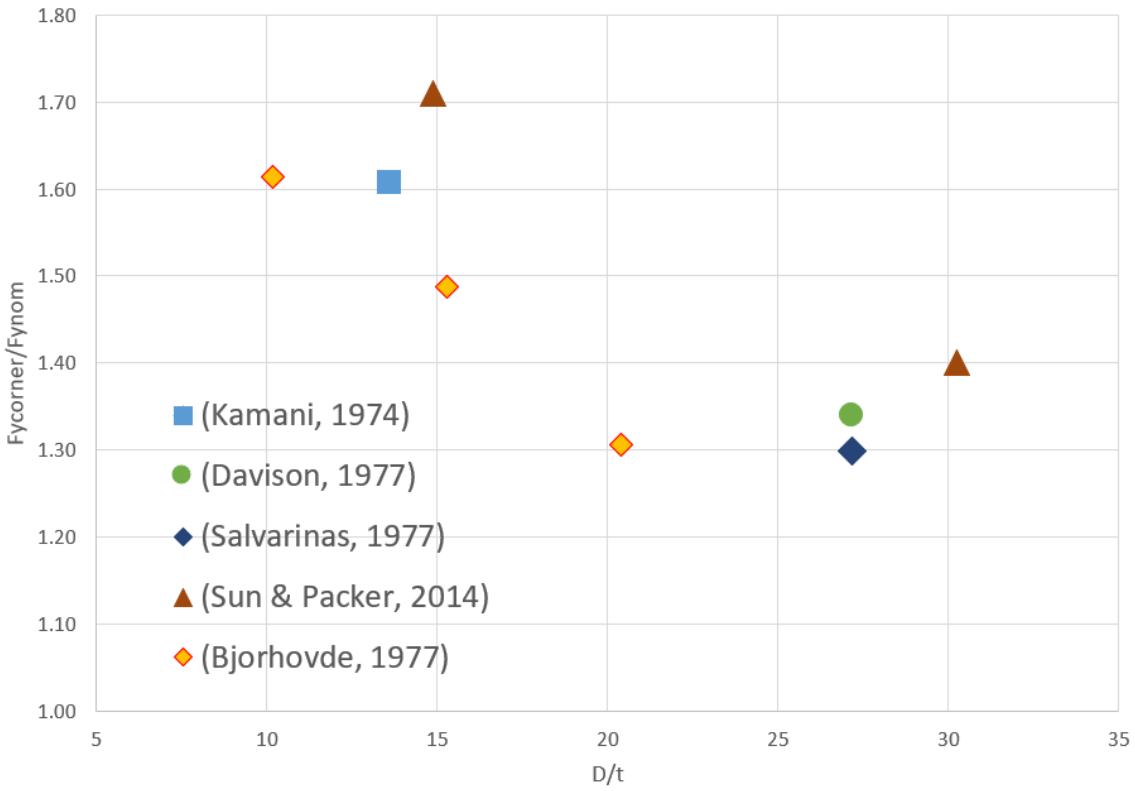


Figure 3-5: Average normalized yield strength of corners – Canadian investigations only

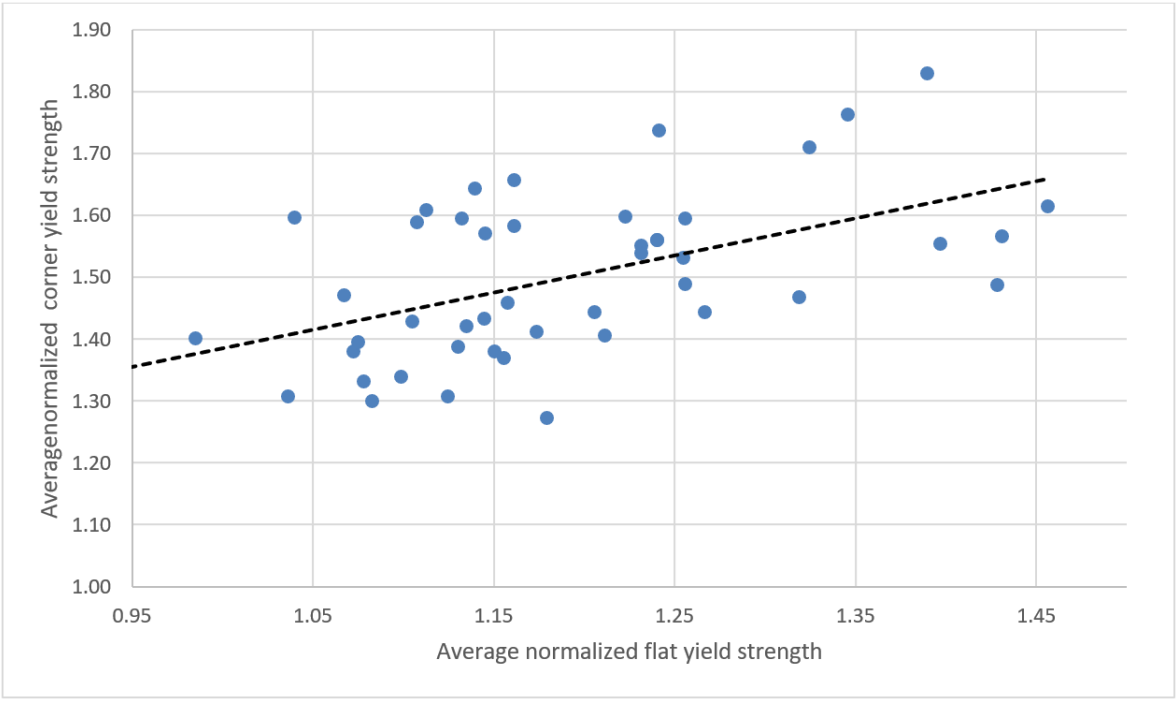


Figure 3-6: Average normalized yield strength of corners versus flats

Figure 3-5 and Figure 3-6 provide the corner yield strength for Canadian sections and the normalized corner yield strength with respect to the normalized flat strength. Sun's (2014) observation, that the yield strength in the section is directly proportional to the amount of cold work the section has sustained seems to be confirmed in this figure. This would imply that a section with a D/t ratio of 10 should have double the cold work than a section with a D/t ratio of 20. By analyzing the results from Bjorhovde (1977) in Figure 3-5, this seems to be the case. For example, the section with a D/t ratio of 10 has a yield strength of 1.6, while the section with a D/t ratio of 20 has a yield strength of 1.3. This means the maximum increase in yield strength for a highly cold worked section cannot be higher than approximately 60% of the nominal yield strength. The lowest increase seems to be at 30%. Figure 3-2, where sections from all over the world were included, seems to confirm this as well since the average yield strength at very low D/t ratios is approximately 60% above the nominal yield strength. This makes it possible to establish a boundary on the maximum and minimum yield strength increase in the corners of HSS cold-formed members. Figure 3-6 shows that a clear linear relationship can be established between the increase in yield strength of corner coupons versus the average increase in yield strength of flat coupons. It is seen that a section subjected to very little cold work, where the yield strength of the flat coupon barely increased ($1.05F_{yn}$ to $1.15F_{yn}$), tends to have a corner yield strength between 30 to 40% above the nominal yield strength. Moderately cold worked sections where the flat yield strength somewhat increased ($1.15F_{yn}$ to $1.25F_{yn}$), tend to have corner yield strength increase ranging from 40 to 60% above the nominal value. Highly worked sections where flat yield strength significantly increased ($1.25F_{yn}$ and above), have a corner yield strength ranging from 50 to 80% above the nominal yield strength. Based on this data, the following corner yield strength distribution is proposed:

- D/t under 30 → $1.60F_{yn}$
- D/t between 30 and 40 → $1.40F_{yn}$
- D/t over 40 → $1.30F_{yn}$

For sections that did not sustain significant cold work and for those that sustained moderate cold work, the lower bound values are taken for the corner yield strength. For sections having sustained significant cold work, a 60% increased is judged to be representative of an average behaviour without underestimating or overestimating the cold work sustained by the members. This is shown in Figure 3-7.

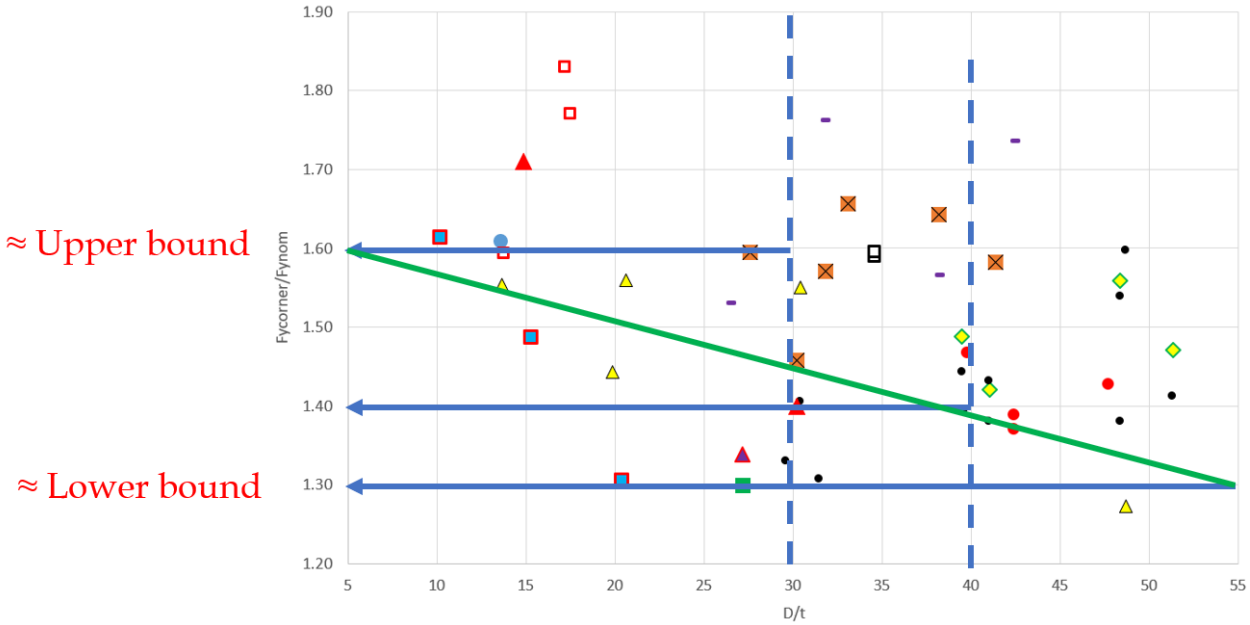


Figure 3-7: Increase in yield strength in the corners normalized with respect to the nominal yield strength with respect to the D/t ratio

## 3.2 Yield strength gradient across the member's section

A yield strength distribution across the perimeter of the HSS's cross-section is proposed in this section of the chapter. It was seen in Chapter 2, Davison and Birkemoe (1983) proposed a linear yield strength distribution for highly cold worked sections and a step function for normal sections. The proposed cut off was at a w/t ratio of 17.3 (D/t = 27) for the highly worked sections to which a linear model would be applied. For lightly worked sections, the cut off was proposed at a w/t of 32.1 (D/t = 41). The step function model was proposed to members with ratios above this cut off. Davison and Birkemoe acknowledged members with w/t ratios between these two cut-offs would have a hybrid behaviour. No attempt was made to model this hybrid behaviour.

For the linear model, the center of the flat has the lowest yield strength. The yield strength then increases linearly by about 20%, above the yield strength of the flat, to the edges near the corners. Several investigations where the full cross section yield strength was determined are presented in Figure 3-8 to Figure 3-15. All of these investigations are Canadian. Figure 3-8 presents the full cross-sectional distribution of one section tested by Davison and Birkemoe (1983), and the same heat-treated section tested by Salvarinas (1974). A few corner and edge coupons for two other sections are also included.

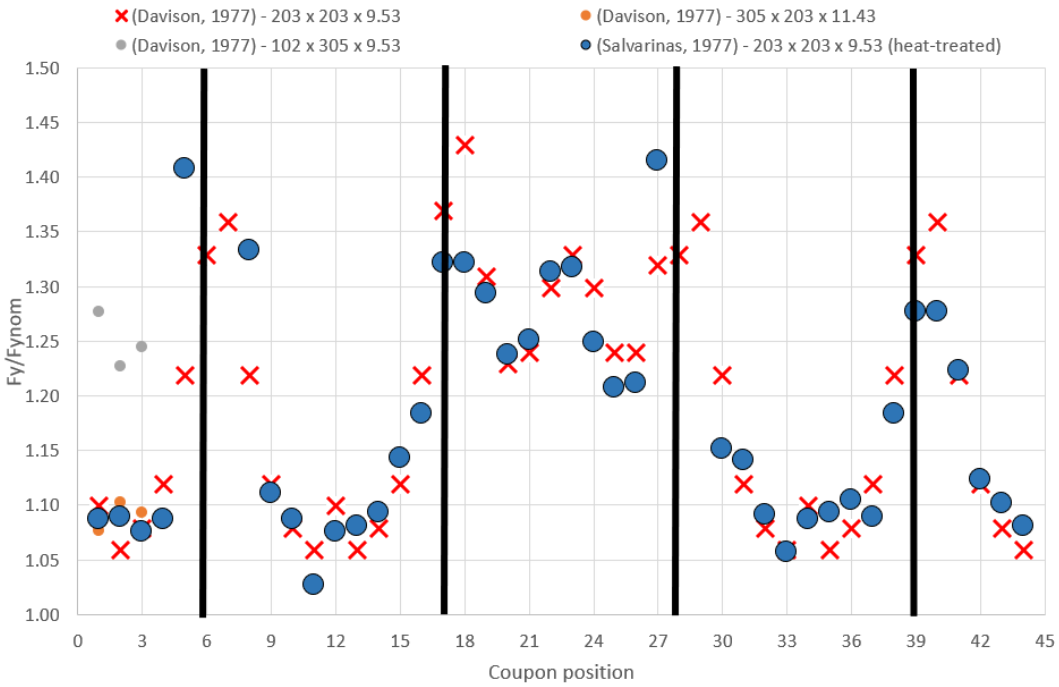


Figure 3-8: Cross section yield strength distribution

A pattern can clearly be observed in Figure 3-8. The center of the flat walls is significantly lower than the edges. The flat wall with the weld does not see this tendency and its yield strength is approximately 25 to 35% higher than the nominal value. It is important to note the w/t ratio of this section is of 21.3 which is significantly higher than the 17.3 cut off proposed by Davison and Birkemoe (1983). Even at this w/t ratio, the edges near the corner are approximately 20% higher than the flat at the center. The flat at the center is only about 5 to 10% higher than the nominal yield strength. Therefore, it can be considered the section was highly cold worked. The face opposite to the weld was at about the same strength as the adjacent faces. It has previously been reported by in a number of investigations the face opposite to the weld should be approximately 10% higher than the adjacent faces. This can be explained by the high D/t ratio of this section. Finally, a somewhat linear increase can be seen from the center of the face up to the edges. The heat-treated section had approximately the same increase.

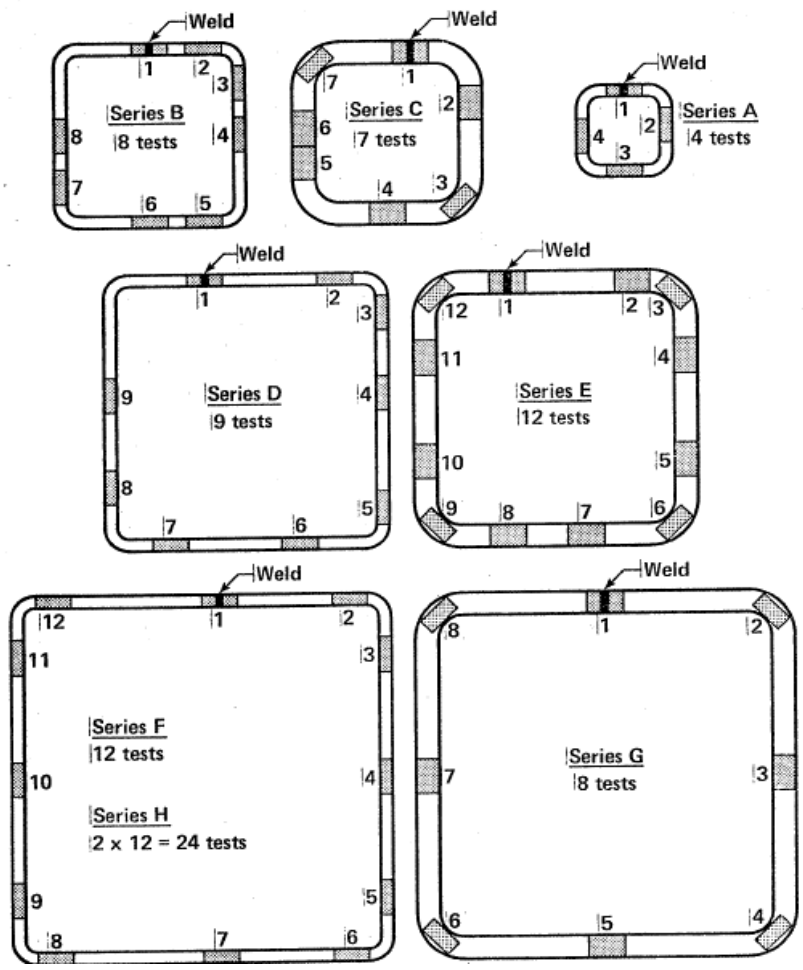


Figure 3-9: Tested coupons - Positions (Bjorhovde, 1977)

Figure 3-10 to Figure 3-15 present the results obtained by Bjorhovde (1977). Bjorhovde tested several sections but the distribution wasn't as detailed as Davison's (1977). The D/t ratio of the tested sections ranged from 10 to 41. It can be seen that even sections with very high D/t ratios display significantly different yield strengths at the center of the flat and the edge. For example, the 203 x 203 x 6 section shows a 25% difference between the flat and the edges. Bjorhovde's results (1977) further reinforce Davison and Birkemoe's (1983) linear yield strength increase model with a 20% difference between the center of the flat and the edges.

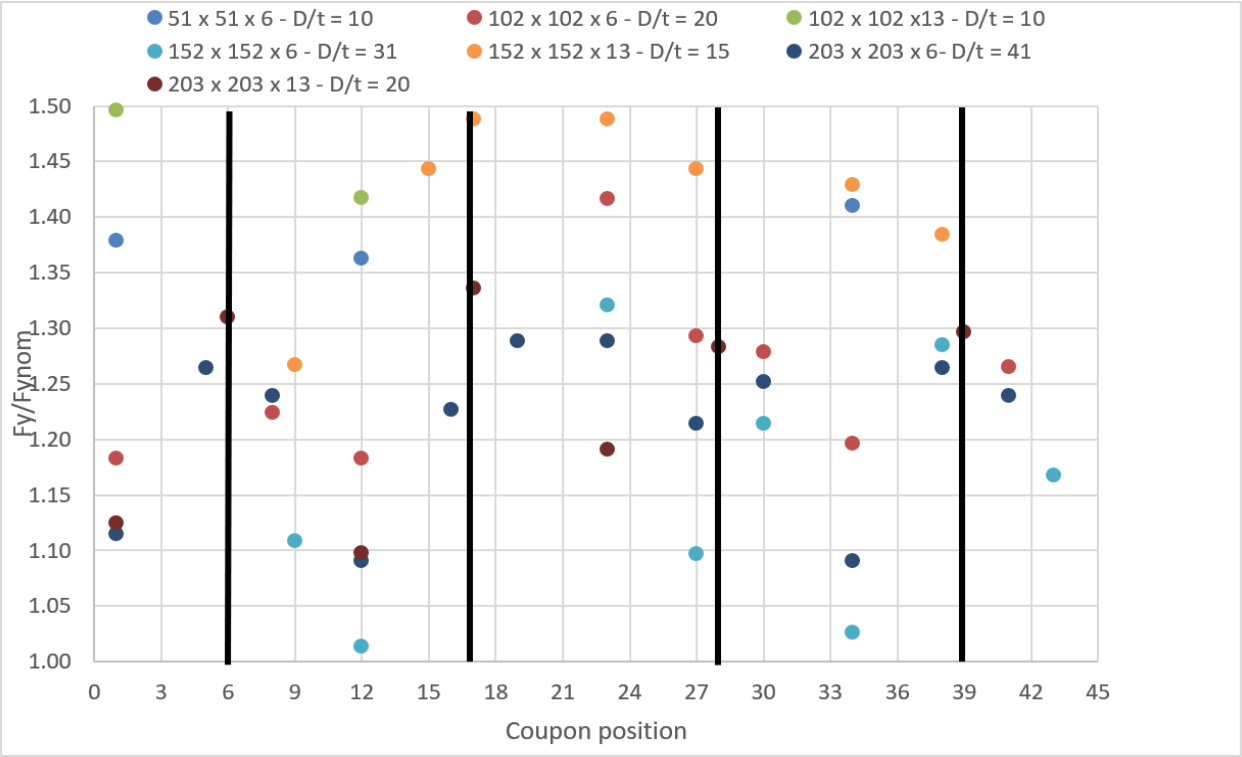


Figure 3-10: Normalized yield strength across the section – All sections (Bjorhovde, 1977)

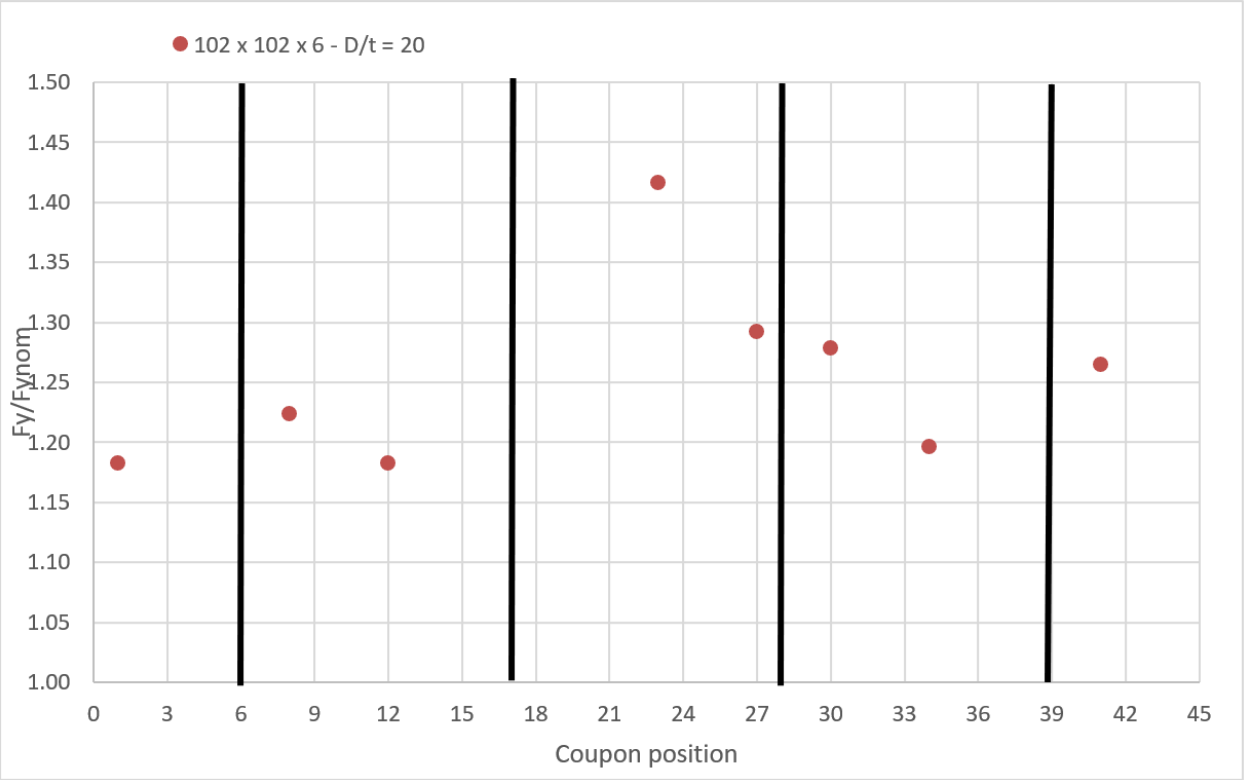


Figure 3-11: Normalized yield strength across the section – 102 x 102 x 6 (Bjorhovde, 1977)

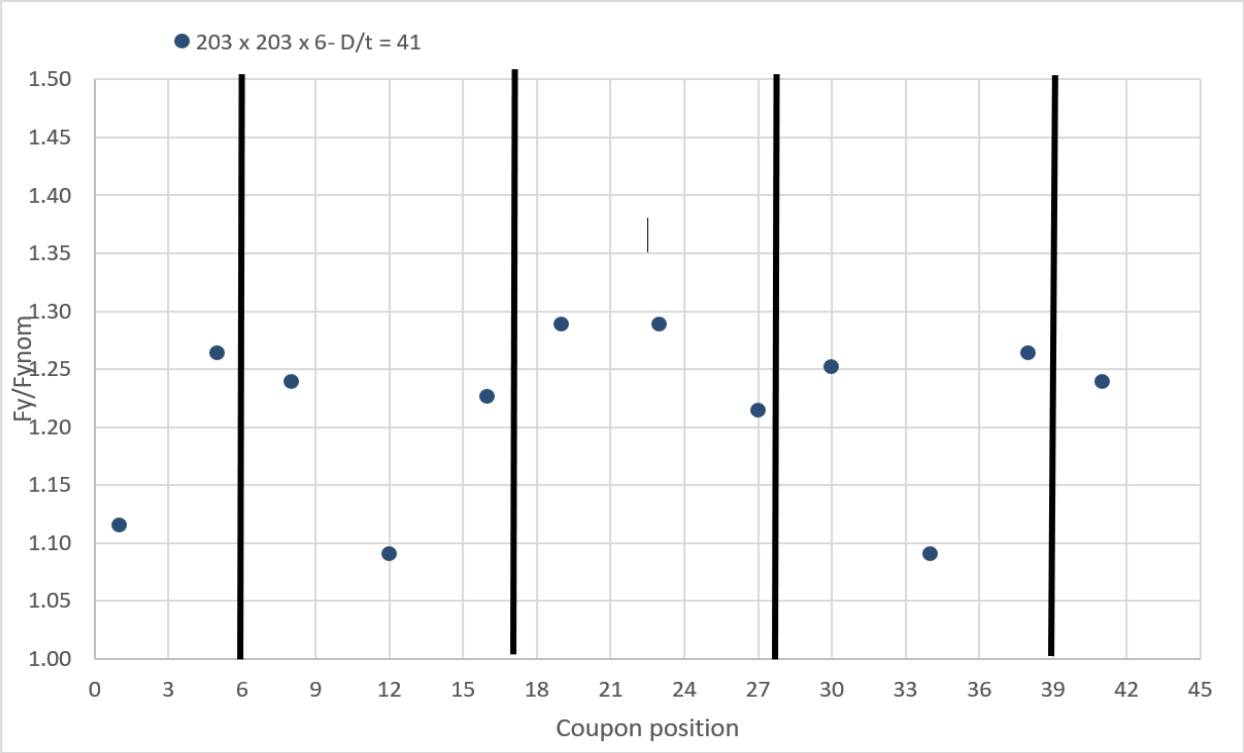


Figure 3-12: Normalized yield strength across the section – 203 x 203 x 6 (Bjorhovde, 1977)

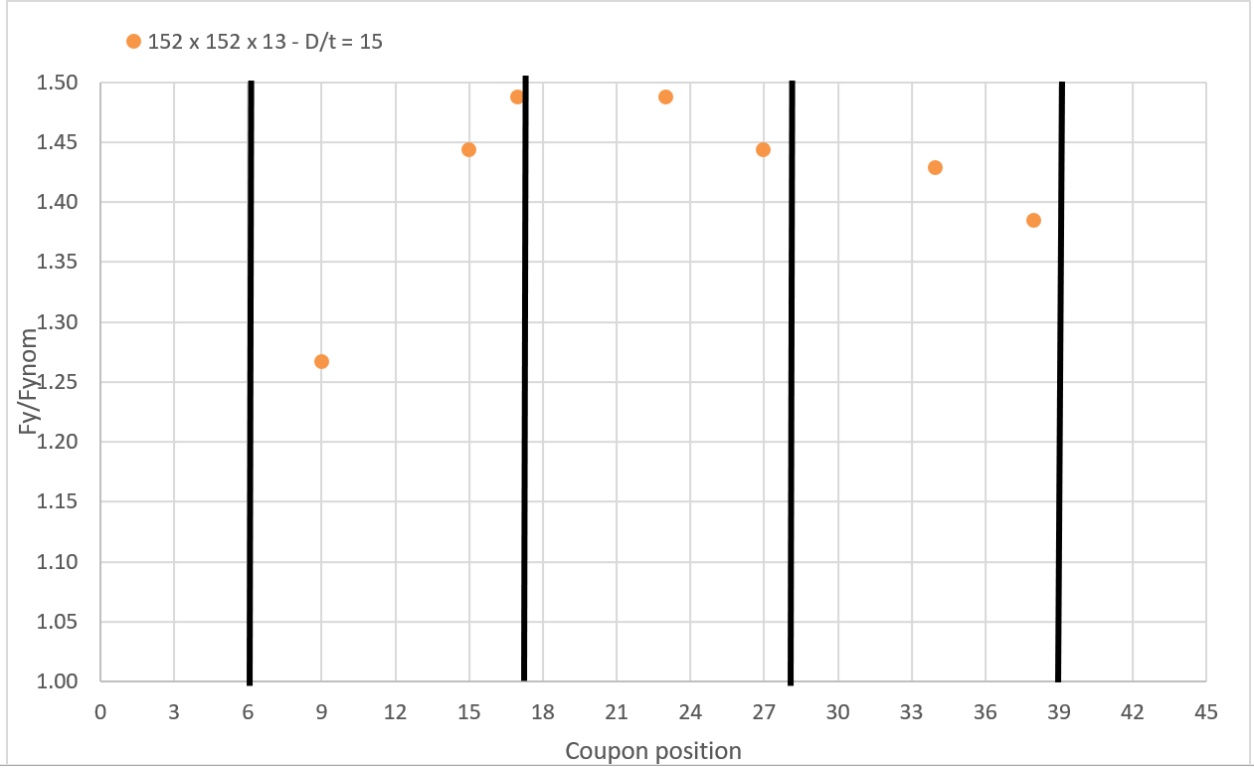


Figure 3-13: Normalized yield strength across the section – 152 x 152 x 13 (Bjorhovde, 1977)

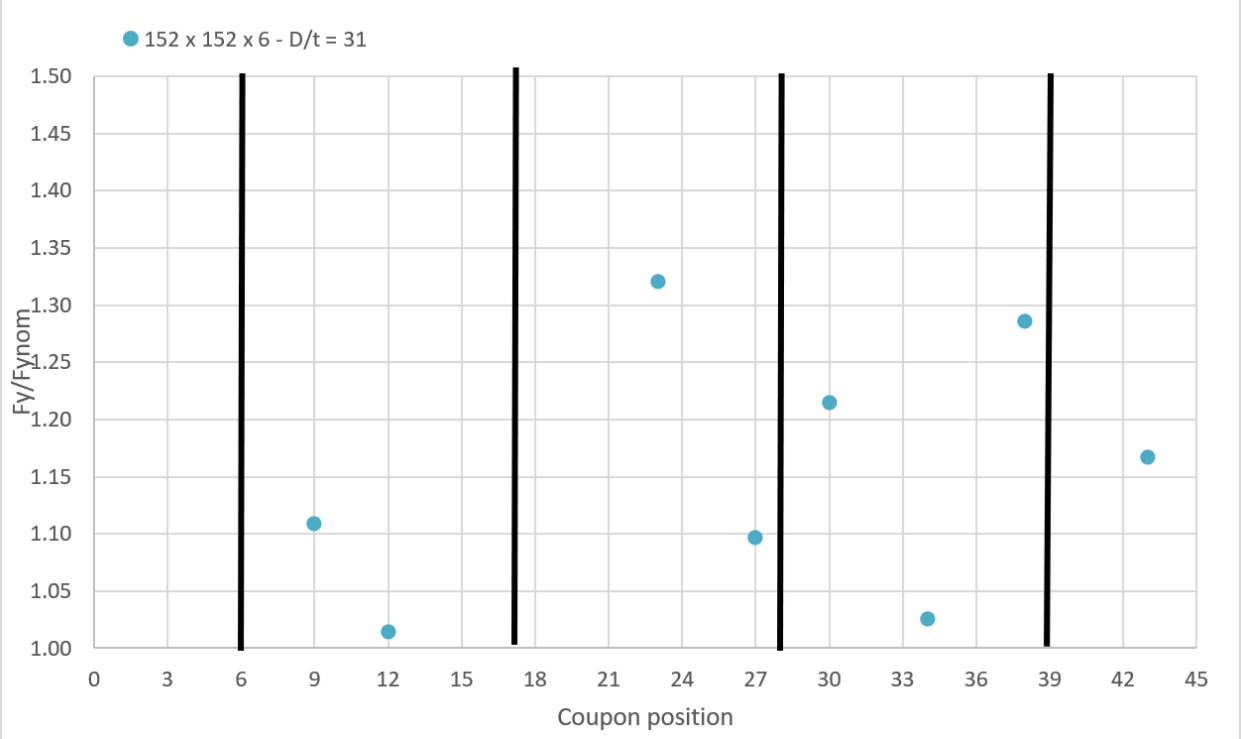


Figure 3-14: Normalized yield strength across the section – 152 x 152 x 6 (Bjorhovde, 1977)

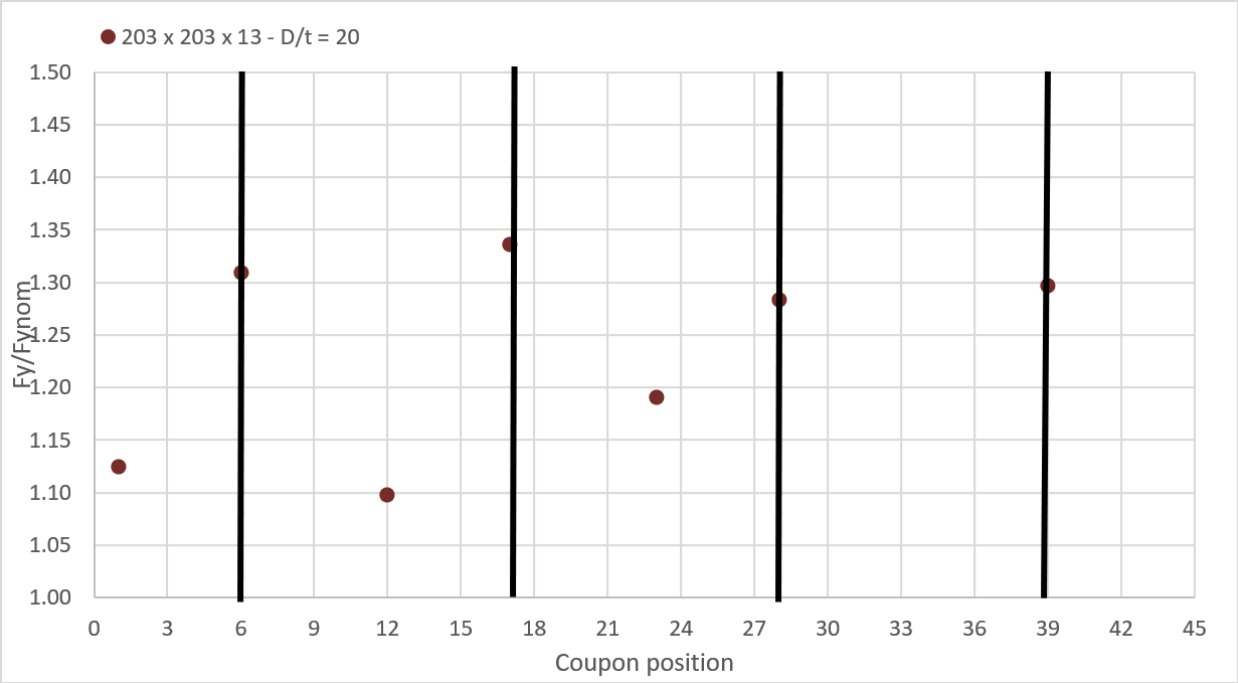


Figure 3-15: Normalized yield strength across the section – 203 x 203 x 13 (Bjorhovde, 1977)

An example of the proposed yield strength distribution model based on the nominal strength is shown in Figure 3-16. If the yield strength of the flat is known, it would be more efficient to increase the yield strength 20% above the known yield strength of the flat coupon at the center of the wall. The proposed corner yield strength is always set at 1.6 of the nominal yield strength as seismic HSS bracing members have to respect slenderness limits. This means the section will always have a D/t below the 30 proposed earlier. The model shows 1/8$^{th}$ of the section. The distribution is perfectly symmetrical on all sides.

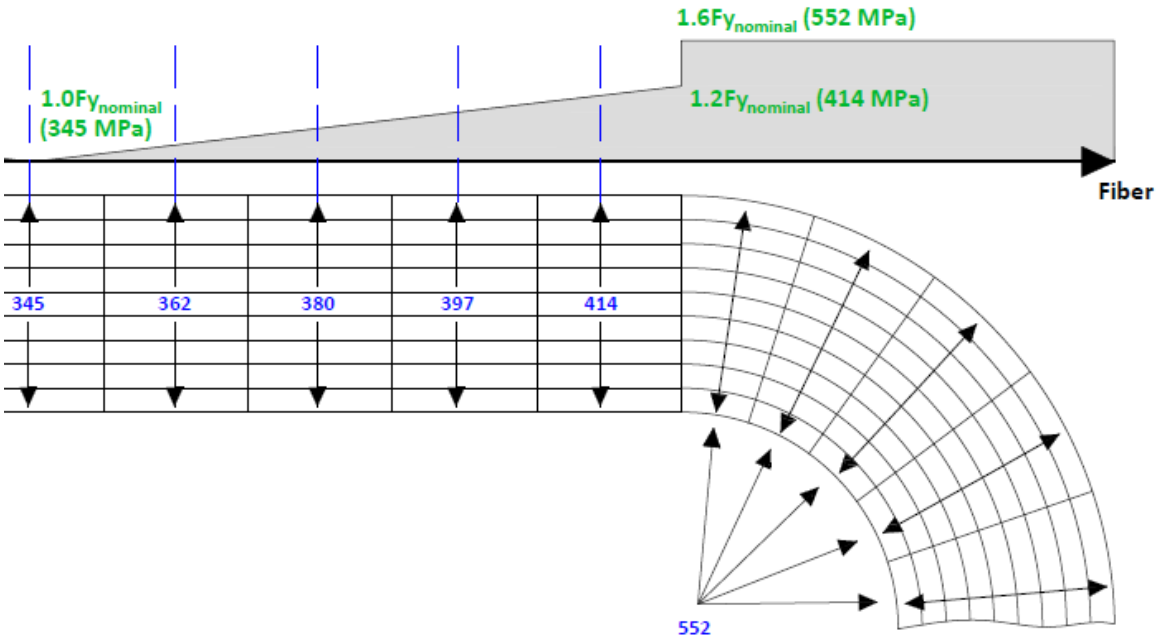


Figure 3-16: Example of yield strength distribution with nominal yield strength

## 3.3 Mill test certificate data from North American manufacturers

In this section, experimental data from North American manufacturers is presented. The test data was collected in the past years, the earliest dating to 2014. The yield and ultimate tensile stress at the center of the flat face opposite to the weld was determined for 18236 sections and several steel grades. The summarized results with respect to the appropriate nominal steel grade are presented in Table 3-3. Detailed results can be found in Appendix A.

Table 3-3: Tensile test results summary from North American manufacturers – Normalized with respect to the nominal yield strength

| | Standard | n samples | Fv (CV) | Fu (CV) |
|---|---|---|---|---|
| ALL | ASTM A500 | 12117 | 1.27 (7.84) | 1.23 (6.25) |
| | ASTM A1085 | 1263 | 1.26 (6.32) | 1.15 (4.86) |
| | G40.21-350W | 4856 | 1.26 (8.77) | 1.15 (5.51) |
| | Standard | n samples | Fy (CV) | Fu (CV) |
| RHS, SHS | ASTM A500 | 11613 | 1.27 (7.80) | 1.23 (6.24) |
| | ASTM A1085 | 1113 | 1.26 (6.18) | 1.15 (4.87) |
| | G40.21-350W | 4806 | 1.26 (8.75) | 1.15 (5.49) |
| | Standard | n samples | Fy (CV) | Fu (CV) |
| CHS | ASTM A500 | 504 | 1.22 (7.82) | 1.21 (6.46) |
| | ASTM A1085 | 150 | 1.26 (7.26) | 1.13 (4.35) |
| | G40.21-350W | 50 | 1.22 (9.62) | 1.12 (6.22) |

It can be seen the overall yield strength obtained from the ASTM A500 grade is 5% lower for circular sections than rectangular (RHS) and square (SHS) sections. There is no difference between the two for the ASTM A1085 grade. The G40.21-350W steel grade presents very close results to the ASTM A500 steel grade. Ultimate tensile stress is about 10% higher for ASTM A500 sections than the other two grades. Table 3-4 shows the results for RHS and SHS sections and Table 3-5 shows the results for CHS sections. The results were then truncated with respect to the b/t ratios for square and rectangular sections and D/t ratios for circular sections.

Table 3-4: Tensile test results summary from North American manufacturers with respect to a b/t ratio for square or rectangular sections

| RHS, SHS | Standard | n samples | Fv (CV) | Fu (CV) |
|---|---|---|---|---|
| b/t<17.7 | ASTM A500 | 6849 | 1.31 (7.44) | 1.23 (6.58) |
| KL/r = 100 | ASTM A1085 | 571 | 1.30 (5.36) | 1.16 (4.78) |
| | G40.21-350W | 2871 | 1.29 (8.66) | 1.16 (5.46) |
| RHS, SHS | Standard | n samples | Fv (CV) | Fu (CV) |
| b/t<19.7 | ASTM A500 | 6903 | 1.31 (7.43) | 1.23 (6.57) |
| KL/r = 140 | ASTM A1085 | 585 | 1.30 (5.34) | 1.16 (4.75) |
| | G40.21-350W | 2944 | 1.29 (8.76) | 1.16 (5.42) |
| RHS, SHS | Standard | n samples | Fv (CV) | Fu (CV) |
| b/t<22.6 | ASTM A500 | 8300 | 1.29 (7.56) | 1.23 (6.45) |
| KL/r = 200 | ASTM A1085 | 708 | 1.29 (5.60) | 1.16 (4.83) |
| | G40.21-350W | 3654 | 1.28 (8.60) | 1.16 (5.34) |

Table 3-5: Tensile test results summary from North American manufacturers with respect to a b/t ratio for circular sections

| CHS | Standard | n samples | Fv (CV) | Fu (CV) |
|---|---|---|---|---|
| D/t<28.9 | ASTM A500 | 265 | 1.24 (7.85) | 1.20 (6.36) |
| KL/r = 100 | ASTM A1085 | 124 | 1.27 (6.59) | 1.13 (4.17) |
| | G40.21-350W | 25 | 1.31 (5.73) | 1.15 (5.62) |
| CHS | Standard | n samples | Fv (CV) | Fu (CV) |
| D/t<32.4 | ASTM A500 | 379 | 1.22 (8.10) | 1.19 (6.35) |
| KL/r = 140 | ASTM A1085 | 139 | 1.26 (7.26) | 1.13 (4.11) |
| | G40.21-350W | 48 | 1.23 (9.65) | 1.11 (6.22) |
| CHS | Standard | n samples | Fv (CV) | Fu (CV) |
| D/t<37.6 | ASTM A500 | 504 | 1.22 (7.82) | 1.21 (6.46) |
| KL/r = 200 | ASTM A1085 | 147 | 1.26 (7.21) | 1.13 (4.18) |
| | G40.21-350W | 50 | 1.22 (9.62) | 1.12 (6.22) |

It can be seen from Table 3-4, RHS and SHS sections with a b/t ratio below 17.7 show an average increase in yield strength of 30% compared to the nominal yield strength. This ratio does not change significantly with b/t ratios of 19.7 and 22.6. The chosen b/t ratios represent interesting

slenderness limits in design. It is also interesting to note there is barely any difference in the average yield strength according to steel grade. The ultimate tensile stress is approximately 7% higher for the ASTM A500 grade than the other two. Yield strength in circular members was approximately 4 to 7% lower for most grades and b/t ratios. An exception can be seen for the G40.21-350W ratio which is almost as high as the SHS and CHS sections. Additional results in form of graphs are presented in  Figure 3-17 to Figure 3-19 for a b/t ratio below 17.7.

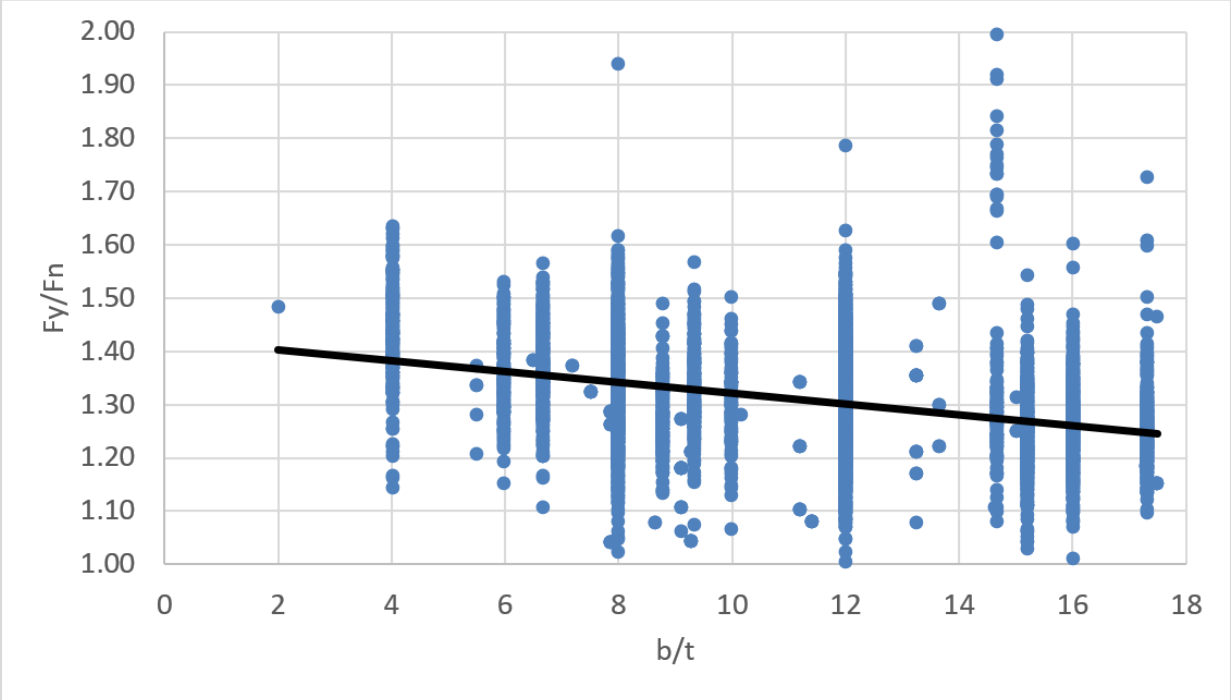


Figure 3-17: Yield ratio - ASTM A500 (SHS and RHS - b/t<17.7 - KL/r = 100)

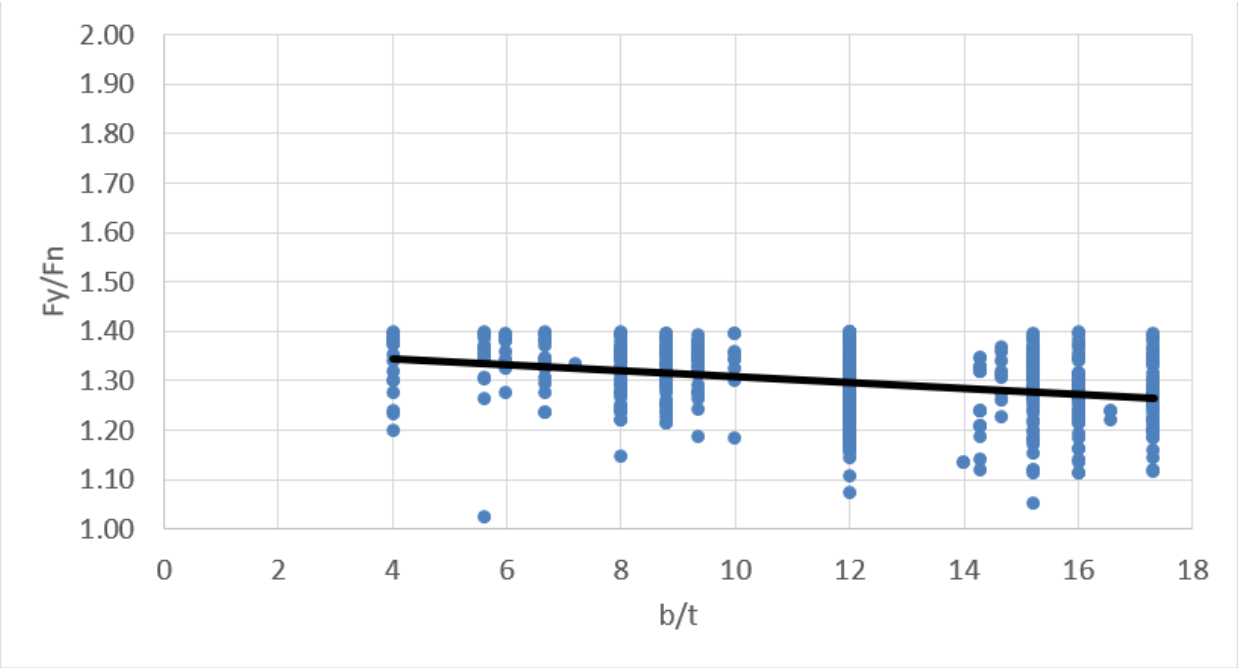


Figure 3-18: Yield ratio - ASTM A1085 (SHS and RHS - b/t<17.7 - KL/r = 100)

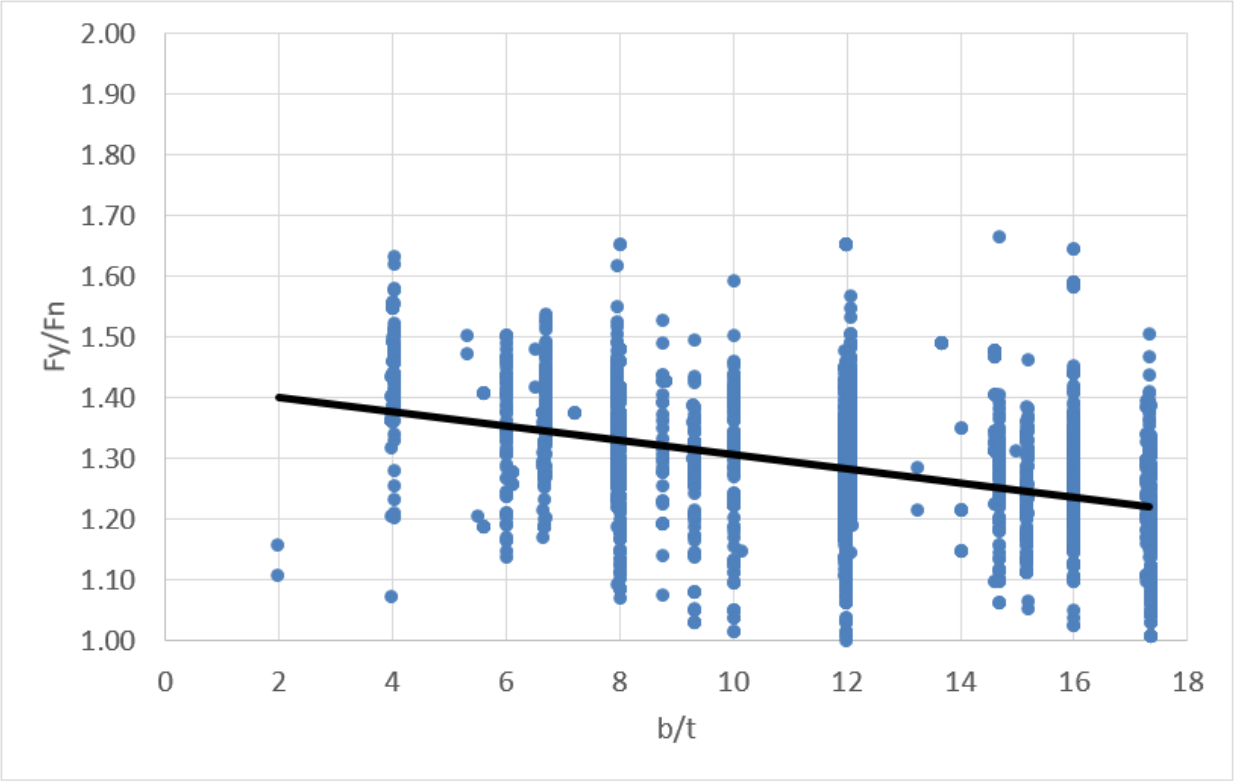


Figure 3-19: Yield ratio - CSA G40.21 (SHS and RHS - b/t<17.7 - KL/r = 100)

It is seen from these figures, the average yield strength for the ASTM A500 grade ranges from 1.40 at the lowest b/t ratio to 1.25 at a b/t ratio of approximately 17. The ASTM A1085 steel grade has a more regular distribution with both extremes going from 1.35 to 1.25. The CSA G40.21 steel grade has by far the widest distribution with an average range going from 1.40 to 1.20. Ultimate tensile stress results are presented in graph form in Appendix A. The average distribution was far more uniform. The ASTM A500 steel grade ranged from 1.25 to 1.20. The ASTM A1085 had an almost flat average distribution around 1.15. The CSA G40.21 grade had a wider distribution ranging from 1.20 to almost 1.10. These results show that the average yield strength of the central flat coupon is proportional to the b/t ratio. The ultimate tensile stress is not significantly affected by cold work as the increase compared to the nominal strength is almost uniform for the ASTM A1085 section with respect to the b/t ratio. Results for circular members can be seen in Appendix A. The ultimate tensile stress increase is almost uniform as was seen for the flats. The yield strength ranges from 1.30 to 1.40 for A500 and CSA G40.21 sections. The ASTM A1085 yield strength varies from 1.30 to 1.35. Based on these data and the slenderness limits, the average yield strength for the central flat coupon of an ASTM A1085 steel grade HSS section in seismic applications can be taken as $1.30F_{yn}$. The increase in yield strength due to the strain rate in mill test certificates was not accounted for. Since this thesis is aimed at seismic applications, the HSS bracing members will be subjected to dynamic loads where strain rate effects are present.

## 3.4 Actual average cross-sectional yield strength (probable yield strength $R_yF_y$)

A yield strength distribution model across the section was established in the previous two sections. It was determined that the flat wall varies linearly from a minimum at the center of the wall to $1.2F_{ycenter}$ at the edges. The corner yield strength is taken as $1.6F_{ynom}$. It was then determined the average coupon from the center of the flat wall for an ASTM A1085 steel grade member is $1.30F_{ynom}$. In this section, the average cross-sectional yield strength is determined for an HSS section based on three different models. The first model is based on a weighted average based on the previously defined model. The distribution is shown in Figure 3-20. The second and third models are based on the CSA S136 standard equation to account for the increased yield strength from cold work forming. This equation has been extensively discussed in Chapter 2. For simplicity, it is repeated as equation (3-2) below. The virgin to ultimate yield ratio, which is normally determined from the coil strip, was determined according to two methods. In the first method, the ratio was taken according to the nominal yield strength to nominal strength. This was named *S136A*. For the second method, the ratio was taken according to the actual measured yield and ultimate tensile stress from the center flat coupon. This method was named *S136B*. Results are presented in Table 3-6.

$$\frac{\mathrm{F}_{yc}}{\mathrm{F}_{yv}} = \frac{B_c}{(\frac{R}{t})^m} \tag{3-2}$$

$$B_c = 3.69\frac{F_{uv}}{F_{yv}} - 0.819\left(\frac{F_{uv}}{F_{yv}}\right)^2 - 1.79$$

$$m = 0.192\frac{F_{uv}}{F_{yv}} - 0.068$$

$$F_{ya} = CF_{yc} + (1-C)F_{yf}$$

$F_{yc} =$ Corner yield stress

$F_{yv} =$ Virgin yield stress

$F_{uv} =$ Virgin ultimate tensile strength

$R =$ Inside bend radius

$F_{ya} =$ Average tensile yield strength of the cross-section

$C =$ Ratio of corner to total cross section area

$F_{yf} =$ Yield strength of flat (uniform throughout the flat wall)

***$F_y$* in corner**

- D/t under 30 → 1.6$F_{ynom}$
- D/t between 30 and 40 → 1.4$F_{ynom}$
- D/t over 40 → 1.3$F_{ynom}$
- $F_y$ corner can never exceed $F_u$ of tested center coupon.

***$F_{yf}$* in flats** (linear distribution)

- Follows linear distribution where center is tested coupon ($F_{ycoup}$).
- Edge near corner is 1.2$F_{ycoup}$.

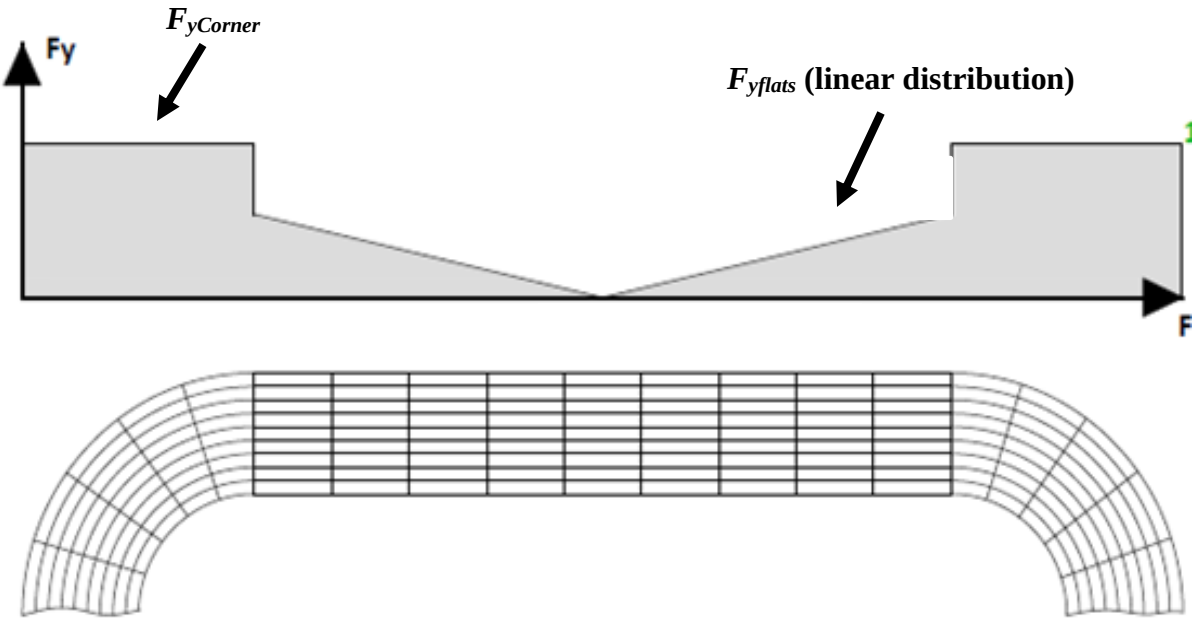


Figure 3-20: Cross sectional yield strength distribution model – Weighted average

Table 3-6: Average cross-sectional yield strength according to weighted average, S136A and S136B methods – Normalized with respect to the nominal yield strength

| | | | RHS, SHS Fy (CV) | | |
|---|---|---|---|---|---|
| KL/r | b/t under | METHOD | ASTM A500 (B&C) | ASTM A1085 | G40.21-350W |
| - | no limit | COUPON DATA | 1.27 (7.84) | 1.26 (6.32) | 1.26 (8.77) |
| | | S136A | 1.36 (5.57) | 1.41 (5.93) | 1.40 (6.42) |
| | | S136B | 1.46 (7.47) | 1.43 (6.44) | 1.45 (7.21) |
| | | WEIGHTED AVERAGE | 1.43 (6.86) | 1.42 (5.94) | 1.42 (7.12) |
| 100 | 17.7 | COUPON DATA | 1.31 (7.44) | 1.30 (5.36) | 1.29 (8.66) |
| | | S136A | 1.41 (4.18) | 1.45 (3.65) | 1.44 (5.18) |
| | | S136B | 1.51 (6.69) | 1.51 (4.84) | 1.50 (6.00) |
| | | WEIGHTED AVERAGE | 1.47 (5.99) | 1.47 (4.44) | 1.46 (6.27) |
| 140 | 19.7 | COUPON DATA | 1.31 (7.43) | 1.30 (5.34) | 1.29 (8.76) |
| | | S136A | 1.40 (4.19) | 1.45 (3.66) | 1.44 (5.22) |
| | | S136B | 1.51 (6.70) | 1.51 (4.81) | 1.50 (5.98) |
| | | WEIGHTED AVERAGE | 1.47 (5.99) | 1.47 (4.42) | 1.46 (6.35) |
| 200 | 22.6 | COUPON DATA | 1.29 (7.56) | 1.29 (5.60) | 1.28 (8.60) |
| | | S136A | 1.39 (4.66) | 1.44 (4.21) | 1.43 (5.51) |
| | | S136B | 1.49 (6.88) | 1.50 (5.23) | 1.48 (6.24) |
| | | WEIGHTED AVERAGE | 1.46 (6.28) | 1.46 (4.88) | 1.45 (6.49) |

The row named "*Coupon Data*" represents the yield strength values determined by the manufacturer (mill certificates) from one central coupon as seen in Section 3.3. For the ASTM A500 steel grade, it can be seen that the weighted average and the *S136B* method (based on measured coupon values) produce very close results for the case where there is no b/t limit. The *S136A* method (with nominal yield and ultimate tensile stress) is in between the results for the *Coupon Data* and the other two methods. For the other b/t limits, the results from the weighted

average and *S136B* methods are approximately 4% apart. The results from the *S136A* method are about 10% above the Coupon Data and 10% below the other two methods for the steel grade of ASTM A500. For the A1085 and G40.21 steel grades, results from all three methods are very close to each other. A maximum difference of about 5% can be seen between these results.

The next step consists of validating the *S136B* method by comparing its results to previously measured corner yield strengths. The method is applied to the HSS members studied in Section 3.1 and results are presented in Figure 3-21. Only members having a nominal yield strength of 345 MPa and an ultimate tensile stress of 450 MPa were included.

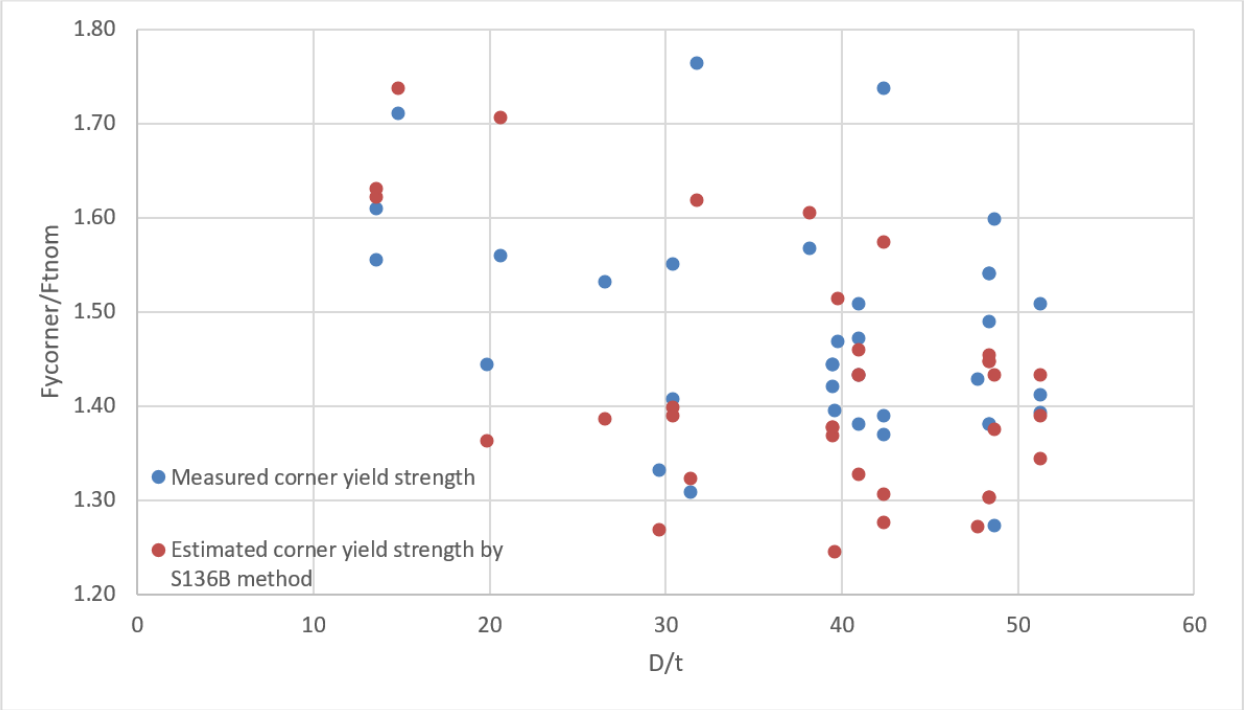


Figure 3-21: Comparison between S136B method and measured corner yield strength

It is seen from Figure 3-21, the *S136B* method seems to give accurate results, but this is not exactly the case. In order to avoid overestimating the strength, an upper bound limit based on the ultimate tensile stress of the flat was added to the *S136B* corner yield strength. By carefully analyzing the obtained values, the corner yield strength was capped by the ultimate tensile stress limit from the flat in every single case. This means all the values shown in Figure 3-21 are actually of the ultimate tensile stress $F_u$ of the flat section. It was seen in Chapter 2, the yield strength of the cold worked material can never exceed the ultimate tensile stress of the virgin coil. It was also seen that the

ultimate tensile stress of the virgin coil does not increase significantly after cold work. Previous investigations usually limited this increase to approximately 10%.

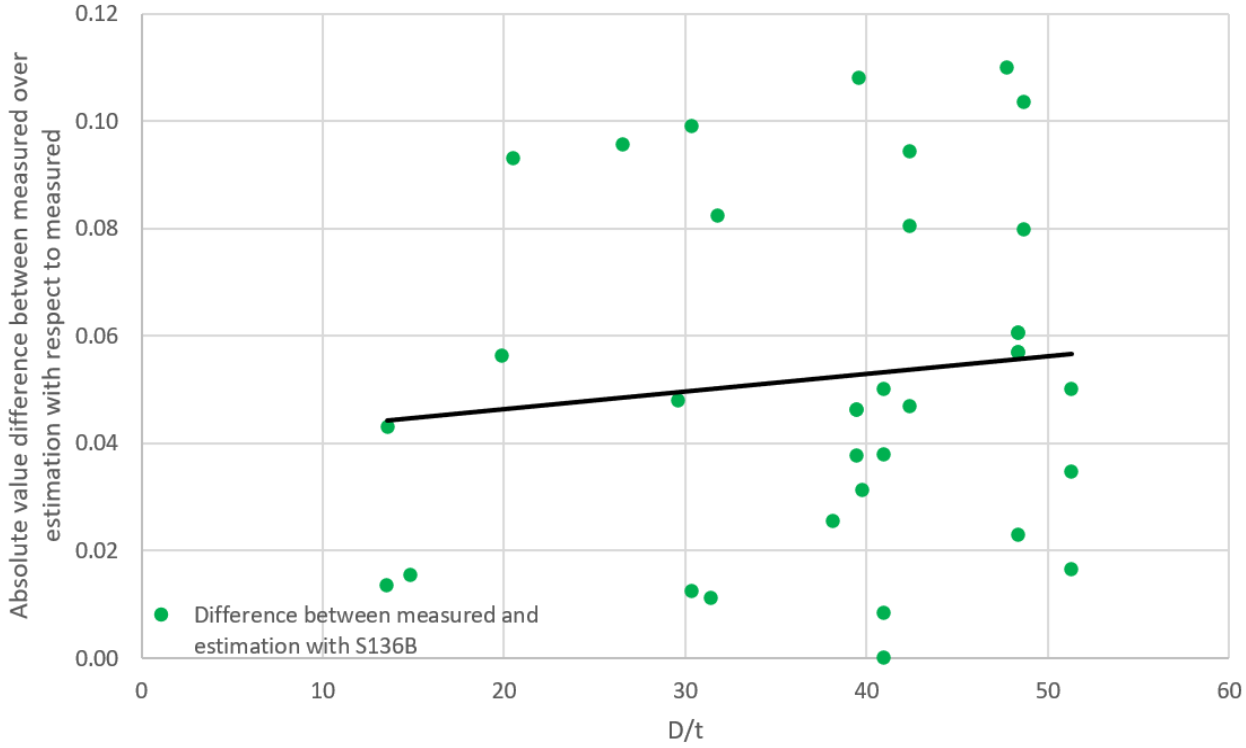


Figure 3-22: Normalized difference between *S136B* method and actual corner yield strength

It can be seen from Figure 3-22, Figure 3-23 and Figure 3-24, the ultimate tensile stress of the corners can be 10 to 40% higher than the ultimate tensile stress of the flat coupon. This does not support conclusions from some previous investigations. Therefore, the *S136B* method to determine the corner yield strength seems too conservative as the ultimate tensile stress of the corner can be higher than the ultimate tensile stress of the flat. This would imply highly cold worked corner yield strength could increase in yield strength up to 40% beyond the ultimate tensile stress of the flat. Nevertheless, judging by Figure 3-22, it appears the yield strength of the corners was generally very close to the ultimate tensile stress of the flats. From Figure 3-25, it seen the ultimate tensile stress of the flat tends to slightly underestimate the yield strength of the corner. From these figures, it can be concluded the yield strength of the corner can be approximated by the ultimate tensile stress of the flat. If the flat strength is not available, the first method, which uses the nominal yield and ultimate tensile stress, always gives a corner yield strength of 562 MPa (63% increase) based

on the S136 standard equation. This can also be considered a reasonable approximation for low D/t ratios based the findings from section 3.1.

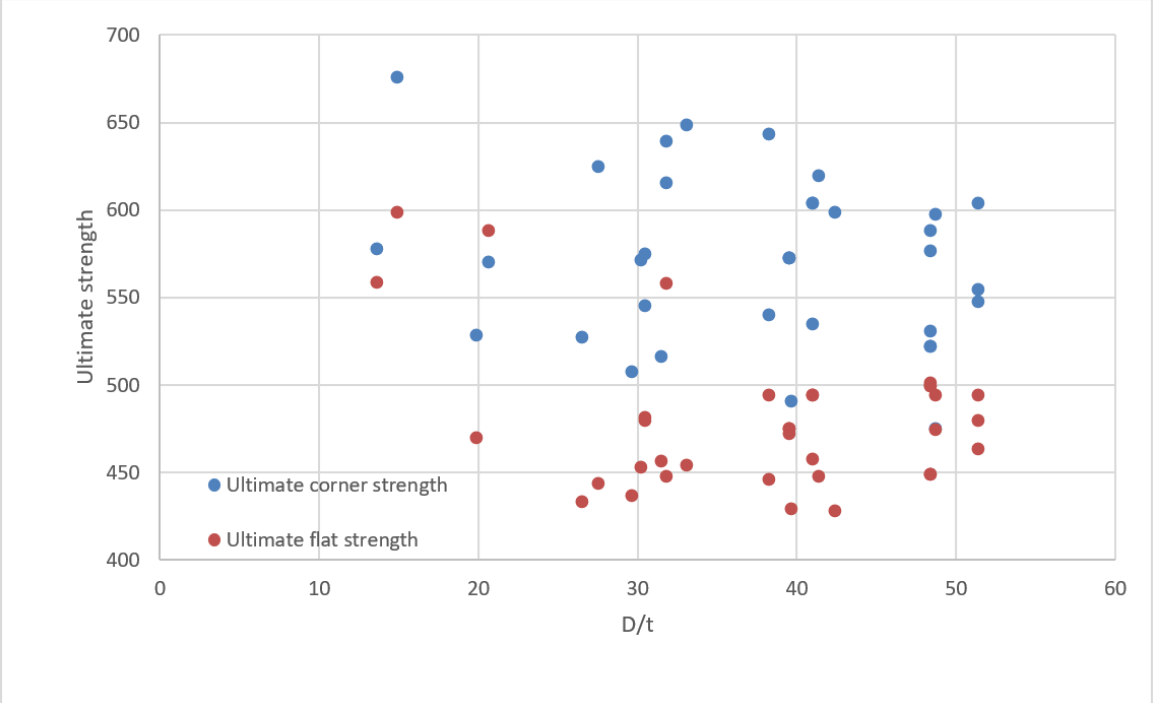


Figure 3-23: Average ultimate tensile stress of corners and flats

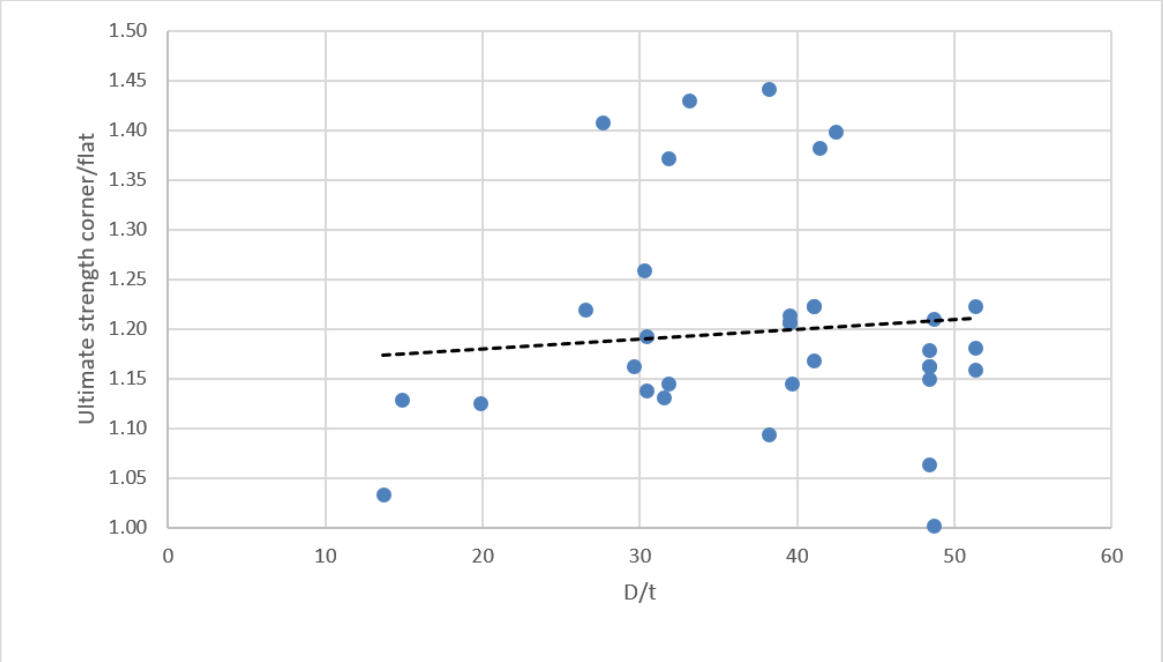


Figure 3-24: Normalized ultimate tensile stress (corner over flat)

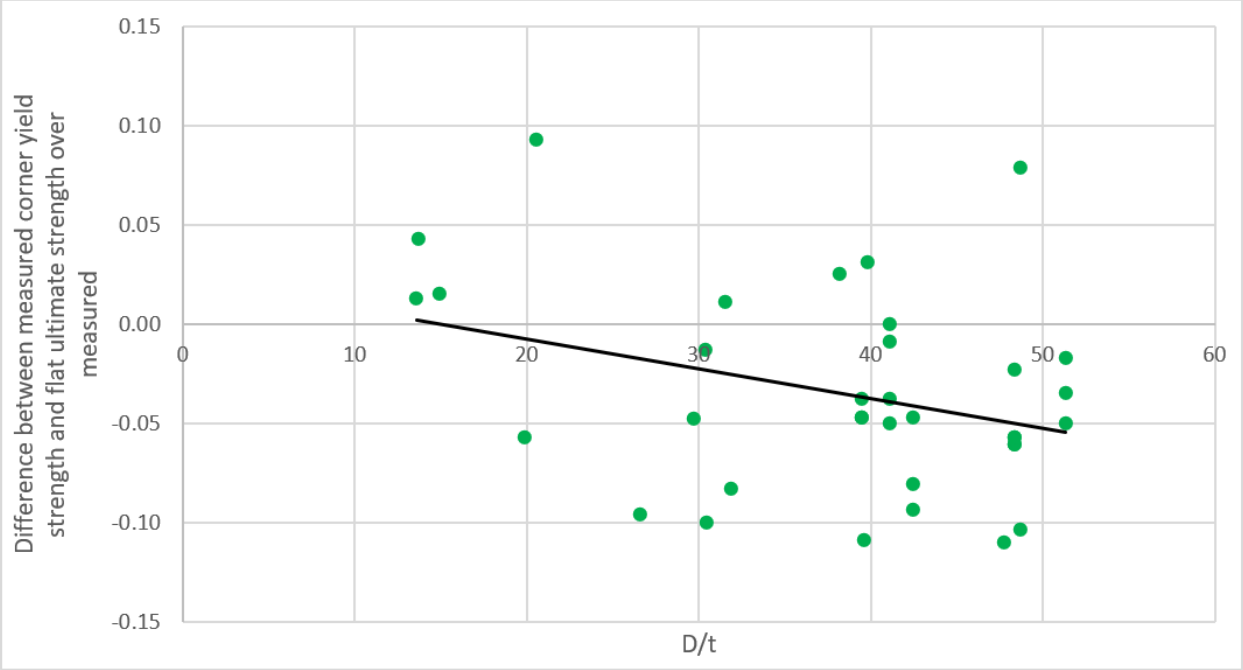


Figure 3-25: Normalized difference between flat ultimate tensile stress and corner yield strength

## 3.5 Predicted equivalent nominal yield strength from reliability analysis

This section consists in an inverted reliability analysis. The equivalent nominal strength to satisfy the steel resistance factor $\phi$ of 0.9 based on the results determined in the previous sections is determined. This equivalent nominal strength can be used to determine the factored tensile resistance $T_r$ by multiplying it by the resistance factor and the nominal area.

Kennedy and Aly (1980) established the resistance factor of steel, $\rho_r$ (mean to nominal resistance), can be determined from equation (2-3).

$$\rho_m \rho_g \rho_p = \rho_r \tag{3-3}$$

Where $\rho_m$ is the material ratio (mean material yield strength over nominal yield strength), $\rho_g$ is the geometric bias ratio (mean geometry over nominal geometry) and $\rho_p$ is the professional ratio (observed capacity in tests over predicted capacity in observed values of the relevant material and geometric properties) (Kennedy & Aly, 1980). The mean material yield strength has been previously determined from current North American manufacturers in Section 3.3 and can be expressed by equation (3-4).

$$F_y^* = \frac{R_y F_y}{\rho_m} \tag{3-4}$$

It was also shown by Kennedy and Aly (1980), the steel resistance factor can be determined by equation (3-5).

$$\varphi = \rho_r e^{(-\beta * \alpha_r * V_r)} \tag{3-5}$$

Where $\phi$ is the well known 0.9 factor, $\rho_r$ is determined from (2-3), $\beta$ is the reliability index, $\alpha_r$ is the coefficient of separation, $V_r$ is the coefficient of variation. Kennedy and Aly (1980) base the coefficient of separation on a study performed by Galambos and Ravindra in 1977. It was shown in this study the coefficient of separation can be taken as a constant of 0.55 for a case of dead, live and wind load. This coefficient of separation also ensures a reliability index of at least 3.0 is achieved at all times (Schmidt and Bartlett, 2002b). The coefficient of variation is based on the

coefficients of variation of the geometric bias and material ratio. The coefficient of variation for the material ratio is determined from section 3.3. The geometric bias and its coefficient of variation is determined from Schmidt and Bartlett (Schmidt and Bartlett, 2002b) for recent HSS members. The coefficient of variation for the resistance factor is expressed by equation(3-6).

$$V_r = \sqrt{V_m^2 + V_g^2 + V_p^2} \tag{3-6}$$

Table 3-7: Example to determine the nominal yield strength to satisfy the resistance factor based on a reliability analysis.

| **Specification (Grouped)** | |
|---|---|
| CSA G40.21 - 350W AND ASTM A500 SINGLE OR DUAL CERTIFIED | |
| **TYPE** | |
| SHAPED | |
| **METHOD** | |
| COUPON DATA | |
| **D/t limit** | |
| 37.6 | |
| **DATA** | |
| Fyn = | 345 |
| **Vm=** | **0.0860** |
| **RyFy (average) =** | **1.28** |
| | 441 MPa |
| Φ = | 0.9 |
| ρg = | 0.971 |
| Vg = | 0.015 |
| ρp = | 1.00 |
| Vp = | 0.00 |
| β = | 3 |
| αr = | -0.55 |
| Vr = | 0.087 |
| ρr = | 1.04 |
| ρm = | 1.07 |
| **Fy* =** | **413 MPa** |

After having determined all the factors, $\rho_r$ is determined from equation (3-5) which then allows to determine $\rho_m$ from equation (3-3). By knowing $\rho_m$ and $R_y F_y$, $F_{nominal}$ can be determined from equation (3-4). An example of a calculation is shown in Table 3-7. Detailed results can be found in Appendix B.

From this result, it can be concluded an equivalent nominal yield strength of 413 MPa in design is enough to satisfy a resistance factor $\phi$ of 0.9. The exercise was repeated for the average full section yield strength determined in Section 3.4.

Table 3-8: Equivalent nominal yield strength ($F_y$*) to be used in the current equation $T_r$ assuming a $\phi$ of 0.9 and the nominal area.

| | | | RHS, SHS Fy* (MPa) | | |
|---|---|---|---|---|---|
| **KL/r** | **b/t under** | **METHOD** | **ASTM A500 (B&C)** | **ASTM A1085** | **G40.21-350W** |
| - | no limit | COUPON DATA | 414 | 421 | 405 |
| | | S136A | 460 | 474 | 467 |
| | | S136B | 479 | 477 | 478 |
| | | WEIGHTED AVERAGE | 474 | 478 | 469 |
| 100 | 17.7 | COUPON DATA | 430 | 441 | 415 |
| | | S136A | 488 | 506 | 490 |
| | | S136B | 502 | 517 | 504 |
| | | WEIGHTED AVERAGE | 494 | 506 | 489 |
| 140 | 19.7 | COUPON DATA | 430 | 442 | 415 |
| | | S136A | 484 | 506 | 490 |
| | | S136B | 502 | 517 | 504 |
| | | WEIGHTED AVERAGE | 494 | 507 | 488 |
| 200 | 22.6 | COUPON DATA | 423 | 436 | 413 |
| | | S136A | 477 | 498 | 484 |
| | | S136B | 494 | 510 | 496 |
| | | WEIGHTED AVERAGE | 489 | 500 | 484 |

## 3.6 Proposed residual stress model

To complete this chapter, a residual stress model is proposed based on the review presented in Chapter 2.

It was seen the first model was proposed by Davison and Birkemoe in 1983. The model was based on the hypothesis that the magnitude of the elastic unloading profile would equal the magnitude of the bending residual stress profile. The total residual stress of the section would equal the sum of the membrane and bending residual stresses. The membrane residual stress would be in tension in the center and in compression at the edge. The maximum values in tension and compression would be of the same magnitude and follow a linear distribution towards each other. The final values proposed by Davison and Birkemoe (1983) were $0.6\sigma_{stub}$ for the maximum through thickness residual stress value and $0.17\sigma_{stub}$ for the maximum membrane residual stress values. Key and Hancock (1993) continued the residual stress research and added a new component named the layering component. This component represents the residual stress remaining within the coupon after the elastic bending stress has been unloaded after the its release from the HSS. This value was implicitly included in the model proposed by Birkemoe, but not explicitly measured. Key and Hancock proposed a new residual stress model slightly different from Davison and Birkemoe's model. Both models are generally equivalent and complement each other. In recent decades, several researchers took additional residual stress measurements with more advanced techniques such as the X-Ray diffraction method and the Photogrid method. A few proposed new residual stress models, however, these were much simpler than the original models proposed by Davison and Birkemoe, and Key and Hancock. In general, no research has disputed the models proposed in 1983 and 1993 and most confirmed their findings through new measurements.

Four through thickness measured or prosed models are shown in Table 3-9. It can be seen the through thickness residual stress profile proposed by Davison and Birkemoe is clearly represented in all four models. Nevertheless, the actual magnitudes proposed in the 1983 paper are average values across the section. It can be noted from more recent investigations, the residual stress at the corner is approximately half of the residual stress of the flat. It was also shown by Somödi and Kovesdi (2016), the average residual stress follows an almost linear profile with respect to section yield strength. This is shown in Figure 3-26.

Table 3-9: Previously proposed residual stress distributions

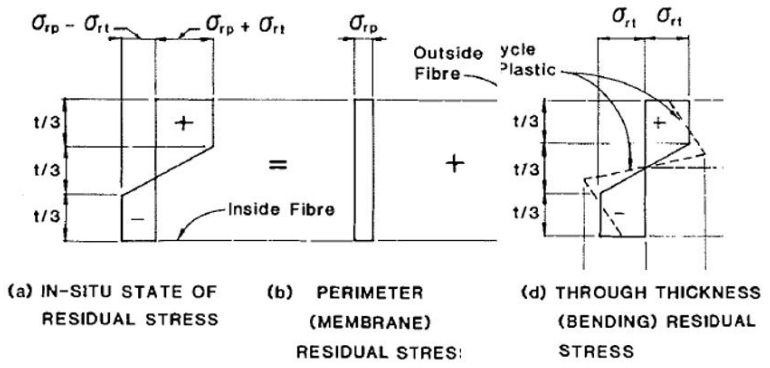


(Davison and Birkemoe, 1983)

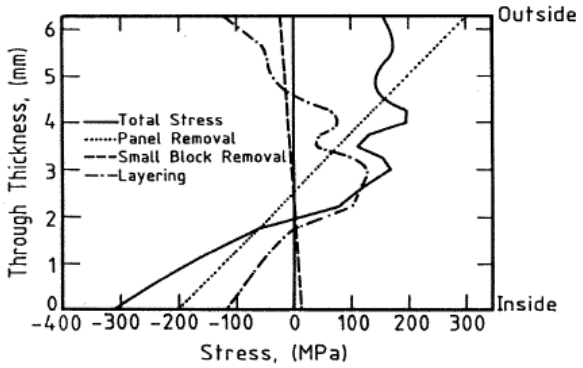


(Key and Hancock, 1993)

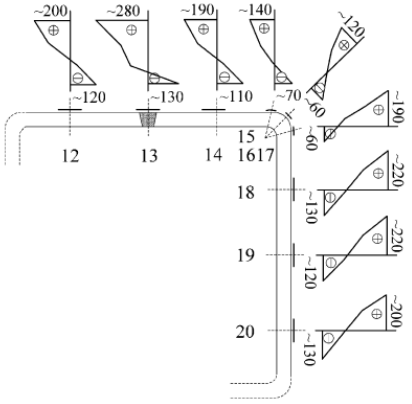


(Li et al., 2009)

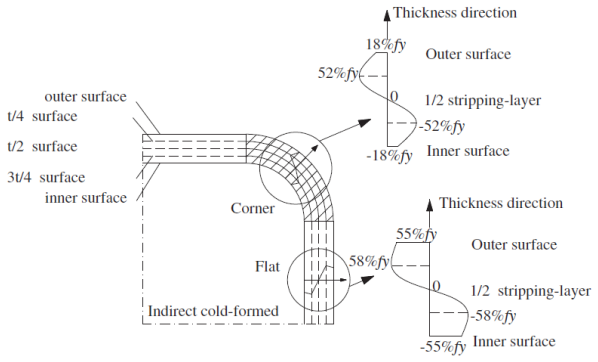


(Tong et al., 2012)

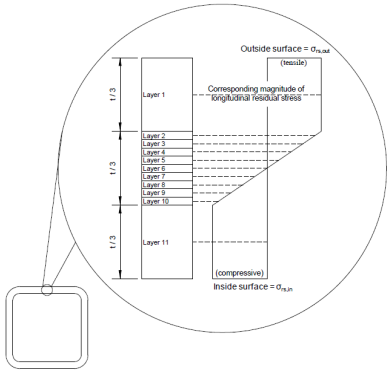


(Sun, 2014)

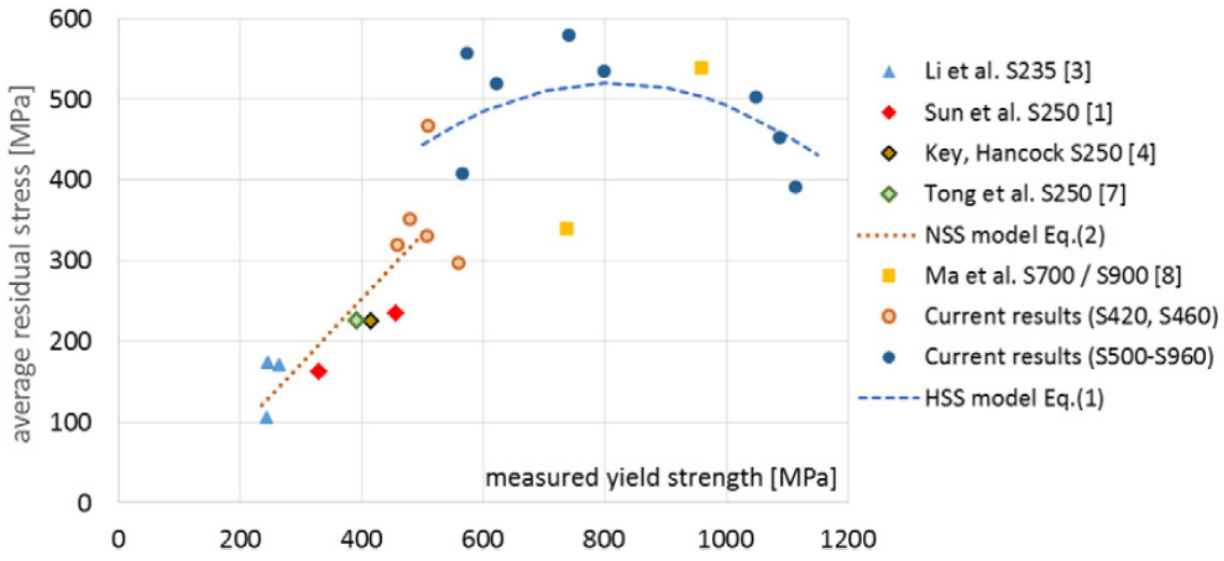


Figure 3-26: Average residual stress with respect to section yield strength (Somödi and Kovesdi, 2016)

Based on these results, two residual stress models are proposed. The first model is used to study the effects of residual stress on the column strength curves and is purely based on the average values proposed by Davison and Birkemoe. The magnitudes of the residual stress are based on $F_{nom}$ for this model. This was due to the lack of more precise values at the time of these analysis. This does not affect the comparison as the yield strength gradient is also based on the nominal value for this model. The second model is based on the same through thickness and membrane distribution, however, the magnitudes are chosen to be more representative of realistic values. The residual stress and yield strength gradient are based on the average cross-sectional yield strength of the section. Equation (3-7) (Somödi and Kovesdi, 2016) is based on the straight line presented in Figure 3-26.

$$RSD_{flat} = 1.2 * (0.75 * 448.5 - 50) \tag{3-7}$$

The 1.2 factor is based on the geometric transformation from the average residual stress profile, represented by a rectangular block, and the trapezoidal model adopted. When comparing the results from this equation to the magnitudes proposed by Davison and Birkemoe (1983), on average, it is seen both are in good agreement with each other. The corner was proposed to be taken as 55% of the flat through thickness residual stress by Somödi and Kovesdi (2016). Davison and Birkemoe

also noticed the residual stress in the corners was somewhat smaller than the residual stress in the flat portions of the cross-section. However, it was judged by Davison and Birkemoe the average representation was good enough for the model and it was not necessary to add the reduction in the corner. In this investigation, the corner reduction is also omitted as the actual percentage has not been universally confirmed and some research did not show a clear reduction (Sun, 2014). It is also considered Davison and Birkemoe's proposed average magnitudes are an accurate representation of residual stresses in the member. However, this value is based on the average cross-sectional yield strength obtained from the proposed yield strength gradient instead of stub column results.

## 3.7 Conclusion

In Chapter 2, an extensive review of a large number of investigations into the cold-formed members over the past 60 years was performed. In this chapter, results from these investigations were presented and analyzed to obtain a proper representation of the material properties of cold-formed HSS members. Based on this representation, a new probable yield strength $R_yF_y$ used to calculate the tensile resistance $T_u$ was established. An equivalent nominal yield strength ($F_y$*) to be used in the current equation of the factored tensile resistance $T_r$ assuming $\phi$ 0.9 and the nominal area was also determined.

The first part consisted in collecting coupon data on the yield strength ($F_y$) and ultimate tensile stress ($F_u$) of flat and corner coupons from several investigations seen in Chapter 2. A total of 18 investigations were included with 81 different sections. Sections with a nominal yield strength of 345 MPa were tested in most investigations. A handful included results for sections with a nominal yield strength of 235 MPa and 317 MPa. Only three investigations included full cross-sectional results on the yield strength gradient (Davison and Birkemoe, 1977; Salvarinas, 1977 and Bjorhovde, 1977). In these three investigations, four HSS sections had detailed readings with several coupons per flat wall, while seven only had partial readings with a few coupons strategically distributed over the flats. Yield strength data in the corners was available for a total of 47 different sections. Some researchers took readings at all four corners, while others only tested one corner or directly provided the average of all tested corners. To simplify the results, except for the three investigations where full cross-sectional readings were taken, only averages of the yield strength of flat coupons at the center of the four walls and the average yield strength of the four corners were provided in the results. These readings were analyzed with respect to the D/t ratio to establish a tendency and a distribution that can be applied to a numerical model. It was determined the yield strength decreases as the D/t ratio increases.

For the corners, results from Canadian investigations suggest there is a linear correlation between the yield strength and the D/t ratio. Sections with low D/t ratios peaked at about 1.6 to 1.7 of $F_{ynom}$, then decreased linearly to $1.3F_{ynom}$ at a D/t ratio of 20. The corner yield strength of $1.3F_{ynom}$ seemed to represent a lower bound. These results from Canadian investigations were very promising, but only five investigations were available with eight different sections which is insufficient to draw definite conclusions.

When analyzing all 47 sections with results from various countries, the lower limit of $1.3F_{ynom}$ seemed to hold as it was seen in the Canadian investigations. The lowest yield strength was found in a section with a D/t ratio of 48 and a corner yield strength of $1.28F_{ynom}$. However, the average yield strength of the corner for the D/t ratio of 50 was approximately $1.45F_{ynom}$ which is slightly above the $1.30F_{ynom}$ limit seen in Canadian investigations. From these findings, it can be concluded that the corner yield strength in cold-formed HSS sections does not decrease below $1.3F_{ynom}$. Several assumptions can be made with respect to the actual decrease with respect to the D/t ratio based on various hypothesis. More corner data from Canadian investigations would be needed to determine a clear pattern.

The average corner yield strength seems to increase up to $1.6F_{ynom}$ for sections with very low D/t ratios. This coincides with Canadian findings. However, there was a significant scatter in the results and it was not possible to confirm the 20 D/t cut off noted in Canadian investigations. The average corner yield strength followed a linear distribution from approximately $1.6F_{ynom}$ to $1.45F_{ynom}$ as mentioned earlier. The maximum yield strength of the corner was $1.85F_{ynom}$ for a D/t ratio of approximately 17.

For flat coupons taken from the center of the walls, the average yield strength obtained from previous investigations ranged from $1.15F_{ynom}$ to $1.25F_{ynom}$. The minimum and maximum were $1.05F_{ynom}$ and $1.50F_{ynom}$. When aligning the flat yield strength to the corner yield strength, the corner yield strength increases linearly with respect to the flat yield strength. This indicates that their increase is directly proportional to the amount of cold work they sustain, which means that there is a direct correlation between the increase in yield strength of the flat and the corner. Finally, it was noted that the increase in corner yield strength is very close to the ultimate tensile stress of the flat. The maximum error between the two was of 11% for large D/t ratios and the average error was about 5%. This leads to the conclusion that the corner yield strength can be approximated from the ultimate tensile stress of the flat coupon.

By analyzing the cross-sectional yield strength of the three investigations, it was possible to confirm the linear gradient proposed by Davison and Birkemoe (1983): the minimum yield strength is located at the center of the flat wall and increases linearly towards the edges up to a value of 20% above the yield strength of the center. The weld face had significantly higher values than the other two faces. Previous research had reported the yield strength of the face opposite to the weld

is about 10% higher than the yield strength of adjacent faces. It was not possible to confirm these findings due to the limited data available.

In the second part of this chapter, mill certificate data was compiled from North American manufacturers on the $F_y$ and $F_u$ properties. A total of 18236 samples of several steel grades of square, rectangular or circular HSS members were included. Of those 18236, 12117 were of the ASTM A500 grade, 1263 were of the ASTM A1085 grade, 4856 were of the G40.21-350W grade. Of the total, 704 sections were round. The steel grades were assembled into three main groups: ASTM A500, ASTM A1085 and G40.21-350W. The mean for the yield strength was at about $1.26F_{ynom}$ for all grades with no b/t limit. The ultimate tensile stress was nearly constant for all HSS members. The mean for the ultimate tensile stress for the ASTM A500 grade was at $1.23F_{unom}$ which was about 10% above the other two grades. The results of the yield strength for the ASTM A1085 grade were similar between shaped (SHS and RHS) and round sections. For the other two grades, the round sections were about 5% below the square and rectangular sections in yield strength but had similar ultimate tensile stress. The results were further truncated by the b/t and D/t ratios. For a b/t ratio below 17.7 (corresponding to KL/r of 100), the average yield strength ratio for the ASTM A500 group ranged from $1.40F_{ynom}$ to $1.25F_{ynom}$ with a mean at $1.31F_{ynom}$. The average for the ASTM A1085 ranged from $1.35F_{ynom}$ to $1.28F_{ynom}$ and the results showed a much smaller scatter than the other two grades. The CSA G40.21 had the widest scatter and the yield strength ranged from $1.40F_{ynom}$ to $1.20F_{ynom}$.

The probable yield strength $R_yF_y$ to determine $T_u$ was found by adjusting mill certificate data determined in the second part of this chapter to account for the increase in yield strength at the corners and across the perimeters of the flat walls determined in the first part of this chapter. This was done by computing an average yield stress over the cross-section to be used as $R_yF_y$ in the calculation of probable brace resistances in seismic design. This average value was obtained using three different yield strength distribution models. The first model, which was named *weighted average*, was based on the $F_y$ gradient across the flat walls perimeter based on literature. In the second and third models, the probable yield strength was based on the CSA S136 standard equation to account for strain hardening. The CSA S136 standard equation requires the $F_u/F_y$ ratio of the coil strip used to form the final profile. This value was unavailable. Therefore, for the second model, which was named *S136A*, this ratio was substituted with the nominal values of yield and

ultimate tensile stress. For the third model, which was named *S136B*, the ratio was determined from the actual mill certificate values taken in the mid-wall. The CSA S136 standard equation does not account for an $F_y$ gradient across the flat wall. The weighted average is computed in all three models once the yield strength is determined for the corners and flat walls. It was determined that the probable resistance $R_yF_y$ increases significantly with all three models compared to the value obtained from the mid-wall tensile coupon in mill certificates.

For rectangular and square profiles, the probable yield strength $R_yF_y$ to determine $T_u$ was established be 1.50Fynom (515 MPa). This new value is superior to the current $R_yF_y$ of 460 MPa specified in the CSA S16 standard. For circular HSS profiles, the probable yield strength $R_yF_y$ should be equal to the yield strength determined from the mill certificate data. Since the circular section does not undergo a second stage of cold work therefore the mill certificate values are representative of the average yield strength. This value is proposed as $1.26F_{ynom}$.

In the third part of this chapter the probable tensile resistance $T_u$ was used to perform a reliability analysis and determine an equivalent nominal yield strength ($F_y$*) to be used in the current equation $T_r$ assuming a $\phi$ of 0.9 and the nominal area. Variables such as the geometric bias, the safety index or the professional ratio were determined from the literature. It was found the tensile yield strength can be taken at: 441 MPa from the coupon data, 506 MPa from the S136A method, 517 MPa from the *S136B* method and 507 MPa for the weighted average method. It can be concluded coupon data represent a lower bound for the actual yield strength in the section, while the *S136B* method represents an upper bound. The final proposed equivalent nominal yield strength $F_{y*}$ is 500 MPa.

Finally, in the fourth part of this chapter, the residual stress model for cold-formed HSS members based on the review presented in Chapter 2 was determined. The models developed by Davison and Birkemoe (1983), and Key and Hancock (1993) were compared to more recent investigations where the residual stress was determined by more advanced methods such as the X-Ray diffraction technique. It is determined that the original through thickness residual stress model developed by Davison and Birkemoe (1983) is an accurate representation of the actual behaviour and recent findings support the proposed profile. The final model for the through thickness residual stresses is a trapezoid split into three equal parts. The membrane residual stresses follow a linear distribution from the edge to the center. The edge and center are at equal magnitudes, but the edge is in compression while the center is in tension. The magnitude for the membrane residual stresses

are +/- $0.17\sigma_{ystub}$. The magnitude for the through thickness residual stresses is +/- $0.60\sigma_{ystub}$. The exterior fiber is in tension while the interior fiber is in compression.

To summarize, the cross-sectional yield strength distribution gradient was determined from previous investigations. The corner yield strength was based on 47 different sections. The flat yield strength gradient was based on 7 Canadian sections from the 1970s. The average yield strength of the center flat coupon of currently manufactured HSS sections was determined from a set of 18236 mill certificates provided by North American manufacturers. The average probable yield strength $R_yF_y$ of the section was determined based on two versions of the CSA S136 standard equation and the cross-sectional yield strength distribution proposed earlier. A reliability analysis was performed on these results to an equivalent nominal yield strength ($F_y$*) to be used in the current equation $T_r$ assuming $\phi$ 0.9 and the nominal area. Finally, a residual stress model was determined based on the findings from the second chapter.

# CHAPTER 4 PROBABLE COMPRESSIVE RESISTANCE

In the capacity based seismic design of steel buildings, the seismic forces experienced by the beams and columns are directly related to the forces that will develop in the HSS bracing members within the seismic force resisting system. These forces are defined as the probable tensile resistance $T_u$ and the probable compressive resistance $C_u$.

The probable yield strength $R_yF_y$ to determine the probable tensile resistance $T_u$ was determined in Chapter 3. In Chapter 2, it was established that the probable yield strength of cold-formed HSS members is dependant on the cross-sectional yield strength gradient of the member. In this chapter, the probable yield strength $R_yF_y$ (average cross-sectional yield strength) is determined from a refined model of the cross-sectional yield strength gradient. The probable compressive resistance $C_u$ is then computed based on the probable yield strength based on the refined model and the residual stress distribution determined in Chapter 3.

A parametric study is first performed to determine the effects of the residual stresses and increased yield strength gradient on the compressive resistance of the HSS member. The effects of these two parameters on the probable compressive resistance of the bracing member are examined using a fiber based OpenSees finite element analysis model. The OpenSees software is an open source engineering program designed to perform large scale parametric analysis and stands for "*Open System For Earthquake Engineering Simulation*". The rights are held by University of California. The 64-Bit version 2.5.0 (rev 6536) was used in this investigation. This parametric study was performed prior to completing the review of the coupon tests in Chapter 3. The increase in yield strength and the residual stresses for the parametric study is therefore based on nominal yield strength values. It is assumed that the effects of the increased yield strength and the residual stresses would be the same whether the increase is based on actual or nominal values of the yield strength of the cross-section. The OpenSees analysis are conducted on typical bracing members having different overall slenderness ratios. The results from the OpenSees analysis are compared to the current column strength curves (CSA S16).

Thereafter, the OpenSees analysis is redone using the refined model of the yield strength and residual stress gradient based on the A1085 steel grade and actual coupon values of Chapter 3. Before the analysis, however, the model is further refined. The refined model is named "*refined weighted average*" and is based on the "*weighted average*" model in Chapter 3. A linear

relationship is determined between the yield strength at the center of the flat walls and the yield strength of the corners for the *refined weighted average* model. In Chapter 3, the yield strength of the corners is based on approximate upper and lower bounds from actual corner data. The residual stresses in the refined model are still based on the same model as determined in Chapter 3, but the magnitudes are based on the average cross-sectional yield strength versus the nominal yield strength taken in the first part of this chapter.

The probable yield strength $R_yF_y$ used to compute the probable compressive resistance $C_u$ is determined from this refined model. The probable compressive resistance $C_u$ is computed for 83 different A1085 HSS sections with slenderness varying from 10 to 250. This second set of analysis is performed for two values of out-of-straightness: L/480, as specified in the ASTM A1085; L/6000 which represents the mean value from reported data (Davison & Birkemoe, 1983; Bjorhovde, 1977; Salvarinas, 1974; Key and Hancock, 1985 and Key et al., 1988). The analysis results are compared to the column strength curves in current provisions (CSA S16-2014).

## 4.1 Parametric study of compressive resistance based on the nominal yield strength

The results of a parametric study performed on several HSS bracing members using a fiber based OpenSees finite element model are presented in this section. This study was performed to determine the effects of the residual stresses and the increased yield strength gradient on the compressive resistance of several HSS bracing members. Obtained compressive resistances were also compared with current column strength curves (CSA S16-14).

Figure 4-1 shows an HSS bracing member which is subjected to a uniform concentric compressive force. The bracing member was discretized into 6 elements. The OpenSees element used for the bracing member was a "*displacement beam column*". It is important to note that moments were not present in the HSS member even if the element used in the software is a beam column.

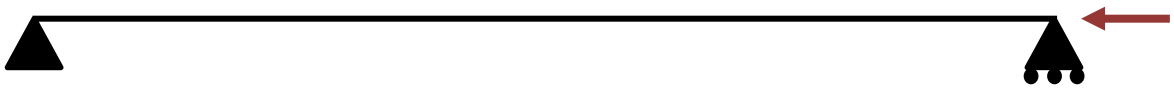

Figure 4-1: HSS bracing member for parametric study subjected to a concentric axial force

The yield strength gradient and residual stress distributions are shown through Figure 4-2 to Figure 4-5. The distributions adopted in this model are based on Davison and Birkemoe's (1983) average values. Davison and Birkemoe proposed an increase in yield strength of approximately 20% for the edges of the flat walls compared to the center of the flat walls. The yield strength of the corners was set to a uniform value of $1.6F_{ynom}$. A more refined distribution had been proposed in Chapter 3 with respect to the D/t ratio. However, the sections tested with this numerical model are all limited by the slenderness limit b/t of 17.3 (D/t ≈ 30) for HSS bracing members subjected to seismic forces (CSA S16-14). According to Chapter 3, a corner yield strength increase of $1.6F_{ynom}$ was proposed for HSS members with a D/t ratio below 30. The through thickness residual stress proposed by Davison and Birkemoe was 60% of the stub column strength and the magnitude of the membrane residual stress was proposed at 17% of the stub column strength. At the time when this investigation was performed, the stub column strength of the modeled sections was not available. Therefore, the same percentages were taken as proposed by Davison and Birkemoe, but they were based on the nominal yield strength of the ASTM A1085 steel grade ($F_{ynom}$ = 345 MPa) instead of the stub column strength. Since both the residual stress and the yield strength are based on the nominal yield

strength, they are kept proportional and using the nominal yield strength should not affect the behaviour of the parameters. The flat portion of the cross section was discretized into 81 fibers (9x9) and the corners were discretized into 45 fibers (9x5). In total, the cross section of the HSS bracing member was composed of 504 fibers. The OpenSees "*uniaxial material steel02*" material was applied to the model. This material uses a uniaxial Giuffre-Menegotto-Pinto steel material nonlinear curve with isotropic strain hardening. A sinusoidal function was applied for the out-of-straightness of the bracing member with a maximum value of L/480. This corresponds to the maximum permitted out-of-straightness in the ASTM A1085 standard.

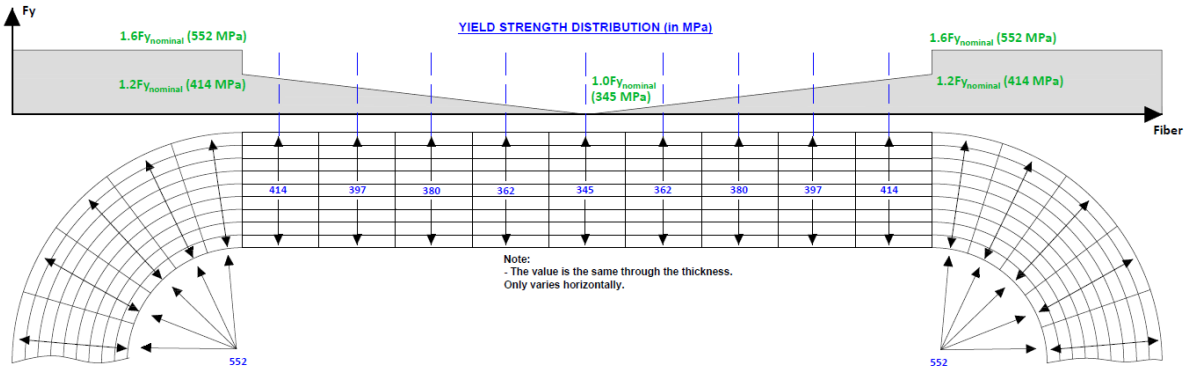


Figure 4-2: Yield strength gradient

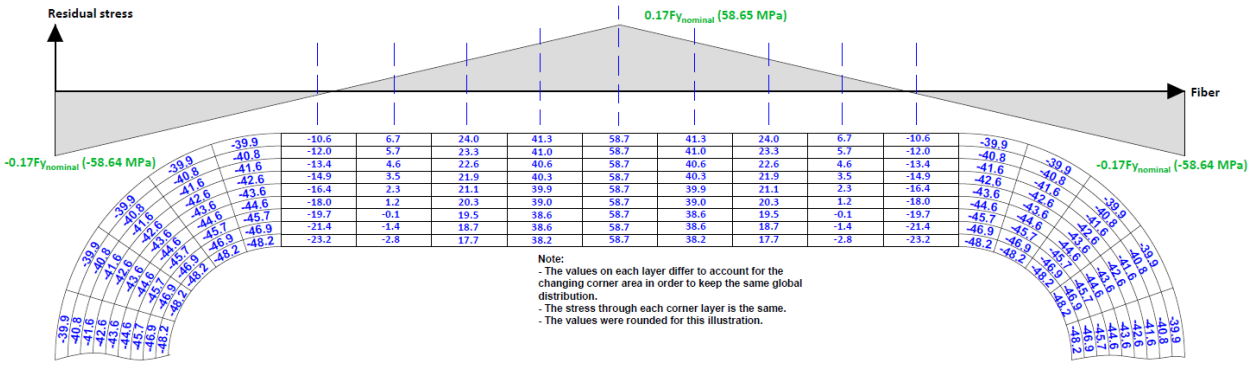


Figure 4-3: Membrane residual stress distribution (perimeter)

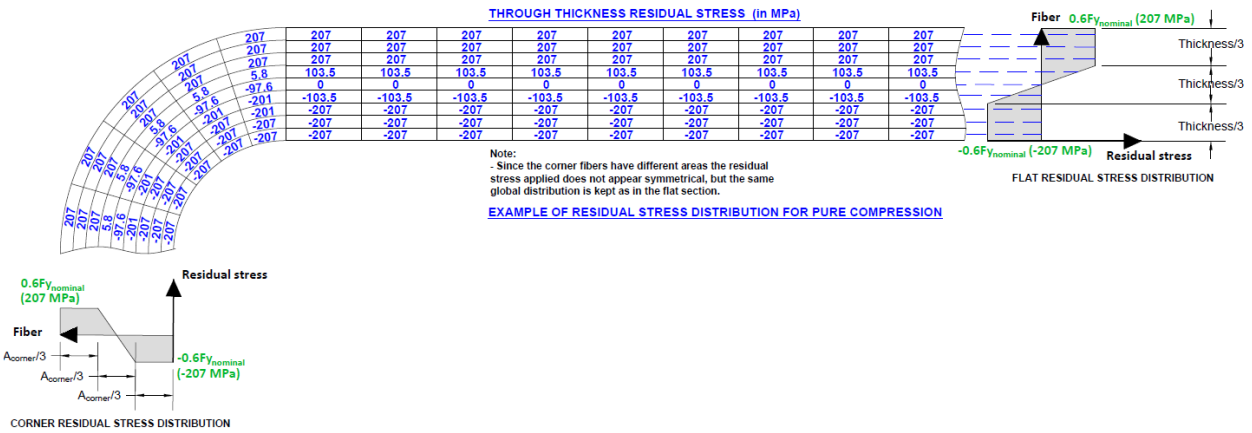


Figure 4-4: Through thickness residual stress distribution (bending)

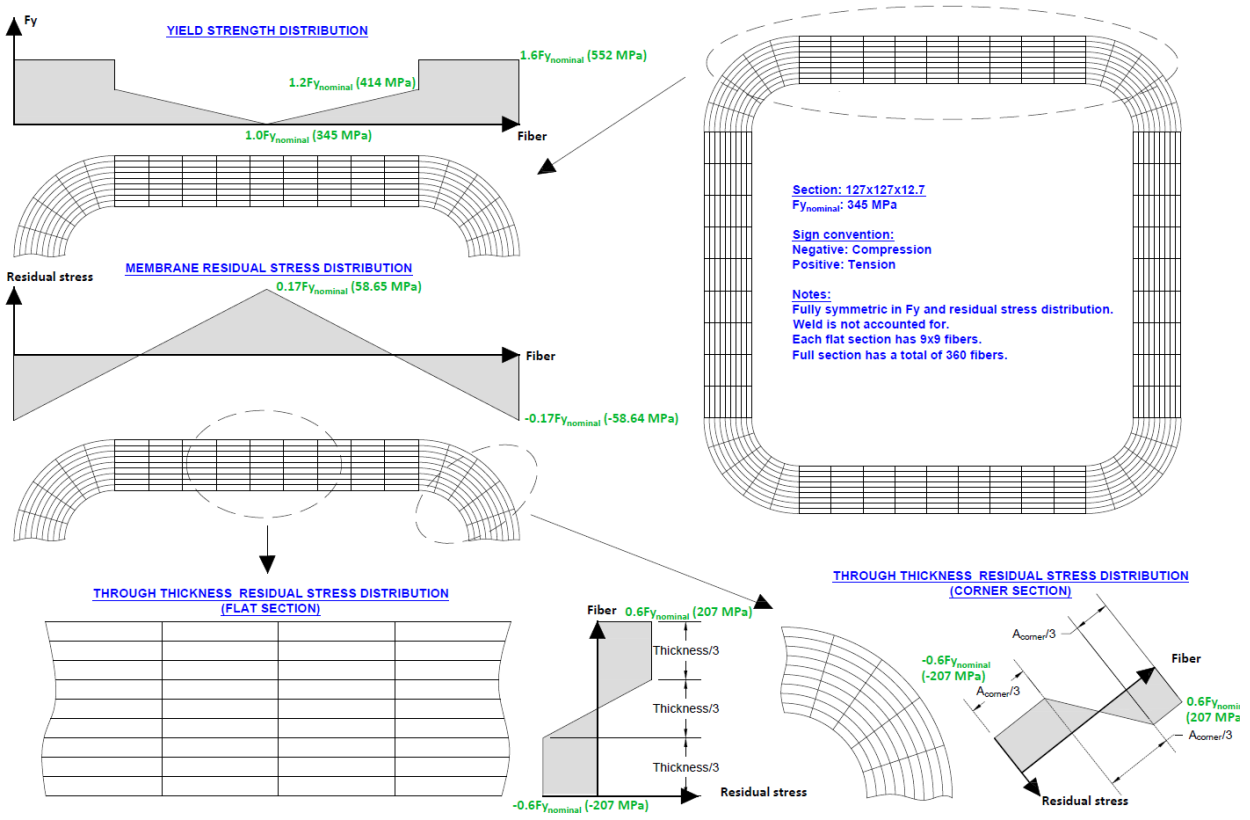


Figure 4-5: Overall view of yield strength and residual stress models

Based on this model, it is seen from Figure 4-2 to Figure 4-5, the maximum yield strength value for the corners is of 552 MPa. The maximum membrane residual stress is of 58 MPa. The maximum through thickness residual stress is of 207 MPa. Residual stress values were applied as initial strain on the model at time 0. An example is shown in Figure 4-6 where the initial through thickness

residual stress is of 208 MPa is applied to the bottom fiber of the corner. It is important to note there is no strain hardening shown in Figure 4-6. This figure was only used for verification purposes and the actual bracing member does have strain hardening in each fiber. The definition of the strain hardening parameters in OpenSees as well as the applied parameters are shown in Figure 4-7 and Figure 4-8. Table 4-1 presents the applied parameters in the model.

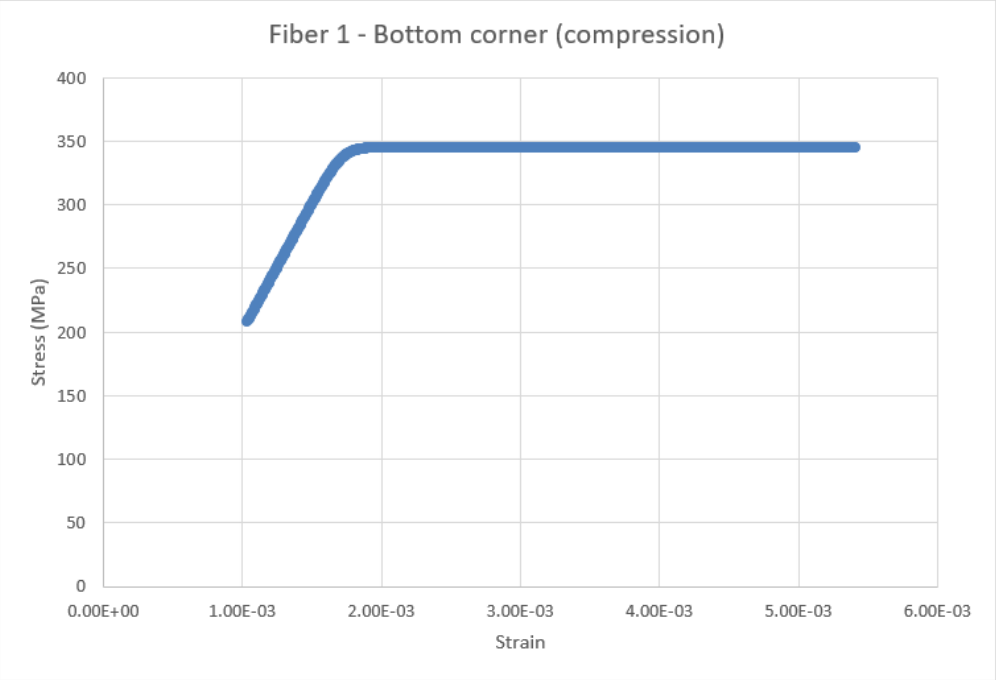


Figure 4-6: Example of residual stress application in OpenSees model (through thickness)

Steel02 Material -- Giuffré-Menegotto-Pinto Model with Isotropic Strain Hardening

Command_Manual

This command is used to construct a uniaxial Giuffre-Menegotto-Pinto steel material object with isotropic strain hardening.

**uniaxialMaterial Steel02 $matTag $Fy $E $b $R0 $cR1 $cR2 <$a1 $a2 $a3 $a4 $sigInit>**

| | |
|---|---|
| **$matTag** | integer tag identifying material |
| **$Fy** | yield strength |
| **$E0** | initial elastic tangent |
| **$b** | strain-hardening ratio (ratio between post-yield tangent and initial elastic tangent) |
| **$R0 $CR1 $CR2** | parameters to control the transition from elastic to plastic branches. Recommended values: **$R0**=between 10 and 20, **$cR1**=0.925, **$cR2**=0.15 |
| **$a1** | isotropic hardening parameter, increase of compression yield envelope as proportion of yield strength after a plastic strain of $a2*($Fy/E0). (optional) |
| **$a2** | isotropic hardening parameter (see explanation under $a1). (optional default = 1.0). |
| **$a3** | isotropic hardening parameter, increase of tension yield envelope as proportion of yield strength after a plastic strain of $a4*($Fy/E0). (optional default = 0.0) |
| **$a4** | isotropic hardening parameter (see explanation under $a3). (optional default = 1.0) |
| **$sigInit** | Initial Stress Value (optional, default: 0.0) the strain is calculated from epsP=$sigInit/$E<br>if (sigInit!= 0.0) { double epsInit = sigInit/E; eps = trialStrain+epsInit; } else eps = trialStrain; |

more on OpenSees uniaxialMaterial Arguments -- Steel02

REFERENCE:

Filippou, F. C., Popov, E. P., Bertero, V. V. (1983). "Effects of Bond Deterioration on Hysteretic Behavior of Reinforced Concrete Joints". Report EERC 83-19, Earthquake Engineering Research Center, University of California, Berkeley.

Figure 4-7: Strain hardening definition in OpenSees uniaxial material steel02 (Mazzoni et al., 2018)

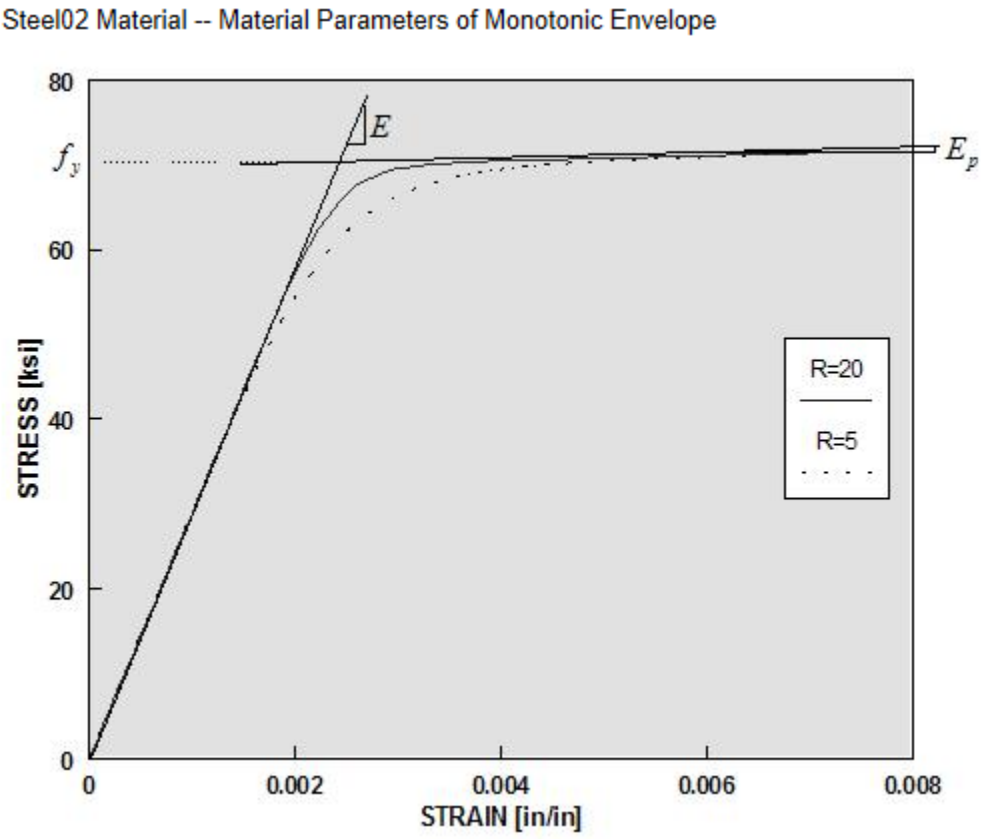


Figure 4-8: Stress strain graph for OpenSees uniaxial material steel02 (Mazzoni et al., 2018)

Table 4-1: Applied strain hardening parameters

| | |
|---|---|
| *b* = | 5.75 |
| *R0* = | 30 |
| *cR1* = | 0.925 |
| *cR2* = | 0.15 |
| *a1* = | 0.4 |
| *a2* = | 22 |
| *a3* = | 0.4 |
| *a4* = | 22 |

Figure 4-9 to Figure 4-15 present the results from the parametric study. The compressive resistance obtained from the defined model, denoted $C_n$ in this study, is normalized with respect to the nominal yield strength (345 MPa). The variable $C_n$ was chosen to represent the compressive resistance obtained in this study since the residual stress and increased yield strength gradient were based on the nominal yield strength as previously explained. The first three analysis were done on

separate sections. These members were selected to represent commonly used HSS bracing members in the seismic design of medium sized buildings in Canada. Different b/t ratios were selected to evaluate its effects on the compressive resistance. It is seen from these figures, the section with the smallest b/t ratio has the highest increase in compressive resistance and the section with the lowest b/t ratio has the smallest increase in compressive resistance compared to the standard case. The standard case borders the n = 1.34 column strength curve which is used to verify the numerical model. The increased yield strength gradient significantly increases the compressive resistance of the HSS bracing member. The residual stress significantly decreases the compressive resistance which counteracts the increase from the yield strength gradient to a certain point. The increase in yield strength can be seen up to a slenderness ratio of approximately 1.00. At very low slenderness values, the increase in yield strength can be up to $1.25F_{ynom}$. The membrane residual stress does not seem to significantly affect results.

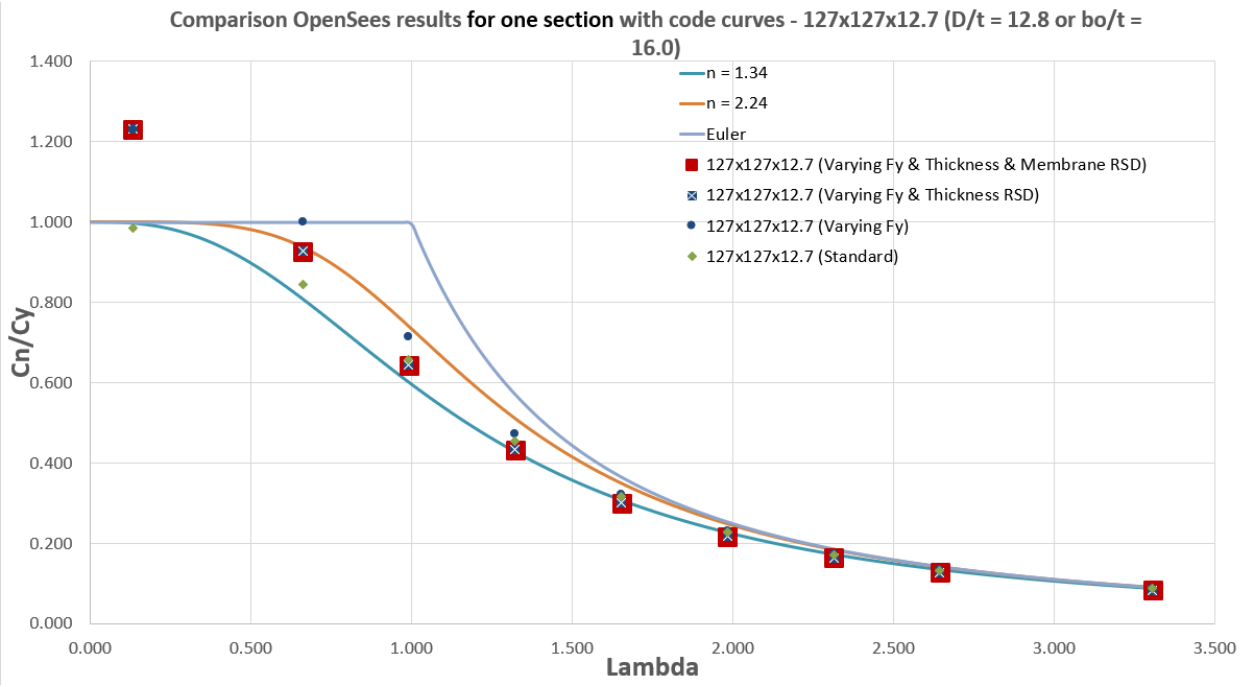


Figure 4-9: HSS bracing member OpenSees results for 127 x 127 x 12.7 section

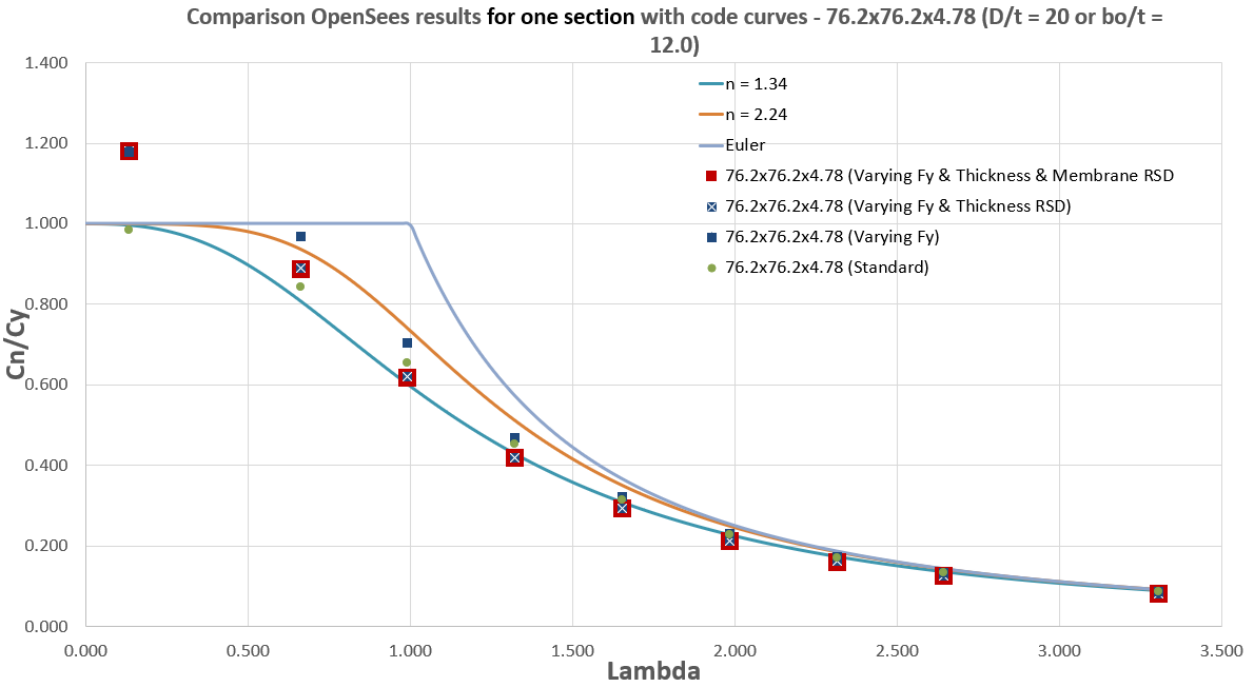


Figure 4-10: HSS bracing member OpenSees results for 76.2 x 76.2 x 4.78 section

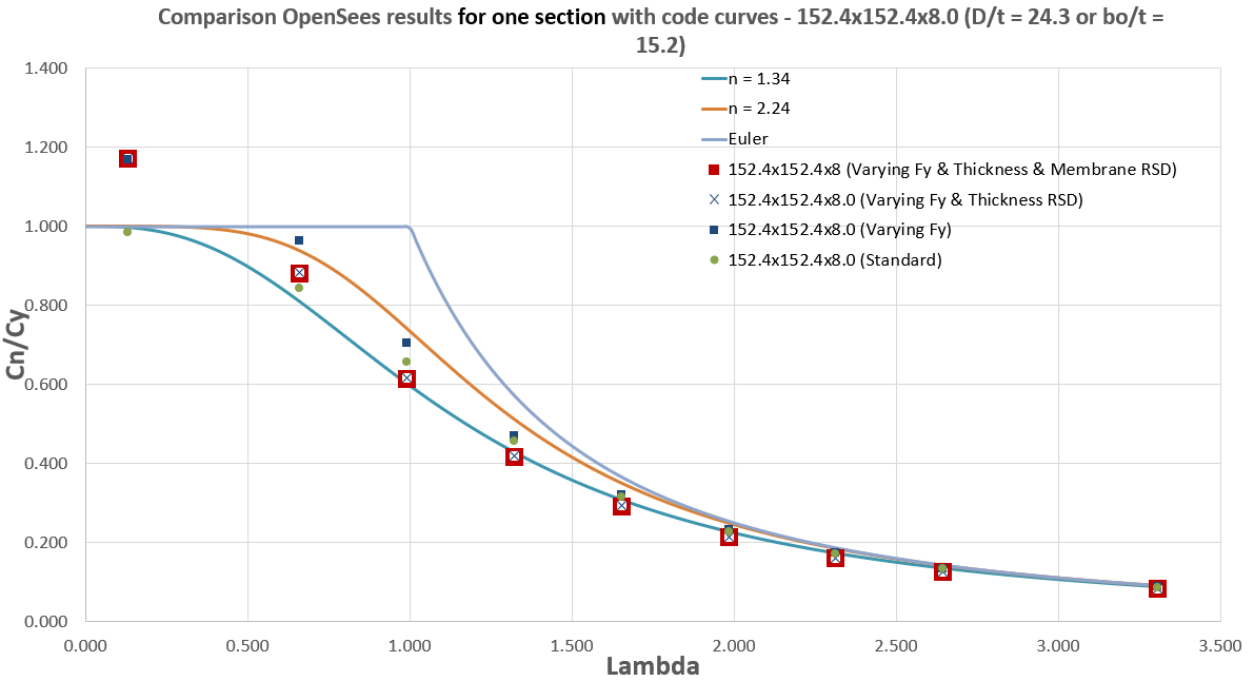


Figure 4-11: HSS bracing member OpenSees results for 152.4 x 152.4 x 8.0 section

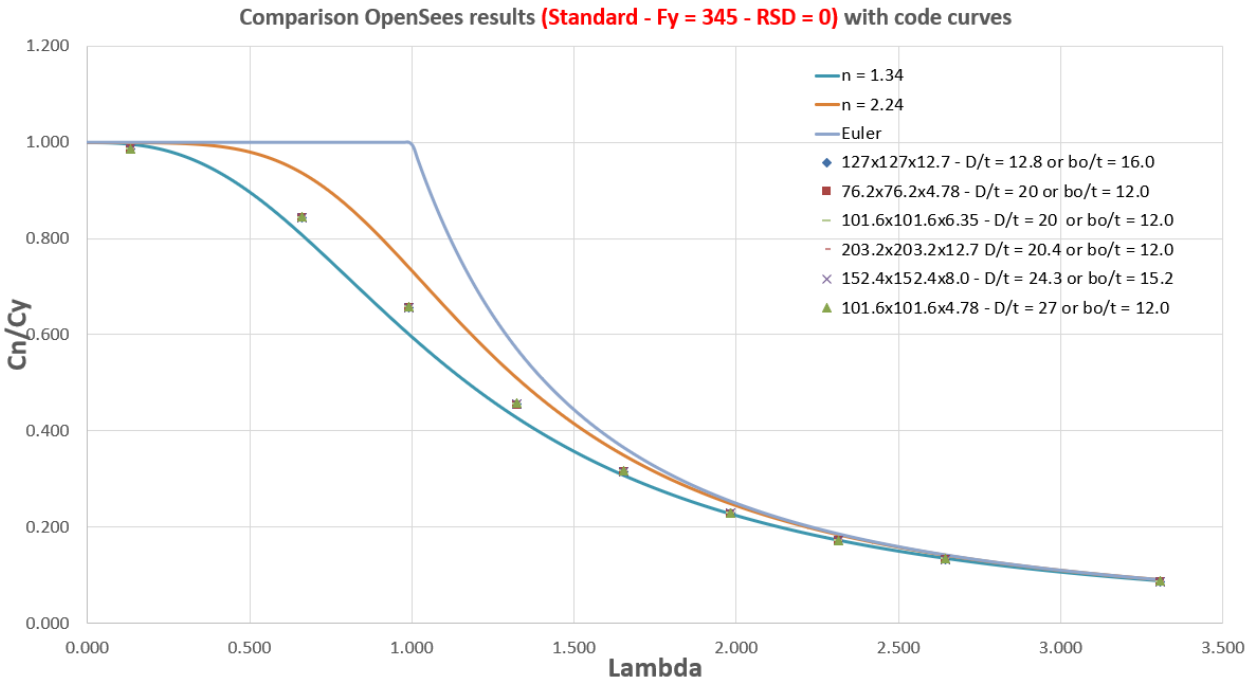


Figure 4-12: HSS bracing member OpenSees results for all sections with standard (345 MPa) uniform yield strength and no residual stresses

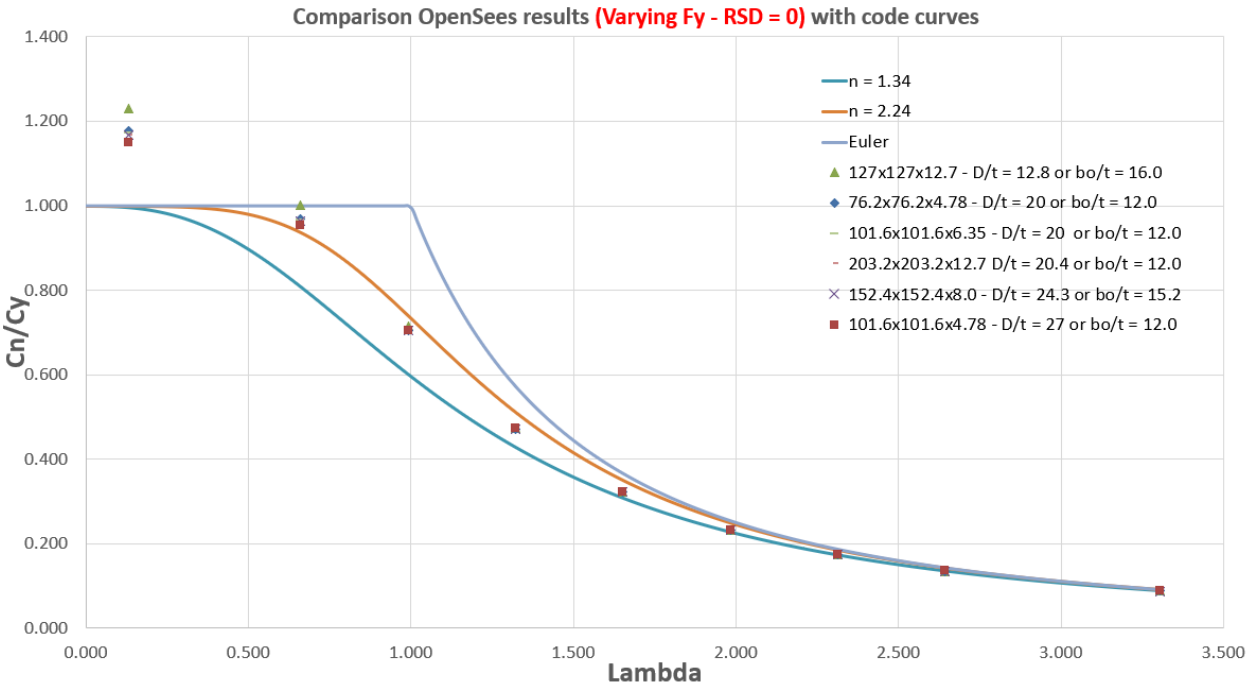


Figure 4-13: HSS bracing member OpenSees results for all sections with a yield strength gradient but no residual stresses

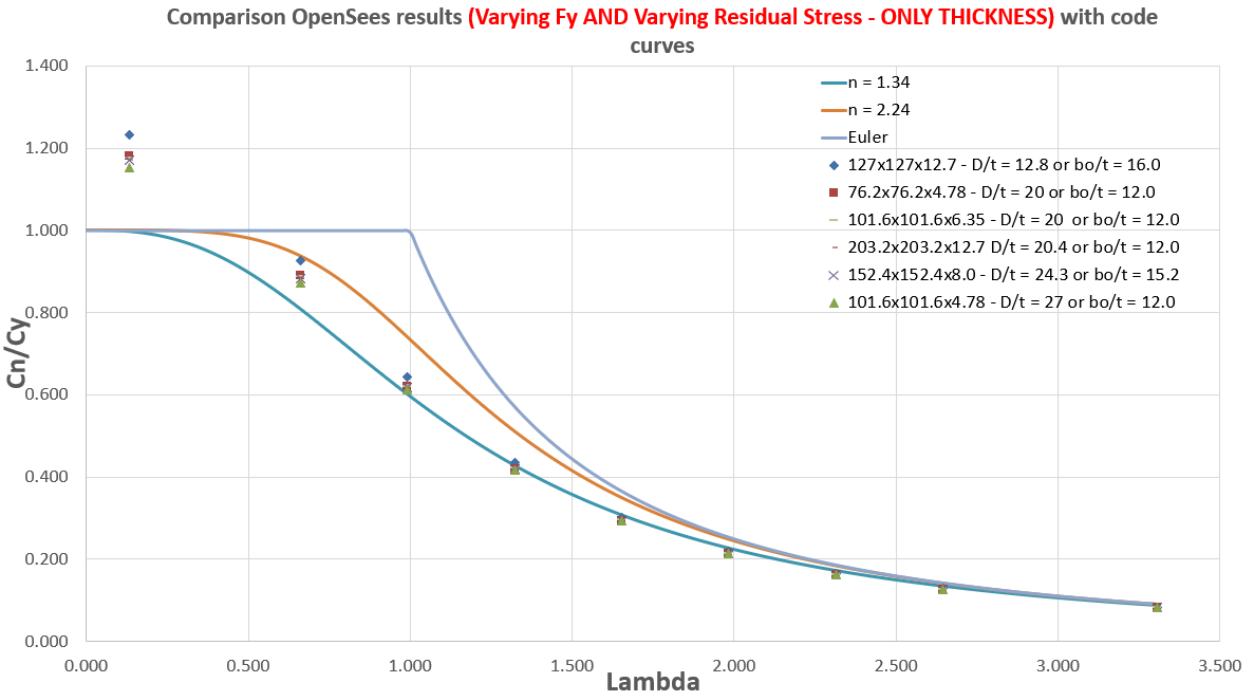


Figure 4-14: HSS bracing member OpenSees results for sections with a yield strength gradient and through thickness residual stress only

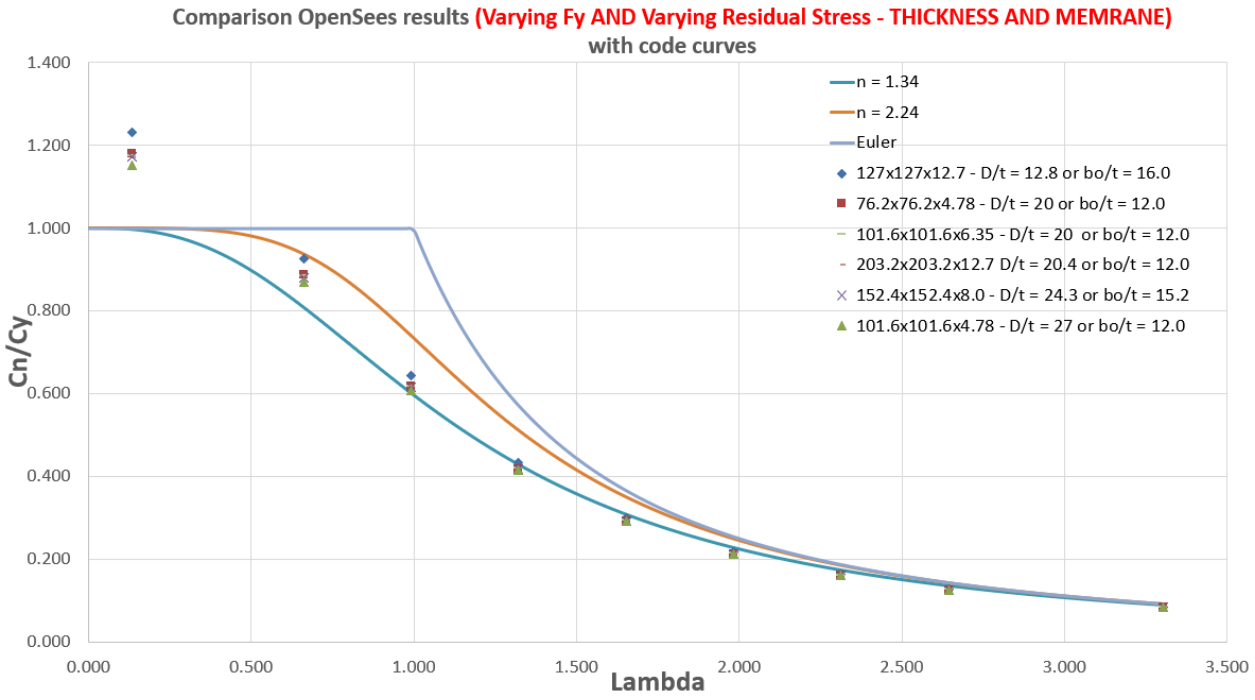


Figure 4-15: HSS bracing member OpenSees results for all sections with both the yield strength gradient and all residual stress components

It is seen in Figure 4-12 representing the standard case (uniform yield strength of 345 MPa and no residual stresses) that all sections overlap on each other and are very close to the $n$ = 1.34 curve, which is expected. When only the increased strength gradient is accounted for, in Figure 4-13, it is seen the $n$ = 2.24 curve is a better representation of the compressive resistance of the member. If all residual stress components are included, in Figure 4-15, it appears the $n$ = 1.34 curve is a better representation for slenderness values approximately above 0.75. The $n$ = 2.24 curve seems to be a better fit for slenderness values below 0.75. When it comes to very low slenderness values, the increase in yield strength ranges from approximately $1.15F_{ynom}$ to $1.25F_{ynom}$, depending on the b/t ratio.

## 4.2 Parametric study of compressive resistance based on the actual yield strength

The compressive resistance of several HSS bracing members based on the nominal yield strength was determined in the previous section of this chapter. This was due to the lack of data at the time of the analysis. In this section, the compressive resistance is determined based on the actual strength of the cross-section.

It is assumed the stub column strength determined by Davison and Birkemoe (1983), on which the increase in yield strength and residual stress distribution was based, can be replaced by an accurate model of the average cross-sectional yield strength based on mill certificate data and previous literature. Such value has already been determined in Chapter 3 based on the three different models that were used to establish the probable yield strength $R_yF_y$ used to compute $T_u$. These models were based on three different hypotheses. It was seen from these three models, the probable yield strength $R_yF_y$ ranged from $1.41F_{ynom}$ (487 MPa) to $1.43F_{ynom}$ (493 MPa) depending on the model if there is no b/t limit. The yield strength in the corners was determined in Chapter 3 according to Figure 4-16 for the "*weighted average*" model. This is the same figure as Figure 3-2 in Chapter 3 and is included again for simplicity.

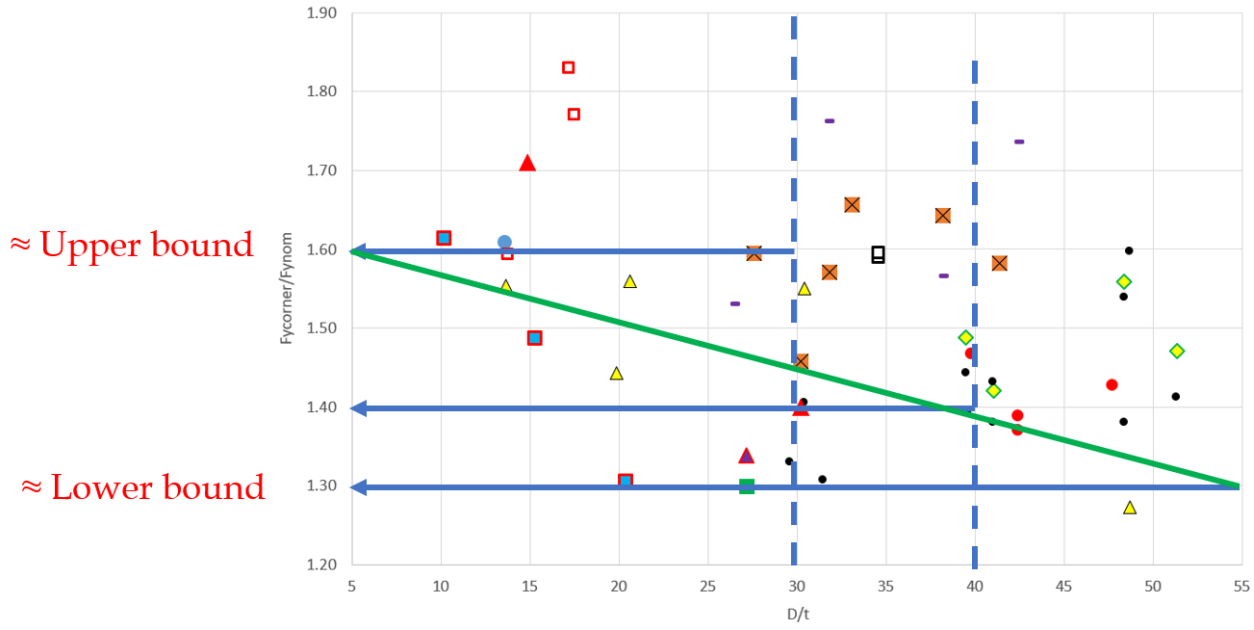


Figure 4-16: Increase in yield strength in the corners normalized with respect to the nominal yield strength with respect to the D/t ratio

Another hypothesis to determine the corner yield strength presented in Chapter 3 was based on the assumption that the corner yield strength can be approximated by the ultimate tensile stress in the center of the flat walls ($F_{ycorner} = F_{uflat}$). This ended up being the assumption for the *S136B* model since the CSA S136 equation always overestimated the corner yield strength when based on the ultimate to yield stress ratio from the mill certificates. The CSA S136 limit stating that the average yield strength of the cross-section cannot be higher than the ultimate tensile stress of the flat coupon was applied.

The new hypothesis applied to this chapter is based on the relationship between the average yield strength of the four flat coupons located at the center of the walls and the increase in the corner yield strength. This was already established in Figure 3-6 in Chapter 3 (included here as Figure 4-17 for simplicity).

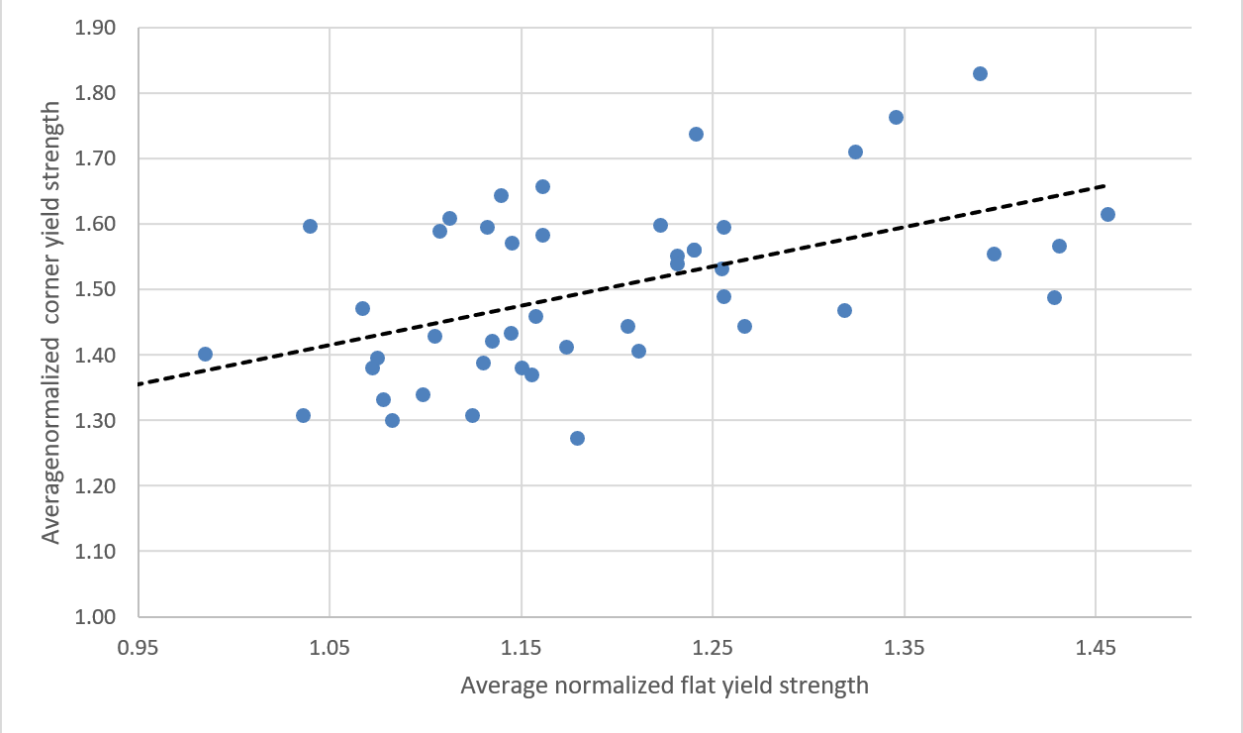


Figure 4-17: Average normalized yield strength of corners versus flats

Based on Figure 4-17 equation (4-1) is established from the trendline.

$$F_{ycorner} = 0.629F_{yflat} + 0.74 \quad (4\text{-}1)$$

The $F_{yflat}$ value represents the average yield strength of the center of the flat walls. This value is determined from Figure 4-18 and changes with respect to the D/t ratio. The trendline can be expressed by equation (4-2).

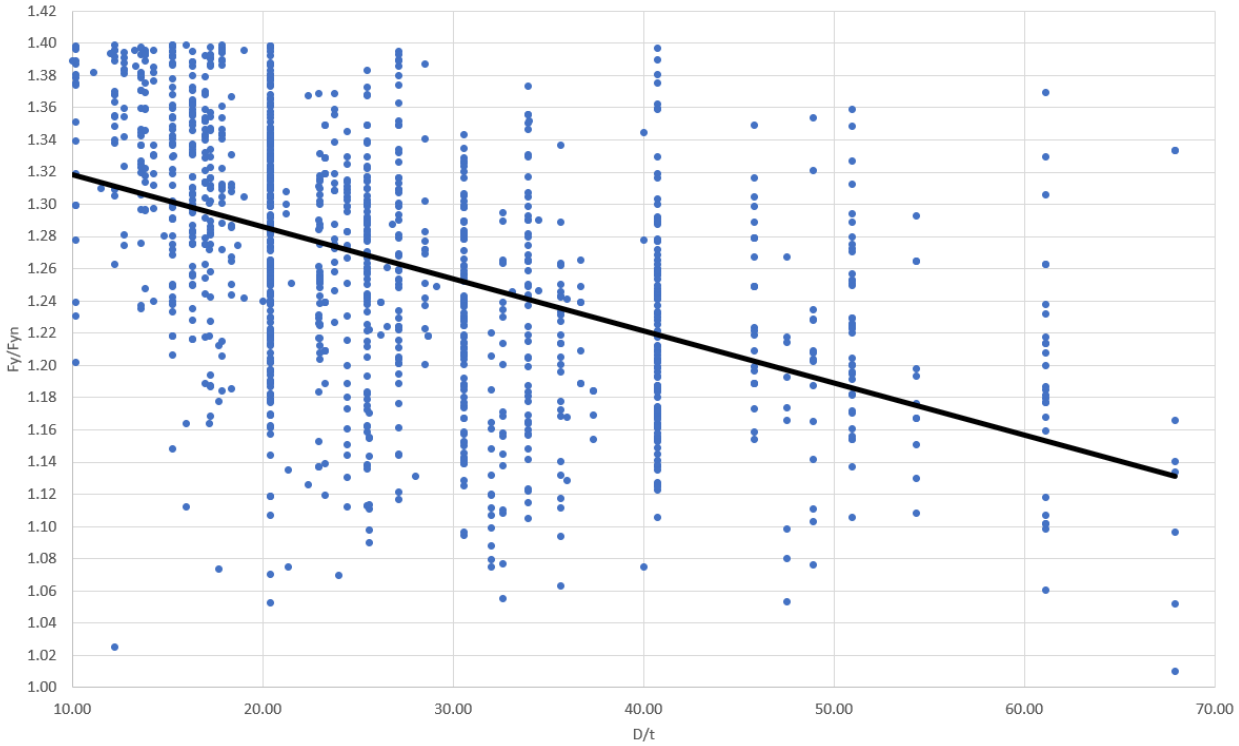


Figure 4-18: Yield strength at the center of the flat wall from mill certificates (A1085)

$$F_{yflat} = -0.00345D/t + 1.358 \quad (4\text{-}2)$$

The yield strength at the edge of the flat walls is 20% above the increase of the center of the flat walls. Two main differences can be seen from this distribution compared to the "*weighted average*" model used in Chapter 3. The corner yield strength is determined from a linear relationship based on the yield strength at the center of the flat walls. The yield strength at the center of the flat wall was available for each individual section in Chapter 3 (scatter in Figure 4-18), while an average trendline was used in this chapter. There is no difference between Chapter 3 and this chapter with respect to the increase in yield strength from the center of the walls up to the edges.

After applying equation (4-1) and (4-2), the normalized corner yield strength is obtained in Figure 4-19 where it is compared to the obtained yield strength values in the corners. These values are the same as presented in Figure 4-16, except, it is not presented for each individual investigation. When

comparing the obtained corner yield strength results (orange line) to the trendline (dashed black line), it can be concluded they are in good agreement with each other. The numerical values for the corner yield strength, the yield strength at the center of the flat walls and the edge of the flat walls is shown in Table 4-2. It is understood it is impossible to have an HSS member with a D/t ratio of 0, this value is included in the table to illustrate the linear equation. The yield strength is normalized with respect to the nominal yield strength.

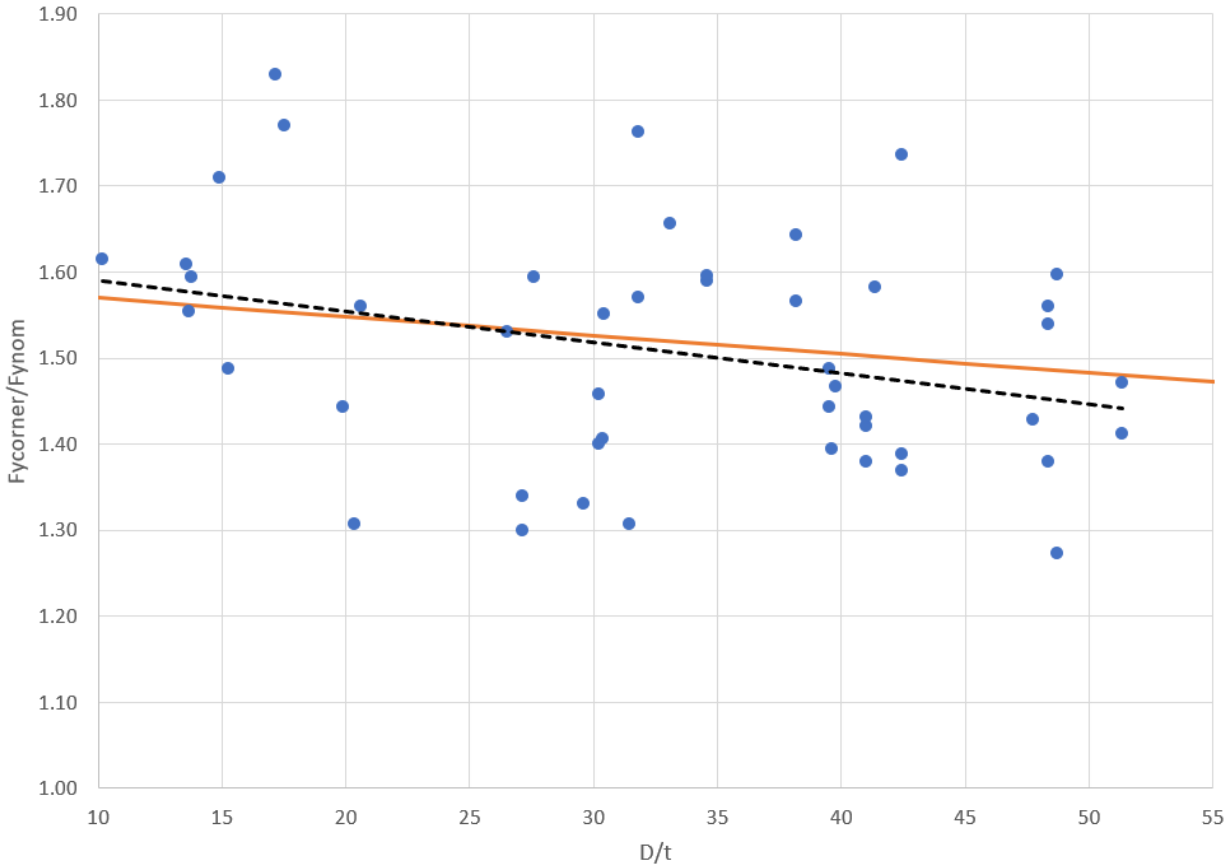


Figure 4-19: Normalized corner yield strength based on Chapter 4 model

Table 4-2: Normalized and numerical results for the yield strength distribution model presented in Chapter 4

| | Normalized yield strength | | | Yield strength (MPa) | | |
|---|---|---|---|---|---|---|
| D/t | flat | edge | corner | flat | edge | corner |
| 0 | 1.35 | 1.55 | 1.59 | 467 | 536 | 549 |
| 5 | 1.34 | 1.54 | 1.58 | 461 | 530 | 545 |
| 10 | 1.32 | 1.52 | 1.57 | 455 | 524 | 542 |
| 15 | 1.30 | 1.50 | 1.56 | 449 | 518 | 538 |
| 20 | 1.29 | 1.49 | 1.55 | 444 | 513 | 534 |
| 25 | 1.27 | 1.47 | 1.54 | 438 | 507 | 530 |
| 30 | 1.25 | 1.45 | 1.53 | 432 | 501 | 527 |
| 35 | 1.23 | 1.43 | 1.52 | 426 | 495 | 523 |
| 40 | 1.22 | 1.42 | 1.50 | 420 | 489 | 519 |
| 45 | 1.20 | 1.40 | 1.49 | 414 | 483 | 515 |
| 50 | 1.18 | 1.38 | 1.48 | 408 | 477 | 512 |
| 55 | 1.16 | 1.36 | 1.47 | 402 | 471 | 508 |
| 60 | 1.15 | 1.35 | 1.46 | 396 | 465 | 504 |
| 65 | 1.13 | 1.33 | 1.45 | 390 | 459 | 500 |
| 70 | 1.11 | 1.31 | 1.44 | 384 | 453 | 497 |
| 75 | 1.10 | 1.30 | 1.43 | 378 | 447 | 493 |
| 80 | 1.08 | 1.28 | 1.42 | 372 | 441 | 489 |

It is seen from Table 4-2 the yield strength at the corners ranges from $1.42F_{ynom}$ (489 MPa) to $1.57F_{ynom}$ (542 MPa). It is seen from Figure 4-20, the average ultimate tensile stress for the A1085 steel grade ranges from $1.12F_{unom}$ (504 MPa) to $1.16F_{unom}$ (522 MPa). It can be considered these results are in a somewhat good agreement with each other.

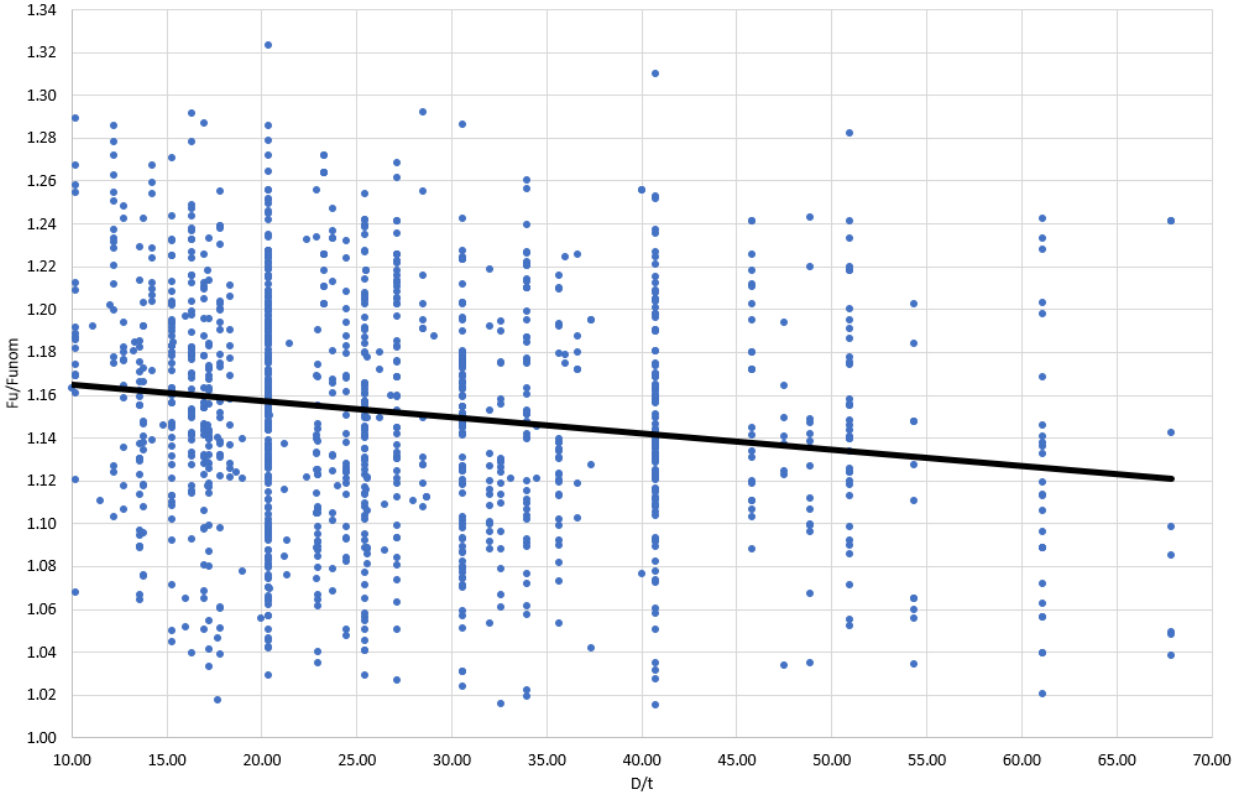


Figure 4-20: Ultimate tensile stress from mill certificates (A1085)

The applied residual stress values are the same as the ones applied in section 4.1. Except that instead of applying them to the nominal yield strength, they are applied to the average cross-sectional yield strength determined from the yield strength gradient model proposed in Table 4-2. This new model is named "*refined weighted average*". The probable yield strength $R_yF_y$ to determine the compressive resistance $C_u$ is established from this model. The probable yield strength was computed for 83 different A1085 steel grade sections. The results are shown in Table 4-3 where the new model is compared with the previous three models presented in Chapter 3. It is concluded the results are in good agreement with each other.

Table 4-3: Comparison between *refined weighted average* model presented in Chapter 4 and previous models presented in Chapter 3 to determine the average cross-sectional yield strength

| No b/t limit | | | |
|---|---|---|---|
| Square and rectangular hollow sections | | | |
| S136A | S136B | Weighted average | Refined weighted average |
| 1.41Fynom | 1.43Fynom | 1.42Fynom | 1.39Fynom |

The final yield strength and residual stress distribution applied to the OpenSees model to determine the compressive resistance $C_u$ is shown in Figure 4-21 through Figure 4-23. The final residual stress in the profile is the arithmetic sum of the membrane and through thickness components as it has been seen in the literature review and previous chapters.

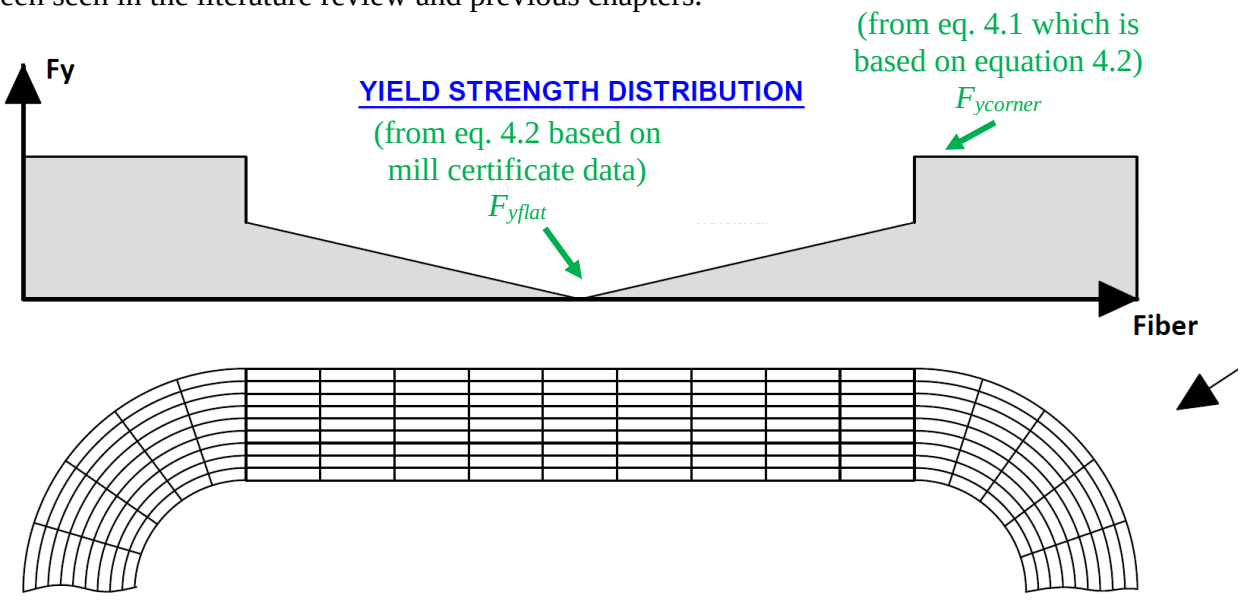


Figure 4-21: Yield strength gradient based on actual mill certificate data

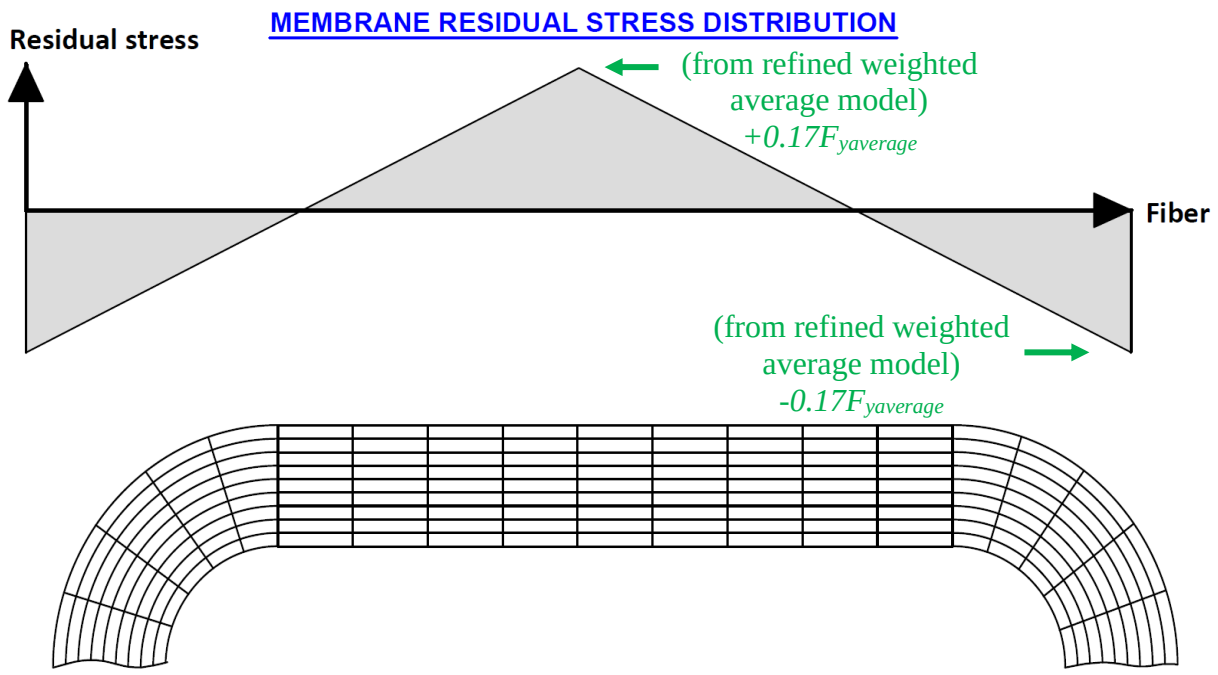


Figure 4-22: Membrane residual stress model based on average cross-sectional yield strength ($R_yF_y$)

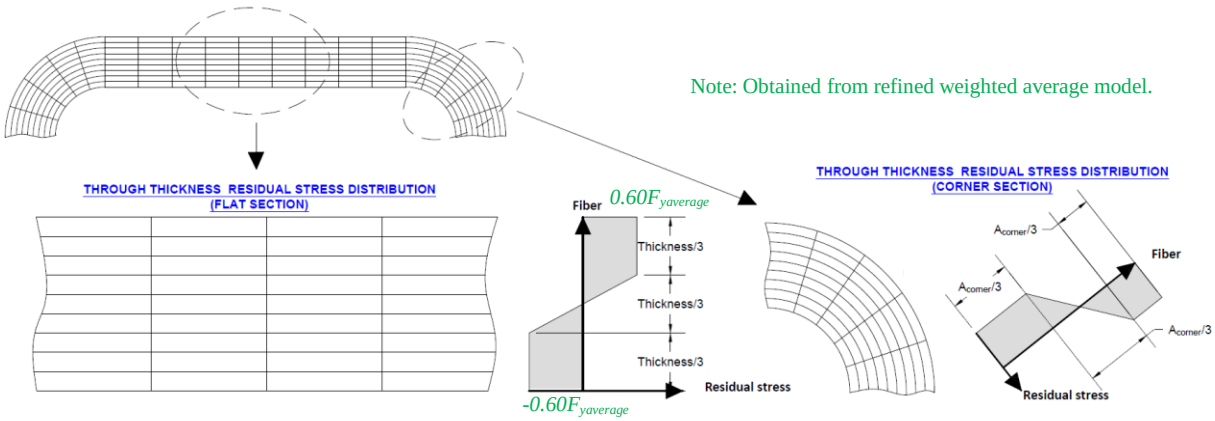


Figure 4-23: Through thickness residual stress model based on average cross-sectional yield strength ($R_yF_y$)

A numerical analysis on the fiber based OpenSees finite element model was performed on the 83 ASTM A1085 sections for which the probable yield strength $R_yF_y$ was determined according to the *refined weighted average* model seen in Table 4-3. The detailed profiles are presented in Appendix C. These sections covered a wide range of D/t ratios. As opposed to section 4.1, the tested members were not limited by the b/t slenderness ratio of 17.3 (CSA S16-14). This limit was omitted in this section to obtain a more generalized behaviour where various D/t ranges can be tested. The

obtained compressive resistance $C_u$ is still to only be used for seismic applications for members which respect proper slenderness limits. Results were obtained for KL/r values ranging from 10 to 250. Two different out-of-straightness's were studied: L/480 which was based on the maximum out-of-straightness specified in the ASTM A1085 standard and L/6000 which was based on an average determined in previous investigations. Results of the probable compressive resistance $C_u$ are presented in Figure 4-24 and Figure 4-26 with respect to KL/r and normalized with respect to the nominal yield strength. Results in Figure 4-25 and Figure 4-27 were normalized with respect to the average yield strength of the cross-section for both $\lambda$ and the compressive resistance.

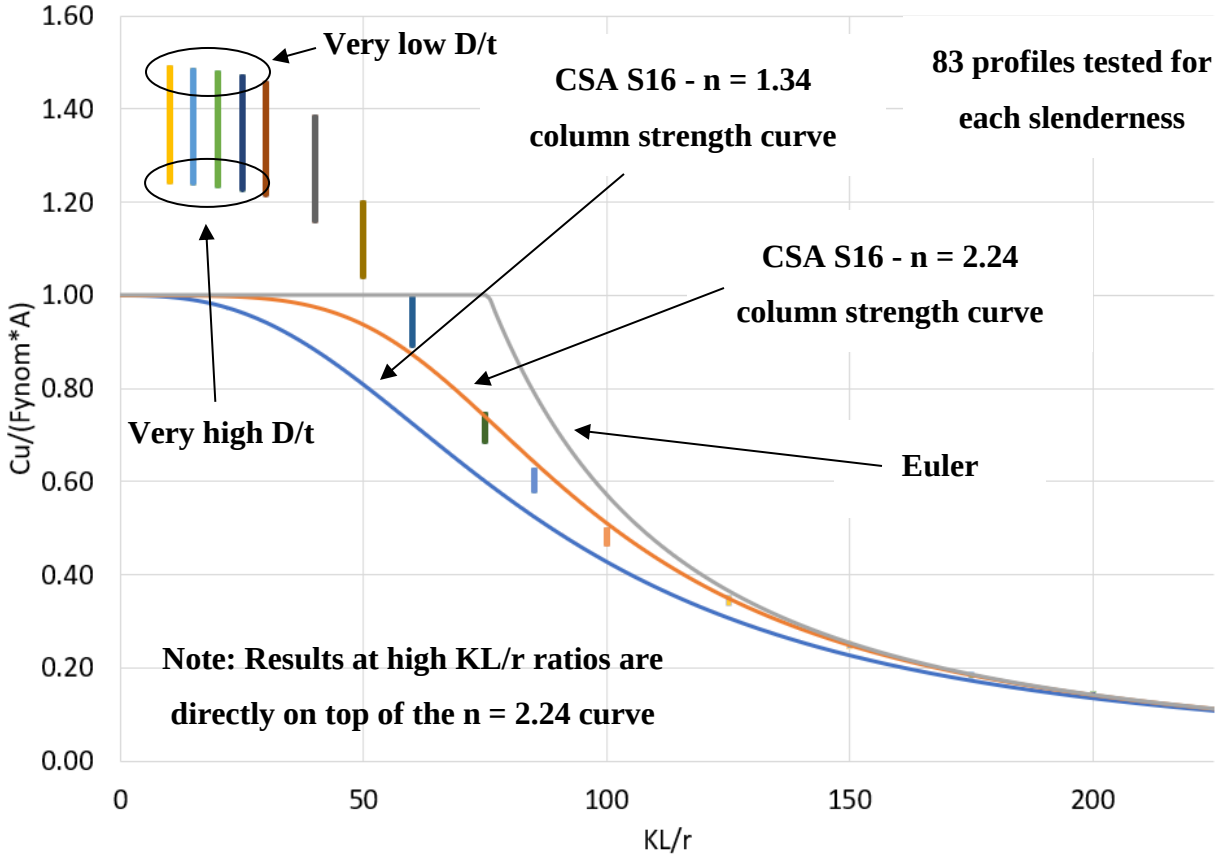


Figure 4-24: Compressive resistance $C_u$ according to KL/r and normalized with respect to the nominal yield strength – Out-of-straightness of L/6000

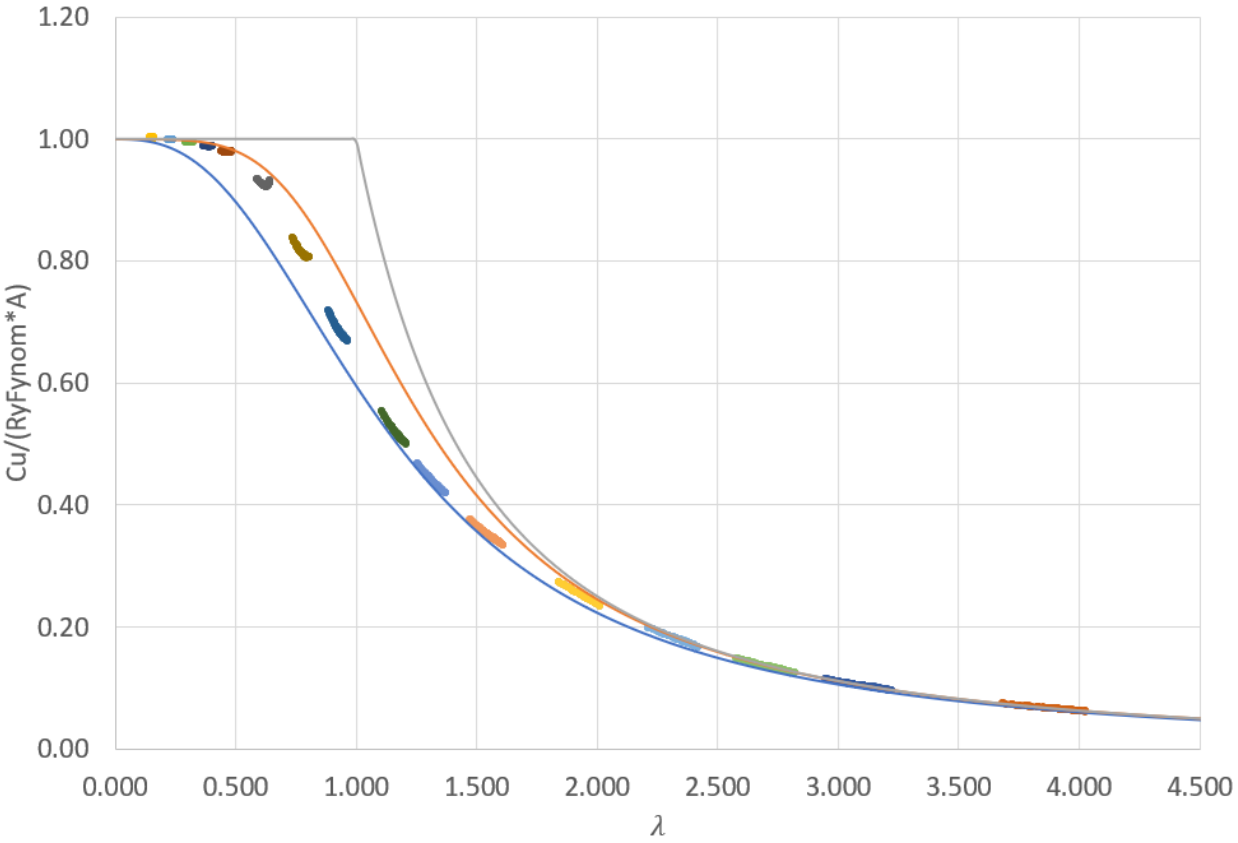


Figure 4-25: Compressive resistance $C_u$ according to $\lambda$ and normalized with respect to average cross-sectional yield strength – Out-of-straightness of L/6000

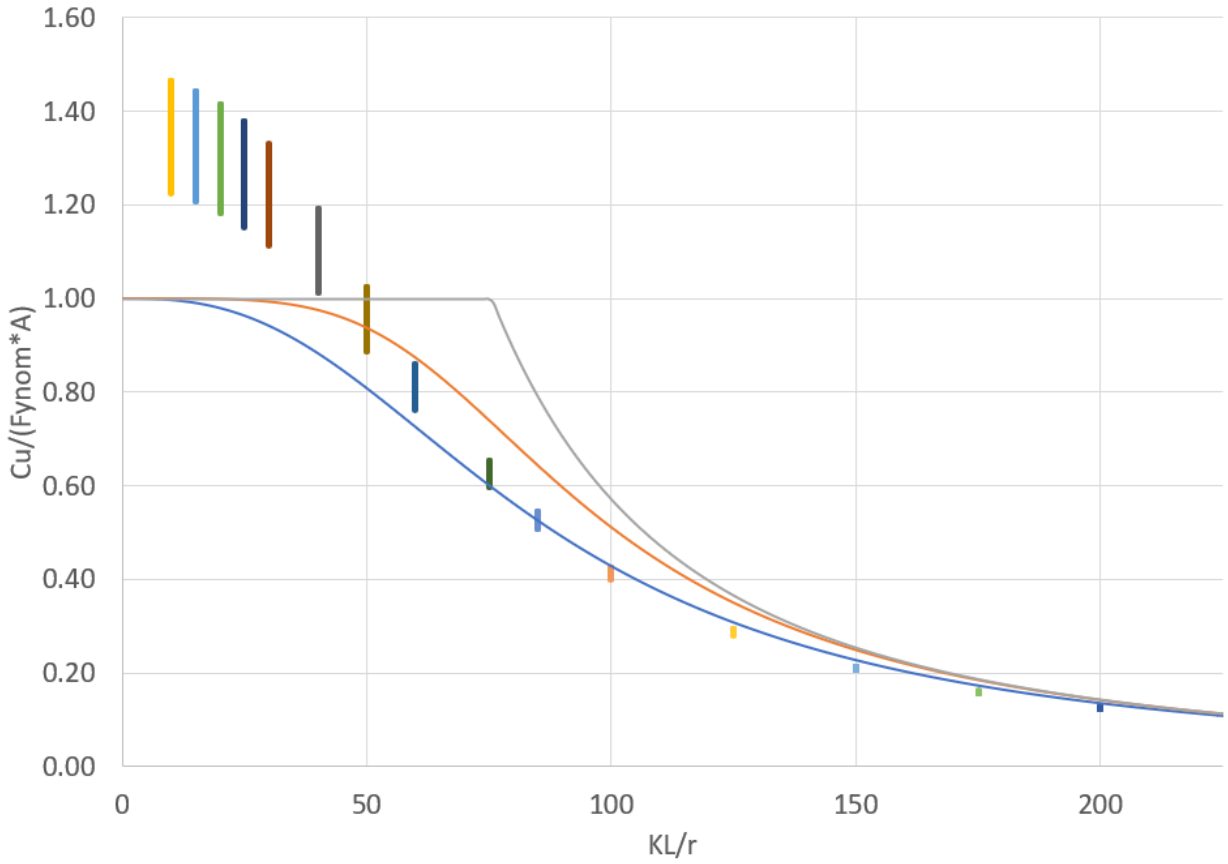


Figure 4-26: Compressive resistance $C_u$ according to KL/r and normalized with respect to the nominal yield strength – Out-of-straightness of L/480

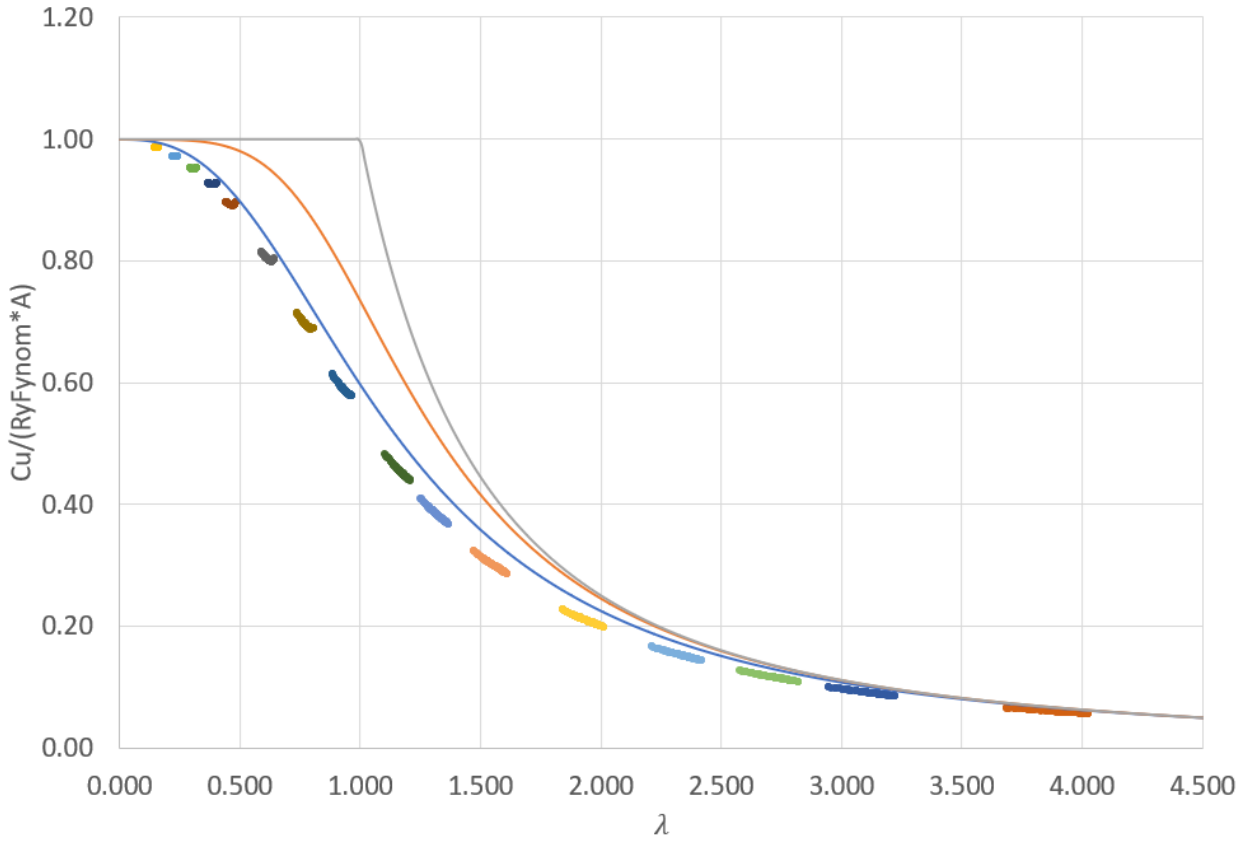


Figure 4-27: Compressive resistance $C_u$ according to $\lambda$ and normalized with respect to average cross-sectional yield strength – Out-of-straightness of L/480

It is seen in Figure 4-24 and Figure 4-26, members with very low KL/r values have significantly higher probable compressive resistances than the nominal yield strength. The average compressive resistance at very low KL/r values approaches the same ratio as the average cross-sectional yield strength determined in Table 4-3. This is to be expected, as the detrimental effect of residual stresses is reduced as the KL/r ratio decreases and the increased average cross-sectional yield strength becomes the dominating component. The vertical spread is explained by the different D/t ratios of the members. Members with higher D/t ratios will be located at the bottom part of the spread, while members with low D/t ratios will be located at the upper part of the spread. As the KL/r ratio increases, the members are more prone to fail by inelastic buckling at intermediate KL/r values, and elastic buckling at very high KL/r values. Therefore, the effects of the increased yield strength are reduced and the compressive strength of the HSS bracing members approaches the well-known n = 1.34 and n = 2.24 column strength curves until eventually reaching the Euler curve. The out-of-straightness has significant effects on the final compressive resistance. The compressive

resistance of members with an L/480 out-of-straightness joins the n = 1.34 curve as the KL/r is increased, while the compressive resistance of members with an out-of-straightness of L/6000 joins the n = 2.24 curve as the KL/r value is increased.

It is seen in Figure 4-25 and Figure 4-26, where everything was normalized with respect to the average cross-sectional yield strength, the n = 1.34 column strength curve provides the best approximation of the probable compressive resistance $C_u$ when an out-of-straightness of L/480 is taken. The n = 1.34 column strength curve even overestimates the probable compressive resistance at intermediate slenderness ratios. This is due to the detrimental effects of the residual stresses. If an out-of-straightness of L/6000 is taken, the probable compressive resistance $C_u$ falls right on top of the n = 2.24 column strength curve for slenderness values below 0.5. For slenderness values from 0.5 to 1.00, the probable compressive resistance decreases gradually from the n = 2.24 column strength curve to the n = 1.34 column strength curve at a value of 1.00. The n = 1.34 column strength curve provides the best approximate of the probable compressive resistance for slenderness values above 1.00.

## 4.3 Conclusion

In this chapter, the probable compressive resistance $C_u$ was determined from a refined model of the probable yield strength $R_yF_y$ (average cross-sectional yield strength) of cold-formed SHS bracing members and the residual stress model determined in Chapter 3. A fiber based OpenSees finite element analysis model was used to compute the probable compressive resistance of cold-formed SHS members, for which the results were further compared to column strength curves in current provisions (CSA S16).

A parametric study was first performed on the fiber based OpenSees model to determine the effects of the residual stresses and increased yield strength gradient on the compressive resistance of the SHS members. The numerical analysis was conducted on typical bracing members having different overall slenderness ratios. The increased yield strength gradient across the section's perimeter and the residual stress components were based on the models proposed in Chapter 2 and 3. However, the mill certificate data in Chapter 3 was not available at this stage of the investigation. Therefore, the yield strength and residual stress gradients were known from the review in Chapter 2, but it was not possible to apply actual yield strength values. For this reason, the values were based on the nominal yield strength at this stage of the investigation. Two residual stress components were included: the bending residual stress (through thickness component) and the membrane residual stress (perimeter component). The final residual stress of the profile is the arithmetic sum of these two components. It was determined that the bending residual stresses have a significant impact on the compressive resistance of SHS bracing members whereas membrane residual stresses have insignificant effects. The yield strength gradient significantly increased the yield strength of the cross-section, but this benefit was counteracted by the detrimental effects of the bending residual stresses. Results at this stage were normalized with respect to the nominal yield strength. It was found the probable compressive resistance of the SHS bracing members was significantly higher than the nominal resistance. The average probable compressive resistance $C_n$ ($C_n$ = compressive resistance based on the nominal yield strength value to compute the yield strength and residual stress gradients) reached approximately $1.20C_y$ ($C_y$ = nominal compressive resistance) for very low slenderness ratios. Thereafter, it gradually decreased until reaching the n=1.34 curve at a slenderness ratio KL/r of approximately 100.

The OpenSees analysis was then redone using the refined model of the yield strength and residual stress gradient based on the ASTM A1085 steel grade and actual coupon values from mill certificates of Chapter 3. The refined average cross-sectional yield strength model was based on the "*weighted average*" model in Chapter 3. The new model was named the "*refined weighted average*" model. The main difference between the two models is in the yield strength of the corners.

In Chapter 3, the yield strength of the corners was based on an approximated upper and lower bound of the corner yield strength based on actual corner yield strength values. In this chapter, a linear relationship was defined between the corner yield strength and the yield strength at the center of the flat wall. Therefore, the corner yield strength varied according to the yield strength of the center of the flat wall. The yield strength at the center of the flat wall was based on an average trendline from the normalized yield strength mill certificate data for the ASTM A1085 grade obtained in Chapter 3. The only difference with Chapter 3 is this value is based on an average trendline instead of the actual coupons. The residual stress distribution was as the one proposed in Chapter 3, however, the magnitudes were computed from the average cross-sectional yield strength instead of the nominal yield strength.

The probable compressive resistance $C_u$ was computed for 83 different ASTM A1085 HSS sections with slenderness varying from 10 to 250. This second set of analysis was performed for two values of out-of-straightness: L/480, as specified in the ASTM A1085; L/6000 which represents the mean value from reported data (Davison & Birkemoe, 1983; Bjorhovde, 1977; Salvarinas, 1974; Key and Hancock, 1985 and Key et al., 1988). The results were normalized with respect to the actual yield strength of the section in this case, versus the nominal yield strength in the first part of this chapter and compared to column strength curves in current provisions (CSA S16). It was determined the probable compressive resistance is slightly below the n=1.34 curve for the out-of-straightness of L/480. For the out-of-straightness of L/6000, the probable compressive resistance is at the n = 2.24 curve up until a dimensionless slenderness ratio of 0.5, and then gradually decreases to the n = 1.34 curve which it reaches at a dimensionless slenderness of approximately 1.0.

To summarize, a parametric study was performed on a fiber based OpenSees model to determine the effects of the residual stresses and increased yield strength gradient on the compressive resistance of the SHS members. This study was based on the nominal yield strength and the yield

strength and residual stress distribution model proposed on Chapter 3. This was due to the lack of mill certificate data at the time of the study. A more refined model based on actual values obtained from mill certificate data was then determined and a second parametric study was performed. This study was done on 83 different ASTM A1085 steel grade members with different slenderness ratios and two different out-of-straightness values.

# CHAPTER 5 CONCLUSION AND RECOMMENDATIONS

## 5.1 Conclusion

The vast majority of cold-formed HSS members used across North America are currently manufactured through a continuous cold-rolling process. A coil is first rolled and welded into a circular section. It is then either sold as an CHS (circular hollow section) or rolled further to form an SHS (square hollow section) or an RHS (rectangular hollow section). This manufacturing method induces a yield strength gradient across the cross-section and significant longitudinal and transversal residual stresses. An equation is proposed in the CSA S136 standard to account for the increase in yield strength in the corners of cold-formed members. However, this equation was based on very thin channel sections from the 1960s and would not reflect to current HSS members. The CSA S136 standard equation is based on the ultimate to yield strength ratio of the virgin coil material used to form the section, and the corner radius to thickness ratio. It only accounts for the increase in the yield strength in the corners based on a weighted average. The yield strength in the walls is either taken from one tensile coupon measured at the center of the walls, or the nominal yield strength. No method is proposed to account for the yield strength gradient across the section and the residual stresses in cold-formed HSS members.

Current seismic provisions are based on probable resistances of HSS bracing members determined from mill certificates taken from the mid-wall cross-section. Based on previous investigations, it was determined that such yield strength is the lowest yield strength of the cross-section. The yield strength increases linearly from the center up to the edges near the corners, and the corners have significantly higher yield strengths than the flat wall. After having compiled a number of investigations on corner yield strength, it was determined that the yield strength can be approximated by the ultimate steel tensile strength from tensile testing of coupons taken from the mid-wall cross-section. An empirical yield strength increase at the corners and a yield strength gradient across the flat walls was proposed based on Canadian investigations. For the numerical model, the corner yield strength was set at $1.60F_y$. The yield strength at the center was set at $1.00F_y$ and the edge of the flat wall near the corner was set at $1.20F_y$.

The residual stresses in cold-formed sections can be approximated by three components in the transverse and longitudinal directions. These are the through thickness (bending), perimeter

(membrane) and layering components. Several investigations have shown that the bending component in the longitudinal direction is the controlling one for member compressive resistance and is sufficient to accurately model cold-formed sections. This was further confirmed in this thesis based on the parametric analysis of several bracing members. A detailed residual stress model based on previous experimental and theoretical investigations was proposed. This model includes the bending and membrane components. The membrane residual stress model follows a linear profile from the corner to the center of the flat walls. The corner is in compression while the center is in tension, and both peak stresses are of the same magnitude. Bending residual stresses were approximated using a trapezoidal shape with residual stresses at the exterior fibre being in tension and residual stress at the interior fibre being in compression. For the numerical model, the magnitude of the exterior fibres was set to $0.6F_y$ in tension and compression at their respective positions for the through thickness component. The membrane component peak residual stress was set at $0.17F_y$.

Yield and ultimate tensile stress data was determined from a large number of Canadian cold-formed HSS manufacturers. The tensile data from a coupon taken at the center of the flat wall was provided in each certificate. A total of 18236 mill certificates were available. The data was divided as a function of HSS b/t ratios and three different steel grades. Trends and mean yield strength values were determined for the ASTM A500 steel grade, the ASTM A1085 steel grade and the G40.20/G40.21 steel grade. The data clearly showed that the yield strength of the section decreases as the b/t ratio increases. For the ASTM A1085 steel grade, no variation was found in the ultimate tensile stress values with respect to the b/t. For the ASTM A500 and CSA G40.21 steel grades, a slight decrease in ultimate tensile stress with an increasing b/t ratio was noticed.

For rectangular and square profiles of the ASTM A1085 and CSA G40.21 steel grades, the average ultimate tensile stress obtained from mid-wall tensile coupons increased to $1.15F_{unom}$. This increase was of $1.12F_{unom}$ for circular profiles. For rectangular and square profiles of the ASTM A500 steel grade, the ultimate tensile stress increased to $1.23F_u$. For circular profiles, this value was $1.21F_{unom}$.

For rectangular and square profiles of all three steel grades and a KL/r limit of 200, the average yield strength obtained from mid-wall tensile coupons was $1.30F_{ynom}$. For circular profiles and a KL/r range of 100 to 200, this was value was $1.22F_{ynom}$ for the ASTM A500 and ASTM A1085 steel grades, and $1.26F_{ynom}$ for the CSA G40.21 steel grade. For circular profiles and a KL/r limit

below 100, this value was $1.24F_{ynom}$ for the ASTM A500 steel grade, $1.27F_{ynom}$ for the ASTM A1085 steel grade and $1.30F_{ynom}$ for the CSA G40.21 steel grade.

The average probable yield strength $R_yF_y$ to determine the probable tensile resistance $T_u$ was found from three models. The first model was based on the $F_y$ distribution proposed for the numerical model based on previous literature. The yield strength varied across the flat wall in this model. In the second and third models, the average probable resistance was based on the CSA S136 standard equation to account for strain hardening. The CSA S136 standard equation requires the $F_u/F_y$ ratio of the coil strip used to form the final profile. This value was unavailable. Therefore, this ratio was substituted with the nominal values for the first second model which was named *S136A*. For the third model named *S136B*, the ratio was determined from the actual values from the mid-wall tensile coupons found in mill certificates. The CSA S136 standard equation does not account for an $F_y$ gradient across the flat wall. All three models, take a weighted average once the yield strength is determined for the corners and flat walls. It was found that the probable resistance $R_yF_y$ increases significantly with all three models compared to the value obtained from the mid-wall tensile coupon in mill certificates.

For rectangular and square profiles, the probable yield strength $R_yF_y$ to determine $T_u$ should be $1.50F_{ynom}$ (515 MPa). This new value is superior to the current $R_yF_y$ of 460 MPa found in the CSA S16 standard. For circular HSS profiles, the probable resistance $R_yF_y$ should be equal to the mid-wall tensile coupon value determined from the mill certificates.

A reliability analysis was performed to determine t an equivalent nominal yield strength ($F_y$*) to be used in the current equation $T_r$ assuming $\phi$ 0.9 and the nominal area. This study was performed on square and rectangular HSS profiles. For these profiles, it was shown an average $F_y$* value of 500 MPa can be used for KL/r ratios below 200.

Finally, two parametric studies were performed on the fiber based OpenSees finite element model. The first study was performed to determine the effects of the residual stresses and increased yield strength gradient on the compressive resistance of the SHS members. The compressive resistance normalized with respect to the nominal compressive resistance was also determined. The second study was performed to determine the probable compressive resistance based on the actual yield strength of the HSS bracing member.

The first numerical study was conducted on typical bracing members having different overall slenderness ratios and the effects of the increased yield strength and residual stresses were determined. This study was based on the yield strength distribution gradient and residual stress model determined in Chapter 2 and Chapter 3. The values were however based on nominal values. It was determined that the bending residual stresses have a significant impact on the compressive resistance of SHS bracing members whereas membrane residual stresses have insignificant effects. The yield strength gradient significantly increased the yield strength of the cross-section, but this benefit was counteracted by the detrimental effects of the bending residual stresses. Results at this stage were normalized with respect to the nominal yield strength. It was found the probable compressive resistance of the SHS bracing members was significantly higher than the nominal resistance. The average probable compressive resistance $C_u$ reached approximately $1.20C_n$ for very low slenderness ratios. Thereafter, it gradually decreased until reaching the n=1.34 curve at a slenderness ratio KL/r of approximately 100.

The second numerical study was based on a refined model of the yield strength and residual stress gradient based on the ASTM A1085 steel grade and actual coupon values from mill certificates of Chapter 3. The study was performed on 83 different sections and two different out-of-straightness values. The results were normalized with respect to the actual yield strength of the section in this case, versus the nominal yield strength in the first part of this chapter, and compared to column strength curves in current provisions (CSA S16). It was determined the probable compressive resistance is slightly below the n = 1.34 curve for the out-of-straightness of L/480. For the out-of-straightness of L/6000, the probable compressive resistance is at the n = 2.24 curve up until a slenderness ratio dimensionless slenderness of 0.5, and then gradually decreases to n = 1.34 curve which it reaches at a dimensionless slenderness of approximately 1.0.

## 5.2 Recommendations and future studies

The following future studies are proposed:

- Very few investigations have performed detailed cross-sectional analysis of tensile coupons. All available investigations were from the 1970s. It would be necessary to test additional sections with different b/t ratios. This would make it possible to determine how the cross-sectional yield strength gradient varies across the flat wall with respect to the b/t ratio.
- While the coupon yield strength was determined from 47 different sections, only 5 were Canadian. Canadian sections showed a clear linear distribution with a lower and upper bound with respect to the b/t ratio. Other investigations had a far greater scatter in the results. It would be interesting to obtain additional corner yield strength values from Canadian sections to verify this trend.
- It would be interesting to compare experimental story shears and brace strengths with results from the numerical model proposed in this investigation. A numerical parametric analysis on full scale buildings would also help understand the effects of b/t ratios, residual stresses and the yield strength gradient on various elements of braced frames.
- The current S136-16 standard equation to account for increased yield strength from the cold work effect needs to be updated to better represent current sections. It would also be interesting to modify this equation to work with respect to the tensile strength of a coupon taken from the mid-wall instead of the coil strip.

# BIBLIOGRAPHY

ASTM. (2015). *A1085-15, Standard Specification for Cold Formed Welded Carbon Steel Hollow Structural Sections (HSS).* American Society for Testing Materials (ASTM), West Conshohocken, Pa.

ASTM. (2013). *A500-13, Standard Specification for Cold Formed Welded Carbon Steel Hollow Structural Sections (HSS).* American Society for Testing Materials (ASTM), West Conshohocken, Pa.

Abdella, K. (2006). Inversion of a full-range stress–strain relation for stainless steel alloys. *International Journal of Non-Linear Mechanics*, 41(3), 456-463.

Afshan, S., Rossi, B., & Gardner, L. (2013). Strength enhancements in cold-formed structural sections—Part I: Material testing. *Journal of Constructional Steel Research*, 83, 177-188.

Bjorhovde, R., & Tall, L. (1971). Maximum column strength and the multiple column curve concept, *Fritz Laboratory Reports*, (345), 75-30.

Bjorhovde, R., Brozzetti, J., Alpsten, G. A., & Tall, L. (1972). Residual stresses in thick welded plates. *WELD J--MIAMI FLA*--, 51(8), 292.

Bjorhovde, R. (1977). *Strength and Behavior of Cold-Formed HSS Columns*. Structural Engineering Report No. 65, University of Alberta, Department of Civil Engineering, Edmonton, Alberta.

Britvec, S. J., Chajes, A., Warren, K. W., Uribe, J., & Winter, G. (1970). Effects of cold work in cold-formed steel structural members, *Cornell Engineering Research Bulletin*, 70(1).

Chajes, A., Britvec, S. J., & Winter, G. (1963). Effects of cold-straining on structural sheet steels. *Journal of the Structural Division*, 89(2), 1-32.

Cruise, R. B., & Gardner, L. (2008). Strength enhancements induced during cold forming of stainless steel sections. *Journal of constructional steel research*, 64(11), 1310-1316.

CSA. (2004). *G40.20-04/G40.21-04, General requirements for rolled or welded structural quality steel/Structural quality steel, Reaffirmed 2009*. Canadian Standards Association (CSA), Toronto, ON.

CSA. (2014). *CSA S16-14, Design of Steel Structures.* Canadian Standards Association (CSA), Toronto, ON.

CSA. (2016). *CSA S136-16, North American Specification for the Design of Cold-Formed Steel Structural Members*. Canadian Standards Association (CSA), Toronto, ON.

Davison, T. A. (1977). A theoretical investigation of the column behaviour of hollow structural steel sections. Master's Degree Theses, Department of Civil Engineering, University of Toronto, Toronto, Ontario, Canada.

Davison, T. A., & Birkemoe, P. C. (1983). Column behaviour of cold-formed hollow structural steel shapes. *Canadian Journal of Civil Engineering*, 10(1), 125-141.

Elghazouli, A. Y., Broderick, B. M., Goggins, J., Mouzakis, H., Carydis, P., Bouwkamp, J., & Plumier, A. (2005). Shake table testing of tubular steel bracing members. *Proceedings of the Institution of Civil Engineers-Structures and Buildings*, 158(4), 229-241.

Feldmann, M., Eichler, B., Kühn, B., Stranghöner, N., Dahl, W., Langenberg, P., ... & Iglesias, G. (2012). *Choice of Steel Material to Avoid Brittle Fracture for Hollow Section Structures.* JRC Scientific and Policy Reports. *Report EUR, 25400*, JRC, Ispra, Italy, 12-14 p.

Filiatrault, A., Tremblay, R., Christopoulos, C., Folz, B., & Pettinga, D. (2013). *Elements of Earthquake Engineering and Structural Dynamics.* Montreal: Presses Internationales Polytechnique, 269-601 p.

Fitzpatrick, M., Fry, A., Holdway, P., Kandil, F., Shackleton, J., & Suominen, L. (2005). Determination of Residual Stresses by X-ray Diffraction - Issue 2. *A NATIONAL MEASUREMENT GOOD PRACTICE GUIDE* (52), 5 p.

Gao, T., & D. Moen, C. (2010). The cold work of forming effect in steel structural members. *Stability and Ductility of Steel Structures*, 8(10.), 1017-1024.

Gardner, L., Saari, N., & Wang, F. (2010). Comparative experimental study of hot-rolled and cold-formed rectangular hollow sections. *Thin-Walled Structures*, 48(7), 495-507.

Giaux, P. (1973). Essais de flambement sur profils creux formés à froid carrés et circulaires. Rept. 72/28/E, made at request of le Comité international pour le développement et l'étude de la construction tubulaire, Université de Liège, Belgium.

Guo, Y.-J., Zhu, A.-Z., Pi, Y.-L., & Ton-Loi, F. (2007). Experimental study on compressive strengths of thick-walled cold-formed sections. *Journal of Constructional Steel Researc*h, 63(5), 718-723.

Han, S.-W., Kim, W. T., & A. Foutch, D. (2007). Seismic Behavior of HSS Bracing Members according to Width–Thickness Ratio under Symmetric Cyclic Loading. *Journal of Structural Engineering*, 133(2), 264-273.

Hancock, G. J., & Key, P. (1986). *Plastic Collapse Mechanisms for Cold Formed Square Hollow Section Columns.* Research Report No. R526 1326-3005, University of Sydney. Sydney, Australia, 1-87 p.

Hu, S.-D., Ye, B., & Li, L.-X. (2011). Materials properties of thick-wall cold-rolled welded tube with a rectangular or square hollow section. *Construction and Building Materials,* 25(5), 2683-2689.

Kamani, P. R. (1974). *Stub column data and the prediction of compression behavior of hollow structural shapes*. Master's Degree Theses, Department of Civil Engineering, University, of Toronto, Toronto, Ontario, Canada, 2-126 p.

Kato, B. (1977). Local buckling of steel circular tubes in plastic region. In *Proc. of International Colloquium on Stability of Structures Under Static and Dynamic Loads, SSRC/ASCE* (pp. 375-391).

Kato, B., & Aoki, H. (1978). Residual stresses in cold-formed tubes. *The Journal of Strain Analysis for Engineering Design*, 13(4), 193-204.

Karren, K. W., & Winter, G. (1965). Effects of cold-forming on light-gage steel members. In *Proc. of Journal of the Structural Divisi*on. ASCE, Vol. 89, No. ST2, Proc. Paper 3477, April, 1963, pp. 1-32.

Karren, K. W. (1967). Corner properties of cold-formed shapes. *Journal of the Structural Division*, 93(1), 401-433.

Kelly. (2012). Mechanics *Lecture Notes: An introduction to Solid Mechanics*. Auckland: University of Auckland. Available from http://homepages.engineering.auckland.ac.nz/~pkel015/SolidMechanicsBooks/index.html

Kennedy, D. J., & Aly, M. G. (1980). Limit states design of steel structures resistance factors. *Canadian Journal of Civil Engineering*, 7(1), 45-77.

Key. (1988). Behaviour of cold-formed square hollow section columns. Doctoral dissertation, Department of Civil Engineering, University, of Sydney, Sydney, New South Wales, Australia, 2-410 p.

Key, P. W., & Hancock, G. J. (1993). A Theoretical Investigation of the Column Behaviour of Cold-Formed Square Hollow Sections. *Thin-Walled Structures*, 16(1-4), 31-64.

Key, P. W., Hasan, S. W., & Hancock, G. J. (1988). Column behavior of cold-formed hollow sections. *Journal of Structural Engineering*, 114(2), 390-407.

Key, P., & Hancock, G. (1985). An experimental investigation of the column behavior of cold formed square hollow sections. Research Report No. 493. University of Sydney. Sydney, Australia, 1-128 p.

Li, S., Zeng, G., Ma, Y., Guo, Y., & Lai, X. (2009). Residual stresses in roll-formed square hollow sections. *Thin-walled structures*, 47(5), 505-513.

Li, Y., Wen, D., Want, L., & Shen, Z. (2012). Cold-forming effect investigation on cold-formed thick-walled steel hollow sections. *International Specialty Conference on Cold-Formed Steel Structures*, 21(3), 27-41.

Lind, N. C., & Schroff, D. K. (1975). Utilization of Cold Work in Cold-Formed Steel. *Journal of the Structural Division*, 101(1), 67-78.

Liu, W., Rasmusse, K. J., & Hao, Z. (2017). Modelling and probabilistic study of the residual stress of cold-formed hollow steel sections. *Engineering Structures*, 150, 986-995.

Mazzoni, S., McKenna, F., Scott, M.H., Fenves, G.L., (2018). *OpenSees Command Language Manual*, Open System for Earthquake Engineering Simulation (OpenSees), Pacific Earthquake Engineering Research Center, University of California Berkeley, CA. Available from http://opensees.berkeley.edu/wiki/index.php/Steel02_Material_--_Giuffré-Menegotto-Pinto_Model_with_Isotropic_Strain_Hardening

Moen, C. D., Igusa, T., & Schafer, B. W. (2008). Prediction of residual stresses and strains in cold-formed steel members. *Thin-walled structures*, 46(11), 1274-1289.

Ringle. (1969). Effects of cold roll-forming on the mechanical properties of square welded steel tubes. National Steel Corp., Research and Development Dept., Project No. 5-501, Weirton, West Virginia.

Rossi, B., Afshan, S., & Gardner, L. (2013). Strength enhancements in cold-formed structural sections - Part II: Predictive models. *Journal of Constructional Steel Research*, 83, 189-196.

Rossi, B., Boman, R., & Degée, H. (2011, September). Effects of the roll forming process on the mechanical properties of thin-walled sections made of non linear metallic materials. In *Proc. of the 6th International Conference on Thin Walled Structures: ICTWS2011, Timisoara 5-7 September 2011* (pp. 633-640).

Rotter, J. M. (1981). A simple approach to multiple column curves. In *National Conference Publication 81/2. Metal Structures Conference 1981. Newcastle, 11-14 May 1981.*

Salvarinas, J. J. (1977). An Experimental Investigation of the Column Behaviour of Hollow Structural Steel Sections. Doctoral dissertation, University of Toronto. Department of Civil Engineering, University, of Toronto, Toronto, Ontario, Canada, 1-114 p.

Schmidt, B. J., & Bartlett, F. M. (2002a). Review of resistance factor for steel: data collection. *Canadian Journal of Civil Engineering*, 29(1), 98-108.

Schmidt, B. J., & Bartlett, F. M. (2002b). Review of resistance factor for steel: resistance distributions and resistance factor calibration. *Canadian Journal of Civil Engineering*, 29(1), 109-118.

Schuster, R. M., & Lind, N. C. (1975). *Cold formed steel design manual: based on CSA standard S136-1974*. Solid Mechanics Division, University of Waterloo.

Sherman, D. R. (1969). Residual stress measurement in tubular members. *Journal of the Structural Division*, 95(4), 635-647.

Somodi, B., & Kovesdi, B. (2016). Residual stress measurements on cold-formed HSS hollow section columns. *Journal of Constructional Steel Research*, 128, 706-720.

Somodi, B., & Kövesdi, B. (2017). Residual stress measurements on cold-formed HSS hollow section columns. *Journal of Constructional Steel Research*, 128, 706-720.

Sun, M., & Packer, A. J. (2014). Direct-formed and continuous-formed rectangular hollow sections - Comparison of static properties. *Journal of Constructional Steel Research*, 92(2014), 67-78.

Tong, L., Hou, G., Chen, Y., Zhou, F., Shen, K., & Yang, A. (2012). Experimental investiation on longitudinal residual stresses for cold-formed thick-walled square hollow sections. *Journal of Constructional Steel Research,* 73(2012), 105-116.

Tremblay, R. (2016). *Notes de cours - Conception parasismique.* Montreal: Polytechnique Montreal. QC, Canada, 15-31 p.

Von Kármán, T., Sechler, E., & Donnell, L. (1932). The Strength of Thin Plates In Compression Transactions of the ASME, 54; 53–57.

Wilkinson. (1999). *The plastic behaviour of cold-formed rectangular hollow sections.* Doctoral dissertation, Department of Civil Engineering, University, of Sydney, Sydney, New South Wales, Australia, 1-482.

# APPENDIX A – MILL CERTIFICATE RESULTS FOR CHAPTER 3

Table A- 5: Steel grade specifications summarized used for mill certificate analysis in Chapter 3

| | | Shaped | | Round | |
|---|---|---|---|---|---|
| Group name | As shown on certificate | Minimum Yield (MPa) | Minimum Tensile (MPa) | Minimum Yield (MPa) | Minimum Tensile (MPa) |
| CSA G40.21 | CSA G40.21-13 50W CLASS C | 345 | 450 | 345 | 450 |
| | CSA G40.21 350W | 345 | 450 | 345 | 450 |
| | CSA G40.21 50W/ASTM A500 GRADE C | 345 | 450 | 345 | 450 |
| | CSA G40.21 350W / ASTM A500-13 GRADE B&C | 345 | 450 | 345 | 450 |
| | A500-C/350W | 345 | 450 | 345 | 450 |
| ASTM A500 | A500 GRADE B&C / ASTM A500 GRADE B&C | 345 | 425 | 315 | 425 |
| | ASTM A500-13 GRADE B&C | 345 | 425 | 315 | 425 |
| | ASTM A500 GR B&C | 345 | 425 | 315 | 425 |
| | ASTM A500 2013 GRADE B/C TYPE 1 | 345 | 425 | 315 | 425 |
| | ASTM A500 GR.C 2021 | 345 | 425 | 315 | 425 |
| | ASTM A500 GR.C 2020 | 345 | 425 | 315 | 425 |
| | ASTM A500 GR.C 2019 | 345 | 425 | 315 | 425 |
| | ASTM A500 GR.C 2018 | 345 | 425 | 315 | 425 |
| | ASTM A500 GR.C 2017 | 345 | 425 | 315 | 425 |
| | ASTM A500 GR.C 2016 | 345 | 425 | 315 | 425 |
| | ASTM A500 GR.C 2015 | 345 | 425 | 315 | 425 |
| | ASTM A500 GR.C 2014 | 345 | 425 | 315 | 425 |
| | ASTM A500 GR.C 2013 | 345 | 425 | 315 | 425 |
| A1085 | ASTM A1085 | 345 | 450 | 345 | 450 |
| | A 1085 | 345 | 450 | 345 | 450 |

Note:

**SHS & RHS (RECTANGULAR OR SQUARE HOLLOW SECTION)**

KL/r = 100 → b/t limit of 17.7 (Fy = 345)

KL/r = 140 → b/t limit of 19.7 (Fy = 345)

KL/r = 200 → b/t limit of 22.6 (Fy = 345)

**CHS (CIRCULAR HOLLOW SECTION)**

KL/r = 100 → D/t limit of 28.9 (Fy = 345)

KL/r = 140 → D/t limit of 32.4 (Fy = 345)

KL/r = 200 → D/t limit of 37.6 (Fy = 345)

Table A- 6: Results for shaped HSS from North American Steel manufacturers – Part 1

## --> b/t no limit – SHAPED – A500

| ASTM A500 | | | Count | Center Coupon Fy | | | | | | Center Coupon Fu | | | | | |
|---|---|---|---|---|---|---|---|---|---|---|---|---|---|---|---|
| | | | | MAX. | MIN. | MED. | AVG. | ST.DEV | CV | MAX. | MIN. | MED. | AVG. | ST.DEV | CV |
| TYPE | Producer A | | 11533 | 2.00 | 1.00 | 1.27 | 1.27 | 0.10 | 7.76 | 1.84 | 1.01 | 1.22 | 1.23 | 0.08 | 6.22 |
| shaped (SHS) | | Plant A | 110 | 1.55 | 1.13 | 1.34 | 1.34 | 0.08 | 5.97 | 1.45 | 1.09 | 1.31 | 1.30 | 0.06 | 4.31 |
| NOMINAL | | Plant B | 4092 | 1.94 | 1.00 | 1.27 | 1.27 | 0.12 | 9.06 | 1.84 | 1.02 | 1.27 | 1.26 | 0.08 | 6.11 |
| Fy (MPa) | | Plant C | 6875 | 2.00 | 1.00 | 1.27 | 1.28 | 0.09 | 6.85 | 1.76 | 1.01 | 1.20 | 1.21 | 0.07 | 5.49 |
| 345 | | Plant D | 261 | 1.49 | 1.00 | 1.21 | 1.21 | 0.08 | 6.68 | 1.30 | 1.02 | 1.17 | 1.16 | 0.06 | 5.29 |
| Fu (MPa) | | Plant undefined | 195 | 1.55 | 1.03 | 1.25 | 1.26 | 0.10 | 7.73 | 1.53 | 1.05 | 1.19 | 1.19 | 0.07 | 5.78 |
| 425 | Producer B | | 6 | 1.21 | 1.01 | 1.18 | 1.16 | 0.07 | 5.76 | 1.16 | 1.05 | 1.16 | 1.12 | 0.05 | 4.40 |
| KL/r limit | Producer C | | - | - | - | - | - | - | - | - | - | - | - | - | - |
| NONE | Producer D | | 8 | 1.45 | 1.33 | 1.40 | 1.39 | 0.05 | 3.42 | 1.40 | 1.27 | 1.33 | 1.33 | 0.05 | 4.00 |
| b/t limit | Producer E | | - | - | - | - | - | - | - | - | - | - | - | - | - |
| NONE | Producer F | | - | - | - | - | - | - | - | - | - | - | - | - | - |
| | Producer G | | 20 | 1.21 | 1.10 | 1.16 | 1.14 | 0.04 | 3.37 | 1.19 | 1.15 | 1.18 | 1.17 | 0.02 | 1.55 |
| | Producer I | | - | - | - | - | - | - | - | - | - | - | - | - | - |
| | Producer J | | 44 | 1.34 | 0.97 | 1.14 | 1.15 | 0.11 | 9.30 | 1.48 | 1.01 | 1.15 | 1.18 | 0.09 | 7.75 |
| | Producer K | | 2 | 1.08 | 1.08 | 1.08 | 1.08 | 0.00 | 0.00 | 1.03 | 1.03 | 1.03 | 1.03 | 0.00 | 0.00 |
| TOTAL | | | 11613 | 2.00 | 0.97 | 1.27 | **1.27** | 0.10 | **7.80** | 1.84 | 1.01 | 1.22 | **1.23** | 0.08 | **6.24** |
| | | D/t | | 67.91 | 7.64 | 24.45 | 26.39 | 11.27 | 42.70 | | | | | | |
| | | b/t | | 60.00 | 2.00 | 15.20 | 18.23 | 10.16 | 55.72 | | | | | | |

| ASTM A500 | | | Count | S136A | | | | | | S136B | | | | | | WEIGHTED AVERAGE | | | | | |
|---|---|---|---|---|---|---|---|---|---|---|---|---|---|---|---|---|---|---|---|---|---|
| | | | | MAX. | MIN. | MED. | AVG. | ST.DEV | CV | MAX. | MIN. | MED. | AVG. | ST.DEV | CV | MAX. | MIN. | MED. | AVG. | ST.DEV | CV |
| TYPE | Producer A | | 11533 | 1.81 | 1.09 | 1.36 | 1.36 | 0.08 | 5.61 | 2.27 | 1.13 | 1.45 | 1.46 | 0.11 | 7.51 | 1.98 | 1.14 | 1.42 | 1.43 | 0.10 | 6.86 |
| shaped (SHS) | | Plant A | 110 | 1.53 | 1.27 | 1.42 | 1.42 | 0.05 | 3.60 | 1.78 | 1.34 | 1.60 | 1.59 | 0.08 | 5.04 | 1.66 | 1.31 | 1.54 | 1.53 | 0.07 | 4.56 |
| NOMINAL | | Plant B | 4092 | 1.71 | 1.09 | 1.36 | 1.36 | 0.09 | 6.56 | 2.27 | 1.13 | 1.49 | 1.49 | 0.13 | 8.62 | 1.86 | 1.14 | 1.43 | 1.43 | 0.11 | 7.98 |
| Fy (MPa) | | Plant C | 6875 | 1.81 | 1.09 | 1.36 | 1.36 | 0.07 | 5.04 | 2.17 | 1.14 | 1.44 | 1.45 | 0.09 | 6.53 | 1.98 | 1.14 | 1.42 | 1.43 | 0.09 | 6.10 |
| 345 | | Plant D | 261 | 1.50 | 1.25 | 1.37 | 1.36 | 0.05 | 3.38 | 1.60 | 1.25 | 1.44 | 1.43 | 0.08 | 5.30 | 1.63 | 1.23 | 1.39 | 1.39 | 0.07 | 5.37 |
| Fu (MPa) | | Plant undefined | 195 | 1.53 | 1.13 | 1.36 | 1.35 | 0.07 | 5.50 | 1.88 | 1.15 | 1.44 | 1.43 | 0.10 | 7.03 | 1.64 | 1.18 | 1.42 | 1.42 | 0.09 | 6.58 |
| 425 | Producer B | | 6 | 1.31 | 1.18 | 1.29 | 1.28 | 0.04 | 3.47 | 1.39 | 1.22 | 1.37 | 1.34 | 0.06 | 4.54 | 1.35 | 1.18 | 1.35 | 1.32 | 0.06 | 4.70 |
| KL/r limit | Producer C | | - | - | - | - | - | - | - | - | - | - | - | - | - | - | - | - | - | - | - |
| NONE | Producer D | | 8 | 1.47 | 1.38 | 1.43 | 1.43 | 0.03 | 2.45 | 1.61 | 1.49 | 1.55 | 1.55 | 0.06 | 3.60 | 1.55 | 1.46 | 1.51 | 1.51 | 0.04 | 2.58 |
| b/t limit | Producer E | | - | - | - | - | - | - | - | - | - | - | - | - | - | - | - | - | - | - | - |
| NONE | Producer F | | - | - | - | - | - | - | - | - | - | - | - | - | - | - | - | - | - | - | - |
| | Producer G | | 20 | 1.34 | 1.18 | 1.26 | 1.24 | 0.05 | 4.30 | 1.43 | 1.23 | 1.34 | 1.32 | 0.07 | 5.49 | 1.39 | 1.23 | 1.32 | 1.30 | 0.05 | 4.01 |
| | Producer I | | - | - | - | - | - | - | - | - | - | - | - | - | - | - | - | - | - | - | - |
| | Producer J | | 44 | 1.42 | 1.20 | 1.33 | 1.33 | 0.06 | 4.51 | 1.65 | 1.25 | 1.41 | 1.44 | 0.10 | 7.21 | 1.53 | 1.17 | 1.36 | 1.36 | 0.10 | 7.68 |
| | Producer K | | 2 | 1.31 | 1.31 | 1.31 | 1.31 | 0.00 | 0.00 | 1.27 | 1.27 | 1.27 | 1.27 | 0.00 | 0.00 | 1.24 | 1.24 | 1.24 | 1.24 | 0.00 | 0.00 |
| TOTAL | | | 11613 | 1.81 | 1.09 | 1.36 | **1.36** | 0.08 | **5.62** | 2.27 | 1.13 | 1.45 | **1.46** | 0.11 | **7.52** | 1.98 | 1.14 | 1.42 | **1.43** | 0.10 | **6.88** |

Table A- 7: Results for shaped HSS from North American Steel manufacturers – Part 2

## --> b/t no limit – SHAPED – A1085

| A1085 | | | Count | Center Coupon Fy | | | | | | Center Coupon Fu | | | | | |
|---|---|---|---|---|---|---|---|---|---|---|---|---|---|---|---|
| | | | | MAX. | MIN. | MED. | AVG. | ST.DEV | CV | MAX. | MIN. | MED. | AVG. | ST.DEV | CV |
| TYPE | Producer A | | 1113 | 1.40 | 1.00 | 1.27 | 1.26 | 0.08 | 6.18 | 1.32 | 1.00 | 1.15 | 1.15 | 0.06 | 4.87 |
| shaped (SHS) | | Plant A | - | - | - | - | - | - | - | - | - | - | - | - | - |
| NOMINAL | | Plant B | - | - | - | - | - | - | - | - | - | - | - | - | - |
| Fy (MPa) | | Plant C | - | - | - | - | - | - | - | - | - | - | - | - | - |
| 345 | | Plant D | - | - | - | - | - | - | - | - | - | - | - | - | - |
| Fu (MPa) | | Plant undefined | 1113 | 1.40 | 1.00 | 1.27 | 1.26 | 0.08 | 6.18 | 1.32 | 1.00 | 1.15 | 1.15 | 0.06 | 4.87 |
| 450 | Producer B | | - | - | - | - | - | - | - | - | - | - | - | - | - |
| KL/r limit | Producer C | | - | - | - | - | - | - | - | - | - | - | - | - | - |
| NONE | Producer D | | - | - | - | - | - | - | - | - | - | - | - | - | - |
| b/t limit | Producer E | | - | - | - | - | - | - | - | - | - | - | - | - | - |
| NONE | Producer F | | - | - | - | - | - | - | - | - | - | - | - | - | - |
| | Producer G | | - | - | - | - | - | - | - | - | - | - | - | - | - |
| | Producer I | | - | - | - | - | - | - | - | - | - | - | - | - | - |
| | Producer J | | - | - | - | - | - | - | - | - | - | - | - | - | - |
| | Producer K | | - | - | - | - | - | - | - | - | - | - | - | - | - |
| TOTAL | | | 1113 | 1.40 | 1.00 | 1.27 | **1.26** | 0.08 | **6.18** | 1.32 | 1.00 | 1.15 | **1.15** | 0.06 | **4.87** |
| | D/t | | | 67.91 | 10.19 | 25.46 | 28.18 | 12.19 | 43.26 | | | | | | |
| | b/t | | | 70.67 | 4.00 | 17.33 | 21.37 | 12.76 | 59.69 | | | | | | |

| A1085 | | | Count | S136A | | | | | | S136B | | | | | | WEIGHTED AVERAGE | | | | | |
|---|---|---|---|---|---|---|---|---|---|---|---|---|---|---|---|---|---|---|---|---|---|
| | | | | MAX. | MIN. | MED. | AVG. | ST.DEV | CV | MAX. | MIN. | MED. | AVG. | ST.DEV | CV | MAX. | MIN. | MED. | AVG. | ST.DEV | CV |
| TYPE | Producer A | | 1113 | 1.56 | 1.11 | 1.40 | 1.40 | 0.08 | 5.77 | 1.68 | 1.12 | 1.46 | 1.45 | 0.10 | 6.67 | 1.58 | 1.15 | 1.43 | 1.42 | 0.09 | 6.02 |
| shaped (SHS) | | Plant A | - | - | - | - | - | - | - | - | - | - | - | - | - | - | - | - | - | - | - |
| NOMINAL | | Plant B | - | - | - | - | - | - | - | - | - | - | - | - | - | - | - | - | - | - | - |
| Fy (MPa) | | Plant C | - | - | - | - | - | - | - | - | - | - | - | - | - | - | - | - | - | - | - |
| 345 | | Plant D | - | - | - | - | - | - | - | - | - | - | - | - | - | - | - | - | - | - | - |
| Fu (MPa) | | Plant undefined | 1113 | 1.56 | 1.11 | 1.40 | 1.40 | 0.08 | 5.77 | 1.68 | 1.12 | 1.46 | 1.45 | 0.10 | 6.67 | 1.58 | 1.15 | 1.43 | 1.42 | 0.09 | 6.02 |
| 450 | Producer B | | - | - | - | - | - | - | - | - | - | - | - | - | - | - | - | - | - | - | - |
| KL/r limit | Producer C | | - | - | - | - | - | - | - | - | - | - | - | - | - | - | - | - | - | - | - |
| NONE | Producer D | | - | - | - | - | - | - | - | - | - | - | - | - | - | - | - | - | - | - | - |
| b/t limit | Producer E | | - | - | - | - | - | - | - | - | - | - | - | - | - | - | - | - | - | - | - |
| NONE | Producer F | | - | - | - | - | - | - | - | - | - | - | - | - | - | - | - | - | - | - | - |
| | Producer G | | - | - | - | - | - | - | - | - | - | - | - | - | - | - | - | - | - | - | - |
| | Producer I | | - | - | - | - | - | - | - | - | - | - | - | - | - | - | - | - | - | - | - |
| | Producer J | | - | - | - | - | - | - | - | - | - | - | - | - | - | - | - | - | - | - | - |
| | Producer K | | - | - | - | - | - | - | - | - | - | - | - | - | - | - | - | - | - | - | - |
| TOTAL | | | 1113 | 1.56 | 1.11 | 1.40 | **1.40** | 0.08 | **5.77** | 1.68 | 1.12 | 1.46 | **1.45** | 0.10 | **6.67** | 1.58 | 1.15 | 1.43 | **1.42** | 0.09 | **6.02** |

Table A- 8: Results for shaped HSS from North American Steel manufacturers – Part 3

## --> b/t no limit – SHAPED – CSA G40.21

| CSA G40.21 – 350W AND ASTM A500 SINGLE OR DUAL CERTIFIED | | | Count | Center Coupon Fy | | | | | | Center Coupon Fu | | | | | |
|---|---|---|---|---|---|---|---|---|---|---|---|---|---|---|---|
| | | | | MAX. | MIN. | MED. | AVG. | ST.DEV | CV | MAX. | MIN. | MED. | AVG. | ST.DEV | CV |
| TYPE | Producer A | | 2932 | 1.67 | 1.00 | 1.28 | 1.29 | 0.09 | 7.04 | 1.37 | 0.97 | 1.15 | 1.15 | 0.06 | 5.04 |
| shaped (SHS) | | Plant A | - | - | - | - | - | - | - | - | - | - | - | - | - |
| NOMINAL | | Plant B | - | - | - | - | - | - | - | - | - | - | - | - | - |
| Fy (MPa) | | Plant C | - | - | - | - | - | - | - | - | - | - | - | - | - |
| 345 | | Plant D | - | - | - | - | - | - | - | - | - | - | - | - | - |
| Fu (MPa) | | Plant undefined | 2932 | 1.67 | 1.00 | 1.28 | 1.29 | 0.09 | 7.04 | 1.37 | 0.97 | 1.15 | 1.15 | 0.06 | 5.04 |
| 450 | Producer B | | - | - | - | - | - | - | - | - | - | - | - | - | - |
| KL/r limit | Producer C | | 10 | 2.17 | 1.17 | 1.68 | 1.71 | 0.28 | 16.14 | 1.74 | 1.10 | 1.59 | 1.57 | 0.17 | 10.79 |
| NONE | Producer D | | - | - | - | - | - | - | - | - | - | - | - | - | - |
| b/t limit | Producer E | | 241 | 1.46 | 1.02 | 1.28 | 1.27 | 0.09 | 7.03 | 1.21 | 1.00 | 1.11 | 1.11 | 0.05 | 4.28 |
| NONE | Producer F | | 130 | 1.65 | 1.07 | 1.24 | 1.29 | 0.17 | 13.25 | 1.38 | 0.96 | 1.18 | 1.20 | 0.11 | 8.97 |
| | Producer G | | - | - | - | - | - | - | - | - | - | - | - | - | - |
| | Producer I | | 1493 | 1.75 | 1.00 | 1.17 | 1.19 | 0.10 | 8.67 | 1.35 | 1.00 | 1.13 | 1.14 | 0.05 | 4.73 |
| | Producer J | | - | - | - | - | - | - | - | - | - | - | - | - | - |
| | Producer K | | - | - | - | - | - | - | - | - | - | - | - | - | - |
| TOTAL | | | 4806 | 2.17 | 1.00 | 1.26 | **1.26** | 0.11 | **8.75** | 1.74 | 0.96 | 1.14 | **1.15** | 0.06 | **5.49** |
| | D/t | | | 101.59 | 7.64 | 25.46 | 26.51 | 10.40 | 39.23 | | | | | | |
| | b/t | | | 75.79 | 2.00 | 16.00 | 17.65 | 8.80 | 49.85 | | | | | | |

| CSA G40.21 – 350W AND ASTM A500 SINGLE OR DUAL CERTIFIED | | | Count | S136A | | | | | | S136B | | | | | | WEIGHTED AVERAGE | | | | | |
|---|---|---|---|---|---|---|---|---|---|---|---|---|---|---|---|---|---|---|---|---|---|
| | | | | MAX. | MIN. | MED. | AVG. | ST.DEV | CV | MAX. | MIN. | MED. | AVG. | ST.DEV | CV | MAX. | MIN. | MED. | AVG. | ST.DEV | CV |
| TYPE | Producer A | | 2932 | 1.65 | 1.12 | 1.42 | 1.42 | 0.08 | 5.76 | 1.78 | 1.15 | 1.46 | 1.47 | 0.10 | 6.58 | 1.75 | 1.15 | 1.44 | 1.44 | 0.09 | 6.37 |
| shaped (SHS) | | Plant A | - | - | - | - | - | - | - | - | - | - | - | - | - | - | - | - | - | - | - |
| NOMINAL | | Plant B | - | - | - | - | - | - | - | - | - | - | - | - | - | - | - | - | - | - | - |
| Fy (MPa) | | Plant C | - | - | - | - | - | - | - | - | - | - | - | - | - | - | - | - | - | - | - |
| 345 | | Plant D | - | - | - | - | - | - | - | - | - | - | - | - | - | - | - | - | - | - | - |
| Fu (MPa) | | Plant undefined | 2932 | 1.65 | 1.12 | 1.42 | 1.42 | 0.08 | 5.76 | 1.78 | 1.15 | 1.46 | 1.47 | 0.10 | 6.58 | 1.75 | 1.15 | 1.44 | 1.44 | 0.09 | 6.37 |
| 450 | Producer B | | - | - | - | - | - | - | - | - | - | - | - | - | - | - | - | - | - | - | - |
| KL/r limit | Producer C | | 10 | 2.04 | 1.30 | 1.66 | 1.69 | 0.20 | 12.12 | 2.27 | 1.33 | 1.97 | 1.93 | 0.25 | 13.07 | 2.13 | 1.33 | 1.73 | 1.76 | 0.22 | 12.66 |
| NONE | Producer D | | - | - | - | - | - | - | - | - | - | - | - | - | - | - | - | - | - | - | - |
| b/t limit | Producer E | | 241 | 1.56 | 1.21 | 1.43 | 1.43 | 0.08 | 5.95 | 1.58 | 1.23 | 1.43 | 1.42 | 0.08 | 5.61 | 1.60 | 1.20 | 1.42 | 1.42 | 0.08 | 5.95 |
| NONE | Producer F | | 130 | 1.64 | 1.21 | 1.41 | 1.44 | 0.12 | 8.67 | 1.80 | 1.25 | 1.46 | 1.52 | 0.17 | 11.07 | 1.73 | 1.22 | 1.41 | 1.46 | 0.15 | 10.08 |
| | Producer G | | - | - | - | - | - | - | - | - | - | - | - | - | - | - | - | - | - | - | - |
| | Producer I | | 1493 | 1.71 | 1.18 | 1.35 | 1.36 | 0.08 | 6.17 | 1.74 | 1.21 | 1.42 | 1.43 | 0.10 | 7.10 | 1.75 | 1.18 | 1.36 | 1.38 | 0.10 | 6.95 |
| | Producer J | | - | - | - | - | - | - | - | - | - | - | - | - | - | - | - | - | - | - | - |
| | Producer K | | - | - | - | - | - | - | - | - | - | - | - | - | - | - | - | - | - | - | - |
| TOTAL | | | 4806 | 2.04 | 1.12 | 1.40 | **1.40** | 0.09 | **6.41** | 2.27 | 1.15 | 1.45 | **1.45** | 0.10 | **7.21** | 2.13 | 1.15 | 1.41 | **1.42** | 0.10 | **7.11** |

Table A- 9: Results for shaped HSS from North American Steel manufacturers – Part 4

## --> b/t up to 22.6 (KL/r = 200) – SHAPED – A500

| ASTM A500 | | | Count | Center Coupon Fy | | | | | | Center Coupon Fu | | | | | |
|---|---|---|---|---|---|---|---|---|---|---|---|---|---|---|---|
| | | | | MAX. | MIN. | MED. | AVG. | ST.DEV | CV | MAX. | MIN. | MED. | AVG. | ST.DEV | CV |
| TYPE | Producer A | | 8245 | 2.00 | 1.00 | 1.29 | 1.29 | 0.10 | 7.50 | 1.84 | 1.01 | 1.22 | 1.23 | 0.08 | 6.42 |
| shaped (SHS) | | Plant A | 103 | 1.55 | 1.13 | 1.34 | 1.35 | 0.08 | 5.99 | 1.45 | 1.09 | 1.31 | 1.30 | 0.06 | 4.31 |
| NOMINAL | | Plant B | 2740 | 1.94 | 1.02 | 1.30 | 1.30 | 0.11 | 8.40 | 1.84 | 1.05 | 1.27 | 1.27 | 0.08 | 6.20 |
| Fy (MPa) | | Plant C | 4994 | 2.00 | 1.01 | 1.29 | 1.29 | 0.09 | 6.82 | 1.76 | 1.01 | 1.20 | 1.21 | 0.07 | 5.74 |
| 345 | | Plant D | 261 | 1.49 | 1.00 | 1.21 | 1.21 | 0.08 | 6.68 | 1.30 | 1.02 | 1.17 | 1.16 | 0.06 | 5.29 |
| Fu (MPa) | | Plant undefined | 147 | 1.55 | 1.07 | 1.30 | 1.28 | 0.10 | 7.71 | 1.53 | 1.08 | 1.21 | 1.20 | 0.07 | 5.87 |
| 425 | Producer B | | 6 | 1.21 | 1.01 | 1.18 | 1.16 | 0.07 | 5.76 | 1.16 | 1.05 | 1.16 | 1.12 | 0.05 | 4.40 |
| KL/r limit | Producer C | | - | - | - | - | - | - | - | - | - | - | - | - | - |
| 200 | Producer D | | - | - | - | - | - | - | - | - | - | - | - | - | - |
| b/t limit | Producer E | | - | - | - | - | - | - | - | - | - | - | - | - | - |
| 22.6 | Producer F | | - | - | - | - | - | - | - | - | - | - | - | - | - |
| | Producer G | | 3 | 1.21 | 1.21 | 1.21 | 1.21 | 0.00 | 0.00 | 1.17 | 1.17 | 1.17 | 1.17 | 0.00 | 0.00 |
| | Producer I | | - | - | - | - | - | - | - | - | - | - | - | - | - |
| | Producer J | | 44 | 1.34 | 0.97 | 1.14 | 1.15 | 0.11 | 9.30 | 1.48 | 1.01 | 1.15 | 1.18 | 0.09 | 7.75 |
| | Producer K | | 2 | 1.08 | 1.08 | 1.08 | 1.08 | 0.00 | 0.00 | 1.03 | 1.03 | 1.03 | 1.03 | 0.00 | 0.00 |
| TOTAL | | | 8300 | 2.00 | 0.97 | 1.29 | **1.29** | 0.10 | **7.56** | 1.84 | 1.01 | 1.22 | **1.23** | 0.08 | **6.45** |
| | | D/t | | 32.59 | 7.64 | 20.37 | 20.86 | 5.74 | 27.51 | | | | | | |
| | | b/t | | 21.60 | 2.00 | 12.00 | 12.94 | 4.57 | 35.29 | | | | | | |

| ASTM A500 | | | Count | S136A | | | | | | S136B | | | | | | WEIGHTED AVERAGE | | | | | |
|---|---|---|---|---|---|---|---|---|---|---|---|---|---|---|---|---|---|---|---|---|---|
| | | | | MAX. | MIN. | MED. | AVG. | ST.DEV | CV | MAX. | MIN. | MED. | AVG. | ST.DEV | CV | MAX. | MIN. | MED. | AVG. | ST.DEV | CV |
| TYPE | Producer A | | 8245 | 1.81 | 1.17 | 1.39 | 1.39 | 0.06 | 4.64 | 2.27 | 1.22 | 1.49 | 1.49 | 0.10 | 6.86 | 1.98 | 1.19 | 1.46 | 1.46 | 0.09 | 6.24 |
| shaped (SHS) | | Plant A | 103 | 1.53 | 1.27 | 1.42 | 1.42 | 0.05 | 3.49 | 1.78 | 1.34 | 1.61 | 1.60 | 0.08 | 4.85 | 1.66 | 1.31 | 1.54 | 1.53 | 0.07 | 4.28 |
| NOMINAL | | Plant B | 2740 | 1.71 | 1.17 | 1.40 | 1.39 | 0.07 | 5.16 | 2.27 | 1.22 | 1.53 | 1.54 | 0.11 | 7.19 | 1.86 | 1.19 | 1.48 | 1.48 | 0.10 | 6.68 |
| Fy (MPa) | | Plant C | 4994 | 1.81 | 1.19 | 1.39 | 1.39 | 0.06 | 4.36 | 2.17 | 1.22 | 1.47 | 1.47 | 0.09 | 6.12 | 1.98 | 1.21 | 1.45 | 1.45 | 0.08 | 5.79 |
| 345 | | Plant D | 261 | 1.50 | 1.25 | 1.37 | 1.36 | 0.05 | 3.38 | 1.60 | 1.25 | 1.44 | 1.43 | 0.08 | 5.30 | 1.63 | 1.23 | 1.39 | 1.39 | 0.07 | 5.37 |
| Fu (MPa) | | Plant undefined | 147 | 1.53 | 1.25 | 1.38 | 1.37 | 0.07 | 4.83 | 1.88 | 1.31 | 1.47 | 1.46 | 0.09 | 6.35 | 1.64 | 1.25 | 1.44 | 1.44 | 0.09 | 6.34 |
| 425 | Producer B | | 6 | 1.31 | 1.18 | 1.29 | 1.28 | 0.04 | 3.47 | 1.39 | 1.22 | 1.37 | 1.34 | 0.06 | 4.54 | 1.35 | 1.18 | 1.35 | 1.32 | 0.06 | 4.70 |
| KL/r limit | Producer C | | - | - | - | - | - | - | - | - | - | - | - | - | - | - | - | - | - | - | - |
| 200 | Producer D | | - | - | - | - | - | - | - | - | - | - | - | - | - | - | - | - | - | - | - |
| b/t limit | Producer E | | - | - | - | - | - | - | - | - | - | - | - | - | - | - | - | - | - | - | - |
| 22.6 | Producer F | | - | - | - | - | - | - | - | - | - | - | - | - | - | - | - | - | - | - | - |
| | Producer G | | 3 | 1.34 | 1.34 | 1.34 | 1.34 | 0.00 | 0.00 | 1.43 | 1.43 | 1.43 | 1.43 | 0.00 | 0.00 | 1.39 | 1.39 | 1.39 | 1.39 | 0.00 | 0.00 |
| | Producer I | | - | - | - | - | - | - | - | - | - | - | - | - | - | - | - | - | - | - | - |
| | Producer J | | 44 | 1.42 | 1.20 | 1.33 | 1.33 | 0.06 | 4.51 | 1.65 | 1.25 | 1.41 | 1.44 | 0.10 | 7.21 | 1.53 | 1.17 | 1.36 | 1.36 | 0.10 | 7.68 |
| | Producer K | | 2 | 1.31 | 1.31 | 1.31 | 1.31 | 0.00 | 0.00 | 1.27 | 1.27 | 1.27 | 1.27 | 0.00 | 0.00 | 1.24 | 1.24 | 1.24 | 1.24 | 0.00 | 0.00 |
| TOTAL | | | 8300 | 1.81 | 1.17 | 1.39 | **1.39** | 0.06 | **4.66** | 2.27 | 1.22 | 1.49 | **1.49** | 0.10 | **6.88** | 1.98 | 1.17 | 1.46 | **1.46** | 0.09 | **6.28** |

Table A- 10: Results for shaped HSS from North American Steel manufacturers – Part 5

## --> b/t up to 22.6 (KL/r = 200) – SHAPED – A1085

| A1085 | | | Count | Center Coupon Fy | | | | | | Center Coupon Fu | | | | | |
|---|---|---|---|---|---|---|---|---|---|---|---|---|---|---|---|
| | | | | MAX. | MIN. | MED. | AVG. | ST.DEV | CV | MAX. | MIN. | MED. | AVG. | ST.DEV | CV |
| TYPE | Producer A | | 708 | 1.40 | 1.03 | 1.30 | 1.29 | 0.07 | 5.60 | 1.32 | 1.02 | 1.16 | 1.16 | 0.06 | 4.83 |
| shaped (SHS) | | Plant A | - | - | - | - | - | - | - | - | - | - | - | - | - |
| | | Plant B | - | - | - | - | - | - | - | - | - | - | - | - | - |
| NOMINAL | | Plant C | - | - | - | - | - | - | - | - | - | - | - | - | - |
| Fy (MPa) | | Plant D | - | - | - | - | - | - | - | - | - | - | - | - | - |
| 345 | | Plant undefined | 708 | 1.40 | 1.03 | 1.30 | 1.29 | 0.07 | 5.60 | 1.32 | 1.02 | 1.16 | 1.16 | 0.06 | 4.83 |
| Fu (MPa) | Producer B | | - | - | - | - | - | - | - | - | - | - | - | - | - |
| 450 | Producer C | | - | - | - | - | - | - | - | - | - | - | - | - | - |
| KL/r limit | Producer D | | - | - | - | - | - | - | - | - | - | - | - | - | - |
| 200 | Producer E | | - | - | - | - | - | - | - | - | - | - | - | - | - |
| b/t limit | Producer F | | - | - | - | - | - | - | - | - | - | - | - | - | - |
| 22.6 | Producer G | | - | - | - | - | - | - | - | - | - | - | - | - | - |
| | Producer I | | - | - | - | - | - | - | - | - | - | - | - | - | - |
| | Producer J | | - | - | - | - | - | - | - | - | - | - | - | - | - |
| | Producer K | | - | - | - | - | - | - | - | - | - | - | - | - | - |
| TOTAL | | | 708 | 1.40 | 1.03 | 1.30 | **1.29** | 0.07 | **5.60** | 1.32 | 1.02 | 1.16 | **1.16** | 0.06 | **4.83** |
| | D/t | | | 32.59 | 10.19 | 20.37 | 20.87 | 5.44 | 26.05 | | | | | | |
| | b/t | | | 21.60 | 4.00 | 12.00 | 13.51 | 4.64 | 34.34 | | | | | | |

| A1085 | | | Count | S136A | | | | | | S136B | | | | | | WEIGHTED AVERAGE | | | | | |
|---|---|---|---|---|---|---|---|---|---|---|---|---|---|---|---|---|---|---|---|---|---|
| | | | | MAX. | MIN. | MED. | AVG. | ST.DEV | CV | MAX. | MIN. | MED. | AVG. | ST.DEV | CV | MAX. | MIN. | MED. | AVG. | ST.DEV | CV |
| TYPE | Producer A | | 708 | 1.56 | 1.23 | 1.44 | 1.44 | 0.06 | 4.21 | 1.68 | 1.28 | 1.50 | 1.50 | 0.08 | 5.23 | 1.58 | 1.24 | 1.47 | 1.46 | 0.07 | 4.88 |
| shaped (SHS) | | Plant A | - | - | - | - | - | - | - | - | - | - | - | - | - | - | - | - | - | - | - |
| | | Plant B | - | - | - | - | - | - | - | - | - | - | - | - | - | - | - | - | - | - | - |
| NOMINAL | | Plant C | - | - | - | - | - | - | - | - | - | - | - | - | - | - | - | - | - | - | - |
| Fy (MPa) | | Plant D | - | - | - | - | - | - | - | - | - | - | - | - | - | - | - | - | - | - | - |
| 345 | | Plant undefined | 708 | 1.56 | 1.23 | 1.44 | 1.44 | 0.06 | 4.21 | 1.68 | 1.28 | 1.50 | 1.50 | 0.08 | 5.23 | 1.58 | 1.24 | 1.47 | 1.46 | 0.07 | 4.88 |
| Fu (MPa) | Producer B | | - | - | - | - | - | - | - | - | - | - | - | - | - | - | - | - | - | - | - |
| 450 | Producer C | | - | - | - | - | - | - | - | - | - | - | - | - | - | - | - | - | - | - | - |
| KL/r limit | Producer D | | - | - | - | - | - | - | - | - | - | - | - | - | - | - | - | - | - | - | - |
| 200 | Producer E | | - | - | - | - | - | - | - | - | - | - | - | - | - | - | - | - | - | - | - |
| b/t limit | Producer F | | - | - | - | - | - | - | - | - | - | - | - | - | - | - | - | - | - | - | - |
| 22.6 | Producer G | | - | - | - | - | - | - | - | - | - | - | - | - | - | - | - | - | - | - | - |
| | Producer I | | - | - | - | - | - | - | - | - | - | - | - | - | - | - | - | - | - | - | - |
| | Producer J | | - | - | - | - | - | - | - | - | - | - | - | - | - | - | - | - | - | - | - |
| | Producer K | | - | - | - | - | - | - | - | - | - | - | - | - | - | - | - | - | - | - | - |
| TOTAL | | | 708 | 1.56 | 1.23 | 1.44 | **1.44** | 0.06 | **4.21** | 1.68 | 1.28 | 1.50 | **1.50** | 0.08 | **5.23** | 1.58 | 1.24 | 1.47 | **1.46** | 0.07 | **4.88** |

Table A- 11: Results for shaped HSS from North American Steel manufacturers – Part 6

## --> b/t up to 22.6 (KL/r = 200) – SHAPED – CSA G40.21

| CSA G40.21 – 350W AND ASTM A500 SINGLE OR DUAL CERTIFIED | | | Count | Center Coupon Fy | | | | | | Center Coupon Fu | | | | | |
|---|---|---|---|---|---|---|---|---|---|---|---|---|---|---|---|
| | | | | MAX. | MIN. | MED. | AVG. | ST.DEV | CV | MAX. | MIN. | MED. | AVG. | ST.DEV | CV |
| TYPE shaped (SHS) | Producer A | | 2285 | 1.67 | 1.02 | 1.30 | 1.31 | 0.09 | 6.84 | 1.37 | 0.97 | 1.16 | 1.16 | 0.06 | 5.12 |
| NOMINAL | | Plant A | - | - | - | - | - | - | - | - | - | - | - | - | - |
| Fy (MPa) 345 | | Plant B | - | - | - | - | - | - | - | - | - | - | - | - | - |
| | | Plant C | - | - | - | - | - | - | - | - | - | - | - | - | - |
| Fu (MPa) 450 | | Plant D | - | - | - | - | - | - | - | - | - | - | - | - | - |
| KL/r limit 200 | | Plant undefined | 2285 | 1.67 | 1.02 | 1.30 | 1.31 | 0.09 | 6.84 | 1.37 | 0.97 | 1.16 | 1.16 | 0.06 | 5.12 |
| b/t limit 22.6 | Producer B | | - | - | - | - | - | - | - | - | - | - | - | - | - |
| | Producer C | | - | - | - | - | - | - | - | - | - | - | - | - | - |
| | Producer D | | - | - | - | - | - | - | - | - | - | - | - | - | - |
| | Producer E | | 219 | 1.46 | 1.03 | 1.28 | 1.29 | 0.08 | 6.21 | 1.21 | 1.00 | 1.12 | 1.11 | 0.05 | 4.35 |
| | Producer F | | 104 | 1.65 | 1.07 | 1.31 | 1.32 | 0.18 | 13.44 | 1.38 | 1.04 | 1.18 | 1.21 | 0.11 | 9.15 |
| | Producer G | | - | - | - | - | - | - | - | - | - | - | - | - | - |
| | Producer I | | 1046 | 1.75 | 1.00 | 1.19 | 1.20 | 0.11 | 9.13 | 1.35 | 1.00 | 1.14 | 1.15 | 0.06 | 4.86 |
| | Producer J | | - | - | - | - | - | - | - | - | - | - | - | - | - |
| | Producer K | | - | - | - | - | - | - | - | - | - | - | - | - | - |
| TOTAL | | | 3654 | 1.75 | 1.00 | 1.28 | **1.28** | 0.11 | **8.60** | 1.38 | 0.97 | 1.15 | **1.16** | 0.06 | **5.34** |
| | | D/t | | 33.86 | 7.64 | 20.45 | 21.95 | 5.93 | 27.00 | | | | | | |
| | | b/t | | 22.60 | 2.00 | 12.06 | 13.65 | 4.74 | 34.73 | | | | | | |

| CSA G40.21 – 350W AND ASTM A500 SINGLE OR DUAL CERTIFIED | | | Count | S136A | | | | | | S136B | | | | | | WEIGHTED AVERAGE | | | | | |
|---|---|---|---|---|---|---|---|---|---|---|---|---|---|---|---|---|---|---|---|---|---|
| | | | | MAX. | MIN. | MED. | AVG. | ST.DEV | CV | MAX. | MIN. | MED. | AVG. | ST.DEV | CV | MAX. | MIN. | MED. | AVG. | ST.DEV | CV |
| TYPE shaped (SHS) | Producer A | | 2285 | 1.65 | 1.21 | 1.44 | 1.44 | 0.07 | 4.83 | 1.78 | 1.19 | 1.49 | 1.49 | 0.09 | 5.78 | 1.75 | 1.17 | 1.46 | 1.47 | 0.08 | 5.74 |
| NOMINAL | | Plant A | - | - | - | - | - | - | - | - | - | - | - | - | - | - | - | - | - | - | - |
| Fy (MPa) 345 | | Plant B | - | - | - | - | - | - | - | - | - | - | - | - | - | - | - | - | - | - | - |
| | | Plant C | - | - | - | - | - | - | - | - | - | - | - | - | - | - | - | - | - | - | - |
| Fu (MPa) 450 | | Plant D | - | - | - | - | - | - | - | - | - | - | - | - | - | - | - | - | - | - | - |
| KL/r limit 200 | | Plant undefined | 2285 | 1.65 | 1.21 | 1.44 | 1.44 | 0.07 | 4.83 | 1.78 | 1.19 | 1.49 | 1.49 | 0.09 | 5.78 | 1.75 | 1.17 | 1.46 | 1.47 | 0.08 | 5.74 |
| b/t limit 22.6 | Producer B | | - | - | - | - | - | - | - | - | - | - | - | - | - | - | - | - | - | - | - |
| | Producer C | | - | - | - | - | - | - | - | - | - | - | - | - | - | - | - | - | - | - | - |
| | Producer D | | - | - | - | - | - | - | - | - | - | - | - | - | - | - | - | - | - | - | - |
| | Producer E | | 219 | 1.56 | 1.22 | 1.44 | 1.44 | 0.07 | 4.79 | 1.58 | 1.23 | 1.44 | 1.44 | 0.07 | 4.82 | 1.60 | 1.20 | 1.44 | 1.43 | 0.07 | 5.15 |
| | Producer F | | 104 | 1.64 | 1.31 | 1.48 | 1.47 | 0.11 | 7.68 | 1.80 | 1.34 | 1.54 | 1.56 | 0.16 | 10.23 | 1.73 | 1.30 | 1.49 | 1.49 | 0.14 | 9.43 |
| | Producer G | | - | - | - | - | - | - | - | - | - | - | - | - | - | - | - | - | - | - | - |
| | Producer I | | 1046 | 1.71 | 1.20 | 1.38 | 1.38 | 0.08 | 5.65 | 1.74 | 1.24 | 1.45 | 1.46 | 0.09 | 6.28 | 1.75 | 1.20 | 1.39 | 1.40 | 0.09 | 6.73 |
| | Producer J | | - | - | - | - | - | - | - | - | - | - | - | - | - | - | - | - | - | - | - |
| | Producer K | | - | - | - | - | - | - | - | - | - | - | - | - | - | - | - | - | - | - | - |
| TOTAL | | | 3654 | 1.71 | 1.20 | 1.42 | **1.43** | 0.08 | **5.51** | 1.80 | 1.19 | 1.48 | **1.48** | 0.09 | **6.24** | 1.75 | 1.17 | 1.44 | **1.45** | 0.09 | **6.49** |

Table A- 12: Results for shaped HSS from North American Steel manufacturers – Part 7

## --> b/t up to 19.7 (KL/r = 140) – SHAPED – A500

| ASTM A500 | | | Count | Center Coupon Fy | | | | | | Center Coupon Fu | | | | | |
|---|---|---|---|---|---|---|---|---|---|---|---|---|---|---|---|
| | | | | MAX. | MIN. | MED. | AVG. | ST.DEV | CV | MAX. | MIN. | MED. | AVG. | ST.DEV | CV |
| TYPE | Producer A | | 6853 | 2.00 | 1.00 | 1.30 | 1.31 | 0.10 | 7.36 | 1.84 | 1.01 | 1.22 | 1.23 | 0.08 | 6.55 |
| shaped (SHS) | | Plant A | 96 | 1.55 | 1.16 | 1.35 | 1.36 | 0.08 | 5.63 | 1.45 | 1.09 | 1.31 | 1.31 | 0.05 | 4.13 |
| NOMINAL | | Plant B | 2259 | 1.94 | 1.04 | 1.32 | 1.32 | 0.11 | 8.02 | 1.84 | 1.05 | 1.27 | 1.27 | 0.08 | 6.30 |
| Fy (MPa) | | Plant C | 4094 | 2.00 | 1.01 | 1.30 | 1.31 | 0.09 | 6.70 | 1.76 | 1.01 | 1.21 | 1.21 | 0.07 | 5.86 |
| 345 | | Plant D | 261 | 1.49 | 1.00 | 1.21 | 1.21 | 0.08 | 6.68 | 1.30 | 1.02 | 1.17 | 1.16 | 0.06 | 5.29 |
| Fu (MPa) | | Plant undefined | 143 | 1.55 | 1.07 | 1.30 | 1.28 | 0.10 | 7.76 | 1.53 | 1.08 | 1.21 | 1.20 | 0.07 | 5.87 |
| 425 | Producer B | | 1 | 1.18 | 1.18 | 1.18 | 1.18 | 0.00 | 0.00 | 1.16 | 1.16 | 1.16 | 1.16 | 0.00 | 0.00 |
| KL/r limit | Producer C | | - | - | - | - | - | - | - | - | - | - | - | - | - |
| 140 | Producer D | | - | - | - | - | - | - | - | - | - | - | - | - | - |
| b/t limit | Producer E | | - | - | - | - | - | - | - | - | - | - | - | - | - |
| 19.7 | Producer F | | - | - | - | - | - | - | - | - | - | - | - | - | - |
| | Producer G | | 3 | 1.21 | 1.21 | 1.21 | 1.21 | 0.00 | 0.00 | 1.17 | 1.17 | 1.17 | 1.17 | 0.00 | 0.00 |
| | Producer I | | - | - | - | - | - | - | - | - | - | - | - | - | - |
| | Producer J | | 44 | 1.34 | 0.97 | 1.14 | 1.15 | 0.11 | 9.30 | 1.48 | 1.01 | 1.15 | 1.18 | 0.09 | 7.75 |
| | Producer K | | 2 | 1.08 | 1.08 | 1.08 | 1.08 | 0.00 | 0.00 | 1.03 | 1.03 | 1.03 | 1.03 | 0.00 | 0.00 |
| TOTAL | | | 6903 | 2.00 | 0.97 | 1.30 | **1.31** | 0.10 | **7.43** | 1.84 | 1.01 | 1.22 | **1.23** | 0.08 | **6.57** |
| | D/t | | | 30.13 | 7.64 | 20.37 | 19.07 | 4.38 | 22.99 | | | | | | |
| | b/t | | | 19.66 | 2.00 | 12.00 | 11.43 | 3.38 | 29.56 | | | | | | |

| ASTM A500 | | | Count | S136A | | | | | | S136B | | | | | | WEIGHTED AVERAGE | | | | | |
|---|---|---|---|---|---|---|---|---|---|---|---|---|---|---|---|---|---|---|---|---|---|
| | | | | MAX. | MIN. | MED. | AVG. | ST.DEV | CV | MAX. | MIN. | MED. | AVG. | ST.DEV | CV | MAX. | MIN. | MED. | AVG. | ST.DEV | CV |
| TYPE | Producer A | | 6853 | 1.81 | 1.20 | 1.40 | 1.40 | 0.06 | 4.17 | 2.27 | 1.24 | 1.50 | 1.51 | 0.10 | 6.68 | 1.98 | 1.23 | 1.47 | 1.48 | 0.09 | 5.94 |
| shaped (SHS) | | Plant A | 96 | 1.53 | 1.32 | 1.43 | 1.43 | 0.04 | 3.15 | 1.78 | 1.34 | 1.61 | 1.61 | 0.07 | 4.44 | 1.66 | 1.31 | 1.55 | 1.54 | 0.06 | 3.89 |
| NOMINAL | | Plant B | 2259 | 1.71 | 1.24 | 1.41 | 1.41 | 0.06 | 4.51 | 2.27 | 1.27 | 1.55 | 1.56 | 0.10 | 6.70 | 1.86 | 1.24 | 1.50 | 1.50 | 0.09 | 5.99 |
| Fy (MPa) | | Plant C | 4094 | 1.81 | 1.20 | 1.40 | 1.40 | 0.05 | 3.90 | 2.17 | 1.24 | 1.48 | 1.49 | 0.09 | 5.95 | 1.98 | 1.23 | 1.46 | 1.47 | 0.08 | 5.57 |
| 345 | | Plant D | 261 | 1.50 | 1.25 | 1.37 | 1.36 | 0.05 | 3.38 | 1.60 | 1.25 | 1.44 | 1.43 | 0.08 | 5.30 | 1.63 | 1.23 | 1.39 | 1.39 | 0.07 | 5.37 |
| | | Plant undefined | 143 | 1.53 | 1.25 | 1.38 | 1.38 | 0.07 | 4.84 | 1.88 | 1.31 | 1.47 | 1.46 | 0.09 | 6.37 | 1.64 | 1.25 | 1.45 | 1.44 | 0.09 | 6.38 |
| Fu (MPa) | Producer B | | 1 | 1.30 | 1.30 | 1.30 | 1.30 | 0.00 | 0.00 | 1.39 | 1.39 | 1.39 | 1.39 | 0.00 | 0.00 | 1.35 | 1.35 | 1.35 | 1.35 | 0.00 | 0.00 |
| 425 | Producer C | | - | - | - | - | - | - | - | - | - | - | - | - | - | - | - | - | - | - | - |
| KL/r limit | Producer D | | - | - | - | - | - | - | - | - | - | - | - | - | - | - | - | - | - | - | - |
| 140 | Producer E | | - | - | - | - | - | - | - | - | - | - | - | - | - | - | - | - | - | - | - |
| b/t limit | Producer F | | - | - | - | - | - | - | - | - | - | - | - | - | - | - | - | - | - | - | - |
| 19.7 | Producer G | | 3 | 1.34 | 1.34 | 1.34 | 1.34 | 0.00 | 0.00 | 1.43 | 1.43 | 1.43 | 1.43 | 0.00 | 0.00 | 1.39 | 1.39 | 1.39 | 1.39 | 0.00 | 0.00 |
| | Producer I | | - | - | - | - | - | - | - | - | - | - | - | - | - | - | - | - | - | - | - |
| | Producer J | | 44 | 1.42 | 1.20 | 1.33 | 1.33 | 0.06 | 4.51 | 1.65 | 1.25 | 1.41 | 1.44 | 0.10 | 7.21 | 1.53 | 1.17 | 1.36 | 1.36 | 0.10 | 7.68 |
| | Producer K | | 2 | 1.31 | 1.31 | 1.31 | 1.31 | 0.00 | 0.00 | 1.27 | 1.27 | 1.27 | 1.27 | 0.00 | 0.00 | 1.24 | 1.24 | 1.24 | 1.24 | 0.00 | 0.00 |
| TOTAL | | | 6903 | 1.81 | 1.20 | 1.40 | **1.40** | 0.06 | **4.19** | 2.27 | 1.24 | 1.50 | **1.51** | 0.10 | **6.70** | 1.98 | 1.17 | 1.47 | **1.47** | 0.09 | **5.99** |

Table A- 13: Results for shaped HSS from North American Steel manufacturers – Part 8

## --> b/t up to 19.7 (KL/r = 140) – SHAPED – A1085

| A1085 | | | Count | Center Coupon Fy | | | | | | Center Coupon Fu | | | | | |
|---|---|---|---|---|---|---|---|---|---|---|---|---|---|---|---|
| | | | | MAX. | MIN. | MED. | AVG. | ST.DEV | CV | MAX. | MIN. | MED. | AVG. | ST.DEV | CV |
| TYPE | Producer A | | 585 | 1.40 | 1.03 | 1.31 | 1.30 | 0.07 | 5.34 | 1.32 | 1.03 | 1.17 | 1.16 | 0.06 | 4.75 |
| shaped (SHS) | | Plant A | - | - | - | - | - | - | - | - | - | - | - | - | - |
| | | Plant B | - | - | - | - | - | - | - | - | - | - | - | - | - |
| NOMINAL | | Plant C | - | - | - | - | - | - | - | - | - | - | - | - | - |
| Fy (MPa) | | Plant D | - | - | - | - | - | - | - | - | - | - | - | - | - |
| 345 | | Plant undefined | 585 | 1.40 | 1.03 | 1.31 | 1.30 | 0.07 | 5.34 | 1.32 | 1.03 | 1.17 | 1.16 | 0.06 | 4.75 |
| Fu (MPa) | Producer B | | - | - | - | - | - | - | - | - | - | - | - | - | - |
| 450 | Producer C | | - | - | - | - | - | - | - | - | - | - | - | - | - |
| KL/r limit | Producer D | | - | - | - | - | - | - | - | - | - | - | - | - | - |
| 140 | Producer E | | - | - | - | - | - | - | - | - | - | - | - | - | - |
| b/t limit | Producer F | | - | - | - | - | - | - | - | - | - | - | - | - | - |
| 19.7 | Producer G | | - | - | - | - | - | - | - | - | - | - | - | - | - |
| | Producer I | | - | - | - | - | - | - | - | - | - | - | - | - | - |
| | Producer J | | - | - | - | - | - | - | - | - | - | - | - | - | - |
| | Producer K | | - | - | - | - | - | - | - | - | - | - | - | - | - |
| TOTAL | | | 585 | 1.40 | 1.03 | 1.31 | **1.30** | 0.07 | **5.34** | 1.32 | 1.03 | 1.17 | **1.16** | 0.06 | **4.75** |
| | D/t | | | 29.10 | 10.19 | 20.37 | 19.26 | 4.31 | 22.37 | | | | | | |
| | b/t | | | 18.86 | 4.00 | 12.00 | 12.05 | 3.71 | 30.80 | | | | | | |

| A1085 | | | Count | S136A | | | | | | S136B | | | | | | WEIGHTED AVERAGE | | | | | |
|---|---|---|---|---|---|---|---|---|---|---|---|---|---|---|---|---|---|---|---|---|---|
| | | | | MAX. | MIN. | MED. | AVG. | ST.DEV | CV | MAX. | MIN. | MED. | AVG. | ST.DEV | CV | MAX. | MIN. | MED. | AVG. | ST.DEV | CV |
| TYPE | Producer A | | 585 | 1.56 | 1.30 | 1.46 | 1.45 | 0.05 | 3.66 | 1.68 | 1.31 | 1.51 | 1.51 | 0.07 | 4.81 | 1.58 | 1.28 | 1.48 | 1.47 | 0.07 | 4.42 |
| shaped (SHS) | | Plant A | - | - | - | - | - | - | - | - | - | - | - | - | - | - | - | - | - | - | - |
| | | Plant B | - | - | - | - | - | - | - | - | - | - | - | - | - | - | - | - | - | - | - |
| NOMINAL | | Plant C | - | - | - | - | - | - | - | - | - | - | - | - | - | - | - | - | - | - | - |
| Fy (MPa) | | Plant D | - | - | - | - | - | - | - | - | - | - | - | - | - | - | - | - | - | - | - |
| 345 | | Plant undefined | 585 | 1.56 | 1.30 | 1.46 | 1.45 | 0.05 | 3.66 | 1.68 | 1.31 | 1.51 | 1.51 | 0.07 | 4.81 | 1.58 | 1.28 | 1.48 | 1.47 | 0.07 | 4.42 |
| Fu (MPa) | Producer B | | - | - | - | - | - | - | - | - | - | - | - | - | - | - | - | - | - | - | - |
| 450 | Producer C | | - | - | - | - | - | - | - | - | - | - | - | - | - | - | - | - | - | - | - |
| KL/r limit | Producer D | | - | - | - | - | - | - | - | - | - | - | - | - | - | - | - | - | - | - | - |
| 140 | Producer E | | - | - | - | - | - | - | - | - | - | - | - | - | - | - | - | - | - | - | - |
| b/t limit | Producer F | | - | - | - | - | - | - | - | - | - | - | - | - | - | - | - | - | - | - | - |
| 19.7 | Producer G | | - | - | - | - | - | - | - | - | - | - | - | - | - | - | - | - | - | - | - |
| | Producer I | | - | - | - | - | - | - | - | - | - | - | - | - | - | - | - | - | - | - | - |
| | Producer J | | - | - | - | - | - | - | - | - | - | - | - | - | - | - | - | - | - | - | - |
| | Producer K | | - | - | - | - | - | - | - | - | - | - | - | - | - | - | - | - | - | - | - |
| TOTAL | | | 585 | 1.56 | 1.30 | 1.46 | **1.45** | 0.05 | **3.66** | 1.68 | 1.31 | 1.51 | **1.51** | 0.07 | **4.81** | 1.58 | 1.28 | 1.48 | **1.47** | 0.07 | **4.42** |

Table A- 14: Results for shaped HSS from North American Steel manufacturers – Part 9

## --> b/t up to 19.7 (KL/r = 140) – SHAPED – CSA G40.21

| CSA G40.21 - 350W AND ASTM A500 SINGLE OR DUAL CERTIFIED | | | Count | Center Coupon Fy | | | | | | Center Coupon Fu | | | | | |
|---|---|---|---|---|---|---|---|---|---|---|---|---|---|---|---|
| | | | | MAX. | MIN. | MED. | AVG. | ST.DEV | CV | MAX. | MIN. | MED. | AVG. | ST.DEV | CV |
| TYPE | Producer A | | 1803 | 1.67 | 1.05 | 1.32 | 1.32 | 0.09 | 6.56 | 1.37 | 1.00 | 1.16 | 1.17 | 0.06 | 5.09 |
| shaped (SHS) | | Plant A | - | - | - | - | - | - | - | - | - | - | - | - | - |
| | | Plant B | - | - | - | - | - | - | - | - | - | - | - | - | - |
| NOMINAL | | Plant C | - | - | - | - | - | - | - | - | - | - | - | - | - |
| Fy (MPa) | | Plant D | - | - | - | - | - | - | - | - | - | - | - | - | - |
| 345 | | Plant undefined | 1803 | 1.67 | 1.05 | 1.32 | 1.32 | 0.09 | 6.56 | 1.37 | 1.00 | 1.16 | 1.17 | 0.06 | 5.09 |
| Fu (MPa) | Producer B | | - | - | - | - | - | - | - | - | - | - | - | - | - |
| 450 | Producer C | | - | - | - | - | - | - | - | - | - | - | - | - | - |
| KL/r limit | Producer D | | - | - | - | - | - | - | - | - | - | - | - | - | - |
| 140 | Producer E | | 185 | 1.46 | 1.13 | 1.29 | 1.30 | 0.07 | 5.70 | 1.21 | 1.00 | 1.13 | 1.11 | 0.05 | 4.46 |
| b/t limit | Producer F | | 96 | 1.65 | 1.07 | 1.35 | 1.34 | 0.18 | 13.34 | 1.38 | 1.04 | 1.19 | 1.22 | 0.11 | 9.26 |
| 19.7 | Producer G | | - | - | - | - | - | - | - | - | - | - | - | - | - |
| | Producer I | | 860 | 1.65 | 1.00 | 1.19 | 1.20 | 0.11 | 9.11 | 1.35 | 1.02 | 1.14 | 1.16 | 0.06 | 4.97 |
| | Producer J | | - | - | - | - | - | - | - | - | - | - | - | - | - |
| | Producer K | | - | - | - | - | - | - | - | - | - | - | - | - | - |
| TOTAL | | | 2944 | 1.67 | 1.00 | 1.29 | **1.29** | 0.11 | **8.76** | 1.38 | 1.00 | 1.15 | **1.16** | 0.06 | **5.42** |
| | D/t | | | 29.28 | 7.64 | 20.37 | 19.97 | 4.69 | 23.49 | | | | | | |
| | b/t | | | 19.00 | 2.00 | 12.00 | 12.02 | 3.76 | 31.25 | | | | | | |

| CSA G40.21 - 350W AND ASTM A500 SINGLE OR DUAL CERTIFIED | | | Count | S136A | | | | | | S136B | | | | | | WEIGHTED AVERAGE | | | | | |
|---|---|---|---|---|---|---|---|---|---|---|---|---|---|---|---|---|---|---|---|---|---|
| | | | | MAX. | MIN. | MED. | AVG. | ST.DEV | CV | MAX. | MIN. | MED. | AVG. | ST.DEV | CV | MAX. | MIN. | MED. | AVG. | ST.DEV | CV |
| TYPE | Producer A | | 1803 | 1.65 | 1.27 | 1.46 | 1.46 | 0.06 | 4.13 | 1.78 | 1.30 | 1.51 | 1.51 | 0.08 | 5.29 | 1.75 | 1.27 | 1.49 | 1.49 | 0.08 | 5.22 |
| shaped (SHS) | | Plant A | - | - | - | - | - | - | - | - | - | - | - | - | - | - | - | - | - | - | - |
| | | Plant B | - | - | - | - | - | - | - | - | - | - | - | - | - | - | - | - | - | - | - |
| NOMINAL | | Plant C | - | - | - | - | - | - | - | - | - | - | - | - | - | - | - | - | - | - | - |
| Fy (MPa) | | Plant D | - | - | - | - | - | - | - | - | - | - | - | - | - | - | - | - | - | - | - |
| 345 | | Plant undefined | 1803 | 1.65 | 1.27 | 1.46 | 1.46 | 0.06 | 4.13 | 1.78 | 1.30 | 1.51 | 1.51 | 0.08 | 5.29 | 1.75 | 1.27 | 1.49 | 1.49 | 0.08 | 5.22 |
| Fu (MPa) | Producer B | | - | - | - | - | - | - | - | - | - | - | - | - | - | - | - | - | - | - | - |
| 450 | Producer C | | - | - | - | - | - | - | - | - | - | - | - | - | - | - | - | - | - | - | - |
| KL/r limit | Producer D | | - | - | - | - | - | - | - | - | - | - | - | - | - | - | - | - | - | - | - |
| 140 | Producer E | | 185 | 1.56 | 1.31 | 1.47 | 1.46 | 0.06 | 4.04 | 1.58 | 1.30 | 1.46 | 1.45 | 0.07 | 4.59 | 1.60 | 1.29 | 1.45 | 1.45 | 0.07 | 4.77 |
| b/t limit | Producer F | | 96 | 1.64 | 1.34 | 1.53 | 1.48 | 0.11 | 7.21 | 1.60 | 1.36 | 1.55 | 1.57 | 0.16 | 9.93 | 1.73 | 1.30 | 1.50 | 1.51 | 0.14 | 9.11 |
| 19.7 | Producer G | | - | - | - | - | - | - | - | - | - | - | - | - | - | - | - | - | - | - | - |
| | Producer I | | 860 | 1.64 | 1.23 | 1.39 | 1.39 | 0.08 | 5.54 | 1.74 | 1.29 | 1.46 | 1.47 | 0.09 | 6.17 | 1.74 | 1.23 | 1.40 | 1.41 | 0.09 | 6.71 |
| | Producer J | | - | - | - | - | - | - | - | - | - | - | - | - | - | - | - | - | - | - | - |
| | Producer K | | - | - | - | - | - | - | - | - | - | - | - | - | - | - | - | - | - | - | - |
| TOTAL | | | 2944 | 1.65 | 1.23 | 1.45 | **1.44** | 0.08 | **5.22** | 1.80 | 1.29 | 1.49 | **1.50** | 0.09 | **5.98** | 1.75 | 1.23 | 1.46 | **1.46** | 0.09 | **6.35** |

Table A- 15: Results for shaped HSS from North American Steel manufacturers – Part 10

## --> b/t up to 17.7 (KL/r = 100) – SHAPED – A500

| ASTM A500 | | | Count | Center Coupon Fy | | | | | | Center Coupon Fu | | | | | |
|---|---|---|---|---|---|---|---|---|---|---|---|---|---|---|---|
| | | | | MAX. | MIN. | MED. | AVG. | ST.DEV | CV | MAX. | MIN. | MED. | AVG. | ST.DEV | CV |
| TYPE | Producer A | | 6799 | 2.00 | 1.00 | 1.30 | 1.31 | 0.10 | 7.36 | 1.84 | 1.01 | 1.22 | 1.23 | 0.08 | 6.56 |
| shaped (SHS) | | Plant A | 96 | 1.55 | 1.16 | 1.35 | 1.36 | 0.08 | 5.63 | 1.45 | 1.09 | 1.31 | 1.31 | 0.05 | 4.13 |
| NOMINAL | | Plant B | 2259 | 1.94 | 1.04 | 1.32 | 1.32 | 0.11 | 8.02 | 1.84 | 1.05 | 1.27 | 1.27 | 0.08 | 6.30 |
| Fy (MPa) | | Plant C | 4094 | 2.00 | 1.01 | 1.30 | 1.31 | 0.09 | 6.70 | 1.76 | 1.01 | 1.21 | 1.21 | 0.07 | 5.86 |
| 345 | | Plant D | 261 | 1.49 | 1.00 | 1.21 | 1.21 | 0.08 | 6.68 | 1.30 | 1.02 | 1.17 | 1.16 | 0.06 | 5.29 |
| Fu (MPa) | | Plant undefined | 89 | 1.55 | 1.07 | 1.30 | 1.30 | 0.11 | 8.39 | 1.53 | 1.08 | 1.20 | 1.20 | 0.08 | 6.37 |
| 450 | Producer B | | 1 | 1.18 | 1.18 | 1.18 | 1.18 | 0.00 | 0.00 | 1.16 | 1.16 | 1.16 | 1.16 | 0.00 | 0.00 |
| KL/r limit | Producer C | | - | - | - | - | - | - | - | - | - | - | - | - | - |
| 100 | Producer D | | - | - | - | - | - | - | - | - | - | - | - | - | - |
| b/t limit | Producer E | | - | - | - | - | - | - | - | - | - | - | - | - | - |
| 17.7 | Producer F | | - | - | - | - | - | - | - | - | - | - | - | - | - |
| | Producer G | | 3 | 1.21 | 1.21 | 1.21 | 1.21 | 0.00 | 0.00 | 1.17 | 1.17 | 1.17 | 1.17 | 0.00 | 0.00 |
| | Producer I | | - | - | - | - | - | - | - | - | - | - | - | - | - |
| | Producer J | | 44 | 1.34 | 0.97 | 1.14 | 1.15 | 0.11 | 9.30 | 1.48 | 1.01 | 1.15 | 1.18 | 0.09 | 7.75 |
| | Producer K | | 2 | 1.08 | 1.08 | 1.08 | 1.08 | 0.00 | 0.00 | 1.03 | 1.03 | 1.03 | 1.03 | 0.00 | 0.00 |
| TOTAL | | | 6849 | 2.00 | 0.97 | 1.30 | **1.31** | 0.10 | **7.44** | 1.84 | 1.01 | 1.22 | **1.23** | 0.08 | **6.58** |
| | D/t | | | 27.37 | 7.64 | 20.37 | 18.99 | 4.30 | 22.66 | | | | | | |
| | b/t | | | 17.50 | 2.00 | 12.00 | 11.37 | 3.32 | 29.22 | | | | | | |

| ASTM A500 | | | Count | S136A | | | | | | S136B | | | | | | WEIGHTED AVERAGE | | | | | |
|---|---|---|---|---|---|---|---|---|---|---|---|---|---|---|---|---|---|---|---|---|---|
| | | | | MAX. | MIN. | MED. | AVG. | ST.DEV | CV | MAX. | MIN. | MED. | AVG. | ST.DEV | CV | MAX. | MIN. | MED. | AVG. | ST.DEV | CV |
| TYPE | Producer A | | 6799 | 1.81 | 1.20 | 1.40 | 1.40 | 0.06 | 4.15 | 2.27 | 1.24 | 1.50 | 1.51 | 0.10 | 6.67 | 1.98 | 1.23 | 1.47 | 1.48 | 0.09 | 5.94 |
| shaped (SHS) | | Plant A | 96 | 1.53 | 1.32 | 1.43 | 1.43 | 0.04 | 3.15 | 1.78 | 1.34 | 1.61 | 1.61 | 0.07 | 4.44 | 1.66 | 1.31 | 1.55 | 1.54 | 0.06 | 3.89 |
| NOMINAL | | Plant B | 2259 | 1.71 | 1.24 | 1.41 | 1.41 | 0.06 | 4.51 | 2.27 | 1.27 | 1.55 | 1.56 | 0.10 | 6.70 | 1.86 | 1.24 | 1.50 | 1.50 | 0.09 | 5.99 |
| Fy (MPa) | | Plant C | 4094 | 1.81 | 1.20 | 1.40 | 1.40 | 0.05 | 3.90 | 2.17 | 1.24 | 1.48 | 1.49 | 0.09 | 5.95 | 1.98 | 1.23 | 1.46 | 1.47 | 0.08 | 5.57 |
| 345 | | Plant D | 261 | 1.50 | 1.25 | 1.37 | 1.36 | 0.05 | 3.38 | 1.60 | 1.25 | 1.44 | 1.43 | 0.08 | 5.30 | 1.63 | 1.23 | 1.39 | 1.39 | 0.07 | 5.37 |
| Fu (MPa) | | Plant undefined | 89 | 1.53 | 1.26 | 1.40 | 1.40 | 0.07 | 4.77 | 1.88 | 1.31 | 1.48 | 1.47 | 0.10 | 6.67 | 1.64 | 1.25 | 1.46 | 1.45 | 0.10 | 6.66 |
| 450 | Producer B | | 1 | 1.30 | 1.30 | 1.30 | 1.30 | 0.00 | 0.00 | 1.39 | 1.39 | 1.39 | 1.39 | 0.00 | 0.00 | 1.35 | 1.35 | 1.35 | 1.35 | 0.00 | 0.00 |
| KL/r limit | Producer C | | - | - | - | - | - | - | - | - | - | - | - | - | - | - | - | - | - | - | - |
| 100 | Producer D | | - | - | - | - | - | - | - | - | - | - | - | - | - | - | - | - | - | - | - |
| b/t limit | Producer E | | - | - | - | - | - | - | - | - | - | - | - | - | - | - | - | - | - | - | - |
| 17.7 | Producer F | | - | - | - | - | - | - | - | - | - | - | - | - | - | - | - | - | - | - | - |
| | Producer G | | 3 | 1.34 | 1.34 | 1.34 | 1.34 | 0.00 | 0.00 | 1.43 | 1.43 | 1.43 | 1.43 | 0.00 | 0.00 | 1.39 | 1.39 | 1.39 | 1.39 | 0.00 | 0.00 |
| | Producer I | | - | - | - | - | - | - | - | - | - | - | - | - | - | - | - | - | - | - | - |
| | Producer J | | 44 | 1.42 | 1.20 | 1.33 | 1.33 | 0.06 | 4.51 | 1.65 | 1.25 | 1.41 | 1.44 | 0.10 | 7.21 | 1.53 | 1.17 | 1.36 | 1.36 | 0.10 | 7.68 |
| | Producer K | | 2 | 1.31 | 1.31 | 1.31 | 1.31 | 0.00 | 0.00 | 1.27 | 1.27 | 1.27 | 1.27 | 0.00 | 0.00 | 1.24 | 1.24 | 1.24 | 1.24 | 0.00 | 0.00 |
| TOTAL | | | 6849 | 1.81 | 1.20 | 1.40 | **1.40** | 0.06 | **4.18** | 2.27 | 1.24 | 1.50 | **1.51** | 0.10 | **6.69** | 1.98 | 1.17 | 1.47 | **1.47** | 0.09 | **5.99** |

Table A- 16: Results for shaped HSS from North American Steel manufacturers – Part 11

## --> b/t up to 17.7 (KL/r = 100) – SHAPED – A1085

| A1085 | | | Count | Center Coupon Fy | | | | | | Center Coupon Fu | | | | | |
|---|---|---|---|---|---|---|---|---|---|---|---|---|---|---|---|
| | | | | MAX. | MIN. | MED. | AVG. | ST.DEV | CV | MAX. | MIN. | MED. | AVG. | ST.DEV | CV |
| TYPE | Producer A | | 571 | 1.40 | 1.03 | 1.31 | 1.30 | 0.07 | 5.36 | 1.32 | 1.03 | 1.17 | 1.16 | 0.06 | 4.78 |
| shaped (SHS) | | Plant A | - | - | - | - | - | - | - | - | - | - | - | - | - |
| | | Plant B | - | - | - | - | - | - | - | - | - | - | - | - | - |
| NOMINAL | | Plant C | - | - | - | - | - | - | - | - | - | - | - | - | - |
| Fy (MPa) | | Plant D | - | - | - | - | - | - | - | - | - | - | - | - | - |
| 345 | | Plant undefined | 571 | 1.40 | 1.03 | 1.31 | 1.30 | 0.07 | 5.36 | 1.32 | 1.03 | 1.17 | 1.16 | 0.06 | 4.78 |
| Fu (MPa) | Producer B | | - | - | - | - | - | - | - | - | - | - | - | - | - |
| 450 | Producer C | | - | - | - | - | - | - | - | - | - | - | - | - | - |
| KL/r limit | Producer D | | - | - | - | - | - | - | - | - | - | - | - | - | - |
| 100 | Producer E | | - | - | - | - | - | - | - | - | - | - | - | - | - |
| b/t limit | Producer F | | - | - | - | - | - | - | - | - | - | - | - | - | - |
| 17.7 | Producer G | | - | - | - | - | - | - | - | - | - | - | - | - | - |
| | Producer I | | - | - | - | - | - | - | - | - | - | - | - | - | - |
| | Producer J | | - | - | - | - | - | - | - | - | - | - | - | - | - |
| | Producer K | | - | - | - | - | - | - | - | - | - | - | - | - | - |
| TOTAL | | | 571 | 1.40 | 1.03 | 1.31 | **1.30** | 0.07 | **5.36** | 1.32 | 1.03 | 1.17 | **1.16** | 0.06 | **4.78** |
| | D/t | | | 27.16 | 10.19 | 20.37 | 19.15 | 4.26 | 22.25 | | | | | | |
| | b/t | | | 17.33 | 4.00 | 12.00 | 11.90 | 3.62 | 30.42 | | | | | | |

| A1085 | | | Count | S136A | | | | | | S136B | | | | | | WEIGHTED AVERAGE | | | | | |
|---|---|---|---|---|---|---|---|---|---|---|---|---|---|---|---|---|---|---|---|---|---|
| | | | | MAX. | MIN. | MED. | AVG. | ST.DEV | CV | MAX. | MIN. | MED. | AVG. | ST.DEV | CV | MAX. | MIN. | MED. | AVG. | ST.DEV | CV |
| TYPE | Producer A | | 571 | 1.56 | 1.30 | 1.46 | 1.45 | 0.05 | 3.65 | 1.68 | 1.31 | 1.51 | 1.51 | 0.07 | 4.84 | 1.58 | 1.28 | 1.48 | 1.47 | 0.07 | 4.44 |
| shaped (SHS) | | Plant A | - | - | - | - | - | - | - | - | - | - | - | - | - | - | - | - | - | - | - |
| | | Plant B | - | - | - | - | - | - | - | - | - | - | - | - | - | - | - | - | - | - | - |
| NOMINAL | | Plant C | - | - | - | - | - | - | - | - | - | - | - | - | - | - | - | - | - | - | - |
| Fy (MPa) | | Plant D | - | - | - | - | - | - | - | - | - | - | - | - | - | - | - | - | - | - | - |
| 345 | | Plant undefined | 571 | 1.56 | 1.30 | 1.46 | 1.45 | 0.05 | 3.65 | 1.68 | 1.31 | 1.51 | 1.51 | 0.07 | 4.84 | 1.58 | 1.28 | 1.48 | 1.47 | 0.07 | 4.44 |
| Fu (MPa) | Producer B | | - | - | - | - | - | - | - | - | - | - | - | - | - | - | - | - | - | - | - |
| 450 | Producer C | | - | - | - | - | - | - | - | - | - | - | - | - | - | - | - | - | - | - | - |
| KL/r limit | Producer D | | - | - | - | - | - | - | - | - | - | - | - | - | - | - | - | - | - | - | - |
| 100 | Producer E | | - | - | - | - | - | - | - | - | - | - | - | - | - | - | - | - | - | - | - |
| b/t limit | Producer F | | - | - | - | - | - | - | - | - | - | - | - | - | - | - | - | - | - | - | - |
| 17.7 | Producer G | | - | - | - | - | - | - | - | - | - | - | - | - | - | - | - | - | - | - | - |
| | Producer I | | - | - | - | - | - | - | - | - | - | - | - | - | - | - | - | - | - | - | - |
| | Producer J | | - | - | - | - | - | - | - | - | - | - | - | - | - | - | - | - | - | - | - |
| | Producer K | | - | - | - | - | - | - | - | - | - | - | - | - | - | - | - | - | - | - | - |
| TOTAL | | | 571 | 1.56 | 1.30 | 1.46 | **1.45** | 0.05 | **3.65** | 1.68 | 1.31 | 1.51 | **1.51** | 0.07 | **4.84** | 1.58 | 1.28 | 1.48 | **1.47** | 0.07 | **4.44** |

Table A- 17: Results for shaped HSS from North American Steel manufacturers – Part 12

## --> b/t up to 17.7 (KL/r = 100) – SHAPED – CSA G40.21

| CSA G40.21 – 350W AND ASTM A500 SINGLE OR DUAL CERTIFIED | | | Count | Center Coupon Fy | | | | | | Center Coupon Fu | | | | | |
|---|---|---|---|---|---|---|---|---|---|---|---|---|---|---|---|
| | | | | MAX. | MIN. | MED. | AVG. | ST.DEV | CV | MAX. | MIN. | MED. | AVG. | ST.DEV | CV |
| TYPE | Producer A | | 1750 | 1.67 | 1.05 | 1.31 | 1.32 | 0.08 | 6.34 | 1.37 | 1.00 | 1.16 | 1.16 | 0.06 | 5.14 |
| shaped (SHS) | | Plant A | - | - | - | - | - | - | - | - | - | - | - | - | - |
| | | Plant B | - | - | - | - | - | - | - | - | - | - | - | - | - |
| NOMINAL | | Plant C | - | - | - | - | - | - | - | - | - | - | - | - | - |
| Fy (MPa) | | Plant D | - | - | - | - | - | - | - | - | - | - | - | - | - |
| 345 | | Plant undefined | 1750 | 1.67 | 1.05 | 1.31 | 1.32 | 0.08 | 6.34 | 1.37 | 1.00 | 1.16 | 1.16 | 0.06 | 5.14 |
| Fu (MPa) | Producer B | | - | - | - | - | - | - | - | - | - | - | - | - | - |
| 450 | Producer C | | - | - | - | - | - | - | - | - | - | - | - | - | - |
| KL/r limit | Producer D | | - | - | - | - | - | - | - | - | - | - | - | - | - |
| 100 | Producer E | | 185 | 1.46 | 1.13 | 1.29 | 1.30 | 0.07 | 5.70 | 1.21 | 1.00 | 1.13 | 1.11 | 0.05 | 4.46 |
| b/t limit | Producer F | | 96 | 1.65 | 1.07 | 1.35 | 1.34 | 0.18 | 13.34 | 1.38 | 1.04 | 1.19 | 1.22 | 0.11 | 9.26 |
| 17.7 | Producer G | | - | - | - | - | - | - | - | - | - | - | - | - | - |
| | Producer I | | 840 | 1.65 | 1.00 | 1.19 | 1.20 | 0.11 | 9.19 | 1.35 | 1.02 | 1.14 | 1.16 | 0.06 | 4.99 |
| | Producer J | | - | - | - | - | - | - | - | - | - | - | - | - | - |
| | Producer K | | - | - | - | - | - | - | - | - | - | - | - | - | - |
| TOTAL | | | 2871 | 1.67 | 1.00 | 1.29 | **1.29** | 0.11 | **8.66** | 1.38 | 1.00 | 1.15 | **1.16** | 0.06 | **5.46** |
| | | D/t | | 27.16 | 7.64 | 20.35 | 19.75 | 4.53 | 22.93 | | | | | | |
| | | b/t | | 17.33 | 2.00 | 12.00 | 11.85 | 3.65 | 30.76 | | | | | | |

| CSA G40.21 – 350W AND ASTM A500 SINGLE OR DUAL CERTIFIED | | | Count | S136A | | | | | | S136B | | | | | | WEIGHTED AVERAGE | | | | | |
|---|---|---|---|---|---|---|---|---|---|---|---|---|---|---|---|---|---|---|---|---|---|
| | | | | MAX. | MIN. | MED. | AVG. | ST.DEV | CV | MAX. | MIN. | MED. | AVG. | ST.DEV | CV | MAX. | MIN. | MED. | AVG. | ST.DEV | CV |
| TYPE | Producer A | | 1750 | 1.65 | 1.27 | 1.46 | 1.46 | 0.06 | 4.06 | 1.78 | 1.30 | 1.51 | 1.51 | 0.08 | 5.29 | 1.75 | 1.27 | 1.49 | 1.49 | 0.08 | 5.07 |
| shaped (SHS) | | Plant A | - | - | - | - | - | - | - | - | - | - | - | - | - | - | - | - | - | - | - |
| | | Plant B | - | - | - | - | - | - | - | - | - | - | - | - | - | - | - | - | - | - | - |
| NOMINAL | | Plant C | - | - | - | - | - | - | - | - | - | - | - | - | - | - | - | - | - | - | - |
| Fy (MPa) | | Plant D | - | - | - | - | - | - | - | - | - | - | - | - | - | - | - | - | - | - | - |
| 345 | | Plant undefined | 1750 | 1.65 | 1.27 | 1.46 | 1.46 | 0.06 | 4.06 | 1.78 | 1.30 | 1.51 | 1.51 | 0.08 | 5.29 | 1.75 | 1.27 | 1.49 | 1.49 | 0.08 | 5.07 |
| Fu (MPa) | Producer B | | - | - | - | - | - | - | - | - | - | - | - | - | - | - | - | - | - | - | - |
| 450 | Producer C | | - | - | - | - | - | - | - | - | - | - | - | - | - | - | - | - | - | - | - |
| KL/r limit | Producer D | | - | - | - | - | - | - | - | - | - | - | - | - | - | - | - | - | - | - | - |
| 100 | Producer E | | 185 | 1.56 | 1.31 | 1.47 | 1.46 | 0.06 | 4.04 | 1.58 | 1.30 | 1.46 | 1.45 | 0.07 | 4.59 | 1.60 | 1.29 | 1.45 | 1.45 | 0.07 | 4.77 |
| b/t limit | Producer F | | 96 | 1.64 | 1.34 | 1.53 | 1.48 | 0.11 | 7.21 | 1.80 | 1.36 | 1.55 | 1.57 | 0.16 | 9.93 | 1.73 | 1.30 | 1.50 | 1.51 | 0.14 | 9.11 |
| 17.7 | Producer G | | - | - | - | - | - | - | - | - | - | - | - | - | - | - | - | - | - | - | - |
| | Producer I | | 840 | 1.64 | 1.23 | 1.39 | 1.39 | 0.08 | 5.58 | 1.74 | 1.29 | 1.46 | 1.47 | 0.09 | 6.21 | 1.74 | 1.23 | 1.40 | 1.41 | 0.10 | 6.77 |
| | Producer J | | - | - | - | - | - | - | - | - | - | - | - | - | - | - | - | - | - | - | - |
| | Producer K | | - | - | - | - | - | - | - | - | - | - | - | - | - | - | - | - | - | - | - |
| TOTAL | | | 2871 | 1.65 | 1.23 | 1.44 | **1.44** | 0.07 | **5.18** | 1.80 | 1.29 | 1.49 | **1.50** | 0.09 | **6.00** | 1.75 | 1.23 | 1.46 | **1.46** | 0.09 | **6.27** |

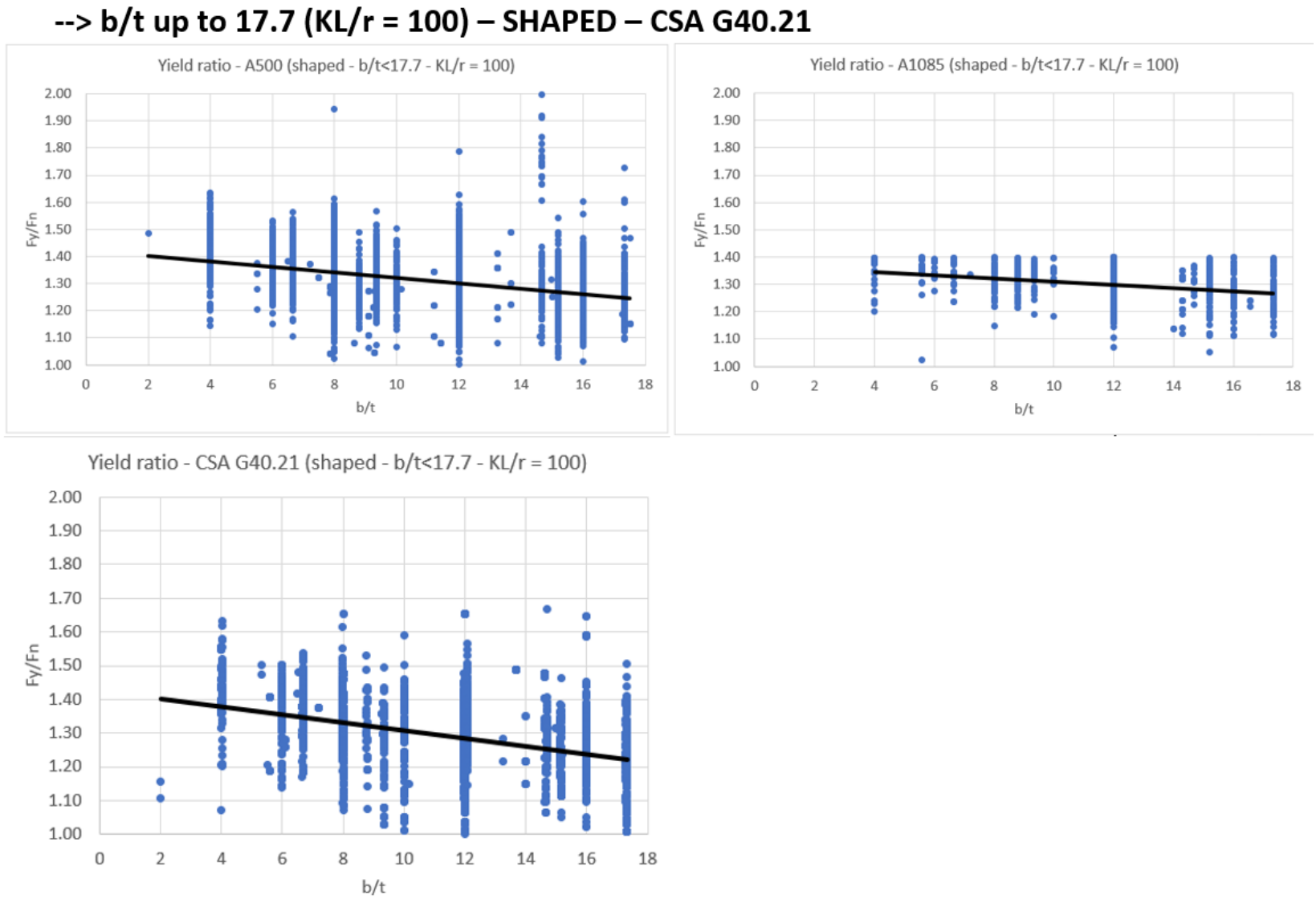


Figure A- 5: Results for shaped HSS from North American Steel manufacturers – Part 1

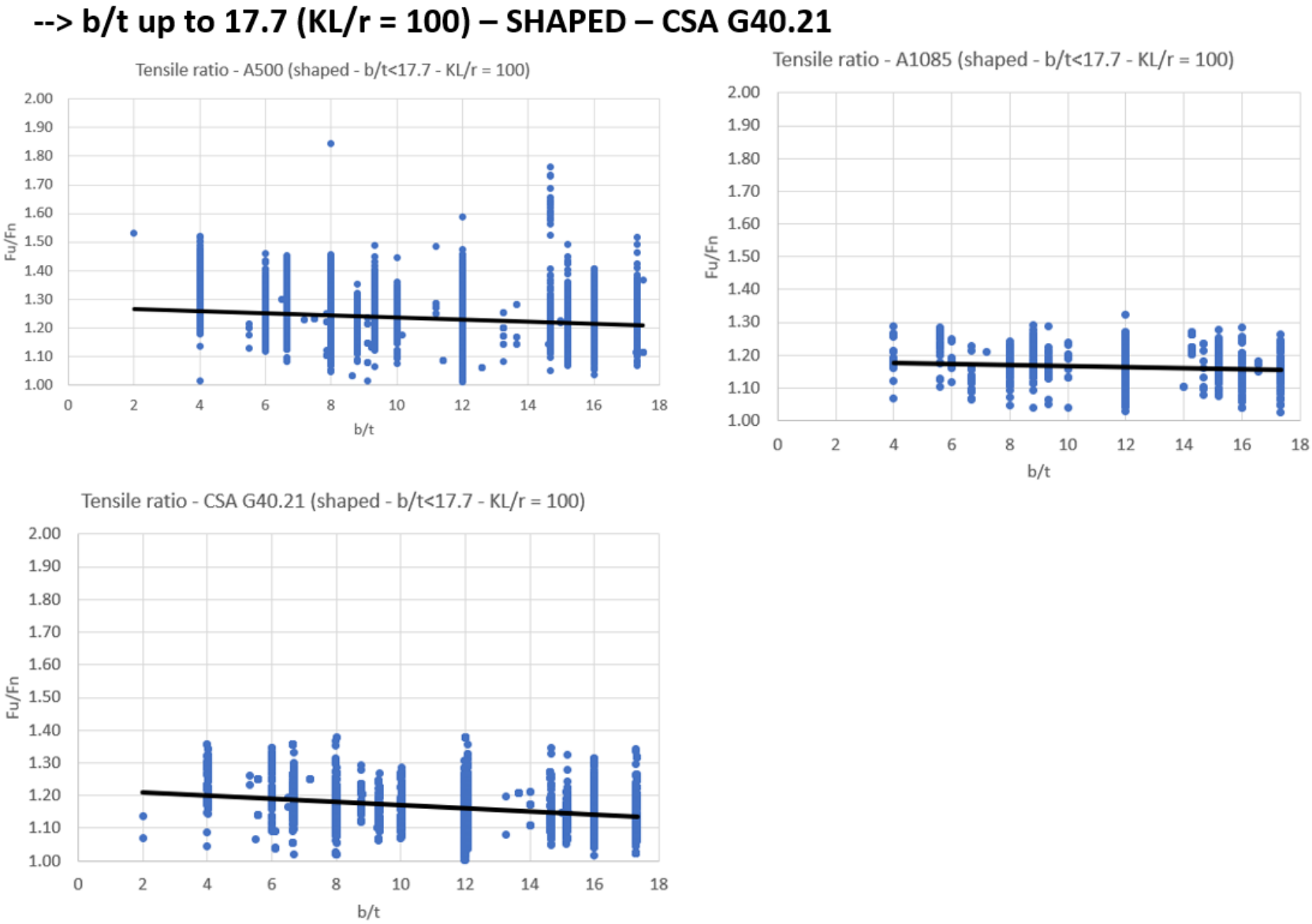


Figure A- 6: Results for shaped HSS from North American Steel manufacturers – Part 2

Table A- 18: Results for round HSS from North American Steel manufacturers – Part 1

## → D/t<37.6 (KL/r = 200) – ROUND – A500

| ASTM A500 | | | Count | Center Coupon Fy | | | | | | Center Coupon Fu | | | | | |
|---|---|---|---|---|---|---|---|---|---|---|---|---|---|---|---|
| | | | | MAX. | MIN. | MED. | AVG. | ST.DEV | CV | MAX. | MIN. | MED. | AVG. | ST.DEV | CV |
| TYPE | Producer A | | 504 | 1.62 | 0.96 | 1.22 | 1.22 | 0.10 | 7.82 | 1.47 | 1.04 | 1.22 | 1.21 | 0.08 | 6.46 |
| round | | Plant A | - | - | - | - | - | - | - | - | - | - | - | - | - |
| NOMINAL | | Plant B | 197 | 1.50 | 1.08 | 1.22 | 1.23 | 0.07 | 5.97 | 1.40 | 1.10 | 1.27 | 1.26 | 0.06 | 4.51 |
| (CHS) | | Plant C | 307 | 1.62 | 0.96 | 1.21 | 1.22 | 0.11 | 8.80 | 1.47 | 1.04 | 1.17 | 1.18 | 0.07 | 6.07 |
| Fy (MPa) | | Plant D | - | - | - | - | - | - | - | - | - | - | - | - | - |
| 315 | | Plant undefined | - | - | - | - | - | - | - | - | - | - | - | - | - |
| Fu (MPa) | Producer B | | - | - | - | - | - | - | - | - | - | - | - | - | - |
| 425 | Producer C | | - | - | - | - | - | - | - | - | - | - | - | - | - |
| KL/r limit | Producer D | | - | - | - | - | - | - | - | - | - | - | - | - | - |
| 200 | Producer E | | - | - | - | - | - | - | - | - | - | - | - | - | - |
| D/t limit | Producer F | | - | - | - | - | - | - | - | - | - | - | - | - | - |
| 37.6 | Producer G | | - | - | - | - | - | - | - | - | - | - | - | - | - |
| | Producer I | | - | - | - | - | - | - | - | - | - | - | - | - | - |
| | Producer J | | - | - | - | - | - | - | - | - | - | - | - | - | - |
| | Producer K | | - | - | - | - | - | - | - | - | - | - | - | - | - |
| TOTAL | | | 504 | 1.62 | 0.96 | 1.22 | **1.22** | 0.10 | **7.82** | 1.47 | 1.04 | 1.22 | **1.21** | 0.08 | **6.46** |
| D/t | | | | 37.33 | 17.25 | 25.60 | 27.28 | 6.79 | 24.90 | | | | | | |

Table A- 19: Results for round HSS from North American Steel manufacturers – Part 2

## → D/t<37.6 (KL/r = 200) – ROUND – A1085

| A1085 | | | Count | Center Coupon Fy | | | | | | Center Coupon Fu | | | | | |
|---|---|---|---|---|---|---|---|---|---|---|---|---|---|---|---|
| | | | | MAX. | MIN. | MED. | AVG. | ST.DEV | CV | MAX. | MIN. | MED. | AVG. | ST.DEV | CV |
| TYPE | Producer A | | 147 | 1.40 | 1.07 | 1.26 | 1.26 | 0.09 | 7.21 | 1.24 | 1.02 | 1.12 | 1.13 | 0.05 | 4.18 |
| round | | Plant A | - | - | - | - | - | - | - | - | - | - | - | - | - |
| (CHS) | | Plant B | - | - | - | - | - | - | - | - | - | - | - | - | - |
| NOMINAL | | Plant C | 50 | 1.40 | 1.07 | 1.26 | 1.26 | 0.08 | 6.43 | 1.20 | 1.02 | 1.12 | 1.12 | 0.05 | 4.08 |
| Fy (MPa) | | Plant D | - | - | - | - | - | - | - | - | - | - | - | - | - |
| 345 | | Plant undefined | 97 | 1.40 | 1.08 | 1.27 | 1.25 | 0.09 | 7.58 | 1.24 | 1.03 | 1.13 | 1.14 | 0.05 | 4.11 |
| Fu (MPa) | Producer B | | - | - | - | - | - | - | - | - | - | - | - | - | - |
| 450 | Producer C | | - | - | - | - | - | - | - | - | - | - | - | - | - |
| KL/r limit | Producer D | | - | - | - | - | - | - | - | - | - | - | - | - | - |
| 200 | Producer E | | - | - | - | - | - | - | - | - | - | - | - | - | - |
| D/t limit | Producer F | | - | - | - | - | - | - | - | - | - | - | - | - | - |
| 37.6 | Producer G | | - | - | - | - | - | - | - | - | - | - | - | - | - |
| | Producer I | | - | - | - | - | - | - | - | - | - | - | - | - | - |
| | Producer J | | - | - | - | - | - | - | - | - | - | - | - | - | - |
| | Producer K | | - | - | - | - | - | - | - | - | - | - | - | - | - |
| TOTAL | | | 147 | 1.40 | 1.07 | 1.26 | **1.26** | 0.09 | **7.21** | 1.24 | 1.02 | 1.12 | **1.13** | 0.05 | **4.18** |
| D/t | | | | 37.33 | 10.00 | 21.20 | 21.52 | 6.48 | 30.12 | | | | | | |

Table A- 20: Results for round HSS from North American Steel manufacturers – Part 3

## → D/t<37.6 (KL/r = 200) – ROUND – CSA G40.21

| CSA G40.21 - 350W AND ASTM A500 SINGLE OR DUAL CERTIFIED | | | Count | Center Coupon Fy | | | | | | Center Coupon Fu | | | | | |
|---|---|---|---|---|---|---|---|---|---|---|---|---|---|---|---|
| | | | | MAX. | MIN. | MED. | AVG. | ST.DEV | CV | MAX. | MIN. | MED. | AVG. | ST.DEV | CV |
| TYPE | Producer A | | 50 | 1.43 | 1.00 | 1.22 | 1.22 | 0.12 | 9.62 | 1.32 | 1.00 | 1.10 | 1.12 | 0.07 | 6.22 |
| round | | Plant A | - | - | - | - | - | - | - | - | - | - | - | - | - |
| (CHS) | | Plant B | - | - | - | - | - | - | - | - | - | - | - | - | - |
| NOMINAL | | Plant C | 50 | 1.43 | 1.00 | 1.22 | 1.22 | 0.12 | 9.62 | 1.32 | 1.00 | 1.10 | 1.12 | 0.07 | 6.22 |
| Fy (MPa) | | Plant D | - | - | - | - | - | - | - | - | - | - | - | - | - |
| 345 | | Plant undefined | - | - | - | - | - | - | - | - | - | - | - | - | - |
| Fu (MPa) | Producer B | | - | - | - | - | - | - | - | - | - | - | - | - | - |
| 450 | Producer C | | - | - | - | - | - | - | - | - | - | - | - | - | - |
| KL/r limit | Producer D | | - | - | - | - | - | - | - | - | - | - | - | - | - |
| 200 | Producer E | | - | - | - | - | - | - | - | - | - | - | - | - | - |
| D/t limit | Producer F | | - | - | - | - | - | - | - | - | - | - | - | - | - |
| 37.6 | Producer G | | - | - | - | - | - | - | - | - | - | - | - | - | - |
| | Producer I | | - | - | - | - | - | - | - | - | - | - | - | - | - |
| | Producer J | | - | - | - | - | - | - | - | - | - | - | - | - | - |
| | Producer K | | - | - | - | - | - | - | - | - | - | - | - | - | - |
| TOTAL | | | 50 | 1.43 | 1.00 | 1.22 | **1.22** | 0.12 | **9.62** | 1.32 | 1.00 | 1.10 | **1.12** | 0.07 | **6.22** |
| D/t | | | | 34.00 | 17.25 | 24.63 | 24.71 | 7.46 | 30.22 | | | | | | |

Table A- 21: Results for round HSS from North American Steel manufacturers – Part 4

## → D/t<32.4 (KL/r = 140) – ROUND – A500

| ASTM A500 | | | Count | Center Coupon Fy | | | | | | Center Coupon Fu | | | | | |
|---|---|---|---|---|---|---|---|---|---|---|---|---|---|---|---|
| | | | | MAX. | MIN. | MED. | AVG. | ST.DEV | CV | MAX. | MIN. | MED. | AVG. | ST.DEV | CV |
| TYPE | Producer A | | 379 | 1.62 | 0.99 | 1.21 | 1.22 | 0.10 | 8.10 | 1.47 | 1.04 | 1.19 | 1.19 | 0.08 | 6.35 |
| round | | Plant A | - | - | - | - | - | - | - | - | - | - | - | - | - |
| (CHS) | | Plant B | 130 | 1.50 | 1.08 | 1.22 | 1.23 | 0.08 | 6.43 | 1.40 | 1.10 | 1.25 | 1.25 | 0.06 | 4.71 |
| NOMINAL | | Plant C | 249 | 1.62 | 0.99 | 1.20 | 1.21 | 0.11 | 8.83 | 1.47 | 1.04 | 1.15 | 1.17 | 0.07 | 5.74 |
| Fy (MPa) | | Plant D | - | - | - | - | - | - | - | - | - | - | - | - | - |
| 315 | | Plant undefined | - | - | - | - | - | - | - | - | - | - | - | - | - |
| Fu (MPa) | Producer B | | - | - | - | - | - | - | - | - | - | - | - | - | - |
| 425 | Producer C | | - | - | - | - | - | - | - | - | - | - | - | - | - |
| KL/r limit | Producer D | | - | - | - | - | - | - | - | - | - | - | - | - | - |
| 140 | Producer E | | - | - | - | - | - | - | - | - | - | - | - | - | - |
| D/t limit | Producer F | | - | - | - | - | - | - | - | - | - | - | - | - | - |
| 32.4 | Producer G | | - | - | - | - | - | - | - | - | - | - | - | - | - |
| | Producer I | | - | - | - | - | - | - | - | - | - | - | - | - | - |
| | Producer J | | - | - | - | - | - | - | - | - | - | - | - | - | - |
| | Producer K | | - | - | - | - | - | - | - | - | - | - | - | - | - |
| TOTAL | | | 379 | 1.62 | 0.99 | 1.21 | **1.22** | 0.10 | **8.10** | 1.47 | 1.04 | 1.19 | **1.19** | 0.08 | **6.35** |
| D/t | | | | 32.00 | 17.25 | 25.50 | 24.64 | 5.70 | 23.11 | | | | | | |

Table A- 22: Results for round HSS from North American Steel manufacturers – Part 5

## → D/t<32.4 (KL/r = 140) – ROUND – A1085

| A1085 | | | Count | Center Coupon Fy | | | | | | Center Coupon Fu | | | | | |
|---|---|---|---|---|---|---|---|---|---|---|---|---|---|---|---|
| | | | | MAX. | MIN. | MED. | AVG. | ST.DEV | CV | MAX. | MIN. | MED. | AVG. | ST.DEV | CV |
| TYPE | Producer A | | 139 | 1.40 | 1.07 | 1.27 | 1.26 | 0.09 | 7.26 | 1.24 | 1.02 | 1.12 | 1.13 | 0.05 | 4.11 |
| round | | Plant A | - | - | - | - | - | - | - | - | - | - | - | - | - |
| (CHS) | | Plant B | - | - | - | - | - | - | - | - | - | - | - | - | - |
| NOMINAL | | Plant C | 48 | 1.40 | 1.07 | 1.26 | 1.26 | 0.08 | 6.56 | 1.20 | 1.02 | 1.11 | 1.12 | 0.05 | 4.15 |
| Fy (MPa) | | Plant D | - | - | - | - | - | - | - | - | - | - | - | - | - |
| 345 | | Plant undefined | 91 | 1.40 | 1.08 | 1.28 | 1.26 | 0.10 | 7.61 | 1.24 | 1.03 | 1.13 | 1.13 | 0.05 | 4.00 |
| Fu (MPa) | Producer B | | - | - | - | - | - | - | - | - | - | - | - | - | - |
| 450 | Producer C | | - | - | - | - | - | - | - | - | - | - | - | - | - |
| KL/r limit | Producer D | | - | - | - | - | - | - | - | - | - | - | - | - | - |
| 140 | Producer E | | - | - | - | - | - | - | - | - | - | - | - | - | - |
| D/t limit | Producer F | | - | - | - | - | - | - | - | - | - | - | - | - | - |
| 32.4 | Producer G | | - | - | - | - | - | - | - | - | - | - | - | - | - |
| | Producer I | | - | - | - | - | - | - | - | - | - | - | - | - | - |
| | Producer J | | - | - | - | - | - | - | - | - | - | - | - | - | - |
| | Producer K | | - | - | - | - | - | - | - | - | - | - | - | - | - |
| TOTAL | | | 139 | 1.40 | 1.07 | 1.27 | **1.26** | 0.09 | **7.26** | 1.24 | 1.02 | 1.12 | **1.13** | 0.05 | **4.11** |
| D/t | | | | 32.00 | 10.00 | 20.00 | 20.70 | 5.66 | 27.37 | | | | | | |

Table A- 23: Results for round HSS from North American Steel manufacturers – Part 6

## → D/t<32.4 (KL/r = 140) – ROUND – CSA G40.21

| CSA G40.21 - 350W AND ASTM A500 SINGLE OR DUAL CERTIFIED | | | Count | Center Coupon Fy | | | | | | Center Coupon Fu | | | | | |
|---|---|---|---|---|---|---|---|---|---|---|---|---|---|---|---|
| | | | | MAX. | MIN. | MED. | AVG. | ST.DEV | CV | MAX. | MIN. | MED. | AVG. | ST.DEV | CV |
| TYPE | Producer A | | 48 | 1.43 | 1.00 | 1.23 | 1.23 | 0.12 | 9.65 | 1.32 | 1.00 | 1.10 | 1.11 | 0.07 | 6.22 |
| round | | Plant A | - | - | - | - | - | - | - | - | - | - | - | - | - |
| (CHS) | | Plant B | - | - | - | - | - | - | - | - | - | - | - | - | - |
| NOMINAL | | Plant C | 48 | 1.43 | 1.00 | 1.23 | 1.23 | 0.12 | 9.65 | 1.32 | 1.00 | 1.10 | 1.11 | 0.07 | 6.22 |
| Fy (MPa) | | Plant D | - | - | - | - | - | - | - | - | - | - | - | - | - |
| 345 | | Plant undefined | - | - | - | - | - | - | - | - | - | - | - | - | - |
| Fu (MPa) | Producer B | | - | - | - | - | - | - | - | - | - | - | - | - | - |
| 450 | Producer C | | - | - | - | - | - | - | - | - | - | - | - | - | - |
| KL/r limit | Producer D | | - | - | - | - | - | - | - | - | - | - | - | - | - |
| 140 | Producer E | | - | - | - | - | - | - | - | - | - | - | - | - | - |
| D/t limit | Producer F | | - | - | - | - | - | - | - | - | - | - | - | - | - |
| 32.4 | Producer G | | - | - | - | - | - | - | - | - | - | - | - | - | - |
| | Producer I | | - | - | - | - | - | - | - | - | - | - | - | - | - |
| | Producer J | | - | - | - | - | - | - | - | - | - | - | - | - | - |
| | Producer K | | - | - | - | - | - | - | - | - | - | - | - | - | - |
| TOTAL | | | 48 | 1.43 | 1.00 | 1.23 | **1.23** | 0.12 | **9.65** | 1.32 | 1.00 | 1.10 | **1.11** | 0.07 | **6.22** |
| D/t | | | | 32.00 | 17.25 | 17.25 | 24.32 | 7.37 | 30.30 | | | | | | |

Table A- 24: Results for round HSS from North American Steel manufacturers – Part 7

## → D/t<28.9 (KL/r = 100) – ROUND – A500

| ASTM A500 | | | Count | Center Coupon Fy | | | | | | Center Coupon Fu | | | | | |
|---|---|---|---|---|---|---|---|---|---|---|---|---|---|---|---|
| | | | | MAX. | MIN. | MED. | AVG. | ST.DEV | CV | MAX. | MIN. | MED. | AVG. | ST.DEV | CV |
| TYPE | Producer A | | 265 | 1.62 | 1.01 | 1.24 | 1.24 | 0.10 | 7.85 | 1.47 | 1.05 | 1.19 | 1.20 | 0.08 | 6.36 |
| round | | Plant A | - | - | - | - | - | - | - | - | - | - | - | - | - |
| (CHS) | | Plant B | 90 | 1.50 | 1.09 | 1.25 | 1.25 | 0.08 | 6.33 | 1.40 | 1.10 | 1.24 | 1.25 | 0.06 | 5.04 |
| NOMINAL | | Plant C | 175 | 1.62 | 1.01 | 1.23 | 1.24 | 0.11 | 8.52 | 1.47 | 1.05 | 1.16 | 1.17 | 0.07 | 5.99 |
| Fy (MPa) | | Plant D | - | - | - | - | - | - | - | - | - | - | - | - | - |
| 315 | | Plant undefined | - | - | - | - | - | - | - | - | - | - | - | - | - |
| Fu (MPa) | Producer B | | - | - | - | - | - | - | - | - | - | - | - | - | - |
| 425 | Producer C | | - | - | - | - | - | - | - | - | - | - | - | - | - |
| KL/r limit | Producer D | | - | - | - | - | - | - | - | - | - | - | - | - | - |
| 100 | Producer E | | - | - | - | - | - | - | - | - | - | - | - | - | - |
| D/t limit | Producer F | | - | - | - | - | - | - | - | - | - | - | - | - | - |
| 28.9 | Producer G | | - | - | - | - | - | - | - | - | - | - | - | - | - |
| | Producer I | | - | - | - | - | - | - | - | - | - | - | - | - | - |
| | Producer J | | - | - | - | - | - | - | - | - | - | - | - | - | - |
| | Producer K | | - | - | - | - | - | - | - | - | - | - | - | - | - |
| TOTAL | | | 265 | 1.62 | 1.01 | 1.24 | **1.24** | 0.10 | **7.85** | 1.47 | 1.05 | 1.19 | **1.20** | 0.08 | **6.36** |
| D/t | | | | 25.60 | 17.25 | 22.40 | 21.48 | 3.62 | 16.84 | | | | | | |

Table A- 25: Results for round HSS from North American Steel manufacturers – Part 8

## → D/t<28.9 (KL/r = 100) – ROUND – A1085

| A1085 | | | Count | Center Coupon Fy | | | | | | Center Coupon Fu | | | | | |
|---|---|---|---|---|---|---|---|---|---|---|---|---|---|---|---|
| | | | | MAX. | MIN. | MED. | AVG. | ST.DEV | CV | MAX. | MIN. | MED. | AVG. | ST.DEV | CV |
| TYPE | Producer A | | 124 | 1.40 | 1.07 | 1.29 | 1.27 | 0.08 | 6.59 | 1.24 | 1.02 | 1.12 | 1.13 | 0.05 | 4.17 |
| round | | Plant A | - | - | - | - | - | - | - | - | - | - | - | - | - |
| (CHS) | | Plant B | - | - | - | - | - | - | - | - | - | - | - | - | - |
| NOMINAL | | Plant C | 48 | 1.40 | 1.07 | 1.26 | 1.26 | 0.08 | 6.56 | 1.20 | 1.02 | 1.11 | 1.12 | 0.05 | 4.15 |
| Fy (MPa) | | Plant D | - | - | - | - | - | - | - | - | - | - | - | - | - |
| 345 | | Plant undefin | 76 | 1.40 | 1.09 | 1.30 | 1.28 | 0.08 | 6.56 | 1.24 | 1.03 | 1.14 | 1.14 | 0.05 | 4.05 |
| Fu (MPa) | Producer B | | - | - | - | - | - | - | - | - | - | - | - | - | - |
| 450 | Producer C | | - | - | - | - | - | - | - | - | - | - | - | - | - |
| KL/r limit | Producer D | | - | - | - | - | - | - | - | - | - | - | - | - | - |
| 100 | Producer E | | - | - | - | - | - | - | - | - | - | - | - | - | - |
| D/t limit | Producer F | | - | - | - | - | - | - | - | - | - | - | - | - | - |
| 28.9 | Producer G | | - | - | - | - | - | - | - | - | - | - | - | - | - |
| | Producer I | | - | - | - | - | - | - | - | - | - | - | - | - | - |
| | Producer J | | - | - | - | - | - | - | - | - | - | - | - | - | - |
| | Producer K | | - | - | - | - | - | - | - | - | - | - | - | - | - |
| TOTAL | | | 124 | 1.40 | 1.07 | 1.29 | 1.27 | 0.08 | 6.59 | 1.24 | 1.02 | 1.12 | 1.13 | 0.05 | 4.17 |
| D/t | | | | 28.67 | 10.00 | 17.25 | 19.33 | 4.32 | 22.34 | | | | | | |

Table A- 26: Results for round HSS from North American Steel manufacturers – Part 9

## → D/t<28.9 (KL/r = 100) – ROUND – CSA G40.21

| CSA G40.21 - 350W AND ASTM A500 SINGLE OR DUAL CERTIFIED | | | Count | Center Coupon Fy | | | | | | Center Coupon Fu | | | | | |
|---|---|---|---|---|---|---|---|---|---|---|---|---|---|---|---|
| | | | | MAX. | MIN. | MED. | AVG. | ST.DEV | CV | MAX. | MIN. | MED. | AVG. | ST.DEV | CV |
| TYPE | Producer A | | 25 | 1.43 | 1.13 | 1.31 | 1.31 | 0.08 | 5.73 | 1.32 | 1.00 | 1.16 | 1.15 | 0.06 | 5.62 |
| round | | Plant A | - | - | - | - | - | - | - | - | - | - | - | - | - |
| (CHS) | | Plant B | - | - | - | - | - | - | - | - | - | - | - | - | - |
| NOMINAL | | Plant C | 25 | 1.43 | 1.13 | 1.31 | 1.31 | 0.08 | 5.73 | 1.32 | 1.00 | 1.16 | 1.15 | 0.06 | 5.62 |
| Fy (MPa) | | Plant D | - | - | - | - | - | - | - | - | - | - | - | - | - |
| 345 | | Plant undefined | - | - | - | - | - | - | - | - | - | - | - | - | - |
| Fu (MPa) | Producer B | | - | - | - | - | - | - | - | - | - | - | - | - | - |
| 450 | Producer C | | - | - | - | - | - | - | - | - | - | - | - | - | - |
| KL/r limit | Producer D | | - | - | - | - | - | - | - | - | - | - | - | - | - |
| 100 | Producer E | | - | - | - | - | - | - | - | - | - | - | - | - | - |
| D/t limit | Producer F | | - | - | - | - | - | - | - | - | - | - | - | - | - |
| 28.9 | Producer G | | - | - | - | - | - | - | - | - | - | - | - | - | - |
| | Producer I | | - | - | - | - | - | - | - | - | - | - | - | - | - |
| | Producer J | | - | - | - | - | - | - | - | - | - | - | - | - | - |
| | Producer K | | - | - | - | - | - | - | - | - | - | - | - | - | - |
| TOTAL | | | 25 | 1.43 | 1.13 | 1.31 | **1.31** | 0.08 | **5.73** | 1.32 | 1.00 | 1.16 | **1.15** | 0.06 | **5.62** |
| D/t | | | | 17.25 | 17.25 | 17.25 | 17.25 | 0.00 | 0.00 | | | | | | |

→ D/t<28.9 (KL/r = 100) – ROUND – CSA G40.21

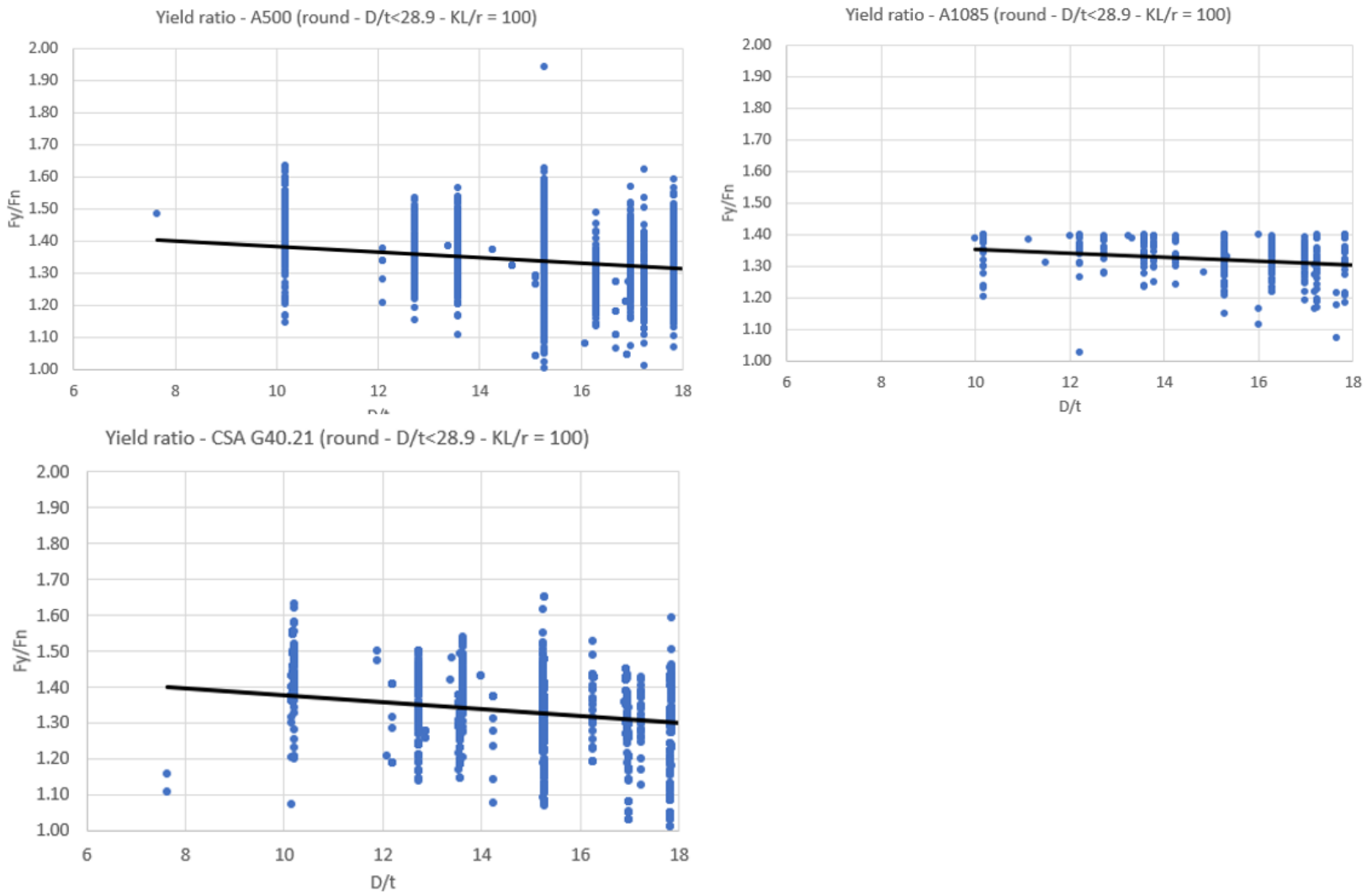


Figure A- 7: Results for round HSS from North American Steel manufacturers – Part 1

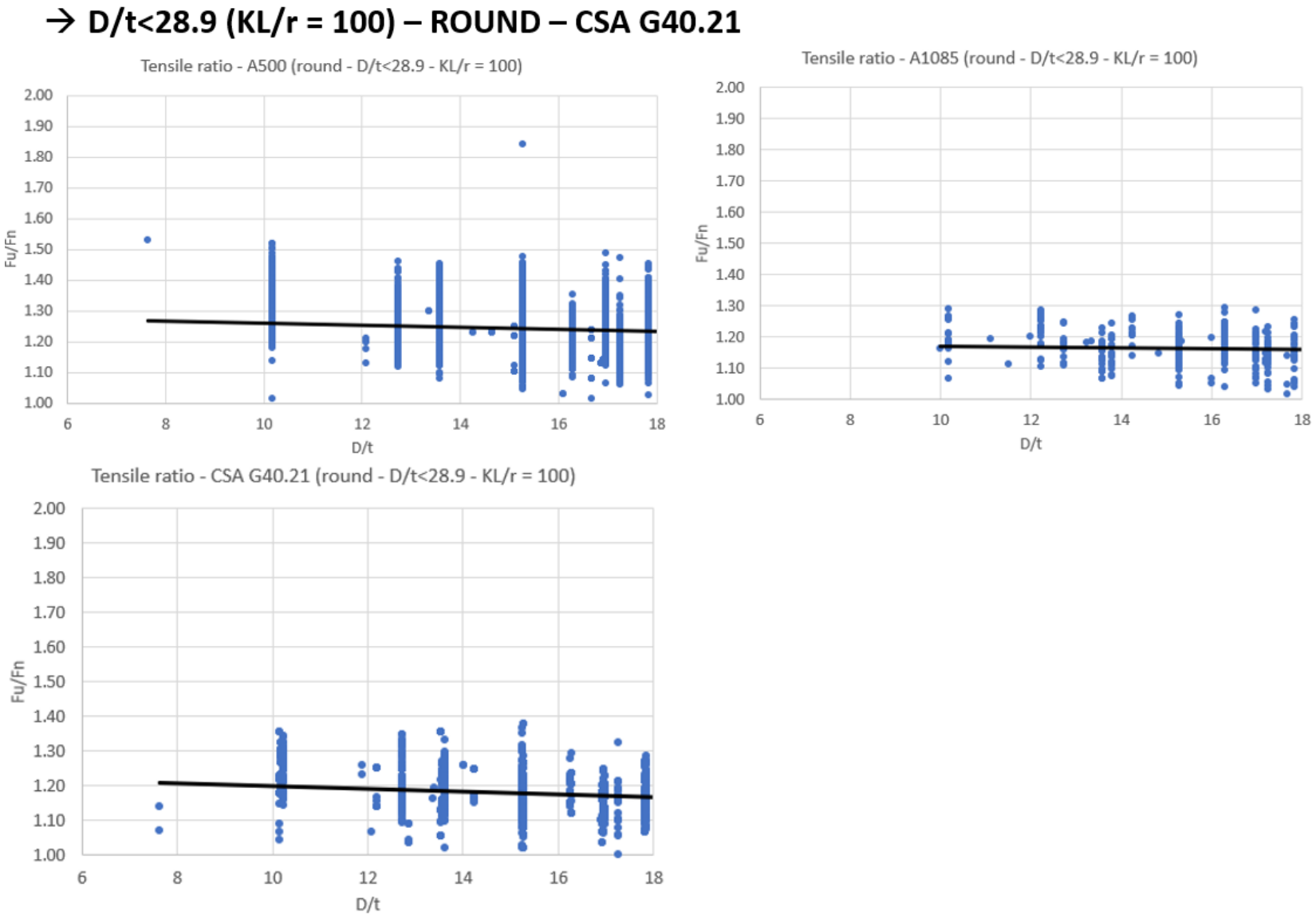


Figure A- 8: Results for round HSS from North American Steel manufacturers – Part 2

# APPENDIX B – DETAILED RESULTS FOR RELIABILITY ANALYSIS IN CHAPTER 3

Table B- 16: Detailed results from reliability analysis – Part 1

**--> b/t no limit (all available data)**

| Specification (Grouped) | ASTM A500 | Specification (Grouped) | ASTM A500 | Specification (Grouped) | ASTM A500 | Specification (Grouped) | ASTM A500 |
|---|---|---|---|---|---|---|---|
| **TYPE** | SHAPED | **TYPE** | SHAPED | **TYPE** | SHAPED | **TYPE** | SHAPED |
| **METHOD** | COUPON DATA | **METHOD** | S136A | **METHOD** | S136B | **METHOD** | WEIGHTED AVERAGE |
| **b/t limit** | none | **b/t limit** | none | **b/t limit** | none | **b/t limit** | none |
| **DATA** | | **DATA** | | **DATA** | | **DATA** | |
| Fyn = | 345 | Fyn = | 345 | Fyn = | 345 | Fyn = | 345 |
| **Vm=** | **0.0784** | **Vm=** | **0.0557** | **Vm=** | **0.0747** | **Vm=** | **0.0686** |
| **RyFy (average) =** | **1.27** | **RyFy (average) =** | **1.36** | **RyFy (average) =** | **1.46** | **RyFy (average) =** | **1.43** |
| | 438.15 | | 469.20 | | 503.70 | | 493.35 |
| Φ = | 0.9 | Φ = | 0.9 | Φ = | 0.9 | Φ = | 0.9 |
| ρg = | 0.971 | ρg = | 0.971 | ρg = | 0.971 | ρg = | 0.971 |
| Vg = | 0.015 | Vg = | 0.015 | Vg = | 0.015 | Vg = | 0.015 |
| ρp = | 1.00 | ρp = | 1.00 | ρp = | 1.00 | ρp = | 1.00 |
| Vp = | 0.00 | Vp = | 0.00 | Vp = | 0.00 | Vp = | 0.00 |
| β = | 3 | β = | 3 | β = | 3 | β = | 3 |
| αr = | -0.55 | αr = | -0.55 | αr = | -0.55 | αr = | -0.55 |
| Vr = | 0.080 | Vr = | 0.058 | Vr = | 0.076 | Vr = | 0.070 |
| ρr = | 1.03 | ρr = | 0.99 | ρr = | 1.02 | ρr = | 1.01 |
| ρm = | 1.06 | ρm = | 1.02 | ρm = | 1.05 | ρm = | 1.04 |
| **Fy =** | **414** | **Fy =** | **460** | **Fy =** | **479** | **Fy =** | **474** |

**Note:** What is referred to in this Appendix as Fy represents Fy* in Chapter 3. This analysis was performed before the final term for the equivalent nominal yield strength was chosen. Fyn refers to the nominal yield strength per grade. RyFy refers to the yield strength obtained from the center coupon from the flat wall of mill certificates.

Table B- 17: Detailed results from reliability analysis – Part 2

**--> b/t no limit (all available data)**

| Specification (Grouped) | |
|---|---|
| A1085 | |
| **TYPE** | |
| SHAPED | |
| **METHOD** | |
| COUPON DATA | |
| **b/t limit** | |
| none | |
| **DATA** | |
| Fyn = | 345 |
| **Vm=** | **0.0632** |
| **RyFy (average) =** | **1.26** |
| | 434.70 |
| Φ = | 0.9 |
| ρg = | 0.971 |
| Vg = | 0.015 |
| ρp = | 1.00 |
| Vp = | 0.00 |
| β = | 3 |
| αr = | -0.55 |
| Vr = | 0.065 |
| ρr = | 1.00 |
| ρm = | 1.03 |
| **Fy =** | **421** |

| Specification (Grouped) | |
|---|---|
| A1085 | |
| **TYPE** | |
| SHAPED | |
| **METHOD** | |
| S136A | |
| **b/t limit** | |
| none | |
| **DATA** | |
| Fyn = | 345 |
| **Vm=** | **0.0593** |
| **RyFy (average) =** | **1.41** |
| | 486.45 |
| Φ = | 0.9 |
| ρg = | 0.971 |
| Vg = | 0.015 |
| ρp = | 1.00 |
| Vp = | 0.00 |
| β = | 3 |
| αr = | -0.55 |
| Vr = | 0.061 |
| ρr = | 1.00 |
| ρm = | 1.03 |
| **Fy =** | **474** |

| Specification (Grouped) | |
|---|---|
| A1085 | |
| **TYPE** | |
| SHAPED | |
| **METHOD** | |
| S136B | |
| **b/t limit** | |
| none | |
| **DATA** | |
| Fyn = | 345 |
| **Vm=** | **0.0644** |
| **RyFy (average) =** | **1.43** |
| | 493.35 |
| Φ = | 0.9 |
| ρg = | 0.971 |
| Vg = | 0.015 |
| ρp = | 1.00 |
| Vp = | 0.00 |
| β = | 3 |
| αr = | -0.55 |
| Vr = | 0.066 |
| ρr = | 1.00 |
| ρm = | 1.03 |
| **Fy =** | **477** |

| Specification (Grouped) | |
|---|---|
| A1085 | |
| **TYPE** | |
| SHAPED | |
| **METHOD** | |
| WEIGHTED AVERAGE | |
| **b/t limit** | |
| none | |
| **DATA** | |
| Fyn = | 345 |
| **Vm=** | **0.0594** |
| **RyFy (average) =** | **1.42** |
| | 489.90 |
| Φ = | 0.9 |
| ρg = | 0.971 |
| Vg = | 0.015 |
| ρp = | 1.00 |
| Vp = | 0.00 |
| β = | 3 |
| αr = | -0.55 |
| Vr = | 0.061 |
| ρr = | 1.00 |
| ρm = | 1.03 |
| **Fy =** | **478** |

Table B- 18: Detailed results from reliability analysis – Part 3

**--> b/t no limit (all available data)**

| Specification (Grouped) | |
|---|---|
| CSA G40.21 - 350W AND ASTM A500 SINGLE OR DUAL CERTIFIED | |
| **TYPE** | |
| SHAPED | |
| **METHOD** | |
| COUPON DATA | |
| **b/t limit** | |
| none | |
| **DATA** | |
| Fyn = | 345 |
| **Vm=** | **0.0877** |
| **RyFy (average) =** | **1.26** |
| | 434.70 |
| Φ = | 0.9 |
| ρg = | 0.971 |
| Vg = | 0.015 |
| ρp = | 1.00 |
| Vp = | 0.00 |
| β = | 3 |
| αr = | -0.55 |
| Vr = | 0.089 |
| ρr = | 1.04 |
| ρm = | 1.07 |
| **Fy =** | **405** |

| Specification (Grouped) | |
|---|---|
| CSA G40.21 - 350W AND ASTM A500 SINGLE OR DUAL CERTIFIED | |
| **TYPE** | |
| SHAPED | |
| **METHOD** | |
| S136A | |
| **b/t limit** | |
| none | |
| **DATA** | |
| Fyn = | 345 |
| **Vm=** | **0.0642** |
| **RyFy (average) =** | **1.40** |
| | 483.00 |
| Φ = | 0.9 |
| ρg = | 0.971 |
| Vg = | 0.015 |
| ρp = | 1.00 |
| Vp = | 0.00 |
| β = | 3 |
| αr = | -0.55 |
| Vr = | 0.066 |
| ρr = | 1.00 |
| ρm = | 1.03 |
| **Fy =** | **467** |

| Specification (Grouped) | |
|---|---|
| CSA G40.21 - 350W AND ASTM A500 SINGLE OR DUAL CERTIFIED | |
| **TYPE** | |
| SHAPED | |
| **METHOD** | |
| S136B | |
| **b/t limit** | |
| none | |
| **DATA** | |
| Fyn = | 345 |
| **Vm=** | **0.0721** |
| **RyFy (average) =** | **1.45** |
| | 500.25 |
| Φ = | 0.9 |
| ρg = | 0.971 |
| Vg = | 0.015 |
| ρp = | 1.00 |
| Vp = | 0.00 |
| β = | 3 |
| αr = | -0.55 |
| Vr = | 0.074 |
| ρr = | 1.02 |
| ρm = | 1.05 |
| **Fy =** | **478** |

| Specification (Grouped) | |
|---|---|
| CSA G40.21 - 350W AND ASTM A500 SINGLE OR DUAL CERTIFIED | |
| **TYPE** | |
| SHAPED | |
| **METHOD** | |
| WEIGHTED AVERAGE | |
| **b/t limit** | |
| none | |
| **DATA** | |
| Fyn = | 345 |
| **Vm=** | **0.0712** |
| **RyFy (average) =** | **1.42** |
| | 489.90 |
| Φ = | 0.9 |
| ρg = | 0.971 |
| Vg = | 0.015 |
| ρp = | 1.00 |
| Vp = | 0.00 |
| β = | 3 |
| αr = | -0.55 |
| Vr = | 0.073 |
| ρr = | 1.01 |
| ρm = | 1.05 |
| **Fy =** | **469** |

Table B- 19: Detailed results from reliability analysis – Part 4

**--> b/t<17.7 (KL/r = 100)**

| Specification (Grouped) | |
|---|---|
| ASTM A500 | |
| **TYPE** | |
| SHAPED | |
| **METHOD** | |
| COUPON DATA | |
| **b/t limit** | |
| 17.7 | |
| **DATA** | |
| Fyn = | 345 |
| **Vm=** | **0.0744** |
| **RyFy (average) =** | **1.31** |
| | 451.95 |
| Φ = | 0.9 |
| ρg = | 0.971 |
| Vg = | 0.015 |
| ρp = | 1.00 |
| Vp = | 0.00 |
| β = | 3 |
| αr = | -0.55 |
| Vr = | 0.076 |
| ρr = | 1.02 |
| ρm = | 1.05 |
| **Fy =** | **430** |

| Specification (Grouped) | |
|---|---|
| ASTM A500 | |
| **TYPE** | |
| SHAPED | |
| **METHOD** | |
| S136A | |
| **b/t limit** | |
| 17.7 | |
| **DATA** | |
| Fyn = | 345 |
| **Vm=** | **0.0418** |
| **RyFy (average) =** | **1.41** |
| | 486.45 |
| Φ = | 0.9 |
| ρg = | 0.971 |
| Vg = | 0.015 |
| ρp = | 1.00 |
| Vp = | 0.00 |
| β = | 3 |
| αr = | -0.55 |
| Vr = | 0.044 |
| ρr = | 0.97 |
| ρm = | 1.00 |
| **Fy =** | **488** |

| Specification (Grouped) | |
|---|---|
| ASTM A500 | |
| **TYPE** | |
| SHAPED | |
| **METHOD** | |
| S136B | |
| **b/t limit** | |
| 17.7 | |
| **DATA** | |
| Fyn = | 345 |
| **Vm=** | **0.0669** |
| **RyFy (average) =** | **1.51** |
| | 520.95 |
| Φ = | 0.9 |
| ρg = | 0.971 |
| Vg = | 0.015 |
| ρp = | 1.00 |
| Vp = | 0.00 |
| β = | 3 |
| αr = | -0.55 |
| Vr = | 0.069 |
| ρr = | 1.01 |
| ρm = | 1.04 |
| **Fy =** | **502** |

| Specification (Grouped) | |
|---|---|
| ASTM A500 | |
| **TYPE** | |
| SHAPED | |
| **METHOD** | |
| WEIGHTED AVERAGE | |
| **b/t limit** | |
| 17.7 | |
| **DATA** | |
| Fyn = | 345 |
| **Vm=** | **0.0599** |
| **RyFy (average) =** | **1.47** |
| | 507.15 |
| Φ = | 0.9 |
| ρg = | 0.971 |
| Vg = | 0.015 |
| ρp = | 1.00 |
| Vp = | 0.00 |
| β = | 3 |
| αr = | -0.55 |
| Vr = | 0.062 |
| ρr = | 1.00 |
| ρm = | 1.03 |
| **Fy =** | **494** |

Table B- 20: Detailed results from reliability analysis – Part 5

**--> b/t<17.7 (KL/r = 100)**

| Specification (Grouped) | |
|---|---|
| A1085 | |
| **TYPE** | |
| SHAPED | |
| **METHOD** | |
| COUPON DATA | |
| **b/t limit** | |
| 17.7 | |
| **DATA** | |
| Fyn = | 345 |
| **Vm=** | **0.0536** |
| **RyFy (average) =** | **1.30** |
| | 448.50 |
| Φ = | 0.9 |
| ρg = | 0.971 |
| Vg = | 0.015 |
| ρp = | 1.00 |
| Vp = | 0.00 |
| β = | 3 |
| αr = | -0.55 |
| Vr = | 0.056 |
| ρr = | 0.99 |
| ρm = | 1.02 |
| **Fy =** | **441** |

| Specification (Grouped) | |
|---|---|
| A1085 | |
| **TYPE** | |
| SHAPED | |
| **METHOD** | |
| S136A | |
| **b/t limit** | |
| 17.7 | |
| **DATA** | |
| Fyn = | 345 |
| **Vm=** | **0.0365** |
| **RyFy (average) =** | **1.45** |
| | 500.25 |
| Φ = | 0.9 |
| ρg = | 0.971 |
| Vg = | 0.015 |
| ρp = | 1.00 |
| Vp = | 0.00 |
| β = | 3 |
| αr = | -0.55 |
| Vr = | 0.039 |
| ρr = | 0.96 |
| ρm = | 0.99 |
| **Fy =** | **506** |

| Specification (Grouped) | |
|---|---|
| A1085 | |
| **TYPE** | |
| SHAPED | |
| **METHOD** | |
| S136B | |
| **b/t limit** | |
| 17.7 | |
| **DATA** | |
| Fyn = | 345 |
| **Vm=** | **0.0484** |
| **RyFy (average) =** | **1.51** |
| | 520.95 |
| Φ = | 0.9 |
| ρg = | 0.971 |
| Vg = | 0.015 |
| ρp = | 1.00 |
| Vp = | 0.00 |
| β = | 3 |
| αr = | -0.55 |
| Vr = | 0.051 |
| ρr = | 0.98 |
| ρm = | 1.01 |
| **Fy =** | **517** |

| Specification (Grouped) | |
|---|---|
| A1085 | |
| **TYPE** | |
| SHAPED | |
| **METHOD** | |
| WEIGHTED AVERAGE | |
| **b/t limit** | |
| 17.7 | |
| **DATA** | |
| Fyn = | 345 |
| **Vm=** | **0.0444** |
| **RyFy (average) =** | **1.47** |
| | 507.15 |
| Φ = | 0.9 |
| ρg = | 0.971 |
| Vg = | 0.015 |
| ρp = | 1.00 |
| Vp = | 0.00 |
| β = | 3 |
| αr = | -0.55 |
| Vr = | 0.047 |
| ρr = | 0.97 |
| ρm = | 1.00 |
| **Fy =** | **506** |

Table B- 21: Detailed results from reliability analysis – Part 6

**--> b/t<17.7 (KL/r = 100)**

| Specification (Grouped) | |
|---|---|
| CSA G40.21 - 350W AND ASTM A500 SINGLE OR DUAL CERTIFIED | |
| **TYPE** | |
| SHAPED | |
| **METHOD** | |
| COUPON DATA | |
| **b/t limit** | |
| 17.7 | |
| **DATA** | |
| Fyn = | 345 |
| **Vm=** | **0.0866** |
| **RyFy (average) =** | **1.29** |
| | 445.05 |
| Φ = | 0.9 |
| ρg = | 0.971 |
| Vg = | 0.015 |
| ρp = | 1.00 |
| Vp = | 0.00 |
| β = | 3 |
| αr = | -0.55 |
| Vr = | 0.088 |
| ρr = | 1.04 |
| ρm = | 1.07 |
| **Fy =** | **415** |

| Specification (Grouped) | |
|---|---|
| CSA G40.21 - 350W AND ASTM A500 SINGLE OR DUAL CERTIFIED | |
| **TYPE** | |
| SHAPED | |
| **METHOD** | |
| S136A | |
| **b/t limit** | |
| 17.7 | |
| **DATA** | |
| Fyn = | 345 |
| **Vm=** | **0.0518** |
| **RyFy (average) =** | **1.44** |
| | 496.80 |
| Φ = | 0.9 |
| ρg = | 0.971 |
| Vg = | 0.015 |
| ρp = | 1.00 |
| Vp = | 0.00 |
| β = | 3 |
| αr = | -0.55 |
| Vr = | 0.054 |
| ρr = | 0.98 |
| ρm = | 1.01 |
| **Fy =** | **490** |

| Specification (Grouped) | |
|---|---|
| CSA G40.21 - 350W AND ASTM A500 SINGLE OR DUAL CERTIFIED | |
| **TYPE** | |
| SHAPED | |
| **METHOD** | |
| S136B | |
| **b/t limit** | |
| 17.7 | |
| **DATA** | |
| Fyn = | 345 |
| **Vm=** | **0.0600** |
| **RyFy (average) =** | **1.50** |
| | 517.50 |
| Φ = | 0.9 |
| ρg = | 0.971 |
| Vg = | 0.015 |
| ρp = | 1.00 |
| Vp = | 0.00 |
| β = | 3 |
| αr = | -0.55 |
| Vr = | 0.062 |
| ρr = | 1.00 |
| ρm = | 1.03 |
| **Fy =** | **504** |

| Specification (Grouped) | |
|---|---|
| CSA G40.21 - 350W AND ASTM A500 SINGLE OR DUAL CERTIFIED | |
| **TYPE** | |
| SHAPED | |
| **METHOD** | |
| WEIGHTED AVERAGE | |
| **b/t limit** | |
| 17.7 | |
| **DATA** | |
| Fyn = | 345 |
| **Vm=** | **0.0627** |
| **RyFy (average) =** | **1.46** |
| | 503.70 |
| Φ = | 0.9 |
| ρg = | 0.971 |
| Vg = | 0.015 |
| ρp = | 1.00 |
| Vp = | 0.00 |
| β = | 3 |
| αr = | -0.55 |
| Vr = | 0.064 |
| ρr = | 1.00 |
| ρm = | 1.03 |
| **Fy =** | **489** |

Table B- 22: Detailed results from reliability analysis – Part 7

**--> b/t<19.7 (KL/r = 140)**

| Specification (Grouped) | |
|---|---|
| ASTM A500 | |
| **TYPE** | |
| SHAPED | |
| **METHOD** | |
| COUPON DATA | |
| **b/t limit** | |
| 19.7 | |
| **DATA** | |
| Fyn = | 345 |
| **Vm=** | **0.0743** |
| **RyFy (average) =** | **1.31** |
| | 451.95 |
| Φ = | 0.9 |
| ρg = | 0.971 |
| Vg = | 0.015 |
| ρp = | 1.00 |
| Vp = | 0.00 |
| β = | 3 |
| αr = | -0.55 |
| Vr = | 0.076 |
| ρr = | 1.02 |
| ρm = | 1.05 |
| **Fy =** | **430** |

| Specification (Grouped) | |
|---|---|
| ASTM A500 | |
| **TYPE** | |
| SHAPED | |
| **METHOD** | |
| S136A | |
| **b/t limit** | |
| 19.7 | |
| **DATA** | |
| Fyn = | 345 |
| **Vm=** | **0.0419** |
| **RyFy (average) =** | **1.40** |
| | 483.00 |
| Φ = | 0.9 |
| ρg = | 0.971 |
| Vg = | 0.015 |
| ρp = | 1.00 |
| Vp = | 0.00 |
| β = | 3 |
| αr = | -0.55 |
| Vr = | 0.045 |
| ρr = | 0.97 |
| ρm = | 1.00 |
| **Fy =** | **484** |

| Specification (Grouped) | |
|---|---|
| ASTM A500 | |
| **TYPE** | |
| SHAPED | |
| **METHOD** | |
| S136B | |
| **b/t limit** | |
| 19.7 | |
| **DATA** | |
| Fyn = | 345 |
| **Vm=** | **0.0670** |
| **RyFy (average) =** | **1.51** |
| | 520.95 |
| Φ = | 0.9 |
| ρg = | 0.971 |
| Vg = | 0.015 |
| ρp = | 1.00 |
| Vp = | 0.00 |
| β = | 3 |
| αr = | -0.55 |
| Vr = | 0.069 |
| ρr = | 1.01 |
| ρm = | 1.04 |
| **Fy =** | **502** |

| Specification (Grouped) | |
|---|---|
| ASTM A500 | |
| **TYPE** | |
| SHAPED | |
| **METHOD** | |
| WEIGHTED AVERAGE | |
| **b/t limit** | |
| 19.7 | |
| **DATA** | |
| Fyn = | 345 |
| **Vm=** | **0.0599** |
| **RyFy (average) =** | **1.47** |
| | 507.15 |
| Φ = | 0.9 |
| ρg = | 0.971 |
| Vg = | 0.015 |
| ρp = | 1.00 |
| Vp = | 0.00 |
| β = | 3 |
| αr = | -0.55 |
| Vr = | 0.062 |
| ρr = | 1.00 |
| ρm = | 1.03 |
| **Fy =** | **494** |

Table B- 23: Detailed results from reliability analysis – Part 8

**--> b/t<19.7 (KL/r = 140)**

| Specification (Grouped) | A1085 | Specification (Grouped) | A1085 | Specification (Grouped) | A1085 | Specification (Grouped) | A1085 |
|---|---|---|---|---|---|---|---|
| **TYPE** | SHAPED | **TYPE** | SHAPED | **TYPE** | SHAPED | **TYPE** | SHAPED |
| **METHOD** | COUPON DATA | **METHOD** | S136A | **METHOD** | S136B | **METHOD** | WEIGHTED AVERAGE |
| **b/t limit** | 19.7 | **b/t limit** | 19.7 | **b/t limit** | 19.7 | **b/t limit** | 19.7 |
| **DATA** | | **DATA** | | **DATA** | | **DATA** | |
| Fyn = | 345 | Fyn = | 345 | Fyn = | 345 | Fyn = | 345 |
| **Vm=** | **0.0534** | **Vm=** | **0.0366** | **Vm=** | **0.0481** | **Vm=** | **0.0442** |
| **RyFy (average) =** | **1.30** | **RyFy (average) =** | **1.45** | **RyFy (average) =** | **1.51** | **RyFy (average) =** | **1.47** |
| | 448.50 | | 500.25 | | 520.95 | | 507.15 |
| Φ = | 0.9 | Φ = | 0.9 | Φ = | 0.9 | Φ = | 0.9 |
| ρg = | 0.971 | ρg = | 0.971 | ρg = | 0.971 | ρg = | 0.971 |
| Vg = | 0.015 | Vg = | 0.015 | Vg = | 0.015 | Vg = | 0.015 |
| ρp = | 1.00 | ρp = | 1.00 | ρp = | 1.00 | ρp = | 1.00 |
| Vp = | 0.00 | Vp = | 0.00 | Vp = | 0.00 | Vp = | 0.00 |
| β = | 3 | β = | 3 | β = | 3 | β = | 3 |
| αr = | -0.55 | αr = | -0.55 | αr = | -0.55 | αr = | -0.55 |
| Vr = | 0.055 | Vr = | 0.040 | Vr = | 0.050 | Vr = | 0.047 |
| ρr = | 0.99 | ρr = | 0.96 | ρr = | 0.98 | ρr = | 0.97 |
| ρm = | 1.02 | ρm = | 0.99 | ρm = | 1.01 | ρm = | 1.00 |
| **Fy =** | **442** | **Fy =** | **506** | **Fy =** | **517** | **Fy =** | **507** |

Table B- 24: Detailed results from reliability analysis – Part 9

**--> b/t<19.7 (KL/r = 140)**

| Specification (Grouped) | |
|---|---|
| CSA G40.21 - 350W AND ASTM A500 SINGLE OR DUAL CERTIFIED | |
| **TYPE** | |
| SHAPED | |
| **METHOD** | |
| COUPON DATA | |
| **b/t limit** | |
| 19.7 | |
| **DATA** | |
| Fyn = | 345 |
| **Vm=** | **0.0876** |
| **RyFy (average) =** | **1.29** |
| | 445.05 |
| Φ = | 0.9 |
| ρg = | 0.971 |
| Vg = | 0.015 |
| ρp = | 1.00 |
| Vp = | 0.00 |
| β = | 3 |
| αr = | -0.55 |
| Vr = | 0.089 |
| ρr = | 1.04 |
| ρm = | 1.07 |
| **Fy =** | **415** |

| Specification (Grouped) | |
|---|---|
| CSA G40.21 - 350W AND ASTM A500 SINGLE OR DUAL CERTIFIED | |
| **TYPE** | |
| SHAPED | |
| **METHOD** | |
| S136A | |
| **b/t limit** | |
| 19.7 | |
| **DATA** | |
| Fyn = | 345 |
| **Vm=** | **0.0522** |
| **RyFy (average) =** | **1.44** |
| | 496.80 |
| Φ = | 0.9 |
| ρg = | 0.971 |
| Vg = | 0.015 |
| ρp = | 1.00 |
| Vp = | 0.00 |
| β = | 3 |
| αr = | -0.55 |
| Vr = | 0.054 |
| ρr = | 0.98 |
| ρm = | 1.01 |
| **Fy =** | **490** |

| Specification (Grouped) | |
|---|---|
| CSA G40.21 - 350W AND ASTM A500 SINGLE OR DUAL CERTIFIED | |
| **TYPE** | |
| SHAPED | |
| **METHOD** | |
| S136B | |
| **b/t limit** | |
| 19.7 | |
| **DATA** | |
| Fyn = | 345 |
| **Vm=** | **0.0598** |
| **RyFy (average) =** | **1.50** |
| | 517.50 |
| Φ = | 0.9 |
| ρg = | 0.971 |
| Vg = | 0.015 |
| ρp = | 1.00 |
| Vp = | 0.00 |
| β = | 3 |
| αr = | -0.55 |
| Vr = | 0.062 |
| ρr = | 1.00 |
| ρm = | 1.03 |
| **Fy =** | **504** |

| Specification (Grouped) | |
|---|---|
| CSA G40.21 - 350W AND ASTM A500 SINGLE OR DUAL CERTIFIED | |
| **TYPE** | |
| SHAPED | |
| **METHOD** | |
| WEIGHTED AVERAGE | |
| **b/t limit** | |
| 19.7 | |
| **DATA** | |
| Fyn = | 345 |
| **Vm=** | **0.0635** |
| **RyFy (average) =** | **1.46** |
| | 503.70 |
| Φ = | 0.9 |
| ρg = | 0.971 |
| Vg = | 0.015 |
| ρp = | 1.00 |
| Vp = | 0.00 |
| β = | 3 |
| αr = | -0.55 |
| Vr = | 0.065 |
| ρr = | 1.00 |
| ρm = | 1.03 |
| **Fy =** | **488** |

Table B- 25: Detailed results from reliability analysis – Part 10

**--> b/t<22.6 (KL/r = 200)**

| Specification (Grouped) | ASTM A500 |
|---|---|
| TYPE | SHAPED |
| METHOD | COUPON DATA |
| b/t limit | 22.6 |
| **COUPON DATA** | |
| Fyn = | 345 |
| **Vm=** | **0.0756** |
| **RyFy (average) =** | **1.29** |
| | 445.05 |
| Φ = | 0.9 |
| ρg = | 0.971 |
| Vg = | 0.015 |
| ρp = | 1.00 |
| Vp = | 0.00 |
| β = | 3 |
| αr = | -0.55 |
| Vr = | 0.077 |
| ρr = | 1.02 |
| ρm = | 1.05 |
| **Fy =** | **423** |

| Specification (Grouped) | ASTM A500 |
|---|---|
| TYPE | SHAPED |
| METHOD | S136A |
| b/t limit | 22.6 |
| **COUPON DATA** | |
| Fyn = | 345 |
| **Vm=** | **0.0466** |
| **RyFy (average) =** | **1.39** |
| | 479.55 |
| Φ = | 0.9 |
| ρg = | 0.971 |
| Vg = | 0.015 |
| ρp = | 1.00 |
| Vp = | 0.00 |
| β = | 3 |
| αr = | -0.55 |
| Vr = | 0.049 |
| ρr = | 0.98 |
| ρm = | 1.00 |
| **Fy =** | **477** |

| Specification (Grouped) | ASTM A500 |
|---|---|
| TYPE | SHAPED |
| METHOD | S136B |
| b/t limit | 22.6 |
| **COUPON DATA** | |
| Fyn = | 345 |
| **Vm=** | **0.0688** |
| **RyFy (average) =** | **1.49** |
| | 514.05 |
| Φ = | 0.9 |
| ρg = | 0.971 |
| Vg = | 0.015 |
| ρp = | 1.00 |
| Vp = | 0.00 |
| β = | 3 |
| αr = | -0.55 |
| Vr = | 0.070 |
| ρr = | 1.01 |
| ρm = | 1.04 |
| **Fy =** | **494** |

| Specification (Grouped) | ASTM A500 |
|---|---|
| TYPE | SHAPED |
| METHOD | WEIGHTED AVERAGE |
| b/t limit | 22.6 |
| **COUPON DATA** | |
| Fyn = | 345 |
| **Vm=** | **0.0628** |
| **RyFy (average) =** | **1.46** |
| | 503.70 |
| Φ = | 0.9 |
| ρg = | 0.971 |
| Vg = | 0.015 |
| ρp = | 1.00 |
| Vp = | 0.00 |
| β = | 3 |
| αr = | -0.55 |
| Vr = | 0.065 |
| ρr = | 1.00 |
| ρm = | 1.03 |
| **Fy =** | **489** |

Table B- 26: Detailed results from reliability analysis – Part 11

**--> b/t<22.6 (KL/r = 200)**

| Specification (Grouped) | |
|---|---|
| A1085 | |
| **TYPE** | |
| SHAPED | |
| **METHOD** | |
| COUPON DATA | |
| **b/t limit** | |
| 22.6 | |
| **COUPON DATA** | |
| Fyn = | 345 |
| **Vm=** | **0.0560** |
| **RyFy (average) =** | **1.29** |
| | 445.05 |
| Φ = | 0.9 |
| ρg = | 0.971 |
| Vg = | 0.015 |
| ρp = | 1.00 |
| Vp = | 0.00 |
| β = | 3 |
| αr = | -0.55 |
| Vr = | 0.058 |
| ρr = | 0.99 |
| ρm = | 1.02 |
| **Fy =** | **436** |

| Specification (Grouped) | |
|---|---|
| A1085 | |
| **TYPE** | |
| SHAPED | |
| **METHOD** | |
| S136A | |
| **b/t limit** | |
| 22.6 | |
| **COUPON DATA** | |
| Fyn = | 345 |
| **Vm=** | **0.0421** |
| **RyFy (average) =** | **1.44** |
| | 496.80 |
| Φ = | 0.9 |
| ρg = | 0.971 |
| Vg = | 0.015 |
| ρp = | 1.00 |
| Vp = | 0.00 |
| β = | 3 |
| αr = | -0.55 |
| Vr = | 0.045 |
| ρr = | 0.97 |
| ρm = | 1.00 |
| **Fy =** | **498** |

| Specification (Grouped) | |
|---|---|
| A1085 | |
| **TYPE** | |
| SHAPED | |
| **METHOD** | |
| S136B | |
| **b/t limit** | |
| 22.6 | |
| **COUPON DATA** | |
| Fyn = | 345 |
| **Vm=** | **0.0523** |
| **RyFy (average) =** | **1.50** |
| | 517.50 |
| Φ = | 0.9 |
| ρg = | 0.971 |
| Vg = | 0.015 |
| ρp = | 1.00 |
| Vp = | 0.00 |
| β = | 3 |
| αr = | -0.55 |
| Vr = | 0.054 |
| ρr = | 0.98 |
| ρm = | 1.01 |
| **Fy =** | **510** |

| Specification (Grouped) | |
|---|---|
| A1085 | |
| **TYPE** | |
| SHAPED | |
| **METHOD** | |
| WEIGHTED AVERAGE | |
| **b/t limit** | |
| 22.6 | |
| **COUPON DATA** | |
| Fyn = | 345 |
| **Vm=** | **0.0488** |
| **RyFy (average) =** | **1.46** |
| | 503.70 |
| Φ = | 0.9 |
| ρg = | 0.971 |
| Vg = | 0.015 |
| ρp = | 1.00 |
| Vp = | 0.00 |
| β = | 3 |
| αr = | -0.55 |
| Vr = | 0.051 |
| ρr = | 0.98 |
| ρm = | 1.01 |
| **Fy =** | **500** |

Table B- 27: Detailed results from reliability analysis – Part 12

**--> b/t<22.6 (KL/r = 200)**

| Specification (Grouped) | |
|---|---|
| CSA G40.21 - 350W AND ASTM A500 SINGLE OR DUAL CERTIFIED | |
| **TYPE** | |
| SHAPED | |
| **METHOD** | |
| COUPON DATA | |
| **b/t limit** | |
| 22.6 | |
| **COUPON DATA** | |
| Fyn = | 345 |
| **Vm=** | **0.0860** |
| **RyFy (average) =** | **1.28** |
| | 441.60 |
| Φ = | 0.9 |
| ρg = | 0.971 |
| Vg = | 0.015 |
| ρp = | 1.00 |
| Vp = | 0.00 |
| β = | 3 |
| αr = | -0.55 |
| Vr = | 0.087 |
| ρr = | 1.04 |
| ρm = | 1.07 |
| **Fy =** | **413** |

| Specification (Grouped) | |
|---|---|
| CSA G40.21 - 350W AND ASTM A500 SINGLE OR DUAL CERTIFIED | |
| **TYPE** | |
| SHAPED | |
| **METHOD** | |
| S136A | |
| **b/t limit** | |
| 22.6 | |
| **COUPON DATA** | |
| Fyn = | 345 |
| **Vm=** | **0.0551** |
| **RyFy (average) =** | **1.43** |
| | 493.35 |
| Φ = | 0.9 |
| ρg = | 0.971 |
| Vg = | 0.015 |
| ρp = | 1.00 |
| Vp = | 0.00 |
| β = | 3 |
| αr = | -0.55 |
| Vr = | 0.057 |
| ρr = | 0.99 |
| ρm = | 1.02 |
| **Fy =** | **484** |

| Specification (Grouped) | |
|---|---|
| CSA G40.21 - 350W AND ASTM A500 SINGLE OR DUAL CERTIFIED | |
| **TYPE** | |
| SHAPED | |
| **METHOD** | |
| S136B | |
| **b/t limit** | |
| 22.6 | |
| **COUPON DATA** | |
| Fyn = | 345 |
| **Vm=** | **0.0624** |
| **RyFy (average) =** | **1.48** |
| | 510.60 |
| Φ = | 0.9 |
| ρg = | 0.971 |
| Vg = | 0.015 |
| ρp = | 1.00 |
| Vp = | 0.00 |
| β = | 3 |
| αr = | -0.55 |
| Vr = | 0.064 |
| ρr = | 1.00 |
| ρm = | 1.03 |
| **Fy =** | **496** |

| Specification (Grouped) | |
|---|---|
| CSA G40.21 - 350W AND ASTM A500 SINGLE OR DUAL CERTIFIED | |
| **TYPE** | |
| SHAPED | |
| **METHOD** | |
| WEIGHTED AVERAGE | |
| **b/t limit** | |
| 22.6 | |
| **COUPON DATA** | |
| Fyn = | 345 |
| **Vm=** | **0.0649** |
| **RyFy (average) =** | **1.45** |
| | 500.25 |
| Φ = | 0.9 |
| ρg = | 0.971 |
| Vg = | 0.015 |
| ρp = | 1.00 |
| Vp = | 0.00 |
| β = | 3 |
| αr = | -0.55 |
| Vr = | 0.067 |
| ρr = | 1.00 |
| ρm = | 1.03 |
| **Fy =** | **484** |

Table B- 28: Detailed results from reliability analysis – Part 13

**-->D/t<28.9 (KL/r = 100)**

| Specification (Grouped) | |
|---|---|
| ASTM A500 | |
| **TYPE** | |
| SHAPED | |
| **METHOD** | |
| COUPON DATA | |
| **D/t limit** | |
| 28.9 | |
| **DATA** | |
| Fyn = | 345 |
| **Vm=** | **0.0744** |
| **RyFy (average) =** | **1.31** |
| | 451.95 |
| Φ = | 0.9 |
| ρg = | 0.971 |
| Vg = | 0.015 |
| ρp = | 1.00 |
| Vp = | 0.00 |
| β = | 3 |
| αr = | -0.55 |
| Vr = | 0.076 |
| ρr = | 1.02 |
| ρm = | 1.05 |
| **Fy =** | **430** |

| Specification (Grouped) | |
|---|---|
| A1085 | |
| **TYPE** | |
| SHAPED | |
| **METHOD** | |
| COUPON DATA | |
| **D/t limit** | |
| 28.9 | |
| **DATA** | |
| Fyn = | 345 |
| **Vm=** | **0.0536** |
| **RyFy (average) =** | **1.30** |
| | 448.50 |
| Φ = | 0.9 |
| ρg = | 0.971 |
| Vg = | 0.015 |
| ρp = | 1.00 |
| Vp = | 0.00 |
| β = | 3 |
| αr = | -0.55 |
| Vr = | 0.056 |
| ρr = | 0.99 |
| ρm = | 1.02 |
| **Fy =** | **441** |

| Specification (Grouped) | |
|---|---|
| CSA G40.21 - 350W AND ASTM A500 SINGLE OR DUAL CERTIFIED | |
| **TYPE** | |
| SHAPED | |
| **METHOD** | |
| COUPON DATA | |
| **D/t limit** | |
| 28.9 | |
| **DATA** | |
| Fyn = | 345 |
| **Vm=** | **0.0866** |
| **RyFy (average) =** | **1.29** |
| | 445.05 |
| Φ = | 0.9 |
| ρg = | 0.971 |
| Vg = | 0.015 |
| ρp = | 1.00 |
| Vp = | 0.00 |
| β = | 3 |
| αr = | -0.55 |
| Vr = | 0.088 |
| ρr = | 1.04 |
| ρm = | 1.07 |
| **Fy =** | **415** |

Table B- 29: Detailed results from reliability analysis – Part 14

**-->D/t<32.4 (KL/r = 100)**

| Specification (Grouped) | |
|---|---|
| ASTM A500 | |
| **TYPE** | |
| SHAPED | |
| **METHOD** | |
| COUPON DATA | |
| **D/t limit** | |
| 32.4 | |
| **DATA** | |
| Fyn = | 345 |
| **Vm=** | **0.0743** |
| **RyFy (average) =** | **1.31** |
| | 451.95 |
| Φ = | 0.9 |
| ρg = | 0.971 |
| Vg = | 0.015 |
| ρp = | 1.00 |
| Vp = | 0.00 |
| β = | 3 |
| αr = | -0.55 |
| Vr = | 0.076 |
| ρr = | 1.02 |
| ρm = | 1.05 |
| **Fy =** | **430** |

| Specification (Grouped) | |
|---|---|
| A1085 | |
| **TYPE** | |
| SHAPED | |
| **METHOD** | |
| COUPON DATA | |
| **D/t limit** | |
| 32.4 | |
| **DATA** | |
| Fyn = | 345 |
| **Vm=** | **0.0534** |
| **RyFy (average) =** | **1.30** |
| | 448.50 |
| Φ = | 0.9 |
| ρg = | 0.971 |
| Vg = | 0.015 |
| ρp = | 1.00 |
| Vp = | 0.00 |
| β = | 3 |
| αr = | -0.55 |
| Vr = | 0.055 |
| ρr = | 0.99 |
| ρm = | 1.02 |
| **Fy =** | **442** |

| Specification (Grouped) | |
|---|---|
| CSA G40.21 - 350W AND ASTM A500 SINGLE OR DUAL CERTIFIED | |
| **TYPE** | |
| SHAPED | |
| **METHOD** | |
| COUPON DATA | |
| **D/t limit** | |
| 32.4 | |
| **DATA** | |
| Fyn = | 345 |
| **Vm=** | **0.0876** |
| **RyFy (average) =** | **1.29** |
| | 445.05 |
| Φ = | 0.9 |
| ρg = | 0.971 |
| Vg = | 0.015 |
| ρp = | 1.00 |
| Vp = | 0.00 |
| β = | 3 |
| αr = | -0.55 |
| Vr = | 0.089 |
| ρr = | 1.04 |
| ρm = | 1.07 |
| **Fy =** | **415** |

Table B- 30: Detailed results from reliability analysis – Part 15

**-->D/t<37.6 (KL/r = 200)**

| Specification (Grouped) | |
|---|---|
| ASTM A500 | |
| **TYPE** | |
| SHAPED | |
| **METHOD** | |
| COUPON DATA | |
| **D/t limit** | |
| 37.6 | |
| **DATA** | |
| Fyn = | 345 |
| **Vm=** | **0.0756** |
| **RyFy (average) =** | **1.29** |
| | 445.05 |
| Φ = | 0.9 |
| ρg = | 0.971 |
| Vg = | 0.015 |
| ρp = | 1.00 |
| Vp = | 0.00 |
| β = | 3 |
| αr = | -0.55 |
| Vr = | 0.077 |
| ρr = | 1.02 |
| ρm = | 1.05 |
| **Fy =** | **423** |

| Specification (Grouped) | |
|---|---|
| A1085 | |
| **TYPE** | |
| SHAPED | |
| **METHOD** | |
| COUPON DATA | |
| **D/t limit** | |
| 37.6 | |
| **DATA** | |
| Fyn = | 345 |
| **Vm=** | **0.0560** |
| **RyFy (average) =** | **1.29** |
| | 445.05 |
| Φ = | 0.9 |
| ρg = | 0.971 |
| Vg = | 0.015 |
| ρp = | 1.00 |
| Vp = | 0.00 |
| β = | 3 |
| αr = | -0.55 |
| Vr = | 0.058 |
| ρr = | 0.99 |
| ρm = | 1.02 |
| **Fy =** | **436** |

| Specification (Grouped) | |
|---|---|
| CSA G40.21 - 350W AND ASTM A500 SINGLE OR DUAL CERTIFIED | |
| **TYPE** | |
| SHAPED | |
| **METHOD** | |
| COUPON DATA | |
| **D/t limit** | |
| 37.6 | |
| **DATA** | |
| Fyn = | 345 |
| **Vm=** | **0.0860** |
| **RyFy (average) =** | **1.28** |
| | 441.60 |
| Φ = | 0.9 |
| ρg = | 0.971 |
| Vg = | 0.015 |
| ρp = | 1.00 |
| Vp = | 0.00 |
| β = | 3 |
| αr = | -0.55 |
| Vr = | 0.087 |
| ρr = | 1.04 |
| ρm = | 1.07 |
| **Fy =** | **413** |

# APPENDIX C – TESTED PROFILES FOR CHAPTER 4

Table C- 5: Profiles used for OpenSees analysis with actual properties – Part 1

| Shape (Square) | Shape | | | Design Wall Thickness, t | Nominal Wt | Area, A | b/t |
|---|---|---|---|---|---|---|---|
| | H | B | $t_{nom}$ | | | | |
| | mm | mm | mm | mm | N/m | mm^2 | |
| **HSS 20 x 20 x 7/8** | 508 | 508 | 22.225 | 22.225 | 3226.13 | 41935.4 | 19.9 |
| **HSS 20 x 20 x 3/4** | 508 | 508 | 19.050 | 19.050 | 2795.90 | 36322.51 | 23.7 |
| **HSS 20 x 20 x 5/8** | 508 | 508 | 15.875 | 15.875 | 2355.46 | 30580.58 | 29.0 |
| **HSS 20 x 20 x 1/2** | 508 | 508 | 12.700 | 12.700 | 1904.80 | 24774.14 | 37.0 |
| **HSS 20 x 20 x 3/8** | 508 | 508 | 9.525 | 9.525 | 1443.92 | 18774.16 | 50.3 |
| **HSS 18 x 18 x 7/8** | 457.2 | 457.2 | 22.225 | 22.225 | 2878.50 | 37419.28 | 17.6 |
| **HSS 18 x 18 x 3/4** | 457.2 | 457.2 | 19.050 | 19.050 | 2497.89 | 32451.55 | 21.0 |
| **HSS 18 x 18 x 5/8** | 457.2 | 457.2 | 15.875 | 15.875 | 2107.21 | 27354.78 | 25.8 |
| **HSS 18 x18 x 1/2** | 457.2 | 457.2 | 12.700 | 12.700 | 1706.17 | 22193.5 | 33.0 |
| **HSS 18 x 18 x 3/8** | 457.2 | 457.2 | 9.525 | 9.525 | 1294.92 | 16838.68 | 45 |
| **HSS 16 x 16 x 7/8** | 406.4 | 406.4 | 22.225 | 22.225 | 2531.02 | 32903.16 | 15.3 |
| **HSS 16 x 16 x 3/4** | 406.4 | 406.4 | 19.050 | 19.050 | 2200.03 | 28580.59 | 18.3 |
| **HSS 16 x 16 x 5/8** | 406.4 | 406.4 | 15.875 | 15.875 | 1858.82 | 24128.98 | 22.6 |
| **HSS 16 x 16 x 1/2** | 406.4 | 406.4 | 12.700 | 12.700 | 1507.55 | 19612.86 | 29.0 |
| **HSS 16 x 16 x 3/8** | 406.4 | 406.4 | 9.525 | 9.525 | 1145.91 | 14903.2 | 39.7 |
| **HSS 16 x 16 x 5/16** | 406.4 | 406.4 | 7.938 | 7.950 | 961.30 | 12516.1 | 48.1 |
| **HSS 14 x 14 x 7/8** | 355.6 | 355.6 | 22.225 | 22.225 | 2183.39 | 28387.04 | 13.0 |
| **HSS 14 x 14 x 3/4** | 355.6 | 355.6 | 19.050 | 19.050 | 1902.02 | 24709.63 | 15.7 |
| **HSS 14 x 14 x 5/8** | 355.6 | 355.6 | 15.875 | 15.875 | 1610.58 | 20903.18 | 19.4 |
| **HSS 14 x 14 x 1/2** | 355.6 | 355.6 | 12.700 | 12.700 | 1308.78 | 17032.22 | 25.0 |
| **HSS 14 x 14 x 3/8** | 355.6 | 355.6 | 9.525 | 9.525 | 996.91 | 12967.72 | 34.3 |
| **HSS 14 x 14 x 5/16** | 355.6 | 355.6 | 7.938 | 7.950 | 837.11 | 10903.2 | 41.7 |

Table C- 6: Profiles used for OpenSees analysis with actual properties – Part 2

| Shape (Square) | Shape | | | Design Wall Thickness, t | Nominal Wt | Area, A | b/t |
|---|---|---|---|---|---|---|---|
| | H | B | $t_{nom}$ | | | | |
| | mm | mm | mm | mm | N/m | mm^2 | |
| **HSS 12 x 12 x 3/4** | 304.8 | 304.8 | 19.050 | 19.050 | 1604.02 | 20838.67 | 13.0 |
| **HSS 12 x 12 x 5/8** | 304.8 | 304.8 | 15.875 | 15.875 | 1362.19 | 17677.38 | 16.2 |
| **HSS 12 x 12 x 1/2** | 304.8 | 304.8 | 12.700 | 12.700 | 1110.16 | 14451.58 | 21.0 |
| **HSS 12 x 12 x 3/8** | 304.8 | 304.8 | 9.525 | 9.525 | 847.91 | 11032.24 | 29.0 |
| **HSS 12 x 12 x 5/16** | 304.8 | 304.8 | 7.938 | 7.950 | 713.06 | 9290.304 | 35.3 |
| **HSS 12 x 12 x 1/4** | 304.8 | 304.8 | 6.350 | 6.350 | 575.44 | 7483.856 | 45.0 |
| **HSS 10 x 10 x 5/8** | 254 | 254 | 15.875 | 15.875 | 1113.95 | 14451.58 | 13.0 |
| **HSS 10 x 10 x 1/2** | 254 | 254 | 12.700 | 12.700 | 911.53 | 11870.94 | 17.0 |
| **HSS 10 x 10 x 3/8** | 254 | 254 | 9.525 | 9.525 | 699.05 | 9096.756 | 23.7 |
| **HSS 10 x 10 x 5/16** | 254 | 254 | 7.938 | 7.950 | 588.86 | 7677.404 | 28.9 |
| **HSS 10 x 10 x 1/4** | 254 | 254 | 6.350 | 6.350 | 476.20 | 6187.084 | 37.0 |
| **HSS 10 x 10 x 3/16** | 254 | 254 | 4.763 | 4.775 | 360.91 | 4703.216 | 50.2 |
| **HSS 9 x 9 x 5/8** | 228.6 | 228.6 | 15.875 | 15.875 | 989.76 | 12838.68 | 11.4 |
| **HSS 9 x 9 x 1/2** | 228.6 | 228.6 | 12.700 | 12.700 | 812.30 | 10580.62 | 15.0 |
| **HSS 9 x 9 x 3/8** | 228.6 | 228.6 | 9.525 | 9.525 | 624.47 | 8129.016 | 21.0 |
| **HSS 9 x 9 x 5/16** | 228.6 | 228.6 | 7.938 | 7.950 | 526.84 | 6851.599 | 25.8 |
| **HSS 9 x 9 x 1/4** | 228.6 | 228.6 | 6.350 | 6.350 | 426.58 | 5541.924 | 33.0 |
| **HSS 9 x 9 x 3/16** | 228.6 | 228.6 | 4.763 | 4.775 | 323.69 | 4219.346 | 44.9 |
| **HSS 8 x 8 x 5/8** | 203.2 | 203.2 | 15.875 | 15.875 | 865.71 | 11225.78 | 9.8 |
| **HSS 8 x 8 x 1/2** | 203.2 | 203.2 | 12.700 | 12.700 | 712.91 | 9290.304 | 13.0 |
| **HSS 8 x 8 x 3/8** | 203.2 | 203.2 | 9.525 | 9.525 | 550.04 | 7161.276 | 18.3 |
| **HSS 8 x 8 x 5/16** | 203.2 | 203.2 | 7.938 | 7.950 | 464.67 | 6045.149 | 22.6 |
| **HSS 8 x 8 x 1/4** | 203.2 | 203.2 | 6.350 | 6.350 | 376.81 | 4896.764 | 29.0 |
| **HSS 8 x 8 x 3/16** | 203.2 | 203.2 | 4.763 | 4.775 | 286.48 | 3729.025 | 39.6 |

Table C- 7: Profiles used for OpenSees analysis with actual properties – Part 3

| Shape (Square) | Shape | | | Design Wall Thickness, t | Nominal Wt | Area, A | b/t |
|---|---|---|---|---|---|---|---|
| | H | B | $t_{nom}$ | | | | |
| | mm | mm | mm | mm | N/m | mm^2 | |
| **HSS 7 x 7 x 5/8** | 177.8 | 177.8 | 15.875 | 15.875 | 741.52 | 9612.884 | 8.2 |
| **HSS 7 x 7 x 1/2** | 177.8 | 177.8 | 12.700 | 12.700 | 613.67 | 7999.984 | 11.0 |
| **HSS 7 x 7 x 3/8** | 177.8 | 177.8 | 9.525 | 9.525 | 475.47 | 6180.633 | 15.7 |
| **HSS 7 x 7 x 5/16** | 177.8 | 177.8 | 7.938 | 7.950 | 402.65 | 5238.699 | 19.4 |
| **HSS 7 x 7 x 1/4** | 177.8 | 177.8 | 6.350 | 6.350 | 327.20 | 4251.604 | 25.0 |
| **HSS 7 x 7 x 3/16** | 177.8 | 177.8 | 4.763 | 4.775 | 249 | 3245 | 34.2 |
| **HSS 6 x 6 x 1/2** | 152.4 | 152.4 | 12.700 | 12.700 | 514 | 6684 | 9.0 |
| **HSS 6 x 6 x 3/8** | 152.4 | 152.4 | 9.525 | 9.525 | 401 | 5213 | 13.0 |
| **HSS 6 x 6 x 5/16** | 152.4 | 152.4 | 7.938 | 7.950 | 341 | 4432 | 16.2 |
| **HSS 6 x 6 x 1/4** | 152.4 | 152.4 | 6.350 | 6.350 | 278 | 3606 | 21.0 |
| **HSS 6 x 6 x 3/16** | 152.4 | 152.4 | 4.763 | 4.775 | 212 | 2761 | 28.9 |
| **HSS 5 x 5 x 1/2** | 127 | 127 | 12.700 | 12.700 | 415 | 5394 | 7.0 |
| **HSS 5 x 5 x 3/8** | 127 | 127 | 9.525 | 9.525 | 326 | 4245 | 10.3 |
| **HSS 5 x 5 x 5/16** | 127 | 127 | 7.938 | 7.950 | 278 | 3626 | 13.0 |
| **HSS 5 x 5 x 1/4** | 127 | 127 | 6.350 | 6.350 | 228 | 2961 | 17.0 |
| **HSS 5 x 5 x 3/16** | 127 | 127 | 4.763 | 4.775 | 175 | 2277 | 23.6 |
| **HSS 4.5 x 4.5 x 3/8** | 114.3 | 114.3 | 9.525 | 9.525 | 289 | 3761 | 9.0 |
| **HSS 4.5 x 4.5 x 5/16** | 114.3 | 114.3 | 7.938 | 7.950 | 248 | 3219 | 11.4 |
| **HSS 4.5 x 4.5 x 1/4** | 114.3 | 114.3 | 6.350 | 6.350 | 203 | 2639 | 15.0 |
| **HSS 4.5 x 4.5 x 3/16** | 114.3 | 114.3 | 4.763 | 4.775 | 156 | 2032 | 20.9 |
| **HSS 4 x 4 x 1/2** | 101.6 | 101.6 | 12.700 | 12.700 | 316 | 4103 | 5.0 |
| **HSS 4 x 4 x 3/8** | 101.6 | 101.6 | 9.525 | 9.525 | 252 | 3277 | 7.7 |
| **HSS 4 x 4 x 5/16** | 101.6 | 101.6 | 7.938 | 7.950 | 216 | 2813 | 9.8 |

Table C- 8: Profiles used for OpenSees analysis with actual properties – Part 4

| Shape (Square) | Shape | | | Design Wall Thickness, t | Nominal Wt | Area, A | b/t |
|---|---|---|---|---|---|---|---|
| | H | B | $t_{nom}$ | | | | |
| | mm | mm | mm | mm | N/m | mm^2 | |
| **HSS 4 x 4 x 1/4** | 101.6 | 101.6 | 6.350 | 6.350 | 178 | 2316 | 13.0 |
| **HSS 4 x 4 x 3/16** | 101.6 | 101.6 | 4.763 | 4.775 | 137 | 1794 | 18.3 |
| **HSS 3.5 x 3.5 x 3/8** | 88.9 | 88.9 | 9.525 | 9.525 | 215 | 2794 | 6.3 |
| **HSS 3.5 x 3.5 x 5/16** | 88.9 | 88.9 | 7.938 | 7.950 | 185 | 2413 | 8.2 |
| **HSS 3.5 x 3.5 x 1/4** | 88.9 | 88.9 | 6.350 | 6.350 | 153 | 1994 | 11.0 |
| **HSS 3.5 x 3.5 x 3/16** | 88.9 | 88.9 | 4.763 | 4.775 | 119 | 1548 | 15.6 |
| **HSS 3 x 3 x 3/8** | 76.2 | 76.2 | 9.525 | 9.525 | 178 | 2310 | 5.0 |
| **HSS 3 x 3 x 5/16** | 76.2 | 76.2 | 7.938 | 7.950 | 154 | 2006 | 6.6 |
| **HSS 3 x 3 x 1/4** | 76.2 | 76.2 | 6.350 | 6.350 | 129 | 1671 | 9.0 |
| **HSS 3 x 3 x 3/16** | 76.2 | 76.2 | 4.763 | 4.775 | 100 | 1303 | 13.0 |
| **HSS 2.5 x 2.5 x 1/4** | 63.5 | 63.5 | 6.350 | 6.350 | 104 | 1348 | 7.0 |
| **HSS 2.5 x 2.5 x 3/16** | 63.5 | 63.5 | 4.763 | 4.775 | 82 | 1065 | 10.3 |
| **HSS 2 x 2 x 1/4** | 50.8 | 50.8 | 6.350 | 6.350 | 79 | 1026 | 5.0 |
| **HSS 2 x 2 x 3/16** | 50.8 | 50.8 | 4.763 | 4.775 | 63 | 819 | 7.6 |

# APPENDIX D – DATA FROM PREVIOUS RESEARCH FOR CHAPTER 3

Table D- 10: Coupon results from previous research – Part 1

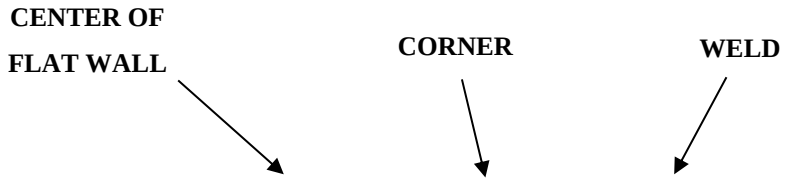


| PROFILE | | | 1 | 2 | 3 | 4 | 5 | 6 | 7 | 8 | 9 | 10 | 11 | 12 | 13 | 14 | 15 | 16 | 17 | 18 | 19 | 20 | 21 | 22 | 23 | 24 | 25 | 26 | 27 | 28 | 29 | 30 | 31 | 32 | 33 | 34 | 35 | 36 | 37 | 38 | 39 | 40 | 41 | 42 | 43 | 44 |
|---|---|---|---|---|---|---|---|---|---|---|---|---|---|---|---|---|---|---|---|---|---|---|---|---|---|---|---|---|---|---|---|---|---|---|---|---|---|---|---|---|---|---|---|---|---|
| 75 | 25 | 1.60 | 487 | | | | | 505 | | | | | | 428 | | | | | 500 | | | | | | | | | | 510 | | | | | | 450 | | | | | 510 | | | | |
| 150 | 50 | 3.00 | 380 | | | | | 465 | | | | | | 369 | | | | | 475 | | | | | | | | | | 480 | | | | | | 421 | | | | | 495 | | | | |
| 100 | 50 | 2.00 | 380 | | | | | 500 | | | | | | 369 | | | | | 485 | | | | | | | | | | 480 | | | | | | 395 | | | | | 505 | | | | |
| 125 | 75 | 3.00 | 403 | | | | | 470 | | | | | | 397 | | | | | 475 | | | | | | | | | | 475 | | | | | | 396 | | | | | 470 | | | | |
| 150 | 50 | 3.00 | 403 | | | | | | | | | | | 383 | | | | | | | | | | | | | | | | | | | | | 380 | | | | | | | | | |
| 125 | 75 | 2.50 | 420 | | | | | | | | | | | 370 | | | | | | | | | (Wilkinson, 1999) | | | | | | | | | | | | 377 | | | | | | | | | |
| 102 | 51 | 4.90 | 437 | | | | | 498 | | | | | | | | | | | | | | | | | | | | | | | | | | | | | | | | | | | | |
| 102 | 51 | 3.20 | 425 | | | | | 535 | | | | | | | | | | | | | | | | | | | | | | | | | | | | | | | | | | | | |
| 102 | 51 | 2.00 | 407 | | | | | 439 | | | | | | | | | | | | | | | | | | | | | | | | | | | | | | | | | | | | |
| 102 | 102 | 9.50 | 482 | | | | | 536 | | | | | | | | | | | | | | | | | | | | | | | | | | | | | | | | | | | | |
| 102 | 102 | 6.30 | 428 | | | | | 538 | | | | | | | | | | | | | | | (Key & Hancock, 1993) | | | | | | | | | | | | | | | | | | | | | |
| 76 | 76 | 2.00 | 428 | | | | | 538 | | | | | | | | | | | | | | | (Key, 1988) | | | | | | | | | | | | | | | | | | | | | |
| 152 | 152 | 4.90 | 435 | | | | 435 | 520 | | 430 | | | | 430 | | | | 430 | 510 | | 450 | | | | 500 | | | 450 | | 510 | | 430 | | | 435 | | | | 435 | | | 435 | | | |
| 203 | 203 | 6.30 | 425 | | | | | 500 | | | | | | 360 | | | | | 500 | | | | | | 560 | | | | | 450 | | | | | 390 | | | | | 510 | | | | |
| 254 | 254 | 6.30 | 400 | | | | 405 | | | 410 | | | | 355 | | | | 390 | | | 410 | | | | 550 | | | 380 | | 485 | | 390 | | | 350 | | | | 400 | 530 | | | | |

Table D- 11: Coupon results from previous research – Part 2

| PROFILE | | | 1 | 2 | 3 | 4 | 5 | 6 | 7 | 8 | 9 | 10 | 11 | 12 | 13 | 14 | 15 | 16 | 17 | 18 | 19 | 20 | 21 | 22 | 23 | 24 | 25 | 26 | 27 | 28 | 29 | 30 | 31 | 32 | 33 | 34 | 35 | 36 | 37 | 38 | 39 | 40 | 41 | 42 | 43 | 44 |
|---|---|---|---|---|---|---|---|---|---|---|---|---|---|---|---|---|---|---|---|---|---|---|---|---|---|---|---|---|---|---|---|---|---|---|---|---|---|---|---|---|---|---|---|---|---|
| 76 | 76 | 2.00 | 425 | | | | | 531 | | | | | | | | | | | | | | (Key et al., 1988) | | | | | | | | | | | | | | | | | | | | | | | |
| 76 | 76 | 2.00 | 370 | | | | | 476 | | | | | | | | | | | | | | | | | | | | | | | | | | | | | | | | | | | | | |
| 152 | 152 | 4.90 | 416 | | | | | 498 | | | | | | | | | | | | | | | | | | | | | | | | | | | | | | | | | | | | | |
| 203 | 203 | 6.30 | 395 | | | | | 494 | | | | | | | | | | | | | | | | | | | | | | | | | | | | | | | | | | | | | |
| 254 | 254 | 6.30 | 405 | | | | | 487 | | | | | | | | | | | | | | | | | | | | | | | | | | | | | | | | | | | | | |
| 102 | 51 | 2.00 | 422 | | | | | 551 | | | | | | | | | | | | | | | | | | | | | | | | | | | | | | | | | | | | | |
| 127 | 51 | 3.60 | 388 | | | | | 451 | | | | | | | | | | | | | | | | | | | | | | | | | | | | | | | | | | | | | |
| 127 | 64 | 4.00 | 418 | | | | | 485 | | | | | | | | | | | | | | | | | | | | | | | | | | | | | | | | | | | | | |
| 152 | 76 | 4.90 | 372 | | | | | 459 | | | | | | | | | | | | | | | | | | | | | | | | | | | | | | | | | | | | | |
| 203 | 102 | 4.90 | 371 | | | | | 481 | | | | | | | | | | | | | | | | | | | | | | | | | | | | | | | | | | | | | |
| 254 | 152 | 6.30 | 397 | | | | | 476 | | | | | | | | | | | | | | | | | | | | | | | | | | | | | | | | | | | | | |
| 76 | 76 | 2.11 | | 390 | 413 | 474 | 555 | | | | | | | | | | | | | | | (Davison & Birkemoe, 1983) | | | | | | | | | | | | | | | | | | | | | | | |
| 203 | 203 | 12.70 | 468 | | | | 544 | | | | | | | | | | | | | | | | | | | | | | | | | | | | | | | | | | | | | | |
| 203 | 203 | 12.70 | 401 | | | | 485 | | | | | | | | | | | | | | | | | | | | | | | | | | | | | | | | | | | | | | |
| 203 | 203 | 9.53 | 431 | | | | 491 | | | | | | | | | | | | | | | | | | | | | | | | | | | | | | | | | | | | | | |
| | | | | | | | | | | | | | | | | | | | | | | | (Kamani, 1974) | | | | | | | | | | | | | | | | | | | | | | | |
| 102 | 102 | 9.53 | 384 | | 401 | | | 585 | | | | | | | | | | 445 | 527 | | | | | | | | | 509 | 553 | | | | 457 | | 381 | | | | | 554 | | | | | |
| 203 | 203 | 9.53 | 379 | 365 | 372 | 386 | 421 | 459 | | 421 | 386 | 372 | 365 | 379 | 365 | 372 | 386 | 421 | 472 | | 452 | 424 | 427 | 448 | 459 | 448 | 427 | 427 | 455 | 459 | | 421 | 386 | 372 | 365 | 379 | 365 | 372 | 386 | 421 | 459 | | 421 | 386 | 372 | 365 |
| 305 | 203 | 11.43 | | | | | | | | | | | 372 | 381 | 377 | | | | | | | | | | | | | | | | | | | | | | | | | | | | | | |
| 102 | 305 | 9.53 | | | | | | | | | | | 441 | 423 | 430 | | | | | | | | (Davison, 1977) | | | | | | | | | | | | | | | | | | | | | | | |

Table D- 12: Coupon results from previous research – Part 3

| PROFILE | | | 1 | 2 | 3 | 4 | 5 | 6 | 7 | 8 | 9 | 10 | 11 | 12 | 13 | 14 | 15 | 16 | 17 | 18 | 19 | 20 | 21 | 22 | 23 | 24 | 25 | 26 | 27 | 28 | 29 | 30 | 31 | 32 | 33 | 34 | 35 | 36 | 37 | 38 | 39 | 40 | 41 | 42 | 43 | 44 |
|---|---|---|---|---|---|---|---|---|---|---|---|---|---|---|---|---|---|---|---|---|---|---|---|---|---|---|---|---|---|---|---|---|---|---|---|---|---|---|---|---|---|---|---|---|---|
| | | | | | | | | | | | | | | | | | | | | | | | (Salvarinas, 1977) | | | | | | | | | | | | | | | | | | | | | | | | | |
| 203 | 203 | 9.53 | 375 | 376 | 371 | 375 | 485 | | | 460 | 383 | 375 | 354 | 371 | 373 | 377 | 394 | 408 | 456 | | 446 | 427 | 432 | 453 | 454 | 431 | 416 | 418 | 488 | | | 397 | 394 | 376 | 365 | 375 | 377 | 381 | 376 | 408 | 441 | | 422 | 387 | 380 | 373 |
| 152 | 152 | 13.00 | 457 | | | | | 590 | | | | | | | | | | | | | | | (Sun & Packer, 2014) | | | | | | | | | | | | | | | | | | | | | | | | |
| 152 | 152 | 6.40 | 340 | | | | | 483 | | | | | | | | | | | | | | | | | | | | | | | | | | | | | | | | | | | | | | |
| 150 | 150 | 6.00 | 592 | | | | | 608 | | | | | | 408 | | | | | | | | | (Afshan et al., 2013) | | | | | | | | | | | | 393 | | | | | | | | | | | |
| 200 | 100 | 5.00 | 624 | | | | | 540 | | | | | | 436 | | | | | | | | | | | | | | | | | | | | | | 421 | | | | | | | | | | |
| 150 | 100 | 6.00 | 561 | | | | | 528 | | | | | | 375 | | | | | | | | | | | | | | | | | | | | | | 363 | | | | | | | | | | |
| 200 | 200 | 6.00 | 417 | | | | | 599 | | | | | | 449 | | | | | | | | | | | | | | | | | | | | | | 419 | | | | | | | | | | |
| 135 | 135 | 10.00 | 394 | | | | | | | | | | | | | | | | | | | | (Tong et al., 2012) | | | | | | | | | | | | | | | | | | | | | | | | |
| 135 | 135 | 10.00 | 374 | | | | | | | | | | | | | | | | | | | | | | | | | | | | | | | | | | | | | | | | | | | |
| 135 | 135 | 10.00 | 404 | | | | | | | | | | | | | | | | | | | | | | | | | | | | | | | | | | | | | | | | | | | |
| 220 | 220 | 16.00 | | | | | | 423 | | | | | | | | | | | 407 | | | | (Li et al., 2012) | | | | | | | 409 | | | | | | | | | | | 426 | | | | |
| 108 | 108 | 10.00 | 460 | | | | | 550 | | | | | | 420 | | | | | | | | | | | 550 | | | | | | | | | | 420 | | | | | | | | | | |
| 135 | 135 | 10.00 | 360 | | | | | 430 | | | | | | 310 | | | | | | | | | | | 460 | | | | | | | | | | 310 | | | | | | | | | | |
| | | | | | | | | | | | | | | | | | | | | | | | (Hu et al., 2011) | | | | | | | | | | | | | | | | | | | | | | | | |
| 250 | 250 | 9.20 | 392 | | | | | 545 | | | | | | 377 | | | | | 550 | | | | | | 535 | | | | | 553 | | | | | 378 | | | | | 545 | | | | |
| 200 | 300 | 9.20 | 392 | | | | | 580 | | | | | | 345 | | | | | 530 | | | | | | 533 | | | | | 523 | | | | | 340 | | | | | 568 | | | | |
| 100 | 100 | 4.00 | 482 | | | | | | | | | | | | | | | | | | | | (Gao & Moen, 2010) | | | | | | | | | | | | | | | | | | | | | | | | |
| 60 | 60 | 4.00 | 361 | | | | | | | | | | | | | | | | | | | | | | | | | | | | | | | | | | | | | | | | | | |
| 40 | 40 | 4.00 | 400 | | | | | | | | | | | | | | | | | | | | | | | | | | | | | | | | | | | | | | | | | | |
| 40 | 40 | 4.00 | 410 | | | | | | | | | | | | | | | | | | | | | | | | | | | | | | | | | | | | | | | | | | |
| 40 | 40 | 3.00 | 451 | | | | | | | | | | | | | | | | | | | | | | | | | | | | | | | | | | | | | | | | | | |

Table D- 13: Coupon results from previous research – Part 4

| PROFILE | | | 1 | 2 | 3 | 4 | 5 | 6 | 7 | 8 | 9 | 10 | 11 | 12 | 13 | 14 | 15 | 16 | 17 | 18 | 19 | 20 | 21 | 22 | 23 | 24 | 25 | 26 | 27 | 28 | 29 | 30 | 31 | 32 | 33 | 34 | 35 | 36 | 37 | 38 | 39 | 40 | 41 | 42 | 43 | 44 |
|---|---|---|---|---|---|---|---|---|---|---|---|---|---|---|---|---|---|---|---|---|---|---|---|---|---|---|---|---|---|---|---|---|---|---|---|---|---|---|---|---|---|---|---|---|---|
| 135 | 135 | 12.00 | 266 | | | | | | | | | | | | | | | | | | | | | | | | | | | | | | | | | | | | | | | | | | | |
| 135 | 135 | 10.00 | 248 | | | | | | | | | | | | | | | | | | | | | | | | | | | | | | | | | | | | | | | | | | | |
| 200 | 200 | 5.00 | 246 | | | | | | | | | | | | | | | | | | | | | | | | | | | | | | | | | | | | | | | | | | | |
| 100 | 100 | 3.20 | 394 | | | | | | | | | | | | | | | | | | | | | | | | | | | | | | | | | | | | | | | | | | | |
| 100 | 100 | 4.00 | 411 | | | | | | | | | | | | | | | | | | | | | | | | | | | | | | | | | | | | | | | | | | | |
| 100 | 100 | 4.50 | 421 | | | | | | | | | | | | | | | | | | | | | | | | | | | | | | | | | | | | | | | | | | | |
| 125 | 125 | 6.00 | 405 | | | | | | | | | | | | | | | | | | | | | | | | | | | | | | | | | | | | | | | | | | | |
| 100 | 100 | 6.00 | 399 | | | | | | | | | | | | | | | | | | | | | | | | | | | | | | | | | | | | | | | | | | | |
| 100 | 100 | 6.00 | 410 | | | | | | | | | | | | | | | | | | | | | | | | | | | | | | | | | | | | | | | | | | | |
| 100 | 100 | 6.00 | 408 | | | | | | | | | | | | | | | | | | | | | | | | | | | | | | | | | | | | | | | | | | | |
| 125 | 125 | 9.00 | 402 | | | | | | | | | | | | | | | | | | | | | | | | | | | | | | | | | | | | | | | | | | | |
| 100 | 100 | 9.00 | 425 | | | | | | | | | | | | | | | | | | | | | | | | | | | | | | | | | | | | | | | | | | | |
| 100 | 100 | 9.00 | 392 | | | | | | | | | | | | | | | | | | | | | | | | | | | | | | | | | | | | | | | | | | | |
| 100 | 100 | 9.00 | 395 | | | | | | | | | | | | | | | | | | | | | | | | | | | | | | | | | | | | | | | | | | | |
| 320 | 200 | 8.00 | 273 | | | | | 372 | | | | | | | | | | | | | | | | | | | | | | | | | | | | | | | | | | | | | | |
| 320 | 200 | 10.00 | 273 | | | | | 389 | | | | | | | | | | | | | | | | | | | | | | | | | | | | | | | | | | | | | | |
| 320 | 200 | 12.00 | 266 | | | | | 375 | | | | | | | | | | | | | | | | | | | | | | | | | | | | | | | | | | | | | | |
| 200 | 180 | 8.00 | 272 | | | | | 343 | | | | | | | | | | | | | | | | | | | | | | | | | | | | | | | | | | | | | | |
| 300 | 300 | 10.00 | 268 | | | | | 386 | | | | | | | | | | | | | | | | | | | | | | | | | | | | | | | | | | | | | | |
| 300 | 300 | 12.00 | 269 | | | | | 369 | | | | | | | | | | | | | | | | | | | | | | | | | | | | | | | | | | | | | | |

| PROFILE | | | 1 | 2 | 3 | 4 | 5 | 6 | 7 | 8 | 9 | 10 | 11 | 12 | 13 | 14 | 15 | 16 | 17 | 18 | 19 | 20 | 21 | 22 | 23 | 24 | 25 | 26 | 27 | 28 | 29 | 30 | 31 | 32 | 33 | 34 | 35 | 36 | 37 | 38 | 39 | 40 | 41 | 42 | 43 | 44 |
|---|---|---|---|---|---|---|---|---|---|---|---|---|---|---|---|---|---|---|---|---|---|---|---|---|---|---|---|---|---|---|---|---|---|---|---|---|---|---|---|---|---|---|---|---|---|
| | | | | | | | | | | | | | | | | | | | | | | | | | | | | | | | | | | | | | | | | | | | | | | |
| 51 | 51 | 6 | 476 | | | | | | | | | | | 470 | | | | | | | | | | | 519 | | | | | | | | | | | 486 | | | | | | | | | | |
| 102 | 102 | 6 | 408 | | | | | | | 422 | | | | 408 | | | | | | | | | | | 489 | | | | 446 | | | 441 | | | | 413 | | | | | | | | 436 | | |
| 102 | 102 | 13 | 516 | | | | | | | | | | 538 | 489 | | | | | 532 | | | | | | 576 | | | | | | | | 587 | | | | | | | | | 581 | | | | |
| 152 | 152 | 6 | | | | 366 | | | | | 382 | | | 350 | | | | | | | | | | | 456 | | | | 378 | | | 419 | | | | 354 | | | | 443 | | | | 403 | |
| 152 | 152 | 13 | | | | 467 | | | | | 437 | | | | | | 498 | | 513 | | | | | | 513 | | | | 498 | | | 523 | | | | 493 | | | | 478 | | | | 528 | |
| 203 | 203 | 6 | 385 | | | | 436 | | | 427 | | | | 376 | | | | 423 | | | 445 | | | | 445 | | | | 419 | | | 432 | | | | 376 | | | | 436 | | | 427 | | |
| 203 | 203 | 13 | 388 | | | | | 452 | | | | | | 379 | | | | | 461 | | | | | | 411 | | | | | 443 | | | | | | 306 | | | | | 447 | | | | |

(Li et al., 2009)

(Han et al., 2007)

(Guo et al., 2007)

(Bjorhovde, 1977)

Table D- 14: Coupon results from previous research – Normalized with respect to nominal yield strength – Part 1

AVERAGE OF FLAT WALLS WITHOUT WELD

AVERAGE OF FLAT WALLS WITH WELD

| | FLT AVRG - Excld wld | FLT AVRG | CRN AVRG | D/t | PROFILE | | |
|---|---|---|---|---|---|---|---|
| (Wilkinson, 1999) | 1.32 | 1.32 | 1.47 | 40 | 75 | 25 | 1.60 |
| | 1.13 | 1.13 | 1.39 | 42 | 150 | 50 | 3.00 |
| | 1.11 | 1.11 | 1.43 | 48 | 100 | 50 | 2.00 |
| | 1.16 | 1.16 | 1.37 | 42 | 125 | 75 | 3.00 |
| | 1.13 | 1.13 | | 42 | 150 | 50 | 3.00 |
| | 1.13 | 1.13 | | 51 | 125 | 75 | 2.50 |
| (Key & Hancock, 1993) | 1.27 | 1.27 | 1.44 | 20 | 102 | 51 | 4.90 |
| | 1.23 | 1.23 | 1.55 | 30 | 102 | 51 | 3.20 |
| | 1.18 | 1.18 | 1.27 | 49 | 102 | 51 | 2.00 |
| | 1.40 | 1.40 | 1.55 | 14 | 102 | 102 | 9.50 |
| | 1.24 | 1.24 | 1.56 | 21 | 102 | 102 | 6.30 |
| (Key, 1988) | 1.24 | 1.24 | 1.56 | 48 | 76 | 76 | 2.00 |
| | 1.26 | 1.30 | 1.49 | 39 | 152 | 152 | 4.90 |
| | 1.14 | 1.26 | 1.42 | 41 | 203 | 203 | 6.30 |
| | 1.07 | 1.20 | 1.47 | 51 | 254 | 254 | 6.30 |

Table D- 15: Coupon results from previous research – Normalized with respect to nominal yield strength – Part 2

| | FLT AVRG - Excld wld | FLT AVRG | CRN AVRG | D/t | PROFILE | | |
|---|---|---|---|---|---|---|---|
| (Key et al., 1988) | 1.23 | 1.23 | 1.54 | 48 | 76 | 76 | 2.00 |
| | 1.07 | 1.07 | 1.38 | 48 | 76 | 76 | 2.00 |
| | 1.21 | 1.21 | 1.44 | 39 | 152 | 152 | 4.90 |
| | 1.14 | 1.14 | 1.43 | 41 | 203 | 203 | 6.30 |
| | 1.17 | 1.17 | 1.41 | 51 | 254 | 254 | 6.30 |
| | 1.22 | 1.22 | 1.60 | 49 | 102 | 51 | 2.00 |
| | 1.12 | 1.12 | 1.31 | 31 | 127 | 51 | 3.60 |
| | 1.21 | 1.21 | 1.41 | 30 | 127 | 64 | 4.00 |
| | 1.08 | 1.08 | 1.33 | 30 | 152 | 76 | 4.90 |
| | 1.08 | 1.08 | 1.39 | 40 | 203 | 102 | 4.90 |
| | 1.15 | 1.15 | 1.38 | 41 | 254 | 152 | 6.30 |
| (Davison & Birkemoe, 1983) | 1.33 | | | 46 | 76 | 76 | 2.11 |
| | 1.36 | 1.36 | | 20 | 203 | 203 | 12.70 |
| | 1.16 | 1.16 | | 20 | 203 | 203 | 12.70 |
| | 1.25 | 1.25 | | 27 | 203 | 203 | 9.53 |
| (Kamani, 1974) | | | | | | | |
| | 1.11 | 1.11 | 1.61 | 14 | 102 | 102 | 9.53 |
| (Davison, 1977) | 1.10 | 1.16 | 1.34 | 27 | 203 | 203 | 9.53 |
| | 1.10 | 1.10 | | 28 | 305 | 203 | 11.43 |
| | 1.23 | 1.23 | | 27 | 102 | 305 | 9.53 |

Table D- 16: Coupon results from previous research – Normalized with respect to nominal yield strength – Part 3

| | FLT AVRG - Excld wld | FLT AVRG | CRN AVRG | D/t | PROFILE | | |
|---|---|---|---|---|---|---|---|
| (Salvarinas, 1977) | | | | | | | |
| | 1.08 | 1.14 | 1.30 | 27 | 203 | 203 | 9.53 |
| (Sun & Packer, 2014) | 1.32 | 1.32 | 1.71 | 15 | 152 | 152 | 13.00 |
| | 0.99 | 0.99 | 1.40 | 30 | 152 | 152 | 6.40 |
| (Afshan et al., 2013) | 1.35 | 1.35 | 1.76 | 32 | 150 | 150 | 6.00 |
| | 1.43 | 1.43 | 1.57 | 38 | 200 | 100 | 5.00 |
| | 1.26 | 1.26 | 1.53 | 27 | 150 | 100 | 6.00 |
| | 1.24 | 1.24 | 1.74 | 42 | 200 | 200 | 6.00 |
| (Tong et al., 2012) | 1.14 | 1.14 | | 17 | 135 | 135 | 10.00 |
| | 1.08 | 1.08 | | 17 | 135 | 135 | 10.00 |
| | 1.17 | 1.17 | | 17 | 135 | 135 | 10.00 |
| (Li et al., 2012) | | | 1.77 | 18 | 220 | 220 | 16.00 |
| | 1.26 | 1.34 | 1.59 | 14 | 108 | 108 | 10.00 |
| | 1.39 | 1.53 | 1.83 | 17 | 135 | 135 | 10.00 |
| (Hu et al., 2011) | | | | | | | |
| | 1.11 | 1.22 | 1.59 | 35 | 250 | 250 | 9.20 |
| | 1.04 | 1.17 | 1.60 | 35 | 200 | 300 | 9.20 |
| (Gao & Moen, 2010) | 1.40 | 1.40 | | 32 | 100 | 100 | 4.00 |
| | 1.05 | 1.05 | | 19 | 60 | 60 | 4.00 |
| | 1.16 | 1.16 | | 13 | 40 | 40 | 4.00 |
| | 1.19 | 1.19 | | 13 | 40 | 40 | 4.00 |
| | 1.31 | 1.31 | | 17 | 40 | 40 | 3.00 |

Table D- 17: Coupon results from previous research – Normalized with respect to nominal yield strength – Part 4

| | FLT AVRG - Excld wld | FLT AVRG | CRN AVRG | D/t | PROFILE | | |
|---|---|---|---|---|---|---|---|
| (Li et al., 2009) | 0.77 | 0.77 | | 14 | 135 | 135 | 12.00 |
| | 0.72 | 0.72 | | 17 | 135 | 135 | 10.00 |
| | 0.71 | 0.71 | | 51 | 200 | 200 | 5.00 |
| (Han et al., 2007) | 1.24 | 1.24 | | 40 | 100 | 100 | 3.20 |
| | 1.30 | 1.30 | | 32 | 100 | 100 | 4.00 |
| | 1.33 | 1.33 | | 28 | 100 | 100 | 4.50 |
| | 1.28 | 1.28 | | 27 | 125 | 125 | 6.00 |
| | 1.26 | 1.26 | | 21 | 100 | 100 | 6.00 |
| | 1.29 | 1.29 | | 21 | 100 | 100 | 6.00 |
| | 1.29 | 1.29 | | 21 | 100 | 100 | 6.00 |
| | 1.27 | 1.27 | | 18 | 125 | 125 | 9.00 |
| | 1.34 | 1.34 | | 14 | 100 | 100 | 9.00 |
| | 1.24 | 1.24 | | 14 | 100 | 100 | 9.00 |
| | 1.25 | 1.25 | | 14 | 100 | 100 | 9.00 |
| (Guo et al., 2007) | 1.16 | 1.16 | 1.58 | 41 | 320 | 200 | 8.00 |
| | 1.16 | 1.16 | 1.66 | 33 | 320 | 200 | 10.00 |
| | 1.13 | 1.13 | 1.59 | 28 | 320 | 200 | 12.00 |
| | 1.16 | 1.16 | 1.46 | 30 | 200 | 180 | 8.00 |
| | 1.14 | 1.14 | 1.64 | 38 | 300 | 300 | 10.00 |
| | 1.15 | 1.15 | 1.57 | 32 | 300 | 300 | 12.00 |

Table D- 18: Coupon results from previous research – Normalized with respect to nominal yield strength – Part 5

| | FLT AVRG - Excld wld | FLT AVRG | CRN AVRG | D/t | PROFILE | | |
|---|---|---|---|---|---|---|---|
| **(Bjorhovde, 1977)** | | | | | | | |
| | 1.38 | 1.41 | | 10 | 51 | 51 | 6 |
| | 1.19 | 1.24 | | 20 | 102 | 102 | 6 |
| | 1.46 | 1.53 | 1.61 | 10 | 102 | 102 | 13 |
| | 1.02 | 1.12 | | 31 | 152 | 152 | 6 |
| | 1.43 | 1.46 | 1.49 | 15 | 152 | 152 | 13 |
| | 1.10 | 1.15 | | 41 | 203 | 203 | 6 |
| | 1.04 | 1.07 | 1.31 | 20 | 203 | 203 | 13 |